Acta Geologica Hungarica

43/2000

VOLUME 43, NUMBER 1, 2000

Akadémiai Kiadó, Budapest

ACTA GEOL. HUNG. AGHUE7 43 (1) 1–106 (2000) HU ISSN 0236–5278

ACTA GEOLOGICA HUNGARICA

A QUARTERLY OF THE HUNGARIAN ACADEMY OF SCIENCES

Acta Geologica Hungarica publishes original studies on geology, crystallography, mineralogy, petrography, geochemistry and paleontology.

Acta Geologica Hungarica is published in yearly volumes of four numbers by

AKADÉMIAI KIADÓ
H-1117 Budapest, Prielle Kornélia u. 4, Hungary
http://www.akkrt.hu

Manuscripts and editorial correspondence should be addressed to the

ACTA GEOLOGICA HUNGARICA

Dr. János Haas
Academical Research Group, Department of Geology, Eötvös Loránd University of Sciences
H-1088 Budapest, Múzeum krt. 4/a, Hungary
Phone/Fax: (36-1) 266 4947
E-mail: haas@ludens.elte.hu

Orders should be addressed to

AKADÉMIAI KIADÓ
H-1519 Budapest, P.O. Box 245, Hungary
Fax: (36-1) 464 8221
E-mail: kiss.s@akkrt.hu

Subscription price for Volume 43 (2000) in 4 issues US$ 180.00, including normal postage, airmail delivery US$ 20.00.

Acta Geologica is abstracted/indexed in Bibliographie des Sciences de la Terre, Chemical Abstracts, GeoRef, Hydro-Index, Mineralogical Abstract

AGeol 43 (2000) 1

Acta Geologica Hungarica, Vol 43/1, pp. 1–14 (2000)

Petrology of the Triassic basaltoid rocks of Vareš (Central Bosnia)

Stevan Karamata
Serbian Academy of Sciences and Arts, Belgrade

Vera Knežević, Vladica Cvetković
Faculty of Mining and Geology, Belgrade

The study represents lithological and geochemical characteristics of the Triassic basaltic rocks of the Vareš area (Central Bosnia). This effusive complex belongs to the NNW–SSE elongated Borovica–Vareš–Čevljanovići–Kalinovik zone which is a part of a large belt of Triassic rift-related igneous provinces in Montenegro, Albania, Greece and Turkey. The Vareš volcanics represent the earliest products of the volcanic activity related to the Triassic rifting. In this volcanic complex two units have been recognized: the lower one is composed of green pillow lavas and subordinate coherent lava flows and dykes; the upper unit consists of in situ and resedimented hyaloclastic deposits interlayered with coherent and pillowed lava flows, rare dykes and sills. Within both units of the Vareš series thin chert intercalations occur. The volcanic activity was characterised by peaceful effusions of basaltic lava either coherent or fragmented by supercooling and quenching. The Vareš basaltic rocks bear evidences of low-Ti tholeiites which differentiation was dominated by fractionation of olivine, clinopyroxene and plagioclase. The parental magma surely originated within the intracontinental rifting geotectonic setting. However, the questions as whether the rift was a mantle plume phenomenon and what is the role of the subduction processes in the rift initiation and in providing the mantle source likely request additional investigation.

Keywords: basalt, rifting, Triassic, hyaloclastic deposits, lava flows, within-plate basalts, volcanic arc basalts, Dinarides, Vareš, Bosnia

Introduction

The basaltoid rocks of the Vareš area, in the earlier literature often refered to as "melaphyres from Vareš" (Karamata 1952), are products of the Triassic rift magmatism of the Borovica–Vareš–Čevljanovići–Kalinovik zone (BVČKZ) (Karamata 1988). This volcanic zone extends from Borovica, Vareš and Zvijezda at the northwest and north, then goes further to the south to Čevljanovići, eastern vicinity of Sarajevo and finally to Igman, Bjelašnica and Kalinovik (Fig. 1). During the second half of this century appeared papers about the Vareš volcanics (e.g. Karamata 1952, 1960, 1988; Pamić 1963) along with some regional investigation (e.g. Karamata 1978; Pamić 1982).

The BVČKZ developed after rifting of the northern margin of the Gondwana-land, i.e. during extensional subsidence in the Paleozoic complex now divided into the Central Bosnian Mts. and Bosnian–Durmitor terranes (?) at the south-west and the Drina–Ivanjica terrane at the northeast (Karamata et al. 1994).

Addresses: S. Karamata: Knez Mihajlova 35, YU-11000 Belgrade, Yugoslavia
V. Knežević, V. Cvetković: Dušina 7, YU-11000 Belgrade, Yugoslavia
E-mail: cvladica@eunet.yu
Received: 13 July, 1999

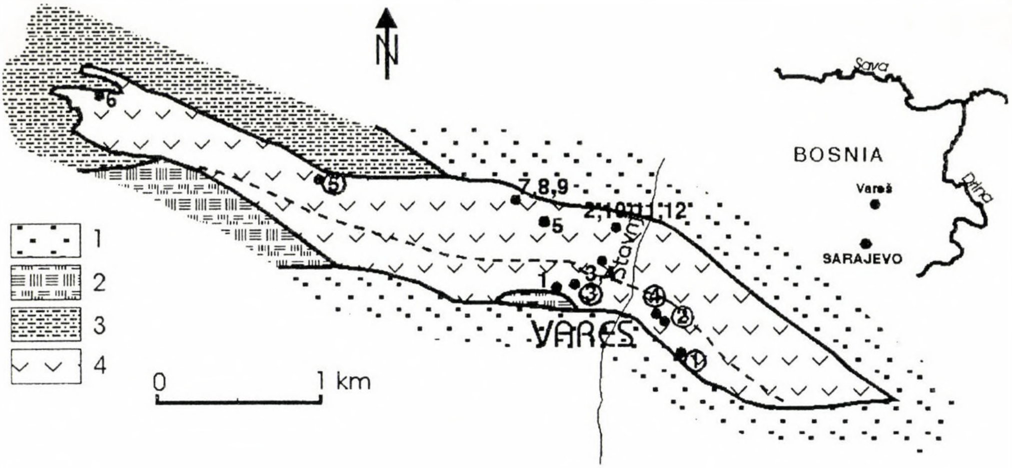

Fig. 1
Simplified geological sketch of the Vareš effusive complex (after Karamata 1956). 1. Werfenian sediments; 2. Anisian limestones; 3. Ladinian sediments; 4. basaltoid rocks of Vareš; I. the Upper unit; II. the Lower unit; numbers – samples analyzed on whole rock; encircled numbers – samples analyzed by microprobe

Consanguineous Triassic rift-related rocks are widespread further to east and southeast in western Serbia, Montenegro, Albania, Greece (e.g. Pe-Piper 1998) and Turkey.

The BVČKZ is composed of different facial members (Karamata, this volume) now exposed close to each other as tectonic slices parallel to the elongation of the zone. Almost in the whole the Triassic is represented by the Lower Triassic sandstones, siltstones, followed by shales and Anisian marls and limestones. This complex is overlained by limestones, basaltoid to rare acid volcanics and cherts of the Ladinian age.

The aim of this study is to present petrographical and geochemical characteristics of the basaltoid rocks of Vareš. They bear very important constrains for understanding paleotectonic conditions during the formation of the whole BVČKZ.

Lithology and petrography

The effusive complex of Vareš is situated on the northernmost part of the BVČKZ; it is WNW–ESE elongated, NNE steeply dipping lens-shaped body, about 5 km long and up to 500 m wide (Fig. 1). Along the tectonic northern and southern margins, where igneous products make sharp contact with Lower Triassic sediments reverse movements occurred. These ruptures intersect each other at the easternmost part of the Vareš body. However, in the western area interfingering of the volcanics and adjacent sediments occur. There can be observed that Ladinian sediments, represented by cherts, chert bearing limestones and dolomitic limestones, either cover or are interlayered within the Vareš efussive rocks.

The effusive complex can roughly be divided into the lower and upper unit. The lower unit is built of green pillow lavas among which sometimes massive and coherent basaltic lava flows and dykes can be found. The upper unit is mainly composed of in situ and resedimented hyaloclastic deposits interlayered with coherent and pillowed lava flows, rare dykes and sills. Within both units of the Vareš series thin chert intercalations occur.

The lower Vareš zone crops out as a section about 100 m wide and at least 90 m thick. It is predominately made by pillow lava piles and sheets which are in uppermost parts at some places separated by rather thin (1–2 m) hyaloclastic layers (Fig. 2a). The pillows are closely packed lacking hyaloclastic matrix in between. They range from few cm to over one m in diameter and show pronounced ellipsoidal forms. Within the pillows of the lower zone large lava piles and dykes (up to 10 m wide) have been found. Figure 2b presents an irregularly jointed and autobrecciated basaltic rock mass which intruded into older pillow lavas. The interior of the body shows pronounced medium-grained ophitic texture indicating subsurface consolidation of a considerably thick mass of basaltic lava. Its margins are more brecciated and not preserved. Within this unit among the pillows occur up to ten cm thick chert layers.

The upper Vareš zone appeared to be much thicker, about 200 m, cropping out along a section of about 300 m. It is mainly composed of volcaniclastic deposits which host numerous thin coherent lava flows which sometimes are found difficult to distinguish from dykes, as well pillowed lavas. Volcaniclastics are mostly represented by in situ and weakly to moderately resedimented basaltic hyaloclastites. The quench fragmentation in response to supercooling of basaltic lava become clearly evident from pronounced chilled rims of lava fragments sometimes displaying jig-saw fit puzzle structure (Fig. 2c). Some parts of hyaloclastites are made of closely packed, poorly sorted angular blocks of moderately vesiculated lava (Fig. 2d). Volcaniclastic material is at many places intruded by coherent basaltic dykes, from 10 cm to about 1 m thick. They often show well developed chilled margins and tiny normal joints perpendicular to cooling surfaces (Fig. 2e). In certain finegrained, undoubtedly redeposited layers, occur merely vesiculated scoriaceous volcaniclastic material, that could primarily originate by periodical phreatomagmatic/magmatic explosive events. After polyphase explosive/effusive volcanic activity unconsolidated pyroclastic and hyaloclastic material would be severely reworked and thereby intimately mixed. Within the upper zone thin intercalations of cherts with different amount of limonite material have been observed. In a pillow a single fragment, up to 30x50 cm, of reddish Upper Anisian limestones has been observed. The limestone does not show any alterations at the margins. At some places typical globular peperite (Busby-Spera and White 1987) have been formed. They are characterized by lensoidal, bulbous or lobate enclosures of the host, muddy calcareous ooze, which recrystallized at the margins (in an up to 1 mm wide zone) in a dense macrocrystalline calcite, in the inner parts into a porous microcrystalline calcite aggregate (Fig. 2f).

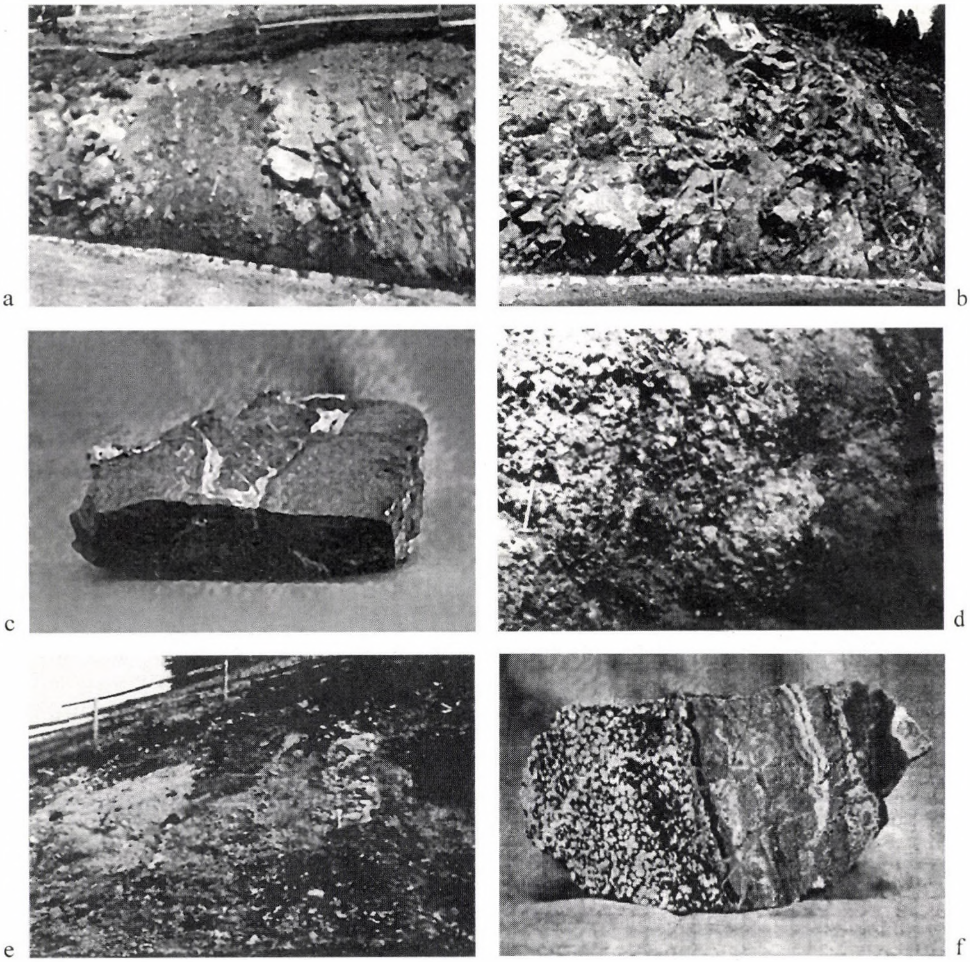

Fig. 2
a – Pillow-lava sheets interlayered by soft hyaloclastic deposits (western bank of the Stavnja R.); b – Irregularly jointed basaltoid rock mass intruding pillow lavas; c – A hand specimen showing pronounced chilled margins and jig-saw fit puzzle structure; d – Hyaloclastic deposits from the western bank of the Stavnja R., where closely packed angular to subangular basaltic fragments predominate; e – A basaltic dyke intruding resedimented hyaloclastites. Left margin of the body shows chilled parts and tiny normal joints; f – A hand specimen of globular peperites from the upper unit of the Vareš mass

Previously, these rocks have been given the names melaphyre or spilite (Karamata 1952). Here we attempt to look through the secondary processes paying our principal attention to their preserved primary igneous features. Thus, it became apparent that the rocks from the whole Vareš series display homogeneous basaltic petrography. They mainly vary in grain size as well as in intensity of vesiculation, metasomatism and secondary alteration processes which more or less have obliterated the primary mineral character, as in case of samples S 44-13, V 46-13 or V 40-4, what strongly affected some major and low field strength element concentration of those samples. The interiors of pillows, thinner dykes and coarser hyaloclastic fragments show porphyritic texture with rounded amygdules filled by calcite and rarely chlorite or chalcedony. Primary intratelluric assemblage is inferred by the presence of clinopyroxene, plagioclase and rare and totally destroyed olivine phenocrysts. Pyroxene is ubiquitous phenocryst phase. It is largely transformed to epidote, chlorite and uralite, but sometimes displays fresh relics. Calcic plagioclase is completely metasomatized (in sense of Hughes 1973); sometimes euhedral albite grains are supressed by aggregates of calcite, phrenite, clinozoisite and chlorite. The groundmass is built of metasomatized plagioclase and altered pyroxene intergrowths with or without completely chloritized volcanic glass. The central parts of the thick dykes and irregular lava piles show medium grained ophitic texture. These facies lack olivine and are characterized by completely albitized plagioclase and mostly fresh pyroxenes which show rather uniform chemical composition. According to microprobe analyses (Table 1) they correspond to transitional field between diopside and augite (Morimoto 1988; Fig. 3) having very similar chemistry (except somewhat higher Mg content) to the pyroxenes of spilites initiators of the Triassic volcanic activity in the Budva–Cukali zone (Bilik et al. 1993). The marginal parts of the dykes and massive lava flows are composed of volcanic glass mostly altered to chlorite and zeolite.

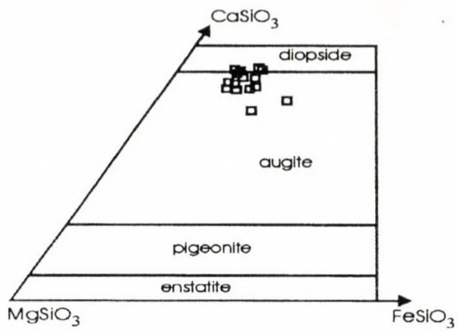

Fig. 3
Quadrilateral diagram for pyroxene classification (Morimoto 1988); empty squares represent pyroxenes from the Vareš basaltic rocks

Geochemical characteristics

A set of five samples were analyzed on major and trace elements by XRF technique at the ETH Zürich (Switzerland). Major elements were determined on additional seven samples in the Laboratory of Petrology of the Faculty of Mining

Table 1
Microprobe analyses of pyroxene from the basaltoid rocks of Vareš

Sample	V-2 (1)			V-18 (2)		V-107 (3)				V-107 (4)			V-54 (5)		
SiO_2	53.58	52.04	52.02	52.95	52.20	52.25	52.24	51.82	52.31	52.26	52.85	53.37	50.24	50.47	53.28
TiO_2	0.37	0.73	0.58	0.52	0.63	0.84	0.71	0.92	0.83	0.52	0.40	0.35	1.40	1.12	0.47
Al_2O_3	1.99	2.48	3.53	2.59	3.93	2.74	2.71	2.42	2.74	3.47	2.57	1.93	5.32	4.72	1.97
FeO	5.15	6.92	5.68	5.77	4.96	7.45	8.55	10.84	7.07	4.90	4.64	4.97	6.36	6.83	5.91
MnO	0.24	0.26	0.38	0.11	0.23	0.19	0.26	0.24	0.18	0.40	0.23	0.17	0.20	0.18	0.29
MgO	17.89	15.97	16.37	17.15	16.43	16.08	17.08	14.94	16.39	16.36	16.78	17.52	14.76	14.93	17.47
CaO	20.41	21.37	21.14	20.74	21.45	20.29	17.91	18.69	20.06	21.86	22.25	20.97	21.24	21.39	20.41
Na_2O	0.35	0.22	0.29	0.15	0.10	0.13	0.49	0.10	0.38	0.19	0.25	0.27	0.44	0.34	0.14
Σ	99.98	99.99	99.99	99.98	99.93	99.97	99.95	99.97	99.96	99.96	99.97	99.55	99.96	99.98	99.94
Si	1.950	1.916	1.904	1.936	1.910	1.927	1.918	1.935	1.922	1.912	1.929	1.953	1.849	1.859	1.949
Ti	0.010	0.020	0.016	0.014	0.017	0.023	0.020	0.026	0.023	0.014	0.011	0.010	0.080	0.031	0.013
Al^{IV}	0.085	0.108	0.152	0.112	0.170	0.119	0.117	0.107	0.119	0.150	0.111	0.083	0.231	0.205	0.085
Al^{VI}	0.035	0.024	0.056	0.048	0.080	0.046	0.036	0.042	0.040	0.061	0.040	0.036	0.080	0.064	0.034
Fe^{2+}	0.137	0.177	0.145	0.176	0.152	0.230	0.221	0.339	0.198	0.138	0.115	0.141	0.172	0.172	0.181
Fe^{3+}	0.020	0.036	0.029	0.000	0.000	0.000	0.042	0.000	0.019	0.012	0.027	0.011	0.024	0.038	0.000
Mn	0.007	0.008	0.012	0.003	0.007	0.006	0.008	0.008	0.006	0.012	0.007	0.005	0.006	0.006	0.009
Mg	0.970	0.876	0.893	0.935	0.896	0.884	0.935	0.831	0.897	0.892	0.913	0.955	0.810	0.820	0.953
Ca	0.796	0.843	0.829	0.813	0.841	0.802	0.705	0.748	0.790	0.857	0.870	0.822	0.838	0.844	0.800
Na	0.025	0.016	0.021	0.011	0.007	0.009	0.035	0.007	0.027	0.013	0.018	0.019	0.031	0.024	0.010
Wo(%)	41.231	43.445	43.460	42.168	44.359	41.732	36.894	38.840	41.346	44.836	45.048	42.491	45.296	44.910	41.190
En(%)	50.266	45.157	46.808	48.498	47.259	46.000	48.936	43.183	46.986	46.671	47.252	49.376	43.780	43.599	49.038
Fs(%)	8.503	11.398	9.732	9.333	8.382	12.269	14.170	17.977	11.667	8.493	7.700	8.133	10.924	11.491	9.772

EXPLANATION: 1 – Pillow-lava, basal part of the lower unit; 2, 3 and 4 – Small intrusive body, middle part of the lower unit; 5 – Fragment, middle part of the upper unit; Locations of the samples are presented in Fig 1 as encircled numbers; all analyses represent the cores of separated mineral grains and Geology (Belgrade) by classical wet analysis. It was complemented by XRF analyses on selected trace elements in the Laboratory of IGEM in Moscow (Russia). The only large discrepancy (more than ten orders of magnitude) show P_2O_5 contents being respectively very low in samples analyzed in the ETH.

All major and trace element analyses are summarized in Table 2. The analysed samples display all the features that often characterize metasomatized basaltoid rocks i.e. enrichment and/or depletion of those elements which are believed to be mobile during the low temperature metamorphism and secondary alteration processes. Hence, they have rather variable CaO (1.25–9.00% – after subtracting $CaCO_3$), MgO (2.01–6.44%) and Na_2O (1.16–5.53%) content and mostly high Fe_2O_3/FeO ratio. It is accompanied by the LILE pattern characterized by large variations of Rb and Ba contents. Consequently our interpretation have been mainly concentrated on the immobile elements which behave either incompatible (e.g. Ti, Nb, Zr, Y) or compatible (Ni, Cr, Co) in respect to partial melting and fractional crystallization processes.

Table 2
Major and trace element analyses of the Vareš basaltoid rocks

Sample	V 40-4	V 77	V 25	V-28	V-42	V 90	V 45-22	S 44-13	V 46-13	V 30	V 33	V 36
No	1	2	3	4	5	6	7	8	9	10	11	12
SiO_2	53.90	47.70	44.58	45.00	50.50	45.45	51.90	58.50	57.25	37.77	37.15	40.36
TiO_2	3.34	0.70	0.68	0.68	1.67	0.99	1.25	1.25	1.00	0.93	0.77	0.73
Al_2O_3	11.35	14.52	14.49	17.92	19.15	15.88	11.93	8.35	13.75	12.05	14.78	14.12
Fe_2O_3	7.29	3.40	4.74	4.05	4.73	5.43	6.80	8.26	3.97	4.63	6.44	4.10
FeO	7.68	4.34	2.58	2.61	4.45	0.78	1.50	1.72	2.01	7.11	1.62	3.06
MnO	0.06	0.10	0.00	0.04	0.09	0.04	0.06	0.09	0.06	0.09	0.07	0.10
MgO	5.30	5.87	6.44	5.70	4.18	2.01	2.75	2.70	3.80	8.96	3.94	5.86
CaO	1.25	13.31	12.73	10.58	4.25	12.48	8.62	2.00	9.00	10.72	18.92	15.51
Na_2O	3.92	3.42	3.18	2.72	5.53	2.87	5.53	2.84	3.35	1.16	1.72	2.16
K_2O	1.19	1.11	1.59	1.36	0.71	2.39	0.40	2.65	1.19	0.63	0.95	0.77
P_2O_5	0.02	0.37	0.20	0.22	0.01	0.30	0.02	0.03	0.02	0.22	0.21	0.20
CO_2	-.-	3.05	5.46	3.24	-.-	6.72	-.-	-.-	-.-	6.19	11.06	8.06
H_2O^+	4.17	2.33	2.64	4.90	3.59	4.14	7.72	6.15	5.43	8.94	2.14	4.59
H_2O^-	0.81	0.42	0.90	0.93	1.15	0.60	1.54	5.52	0.49	0.86	0.34	0.45
Σ	100.28	100.64	100.21	99.95	100.01	100.08	100.02	100.06	101.32	100.26	100.11	100.07
ppm												
Nb	29	9	6	5	14	8	0	14	0	10	6	5
Zr	127	78	85	81	105	90	82	103	77	115	79	76
Y	52	21	20	18	31	22	16	28	19	23	20	22
Sr	88	117	77	99	198	116	148	114	161	64	107	112
Rb	42	11	3	4	7	12	0	46	11	48	7	4
Th	18				8		0	8	0			
Pb	30				19		55	4	0			
Ga	25				14		5	13	3			
Zn	162				211		1032	88	25			
Cu	0				50		0	22	0			
Ni	11	62	246	394	108	<50	209	212	51	161	112	161
Co	30				23		25	26	7			
Cr	19	309	375	651	174	270	352	313	160	371	221	218
V	121				158		95	284	222			
Ce	20				0		0	26	10			
Nd	13				0		0	26	10			
Ba	134	142	<100	<100	61	181	44	145	106	139	140	103
La	13				0		0	27	15			
Sc	49				35		27	31	22			

1, 2. pillow-lava, basal part of the lower unit; 3, 4. rim (3) and interior (4) of a pillow in the lower part of the upper unit; 5, 6. basaltic fragments in the middle part of the upper unit; 7, 8, 9. fragments within hyaloclastites and lava blocks, upper part of the upper unit; 10, 11, 12. pillow upper part of the upper unit; Locations of the samples are represented in Fig. 1 as numbers

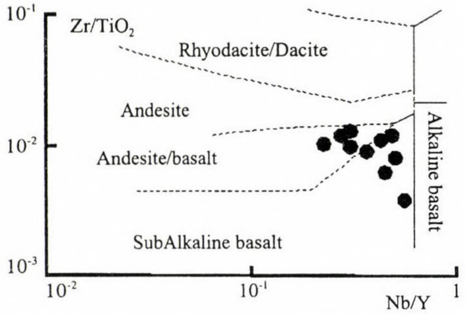

Fig. 4
The classification of the Vareš volcanic rocks according to immobile trace elements (Winchester and Floyd 1977)

From the Nb/Y vs Zr/TiO_2 classification diagram (Winchester and Floyd 1977), presented in Fig. 4, the basaltoid rocks of Vareš plot in the subalkaline basalts and the transitional andesite/basalt field.

According to the contents of compatible elements a vast majority of the samples analysed represents evolved basalts with few of them which could be candidates for primitive magma (e.g. V-28: Ni=394 ppm, Cr=651 ppm). In Fig. 5. are presented variation diagrams with Zr (ppm) as index of fractionation. Although there is obvious scattering of data plots, most probably due to effects of crystal accumulation, it is apparent that Cr, Ni and Sr all behaved compatible. It depicts the role of olivine, clinopyroxene and plagioclase fractionation what is in strong agreement with the observed phenocryst assemblage. Sr contents show slight but mostly regular negative correlation with Zr, thereby suggesting that strontium largely survived the mobilization effects during the secondary processes. TiO_2, Nb and Y all have incompatible trend showing the highest contents in the sample V 40-4 with the lowest concentration of Ni and Cr. Furthermore, the incompatible trend for TiO_2 is similar to the LPT rocks of some tholeiitic flood provinces (e.g. Parana, Columbia River; Wilson 1989). From the variation pattern of Ni and Cr contents, which are believed to be relatively insensitive to the partial melting processes, it can be inferred that fractional crystallization was of principal importance for the rock petrogenesis. Unfortunately, secondary processes have affected some samples decreasing their Ni and Cr contents what in certain extent have obliterated their strongly compatible variation pattern. The hypothesis of only limited role of degree of partial melting in the evolution of the Vareš basaltic rocks supports mostly the flat pattern with only slight increase of Nb/Y and decrease of Ti/Nb ratio in respect with increasing of Zr content.

In order to elaborate some petrogenesis aspects we plot the sample S 44-13 (given the high silika content is a result of postmagmatic processes it is one of the most primitive samples analyzed on the full set of trace elements) on a multielement spider diagram (Sun and McDonough 1989; Fig. 6). The trend of decreasing trace element contents toward the right approaching ten times chondritic for the least incompatible elements (i.e. Ti, Zr, Y) shows that the Vareš basaltic rocks originated from the undepleted mantle source. Even this sample with very high Cr and Ni content expresses evolved character, for instance a distinctive Sr trough, characteristic of other samples too, as evidence of low

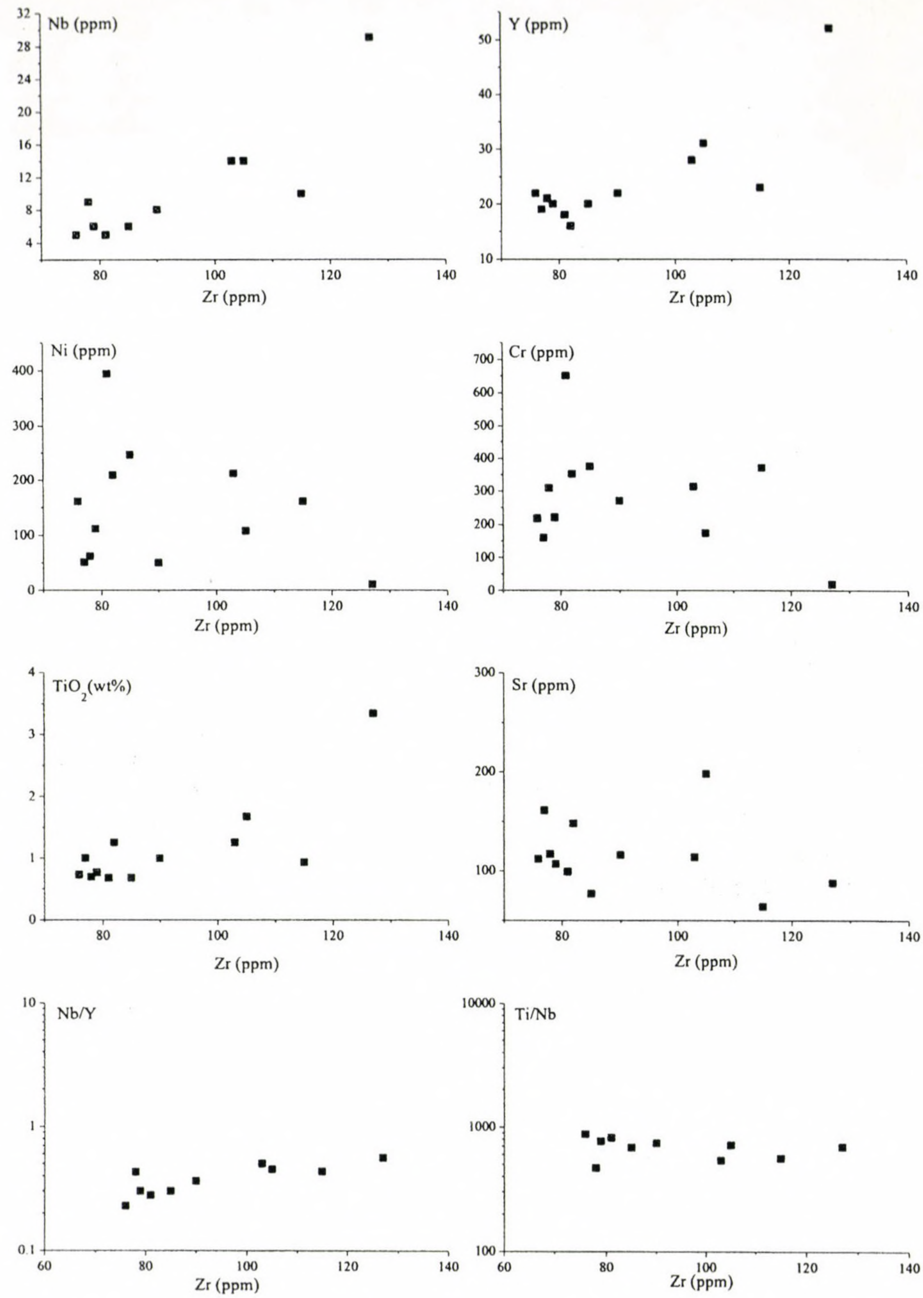

Fig. 5
Variation diagrams of selected trace element contents and ratios of the Vareš basaltoid rocks; Zr content was used as differentiation index

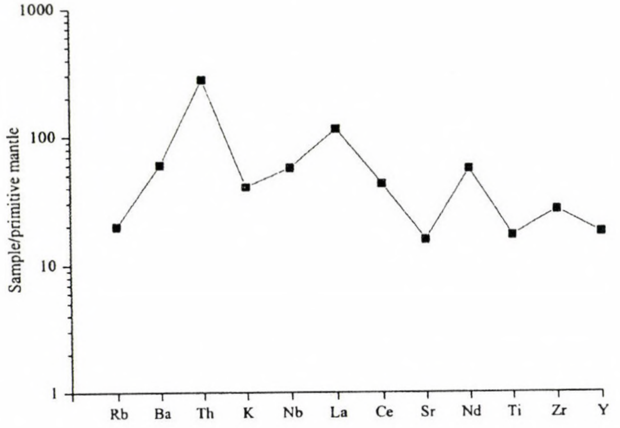

Fig. 6
Multielement spider-diagram for the S 44-13 sample of the Vareš basaltic rocks. Coefficient of normalization according to Sun and McDonough (1989)

pressure plagioclase fractionation. It is generally accepted that Th peak coupled with weak Nb and Ti trough could be explained by at least two possibilities (1) the role of subduction component in the mantle source and/or (2) the incorporation of upper crustal material. Both consequences would produce higher concentration of the LILE as well as higher LILE/HFSE ratio but, as we mentioned earlier, we have to abandon these elements as strongly mobile during the alteration processes.

Zr vs Zr/Y discrimination diagram (Pearce and Norry 1979) for determining paleotectonic conditions of basaltic rocks is presented in Fig. 7a. It was used by an important approximation in that all the plotted rocks do not meet the requirement of CaO+MgO>12% due to alteration and not their primary composition. From this diagram, as well as from Zr/4-Y-2Nb plot (Meshede 1986; Fig. 7b) within plate setting and undepleted mantle source appear as the most probable. On the contrary, the discrimination diagram after Pearce and Gale (1977), that uses ratios of Ti (ppm) and Zr (ppm) vs Y (ppm) (Fig. 7c) reveal mixed VAB and MORB affinity of the Vareš basaltic rocks. In order to put further constraints on geotectonic setting of these rocks we used F1-F2 discrimination diagram for based on pyroxene composition (Nisbet and Pearce 1977; Fig. 8), which is most suitable for metamorphosed and weathered basalts. The Vareš clinopyroxenes concentrate on the field where basalts of WPT, VA and OF affinity cannot be unambiguously distinguished.

Discussion and conclusion

In respect to other occurrences of the Triassic volcanic rocks of the BVČKZ the Vareš effusive complex shows considerable lithological and geochemical uniformity for it consists mainly of subalkaline basalts. Assuming the observed lithology the Vareš rock mass originated in a shallow water environment where predominately pillow-lavas and hyaloclastic facies formed. Coherent volcanic products are represented by dykes and smaller irregular bodies intruding earlier hyaloclastites, as well as by rare massive lava flows. The volcanic activity was dominated by peacefull outpourings of basaltic lava either coherent and massive or fragmented by supercooling and quenching. Initially low water pressure produced moderate vesiculation of the magma which might have given rise to phreatomagmatic/magmatic explosive events. However, they have had to be of limited extent taking into account a lack of volcanic fragments of unequivocal pyroclastic origin.

Although displaying some calc-alkaline features the Vareš basaltic rocks bear evidences of low-Ti tholeiites: (1) strongly incompatible TiO_2 trend, (2) higher Ni and Cr, as well as Nb and lower Sr content (assuming that Sr content was not severely lowered by alteration and low temperature metamorphism) then it would be expected for CAB, and (3) lack of intermediate and/or acid equivalents. Some major and trace elements variation patterns emphasise fractionation as the most important differentiation mechanism during which olivine, clinopyroxene and plagioclase were precipitated. Almost unchanged Nb/Y or Ti/Nb ratios along with increasing differentiation show no significance of partial melting but it does not account to the effects of possible contamination processes. Hence, its role remains an open question which ought to be emphasised in further studies.

Most plate tectonic reconstructions place all the terranes presently west of the Vardar zone composite terrane on the south side of Palaeotethys, i.e. as

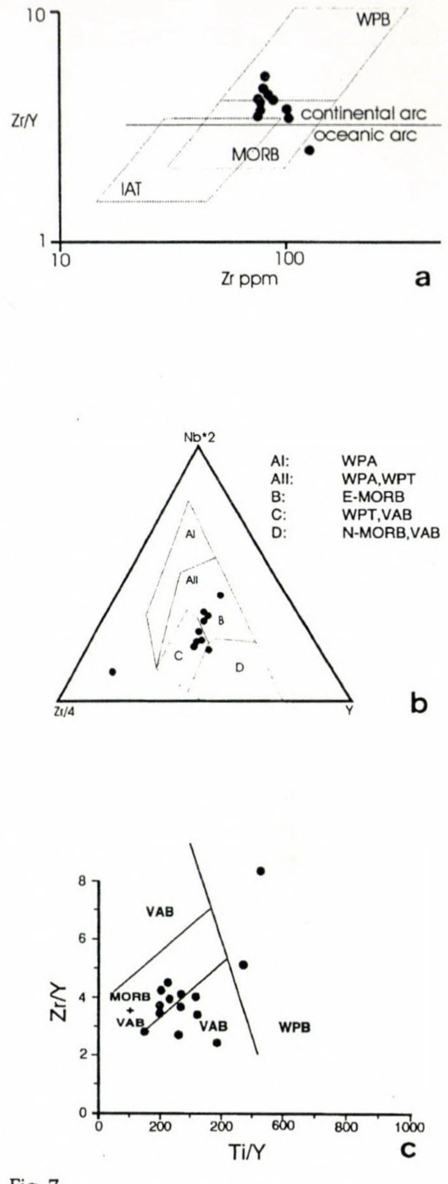

Fig. 7
Discrimination diagrams for distinguishing basaltoid rocks from different tectonic setting. a – Zr vs Zr/Y (Pearce and Norry 1979); b – Nb*2-Zr/4-Y diagram (Meshede 1986); c – Zr/Y vs Ti/Y (Pearce and Gale 1977); dots represent the Vareš basaltic rocks

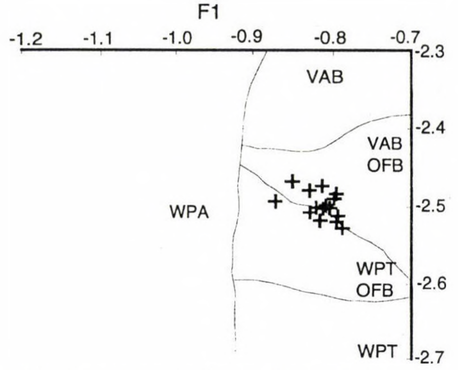

Fig. 8
F1–F2 discrimination diagrams for distinguishing basaltoid rocks from different tectonic setting on the basis of pyroxene chemical composition (Nisbet and Pearce 1977); WPA – within-plate alkaline; WPT – within-plate tholeiite; VAB – volcanic arc basalts; OFB – ocean floor basalts, crosses represent the Vareš basaltic rocks

rifted segments from the northern parts of the Gondwanaland (e.g. Karamata et al. 1994). The Vareš effusive complex together with the whole BVČKZ make a northwestern part of the large belt containing volcanic rocks related to the Triassic rifting processes. The belts continues further to south and southeast through western Serbia, Montenegro, Albania, Greece and western Anatolia.

Taking into consideration their petrographical and geochemical evidence the Vareš rocks have differentiated from a primitive basaltic magma which nature strongly depended on the character of the mantle source. The parental magma originated within the intracontinental rifting geotectonic setting, but some problems indeed request further elaboration. If the rift was associated with a mantle plume and what was the role of the subduction processes in the rift initiation and in providing the mantle source represent main questions still waiting for a consensus of most authors (e.g. Pe-Piper 1982; Wooler et al. 1992, Robertson et al. 1991, etc.). Either the small rock volume and the lack of uplift during the evolution of the Vareš effusive complex (all products are clearly shallow undersea facies) it is very unlikely that its origin could be connected to a mantle plume but it is not to exclude introduction of astenospheric melts. Moreover, within-plate geochemical character of some samples (higher HFSE, especially Nb, samples: V 40-4, V 45-22, V 44-13) leave possibility that partial melts from astenosphere were of at least limited importance in the genesis of the primary magma. Contemporaneously, some geochemical features of the Vareš rocks indicate their volcanic arc-affinity (e.g. Nb-Ti through coupled with Th peak; Sun and McDonough 1989; Fig. 6) arguing in favor of a back-arc setting with respect to Palaeotethys. This ambiguity becomes more obvious further to south of the BVČKZ in the areas of the Triassic rift-related rocks in Montenegro (e.g. Knežević et al. 1998).

Acknowledgement

This study is a part of the Project GEODYNAMICS of the Serbian Academy of Sciences and Arts. The authors greatly acknowledge to Tatjana Marchenko for the trace element analyses in the Laboratories of the IGEM in Moscow (Russia).

References

Bilik, I., V. Knežević, E. Árvá-Sós, M. Jánosi, S. Karamata 1993: The spilites of Becići, in the neighbourhood of Budva, initiators of the rifting in Budva-Cukali zone. – Ann. Geol. Penins. Balk., 57/1, pp. 215–238.

Busby-Spera, C.J., J.D.L. White 1987: Variation in peperite textures associated with differing host-sediment properties. – Bull. Volcanol., 49, pp. 765–775.

Hughes, C.J. 1973: Spilites, keratophyres, and the igneous spectrum. – Geol. Mag., 109/6, pp. 513–527.

Karamata, S. 1952: Opšta karakteristika melafira okoline Vareša (Bosna). (Allgemeine Charakteristik der Melaphyre in der Umgebung von Vareš [Bosnien]). – Spomenica Miše Kišpatića, Jug. Akad. Znan. i Umjet., pp. 237–247, Zagreb.

Karamata, S. 1960: Melafiri Vareša (Die Melaphyre von Vareš). – Simpozijum o problemima alpijskog inicijalnog magmatizma, Ilidža-Vareš, 1960, III-1-III-20.

Karamata, S. 1978: Magmatske stijene područja Borovica-Vareš-Čevljanovići-Bjelašnica-Kalinovik (Igneous rocks of the Borovica–Vareš–Čevljanovici–Bjelanšnica–Kalinovik). – Geologija Bosne i Herceg., IV, Magmatizam i metalogenija, pp. 69–82, Sarajevo.

Karamata, S. 1988: Trijaski rifting i s njim vezane geološke tvorevine u zoni Borovica-Cevljanovići. (Triassic rifting processes and related geological formations in the Borovica-Cevljanovići area). – Zbornik ref. skupa "Minerali, stijene, izumrli i živi svijet BiH", Sarajevo 7-8.10.1988, Zemaljski muzej Bosne i Hercegovine, pp. 105–110, Sarajevo.

Karamata, S. (this volume): Mineralization related to the Triassic rifting initiating the formation of the Dinaridic Ophiolitic Belt. – Acta Geol. Hung., Budapest.

Karamata, S., B. Krstić, M.D. Dimitrijević, I. Filipović, M.N. Dimitrijević, V. Kneževic 1994: Terranes between the Adriatic and the Carpatho-Balkanian arc (Triassic igneous rocks from the Yugoslavian Dinarides). – Bull. CVIII de l'Acad. Serbe des Sci. et des Arts, Class. des Sci. math. et natur., 34, pp. 47–66.

Knežević, V., V. Jovanović, E. Memović, K. Resimić 1998: Trijaske magmatske stene jugoslovenskih Dinarida. – XIII Kongr. geol. Jugosl. Herceg Novi, Petrologija, mineralogija i geohemija, III, pp. 61–66.

Meshede, M. 1986: A method of discriminating between different types of mid-ocean ridge basalts and continental tholeiites with Nb-Zr-Y diagrams. – Chem. Geol., 56, pp. 207–218.

Morimoto, N. 1988: Nomenclature of Pyroxenes. – Miner. Petrol., 39, pp. 55–76.

Nisbet, E.G., J.A. Pearce 1977: Clinopyroxene Composition in Mafic Lavas from Different Tectonic Settings. – Contrib. Mineral. Petrol., 63, pp. 149–160.

Pamić, J. 1963: Trijaski vulkaniti okolice Čevljanovića i kratak osvrt na trijaski vulkanizam zone Borovica-Vareš-Čevljanovići (Triassic volcanic rocks of Čevljanovici and short regards to Triassic volcanism of the Borovica–Vareš–Čevljanovici zone). – Geol. glasn., 7, pp. 9–20, Sarajevo.

Pamić, J. 1982: Trijaski magmatizam Dinarida (Triassic magmatism of Dinarides). – Nafta, 236 p. Zagreb.

Pearce, J.A., G.M. Gale 1977: Identification of ore-deposition environment from trace element geochemistry of associated igneous host rocks. – In: Volcanic Processes in Ore Genesis. – Geol. Soc. Spec. Publ., 7, pp. 14–24.

Pearce, J.A., M.J. Norry 1979: Petrogenetic implications of Ti, Zr, Y and Nb variations in volcanic rocks. – Contrib. Mineral. Petrol., 69, pp. 33–47.

Pe-Piper, G. 1998: The nature of Triassic extension-related magmatism in Greece: evidence from Nd and Pb isotope geochemistry. – Geol. Mag., 135/3, pp. 331–348.

Robertson, A.H.F,. P.D. Clift, P. Degnan, G. Jones 1991: Paleoceanography of the Eastern Mediterranean Neotethys. – In: Chanel, J., E. Winterer, L.F. Jansa (Eds): Palaeogeography and paleooceanography of Tethys. – Paleogeography, Paleoclimatology, Paleoecology, 87, pp. 289–343.

Sun, S., W.F. McDonough 1989: Chemical and isotopic systematics of oceanic basalts: implications for mantle composition and processes. – In: Saunders, A.D., M.J. Norry (Eds): Magmatism in the Ocean Basins – Geol. Soc. Spec. Publ., 42, pp. 313–345.
Wilson, M. 1989: Igneous Petrogenesis. – Unwin Hyman, London–Boston–Sydney–Wellington, 466 p.
Winchester, J.A., P.A. Floyd 1977: Geochemical discrimination of different magma series and their differentiation products using immobile elements. – Chem. Geol., 20, pp. 325–343.
Wooler, D.A., A.G. Smith, N. White 1992: Measuring lithosphering stretching on Tethyan passive margins. – Jour. Geol. Soc., 149, pp. 517–532.

Acta Geologica Hungarica, Vol. 43/1, pp. 15–23 (2000)

Mineralization related to the Triassic rifting in the Borovica–Vareš–Čevljanovići–Kalinovik zone (Bosnia)

Stevan Karamata
Serbian Academy of Sciences and Arts, Belgrade

In the Borovica–Vareš–Čevljanovići–Kalinovik zone (Central Bosnia) remnants of sedimentary and magmatic formations, which originated in basins related to the embryonic phases of the Lower and Middle Triassic rifting, are well exposed. These basins underwent different evolutions related to variation in depth, input of clastic material from the neighboring land area, connection with the open sea, redox conditions, occurrence of volcanism, etc. As a result of this different mineralization conditions obtained in these basins. The events leading to their formation are analyzed.

Keywords: rifting, basins conditions, Fe-Mn- and sulfide mineralization, Lower-Middle Triassic, Central Bosnia

Introduction

The beginning of the Triassic was characterized by rifting in many parts of the Dinarides, but these areas are mostly covered by tectonic nappes or post-collisional formations. In Central Bosnia, in the Borovica–Vareš–Čevljanovići–Kalinovik zone (BVČKZ) at the northern margin of the Central Bosnian Mts. Terrane, illustrative examples of formations developed during this period are exposed. In the area, because of imbricated structure, Lower and Middle Triassic formations originated in different geologic environments and are thus characterized by distinct sedimentary and magmatic rocks, as well as mineralization.

The areas with preserved and exposed traces of initial rifting are generally rare worldwide. In the before-mentioned area they are, however, well exposed (Karamata 1988) and, because of the diversity in composition and evolution of the units, very instructive. For this reason they will be presented here.

The author began to study these areas in 1950, and with some interruptions he investigated them until a few years ago. This paper presents a short synthesis of that work.

Address: S. Karamata: Knez Mihajlova 35, YU-11000 Belgrade, Yugoslavia
Received: 14 July, 1999

0236–5278/2000/$ 5.00

Short geologic review

The BVČKZ represents the tectonically deformed northern margin of the Central Bosnian Mts. Terrane (CBMT), docked to the basement of the Dalmatian-Herzegovinian Composite Terrane prior to the Permian. From the Upper Permian to the Upper Triassic this was the southern part of an intracontinental rifting zone, becoming in the Upper Triassic the southern margin of the Dinaridic ophiolite belt (Karamata and Krstić 1996). The present geologic position of the BVČKZ is presented in Fig. 1.

The Lower and the Middle Triassic formations of the BVČKZ occur between the formations of the Dinaride ophiolite belt in the north, and at the northern margin of the CBMT in the south. The Upper Cretaceous and Oligocene–Miocene sediments were later deposited in a trench, and a lacustrine basin imposed upon the northern marginal part of the CBMT, between the exposed BVČKZ and the Paleozoic core of the CBMT. The geologic framework is additionally complicated by the occurrence of Upper Jurassic to Berriasian marls and fine-grained clastics, occurring now on both sides of the BVČKZ because of later tectonic activity. An important point is that in the BVČKZ, beneath the Lower and Middle Triassic sedimentary rocks with intercalated Middle Triassic volcanics, locally Paleozoic low-grade metamorphic rocks are exposed (Fig. 2, after Veljković, 1979).

The BVČKZ zone

In the area of interest (Fig. 1), or in the northern and northeastern parts of the CBMT, subsidence began in the Upper Permian with the deposition of shallow water clastics and "porous" limestones on metamorphic rocks of the Paleozoic core of the terrane. The subsidence, expressed mostly by listric faulting, was intensified through time at the margin of the terrane and locally associated with volcanism.

The listric faulting initiated the formation of shallow to very shallow basins, where different sediments were accumulated. The basins were mostly connected with the open sea but some were locally or temporally isolated, i.e. the conditions were mostly oxidizing, only occasionally becoming reducing. They were situated at varying distances from land, the most distal ones being separated from dry land by other basins. The land, or denudation area, was distinct in morphology and vegetation; thus, the input of material into the basins was different in amounts as well as in composition. From the Lower to Upper Triassic conditions in some basins changed: they were deepened or uplifted, or the redox potential changed. Magmatic masses intruded beneath some basins, heating up the overlying rocks and the deep circulating waters; in others basaltic rocks (of WPB affinity) and rare keratophyric lava reached the surface along deep faults. Such geologic evolutions and conditions are reflected in the presence/absence of different ore deposits.

As examples the following evolutions of the Lower and Middle Triassic formations in selected basins can be presented:

i) *The Fe ore-bearing basin.* The iron ore-bearing development occurs on both sides of the Stavnja River, close to the management office of the "Vareš" mine (Katzer 1910; Cissarz 1956; Ramović 1979; Bodulić 1979 with additions of Karamata).

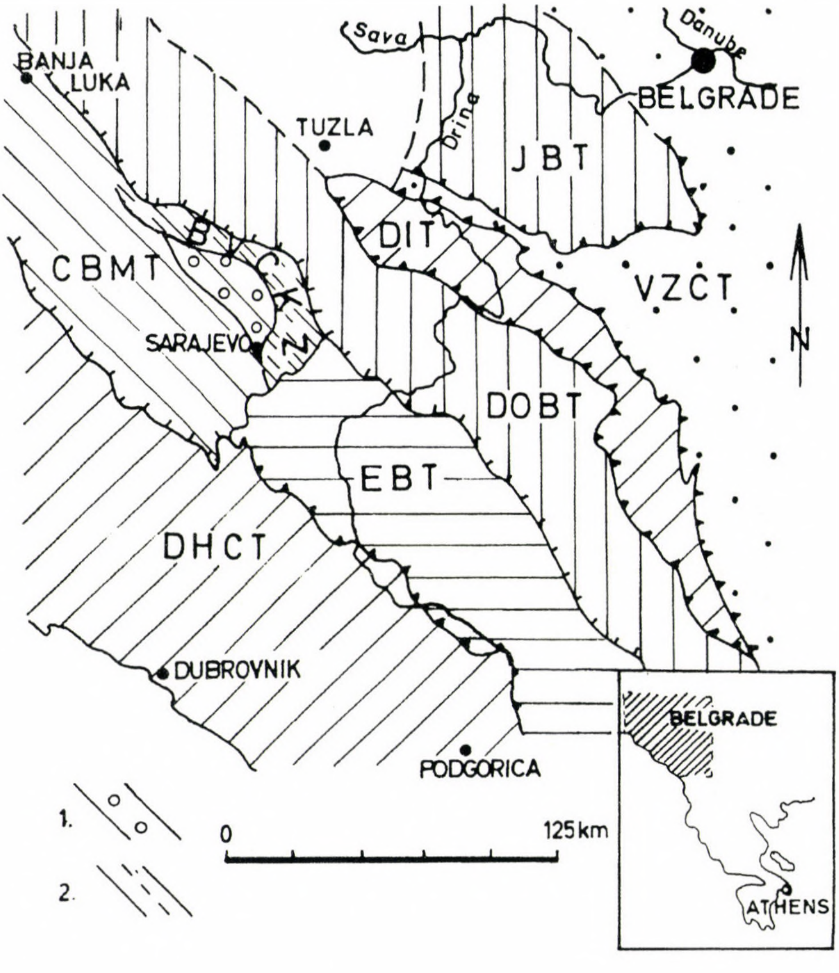

Fig. 1
The position of the Borovica–Vareš–Čevljanovići–Kalinovik Zone (BVČKZ) in the geotectonic framework of the western part of the Balkan peninsula. VZCT – Vardar Zone Composite Terrane; JBT – Jadar Block Terrane; DIT – Drina-Ivanjica Terrane; DOBT – Dinaride Ophiolite Belt Terrane; CBMT – Central Bosnian Mts. Terrane; EBT – East Bosnian Terrane; DHCT – Dalmatian-Herzegovinian Composite Terrane; 1. (Oligocene–)Miocene Sarajevo – Zenica Basin; 2. The BVČKZ area, including the Upper Jurassic – Berriasian continental slope sediments. Terranes after Karamata and Krstić 1996

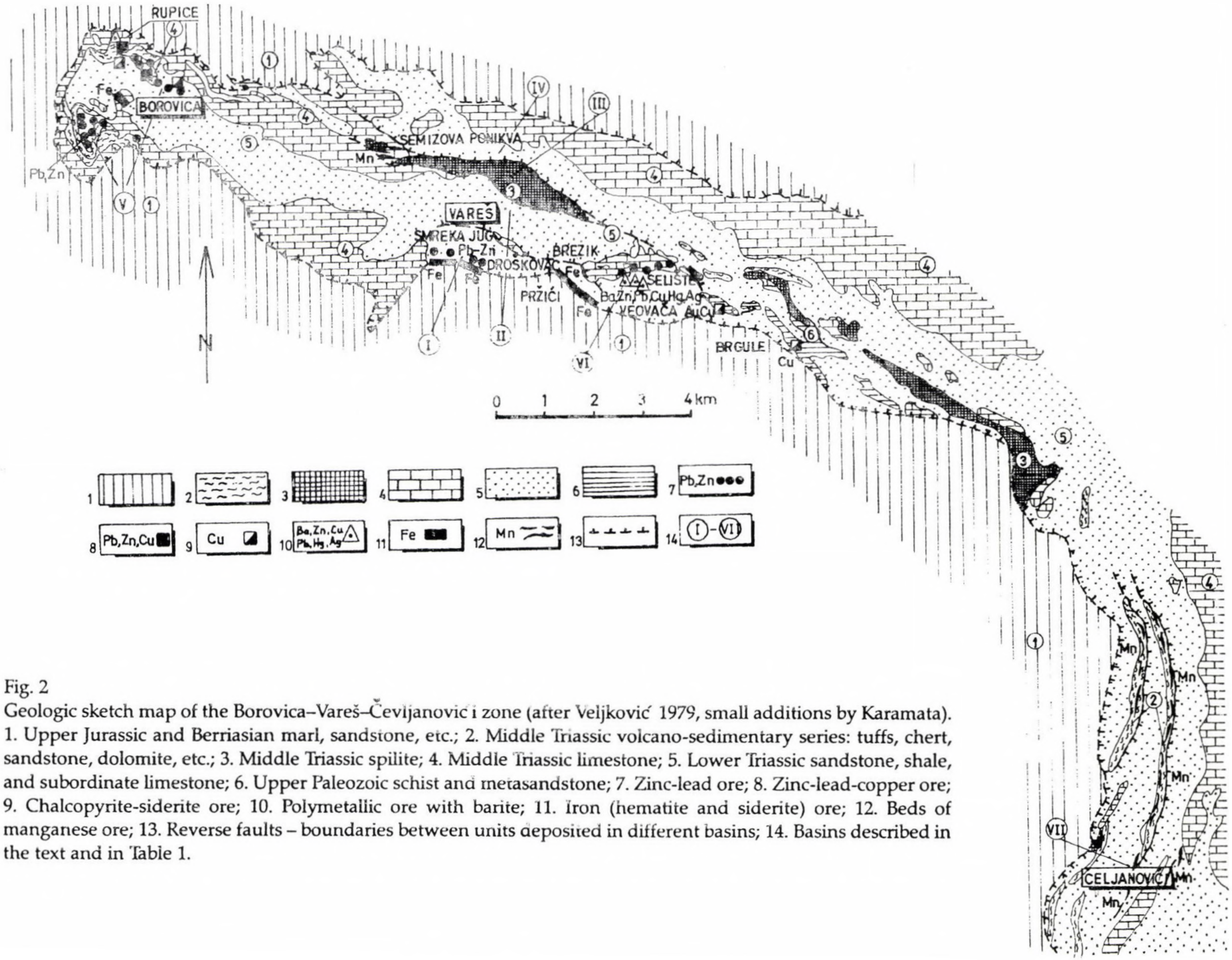

Fig. 2

Geologic sketch map of the Borovica–Vareš–Čevljanovići zone (after Veljković 1979, small additions by Karamata). 1. Upper Jurassic and Berriasian marl, sandstone, etc.; 2. Middle Triassic volcano-sedimentary series: tuffs, chert, sandstone, dolomite, etc.; 3. Middle Triassic spilite; 4. Middle Triassic limestone; 5. Lower Triassic sandstone, shale, and subordinate limestone; 6. Upper Paleozoic schist and metasandstone; 7. Zinc-lead ore; 8. Zinc-lead-copper ore; 9. Chalcopyrite-siderite ore; 10. Polymetallic ore with barite; 11. Iron (hematite and siderite) ore; 12. Beds of manganese ore; 13. Reverse faults – boundaries between units deposited in different basins; 14. Basins described in the text and in Table 1.

- Lower Triassic bituminous shale with plant relics – marsh sediments reducing conditions. Grading into:
- siderite, bedded, with at the base locally developed barite, pyrite, Cu-, Zn- and Pb-sulfide beds, and impregnated with the same minerals reducing conditions, almost without input of terrigenous material (the neighboring land was probably flat and covered by vegetation). The siderite is covered by
- green shale, with an intercalated layer composed of limestone nodules or lenses in a clayey to marly matrix, grading upward into reddish shale. These sediments originated during deepening of the basin when the reducing conditions changed to oxidizing, and weak input of terrigenous material took place. It grades into
- beds of hematite, often enriched in manganese, with Anisian to Ladinian ammonites. Upward the hematite beds become richer in silica, and later jasper occurs as interlayers, becoming finally the main member. This unit originated under oxidizing conditions. It passes into
- chert, tuffaceous in the upper levels, with a layer enriched in pyrite, Zn-, Pb-, and Cu-sulfides. This unit again originated under reducing conditions, probably simultaneously with volcanic activity. The later evolution of this basin cannot be interpreted, and it is not clear if the basin existed any longer.

ii) The southern Vareš basin with pelitic development is exposed in the Stavnja river valley north of the ore-bearing zone as far as the town of Vareš. It contains:
- greenish to reddish Lower Triassic shale, with subordinate fine-grained sandstone, originating in a basin with input of terrigenous material from a mainly flat land area, covered by vegetation. It grades upward into:
- Anisian black limestone, becoming white upward white, and
- Ladinian and younger deposits are presently absent, but probably existed and were analogous to those deposited in other basins connected to the open sea.

iii) Basin with spilites of (Anisian–) Ladinian age and some coeval limestone, dolomite and chert situated between the basins with pelitic and psammitic evolutions, presented as "ii" and "iv". It is not clear if this basin existed earlier and later, or whether its formation and development were mainly related to the fracturing enabling the rise of magma.

iv) The northern Vareš basin with psammitic development, exposed in the Stavnja river valley to the north of the town of Vareš, consisting of
- red, with subordinate white, medium to coarse-grained Lower Triassic sandstone, originating by rapid input of clastic material in a basin situated in front of an intensely weathered area. The conditions in the basin were oxidizing. Above the sandstone were deposited:
- Anisian black to gray limestone, a few meters thick, grading into white, massive limestone of Anisian to Ladinian age. Later evolution of the basin can

be only presumed, but considering that, to the East, the lowest levels of Upper Triassic limestone overlie the Middle Triassic ones, the basin continued to exist as a shallow water marine area. This basin was connected to the open sea.

v) The Borovica basin – the Triassic deposits near Borovica. Above the Lower Triassic sandstone, Anisian and Ladinian shale, sandstone, chert, dolomite, siliceous limestone, and tuff with occurrences of metabasalt and keratophyre, were deposited. The Ladinian series contains beds of barite with pyrite, sphalerite, galena, chalcopyrite, sulfosalts and rare cinnabar (i.e. a polymetallic sulfide mineralization). The Middle Triassic sediments were deposited in a basin poorly and only sporadically some periods connected with the open sea. The ore deposition corresponds to periods of isolation of the basin when strong reducing conditions existed. The evolution of the basin following the Ladinian cannot be determined.

vi) Barite and sulfide-rich sediments occurring *near Veovaca* (studied by Veljković 1979). Lower Triassic sandstone passes into porous dolomitic limestone grading into gray to black dolomite of Lower Anisian age. This in turn passes into Fe-Mn-rich shale, chert and tuffaceous sandstone corresponding to the Uppermost Anisian – Lowermost Ladinian, when basaltic volcanism took place in this area. Simultaneously with this series sulfide-bearing breccia originated, in an area subsided between faults. It is composed of fragments of Paleozoic low-grade schist, Lower Triassic sandstone and Anisian limestone, with rare basaltic volcanic bombs, in a sandy mudstone, locally very rich in micro-crystalline gray barite. The barite is associated with sphalerite, galena, pyrite (partly representing recrystallized gel), sulfosalts, antimonite, cinnabar, etc. The mineralization represents a metal-rich mud deposited in a closed basin partly bordered by faults. Hydrothermal solutions ascending along the faults delivered their metal content to the sea-water and the mud, where, because of strong reducing conditions, the polymetallic mineralization occurred. The basin was similar to the one near Borovica, and the same conclusion on its further development can be made.

vii) The manganese ores of Čevljanovići at the eastern part of the BVČKZ (described by Kulenović 1979) deposited in the *Čevljanovići Basin*. The Lower Triassic, developed in its usual form in the BVČKZ, is covered by Anisian limestone grading upward into a Ladinian series composed of shale, red and green chert, tuff and tuffaceous sandstone with interlayered spilite. Between the chert, beds of manganese ore are interlayered. The principal ore mineral is psilomelane, associated with braunite, manganite, etc., hematite or rare pyrite; chalcopyrite, sphalerite and other sulfides occur as well. The mineralization originated in the basin during periods of very reduced input of terrigenous material and of transitional oxidizing/reducing conditions.

The further evolution of the basin is linked to its connection with and adjustment to the conditions of a shallow open sea, with a very low input of clastic material from the margins, when Upper Triassic limestone was deposited.

Discussion

It is clear that the formation of the mineralization in the BVČKZ depended on the conditions in the basins and in the surrounding dry land. Of primary importance for basin development was the input of material from the neighboring land, i.e. its character and the amount. The emerged areas land could be flat or with steep slopes, with poor vegetation and undeveloped soil or covered by abundant vegetation and with thick soil, or even with marshes at the basin margins. Given that the input of clastic material was low, the question of how the basin communicated with the open sea, i.e. whether oxidizing or reducing conditions existed, is of great significance. The presence of volcanic activity in the basin or at its margin could promote the formation of different mineralizations. For the BVČKZ all these factors are summarized in Table 1.

According to the data presented above and given in Table 1, the most important factor for the formation of mineralization is the absence or a very weak input of clastic material. This means that a basin where ore can be concentrated must be separated from emerged land by other basins or narrow (mainly submarine) ridges. If, however, the basin is close to the land, a condition for the formation of mineralization is that the coastal land be flat and covered by thick soil and vegetation. If such circumstances exist mineralization can occur and its type and ore minerals willdepend on the redox conditions in the basin and the presence or absence of volcanism. Such convenient conditions are rarely found and occur in special conditions only, mostly in small areas. Therefore mineralization in BVČKZ is encountered in the small basins mentioned previously, i.e. in the Veovaca basin and the Borovica basin, as well as in some middle-sized ones: the iron ore-bearing basin in the Vareš area and the Cevljanovići basin during some periods of their evolution.

Acknowledgement

I extend my sincere thanks to all the co-workers during my more than 40 year-long work in the BVČKZ. The suggestions of Prof. D. Hovorka are highly appreciated.

Table 1

Conditions by formation of mineralization in the Borovica–Vareš–Čevljanovici–Kalinovik zone (BVČKZ) during the lower–middle Triassic rifting phase

Basin	Time	Clastic input	REDOX condition	Volcanic activity	Sediments	Mineralization
Fe-ore bearing basin	LT	negl.	RED	-	bituminous shale	-
	LT-AN	-.-	RED	-	barite, pyrite, Cu-, Zn-, Pb-sulphide	
	AN	-.-	RED	-	siderite with former minerals	
	AN	weak	RED to OX	-	shale and nodular marl	-
	(AN) LAD	negl.	OX	?	haematite	
	LAD	weak	OX to RED	weak	cherts with pyrite, Cu-, Zn-, Pb-sulphides	
Southern Vareš basin	LT	yes	(RED) OX	-	shale +/- sandstone	-
	AN	negl.	OX	-	limestone	-
Basin with spilites	(AN) LAD	-	OX	basaltic, strong	rare cherts + limestone	-
Northern Vareš basin	LT	yes	OX	-	sandstone	-
	AN-LAD	negl.	OX	-	limestone	-
Borovica basin	LT	strong	OX	-	sandstone	-
	(AN) LAD	strong to weak	OX to RED	weak to strong	limestone, shale, chert	-
					barite, pyrite, Cu-, Zn-, Pb-etc. sulphides	
Veovača	similar, in Ladinian submarine hydrothermal solutions contributed to the ore formation					
Čevljanovići basin	LT	strong	OX	-	sandstone	-
	AN	weak	OX	-	limestone, shale, chert	-
	LAD	weak to negl.	OX trans. to RED	weak to strong	Mn-oxides and hydroxides	

EXPLANATION: LT - Lower Triassic, AN - Anisian, LAD - Ladinian, negl. - negligible, OX - Oxidizing conditions, RED - Reducing conditions

References

Bodulić, G., 1979: Područje Vareša (The Vareš Area). – In: Jurić M. (Ed.): Mineralne sirovine Bosne i Hercegovine – Ležišta crnih metala (Mineral xources of Bosnia and Hercegovina – Ore deposits of black metals). – Geoinženjering, Sarajevo, pp. 221–239 (in Serbo-Croat).

Cissarz, A., 1956: Lagerstätten und Lagerstättenbildung in Jugoslawien in ihre Beziehungen zu Vulkanismus und Geotektonik. – Mem. Service geol. geophys. Serb., Belgrade, 6, 152 p.

Janković, S. 1987: Genetic types and Major Triassic Deposits of the Dinarides, Yugoslavia. – In: Janković S. (Ed): Mineral Deposits of the Tethyan Eurasian Metallogenic Belt between the Alps and the Pamirs. UNESCO/IGCP Project no 169. Dept. of Mineral Exploration, Fac. Of Mining and Geology, Belgrade University, pp. 11–33.

Karamata, S. 1988: Trijaski rifting i s njim vezane geološke tvorevine u zoni Borovica–Čevljanovići (Triassic rifting processes and related geologic formations in the Borovica – Čevljanovići area). – Zemaljski muzej Bosne i Hercegovine, Zbornik sa naucnog skupa "Minerali, stijene, izumrli i živi svijet B i H", Sarajevo, pp. 105–110 (in Serbian).

Karamata, S., B. Krstić 1996: Terranes of Serbia and neighbouring areas. – In: Knežević V., Krstić B. (Eds): Terranes of Serbia, Fac. of Mining and Geology, Univ. Belgrade, pp. 25–40.

Katzer, F. 1910: Die Eisenerzvorräte Bosniens und Herzegovina. – Sonderband, Berg. – u. Hüttenmänn usw. 58, 343 p.

Kulenović, E. 1979: Trijaska nalazišta Borovice i Čevljanovića (Triassic ore occurrences between Borovica and Čevljanović). – In: Jurić M. (Ed): Mineralne sirovine Bosne i Hercegovine – Ležišta crnih metala, Geoinženjering, Sarajevo, pp. 375–380 (in Serbo-Croat).

Pamić, J., O. Pamić, J. Olujić, R. Milojević, D. Veljković, I. Kapeler 1978: Tumac za geol. kartu list Vareš (Geology of the sheet Vareš) 1:100.000. – Savezni geološki zavod, Beograd, 68 p. (in Serbo-Croat).

Ramović, M., 1979: Trijaska cinko-olovna rudišta (Triassic zinc-lead ore deposits). – In: M. Ramović (Ed): Mineralne sirovine Bosne i Hercegovine. – Ležišta obojenih metala, Sarajevo, pp. 24–36, 48–58 (in Serbo-Croat).

Veljković, D. 1979: Veovaca – Dahštansko istocno od Vareša (Veovaca – Dahštansko to the east of Vareš). – In: M. Ramović (Ed.): Mineralne sirovine Bosne i Hercegovine – Ležišta obojenih metala. – Geoinženjering, Sarajevo, pp. 36–48, 54–55 (in Serbo-Croat).

Acta Geologica Hungarica, Vol. 43/1, pp. 25–41 (2000)

Lamprophyric rocks of the Miocene Borač Eruptive Complex (Central Serbia, Yugoslavia)

Vladica Cvetković, Dejan Prelević
Faculty of Mining and Geology, Belgrade

Zoltán Pécskay
ATOMKI, Debrecen

The aim of this study is to emphasize the petrogenetic significance of the lamprophyric rocks of the Borac Eruptive Complex (BEC) in order to explain magma evolution processes. The largest occurrences of these rocks crop out in the northwestern parts of the BEC as hypabyssal bodies, but in some areas they are represented by autobrecciated lava flows as well as resedimented volcanic breccias. These rocks correspond to calc-alkaline phlogopite lamprophyres consisting of diopside (Wo_{45-49}), phlogopite (> 0.5% Cr_2O_3, Mg# up to 0.86), sanidine ($Or_{54.6-54.9}$), ± oligoclase, ± altered olivine, ± leucite, apatite and opaque minerals, as well as quartz and zoned plagioclase ($An_{47.3}$) of xenocrystic origin. K/Ar ages (22.78±0.88 Ma and 22.65±0.89 Ma – phlogopites; 22.72±0.86 Ma – w.r.) show that the hypabyssal lamprophyres of the Borač area formed during the first volcanic phase. These rocks correspond to potassic series (Foley et al. 1987) displaying a high content of K_2O, MgO, TiO_2, incompatible (Ba, Sr, Zr, Y, Nb, Th and ΣREE) as well as compatible trace elements (Cr, Ni, Co, V and Sc). Their parental melts probably originated within the subcontinental mantle, i.e. by melting of the parts previously enriched by the subduction component.

Keywords: lamprophyric rock, volcanic succession, volcanoclastic deposits, phlogopite lamprophyre, Miocene, Borac

Introduction

About 2000 km^2 of the territory of Serbia is covered by Tertiary volcanics which are mostly represented by intermediate to acid calc-alkaline rock series. In almost all of the volcanic provinces small subvolcanic bodies occur, rarely lava flows of melanocratic volcanic rocks (often referred to as latites by earlier authors), feldspatoid rocks or trachyandesites. Sporadically the word 'lamprophyre' has also been attached to those rocks – either as a noun or an adjective.

Lamprophyres and related rocks have been extensively studied during the past two decades, being the subject of considerable debate especially on the issues of their classification and petrogenesis. However, only a few authors paid attention to the origin of these rocks in Serbia (e.g. Majer and Karamata 1983). The nature of these volcanic rocks, however, is still not fully understood and their investigation could provide very important petrogenetic evidence. The aim of this paper is to emphasize lamprophyric rocks of Serbian terrains, with these volcanic products from the BEC serving as an example.

Addresses: V. Cvetković, D. Prelević: Dušina 7, YU-11000 Belgrade, Yugoslavia;
E-mail: cvladica@eunet.yu
Z. Pécskay: ATOMKI, H-4001 Debrecen, Hungary; E-mail: pecskay@moon.atomki.hu
Received: 9 December 1998

0236–5278/2000/$ 5.00

Geologic setting

The Borač Eruptive Complex (BEC) is a volcanic area of about 120 km^2 where many types of volcanic rocks and various volcanic landforms and structures crop out; it is situated in Šumadija, about 100 km south of Belgrade. The BEC is part of the Vardar Zone Composite Terrane (Karamata et al. 1994), forming its western subzone (Dimitrijević 1995), which became tectonically complicated as a result of the docking of the Jadar Block Terrane before the Oligocene. The basement rocks are represented by Upper Cretaceous flysch which corresponds to relic trough deposits originating during and after the main phases of closure of the ancient Vardar Ocean.

On the basis of their relationship with the lacustrine sediments of the adjacent Gornji Milanovac, Kragujevac and Zapadna Morava Basins the stratigraphic position of the Borač volcanic succession is difficult to interpret, largely because of lack of knowledge about the age of the sediments (i.e. Early or Middle Miocene?). Given the available data it seems inevitable that the oldest volcanic products originated during or after the Early Miocene (e.g. Ilić 1961). A simplified volcanological map of the BEC as well as the geotectonic sketch of central Serbia are presented in Fig. 1.

During the past three decades a large amount of data concerning the areal distribution and petrographic characteristics of the Borac volcanic rocks has been published (e.g. Marković and Pavlović 1967). Cvetković (1997) pointed out relics of two caldera structures of which the older one originated after a plinian/subplinian eruptive phase. The author recognized different coherent and volcanoclastic facies of volcanic rocks ranging from rhyodacites to basaltic andesites, which all express medium to high potassium calc-alkaline geochemistry. Apart from the calc-alkaline volcanics there occur high to ultrapotassic volcanic rocks of apparent lamprophyric character that are the main focus of this paper.

Analytical techniques

Mineral analyses on a set of samples were carried out using two machines: "Camebax" with the "Link" energo-dispersive unit and conditions of 20 kV, 1.3–1.5 mA, 70–100 s (Institute of Experimental Mineralogy of the Russian Academy of Sciences – IEM RAN, Moscow) and "AMRAY 18301" together with the EDAX PV 9800 EDS detector, under conditions of 15 kV, 1.5 nA and 30 s (Department of Petrology and Geochemistry, Eötvös Loránd University, Budapest).

Major element analyses were made by wet analysis in the Laboratory of Petrology and Geochemistry, Faculty of Mining and Geology, Belgrade.

Ba, Nb, Zr, Rb, Sr, Y, Ni and Cr contents were determined by XRF in the IGEM RAN Laboratory (Moscow), with Rh-anode, under conditions of 40–60 kV and 30–35 mA respectively, using a LiF-200 crystal analyzer.

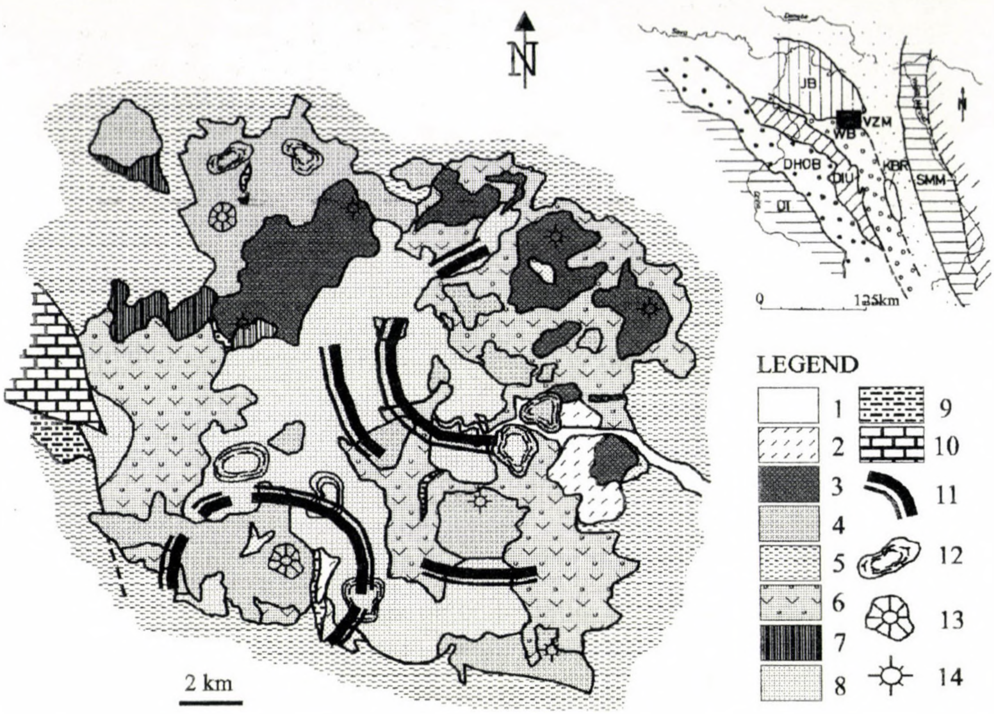

Fig. 1
Simplified volcanological map of the Borač eruptive complex (after Cvetković 1997) with the geotectonic sketch of the Balkan Peninsula (after Karamata et al. 1998). 1. alluvium; 2. delluvium; 3. andesites and basaltic andesites; 4. quartzlatites, 5. Middle Miocene(?) sediments; 6. quartzlatite-rhyodacite pyroclastics; 7. lamprophyres; 8. dacites; 9. Early Miocene sediments; 10. Cretaceous sediments; 11. caldera relics; 12. lava dome; 13. volcanic neck; 14. supposed volcanic center. JB – the Jadar Block; VZM – the Main Branch of the Vardar Zone; WB – the western Branch of the Vardar Zone; KBR – the Kopaonik Block Rise; DIU – the Drina-Ivanjica Unit; DHOB – the Dinaridic–Hellenidic Ophiolite Belt; DT – the Dinaridic Trunc; SMM – the Serbo Macedonian Mass

REE analyses were carried out by INAA at the Laboratories of the KFKI (Budapest, Hungary). For the short irradiation (about 2 min) Whatman 41 filter and for the long irradiation (48 hours) clean, sealed Suprasil (Hearaeus) quartz tubes were used. Measuring was carried out with a high-resolution HPGe detector, with an 8K ADC gamma-spectrometer.

Sr-Nd isotope ratios were determined at the Laboratory of Institute of Experimental Mineralogy of the Russian Academy of Sciences – IEM RAN (Moscow, Russia). Rb contents were measured by a MI 1320-type mass-spectrometer, with one collector and ion source 2*Ta. Sr, Nd and Sm analyses were performed by a Finnigan MAT-262 mass-spectrometer with static collectors and ion source 2*Re; Normalization values were: $^{146}Nd/^{144}Nd=0.7219$ and

$^{86}Sr/^{88}Sr$=0.1194; standards for evaluation of the results: La Jolla: $^{143}Nd/^{144}Nd$ = 0.511841 +/- 14, BCR-1: $^{143}Nd/^{144}Nd$ = 0.512628 +/- 7 and Elmer and Amend: $^{87}Sr/^{86}Sr$ = 0.708051 +/- 18.

K-Ar age determinations were carried out on whole rock samples and phlogopites. Specimens showing alteration were eliminated after thin section examination.

The samples were degassed in a conventional extraction system using induction heating and measured by mass spectrometric isotope dilution with a ^{38}Ar spike. Data handling and recording were controlled by a microcomputer.

Potassium analyses were made using standard flame photometric techniques. Potassium and argon determinations were checked regularly by interlaboratory standards HD-B1, LP-6, GL-0 and Asia 1/65. Atomic constants suggested by Steiger and Jäger (1977) were used for calculating the radiometric age. All analytical errors represent one standard deviation (68% confidence level). Details of the instruments, the applied methods and results of calibration have been described elsewhere (Balogh 1985).

Petrography and age of the Borač lamprophyric rocks

The Borač calc-alkaline lamprophyres appear both as hypabyssal and surface volcanic phenomena. In addition, they appear as numerous xenoliths within younger quartz-latites of subvolcanic and lava flow facies.

Their largest occurrence is observed in the northwestern part of the complex where they are represented by hypabyssal phlogopite lamprophyres. It is a dark gray, massive to slightly vesicular volcanic rock, which expresses holocrystalline porphyritic texture. Phlogopite flakes, along with pyroxene phenocrysts and rare quartz and feldspar xenocrysts, are often observable macroscopically.

In the close vicinity of the village of Borač a small (several tens of m^2) outcrop of an autobrecciated lava plug of leucite-bearing phlogopite lamprophyre was found. The fragmented lava overlies resedimented quartz-latite/rhyodacite pyroclastic deposits producing a clear zone of reddish color, which is built of mixed effusive and wet, redeposited pyroclastic material. The autoclastic deposit is fairly unsorted. The fragments of lamprophyric lava are subangular to angular and their size ranges from above half of a meter to below a cm in diameter, and when strongly vesiculated they resemble a typical scoria. The matrix is subordinated, being composed of the same small fragments of brecciated lava.

Many potassic/ultrapotassic(?) varieties, which could be genetically related to the lamprophyres have been observed within epiclastic breccias, e.g. phlogopite-leucite melaphonolite, phlogopite-feldspar leucitite and olivine melaleucitite, but this rock material was not suitable for chemical analysis. Therefore, only phlogopite calc-alkaline lamprophyres of subvolcanic and effusive origin have been subjected to mineralogical and geochemical investigation. It should be emphasized that the main mineralogical difference between volcanic and subvolcanic lamprophyric occurrences in the Borač area is the presence of leucite in the former and absence in the latter (Table 1).

Table 1
Modal composition of the Borač lamprophyres

No/mineral	Phl	Py	Ol	Lc	Opq	Ap	GM		Xen
							San+Pl	Gl	
T-116	19.11	27.26	-	-	6.16	1.98	39.21	-	6.28
T-117	18.11	31.15	1.22	-	5.84	2.31	35.81	-	5.56
D-214a	11.95	42.56	9.87	-	3.59	1.76	29.70	-	0.57
T-318	17.32	26.81	-	-	5.56	3.02	42.53	-	4.76
S-4	19.16	34.52	6.71	7.18	3.98	1.99	-	-	-
Gl-639	1.96	30.14	16.11	40.94	3.00	2.85	-	5.94	-

T-116 and T-117 – hypabyssal phlogopite lamprophyre; D-214a – effusive leucite-bearing phlogopite lamprophyre; T-318 – hypabyssal phlogopite lamprophyre; S-4 – effusive phlogopite lamprophyre with olivine and leucite; GI-639 – effusive phlogopite lamprophyre with olivine and leucite, Abbreviations: Phl – phlogopite, Py – pyroxene, Ol – olivine, Lc – leucite, Opq – opaque minerals, Ap – apatite, GM – groundmass, San+Pl – sanidine and plagioclase within the groundmass, Gl – glass, Xen – xenocrysts

Within the quartz-latites situated in the northwestern part of the Borac complex occur frequent xenoliths of olivine and leucite-bearing lamprophyres. The size of these subrounded to rounded lamprophyric fragments ranges from a few cm to less than one mm in diameter. Around the xenoliths, which form very sharp borders without reaction rims, plagioclase and alkali feldspar microlites within the quartz-latitic groundmass sometimes show tangential orientation.

The Borac lamprophyric rocks show porphyritic texture with holocrystalline to hypocrystalline groundmass. The main constituents which appear as phenocrysts are clinopyroxene, phlogopite, and when present leucite and relics of olivine. The groundmass is built of sanidine, apatite and opaque minerals, while in some varieties plagioclase and leucite occur as microlites as well. Zeolites, calcite and rarely epidote are the main secondary minerals. Quartz and sometimes plagioclase are present as xenocrysts. Selected microprobe analyses of minerals of the BEC are presented in Table 2.

Clinopyroxene is the most abundant phenocryst, except in the above-mentioned olivine melaleucitite where olivine and leucite predominate. It appears as small prismatic phenocrysts, from 2 × 0.5 mm to below 0.5 mm in diameter, which sometimes build glomeroporphyritic aggregates. According to chemical analyses it is diopside (Morimoto et al. 1988) which expresses a rather uniform CaO content (23.81–22.29%, Wo_{45-49}), while Al-Si substitution shows an upper limit (about 10%) according to theoretical values (Deer et al. 1966). Three analyses of the same clinopyroxene phenocryst (Fig. 2) revealed a change in MgO, FeO, Al_2O_3 and TiO_2 contents with oscillatory manner.

Table 2

Selected chemical mineral analyses of the Borac lamprophyric rocks

No	T-117			D-214a		No	D-214a		No	T-117	D-214a				
	Phl1	Phl2		Phl1			San1	San2		Cpx1		Cpx1		Cpx2	
	core	core	rim	core	Core		microlite	microlite		core	core	middle	rim	core	rim
SiO_2	39.71	40.05	36.70			**SiO_2**			**SiO_2**	54.78	52.13	50.92	51.86	51.82	53.14
TiO_2	2.59	2.53	4.80	2.63	2.74				**TiO_2**	0.19	0.37	0.80	0.53	0.56	0.43
Al_2O_3	15.39	14.99	16.55	14.97	15.09	**Al_2O_3**	19.04	19.41	**Al_2O_3**	1.47	2.79	4.26	3.12	3.17	2.20
FeO	7.50	8.38	11.55	6.32	6.14				**FeO**	3.04	5.19	7.60	5.54	6.68	3.46
Cr_2O_3	0.89	0.72	0.52	0.87	0.37										
MnO	0.06	0.20	0.03						**MnO**	0.17	0.05	0.09	0.11	0.02	0.15
MgO	21.14	20.33	17.31	20.69	21.01				**MgO**	17.73	15.26	13.87	14.84	14.19	16.73
CaO	0.06	0.02	0.11			**CaO**	0.00	0.00	**CaO**	22.29	23.59	23.06	23.60	23.84	23.81
Na_2O	0.94	0.64	0.82			**Na_2O**	5.22	5.02							
K_2O	8.94	8.98	8.92	9.91	9.96		9.66	9.19							
BaO	0.55	0.65	0.61	0.43	0.51										
Σ	97.77	97.49	97.92	95.2	95.53	**Σ**	99.19	99.33	**Σ**	99.66	99.33	100.51	99.47	100.25	100.10
Si	5.583	5.632	5.274	5.664	5.681	**Si**	2.9627	2.9857	**Si**	1.998	1.930	1.881	1.921	1.915	1.943
Ti	0.285	0.283	0.544	0.302	0.312				**Ti**	0.005	0.010	0.022	0.015	0.016	0.012
Al^t	2.556	2.484	2.803	2.541	2.542	**Al^t**	1.0186	1.0394							
Al^{IV}									**Al^{IV}**	0.063	0.122	0.186	0.136	0.138	0.095
Al^{vi}									**Al^{vi}**	0.062	0.051	0.067	0.057	0.053	0.038
Fe^t	0.881	0.995	1.394	0.761	0.731				**Fe^t**	0.093	0.161	0.235	0.172	0.206	0.106
Mn	0.012	0.023	0.002	0.000	0.000				**Mn**	0.005	0.002	0.003	0.003	0.000	0.004
Mg	4.430	4.261	3.711	4.443	4.483				**Mg**	0.964	0.842	0.764	0.819	0.781	0.912
Ca	0.012	0.001	0.021	-.-	-.-	**Ca**	0.0000	0.0000	**Ca**	0.871	0.936	0.913	0.937	0.944	0.933
Na	0.262	0.171	0.232	-.-	-.-	**Na**	0.4594	0.4422	**Q**	1.928	1.938	1.903	1.928	1.930	1.950
K	1.607	1.612	1.633	1.822	1.823	**K**	0.5593	0.5327	**Wo**	45.096	48.275	47.760	48.595	48.862	47.831
Cr	0.101	0.083	0.062	0.101	0.043	**Ab**	0.451	0.454	**En**	49.861	43.435	39.955	42.501	40.452	46.744
Ba	0.031	0.041	0.031	0.021	0.034	**Or**	0.549	0.546	**Fs**	5.069	8.290	12.286	8.904	10.686	5.425

Petrography of the samples is given in the Table 1; Formulae are calculated on the basis of 22 (Phl – phlogopite), 32 (San – sanidine), and 6 oxygens (Cpx – clinopyroxene)

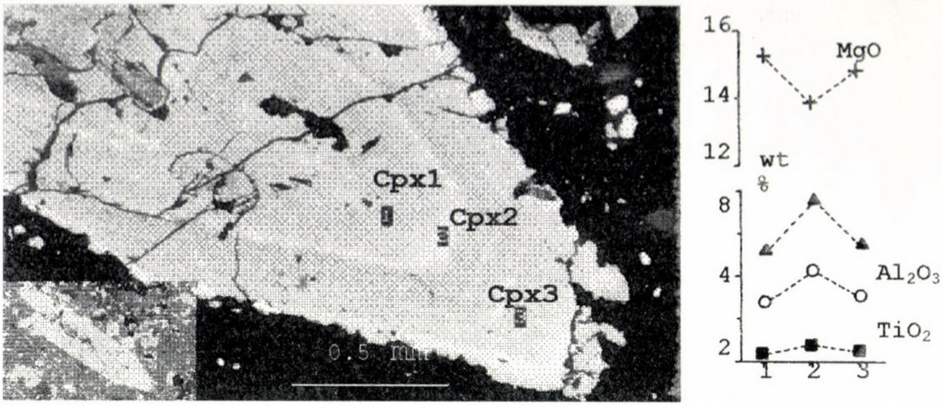

Fig. 2
Photomicrograph of zoned diopside phenochryst from a Borač phlogopite lamprophyre; analyzed spots and some oxide variations indicated are on the left (N+)

Phlogopite occurs as elongated, rarely isometric flakes (2×0.5 mm–0.3×0.2 mm) often having inhomogeneous pigmentation and bearing needle-shaped sagenite inclusions. The abundance of phlogopite phenocrysts decreases with appearance of olivine; hence, in some varieties it makes up no more than 1% of phenocryst population. On the quadrilateral Al^{tot} vs. Fe/Fe+Mg classification diagram (Fig. 3) analyzed micas from the Borač lamprophyres fall in the phlogopite field, distinct from those of other volcanics from the area. Furthermore, the phlogopite core is relatively primitive with high Mg# (up to 0.86), low TiO_2, high Al_2O_3 (Fig. 4) and Cr_2O_3 content, whereas the rim presents lower Mg# and Cr_2O_3 and higher TiO_2 contents.

Fresh olivine phenocrysts have not been observed. Olivine is represented by euhedral grains always altered to iddingsite. Pseudomorphism of phlogopite and pyroxene crystals over olivine is also found.

When present leucite appears as equidimensional phenocrysts 1–0.5 mm in diameter, or as a groundmass constituent when it is regularly more fresh. Leucite and sanidine contents are reversely related.

Sanidine ($Or_{54.6\text{-}54.9}$) is a major constituent of the holocrystalline groundmass; in leucite-free varieties it can make up over 35% (vol) of the rock. It is developed as tiny microlites, about 0.2×0.05 mm in length, which often show fluidal orientation. Oligoclase ($An_{28.8}$) microlites are strongly subordinated.

Xenocrysts of quartz and rarely plagioclase are abundant, making representative sampling a very delicate task. They often have clear reaction rims composed of small grains of pyroxene and opaque minerals. Plagioclase of xenocrystic origin has a more basic composition ($An_{47.3}$) than the same mineral within the groundmass but of primary origin.

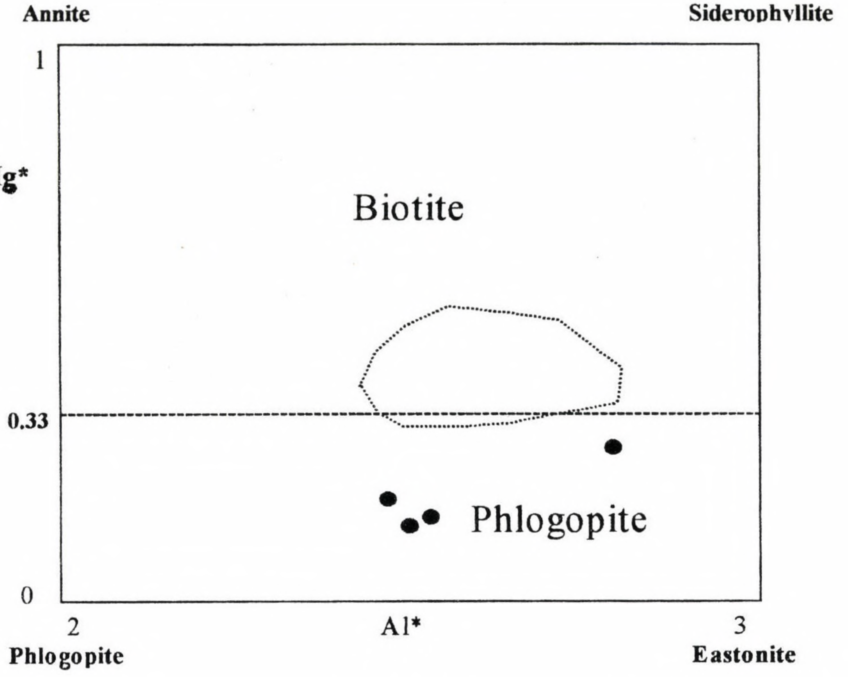

Fig. 3

Quadrilateral classification diagram for trioctahedral micas (Deer et al. 1966). Dotted circles – micas from Borac lamprophyres, dashed line represents the field of micas from the Borac calc-alkaline volcanics. *Number of atoms per crystallochemical formulae

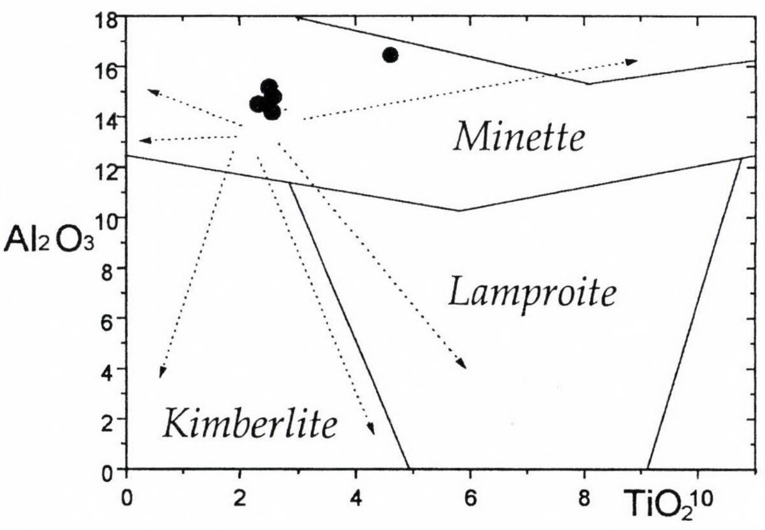

Fig. 4
Al_2O_3 versus TiO_2 (%) diagram for the Borac phlogopites. Variation trends and compositional fields are taken from Mitchell and Bergman (1991)

Often the stratigraphic position of the BEC hypabyssal lamprophyric bodies is not clear; however, the autobrecciated lamprophyre plug-flow surely postdates rhyodacite/quartz-latite pyroclastic deposits, which itself are thought to be Ottnangian-Eggenburgian in age (Cvetković 1997). However, on the basis of the first obtained radiometric data, together with an already published age (Table 3) it is by no means easy to interpret the age of the Borac lamprophyric rocks unequivocally. It should be emphasized that new analyses, made in the K-Ar Laboratory of the Institute of Nuclear Research of the Hungarian Academy of Sciences (ATOMKI, Debrecen, Hungary) do not scatter. However, it appears that

Table 3
Radiometric data for the Borač lamprophyric rocks

Lab.No/ Sam. No	Petrography	Analyzed fraction	K (%)	^{40}Ar (rad) (%)	^{40}Ar (rad) (10^{-6} ccSTP/g)	Age (Ma)
3836/ T-119	hypabyssal phlogopite lamprophyre	w.r.	3.56	84.5	3.1654	22.72±0.86
4427/Q	olivine bearing phlogopite lamprophyre (xenolith in quartzlatite)	Phl	7.68	74.1	6.846	22.78±0.88
4429/ 237A	hypabyssal phlogopite lamprophyre	Phl	5.28	68.2	4.678	22.65±0.89
Ka-305*/ 60664	hypabyssal phlogopite lamprophyre	Bi (Phl?)	7.20	-	4.262	33.82±?

* Sample analyzed in ETF Zuerich (Divljan et al. 1986)

the investigated lamprophyres originated between the Egerian and Eggenburgian, i.e. they are older than the calc-alkaline pyroclastic (?). Although we could take into consideration the possibility of higher Ar retention by mostly primitive phlogopites, it will be necessary to make another set of measurements of both lamprophyric and calc-alkaline acid to intermediate volcanics of the Borač area.

Geochemistry of the lamprophyres

Chemical analyses on major and selected trace elements of the Borač calc-alkaline lamprophyres are presented in Table 4.

Among the major elements with rather high contents are K_2O (4.80–7.29%), MgO (4.06–6.21%), CaO (6.00–7.44%) and TiO_2 (1.10–1.88%). Relatively high

Table 4
Major and selected trace element analyses of the Borač lamprophyres and related potassic rocks

No	1	2	3	B-237	T-116	T-117	T-119	D-214a
SiO_2	56.72	54.20	50.27	53.18	52.35	54.02	54.54	52.50
TiO_2	1.00	0.86	1.20	1.45	1.32	1.21	1.10	1.88
Al_2O_3	14.35	15.96	12.25	14.11	14.62	14.69	14.12	13.04
Fe_2O_3	6.90	6.79	5.82	4.81	5.37	6.10	5.55	4.28
FeO	2.27	0.61	1.84	1.80	2.44	1.59	2.48	2.00
MnO	0.20	0.10	0.07	0.12	0.05	0.05	0.06	0.10
MgO	4.50	3.81	6.04	6.17	5.46	6.06	4.06	6.21
CaO	5.75	6.22	8.37	6.75	7.00	6.00	7.44	7.12
Na_2O	3.00	2.62	2.28	2.88	2.80	2.00	2.90	3.15
K_2O	4.20	5.67	4.87	5.99	5.90	5.57	4.80	7.29
P_2O_5	0.32	0.72	0.68	0.88	0.90	0.93	0.81	0.90
H_2O^+	0.42	1.96	3.18	1.95	1.80	1.46	2.20	1.00
H_2O^-	0.75	0.73	3.00	0.40	0.70	0.47	0.28	0.66
S %	100.38	100.25	99.87	100.49	100.71	100.15	100.34	100.13
ppm								
Zr				233	262	206	194	218
Nb				13	12	18	15	18
Y				29	34	30	32	31
Sr				450	866	921	388	860
Rb				113	117	96	98	85
Ba				688	1236	858	673	990
Ni				202	259	260	212	218
Cr				98	86	111	135	95

1. analysis taken from Brković et al. (1978), the rock named 'latite'; 2. 'trachyandesite' (Marković et al. 1967); 3. 'leucite-basalt' (Filipović et al. 1978); B-237. hypabyssal phlogopite lamprophyre; T-117, T-118 and T-119 – hypabyssal phlogopite lamprophyres; D-214a – effusive olivine bearing phlogopite lamprophyre

Fe_2O_3 is due to oxidation effects, while somewhat increased SiO_2 is to be expected, for sometimes it was not possible to omit submillimetric quartz xenocrysts during sampling. Compared to the BEC calc-alkaline rocks the lamprophyres show distinctive alkaline affinity, corresponding to a shoshonitic series (e.g. Peccerillo and Taylor 1976). All the samples analyzed display potassic character (with mol. $K_2O/Na_2O < 3$, mainly 2; Foley et al. 1987).

Both incompatible (e.g. Zr=194–266 ppm; Nb=12–18 ppm; Sr=388–866 ppm; Ba=673–1236 ppm) and compatible (Ni=202–260 ppm, Cr=86–135 ppm) trace elements show relatively high contents. With respect to the calc-alkaline rocks they have somewhat lower Zr/Nb (11.44–21.83) and considerably higher K/Rb (31.50–57.46) ratios. A similar trend of comparison between the lamprophyres and calc-alkaline Borac volcanic rocks are inferred from higher contents of Th and REE as well as of Co, V and Sc in the former.

Discussion

It is the petrogenesis of the Borač lamprophyric rocks that could bear very important constraints for the explanation of the evolution of the entire eruptive complex. Hence, the attention which has been paid to these rocks overrides their abundance.

In order to make an approach for understanding the paleotectonic conditions during the primary magma formation it is first necessary to take into consideration some geologic evidence which is available: (1) the BEC was formed in a continental environment; the total thickness of the continental crust could have reached about 40 km, what may be inferred from the recent thickness of about 35 km (Aljinović 1986); (2) the subduction processes, i.e. the closure of the Vardar Ocean, ceased during the Upper Jurassic, only in some westernmost parts during the Upper Cretaceous (Karamata et al. 1994) and (3) at the beginning of

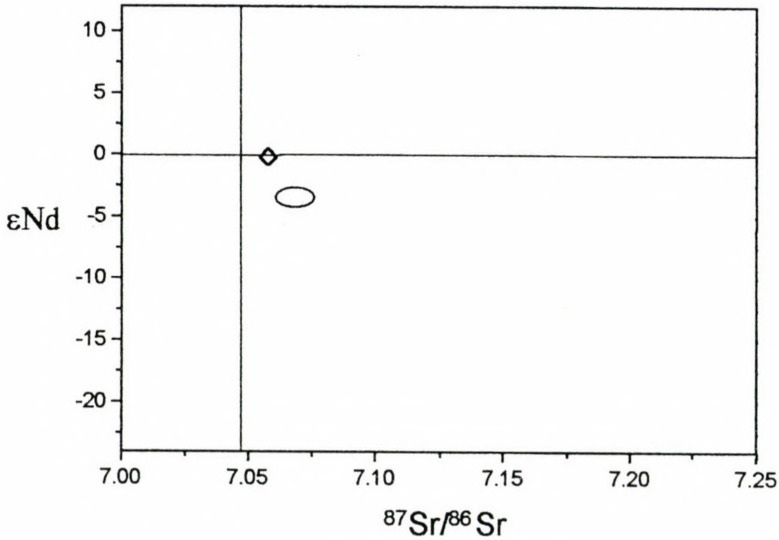

Fig. 5
$^{87}Sr/^{86}Sr$ vs εNd diagram for the Borač lamprophyre (romb) with the position of the Borač calc-alkaline eruptives (ellipse)

Table 5
Sr and Nd isotope ratios for the sample T-119 (phlogopite lamprophyre)

Sr ppm	**Rb** ppm	$^{87}Rb/^{86}Sr$	$^{87}Sr/^{86}Sr$	**εSr**
1027	171	0.482±2	0.705778	+18.5±.3
Nd ppm	**Sm** ppm	$^{147}Sm/^{144}Nd$	$^{143}Nd/^{144}Nd$	**εNd**
63.0	10.8	0.10351	0.512616±7	-0.2±.3

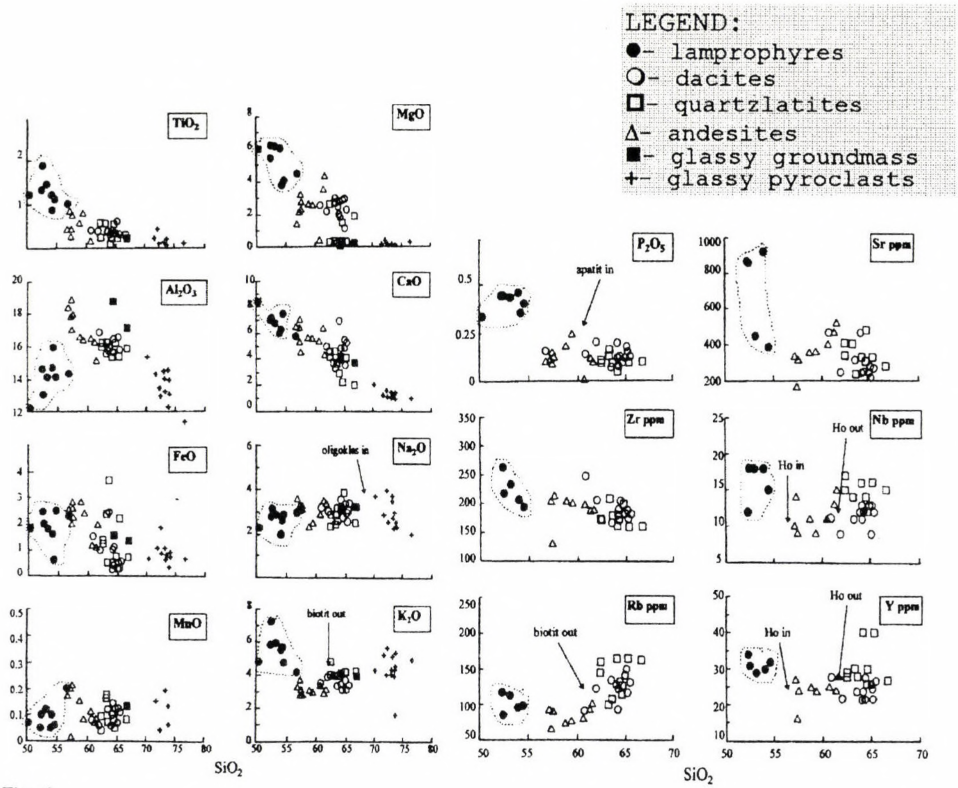

Fig. 6
Harker`s variation diagrams for the lamprophyric and calc-alkaline rocks of the Borač eruptive complex

Paleogene this suture zone was subjected to dextral transpression of NW–SE orientation (Brunn 1960; Grubić 1966).

In Table 5 and in Figure 5 it can be seen that the isotope values for the lamprophyric rocks are very close to the Bulk Earth. They are clearly distinct from the coeval calc-alkaline Borac volcanics which bear evidence of inevitable crustal contribution in their magma genesis. The presence of at least two different primary magmas also becomes apparent from the Harker's variation diagrams (Fig. 6). The major and trace element contents of the lamprophyres show inclination from the liquid line of descent which outline the calc-alkaline rocks, which could certainly not be explained by a change in fractionation assemblage. Furthermore, the REE pattern (Fig. 7) of the lamprophyric rocks lacks a Eu-anomaly.

Some petrographic evidence indicates that magma mingling and even mixing have occurred in the evolution of the BEC: (1) presence of xenoliths and rare xenocrysts of lamprophyric origin within the evolved quartz-latites; (2) presence of numerous xenocrysts (mostly resorbed) within the most primitive calc-alkaline

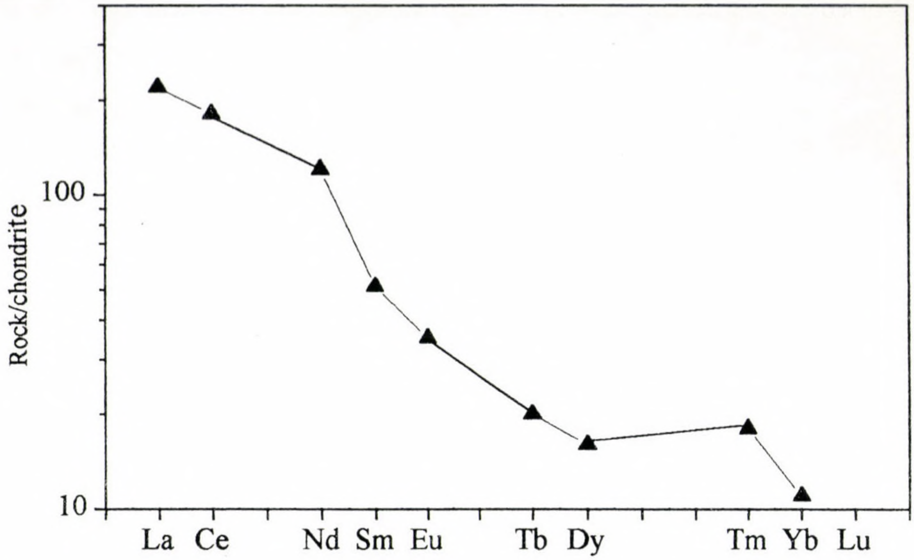

Fig. 7
REE pattern for the lamprophyric rocks of the Borač eruptive complex (coef. norm. after Nakamura 1974)

volcanics represented by andesites and basaltic andesites and (3) the fact that the generation of lamprophyric lava flows and hypabyssal bodies is contemporaneous with the paroxysm of the calc-alkaline volcanism, i.e. with a plinian to sub-plinian explosive event. Scarce though geochemical data are it is evident that the second eruptive calc-alkaline phase in the BEC, which is clearly coeval with the lamprophyric rocks, was more potassic and had higher REE in respect to the older dacites. Notwithstanding all the before mentioned the role of magma mixing and mingling processes still remains an open question.

The trace element distribution illustrated by the primitive mantle normalized multi-element spider diagram (Fig. 8) depicts inevitable conformity between the Borac lamprophyres and ultrapotassic volcanic rocks of the Roman Province (Conticeli and Peccerillo 1992). Three main negative anomalies are noticeable: Rb, Ba, K; Sr, then Ta, Nb, Ti and, to a lesser extent, Zr and Hf. The negative anomaly of Rb, Ba and K suggest some phlogopite fractionation. This is apparent from the petrographic evidence as well, with the variable modal content of phlogopite. As plagioclase is not found as an early crystallizing phase, but in the form of rare xenocrysts, Sr in the Borac lamprophyres will be unaffected by the variations in plagioclase fractionation. Its negative anomaly could be explained by possible mixing of lamprophyric and a magma-bearing negative Sr anomaly (?). Coupled Ta-Nb-Ti (TNT) troughs form a noticeable feature on spider diagrams derived from all subduction-related rocks (andesites and arc-related alkaline rocks) (e.g. Pearce 1983). This feature is widespread, but not exclusive, among calc-alkaline

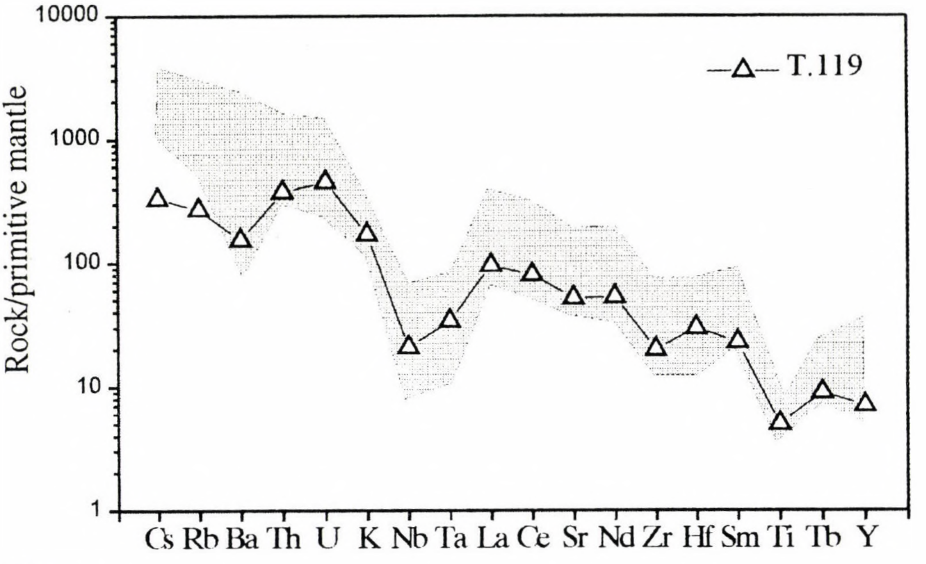

Fig. 8
Multielement spider diagram for the Borač lamprophyric rocks (triangle) normalized to primitive mantle (McDonough et al. 1991). The shaded area represents ultrapotassic and potassic volcanic rocks of the Roman Province (Conticelli and Pecerillo 1992)

lamprophyric rock of all ages. There are three explanations for generating these anomaly (e.g. Sheppard and Taylor 1992):

– partial melting of lithospheric mantle modified by fluids and melts generated from the (fossil) subduction zone;

– retention of Ta-Nb-Ti by some titanium phase (rutile) in the source suggesting its oxidizing and low heat flow environment;

– crustal contamination processes.

The main problem arises with the existence of TNT anomalies in a continental tectonic environment that is remote from subduction zones in space/or time. So, although it is early to attach a clear genetic significance to TNT anomalies, it is reasonable to regard them as a broad subduction tracer (Rock 1991).

In order to further elaborate evidence of the role of the subduction component in the Borac lamprophyre magma genesis, a Nb vs. Zr diagram for potassic and ultrapotassic rocks (Thompson and Fowler 1986) has also been used (Fig. 9); the investigated rocks cluster within the post-collision field indicating that they originated in an area that was neither spatially nor temporally remote from the subduction processes.

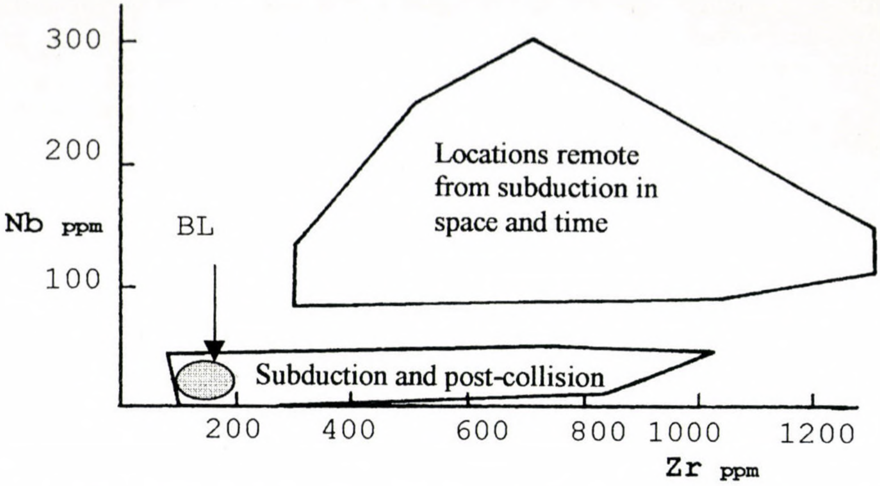

Fig. 9
Nb vs Zr (ppm) diagram for potassic and ultrapotassic rocks with silica lower than 60% (Thompson and Fowler 1986). Shaded area represents the field of the Borač lamprophyres (BL)

Conclusion

In terms of petrochemical and isotope data it can be generally accepted that the Borac lamprophyres originated from a distinctive potassic/ultrapotassic magma as compared to the coeval calc-alkaline volcanic products. Their parental melts probably originated from previously enriched parts of the subcontinental mantle. From the Nd-Sr isotope ratios and some incompatible trace element contents and ratios it appears that the subduction component is responsible for the uppermost mantle inhomogeneity. These components have formed parts of amphibole (?) and phlogopite peridotite within the mantle beneath the Vardar Zone. Lamprophyres lack a Europium anomaly and display only some evidence of phlogopite fractionation and a negligible contribution of crustal material. Whether magma mingling-mixing processes have played any significant role in the petrogenesis remains an open question.

Comparing similar petrochemical characteristics of the Borač lamprophyres with the volcanic rocks of the Roman Province as well as considering the trace element pattern of the contemporaneous acid volcanics, it was concluded that the Miocene BEC as a whole developed in a continental environment under post-collisional geotectonic conditions.

Acknowledgements

This study is a part of the Project of GEODYNAMICS of the Serbian Academy of Sciences and Arts. It resulted during the collaboration between Serbian

Academy of Sciences and Arts and Hungarian Academy of Sciences. The authors express their sincere appreciation to Cs. Szabo and S. Karamata for their reviews of the manuscript.

References

Aljinović, B. 1986: Karta dubina Mohorovičičevog diskontinuiteta na području Jugoslavije (The map of the Mohorovicic discontinuity of Jugoslavia). – Nafta, 37/3, pp. 127–130. Zagreb.

Balogh, K. 1985: K-Ar dating of Neogene volcanic activity in Hungary: experimental technique, experiences and methods of chronologic studies. ATOMKI Rep. D/1, pp. 277–288.

Brković, T., M. Malesević, M. Urosević, S. Trifunović, Z. Radovanović, Z. Pavlović, M. Rakić 1978: Geologic map and explanatory text for the Čaćak Sheet. – Savezni geološki zavod, p. 64, Beograd.

Brunn, J.H. 1960: Les zones helléniques internes et leur extension. Réflexions sur l'orogenése alpine. – Bull. Soc. Géol. France, 7, II, 4, pp. 471–486, Paris.

Conticeli, S., A. Peccerillo 1992: Petrology and geochemistry of potassic and ultrapotassic volcanism in central Italy: petrogenesis and inferences on the evolution of the mantle sources. – Lithos, 28, pp. 221—40.

Cvetković, V. 1997: Petrostrukturne i vulkanološke karakteristike boračkog eruptivnog kompleksa (Petrostructural and volcanological characteristics of the Miocene Borač eruptive complex). – PhD Thesis, Fac. of Mining and Geology, Univ. of Belgrade, 242 p.

Deer, W.A., R.A. Howie, J. Zussman 1966: An Introduction to the Rock Forming Minerals. – Longman Group Limited, 528 p, London.

Dimitrijević, M.D. 1995: Geologija Jugoslavije. – Geoinstitut, 205 p, Beograd.

Divljan, S., G. Martinović, S. Cvetić 1986: Novi pogledi na genezu vulkanskih stena boracke oblasti (New aspects on the genesis of volcanic rocks of Borač region). – XI Kongres geol. Jugoslavije, 3, pp. 63–80, Tara.

Filipović, I., B. Marković, Z. Pavlović, V. Rodin, O. Marković 1978: Geological map and explanatory text for the sheet Gornji Milanovac. – Savezni geoloski zavod, p. 71, Beograd.

Foley, S.F., G. Venturelli, D.H. Green, L. Toscani 1987: The ultrapotassic rocks: characteristics, classification and constraints for petrogenetic models. – Earth Sci. Rev., 24, pp. 81–134.

Grubić, A. 1966: Tektonske karakteristike Vardarske zone. – Referati VI savetovanja geologa Jugoslavije, I, pp. 475–481, Ohrid.

Ilić, M. 1961: Geologija gornjomilanovackog tercijarnog basena i okolnih formacija (Geology of the Gornjii Milanovac Tertiary basin and of the neighbouring formations). – Vesnik Zavoda za geol. i geof. istraz., XIX/A, pp. 125–157, Beograd.

Karamata, S., M.N. Dimitrijević, MD. Dimitrijević, 1998: Mesozoic oceanic realms in the recent framework of the Balkan Peninsula. XVI Congress CBGA, Vienna, Abstracts, p. 263.

Karamata, S., B. Krstić, M.D. Dimitrijević, V. Knežević, M.N. Dimitrijević, I. Filipović 1994: Terranes between the Adriatic and the Carpatho-Balkanian arc. – Bull. CVIII de l'Acad. Serbe des Sci. et des Arts, Classe des Sci. math. et natur. Sci. natur., 34, pp. 47–66, Beograd.

Le Maitre, R.W., P. Bateman, A. Dudek, J. Keller, J. Lameyre, M.J. Le Bas, P.A. Sabine, R. Schmidt, H. Srrensen, A. Streickeisen, A.R. Woolley, B. Zanettin 1989: A Classification of Igneous Rocks and Glossary of Terms. Recommendations of the International Union of Geological Sciences Sub-commission on the Systematics of Igneous Rocks. – Blackwell Scientific Publications, 193 p.

Majer, V., S. Karamata 1983: Mogucnosti novog tumacenja geneze K-bogatih lamprofira i bazalta u Jugoslaviji (Possibility of new interpretation of genesis K-rich lamprophyres and basalts in Yugoslavia). – Geol. vjesnik, 36, pp. 183–188, Zagreb.

Marković, M., Z. Pavlović 1967: Fotogeoloska ispitivanja vulkanita u eruptivnoj zoni Kotlenik-Borač (Recherces photogeologiques des roches volcaniques dans la zone eruptive Kotlenik–Borač). – Geol. an. Balk. poluos., 33, pp. 77–92, Beograd.

Marković, B., M. Urosević, Z. Pavlović, V. Terzin, Z. Jovanović, J. Karović, T. Vujisić, R. Antonijević, M. Malesević, M. Rakić 1968: Geological map and explanatory text for the sheet Kraljevo. – Savezni geoloski zavod, 63 p, Beograd.

McDonough, W.F., S. Sun, A.E. Ringwood, E. Jagoutz, A.W. Hofmann 1991: K, Rb and Cs in the earth and moon and the evolution of the earth's mantle. – Geochim. Cosmochim. Acta, Ross Taylor Symposium volume.

Mitchell, R.H., S.C. Bergman 1991: Petrology of lamproites. – Plenum Press, 477 p, New York.

Morimoto, N., J. Fabries, A.K. Ferguson, I.V. Ginzburg, M. Ross, F.A. Seifert, J. Zussman, K. Aoki, G. Gottardi 1988: Nomenclature of pyroxenes. Mineral. Mag., 52, pp. 535–550.

Nakamura, N. 1974: Determination of REE, Ba, Fe, Mg, Na and K in carbonaceous and ordinary chondrites. – Geochim. Cosmochim. Acta, 38, pp. 757–773.

Pearce, J.A. 1983: The role of sub-continental lithosphere in magma genesis at destructive plate margins. – In: Hawkesworth, C.J., M.J. Norry (Eds): Continental basalts and mantle xenoliths,. pp. 230–249.

Peccerillo, A., S.R. Taylor 1976: Geochemistry of Eocene calc-alkaline volcanic rocks from the Kastamonu area, Northern Turkey. – Contrib. Mineral. Petrol., 58, pp. 63–81.

Rock, N.M.S. 1991: Lamprophyres. – Bleckie & Son Ltd, 285 p, London.

Sheppard, S., W. Taylor 1992: Barium- and LREE-rich, olivine-mica-lamprophyre with affinities to lamproites, Mt. Bundey, Northern Territory, Australia. – Lithos, 28, pp. 303–325.

Steiger, R.H., E. Jäger 1977: Subcommision on geochronology: convention on the use of decay constants in geo- and cosmochronology. – Earth Planet. Sci. Lett., 36, pp. 359–362.

Thompson, R.N., M.B. Fowler 1986: Subduction related soshonitic and ultrapotassic magmatism: a study of Siluro-Ordovician syenites from the Scottish Caledonides. – Contrib. Mineral. Petrol., 94, pp. 507–522.

Acta Geologica Hungarica, Vol. 43/1, 43–63 (2000)

Alpine low-T prograde metamorphism in the post-Variscan basement of the Great Plain, Tisza Unit (Pannonian Basin, Hungary)

Péter Árkai
Laboratory for Geochemical Research, Hungarian Academy of Sciences

Anikó Bérczi-Makk
MOL Hungarian Oil & Gas Plc.

Kadosa Balogh
Institute of Nuclear Research, Hungarian Academy of Sciences

Traditionally, the Tisza Unit in the Pannonian Basin has been considered a very stable, refractory crustal block or microplate, the pre-Tertiary basement of which escaped Alpine prograde metamorphism. After describing sporadic occurrences of Alpine metamorphism from the Mesozoic (Árkai 1990; Balogh et al. 1990; Árkai et al. 1998), a systematic regional study applying microstructural, mineral paragenetic, illite and chlorite crystallinity, white K-mica geobarometric and K-Ar isotope geochronological methods was carried out on the post-Variscan (mainly Mesozoic) part of the pre-Tertiary basement of the Great Plain (Tisza Unit). New data prove that prograde metamorphism affected considerable parts of the post-Variscan basement beneath the overthrusted polymetamorphic Variscan – pre-Variscan (?) formations, or in a disrupted, allochthonous tectonic position along the main Alpine thrust zones. The regional metamorphism was of an orogenic (dynamothermal) type. Its grade culminated in the epizone (greenschist facies chlorite zone) in the easternmost part (Sáránd area). In addition, anchizonal rocks have also been described from various parts of the basement. The age of the ca. 200–350 °C prograde, medium, transitional low-medium pressure-type metamorphism is Cretaceous. Thus, the Tisza Unit formed an organic part of the Mediterranean orogenic belt, also from the point of view of regional metamorphism.

Keywords: low-T metamorphism, illite crystallinity, chlorite crystallinity, isotope geochronology, K-Ar dating, Alpine metamorphism, Tisza Unit, Pannonian Basin, Hungary

Introduction

Until recently the Tisza Unit had been traditionally considered one of the most stable, refractory parts of the Pannonian Basin, a part that – disregarding the locally occurring, mostly Cretaceous retrograde overprint in the pre-Alpine polymetamorphic basement – practically escaped Alpine prograde metamorphism. This view was rooted historically in the "median mass" concept

Addresses: P. Árkai: H-1112 Budapest, Budaörsi út 45, Hungary. E-mail: arkai@sparc.core.hu
A. Bérczi-Makk: H-1039 Budapest, Batthyány u. 45, Hungary
K. Balogh: H-4001 Debrecen, Bem tér 18/c, Hungary
Received: 27 March, 2000

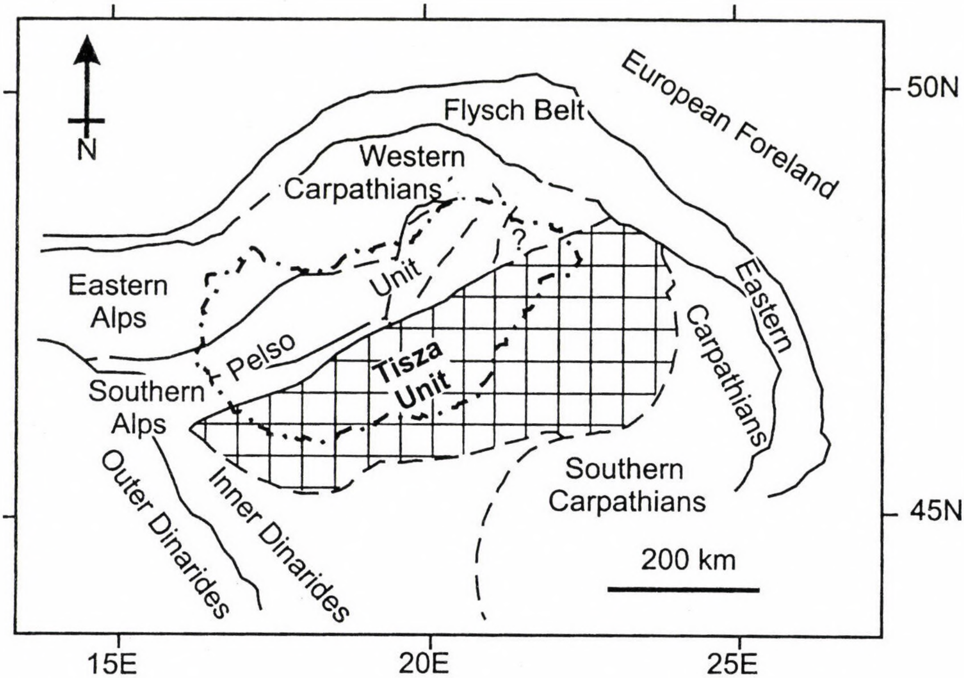

Fig. 1
Tectonic sketch of the Alpine-Carpathian-Pannonian realm with the location of the Tisza Unit. Dash-dotted line indicates the state boundary of Hungary

elaborated and applied to the Carpathian or Pannonian Basin by Lóczy (1918, 1924) and Kober (1921, 1923), mostly on the basis of geomorphological considerations; taking into account the bifurcation, the sudden change of strikes of the Mediterranean orogenic belt at the eastern termination of the Alps and the curvature of the Carpathian chain. Prinz (1926) was the first to introduce the term *Tisia* for the *median mass* surrounded by the Alps, Carpathians and Dinarides. The extent and geotectonic interpretation of Tisia within the pre-Tertiary basement of the Carpathian Basin have changed remarkably during the past century (for recent reviews see Fülöp 1989; Kovács 1996 and Árkai 1999).

On the basis of core samples from hydrocarbon exploration boreholes Szederkényi (1984, 1996) demonstrated Alpine overthrust (nappe) structures within the *Tisza Unit* (the Tisza Unit is used in the present paper in the sense of Csontos et al. 1992, corresponding to the *Tisia Composite Terrane* of Kovács et al. 1996–97, see also Fig. 1). Árkai (1990) described an exotic (Dinaric-type) medium pressure, very low to low-grade Mesozoic sequence in the Barcs-West area, in the Drava Basin, southern Transdanubia (Fig. 2). This complex is in an overthrusted position, overlying the Variscan – pre-Variscan (?) medium grade, polymetamorphic complex. The age of the low-T prograde metamorphism of the Mesozoic

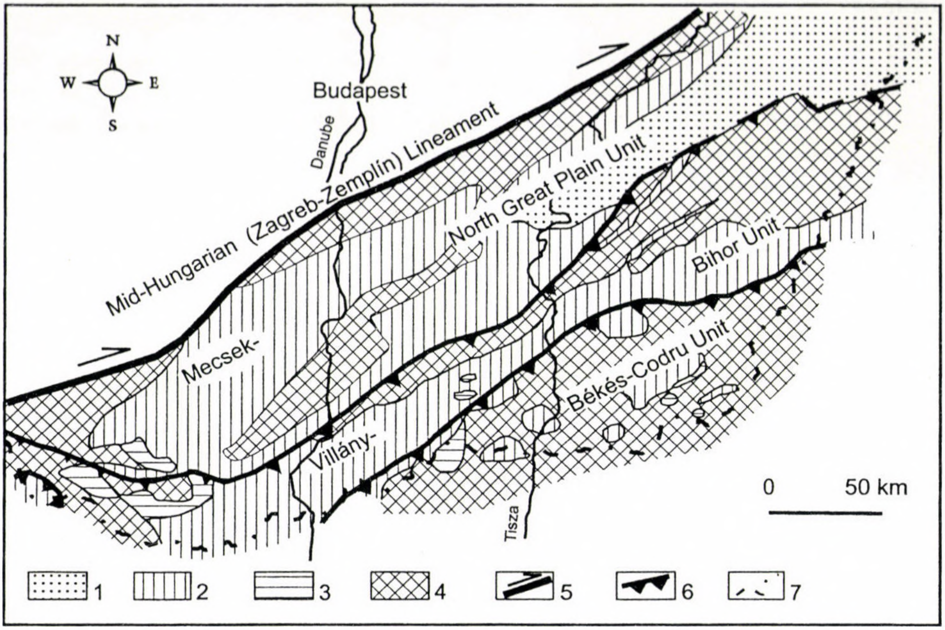

Fig. 2.
Geologic map sketch of the basement of the Hungarian part of the Tisza Unit after Fülöp (1989), strongly simplified, with the locations of boreholes and borehole groups used in this study. Legend: 1. Upper Cretaceous–Paleogene flysch; 2. Mesozoic in general; 3. post-Variscan Upper Paleozoic (Upper Carboniferous–Permian); 4. mostly Variscan, medium grade polymetamorphic complex, locally with syn-kinematic Variscan granitoids; 5. major strike-slip fault; 6. main overthrust; 7. state boundary

complex is Cretaceous, overprinted by a Tertiary (ca. 30 Ma) thermal event (Balogh et al. 1990). Alpine (Cretaceous) prograde, transitional low-medium pressure type, very low- to low-grade (anchizonal, epizonal) metamorphism of Mesozoic basement rocks was reported by Árkai et al. (1998) from the eastern part of the Tisza Unit, in the neighborhood of the so-called Derecske Depression (borehole Sáránd-I, etc.). Here the low-T prograde metamorphic Mesozoic is in a parautochthonous position, having been overthrusted by a ca. 1 km-thick, medium grade polymetamorphic complex that simultaneously retrogressed in the Cretaceous. These results proved that Alpine prograde metamorphism also occurred in the post-Variscan basement of the Tisza Unit. However, the regional extent of this metamorphism remained unknown.

The aim of the present paper is to provide new metamorphic petrological data on the nature and regional distribution on the Alpine prograde metamorphism that affected the post-Variscan (Permian and Mesozoic) formations of the Tisza Unit. For this purpose core samples taken from boreholes located along main overthrust zones of the Great Plain's basement were studied.

Geology

Figure 1 shows that, according to recent plate tectonic reconstructions, the Pre-Tertiary basement of the Pannonian Basin is made up of different blocks that originated from various parts and bordering areas of the Tethyan realm and came into close geographic relation through large-scale horizontal displacements. The Tisza Unit represents a certain fragment of the northern ("stable", Variscan European) margin of the Tethys, which was detached from the continent during the Early-Middle Jurassic and occupied its present tectonic position mostly during the Tertiary, not later than the Middle Miocene (Géczy 1973; Kovács 1982; Kázmér and Kovács 1985; Csontos et al. 1992; Kovács et al. 1996–97).

The simplified basement map of the Hungarian part of the Tisza Unit is shown in Fig. 2. The polymetamorphic basement is characterized by an older (early Variscan (?) or pre-Variscan (?)) medium thermal gradient amphibolite facies event, a younger (Variscan) high thermal gradient, mainly amphibolite facies event and late Variscan and/or Alpine retrogression, mylonite and cataclasite formation (Szederkényi 1984, 1996; Árkai 1984, 1987; Árkai et al. 1985; Szederkényi et al. 1991; Kovács et al. 1996–97).

This polymetamorphic basement is separated by erosional unconformity from the overlying post-orogenic Upper Carboniferous and Permian, mostly molasse-type terrigenous clastic formations and Permian acidic volcanics and volcaniclastics (for a summary see Fülöp 1994).

In the Hungarian part of the Tisza Unit two main overthrust zones subdivide the basement into three parts (Fig. 2), i.e., the so-called Mecsek – North Great Plain, the Villány – Bihor and the Békés – Codru subunits (for details see Bérczi-Makk et al. 1996; Bleahu et al. 1994; Haas 1994 and Kovács 1987). The Mesozoic sedimentary and tectonic evolution paths of these subunits differ from each other, indicating the regional extent of the overthrust structures. The Mesozoic formations, covered by several kilometer thick Neogene sediments, display regular, SW-NE striking zonal distribution (Fig. 3).

In the basement of the Great Plain the Mesozoic of the Mecsek – North Great Plain subunit is characterized by intensive, widespread Lower Cretaceous alkali basaltic volcanism. The northeastern part of this zone comprises an Upper Cretaceous – Paleogene flysch belt (Szolnok – Maramures Flysch Trough) mirroring the Cretaceous orogeny. South of this flysch belt there are two SW–NE striking zones where Mesozoic formations are found beneath the overthrusted polymetamorphic basement. In the northernmost zone (Tázlár-N, Ebes, etc.) Mecsek-type Jurassic formations were always intersected by the hydrocarbon exploration wells. These are typical slope sediments represented predominantly by dark-gray marls with limestone intercalations. On the basis of their rather poor radiolarian fauna their age is Late Dogger and Malm.

South of this zone, beneath or between the polymetamorphic rocks, Mecsek-type Mesozoic (predominantly Jurassic, subordinately Triassic and Lower Cretaceous) formations are also found (Öcsöd, Endrőd, Sáránd, Bagamér,

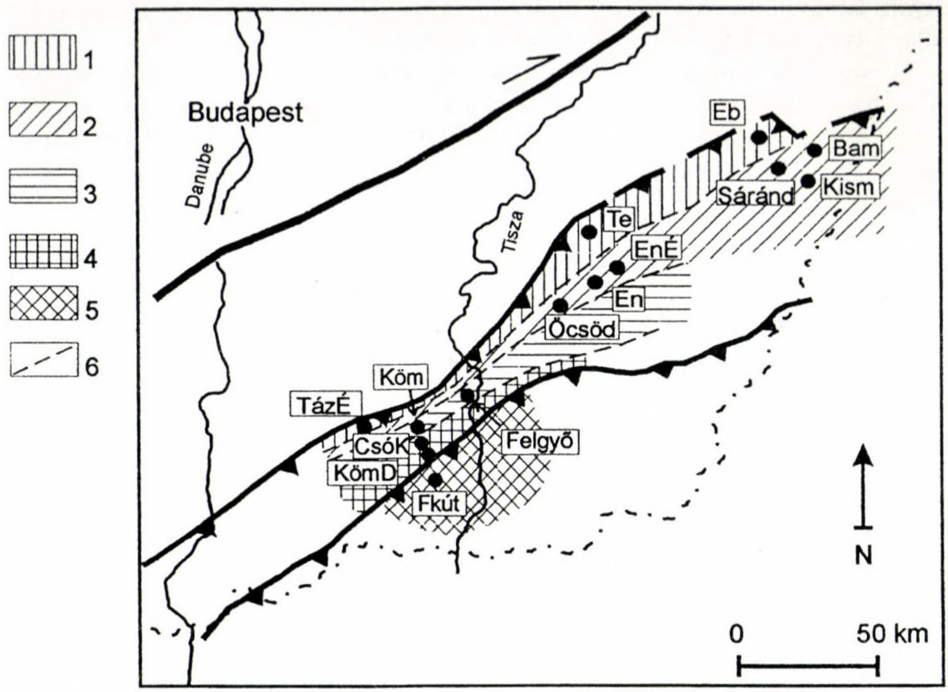

Fig. 3.
Characteristics of the Mesozoic rocks in the boreholes studied (Great Plain). Legend: 1. Mecsek-type Jurassic in the footwall of Variscan polymetamorphic nappes of scales (VPN); 2. Mecsek-type Mesozoic (Triassic, Jurassic and Cretaceous) rocks below the VPN; 3. Overthrusted, scaly Mesozoic sequences: Mecsek- and Villány-type Mesozoic sequences in allochthonous tectonic position; 4. Overthrusted, scaly Mesozoic and Variscan polymetamorphic sequences; 5. Overthrusted, scaly Triassic sequences; 6. Boundary separating various Mesozoic lithofacies. For other symbols see the Legend of Fig. 2

Kismarja-W). These are Triassic (Anisian) lagoonal dolomite and limestone, Jurassic, grayish-green, strongly tectonized radiolarian chert, cherty limestone, marl and marly slate that most probably was formed during the post-Bajocian deep-water sedimentation. Very recent nannoplankton (*Ellipsagelosphaera* sp., *Cyclagelosphaera margereli* Noäl) and radiolaria (*Archaeospongoprunum* sp., *Setohocapsa* sp., *Parvicingula* sp., *Stichocapsa robusta* Matsuoka) studies have proved Late Dogger and Malm sedimentation (Bérczi-Makk 1998). The Lower Cretaceous is represented by metatuff of basic to intermediate chemistries and alkali basalts.

In the Villány – Bihor Sub-unit overthrusted, scaly Mesozoic and subordinate polymetamorphic Variscan – pre-Variscan (?) formations are found. The boreholes intersected Villány and Mecsek-type Triassic and Jurassic formations, all being in allochthonous positions (Kömpöc, Felgyő). For example, Mecsek-type

Lower Cretaceous basic volcanites and Jurassic pelitic rocks are overlain by Villány-type Triassic carbonate platform formation.

The studied occurrences of the Békés – Codru (Lower Codru) Sub-unit are characterized by relatively thin, locally strongly brecciated Lower and Middle Triassic (mostly Anisian) carbonate formations. Repetitions, inverse successions as well as overthrusted, scaly structures indicate their allochthonous tectonic positions (Forráskút).

Methods

In order to determine the rock types with special reference to their microstructural features, diagenetic – metamorphic and post-metamorphic alterations, distinction between inherited (detrital) and newly-formed (authigenic) minerals, detailed mesoscopic, petrographic microscopic, X-ray powder diffractometric (XRD) and K-Ar isotope geochronological methods were applied.

Vitrinite reflectance values (R_{max}, R_{min}, R_{random}) characteristic of the thermal maturity of the fine disperse coalified organic matter were measured as described by Árkai (1983). *Modal composition* was determined by a combination of petrographic microscopic observations and XRD results, the latter obtained from whole rock, acid insoluble residue and <2 μm SED (spherical equivalent diameter) fraction powder samples. For determining diagenetic - incipient metamorphic grades, XRD-measured *phyllosilicate crystallinity parameters* were applied. The procedures and instrumental conditions used in XRD work of the present study were the same as described in detail by Árkai et al. (1997, 1998). The actual boundary ranges of illite crystallinity [IC, i.e., the full width at half maximum (FWHM) values of the first, 10-Å basal reflection of illite-muscovite] and chlorite crystallinity indices [i.e., the FWHM values of the first (14-Å) and second (7-Å) basal reflections of chlorite indicated as ChC(001) and ChC(002)] of the present paper, which correspond to Kübler's (1968, 1990) original anchizone, are 0.284–0.435°, 0.309–0.390° and 0.284–0.348° $\Delta 2\Theta$, respectively (see also Árkai et al., 1995b). All of these boundary values refer to air-dried (AD) mounts. *White K-mica geobarometry* elaborated for lower greenschist facies pelitic rocks by Sassi (1972) and also extended by Padan et al. (1982) to the high-T part of the anchizone was applied for qualitative estimation of metamorphic pressure conditions. For these geobarometric estimations the constraints given by Guidotti and Sassi (1976, 1986) for appropriate modal composition were also taken into consideration. The $b \cong 6x(d_{331,060})$ value was measured on disorientated whole rock and acid insoluble residue powder mounts as described by Árkai et al. (1991). Detailed description of *K-Ar isotopic dating* applied to illite-muscovite-rich <2 μm grain-size fraction samples was presented by Árkai et al. (1995a).

Results

Out of 27 boreholes a total of 109 core rock samples form the objective of the present study. Geographic position of the boreholes, depth, lithology, stratigraphic age and tectonic settings of the rocks are listed in Table 1 (for orientation see also Fig. 3). Modal composition of the rock samples is summarized in Table 2. Table 3 contains the corrected IC and ChC values determined on <2 μm grain-size fraction, air dried mounts and the *b* values of white K-mica measured on whole rock and acid insoluble residue mounts by XRD. K-Ar ages obtained on the <2 μm grain-size fraction samples are given in Table 4.

Discussion

Comparing the data of Tables 1, 2 and 3 it is obvious that not only the lithotypes but also the diagenetic – metamorphic grade-indicating parameters are strongly variable over the studied area.

As is shown in Fig. 4 displaying *the regional distribution of average IC values*, the Mecsek-type Jurassic formations overthrusted by pre-Alpine polymetamorphic rocks suffered only diagenetic alterations. In *borehole Eb-1* the marly shale displays rough fracture cleavage with rare crenulation of certain cleavage surfaces. The sandstone sample is fractured and the fractures are filled with carbonate minerals. The clay mineral assemblages of illite-muscovite + chlorite + kaolinite in the shale and illite-muscovite + chlorite + smectite in the sandstone are in agreement with the IC data, indicating only diagenetic alterations. The silty, marly shale from *well Te-19* shows crenulated cleavage; the limestone is moderately fractured. Their phyllosilicates are represented by illite-muscovite and chlorite, the former being predominant. In the *Tázlár-North area* the pelitic, marly shale displays rough fracture cleavage without appreciable white K-mica neoformation on the cleavage surfaces. In general cleavage planes are parallel to sedimentary layering. Illite-muscovite and chlorite are the common phyllosilicates, while kaolinite and mixed-layered illite/smectite occur only in few samples in subordinate quantities. The large scatter of IC values indicates variable conditions ranging from typical diagenetic to transitional diagenetic/anchizonal circumstances. Mean vitrinite reflectance data obtained from a marly shale sample from core Táz-É-2.5 (R_{max} = 1.52%, R_{min} = 0.89%, R_{random} = 1.30%, n = 13) confirm the conclusion of mainly diagenetic alteration.

South of the zone discussed above the degree of regional alteration of the Mecsek-type Mesozoic rocks varies strongly. In eastern Hungary, in the *Sáránd-Bagamér* area, the upper, dolomitic–fine clastic Triassic sequence suffered low-T anchizonal, while the middle, calcareous – fine clastic Jurassic and the lower, calcareous – basic to intermediate volcaniclastic subunits were subjected to epizonal (greenschist facies chlorite zone) and transitional anchizonal and epizonal regional metamorphism (for further details see Árkai et al. 1998). In the *Kismarja-West area* (well Kism-Ny-1) the slates with penetrative crenulation

Table 1
List of the Late Paleozoic and Mesozoic samples investigated

Locality, borehole	Core	Depth (m)	Rock type	Strat. age	Zone
Bagamér					
Bam-2	3/a-c	2644.7-2645.6	banded, schistose metatuffite (basic-intermediate)	Cr_1?	Mecsek
Bam-2	4/a-c	2702.4-2704.7	metadiorite (porphyric)	Cr_1?	Mecsek
Bam-1	5	2862.1	brecciated calcschist	J?	Mecsek
Bam-1	6/a-d	2888.0-2894.0	banded, calcite-bearing pelitic (silty) slate	J?	Mecsek
Bam-1	7/a-b	2959.0-2960.0	banded, calcite-bearing pelitic slate	J?	Mecsek
Bam-1	7/c	2960.4	brecciated, calcite-bearing pelitic slate	J?	Mecsek
Bam-1	8/a	3146.1	psammitic calcschist with muscovite bands	J?	Mecsek
Bam-1	8/b	3147.0	banded, calcite-bearing pelitic, silty slate	J?	Mecsek
Bam-1	8/c	3147.6	banded slate (with carbonatic, psammitic and pelitic-silty bands)	J?	Mecsek
Bam-1	8/d	3149.1	calcschist with pelitic bands	J?	Mecsek
Bam-1	9/a	3188.0	marble (schistose)	J?	Mecsek
Bam-1	9/b	3189.5	banded calcschist	J?	Mecsek
Bam-1	9/c	3189.8	brecciated marble	J?	Mecsek
Bam-1	9/d	3191.6	pelitic calcschist	J?	Mecsek
Bam-1	10/a-b	3410.0-3410.7	calcschist	J?	Mecsek
Bam-1	11/a-c	3438.8-3439.8	metatuffite (basic?, slatey, banded, dolomitic)	Cr_1?	Mecsek
Bam-1	12/a-b	3496.5-3497.2	brecciated, recrystallized limestone	Cr_1?	Mecsek
Kismarja-West					
Kism-Ny-1	6/a	2081.55	banded marly slate/calc-slate	Mes?	Mecsek?
Kism-Ny-1	6/b	2082.5	limestone	J_{2-3}	Mecsek
Kism-Ny-1	6/c	2083.1	brecciated limestone	J_{2-3}	Mecsek
Sáránd					
Sáránd-I	6/a	3941.0	calcitic dolomite marble with muscovite network (cipollino)	T_2	Mecsek
Sáránd-I	6/b	3942.2	pelitic-silty slate	T_2	Mecsek
Sáránd-I	6/c	3942.8	silty-pelitic slate	T_2	Mecsek
Sáránd-I	7/a	3989.0	dolomite schist with muscovite bands	T_2	Mecsek
Sáránd-I	7/b	3990.2	dolomite marble	T_2	Mecsek
Sáránd-I	7/c	3991.6	dolomite-bearing pelitic-silty slate	T_2	Mecsek
Sáránd-I	8/a-c	4048.1-4048.3	banded calcschist	J?	Mecsek
Sáránd-I	9/a	4130.6	schistose marble with chlorite+ muscovite network	J?	Mecsek
Sáránd-I	9/b	4131.0	banded, recrystallized limestone	J?	Mecsek
Sáránd-I	9/c	4131.2	marble with muscovite bands	J?	Mecsek
Sáránd-I	9/d	4132.3	calcitic metatuffite (cipollino-like)	J?	Mecsek
Sáránd-I	9/e	4134.0	marble with chlorite+muscovite network	J?	Mecsek
Sáránd-I	11/a-c	4400.1-4402.0	schistose, banded, (calcitic) metatuffite (intermediate comp.)	Cr_1?	Mecsek
Sáránd-I	13/a-c	4728.1-4730.2	schistose, banded (intermediate-basic) metatuffite	Cr_1?	Mecsek
Sáránd-I	14/a-e	4795.0-4799.2	schistose, banded (carbonatic) metatuffite (intermediate-basic comp.)	Cr_1?	Mecsek

Table 1
(cont.)

Locality, borehole	Core	Depth (m)	Rock type	Strat. age	Zone
Ebes					
Eb-1	6	1555.3	marly shale	J_{1-2}?	Mecsek
Eb-1	7	1600	carbonate-bearing sandstone	J_{1-2}?	Mecsek
Túrkeve					
Te-19	6/a	2200	silty, marly shale with calcareous bands	J_{1-2}	Mecsek
Te-19	6/b	2201.85	limestone	J_{1-2}	Mecsek
Endrõd-North					
En-É-6	3	2956.2	carbonate-bearing sandstone	K_2	Mecsek
En-É-8	4	2998	banded, carbonatic siltstone/sandstone	J_2	Mecsek
En-É-2	2/a	2886	marl	K_2	Mecsek
En-É-2	2/b	2886	lapilli tuff	?	Mecsek
Endrõd					
En-7	16/1a-b	2821	psammitic, marly shale	J_{2-3}	Mecsek
Öcsöd					
Öcsöd-3	2	2483	metabasalt	K_1	Mecsek
Öcsöd-3	3	2595	metabasalt	K_1	Mecsek
Felgyõ					
Felgyõ-I	16	3322	metabasalt	K_1	Mecsek
Felgyõ-I	17/a-b	3433	sandstone	J_{1-2}	Mecsek
Felgyõ-I	18/a-b	3495	psammitic, silty, marly shale	J_{1-2}	Mecsek
Tázlár-North					
Táz-É-2	5	2375	marly shale	J_1	Mecsek
Táz-É-2	6	2459	marl	J_1	Mecsek
Táz-É-6	4	2273	pelitic, marly shale	J_1	Mecsek
Táz-É-6	5/I	2336	banded marly shale	J_1	Mecsek
Táz-É-12	6	2497	dolomitic marly shale	J_1	Mecsek
Táz-É-14	3/t-a	2210	pelitic, silty, marly shale	J_1	Mecsek
Kömpöc					
Köm-5	4	2869	banded silty, marly shale	Mes?	Villány?
Köm-5	5	3145	limestone	Mes?	Villány?
Köm-6	4	2717	brecciated dolomitic limestone	T_2	Villány?
Köm-8	4	2658.2	brecciated dolomitic limestone	T_2	Villány?
Köm-8	5/I	2710	brecciated dolomitic, sideritic limestone	T_2	Villány?
Köm-8	5/II	2710	brecciated dolomite	T_2	Villány?
Csólyospálos-East					
Csó-K-6	3/a	3237.5	silty, pelitic shale	T_1	Villány?
Csó-K-6	3/b	3238	silty, pelitic shale	T_1	Villány?
Csó-K-6	3/c	3238.55	sandstone with silty bands	T_1	Villány?
Csó-K-6	3/d	3241.9	dolomitic, pelitic, silty shale	T_1	Villány?
Csó-K-6	3/e	3243.4	silty sandstone	T_1	Villány?
Csó-K-6	3/f	3244	breccia (polymictic)	T_1	Villány?
Kömpöc-South					
Köm-D-4	2/1	3640	metarhyolite tuff	P	Villány?
Köm-D-4	2/9	3640	metarhyolite	P	Villány?
Köm-D-4	2/16	3640	metarhyolite tuff	P	Villány?
Köm-D-2	4	3370	sandstone	T_1	Villány?
Köm-D-2	5/5/a-b	3468	metarhyolite	P	Villány?
Köm-D-3	6	3782	dolomitic limestone	P_2	Villány?
Köm-D-3	7/I	3845	calcite-bearing dolomite	P_2	Villány?
Köm-D-3	7/II/a	3845	dolomite with siderite and pyrite	P_2	Villány?
Forráskút					
Fkút-2	7	2992.4	sandstone	T_1	Békés
Fkút-3	7/a	3297	carbonatic, psammitic, pelitic-silty slate	T_1	Békés
Fkút-3	7/b	3297	carbonatic, psammitic, pelitic-silty slate	T_1	Békés
Fkút-9	4/a-b	3416.2	brecciated sandstone with hematitic infiltration	T_1	Békés
Fkút-9	5	3470.2	brecciated, recrystallized dolomite	T_2	Békés
Fkút-10	5	3412.2	brecciated limestone with dolomite marble clasts	T_2	Békés

Table 2
Modal composition of the samples

Borehole	Core	Qtz	Pl	Kfs	Ill-Ms	Chl	Kln	Sm	Ill/Sm	Cal	Dol	Sd	Py	Hem	Rt	Ep	Stp	Aug	Gp	Brt
Bam-2	3/a	x	x		x	x				0				0						
Bam-2	3/b	0	x		x	x				x				0						
Bam-2	3/c	0	x		x	x				x				0						
Bam-2	4/a	0	x		0	x								0	0	x				
Bam-2	4/b	0	+		0	x				0				0	0	0		0		
Bam-2	4/c	0	x		tr	x				tr			tr	0	0	x				
Bam-1	5	x			0	(a)	0			+					tr					
Bam-1	6/a	x			0		tr		(a)	x			tr		tr					
Bam-1	6/b	x			x					x			tr		tr					
Bam-1	6/c	+			x	(a)	(a)			x			0		tr					
Bam-1	6/d	+	tr		x		(a)			x			0		tr					
Bam-1	7/a	x			x	0	tr			x	0		0		tr					
Bam-1	7/b	x			x	0	tr			x	0		0		tr					
Bam-1	7/c	x			0	0				x	0		0		tr					
Bam-1	8/a	x			0		tr	(a)		+		0			tr					
Bam-1	8/b	x			x		tr	(a)		x	0	0			tr					
Bam-1	8/c	x			x		tr	(a)		x	x		0		0					
Bam-1	8/d	x			0		0	(a)		+	0		0							
Bam-1	9/a	0			0	(a)				+			tr							
Bam-1	9/b	0			0	(a)	(a)			+	0		tr							
Bam-1	9/c	x			0					+	0		0							
Bam-1	9/d	x			0	(a)		(a)		+			tr							
Bam-1	10/a	0			0	(a)	(a)			+	0									
Bam-1	10/b	0			0		(a)			+										
Bam-1	11/a	x	x		0	x				tr	x									
Bam-1	11/b	x	x			x					0									
Bam-1	11/c	x	x			+				0	0									
Bam-1	12/a	0			(a)	(a)	(a)			+										
Bam-1	12/b	x			0	tr	tr	(a)		+										
Kism-Ny-1	6/a	x			x					+	0		0							
Kism-Ny-1	6/b	x			0					+	0									
Kism-Ny-1	6/c	x			x	(a)				+	0		0							
Sáránd-I	6/a	0	tr		0	(a)		(a)		x	+		tr							
Sáránd-I	6/b	x	0		x	0				0	0		x		0					
Sáránd-I	6/c	x	0		x	0					0		0		0					
Sáránd-I	7/a	0			x	(a)				0	+	0	tr		tr					
Sáránd-I	7/b	0			0	(a)				0	+		tr							
Sáránd-I	7/c	x			+	(a)					0		0		0					
Sáránd-I	8/a	0			0	0				+	0		tr							
Sáránd-I	8/b	0			0	0				+	0									
Sáránd-I	8/c	0			tr	0				+	0				tr					
Sáránd-I	9/a	x			0	0			(a)	+			tr		tr					
Sáránd-I	9/b	x			0				(a)	+	0								0	
Sáránd-I	9/c	x			0	tr				+	tr		tr							
Sáránd-I	9/d	x			x	x			(a)	0	tr		0		tr					0
Sáránd-I	9/e	0			0	0				+	tr		0							
Sáránd-I	11/a	x	x		x	x				0				0					tr	
Sáránd-I	11/b	x	x		x	x				0				0						
Sáránd-I	11/c	x	+		0	x				0				0						
Sáránd-I	13/a	x	x		0	+				0			tr							
Sáránd-I	13/b	x	x		0	+				x				0						
Sáránd-I	13/c	x	0			+				0				tr	0					
Sáránd-I	14/a	0	x			x				x				tr			x			
Sáránd-I	14/b	x	0		x	x				x				tr	0					
Sáránd-I	14/c	x	x			x				x				0	0					
Sáránd-I	14/d	x	x		0	x				x	0			tr	0					
Sáránd-I	14/e	x	0		0	x				x	0			0	0					

Table 2
(cont.)

Borehole	Core	Qtz	Pl	Kfs	Ill-Ms	Chl	Kln	Sm	Ill/Sm	Cal	Dol	Sd	Py	Hem	Rt	Ep	Stp	Aug	Gp	Brt
En-E-6	3	x	x	tr	0	0				x	0									
En-E-8	4	x	x		x	x				x	0									
En-E-2	2/a	x			0	0			(a)											
En-E-2	2/b	0	+			0			0	x				0						
En-7	16/1/a	x			x	0				x	0		0							
En-7	16/1/b	x	0		x	0				x	0		0							
Öcsöd-3	2	0	x			x				x	0	tr		0						
Öcsöd-3	3	0	x			x			(a)	0				0						
Felgyő-I	16	0	x			x				x		0		0						0
Felgyő-I	17/a	+			0		0				0		tr							
Felgyő-I	17/b	+			x		0						0							
Felgyő-I	18/a	x	0		x	0				x	0		0							
Felgyő-I	18/b	x	0		0	0				+	0		0							
Táz-E-2	5	x			0	tr			0	+	0		0							
Táz-E-2	6	x			0	0	0			x										
Táz-E-6	4	+			0	0				x	0		0							
Táz-E-6	5/I	x			x	0	0			x	0		0							
Táz-E-12	6	x			0	tr				+	0		0							
Táz-E-14	3/t	+			0	0			0	x	0		0		tr					
Táz-E-14	3/a	x			0	0			0	x	0		0							
Köm-5	4	x	tr	0	x	0			(a)	0	x		0							
Köm-5	5	0			(a)				(a)	+	0		tr							
Köm-6	4	tr								+	0									
Köm-8	4	x			0	(a)			(a)	+	0									
Köm-8	5/I	x			tr		0	(a)	(a)	x	0	x	0							0
Köm-8	5/II	0			tr	(a)					+									
Csó-K-6	3/a	x	0		+		(a)			0	0			0						
Csó-K-6	3/b	x	0		x		(a)				x			0						
Csó-K-6	3/c	+		x	x		tr				0			0						
Csó-K-6	3/d	x		x	x		(a)				x									
Csó-K-6	3/e	+	x	0	0						0			0						
Csó-K-6	3/f	+	x	0	0		(a)				0			0						
Köm-D-4	2/1	+		0	x						0	0								
Köm-D-4	2/9	+	0	x	x						0	0		0						
Köm-D-2	4	x			x								0		0					
Köm-D-2	5/5/a	+	0	0	x						0	0								
Köm-D-2	5/5/b	x	x	x	x							0		tr						
Köm-D-3	6	0			(a)		(a)		(a)	x	x									
Köm-D-3	7/I	0			0		(a)			x	+									
Köm-D-3	7/I/a	x									x	x	x							0
Fkút-2	7	+			0					tr	0		tr							
Fkút-3	7/a	x	0	tr	x		0				0	0		0						
Fkút-3	7/b	x	0	tr	+		0				0	0		0						
Fkút-9	4/a	+			0							0		tr	tr					
Fkút-9	4/b	+			0							0		0						
Fkút-9	5	0			tr	(a)	tr				+									
Fkút-10	5	x				x				x	x									

Abbreviations: Qtz – quartz; Pl – plagioclase; Kfs – K-feldspar; Ill-Ms – illete-muscovite; Chl – chlorite; Kln – kaolinite; Sm – smectite; Ill/Sm – illite/smectite mixed-layer mineral; Cal – calcite; Dol – dolomite; Sd – siderite; Py –pyrite; Hem – hematite; Rt – rutile; Ep – epidote; Stp – stilpnomelane; Aug – augite; Gp – gypsum; Brt – baryte

Table 3
Illite crystallinity (IC) and chlorite crystallinity [ChC(001) and ChC(002)] values obtained on <2 μm SED grain-size fraction samples and *b* values of white K-mica determined on whole rock samples

Borehole	Core	IC	ChC(001)	ChC(002)	b_o
Bam-2	3/a	0.232	0.256	0.279	-
Bam-2	3/b	0.214	0.232	0.253	-
Bam-2	3/c	0.241	0.254	0.276	-
Bam-2	4/a	0.300	0.312	0.284	-
Bam-2	4/b	0.276	0.236	0.242	-
Bam-2	4/c1	-	0.238	0.246	-
Bam-2	4/c2	-	0.286	0.263	-
Bam-1	5	0.277	-	-	-
Bam-1	6/a	0.292	-	0.289	8.998
Bam-1	6/b	-	-	-	9.005; 9.001
Bam-1	6/c	0.331	-	-	9.005; 9.002
Bam-1	6/d	0.241	-	-	9.005
Bam-1	7/a	0.290	-	0.368	9.011; 9.006
Bam-1	7/b	0.289	0.258	0.318	9.011; 9.007
Bam-1	7/c	0.317	-	0.371	9.003
Bam-1	8/a	0.261	-	-	9.047; 9.005
Bam-1	8/b	0.262	-	-	9.001
Bam-1	8/c	0.313	-	-	9.002; 8.999
Bam-1	8/d	0.267	-	-	8.998
Bam-1	9/a	0.232	-	-	8.990; 9.013
Bam-1	9/b	0.269	-	-	8.992
Bam-1	9/c	0.312	-	-	-
Bam-1	9/d	0.314	-	-	-
Bam-1	10/a	0.222	-	-	9.025
Bam-1	10/b	0.239	-	-	9.020
Bam-1	11/a	-	0.248	0.254	-
Bam-1	11/b	-	0.257	0.243	-
Bam-1	11/c	-	0.239	0.245	-
Bam-1	12/a	0.280	-	-	-
Bam-1	12/b	0.314	-	-	-
Kism-Ny-1	6/a	0.304	-	-	9.006
Kism-Ny-1	6/b	0.266	-	-	8.994
Kism-Ny-1	6/c	0.330	-	-	8.998
Sáránd-I	6/a	0.335	-	-	8.990
Sáránd-I	6/b	-	-	-	8.976
Sáránd-I	6/c	0.410	-	-	8.978
Sáránd-I	7/a1	-	-	-	9.028
Sáránd-I	7/a2	0.335	-	-	9.022
Sáránd-I	7/b	-	-	-	9.003
Sáránd-I	7/c	0.332	-	-	9.022
Sáránd-I	8/a	0.300	0.279	0.251	9.011
Sáránd-I	8/b	0.265	0.250	0.234	9.008
Sáránd-I	8/c	0.279	0.250	0.239	9.008
Sáránd-I	9/a	0.332	0.308	0.266	9.050
Sáránd-I	9/b	0.221	0.210	0.229	9.016
Sáránd-I	9/c	0.233	0.215	0.230	9.040
Sáránd-I	9/d	-	-	0.271	-
Sáránd-I	9/e	0.273	0.242	0.243	9.019
Sáránd-I	11/a	0.223	-	0.236	9.051
Sáránd-I	11/b1	0.216	-	-	9.048
Sáránd-I	11/b2	0.240	-	0.251	9.050
Sáránd-I	11/c	0.215	0.248	0.230	9.025
Sáránd-I	13/a	-	0.277	0.269	-
Sáránd-I	13/b1	0.236	0.244	0.248	9.048
Sáránd-I	13/b2	-	0.302	0.295	-
Sáránd-I	13/c	-	0.269	0.268	-
Sáránd-I	14/a	-	-	0.300	-
Sáránd-I	14/b	0.261	0.245	0.247	9.039
Sáránd-I	14/c	-	0.282	0.277	-
Sáránd-I	14/d	0.284	0.195	0.266	-

Table 3
(cont.)

Borehole	Core	IC	ChC(001)	ChC(002)		b_o
Te-19	6/b	0.505	-	-	9.008	
En-E-6	3	0.368	0.389	0.323	9.007	
En-E-8	4	0.432	0.403	0.365	9.025	
En-E-2	2/a	0.979	-	0.311		-
En-E-2	2/b	0.838	-	0.389	8.987	
En-7	16/1/a	0.495	-	0.282		-
En-7	16/1/b	0.501	0.267	0.271	8.997	
Ocsöd-3	2	-	0.377	-		-
Ocsöd-3	3	-	0.355	0.338		-
Felgyő-I	16	-	0.371	0.387		-
Felgyő-I	17/a	0.554	-	-		-
Felgyő-I	17/b	0.579	-	-		-
Fegyő-I	18/a	0.508	-	0.372		-
Felgyő-I	18/b	0.485	-	0.361		-
Táz-E-2	5	0.710	-	0.349		-
Táz-E-2	6	0.425	-	0.385		-
Táz-E-6	4	0.774	-	0.342		-
Táz-E-6	5/I	0.421	-	0.323		-
Táz-E-12	6	1.121	-	0.323		-
Táz-E-14	3/t	0.994	-	0.306		-
Táz-E-14	3/a	1.128	-	0.331		-
Köm-5	4	0.570	-	-		-
Köm-5	5	0.487	-	-		-
Köm-6	4	0.501	-	-		-
Kőm-8	4	1.118	-	0.287		-
Kőm-8	5/I	0.741	-	-		-
Kőm-8	5/II	0.878	-	-	9.005	
Csó-K-6	3/a	0.538	-	-	9.014	
Csó-K-6	3/b	0.544	-	-	9.014	
Csó-K-6	3/c	0.615	-	-	9.010	
Csó-K-6	3/d	0.608	-	-	9.011	
Csó-K-6	3/e	0.673	-	-	9.007	
Csó-K-6	3/f	0.578	-	-		-
Köm-D-4	2/1	0.444	-	-	9.010	
Kőm-D-4	2/9	0.442	-	-	9.016	
Köm-D-4	2/16	-	-	-		-
Köm-D-2	4	0.439	-	-		-
Köm-D-2	5/5/a	0.383	-	-		-
Köm-D-2	5/5/b	0.372	-	-		-
Köm-D-3	6	0.783	-	-		-
Köm-D-3	7/I	0.882	-	-		-
Köm-D-3	7/II/a	-	-	-		-
Fkút-2	7	0.336	-	-		-
Fkút-3	7/a	0.263	-	-	9.029	
Fkút-3	7/b	0.270	-	-	9.039	
Fkút-9	4/a	0.405	-	-	8.990	
Fkút-9	4/b	0.374	-	-		-
Fkút-9	5	0.306	-	-		-
Fkút-10	5	-	0.278	0.284		-

-IC and ChC values are expressed in $\Delta^{\circ} 2\Theta$, CuK_{α}. As calibrated against Kübler's (1968, 1990) IC scale, the boundary values of the anchizone in the sense of Kübler (1990) are the followings:

	IC	ChC(001)	ChC(002)
diagenetic zone	>0.435	>0.390	>0.348
anchizone	0.284-0.435	0.309-0.390	0.284-0.348
epizone	<0.284	<0.309	<0.284

- $b_o \sim 6 \times d(060, 331)$ in A

Table 4
K-Ar isotopic ages calculated on <2 μm fraction samples

Borehole	Core	K (weight-%)	$^{40}Ar_{rad}$ (cm^3/g)	$^{40}Ar_{rad}$	age (MA)*±16
Bam-2	3	5.99	$2.032x10^{-5}$	80.0	85.3 ± 3.3
Bam-2	4	2.00	$7.306x10^{-6}$	34.9	91.7 ± 4.6
Bam-1	6	5.49	$1.956x10^{-5}$	60.5	89.4 ± 3.6
Kism-Ny-1	6/a	4.92	$8.222x10^{-6}$	58.6	42.5 ± 1.7
Sáránd-I	6/a	6.43	$2.069x10^{-5}$	59.7	81.0 ± 3.3
Sáránd-I	6/b	5.32	$1.718x10^{-5}$	62.4	81.3 ± 3.3
Sáránd-I	7/c	7.76	$2.099x10^{-5}$	67.0	68.4 ± 2.7
Sáránd-I	9/d	4.31	$1.165x10^{-5}$	43.7	68.3 ± 3.0
Sáránd-I	9/e	5.38	$1.690x10^{-5}$	32.1	79.0 ± 4.1
Sáránd-I	11/b	5.36	$1.602x10^{-5}$	51.4	75.4 ± 4.2
Sáránd-I	13/a	1.60	$5.814x10^{-6}$	33.5	91.2 ± 4.6
Sáránd-I	14/a	4.34	$1.393x10^{-5}$	55.7	80.8 ± 3.5
Eb-1	6	4.72	$2.066x10^{-5}$	87.1	109.2 ± 4.2
Te-19	6	5.09	$2.277x10^{-5}$	92.3	111.6 ± 4.3
En-7	16/1/a	3.92	$1.376x10^{-5}$	88.0	88.1 ± 3.4
Táz-É-2	5	3.07	$1.371x10^{-5}$	80.9	109.0 ± 4.3
Táz-É-14	3/t	2.48	$1.153x10^{-5}$	78.2	115.8 ± 4.5
Csó-K-6	3/a	6.12	$4.128x10^{-5}$	95.8	165.6 ± 6.4
Fkút-3	7/a	6.36	$1.967x10^{-5}$	86.8	77.9 ± 3.1

* Calculated using atomic constants of Steiger and Jäger (1977)

cleavage and the (brecciated) limestone show signs of high-T anchizonal regional metamorphism, transitional to the epizone. By contrast, the various lithotypes of the *Endrőd and Endrőd-North areas* that display rough fracture cleavage and brecciation, suffered only diagenetic alteration. Their dominant illite-muscovite + chlorite assemblage (with rare illite/smectite mixed layers) contains various amounts of inherited (well-crystallized) mica and chlorite. The metabasalt from *well Öcsöd-3* shows signs of hydrothermal spilitization, the temperature of which might have been about 200–250 °C, judging from the chlorite properties. No remarkable deformation followed the hydrothermal activity. This rock type is very similar to the metabasalt described from *well Felgyő-I.*

In the next zone to the south represented by mixed (Mecsek- and Villány-type) Mesozoic formations in allochthonous position (*well Felgyő-I* and the *Kömpöc area*), shale displays embryonic forms of rough fracture cleavage, while the carbonate sedimentary rocks and sandstone are more or less brecciated. Their mixed clay mineral assemblages as well as their IC values indicate diagenetic alterations. Similarly, only diagenetic effects were proved in the zone represented by scaly, overthrusted Permian and Triassic (*Csólyospálos-East and Kömpöc-South areas*).

The Lower Triassic (?), strongly tectonized sandstone, slate, dolomite and limestone series of the *Forráskút area* representing the Békés-Codru Zone of the basement, shows high-T anchizonal, transitional anchizonal and epizonal IC

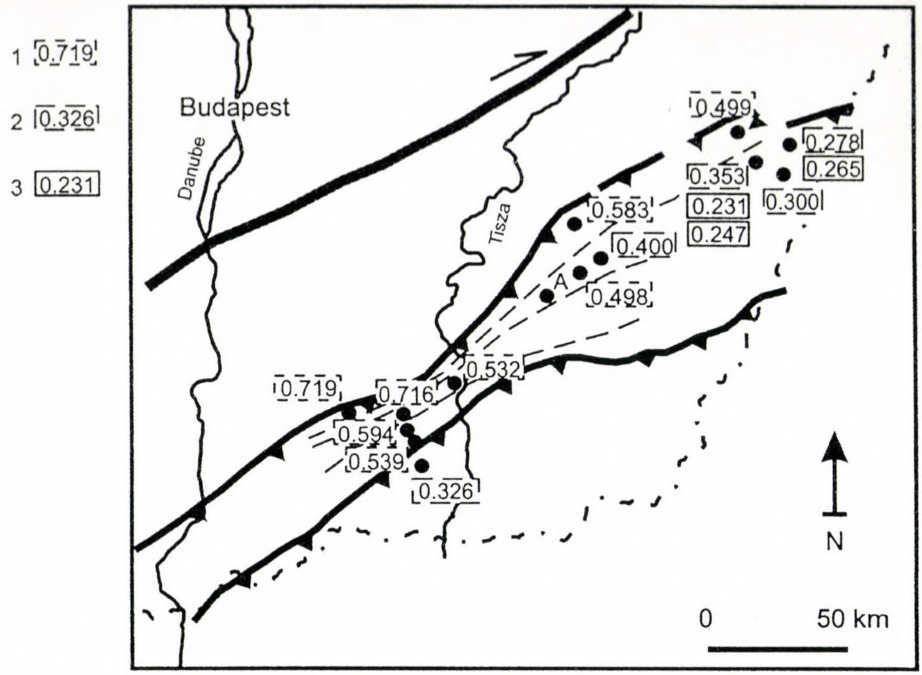

Fig. 4
Average IC values of the Mesozoic formations, measured on < 2 μm fraction samples. 1. diagenetic; 2. anchizonal; 3. epizonal rocks

indices. The appearance of ordered kaolinite was connected to post-metamorphic hydrothermal alteration.

Summarizing the results on grades one may conclude that the Jurassic formations in the northernmost zone suffered only diagenetic alterations. Farther south of the main thrust plane, where not only Jurassic but also Triassic and Lower Cretaceous are found beneath the polymetamorphic nappes, grades vary strongly from diagenesis (ca. <200 °C) through the anchizone up to the epizone (ca. >300 °C). The highest-grade regional metamorphism was observed in the easternmost part of the studied area. Nevertheless, anchizonal sequences were also found sporadically in the central and southwestern parts, where the majority of the samples underwent only diagenesis.

Figure 5 displays the regional distribution of mean b ($\cong 6 \times d_{33\bar{1},060}$) values of white K-micas. The mean values scatter between 8.999 and 9.044Å, indicating a wide range of celadonitic [$Al^{IV}Al^{VI} \leftrightarrow Si(Mg,Fe^{2+})$] substitution in illite-muscovite. In Fig. 5 mean b values are discriminated according to grades (diagenetic and metamorphic IC zones). Figure 5 shows that, presumably because of lithological and bulk chemical effects (see also Árkai & Lelkes-Felvári, 1993), there is no significant relation between the mean b values (celadonite content) and grade-indicating IC (≈temperature).

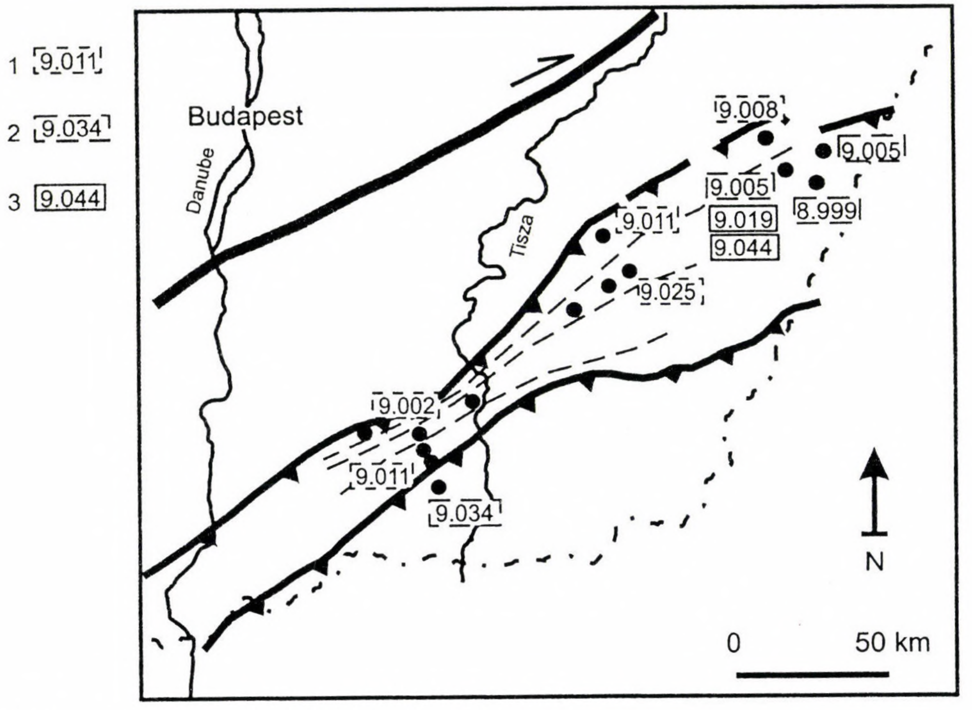

Fig. 5
Average b ($\cong 6 \times d_{\bar{3}31,060}$) values of white K-micas. 1. diagenetic; 2. anchizonal; 3. epizonal rocks

According to theoretical and empirical limitations outlined by Guidotti & Sassi (1976, 1986) and Padan et al. (1982), only epizonal (greenschist facies chlorite zone) and medium and high-T anchizonal fine-clastic metasedimentary rocks with common mineral assemblages consisting of quartz, albite, white K-mica ± chlorite and carbonate minerals (the latter being present in moderate quantities) can be taken into consideration for evaluating pressure conditions. Among the areas investigated there are only two boreholes from which rocks of adequate lithology and modal composition were found. In *borehole Sáránd-I* a high-T anchizonal slate sample from the upper (dolomitic - fine-clastic) subunit is characterized by b = 9.005Å, implying transitional low-medium pressure range. The high-T anchizonal, partly epizonal slate samples from the *Forráskút area* (Danube-Tisza Interfluve) indicate typical medium-pressure metamorphic conditions. Their b values range between 9.029 and 9.039Å, giving an average of 9.034Å. The b averages of the other localities do not support, but neither do they contradict, the above-mentioned conclusion on the medium, transitional low-medium pressure type of regional metamorphism, being rather similar to the pressure-indicating b values.

When evaluating the K-Ar ages obtained on the <2 μm grain-size fraction illite-muscovite-rich samples (Fig. 6 and Table 4) for estimating age relations of

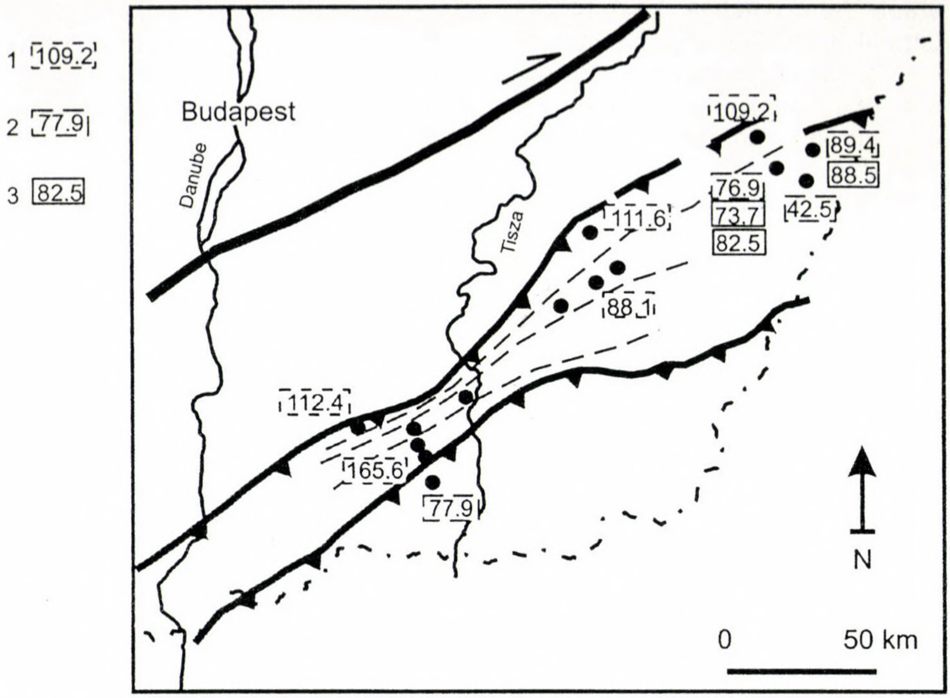

Fig. 6
K-Ar ages obtained on the illite-muscovite-rich, < 2 μm grain-size fraction samples separated from diagenetic (1), anchizonal (2) and epizonal (3) rocks

regional metamorphism the following must be taken into consideration. The effect of inherited detrital (old) micas has resulted in higher ages. This effect decreases with increasing grade. However, this effect, although very slight, can be observed even in epizonal rocks (Ahrendt et al. 1978; Hunziker et al. 1986; Árkai et al. 1995a). In the geologic sense relatively short-lived Neogene (mostly Pliocene) burial and heating might cause an opposite effect, i.e., decrease of apparent K-Ar ages. Considering an effective heating time of ca. 2–3 Ma, a maximum burial temperature of about 200 °C at 4000 m and a closure temperature of 260±20 °C for <2 μm illite-muscovite during 10±5Ma (Hunziker et al. 1986), the K-Ar ages might decrease no more than 10–20 relative % (see Balogh et al. 1990).

Disregarding a single Tertiary age value from the *Kismarja-West area* (eastern Hungary), all of the K-Ar ages of the anchizonal and epizonal metamorphic samples scatter between 68.3 and 91.7 Ma, giving an average of 80.8 Ma (s = 7.8 Ma, n = 12). Thus, the regional metamorphism most probably took place in the Cretaceous and might be related to the Austrian and/or Subhercynian phases that were responsible for the main nappe-forming compressional events in the Pannonian Basin and the Carpathians. The age value of 42.5 Ma obtained from a sample from borehole Kism-Ny-1 may be connected to a local meso-Alpine thermal effect. The K-Ar ages of the diagenetic samples are generally higher than those of the anchizonal and epizonal samples. Their values – depending on the ratios of inherited mica and authigenic illite in the <2 μm fractions – are scattered between 88.1 and 165.6 Ma. The oldest age was obtained from a supposed Permian sample from the *Csólyospálos-East area* (Danube-Tisza Interfluve). The K-Ar values of the diagenetic samples suggest mixed ages between the Cretaceous, which may be considered the main phase of illite neoformation, and the ages of inherited detrital muscovites.

Conclusions

The new petrographic data presented here prove that the metamorphism of the post-Variscan (mainly Mesozoic) part of the pre-Tertiary basement of the Tisza Unit (southern Hungary) was much more widespread than had been previously anticipated. It was not restricted to the two localities (Barcs-West area in southern Transdanubia and the Sáránd area in the eastern Great Plain) characterized by Árkai (1990), Balogh et al. (1990) and Árkai et al. (1998); on the contrary, regional metamorphism affected a considerable part of the post-Variscan basement underlying the overthrusted polymetamorphic nappes or which was in imbricated, scaly, allochthonous tectonic positions along the main thrust zones of the basement.

The relatively highest-grade (epizonal – greenschist facies chlorite zone) alteration is observed in eastern Hungary (Sáránd area). Nevertheless, anchizonal rocks are found in various parts of the Tisza Unit, also in the Békés-Codru zone of the Danube–Tisza Interfluve. However, the present dataset does not allow drawing further conclusions on eventual regularity in distribution of metamorphic grades.

The metamorphism, the temperature of which varied between about 200 and 350 °C, proved to be of orogenic (regional dynamothermal) type. Judging from the sporadic white K-mica geobarometric data metamorphism proceeded most probably in a medium or transitional low-medium pressure system.

The age of metamorphism is Cretaceous. This event might be related to (slightly preceding or contemporaneous with) the compressional events of the Austrian and Subhercynian phases.

The results of the present paper confirm the earlier statements of Árkai et al. (1998) and Árkai (1999). Thus, the Tisza Unit did not escape the Alpine (Cretaceous) prograde regional metamorphism. As the temperature of this event might exceed 300 °C in the level of the Mesozoic, it might cause even higher temperature alterations in the underlying polymetamorphic complex of the Tisza Unit than has been generally supposed so far. Consequently, the present results may also open new perspectives for a more reliable petrogenetic interpretation of the polymetamorphic complex.

Acknowledgements

The metamorphic petrological and isotope geochronological research that provided the database of the present paper was initiated and financially supported by MOL Hungarian Oil & Gas Plc., Budapest. Thanks are due for permitting the publication. The authors are indebted to Mrs. H. Bohn-Vajk (Lab. for Geochemical Research, Hung. Acad. Sci.) for vitrinite reflectance measurements and Mrs. O. Komoróczy, Cs. M. Sándor, Ms. K. Temesvári and N. Szász (all in Lab. for Geochemical Research, Hung. Acad. Sci.) for their technical assistance. This work was also supported by the Hungarian Research Fund (OTKA), Budapest, by programs Nos. T-022773/1997-2000 to P.Á. and T-014961/1995-1998 to K.B.

References

Ahrendt, H., J.C. Hunziker, K. Weber 1978: K/Ar-Altersbestimmungen an schwachmetamorphen Gesteinen des Rheinischen Schiefergebirges. – Zeitschrift der Deutschen Geologischen Gesellschaft, 129, pp. 229–247.

Árkai, P. 1983: Very low- and low-grade Alpine regional metamorphism of the Paleozoic and Mesozoic formations of the Bükkium, NE-Hungary. – Acta Geol. Hung., 26, pp. 83–101.

Árkai, P. 1984: Polymetamorphism of the crystalline basement of the Somogy-Dráva Basin (Southwestern Transdanubia, Hungary). – Acta Miner. Petr. Szeged, 26, pp. 129–153.

Árkai, P. 1987: Contributions to the knowledge of the polymetamorphic basement of the Great Plain (Pannonian Basin, East Hungary): the environment of the Derecske Depression. – Fragmenta Mineralogica et Palaeontologica, Budapest 13, pp. 7–30.

Árkai, P. 1990: Very low- and low-grade metamorphic rocks in the pre-Tertiary basement of the Drava Basin, SW-Hungary: mineral assemblages, illite "crystallinity", b_0 data, and problems of geological correlation. – Acta Geol. Hung., 33, pp. 43–67.

Árkai, P. 1999: The basement of the Carpathian Basin. – In: Pécsi, M. (ed.): Landform evolution studies in Hungary. Akadémiai Kiadó, Budapest, pp. 13–28.

Árkai, P., K. Balogh, I. Dunkl 1995a: Timing of low-temperature metamorphism and cooling of the Paleozoic and Mesozoic formations of the Bükkium, innermost Western Carpathians, Hungary. – Geol. Rundschau, 84, pp. 334–344.

Árkai, P., K. Balogh, M. Frey 1997: The effects of tectonic strain on crystallinity, apparent mean crystallite size and lattice strain of phyllosilicates in low-temperature metamorphic rocks. – Schweiz. Mineral. Petrogr. Mitt., 77, pp. 27–40.

Árkai, P., A. Bérczi-Makk, D. Hajdu 1998: Alpine prograde and retrograde metamorphisms in an overthrusted part of the basement, Great Plain, Pannonian Basin, Eastern Hungary. – Acta Geol. Hung., 41, pp. 179–210.

Árkai, P., Gy. Lelkes-Felvári 1993: The effects of lithology, bulk chemistry and modal composition on illite "crystallinity" – A case study from the Bakony Mts., Hungary. – Clay Minerals, 28, pp. 417–433.

Árkai, P., G. Nagy, G. Dobosi 1985: Polymetamorphic evolution of the South-Hungarian crystalline basement, Pannonian Basin: geothermometric and geobarometric data. – Acta Geol. Hung., 28, pp. 165–190.

Árkai, P., F.P. Sassi, R. Sassi 1995b: Simultaneous measurements of chlorite and illite crystallinity: a more reliable tool for monitoring low- to very low-grade metamorphisms in metapelites. A case study from the Southern Alps (Italy). – Eur. J. Mineral., 7, pp. 1115–1128.

Árkai, P., R. Sassi, G. Zirpoli 1991: On the boundary between the low- and very low-grade South-Alpine basement in Pustertal: X-ray characterization of white mica in metapelites between Dobbiaco (Toblach, Italy) and Leiten (Austria). – Mem. Sci. Geol. Padova, 63, pp. 293–304.

Balogh, K., Á. Kovách, Z. Pécskay, É. Svingor, P. Árkai 1990: Very low- and low-grade metamorphic rocks in the pre-Tertiary basement of the Drava Basin, SW-Hungary, II: K-Ar and Rb-Sr isotope geochronologic data. – Acta Geol. Hung., 33, pp. 67–76.

Bérczi-Makk, A. 1998: Az Alföld és a Tokaji-hegység triász és jura képződményeinek rétegtana. (Stratigraphy of Triassic and Jurassic formations in the Great Plain and Tokaj Mts.) – In: Bérczi, I., Á. Jámbor (Eds): Magyarország geológiai képződményeinek rétegtana. (Stratigraphy of Hungary.), Publication of the MOL Plc. and the Hungarian Geological Institute, Budapest, pp. 281–298 (in Hungarian).

Bérczi-Makk, A., G. Császár, A. Nusszer 1996: A Mecseki Zóna közép-alföldi mezozóos aljzatának sztratigráfiai értékelése és fejlődéstörténeti vázlata. (Stratigraphy and geological evolution of the Mesozoic basement of the Mecsek Zone in the central part of the Great Hungarian Plain (East Central Hungary).) – Földt. Közl., 126, pp. 185–207 (in Hungarian).

Bleahu, M., G. Mantea, S. Bordea, S. Panin, M. Stefanescu, K. Sikic, J. Haas, S. Kovács, Cs. Péró, A. Bérczi-Makk, Gy. Konrád, E. Nagy, E. Rálisch-Felgenhauer, Á. Török 1994: Triassic facies types, evolution and paleogeographic relations of the Tisza Megaunit. – Acta Geol. Hung., 37, pp. 187–234.

Csontos, L., A. Nagymarosy, F. Horváth, M. Kovac 1992: Tertiary evolution of the Intra-Carpathian area: a model. – Tectonophysics, 208, pp. 221–241.

Fülöp, J. 1989: Bevezetés Magyarország geológiájába (Introduction to the geology of Hungary). – Akadémiai Kiadó, Budapest, p. 246 (in Hungarian).

Fülöp, J. 1994: The geology of Hungary, Paleozoic II. – Monograph, Akadémiai Kiadó, Budapest, p. 445 (in Hungarian).

Géczy, B. 1973: The origin of the Jurassic faunal provinces and the Mediterranean plate tectonics. – Ann. Univ. Sci. Budapest. R. Eötvös Nom. Sect. Geol., 16, pp. 99–114.

Guidotti, C. V., F. P. Sassi 1976: Muscovite as a petrogenetic indicator mineral in pelitic schists. – N. Jb. Miner. Abh., 127, pp. 97–142.

Guidotti, C. V., F. P. Sassi 1986: Classification and correlation of metamorphic facies series by means of muscovite bo data from low-grade metapelites. – N. Jb. Miner. Abh., 153, pp. 363–380.

Haas, J. 1994: Magyarország földtana. Mezozoikum. (Geology of Hungary. Mesozoic.) – Eötvös University, Budapest, 119 p (in Hungarian).

Hunziker, J. C., M. Frey, N. Clauer, R. D. Dallmeyer, H. Friedrichsen, W. Flehmig, K. Hochstrasser, P. Rogwiller, H. Schwander, 1986: The evolution of illite to muscovite: mineralogical and isotopic data from the Glarus Alps, Switzerland. – Contrib. Mineral. Petrol., 92, pp. 413–427.

Kázmér, M., S. Kovács 1985: Permian–Paleogene paleogeography along the Eastern part of the Insubric–Periadriatic lineament system: evidence for the continental escape of the Bakony–Drauzug Unit. – Acta. Geol. Hung.,28, pp. 71–84.

Kober, L. 1921: Der Bau der Erde. – Berlin, Borntraeger.

Kober, L. 1923: Bau und Entstehung der Alpen. – Berlin, Borntraeger, p. 203.

Kovács, S. 1982: Problems of the "Pannonian Median Massif" and the plate tectonic concept. Contributions based on the distribution of Late Paleozoic–Early Mesozoic isopic zones. – Geol. Rundschau 71, pp. 617–640.

Kovács, S. 1987: Az Alföld medencealzatának szerkezet fejlődése. (Tectonic evolution of the basement of the Great Hungarian Plain.) – Publication of the Szeged Regional Committee of the Hungarian Academy of Sciences, Szeged, pp. 17–29 (in Hungarian).

Kovács, S. 1996: Magyarország nagyszerkezeti helyzete és geológiai környezetének fő vonásai (Megastructural position of Hungary and outlines of its geological environment). – In: Haas, J. (ed.): Magyarázó Magyarország földtani térképe a kainozoikum elhagyásával és Magyarország szerkezetföldtani térképe című térképlapokhoz. 1:500,000. Budapest, Magyar Állami Földtani Intézet, pp. 43–73 (in Hungarian).

Kovács, S., T. Szederkényi, P. Árkai, Gy. Buda, Gy. Lelkes-Felvári, A. Nagymarosi 1996–97: Explanation to the terrane map of Hungary. – Annales Geol. des Pays Helleniques, Athens, 37, pp. 271–330.

Kübler, B. 1968: Evaluation quantitative du métamorphisme par la cristallinité de l'illite. – Bull. Centre Recherche Pau-SNPA, 2, pp. 385–397.

Kübler, B. 1990: "Cristallinité" de l'illite et mixed-layers: brève révision. – Schweiz. Mineral. Petrogr. Mitt. 70, pp. 89–93.

Lóczy, L. 1918: Magyarország földtani szerkezete (Geological structure of Hungary). – In: Lóczy, L. (ed.): A magyar szent korona országainak földrajzi, társadalomtudományi, közművelődési és közgazdasági leírása. – Kilián Frigyes utóda, Budapest, pp. 5–3 (in Hungarian).

Lóczy, L. 1924: Geologische Studien in westlichen Serbien. – Die Ergebnisse der von der Orientkommission der Ungarischen Akademie der Wissenschaften organisierten Balkan-Forschungen. II. Geologie. Berlin/Leipzig.

Padan, A., H.J. Kisch, R. Shagam 1982: Use of the lattice parameter b_0 of the dioctahedral illite/muscovite for the characterization of P/T gradients of incipient metamorphism. – Contrib. Mineral. Petrol., 79, pp. 85–95.

Prinz, Gy. 1926: Magyarország földrajza. I. Magyarország földjének származása, szerkezete és alakja (The geography of Hungary). – Danubia Könyvkiadó, Pécs (in Hunagrian).

Sassi, F. P. 1972: The petrologic and geologic significance of the bo value of potassic white micas in low-grade metamorphic rocks. An application to the Eastern Alps. – Tschermaks Mineral. Petrogr. Mitt., 18, pp. 105–113.

Steiger, R.H., E. Jäger 1977: Subcommission on Geochronology: Convention on the use of decay constants in geo- and cosmochronology. – Earth Planet. Sci. Lett. 36, pp. 359–362.

Szederkényi, T. 1984: Crystalline basement of the Great Hungarian Plain and its geological connections. – D.Sc. Thesis, Budapest (in Hungarian).

Szederkényi, T. 1996: Metamorphic formations and their correlation in the Hungarian part of the Tisia megaunit (Tisia megaunit terrane). – Acta Miner. Petr. Szeged., 37, pp. 143–160.

Szederkényi, T., P. Árkai, Gy. Lelkes-Felvári 1991: Crystalline basement of the Great Hungarian Plain and South Transdanubia, Hungary. – In: Karamata, S. (ed.): Geodynamic evolution of the Pannonian Basin. – Serb. Acad. Sci. Arts, Acad. Conf., 62, Dept. Nat. and Math. Sci. , 4, pp. 261–273, Beograd.

Acta Geologica Hungarica, Vol 43/1, pp. 65–84 (2000)

Late Variscan ultramylonite from the Mórágy Hills, SE Mecsek Mts., Hungary

Gyöngyi Lelkes-Felvári
Hungarian Natural History Museum, Department of Mineralogy and Petrology, Budapest

Péter Árkai
Laboratory for Geochemical Research Hungarian Academy of Sciences, Budapest

Wolfgang Frank
Institut für Geologie, Universität Wien, Austria

Géza Nagy
Laboratory for Geochemical Research Hungarian Academy of Sciences, Budapest

A regional shear zone developed during a late stage of the Variscan orogeny in the Mórágy Hills, SE Mecsek Mts., Tisza Unit, Hungary. This shear zone brought in contact a Variscan granite suite of Moldanubian lithological affinity (Mórágy Granitoid) and a regional metamorphic series (Ófalu series) in which different lithologies with various metamorphic grades are interlaced, displaying a broad range of deformational microtextures. Polyphase garnet-bearing ultramylonites are for the first time petrologically described from this shear zone. Splintery cores of idioblastic garnets are interpreted as relic porphyroclasts from precursor gneiss. Their strongly varying chemical composition indicates amphibolite facies conditions for the parent rock. A new idioblastic garnet generation around these cores reflects compositional growth zoning with a contrasting, homogeneous chemistry pointing to equilibrium conditions. Mineral parageneses and thermobarometric calculations indicate 5.7–6.3 kbar and 450°C peak postkinematic conditions. According to the $^{40}Ar/^{39}Ar$ analyses on whole rock and biotite-rich concentrates this shearing event took place between 303 Ma (maximum age) and 270 Ma.

Keywords: ultramylonite, greenschist facies metamorphism, thermobarometry, mineral chemistry, $^{40}Ar/^{39}Ar$ analyses, Mecsek Mts., Hungary

Introduction

The aim of this paper is to present new data on ultramylonite formation and to characterize the temperature and pressure conditions of shear-related metamorphism in the metamorphic basement of the Mecsek Mountains. For this purpose detailed microstructural, mineral paragenetic, mineral chemical, thermobarometric and isotope geochronological studies were carried out on the continuous core material from borehole Mőcsény-I.

This shear zone is of regional significance because it separates the Mórágy Variscan granitic rocks (with strong Moldanubian lithological affinities) from

Addresses: Gy. Lelkes-Felvári: H-1431 Budapest, Pf. 137, Hungary
E-mail: felvari@zoo.zoo.nhmus.hu
P. Árkai, G. Nagy: H-1112 Budapest, Budaörsi út 45, Hungary
W. Frank: 3A-1090 Wien, Althanstr. 14, Austria
Received: 17 November, 1999

0236–5278/2000/$ 5.00

Silurian rocks with very-low-grade metamorphism. Detailed knowledge of the basement rocks in the Tisza Unit can yield additional arguments to the ongoing discussion on where this large unit was located at the former European margin of the Tethys.

Geologic outline

The Mecsek Mountains form part of the Tisza Unit (Fig. 1) which originated from the northern, European margin of Tethys, mostly by Meso-Alpine horizontal block (microplate) displacements (Géczy 1973; Kovács 1982; Kázmér and Kovács 1985; Balla 1988; Haas et al. 1990).

In general, the major part of the basement in the Tisza Unit is characterized by early Variscan(?), medium-pressure, amphibolite-facies regional metamorphic rocks overprinted by a low-pressure Variscan event ranging from subgreenschist to amphibolite facies. The formation of syn and late-kinematic migmatites and granitoids was connected to the axes of thermal maxima of this low-pressure event, as typified by the Mecsek granitoids (Lelkes-Felvári and Sassi 1981; Árkai 1984; Szederkényi 1984; Árkai et al. 1985; Szederkényi et al. 1991). The Tisza Unit was one of the most stable blocks of the Pannonian Basin during the Alpine tectonometamorphic cycle (Árkai 1991); however, locally it was also affected by subgreenschist and greenschist facies Alpine metamorphism (Árkai 1990; Balogh et al. 1990; Árkai et al. 1998).

The investigated borehole Mőcsény-I is located in the Mórágy Hills, an isolated outcrop of basement rocks in the southeastern part of Mecsek Mts. In this area two basement complexes can be distinguished. The main body of the area is built up by granitoid rocks (Mórágy Granitoid Formation). Northwest of the granitoid body, in a narrow (1.5 km) NE–SW trending zone, metamorphic rocks are exposed called the Ófalu Series (Ghoneim and Szederkényi 1977). To the NW a widespread Mesozoic carbonate and clastic sedimentary sequence is developed, the contact with the shear zone of which is tectonic (a later thrust). In surrounding areas granite and metamorphic rocks are unconformably overlain by Triassic, Miocene and Quaternary sediments. North of the Ófalu Shear Zone Silurian rocks of variable lithology and considerable thickness, with very low-grade metamorphic overprint, are known from boreholes (Szederkényi 1977; Árkai et al. 1995). It is generally accepted that such rocks (at least partly) underlie the Mecsek Mesozoic series.

The Mórágy Granitoid is heterogeneous in composition, monzonite, quartz monzonite and monzogranite being the most common rock types, showing prevailing metaluminous and slightly peraluminous character. They belong to a potassic calc-alcaline series (Buda 1985). Recent single-zircon ages on two typological groups from the granitoid provided ages of 377±13 Ma and 363±13 Ma; a rare 619±18 Ma old generation was also demonstrated (Buda et al. 1999). Variscan ages scattered in the range of 323–365 Ma were also obtained by means

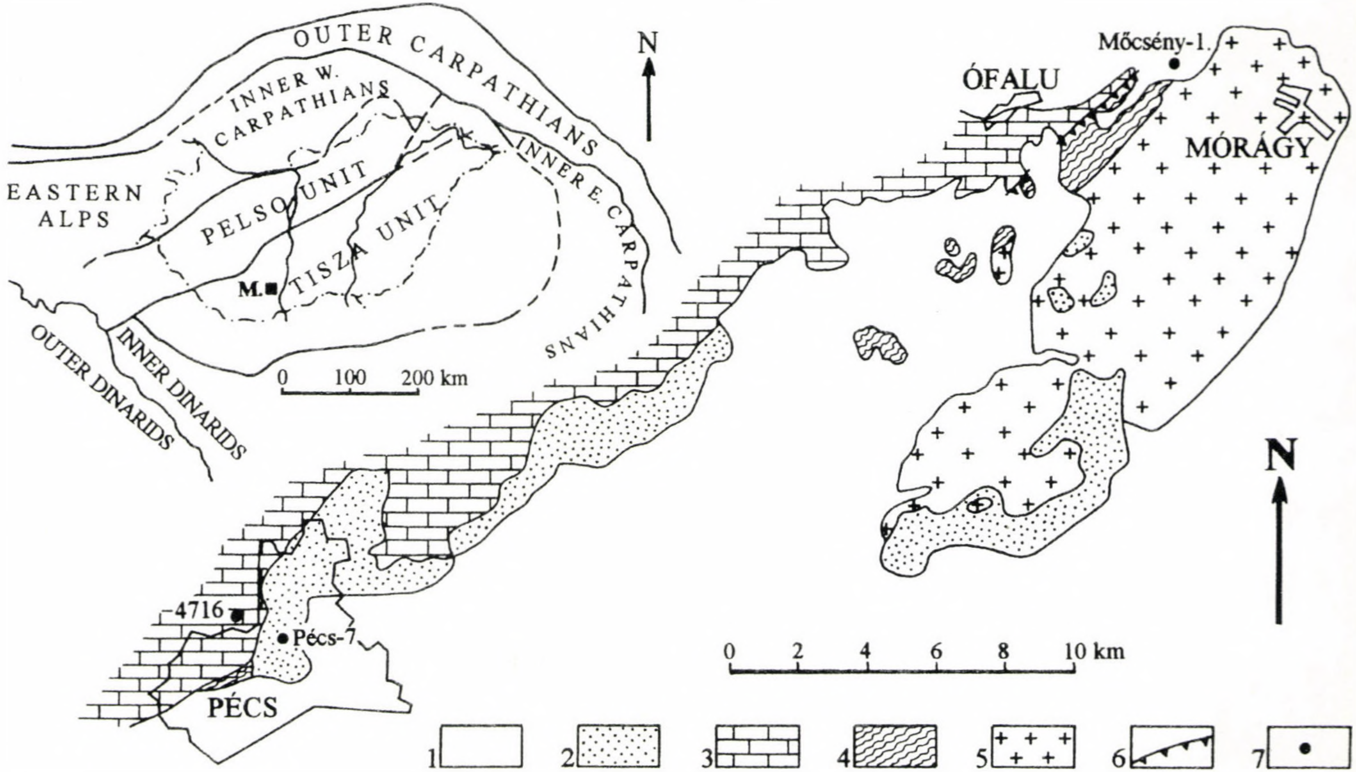

Fig. 1
Geologic sketch of the basement of the Mecsek Mountains, with the location of borehole Mőcsény-I. Inlet: Tectonic position of the Mecsek Mts. in the Alpine–Carpathian system (after Haas et al. 1990) 1. Quaternary; 2. Miocene; 3. Mesozoic; 4. Ófalu Shear Zone; 5. Mórágy Granodiorite; 6. fault; 7. borehole

of Rb-Sr whole rock analyses and by Rb/Sr and K/Ar analyses of biotite concentrates (Svingor and Kovách 1981; Balogh et al. 1983). Lelkes-Felvári and Sassi (1981) pointed out that the high-grade metamorphism developed under a relatively high (>34 °C km^{-1}) thermal gradient indicated by the occurrence of cordierite + sillimanite. The porphyric granodioritic rocks of Mórágy have strong analog features to certain magmatic rocks of the Moldanubian Massif, e.g. the Rastenberg Granodiorite (Buda 1996). They have very similar macroscopic aspects in the field and both are characterized by very special and rare zircon typology, geochemistry and similar ages (kind pers. communication by Klötzli).

From the Ófalu Series metapelite, different types of metavolcanic rocks, amphibolites, serpentinite, and marbles were described, with grades ranging from greenschist to amphibolite facies. From this complex only two K/Ar data from amphibole concentrates coming from amphibolites (lacking any petrographic description) are available: 333 and 350 Ma (Balogh et al. 1983).

In the literature two main contrasting views exist about the origin of these rocks. In several papers the Ófalu Series is considered as part of a prograde metamorphic series ranging from greenschist to amphibolite facies with various features of migmatisation (Szádeczky-Kardoss et al. 1969; Ghanem and Ravasz-Baranyai 1969; Jantsky 1979). The other view – which is proposed in this paper – interprets all these rocks as highly transformed tectonites with some relics of earlier higher-grade metamorphic stages. Jantsky (1953) was the first author who recognized a strong tectonic imprint in this area. Szederkényi (1975) interpreted part of the metamorphic rocks as mylonites formed during early Variscan transcurrent faulting with temperatures causing the formation of anatectic melts.

Main characteristics of the shear zone

The shear zone reaches a width of 1.5–2 km and extends for 35 km from the outcrops at Ófalu. Further westward, up to the town of Pécs, it is known only from boreholes, but is supposed to be much more extensive; however, no detailed knowledge exists about the continuation of this shear zone to the west of Pécs, where it is cut and offset by a complicated system of Mesozoic and younger tectonic lines. In the area of Pécs two boreholes traverse the sheared contact of the regional metamorphic series with granitoids. In borehole Pécs-7 andalusite-bearing schist was found, and in borehole No. 4716 metapelite is characterized by biotite + muscovite ± garnet ± andalusite ± sillimanite mineral assemblage (Lelkes-Felvári and Sassi 1981).

In its outcropping part the shear zone is parallel to the various lineations in the granite. The different lithologies and metamorphic grades of the regional metamorphic series occurring in narrow, discontinuous stripes are also parallel to the trend of the shear zone. Sheared rocks exhibit a heterogeneous nature of deformation, with a broad range of microstructural development. A whole series of mylonitic and cataclastic rocks occur. Different types of mylonitic rocks are widespread and display a late-stage folding of the mylonitic foliation. Cataclastic rocks can be attributed to later phases of deformation.

From the outcropping portion of the shear zone there are only sporadic data available on temperature and pressure conditions. According to Jantsky (1953) and our observations the recrystallization of granitoids can be characterized by ubiquitous, newly grown biotite. Árkai and Nagy (1994) described mylonitization of high-T greenschist-facies / low-T amphibolite-facies amphibolites (Erdősmecske and Mórágy) in a prograde system: ca. 540 °C and 3 kbar for the regional metamorphic amphibolite and ca. 580 °C and 4 kbar for its mylonitized variety.

At present no detailed structural data are available and no kinematic analysis has yet been performed – although it would be very important – from this shear zone. Along Goldgrund valley (SW of Ófalu) the following reconnaissance observations could be made. All outcropping rocks show a nearly vertical dip (S=105–125/85–90°). Over a width of nearly 1,500 m the shear zone is largely composed of extremely deformed to fine-grained rocks of phyllitic appearance. Relics of former coarse-grained rocks are preserved as porphyroclastic muscovite-flakes (up to 3–4 mm) and feldspars in some layers. Most rocks have a new mineral assemblage, of which white mica and biotite flakes are visible to the naked eye. Usually the schistosity is very pronounced and often developed on a millimetric scale. A pronounced lineation is developed only in a few layers and some lithologies (e.g. the carbonate rocks). In spite of their pronounced schistosity, most of the rocks do not exhibit a linear fabric. A dextral shear sense was deduced for this area.

Methods and analytical procedure

In addition to macroscopic and microscopic observations, bulk chemical, XRD, electron microprobe and $^{40}Ar/^{39}Ar$ analyses have been performed and utilized.

Element concentrations were determined by AAS (Perkin-Elmer 5000) using a flame technique after digesting the rock samples in lithium metaborate. Gravimetric (SiO_2, H_2O^+ and H_2O^-), spectrophotometric (SiO_2, TiO_2 and P_2O_5), permanganometric (FeO) and volumetric (CO_2) methods completed the major element analyses.

The XRD powder analyses were undertaken with a Philips PW-1730 diffractometer with CuK radiation, using the computerized APD-1700 system. Measuring conditions were: 45 kV, 35 mA, proportional counter, graphite monochromator, divergency and detector slits of 1°, and collection of data with 0.05°2 steps, using measuring time intervals of 1s.

Chemical analyses of minerals were carried out with a JEOL JCXA-733 electron microprobe equipped with 3 WDS, using the measuring program of Nagy (1984; 1990). For the detailed description of measuring conditions and precision of analyses the authors refer to Árkai and Nagy (1994).

For age determinations: biotite concentrates processed in the usual way were ground in an agate mortar mill to destroy mineral grains others than mica, to split up intergrown flakes and remove inclusions of apatite, etc. Magnetic separation yielded concentrates of typical purity around 99% and better. The mineral concentrates were enclosed in high-purity quartz vials and irradiated at the 9MW ASTRA reactor at the Austrian Research Center in Seibersdorf. Detailed description of the analytical techniques can be found in Frimmel and Frank (1998).

Results and discussion

Petrography of the ultramylonite

The investigated borehole (for location see Fig. 1) cut across dark brown to black banded ultramylonite between 67.4 and 71 m (Fig. 2); it is covered by Pannonian sediments. We investigated this core material because sheared rocks with newly formed garnets had not been detected in this area so far; moreover they are fresh, while those of outcropping rocks are weathered.

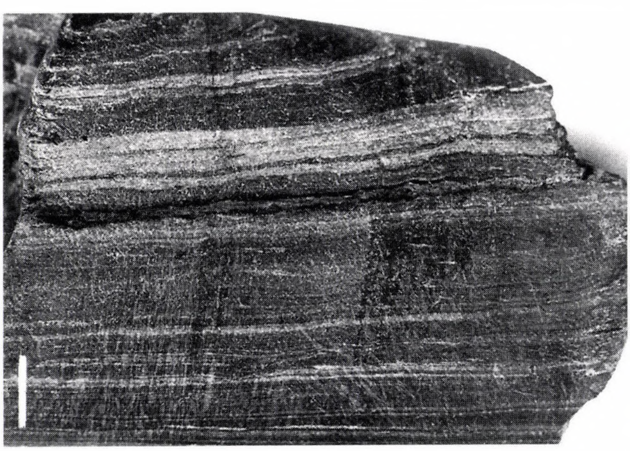

Fig. 2: Banded ultramylonite from borehole Mőcsény-I, core sample, 68.4–68.5 m (bar scale: 1 cm)

To the naked eye they are banded, aphanitic, very fine grained rocks: darker and lighter bands of a few mm thickness and laminae alternate with sharp contacts. Some bands are slightly undulatory and wedge-shaped. The dip of the mylonitic schistosity (Sm) is 80° in the cores.

Under the microscope they are made up of a very fine-grained matrix and some elongate lenses and ribbons of quartz. A weak compositional layering is due to layers also containing porphyroclasts. A very pronounced continuous cleavage is characteristic, which is transsected by a later set of weak, wavy, anastomosing cleavage. The transition from these cleavage domains into the Sm is gradational.

The matrix is composed of fine-grained biotite and subordinate chlorite, quartz, plagioclase and K-feldspar. Biotite crystals in the matrix are mostly aggregates, with single crystals 10–40 μm in length, having irregular grain boundaries and distinct preferred orientation. They are frequently intergrown with chlorite. Coarser biotite and chlorite flakes occur in the pressure shadows of porphyroclasts.

Porphyroclasts (quartz, plagioclase, K-feldspar, garnet, white mica) are up to 150 μm in diameter; their quantity is subordinate. They occur as dispersed single monocrystals or polycrystalline aggregates. The matrix wraps around the bigger ones and pressure shadows, composed mainly of biotite, quartz, chlorite and pyrite, appear. Feldspars are the most common among the porphyroclasts; they have irregular shapes (mainly round) and some of them are partially altered to sericite. A few mica flakes with opacitic border can be considered to be former biotite. A few mantled quartz porphyroclasts also occur. Garnet, apatite, tourmaline and zircon are accessory components. Garnets (40–150 μm in diameter) generally display regular crystal faces, but grains with irregular angular cores and euhedral rims also occur (Fig. 3a). These rims may contain inclusions from the matrix at their border. Some of the garnets have pressure shadows composed of biotite and chlorite. Fine, dispersed opacitic dust (leukoxene and hematite) is always present as elongated seams parallel to Sm, concentrated in micaceous-chloritic layers. The polycrystalline quartzitic microlayers and lenses (up to 0.6 mm in width) are mainly monomineralic (Fig. 3b); they rarely contain feldspar porphyroclasts and single, dispersed sericite flakes or an anastomozing micaceous film.

Bulk rock chemistry

Ultramylonites are represented by samples from 69.0, 70.4 and 70.6 m. Differences in bulk rock chemistry can be attributed to different matrix porphyroclast ratios in different layers (Table 1).

Mineral chemistry

The compositions of plagioclase from samples 69.0 m, 70.4 m and 70.6 m are given in Table 2. They are transitional between oligoclase and andesine with ca. 30% An and <1% Or. The K-feldspar contains 2–3% Ab and is lacking in An. As no variations in the chemistry of plagioclase and K-feldspar could be demonstrated as zoning within the porphyroclasts on one hand, or between porphyroclasts and the fine-grained matrix at the other, the assumption that feldspar porphyroclasts were completely re-equilibrated during the shear-related metamorphism seems to be a reasonable explanation. Together with the matrix

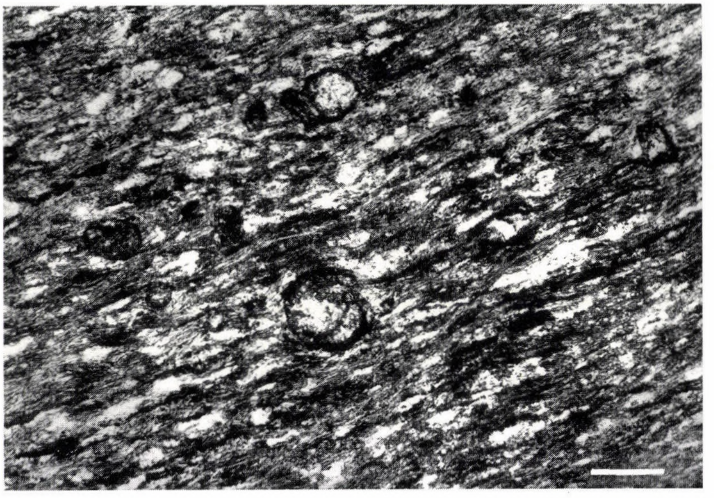

Fig. 3a, b: Photomicrographs of ultramylonite from borehole Mő-csény-I: (plane polarized light). a) 68.8 m: garnet crystal with euhedral rim in ultramylonite (bar scale 0.25 mm)

b) 70.1 m: quartz ribbons in ultramylonite (bar scale: 1 mm).

feldspars, the garnet rim, biotite, chlorite, hematite and quartz they make up an equilibrium assemblage.

The chemistry of chlorite from ultramylonite (sample 70.4 m) corresponds to ripidolite (Table 3), using the chlorite nomenclature of Foster (1962). Chlorite is frequently associated with small-grained biotite and other, matrix-forming minerals suggesting an equilibrium assemblage rather than an alteration product.

According to microtextural features flakes of biotite in the matrix formed during the shear-related metamorphism. Its chemical composition is rather homogeneous (Table 3).

The chemistry of garnets from ultramylonite was studied in detail (Table 4). As seen in Fig. 4 the garnet grains of several ten μm diameter display composite chemical zoning that indicates their polyphase evolution. BSE and composition pictures prove that most of the garnet grains consist of anhedral, fractured, splintery cores (usually rich in Ca and poor in Mn) overgrown by a new idioblastic generation of garnet showing contrasting chemistry (Ca-poor and Mn-rich, as compared to the core), and compositional growth zoning.

he composition of the cores is strongly variable (Prp = 5.1–13.4%, Alm = 45.6–58.5%, Sps = 2.5–39.7% and Grs = 9.6–29.3%). Thus, these cores may represent fragments originated from various parts of strongly zoned garnet porphyroblasts of the precursor gneiss. The cores were not re-equilibrated during the shear-related metamorphism.

Table 1
Bulk rock major element chemical compositions of ultramylonite (weight-%)

sample	69.0 m	70.4 m	70.6 m
SiO_2	59.22	56.68	60.36
TiO_2	0.81	0.90	0.80
Al_2O_3	16.51	17.18	16.07
Fe_2O_3	2.33	3.69	2.70
FeO	4.57	3.52	3.99
MnO	0.14	0.15	0.16
MgO	3.80	3.99	3.80
CaO	1.82	0.95	1.45
Na_2O	2.72	3.19	2.62
K_2O	2.22	0.95	1.88
^-H_2O	0.55	1.28	0.73
^+H_2O	4.39	6.32	4.91
CO_2	<0.05	<0.05	<0.05
P_2O_5	0.17	0.22	0.18
total	99.25	99.02	99.65

The compositional growth zoning in the newly formed, outer parts of the garnet crystals displays certain regularity: the shape of the zones can be related to crystal faces. In contrast to the cores the composition of the rims is rather homogeneous, indicating equilibrium conditions (Prp = 4.8–5.1%; Alm = 43–44.1%; Sps = 32.4–34.2%; Grs = 17.6–19.8%). The transitional growth zone (between the core and the rim) differs in its somewhat lower Ca and higher Mn content from the rim. It is worth mentioning that in addition to overgrowths the chemistry of garnet clasts was also changed along micro-cracks (see Figs 4c and 4f) as evidenced by very small-scale Mn diffusion into the clasts along the cracks. At the rims of the grains other minerals, mainly quartz grains, were partially or completely incorporated (irregular grain boundaries).

P-T conditions of the shear-related metamorphism

Thermobarometric data on shear-related equilibrium mineral assemblages proved by microstructural and mineral chemical criteria were estimated using the mineral reactions given by Bucher and Frey (1994) for metapelite and were also calculated using the TWEEQU 1.02 program of Berman (1991).

No exact data are available for the P-T conditions of the precursor garnet-bearing biotite-muscovite-K-feldspar-plagioclase gneiss. On the basis of higher Prp and lower Alm contents of the cores (as compared to the outer zones) amphibolite facies conditions can be supposed.

Considering the assemblage of ultramylonites (samples 69.0 m, 70.4 m and 70.6 m) containing Mn-rich garnet, biotite, plagioclase, K-feldspar, chlorite, quartz and

Table 2
Average compositions of feldspars

	plagioclase			K-feldspar		
Sample	69.0 m	70.4 m	70.6 m	69.0 m	70.4 m	70.6 m
n	*4*	*3*	*4*	*2*	*3*	*3*
SiO_2	59.94	59.89	59.87	64.30	63.19	63.51
Al_2O_3	26.22	26.25	25.94	19.56	19.69	19.36
CaO	6.09	6.84	6.08	0.01	0.00	0.01
Na_2O	7.85	7.79	7.47	0.23	0.27	0.28
K_2O	0.10	0.11	0.11	14.27	14.11	15.07
Total	100.20	100.88	99.47	98.37	97.26	98.23
		Number of cations per 8 oxygens				
Si	2.66	2.64	2.67	2.98	2.96	2.96
Al	1.37	1.37	1.36	1.07	1.09	1.06
Ca	0.29	0.32	0.29	0.00	0.00	0.00
Na	0.67	0.67	0.64	0.02	0.03	0.03
K	0.01	0.01	0.01	0.84	0.84	0.90
Total	5.00	5.01	4.97	4.91	4.92	4.95
An	29.9	32.5	30.9	0.0	0.0	0.1
Ab	69.5	66.9	68.5	2.4	2.8	2.7
Or	0.6	0.6	0.6	97.6	97.2	97.2

n = number of measurements

hematite, the temperature climax may be put at around 450 °C (see Bucher and Frey 1994) on the basis of the first appearance of garnet and the lack of staurolite. This estimate is in agreement with the TWEEQU calculations that yield 445–448 °C and 5.70–6.28 kbar for the association of the ultramylonites (Table 5), implying a medium (Barrovian type) pressure range. Although the transitional growth zone of the garnet was not in equilibrium with the matrix assemblage of the ultramylonites the calculations using the chemistry of garnet transitional zones gave similar T, but somewhat lower (ca. 5 kbar) P, suggesting that the growth of the garnet rim may have proceeded in quasi-isothermal conditions characterized by increasing pressure. According to Bucher and Frey (1994) the chlorite+K-feldspar assemblage may be stable below ca. 500 °C, producing annite, muscovite and quartz depending on the Fe/Mg ratio between 420 and 460 °C. If chlorite and biotite are in equilibrium, the XFe of biotite is higher than that of the chlorite, which is the case for the ultramylonite samples investigated. The muscovite formed in this way may have been used for producing garnet and biotite according to the reaction of 1Ms+3Chl+3Qtz=4Alm+1Ann+12H_2O (see Bucher and Frey 1994).

According to Árkai and Nagy (1994) the mylonitization of high-T greenschist-facies / low T amphibolite-facies amphibolites was accompanied by prograde recrystallization, as proved by chemical zoning of amphibole porphyroclasts and newly formed amphibole and plagioclase matrix grains. The shear-related metamorphism reached its climax at ca 580 °C and 4 kbar. Comparing these results to those of the present study it is obvious that various P-T conditions were operating in different parts of the shear zone.

Table 3
Average compositions of biotite and chlorite

Sample	biotite			chlorite
	69.0 m	70.4 m	70.6 m	70.4 m
n	*3*	*3*	*5*	*2*
SiO_2	35.56	36.73	34.81	26.38
TiO_2	1.86	1.67	1.49	0.08
Al_2O_3	20.41	20.26	19.86	22.65
FeO	16.57	15.78	16.58	21.40
MnO	0.26	0.27	0.30	0.48
MgO	10.68	10.82	10.98	17.89
CaO	0.14	0.21	0.12	0.07
Na_2O	0.03	0.01	0.03	0.01
K_2O	7.89	6.33	7.29	0.02
Total	93.40	92.09	91.45	88.95
	Number of cations per 22 oxygens			28 oxygens
Si	5.39	5.55	5.38	5.35
Al^{iv}	2.61	2.45	2.62	2.65
Al^{vi}	1.03	1.16	1.00	2.77
Ti	0.21	0.19	0.17	0.01
Fe	2.10	2.00	2.15	3.63
Mn	0.03	0.03	0.04	0.08
Mg	2.41	2.44	2.53	5.41
Ca	0.02	0.04	0.02	0.01
Na	0.01	0.00	0.01	0.00
K	1.53	1.22	1.44	0.00
Total	15.34	15.08	15.36	19.91

n = number of measurements

Fig. 4 a–h →
Back-scattered electron (BSE) images from, and distribution of Ca and Mn, in sample 70.6 m. (a): Microstructure of ultramylonite with fractured garnet (center) and quartz and plagioclase clasts (upper part) in the fine-grained, foliated matrix composed of biotite, chlorite, quartz, plagioclase and K-feldspar. The white bar on the right corresponds to 100 μm (BSE image); (b): anhedral, splintery garnet porphyroclast (central, medium-gray part) with post-tectonic, zoned, euhedral garnet overgrowth (light-gray rim). Note the sharp difference in composition between core and rim (BSE image); (c): distributions of Mn and (d) of Ca in the garnet grain of picture b; (e): overgrowth of zoned, euhedral garnet around an elongated, fractured garnet clast (BSE image); (f): Mn in garnet e. Note the enrichment of Mn not only in the outer part but also along a thin crack traversing the elongated clast (inner, dark part); (g): Ca in garnet e. The Ca-rich clast is surrounded by a Ca-poor transitional zone; (h): euhedral, post-tectonic overgrowth zones around an anhedral garnet clast. Note that near the rim of the garnet, quartz and other grains are partially or completely incorporated; see also the rims of grains b and e (BSE image). The white bar on the right of Figures b – h corresponds to 10 μm.

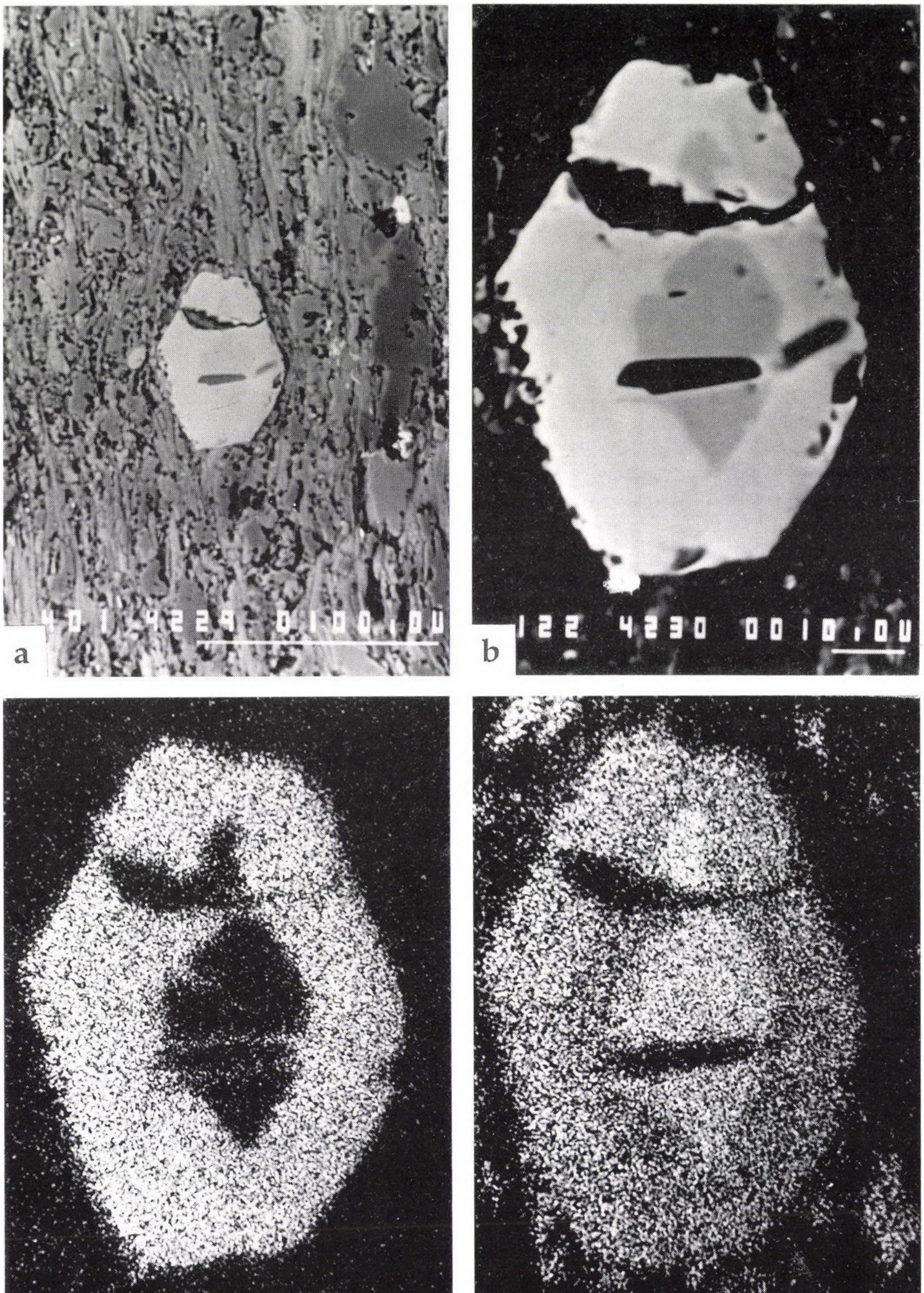
a
b
c
d

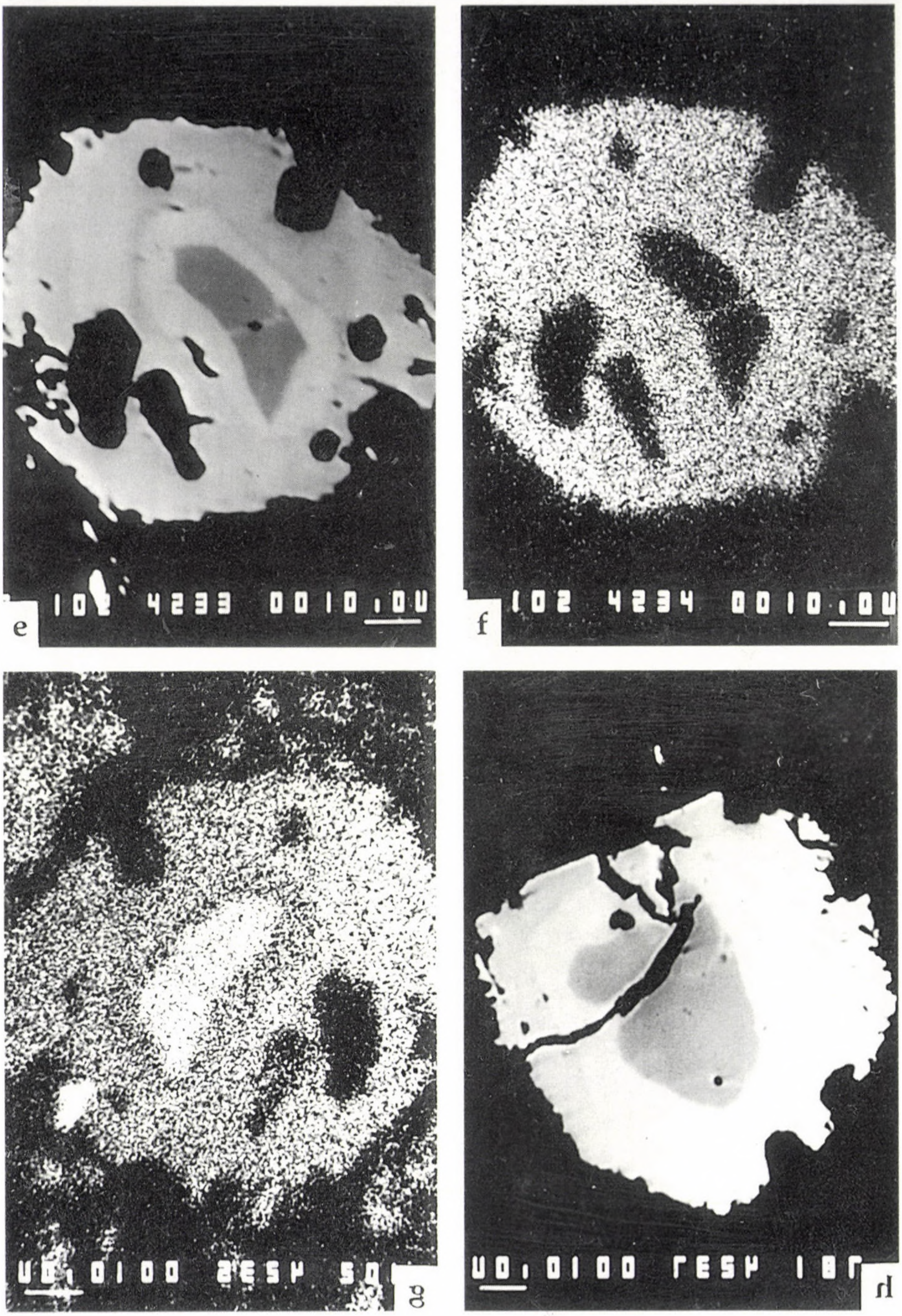
e
f
g
h

Table 4
Average compositions of garnet

Sample	69.0 m			70.4 m		70.6 m		
Grain part	core	transitional	rim	core	rim	core	transitional	rim
n	*2*	*2*	*2*	*2*	*5*	*6*	*11*	*7*
SiO_2	36.14	35.11	37.01	37.13	37.77	37.87	36.95	37.47
TiO_2	0.04	0.13	0.14	0.07	0.15	0.11	0.07	0.11
Al_2O_3	21.24	20.68	20.85	21.20	21.51	21.45	21.06	21.16
FeO	24.07	18.89	18.81	19.45	18.88	26.91	19.02	19.48
MnO	3.94	16.09	13.97	16.71	14.79	1.12	16.02	14.50
MgO	3.41	1.16	1.17	1.22	1.18	2.50	1.16	1.27
CaO	8.83	4.59	6.73	3.20	6.10	10.53	4.70	6.08
Total	97.65	96.68	98.67	98.96	100.38	100.48	98.98	100.07
	Number of cations per 24 oxygens							
Si	5.87	5.89	6.02	6.04	6.03	5.97	6.01	6.01
Ti	0.01	0.02	0.02	0.01	0.02	0.01	0.01	0.01
Al	4.06	4.09	4.00	4.07	4.05	3.99	4.04	4.01
Fe	3.27	2.65	2.56	2.65	2.52	3.55	2.59	2.62
Mn	0.54	2.29	1.92	2.30	2.00	0.15	2.21	1.97
Mg	0.83	0.29	0.28	0.30	0.28	0.59	0.28	0.30
Ca	1.54	0.83	1.17	0.56	1.04	1.78	0.82	1.05
Total	16.12	16.06	15.97	15.93	15.94	16.04	15.96	15.97
Prp	13.4	4.8	4.8	5.1	4.8	9.7	4.8	5.1
Alm	52.9	43.8	43.0	45.6	43.1	58.5	43.9	44.1
Sps	8.8	37.8	32.4	39.7	34.2	2.5	37.4	33.2
Grs	24.9	13.7	19.8	9.6	17.9	29.3	13.9	17.6

n = number of measurements
Prp=pyrope, Alm=almandine, Sps=spessartine, Grs=grossularite, all in mol-%

Geothermometric and -barometric data calculated by the TWEEQU program of Berman (1991)

sample	69.0 m		70.4 m		70.6 m		number of independent reactions
mineral assemblage/ P, T	P	T	P	T	P	T	
Grt(r), Bt, Pl, Kfs, Chl, Qtz, Hem	6.28±0.53	445±13	5.70±0.01	446±0	6.01±0.42	448±10	(3)
Grt(t), Bt, Pl, Kfs, Chl, Qtz, Hem	5.08±0.11	442±1	-	-	5.09±0.12	443±1	(3)

Legend: T in °C and P in kbars; Grt – garnet; (r) – rim; (t) – trtansitional zone; Bt-biotite; Pl – plagioclase; Kfs – K-feldspar, Chl – chlorite; Qtz – quartz; Hem – hematite

The thermodynamic data of Berman (1988, 1990) and the solid solution models of Fuhrman and Lindsley (1988) for plagioclase, McMullin et al. (1991) and Ferry and Spear (1978) and Chatterjee and Froese (1975) for micas were applied

Geochronology

Due to the fine grain size of the ultramylonite (70.5 m) no pure mineral concentrate could be separated. Therefore three different grain size fractions were investigated by the $^{40}Ar/^{39}Ar$ step heating method: a whole rock sample (0.2–0.4 mm), a 6–11 μm and a 2–6 μm fraction obtained by sedimentation. Due to the different mineralogy and individual grain size of the constituents the results of the different grain size fractions differ distinctly. The whole rock sample supplied the most consistent age information (Fig. 5a). The first third of the diagram yielded Permian ages of about 270 Ma. Consistent ages of 303 Ma were obtained between 860 and 1020 °C. According to the K/Ca ratio these ages should be mainly correlated with the breakdown of the coarse biotite in the mylonite.

Saddle-shaped spectra of Permian to lowermost Triassic ages were obtained from the fine fractions of 6–11 μm and 2–6μm (Figs 5b, c). The low-temperature portion of the diagram seems to represent the Ar content from fine-grained, biotite-dominated fractions, which yielded similar Permian ages as the low-temperature part of the whole rock sample. The saddle-shaped portion of the diagram with ages down to 220 Ma is obviously caused by a higher amount of feldspars in these fine fractions, which due to their small grain size and sericitization exhibit a more pronounced Ar loss than the whole rock sample.

Mőcsény-I, 70.5 m; ultramylonite, whole rock

J = 0.005108 ± 0.4%

Step	T[°C]	%39	40*	%rad	39/37	%36Ca	40*/39	age
1	580	7.6%	569.58 mV	95.5%	15	0.53%	27.71 ± 0.7%	249.6 ± 1.7
2	610	4.7%	388.24 mV	97.1%	16	0.70%	30.37 ± 0.4%	271.8 ± 1.0
3	640	4.8%	397.97 mV	97.4%	15	0.84%	30.69 ± 0.5%	274.5 ± 1.2
4	680	4.7%	376.36 mV	97.4%	13	0.97%	29.61 ± 0.5%	265.5 ± 1.3
5	730	4.9%	392.24 mV	97.6%	12	1.19%	29.49 ± 0.6%	264.5 ± 1.5
6	790	4.9%	420.33 mV	97.8%	12	1.19%	31.60 ± 0.6%	282.1 ± 1.6
7	860	29.3%	2706.15 mV	98.7%	21	1.17%	34.12 ± 0.5%	302.8 ± 1.3
8	1020	29.3%	2721.06 mV	98.9%	20	1.38%	34.31 ± 0.2%	304.4 ± 0.5
9	1100	6.2%	530.95 mV	97.9%	5	2.98%	31.38 ± 0.4%	280.3 ± 1.1
10	1250	3.5%	323.98 mV	94.3%	6	0.86%	33.89 ± 0.9%	300.9 ± 2.5
							total gas age:	**290.3 ± 2.5**

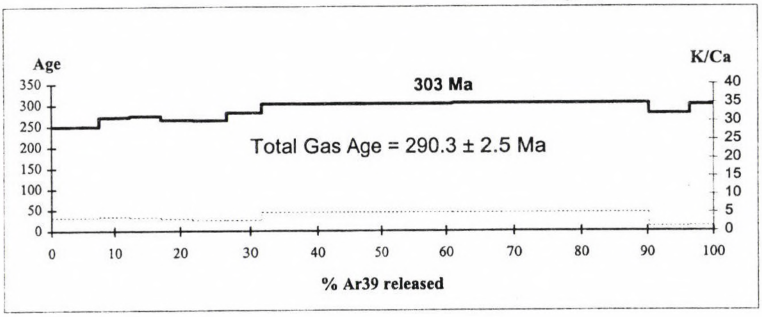

Mőcsény-I, 70.5 m; 2-6 µ, ultramylonite

J = 0.005108 ± 0.4%

Step	T[°C]	%39	40*	%rad	39/37	%36Ca	40*/39	age
1	580	25.0%	798.66 mV	94.8%	10	0.62%	30.48 ± 0.3%	272.8 ± 0.7
2	610	18.4%	569.25 mV	96.9%	10	1.14%	29.56 ± 0.4%	265.1 ± 0.9
3	640	13.6%	384.43 mV	97.3%	8	1.82%	26.93 ± 0.4%	242.9 ± 1.0
4	680	11.5%	305.22 mV	97.2%	6	2.42%	25.43 ± 0.5%	230.2 ± 1.1
5	730	8.9%	228.75 mV	95.2%	4	1.89%	24.42 ± 0.6%	221.6 ± 1.3
6	790	6.7%	178.17 mV	91.4%	4	1.00%	25.41 ± 1.3%	230.0 ± 2.8
7	860	5.8%	194.82 mV	91.0%	5	0.69%	32.05 ± 2.1%	285.8 ± 5.6
8	1020	9.6%	332.44 mV	94.6%	5	1.10%	33.14 ± 0.7%	294.8 ± 1.8
9	1120	0.5%	9.11 mV	80.9%	2	1.31%	18.88 ± 14.8%	173.6 ± 24.5
							total gas age:	**257.4 ± 3.1**
						100%	**'plateau age:**	**257.4 ± 3.1**

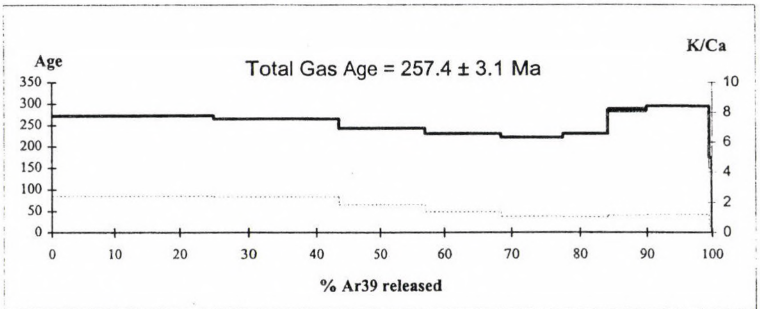

Fig. 5 a – c
$^{40}Ar/^{39}Ar$ release spectra of whole rock sample (a) and mica concentrates 2–6 µm and 6–11 µm (b–c) from ultramylonite from borehole Mőcsény-I 70.5 m

Mőcsény-I, 70.5 m; 6-11 μ, ultramylonite

J = 0.005108 ± 0.4%

Step	T[°C]	%39	40*	%rad	39/37	%36Ca	40*/39	age
1	580	4.1%	40.70 mV	95.2%	11	0.70%	26.63 ± 4.4%	240.4 ± 9.9
2	610	8.3%	85.58 mV	96.4%	10	0.94%	27.80 ± 1.8%	250.3 ± 4.3
3	640	12.9%	135.15 mV	97.1%	9	1.39%	28.31 ± 1.6%	254.6 ± 3.9
4	680	15.8%	153.01 mV	96.8%	6	1.89%	26.23 ± 1.5%	237.0 ± 3.3
5	730	15.5%	135.90 mV	95.4%	4	2.06%	23.74 ± 0.6%	215.7 ± 1.2
6	790	11.8%	108.06 mV	92.4%	4	1.32%	24.90 ± 1.5%	225.7 ± 3.2
7	860	9.6%	102.16 mV	91.4%	4	0.91%	28.85 ± 1.4%	259.1 ± 3.4
8	1020	19.9%	229.95 mV	95.3%	5	1.24%	31.28 ± 0.8%	279.4 ± 2.2
9	1100	2.0%	24.34 mV	93.6%	1	4.41%	33.70 ± 2.5%	299.4 ± 6.8
							total gas age:	**247.7 ± 4.8**
						100%	**'plateau age:**	**247.7 ± 4.8**

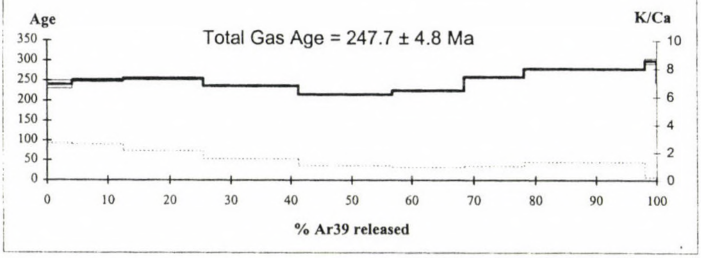

303 Ma may represent the cooling age for the biotite-dominated whole rock sample. However, as a uniform incorporation of excess Ar in biotite is a very common feature, especially in mylonitized rocks, this date should be considered as a maximum cooling age. The minimum age of the mylonitization is considered to be not younger than approximately 270 Ma. Younger ages of individual steps are interpreted as effects of alterations and Ar loss due to the small grain size in the feldspar-dominated samples.

Conclusions

In the Mórágy Hills a regional, steeply dipping shear zone developed, which traverses the porphyric Mórágy Granitoid and the Ófalu regional metamorphic series, producing a great variety of sheared rocks. They had been frequently misinterpreted and their importance had been underestimated in the majority of the earlier publications.

In case of mylonitic rocks derived from serpentinite, amphibolite and marbles the original lithologies can easily be recognized. On the other hand, the shearing of the Mórágy Granitoid and gneisses of the Ófalu regional metamorphic series resulted in very similar rock types: quartz-feldspar-biotite mylonites to ultramylonites, rendering difficult the differentiation of their precursor rock. From the banded ultramylonites encountered by borehole Mőcsény-I a reconstruction was possible: they contain garnet porphyroclasts in a very fine-grained biotite matrix. The varying chemical composition of the splintery cores of garnet porphyroclasts indicates a precursor rock containing strongly zoned garnet crystals. Their compositions reflect amphibolite facies conditions. The crystallization of the rims during ultramylonite generation took place at ca. 450 °C, with pressure conditions attaining ca. 5.7–6.3 kbar.

The regional geologic setting indicates that this Ófalu Shear Zone is of regional importance, since it separates very contrasting lithological units with different metamorphic grades in the basement. According to $^{40}Ar/^{39}Ar$ analyses of banded ultramylonite this shearing event took place between 303 Ma (maximum age) and 270 Ma. This time interval can be very well correlated with the regional framework, namely the formation of Late Variscan sedimentary basins.

Acknowledgements

The authors are indebted to the Hungarian Geological Institute for providing the borehole samples. The present work forms part of metamorphic petrological research programs Nos. T 023940 (Gy L-F) and T 022773 (P. Á) (1997–2000) sponsored by the Hungarian Scientific Research Fund (OTKA), Budapest. Thanks are due to Mr. Z. Wieszt and Mrs. V. Varga (Laboratory for Geochemical Research Hungarian Academy of Sciences) for major element bulk chemical analyses.

References

Árkai, P. 1984: Polymetamorphism of the crystalline basement of the Somogy-Drava Basin (Southwestern Transdanubia, Hungary). – Acta Miner. Petr. Szeged., 26, pp. 129–153.

Árkai, P. 1990: Very low- and low-grade metamorphic rocks in the pre-Tertiary basement of the Drava basin, SW Hungary: mineral assemblages, illite crystallinity, b_0 data, and problems of geological correlation. – Acta Geol. Hung., 33, pp. 43–67.

Árkai, P. 1991: Alpine regional metamorphism of the different tectonic domains in the Hungarian part of the Pannonian Basin. – In: Baud, A., P. Thélin, G. Stampfli (Eds): Paleozoic geodynamic domains and their alpidic evolution in the Tethys. IGCP Project No. 276 Newsletter No. 2. Mémoires de Géologie (Lausanne) 10, pp. 5–13.

Árkai, P., A. Bérczi-Makk, D. Hajdu 1998: Alpine prograde and retrograde metamorphisms in an overthrusted part of the basement, Great Plain, Pannonian Basin, Eastern Hungary. – Acta Geol. Hung. 41, pp. 179–210.

Árkai, P., Gy. Lelkes-Felvári, Cs. Lantai, G. Nagy 1995: Biotite in a Paleozoic metagreywacke complex, Mecsek Mountains, Hungary: conditions of low-T metamorphism deduced from illite and chlorite crystallinity, coal rank, white mica geobarometric and microstructural data. – Acta Geol. Hung. 38, pp. 293–318.

Árkai, P., G. Nagy 1994: Tectonic and magmatic effects on amphibole chemistry in mylonitized amphibolites and amphibole-bearing enclaves associated with granitoid rocks, Mecsek Mountains, Hungary. – Acta Geol. Hung. 37, pp. 235–268.

Árkai, P., G. Nagy, G. Dobosi 1985: Polymetamorphic evolution of the South-Hungarian crystalline basement, Pannonian Basin: geothermometric and geobarometric data. – Acta Geol. Hung. 28, pp. 165–190.

Balla, Z. 1988: On the origin of the structural pattern of Hungary. – Acta Geol. Hung. 31, pp. 53–63.

Balogh, K., E. Árva-Sós, Gy. Buda 1983: Chronology of granitoid and metamorphic rocks of Transdanubia, Hungary. – Anuarul Institutului de geol. si geofiz, 61, pp. 359–364, Bucharest.

Balogh, K., Á. Kovách, Z. Pécskay, É. Svingor, P. Árkai. 1990: Very low- and low-grade metamorphic rocks in the pre-Tertiary basement of the Drava Basin, SW-Hungary, II: K-Ar and Rb-Sr isotope geochronologic data. – Acta Geol. Hung., 33, pp. 67–76.

Bence, A.E., A. Albee 1968: Empirical correction factors for electron microanalysis of silicates and oxydes. – J. Geol. 76, pp. 382–403.

Berman, R.G. 1988: Internally-consistent thermodynamic data for stoichiometric minerals in the System Na_2O–K_2O–CaO–MgO–FeO–Fe_2O_3–Al_2O_3–TiO_2–HH_2O–CO_2. – J. Petrol. 29. pp. 445–522.

Berman, R. G. 1990: Mixing properties of Ca–Mg–Fe–Mn garnets. – Amer. Mineralogist 75, pp. 328–344.

Berman, R. G. 1991: Thermobarometry using multiequilibrium calculations: a new technique with petrologic applications. – Can. Mineral. 29, pp. 833–885.

Buda, Gy. 1985: Origin of collision-type Variscan granitoids as exemplified by the granitoids of Hungary, the Western Carpathians and the Central Bohemian Massif. – C. Sc. Thesis, Budapest. (In Hung.)

Buda, Gy. 1996: Correlation of Variscan granitoids occurring in Central Europe. – Acta Min. Petr. Szeged, 37, Suppl. p. 24.

Buda, Gy., Gy. Lovas, U. Klötzli, B.L. Cousens 1999: Variscan granitoids of the Mórágy Hills (South Hungary). – Beih. z. Eur. J. Mineral. No. 2, 11, pp. 21–32

Bucher, K., M. Frey 1994: Petrogenesis of Metamorphic rocks. – Springer, Berlin.

Chatterjee, N.D., E.F. Froese 1975: A thermodynamic study of the pseudobinary joint muscovite-paragonite in the system $KAlSi_3O_8$–$NaAlSi_3O_8$–Al_2O_3– SiO_2–H_2O. – Amer. Mineralogist, 60, pp. 985–993.

Ferry, J.M., F.S. Spear 1978: Experimental calibration of partitioning of Fe and Mg between biotite and garnet. – Contrib. Mineral. Petrol., 66, pp. 113–117.

Foster, M.D. 1962: Interpretation of the composition and a classification of the chlorites. – U. S. Geol. Surv. Prof. Paper, 414–A, pp. 1–33.

Fuhrman, M.L., D.H. Lindsley 1988: Ternary-feldspar modeling and thermometry. – Amer. Mineralogist 73, pp. 201–216.

Frimmel, H.E., W. Frank 1998: Neoproterozoic tectono-thermal evolution of the Gariep belt and its basement, Namibia and South Africa. – Precambrian Research 90, pp. 1–28.

Géczy, B. 1973: The origin of the Jurassic faunal provinces and the Mediterranean plate tectonics. – Ann. Univ. Sci. Budapest R. Eötvös Nom. Sect. Geol., 16, pp. 99–114.

Ghanem, M.A., L. Ravasz-Baranyai 1969: Petrographic study of the crystalline basement rocks, Mecsek Mountains, Hungary. – Acta Geol. Acad. Sci. Hung., 13, pp. 191–219.

Ghoneim, M.F., T. Szederkényi 1977: Preliminary petrological and geochemical studies of the area Ófalu, Mecsek Mountains, Hungary. – Acta Miner. Petr. Szeged, 23, pp. 15–28.

Haas, J., G. Császár, S. Kovács, A. Vörös 1990: Evolution of the western part of the Tethys as reflected by the geological formations of Hungary. – Acta Geod. Geoph. Mont. Hung., 25, pp. 25–344.

Jantsky, B. 1953: A mecseki kristályos alaphegység földtani viszonyai (Geologic conditions of the Mecsek crystalline substratum). – MÁFI Évi Jel. 1950, pp. 65–77.

Jantsky, B. 1979: Géologie du socle cristallin granitisé de la montagne Mecsek. – Annales Hung. Geol. Inst., 60, pp. 1–385.

Kázmér, M., S. Kovács 1985: Permian–Paleogene paleogeography along the Eastern part of the Insubric–Periadriatic lineament system: evidence for the continental escape of the Bakony–Drauzug Unit. – Acta Geol. Hung., 28, pp. 71– 84.

Kovács, S. 1982: Problems of the "Pannonian Median Massif" and the plate tectonic concept. Contributions based on the distribution of Late Paleozoic–Early Mesozoic isopic zones. – Geol. Rundschau, 71, pp. 617–640.

Kretz, R. 1983: Symbols for rock-forming minerals. – Amer. Mineralogist, 68, pp. 277–279.

Lelkes-Felvári, Gy., F.P. Sassi 1981: Outlines of the pre-Alpine metamorphism in Hungary. – In: Karamata S., F.P. Sassi (Eds): IGCP Project No. 5. Newsletter No. 3, pp. 89–99.
McMullin, D., R.G. Berman, H.J. Greenwood 1991: Calibration of the SGAM thermobarometer for pelitic rocks using data from phase equilibrium experiments and natural assemblages. – Can. Mineral. 29, pp. 889–908.
Nagy, G. 1984: Computer programs for quantitative electron microprobe analysis developed for geological applications. – EUREM 84: Proc. 8th Eur. Congr. on Electron Microscopy, Budapest, pp. 1041–1042.
Nagy, G. 1990: Quantitative analysis by electron microprobe: Methods and applications in the Laboratory for Geochemical Research (in Hung). – Izotóptechnika, Diagnosztika 33, pp. 133–139.
Svingor, É., Á. Kovách 1981: Rb–Sr isotopic studies on granodioritic rocks from the Mecsek Mountains, Hungary. – Acta Geol. Hung., 24, pp. 295–307.
Szádeczky-Kardoss, E., Á. Juhász, E. Balázs 1969: Erläuterung zur Karte der Metamorphiten von Ungarn. – Acta Geol. Acad. Sci. Hung., 13, pp. 27–34.
Szederkényi, T. 1975: Rare element research of the Early Paleozoic formations in SW-Transdanubia. – C. Sc. Thesis, Budapest, (in Hungarian)
Szederkényi, T. 1977: Geological evolution of South Transdanubia (Hungary) in Paleozoic time. – Acta Min.-Petr., Szeged, 23, pp. 3–14.
Szederkényi, T. 1984: Crystalline basement of the Great Hungarian Plain and its geological connections. – D. Sc. Thesis, Budapest (in Hungarian)
Szederkényi, T., P. Árkai, Gy. Lelkes-Felvári 1991: Crystalline basement of the Great Hungarian Plain and South Transdanubia, Hungary. – In: Karamata S. (Ed.): Geodynamic evolution of the Pannonian Basin. – Serb. Acad. Sci. Arts Acad. Conf., 62, Dept. Nat. and Math. Sci., 4, pp. 261–273, Beograd.

Acta Geologica Hungarica, Vol. 43/1, pp. 85–106 (2000)

Results of the modern depositional process and hydrogeologic investigations in Szigetköz, Hungary

Operation of a geologic monitoring system by the Geological Institute of Hungary

Péter Scharek, György Don
Geological Institute of Hungary, Budapest

István Horváth, György Tóth
Geological Institute of Hungary, Budapest

Human intervention into the Hungarian upper reach of the Danube modified and still modifies the flow velocity and quality of surface water as well as the state of channels. In reaches where surface water recharges groundwater these changes can be traced in wells and soundings placed as near to the active riverbed as possible. Contracted by the Ministry for Environment and Regional Policy, the Geological Institute of Hungary has been performing regular geologic monitoring since 1994 in the area of the Danube between Rajka and Sap. It is aimed at documenting the relationship between the surface and groundwater along the affected reach, as well as determining their connection with geologic formations. The results of regular (seasonal) sampling provided us with data on temporal and spatial distribution of the most important changes (relationship between the groundwater and overburden, effect of diversion and the underwater weir, etc.). These results have been made available for decision-makers and representatives of other scientific disciplines. By summarizing geologic data in a uniform system we started with building a geologic information system.

Keywords: Danube, Szigetköz, actual geology, monitoring, hydrogeology

Geologic setting of Szigetköz

History of geologic and geophysical evaluation

As elsewhere in the country the detailed geologic survey of Szigetköz (the largest island of the Danube in the northwestern part of Hungary) and its surroundings began in the sixties of the last century. At that time 1:28 800-scale maps were prepared, serving as a basis for the compilation of the 1:144 000 manuscript geologic map of Transdanubia in the Geological Institute of Hungary that provided a detailed description even of lowland areas. L. Róth, E. Pávai, K. Hoffmann, J. Böckh and I. Stürzenbaum carried out this project.

The end of the century marks the beginning of pedological and agrogeologic mapping in Hungary led by H. Horusitzky, G. László and I. Timkó. Upon results furnished by the 1st Agrogeological Congress held in 1909, P. Treitz compiled in 1918 the pedological map of Hungary based on the conception of climatic zones and published with explanatory text following World War I.

Addresses: P. Scharek, Gy. Don, I. Horváth, Gy. Tóth: H-1143 Budapest, Stefánia u. 14, Hungary
Received: 11 June, 1999

Between the two World Wars geologic research in the Little Hungarian Plain and adjacent territories also received an impetus. Investigation of coarse clastic sediments was launched by E. Szádeczky-Kardoss, creating a tradition with his methodology. L. Kreybig initiated pedological mapping in this area that was not, however, finished before the fifties of this century, at the scale of 1:25 000. The 1:200 000 pedological map of Hungary compiled by P. Stefanovits and L. Szücs was accomplished by 1955.

The initiation and completion of detailed geologic mapping of lowland areas is the merit of J. Sümeghy. These 1:25 000-scale maps prepared by 1952 cover the major part of the area and they provided the only unified geologic data collection up to the start of our remapping.

At the end of the 1950s morphological and hydrological surveying, including the area of Szigetköz, received an impetus. In this respect the morphological research of S. Láng, L. Kárpáti, M. Pécsi, L. Góczán and L. Ádám, as well as the hydrogeologic activity of K. Ubell and A. Rónai, should be emphasized. Results of geophysical surveying were reported by J. Lányi and V. Scheffer. Within the framework of the 1:200 000 mapping of the entire country the remapping of the Győr sheet (including Szigetköz) ended in 1966, followed by its publication in print (F. Franyó et al. 1971).

Several comprehensive studies were prepared in association with this latter project. Quaternary deposits and tectonic features were described by F. Franyó and Gy. Wein, respectively. Deep-seated geologic structures were summarized for the first time by L. Kőrössy. Hydrogeologic investigations carried out recently in the Little Hungarian Plain were summarized by M. Erdélyi and K. Korim, supplemented by the study of ecological problems emerging in Szigetköz.

Within the framework of the map series representing geographical land units of Hungary, L. Ádám and S. Marosi published a geographic summary, followed by the morphological study of I. Göcsei on Szigetköz.

Recognizing the lack of proper geologic and hydrogeologic surveying in association with the Gabčikovo-Nagymaros dam system the Geological Institute of Hungary initiated a complex geologic mapping of the concerned region, as well as of the entire Little Hungarian Plain including Szigetköz, prompted by the resumption of construction in 1977 (Don et al. 1993).

Thickness and description of Quaternary deposits

In the eastern part of the concerned area the thickness of Quaternary deposits rarely surpasses 20 m. It allows us to offer a more precise picture of thickness characteristics there then in the interior of the basin. The base of Quaternary sediments breaks surface in the area between Győrszabadhegy and Bábolna. The subsidence of the pre-Quaternary basement N of this area up to the Danube cannot be determined precisely. A distinct tendency of sinking is exhibited in a northward-striking direction from Bábolna and Bana, undoubtedly brought about by the wandering of the Bakony brook in Quaternary time.

Simultaneously, Pannonian deposits are recovered by the lateral cutting of the Danube at Gönyű. Westward and northward from the line of the Rába and Moson-Danube rivers a sharp increase in thickness of Quaternary sediments can be noted, reaching its highest value in the surroundings of the villages of Sérfenyősziget and Püski, where it exceeds 700 m. According to our present knowledge it can be suggested that the Moson depression discovered during previous surveying is well divided into two parts. In order to elucidate stratification and lithological properties of Quaternary deposits, two structural exploratory drillings were carried out in the region by our Institute (at the villages of Arak, Arak-1; and of Tárnokréti, Trt-1).

Up to the present day the overall characteristic lack of fauna in coarse clastic sediments renders the lithological and chronostratigraphic classification of the thick Pleistocene-Holocene, principally also the coarse clastic fluvial sedimentary sequence of Szigetköz, virtually impossible. Although the comparative abundance in hydrogeologic exploratory boreholes furnishes some information on structural aspects of these sequences, core sampling bound to a limited number of intervals and a deficiency in data provided by surface geophysical measurements, inhibit a precise stratigraphic interpretation.

The structural exploratory well at Arak drilled within the framework of the Little Hungarian Plain Project with continuous core sampling, reached the base of Quaternary deposits at a depth of 358.0 m. It was stopped in Upper Pannonian formations, 400.0 m below the surface. This drilling brought some important results from stratigraphic point of view, since it revealed the existence of fine-grained horizons with irrelevant thicknesses as compared to that of the entire profile but enabled us to subdivide the coarse, clastic sequence (described so far as a homogeneous complex) by geophysical methods. These thin horizons shelter the remains of some vertebrates and mollusks preserved from mechanical deformation. They were deposited in a low-velocity, rather shallow fluvial environment subdividing the coarse clastic sequence into 10 levels.

The substantial lithological contrast allowed determining with high precision the thickness of coarse-grained sediments by geophysical methods even before the drilling at Arak. In conjunction with the information provided by this well the related lithological transition can simultaneously be interpreted as the Pleistocene-Pannonian boundary in intrabasinal areas. Additionally, on the basis of this well data, the presence of thicker Holocene sediments in Szigetköz can also be justified. Tracing layers of conglomerate and sandstone recovered at certain levels of this well proves to be difficult by geophysical methods, for they have not yet been encountered in any structural exploratory drilling. They cannot therefore be counted on for the time being for the lithological classification of Pleistocene complexes. We assume that they occur only locally and that they pinch out fairly rapidly, and thus presumably cannot be used for the subdivision of these sequences.

Hydrogeologic conditions in Szigetköz

The Little Hungarian Plain's wide-ranging Quaternary clastic complex, of considerable thickness can be referred to as the most important drinking-water reservoir to be found in Hungary. Groundwater constituting a strongly interrelated entity with other subsurface aquifer horizons communicates intensively with surface water bodies, like the Danube, Moson-Danube and Rábca rivers as well as the Hanság canal.

Studying the ground-water regime of the area became a priority from the early 1950s, begun with the establishment of 8 observation well series between Rajka and Győr for the carrying out of a preliminary study concerning the projected hydroelectric power plant. Initially, they were observed by VITUKI, presently they are recorded by Regional Water Management Offices. The series of data acquired from these observations constitutes a most valuable database concerning the groundwater level of the area.

Acceleration of the construction of the Gabčikovo power plant gave a new impetus for surveying, leading to the establishment of a denser grid of groundwater observation sites as well as to the drilling of wells, with several screened intervals, within the framework of the observation network of deep aquifer horizons. From the 1960s up to present several studies discussing the effects of the projected water barrage have been published. The Geological Institute of Hungary launched its mapping project in the area in 1982, including the implantation of new groundwater observation wells together with a well series for the investigation of relationships between deep subsurface aquifers and groundwater.

Hydrogeologic conditions in Szigetköz are essentially determined by the fact that Danube runs its course through the most elevated sequence of its own alluvial fan in a so-called hanging valley. Water filtrating into its gravel bed percolates in a south-southeastern direction and through the line of the Moson-Danube it reaches the belt of the Hanság canal and the Rábca river. Simultaneously, the baseline of water entering the NE bank of the Danube is represented by its northern by-channel extending to Csallóköz, in Slovakia.

Setting up the Geologic Monitoring System, methodology of investigation

The 1:100.000-scale investigation of Szigetköz began in 1982 within the framework of the detailed geologic mapping of the Little Hungarian Plain (Kisalföld). Geologic source maps were compiled at 1:25.000 scale, whereas final, summarized versions were printed at 1:100.000 and 1:200.000 scales in 1991 (map sheets Mosonmagyaróvár and Győr-Észak). Between 1982 and 1987, 364 shallow, no more than 10 m-deep boreholes were completed in a network with an average spacing of 1,000–1,500 m. They were supplemented by 24 boreholes of minor depth (<= 50 m) and one of intermediate depth (400 m). One part of the these 24 boreholes was completed as groundwater observation wells serving as the basis for the water level observation network of the Geological Institute of Hungary (MÁFI), established in Szigetköz. The Arak-1 intermediately deep borehole was also transformed to an observation well for both shallow and deep groundwater.

GIS processing and summary of geologic data (Scharek et al. 1994a) together with the modern depositional process study of sedimentation in river channels (Molnár 1991) already began during the final stage of investigation. The main objective of modern process investigation was the mapping of sedimentary and erosion processes occurring in the main channel and side-branches.

As a result of a contract from the Ministry for Environment and Regional Policy following the diversion of the Danube in 1992, the geologic investigation of Szigetköz gained new impetus. Descriptions of surface and basin sediments were published, also in English (Don et al. 1993), thus providing help for invited EU experts. As a result of the expert reports we were contracted to carry out further hydrogeologic and modern process investigations and to summarize the results in GIS format (Molnár 1994; Scharek et al. 1994, 1994a).

In 1995 we completed the observation network of the Geologic Monitoring System in Szigetköz, which was in operation until the end of 1998 (Horváth et al. 1995; Don et al. 1996; Horváth et al. 1997; Don et al. 1998).

Within the framework of Geologic Monitoring samples were taken in pairs, at first from 29, then (following financial restrictions in 1998) from 16 sites from surface and groundwater (recovered in soundings). Additional samples were collected from observed natural springs and new observation wells established in 1995 for tracing the effect of the underwater weir constructed in the same year (Fig. 1, Table 1).

The collected water samples were analyzed in situ and in MÁFI's laboratory for the following components:

In situ field analyses:

Hydrostatic groundwater level, water and air temperature, alkalinity, pH, electric conductivity, dissolved oxygen content.

Laboratory analyses of the in situ conserved samples:

Routine and ICP MS measurements were performed for the following components and elements:

Main components

pH, alkalinity, specific conductivity, temperature, total hardness, carbonate hardness

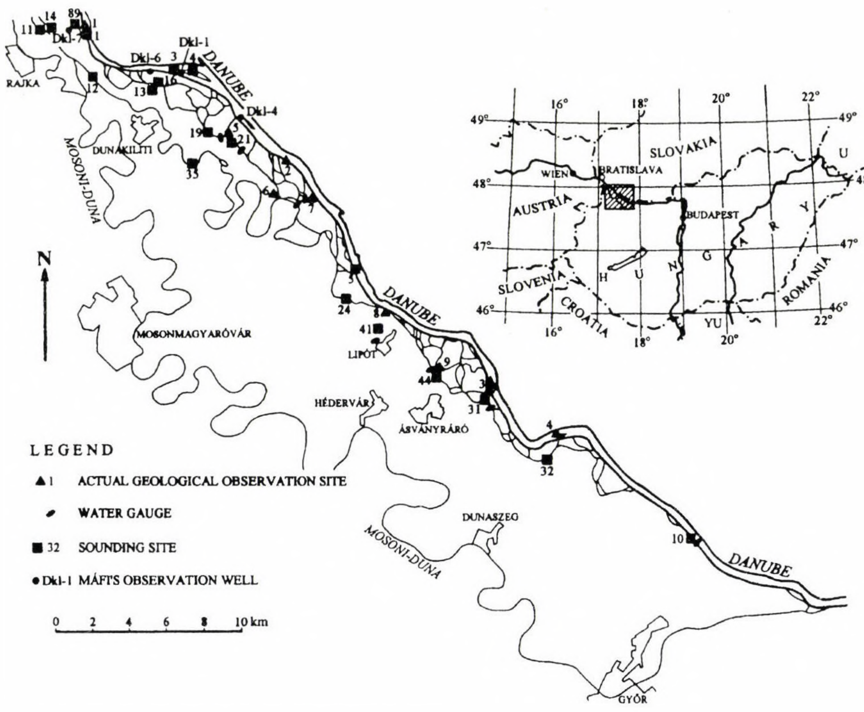

Fig. 1
Observation sites of the Geologic Monitoring (1998)

Determination of Na^{+}, K^{+}, Ca^{++}, Mg^{++}, Fe^{++}, Mn^{++}, NH^{+}, Cl^{-}, HCO_3^{-}, SO_4^{--}, NO_3^{--}, NO_2^{--}, PO_4^{--}, $H_2SiO_3^{-}$

Trace elements

Li, Be, B, Al, V, Cr, Mn, Co, Ni, Cu, Zn, As, As,H, Rb, Sr, Mn, Ag, Cd, Sb, Cs, Ba, La, Tl, Pb, Bi, Th, U

In 1997 and 1998 in co-operation with the experts of the Northern-Transdanubian Environmental Inspectorate's Measuring Station we collected a further 10 single samples for chemical and microbiological studies. They were analyzed in the Measuring Station's laboratory and the Győr-Moson-Sopron county branch of the National Public Health Care and Medical Officer Services (ÁNTSZ). The measurements concerned components specified in the Hungarian-Slovak cross-border river agreement. It provided an opportunity to compare the analyses of the same laboratory with the cross-border river data. Furthermore, the relationship between data of the specific laboratories could also be determined on the basis of samples taken from the same site at the same time and analyzed in MÁFI's laboratory.

Table 1
Position of the 1998 sampling sites

Sampling site	X (EOV)	Y (EOV)
Measuring of the influence of the Čunovo reservoir		
Dkl–7 well	298255	514660
MÁFI Sz–1 sounding site (1849 km)	297950	515570
Jónás-branch	298390	515050
Measuring of the influence of the Somorín reservoir		
Dkl–6 well	295880	518855
MÁFI Sz–16 sounding site	295300	519100
MÁFI Sz–4 sounding site (1842 km)	295950	521670
Measuring of the influence of the Danube between Rajka and Dunakiliti		
Dkl–1 well	295940	520585
MÁFI Sz–3 sounding site (1843.15 km)	295950	520540
Measuring of the influence of the Mosoni-Danube between Čunovo and Rajka		
MÁFI Sz–14 sounding site	298380	513540
Measuring of the influence of the water recharge system between Čunovo and Rajka		
MÁFI Sz–11 sounding site	298395	512840
Measuring of the influence of the water recharge system between Z3 and Z5 locks		
MÁFI Sz–12 sounding site	295790	515640
MÁFI Sz–13 sounding site	294600	518740
Measuring of the influence of the active floodplain between Dunakiliti and Cikolasziget		
MÁFI Sz–21 sounding site	292050	523640
Dkl–4 well	293255	524030
Measuring of the influence of the active floodplain between Cikolasziget and Dunaremete		
MÁFI Sz–24 sounding site (Mosó-Danube)	283540	529560
Measuring of the influence of the active floodplain between Ásványráró and Bagamér		
Spring under the B11 dam	278970	534575
MÁFI Sz–31 sounding site (Ásványi-Danube)	278120	537000
MÁFI Sz–32 sounding site (Bagoméri-Danube)	274600	540150
Measuring of the influence of the water recharge system between Dunakiliti and Dunasziget		
MÁFI Sz–35 sounding site (Zátonyi-Danube)	290700	521250
Measuring of the influence of the water recharge system downstream from Dunasziget		
MÁFI Sz–41 sounding site (oxbow at Lipót)	281760	531020
Measuring of the influence of the Danube between Dunakiliti and Sap		
MÁFI Sz–5 sounding site (1828 km)	285150	530080
Measuring of the influence of the Danube between Sap and Gönyű		
MÁFI Sz–10 sounding site (Nagybajcs)	270610	548345

Simultaneously with water sample collecting in sounding sites, regular observations of the character of sedimentation versus erosion in specific channel reaches in modern process observation sites also took place, together with sample taking and analyzing their sedimentary features.

In 1998 modern depositional/erosional process investigations were carried out at the following sites:

Main channel
1. 1850.0 km, Rajka
2. 1834.7 km, Cikolasziget
3. 1817.3 km, Ásványráró
4. 1812.3 km, Bagomér

Water recharge system of the active floodplain
5. Kormosi-Danube at the branching of the Doborgaz-cutoff
6. Görbe-Danube, 600 m upstream the Z3 lock
7. Denkpáli mouth
8. Mosó-Danube, 100 m downstream of the B8 cross-dyke
9. Halrekesztő-Danube, downstream of the B11 cross-dyke

Main trends of channel development on the basis of modern process observations

In the reach of the main channel upstream of the underwater weir (1851–1843 km) the water level is regulated by the Dunakiliti dam. At the Rajka water gauge (km 1848.4) annual water level fluctuation ranges between 122.9 and 123.3 m aBsl (m above Baltic Sea level). In this reach flow velocity in the main channel remains below 0.1–0.2 m/s.

In the reach of the main channel downstream of the underwater weir (1843–1841 km) a stable flow pattern can be observed. On the Dunakiliti water gauge data (1,842.4 km) backwater level, upstream of the underwater weir, data fluctuated between 118.4 and 119.1 m aBsl with higher values occurring in summer. Most of the main channel's water yield falls over the underwater weir resulting in very high flow velocity.

In the middle reach of the main channel between 1841 and 1825 km water level is basically controlled by the water volume transmitted at Dunacsún (Čunovo). Early spring and late autumn water levels at the Doborgaz water gauge (1839.5 km) fluctuated between 117.3 and 117.5 m aBsl, whereas spring and summer values changed between 117.9 and 118.2 m aBsl.

In the reach of the main channel between 1825 and 1820 km a more important water level fluctuation can be observed. The water regime is comparatively stable during early spring and late autumn, with monthly fluctuation not exceeding 40 cm at the Dunaremete water gauge (113.4–113.8 m aBsl.). Slightly higher water levels can be experienced during spring and summer, brought about by floods and the backwater effect of the Gabcikovo tailrace canal.

The water regime of the main channel between 1820 and 1811 km is fully controlled by the backwater effect of the Gabcikovo power plant's tailrace canal. Flow velocity diminishes progressively downstream. At the Ásványráró water gauge water levels in early spring and late autumn are near 111 m aBsl, whereas in the spring-summer period they rise to 112 m aBsl or even higher.

The water level of the side-branch system in the active floodplain is entirely controlled by artificial factors. The annual difference between the highest and lowest values does not exceed 1.0–1.2 m. The water regime can essentially be described by longer periods of stable water level, occasionally interrupted by sudden, more important fluctuations.

The water regime of the recharge system in the active floodplain can be assumed as stable: flow velocity achieving 1.0–1.2 m/s in channels occurs only in the reach between Dunakiliti and Doborgazsziget. Further downstream, reaches with equally high velocity occur solely immediately downstream of the cross-dykes and sluices, as well as in some smaller crosscutting side-branches. As a result of artificial intervention severe lateral erosion and in some other parts rapid sediment accumulation occur sporadically (Photos 1–2).

The lower reach of the side-branch system in the active floodplain not involved in water recharge, namely the Ásványi-Danube and the Bagomér branch-system, can also be attributed to the reach influenced by the backwater effect of the Gabcikovo tailrace canal. Its water regime and flow pattern is identical with that of the reach of the main channel between 1820 and 1811 km.

The water level fluctuation in channels of the recharge system in the protected side remains essentially below 0.5 m. The water volume flowing into this system is influenced through the backwater level of the Rajka-5 sluice. The size of specific channel reaches varies over a wide range. All the same, slowly flowing parts or stagnant, backwater tables prevail. Faster water flow can only be experienced in short segments directly downstream of the sluices and cross-dykes.

The water regime of the upper reach of Mosoni-Danube extending up to Mosonmagyaróvár is fully under artificial control. The water yield flowing through the Rajka-6 sluice into the Mosoni-Danube can be regarded essentially as the difference between the water transmitted from Slovakia and that taken from the infiltration canal for supplying the branches in the active floodplain.

In the upper reach of the Mosoni-Danube flow velocity is invariably high. As compared to the situation before diversion long, low-water-level- and dry periods ceased but Danubian floods also ceased. Water level stabilized at an interval slightly above earlier average level.

Photo 1
Riverbank scoured by local swift current (actual geologic site 5, 29. 07. 1998)

Photo 2
Alluvial fan built by the current loosing its energy under the artifical cross-dyke (actual geologic site 9, 19. 02. 1998)

Results of water quality analyses

In our yearly reports on the results of the geologic monitoring in Szigetköz we regularly made an overview of the significant phenomena that can be studied through special sounding along the channels and characterize the relationship in the quality of surface and groundwater. This sounding method is capable essentially of studying short-distance (1–2 m) and short-term (some days) changes in water quality occurring during infiltration from channels toward groundwater. Simultaneously, it can indicate some later-occurring changes in flow direction and in water quality occurring in more remote and deeper aquifers. Additionally, in channel reaches draining groundwater it reveals the quality of water coming from longer distances.

Seasonal fluctuation of water quality can easily be traced in time series. Of the results of investigations between 1995 and 1998, Figure 2 displays the nitrate content ratio measured in the related sounding and surface water sample pairs

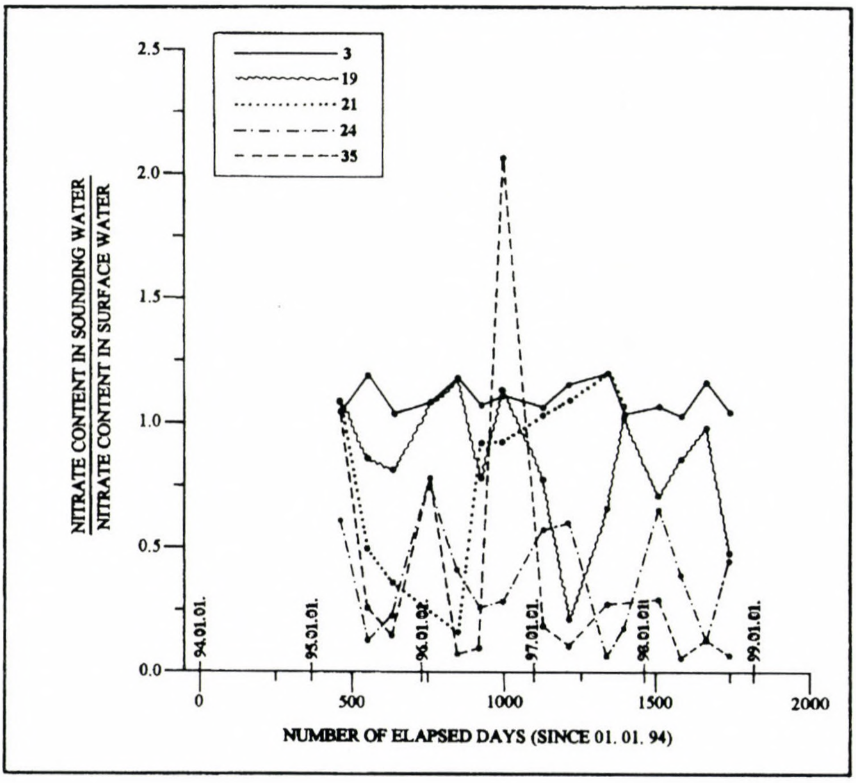

Fig. 2
Nitrate reduction characteristic of different infiltration sites

in 19 sampling sites characterized by stable infiltration. This quotient clearly describes the degree of reduction, i.e. the quality of the screening surface. The figure shows no notable reduction in Sample Site 3 in the entire period during infiltration, whereas in Sites 24 and 35 it was constantly prominent (the positive anomaly occurring in Sampling Site 35 is probably due to local pollution. The seasonal change in the quotient of nitrate content can be associated with a temperature effect influencing the production of bacterium flora.

The lack or appearance of seasonal changes in time series can provide help to assume the time and distance covered by water flow. Lacking quantitative data we can only suggest that the effect of seasonal changes in surface water quality can be observed in groundwater within a year of infiltration. Presuming average flow velocity, the lack of seasonal changes in groundwater indicates that infiltration occurred more than a year earlier, or over a flow track longer than 300-500 m. These results can be concluded from Figs 3–6. Sample Sites 1 and 3 lie beside a draining and infiltrating channel reach, respectively. In sample pairs taken from Site 3 the nitrate content in sounding water is invariably higher than in the respective samples taken from surface water. Consequently, favorable infiltration conditions, which subdue nitrate reduction, are proved by the only very slight decrease in dissolved oxygen content. Nevertheless, we have no explanation for the inverse character of nitrate content (Fig. 3). The following list shows the screened intervals in some boreholes: Dkl-1: 10-15 m; Dkl-6 and 7: 45-50 m. The results of analyses of surface waters from the two sounding sites have also been indicated.

It can be noted that dissolved oxygen content in sounding and borehole water samples decreases invariably in all presented sites as compared to surface waters (Fig. 4). A more significant decrease in nitrate content was reported from borehole Dkl-7 and Sounding Site 1. In both cases this can be explained by the appearance of reductive waters through remote infiltration. Borehole Dkl-1 and Sounding Site 3 are situated directly beside the upstream reach of the underwater weir. As a result they are hydrogeologically in a heavily undersucked position. Water infiltrating through the gravel-bearing riverbed maintains its oxygen content. Analyses of sounding water show regularly higher nitrate content than in surface water. The water quality data of borehole Dkl-6 does not correspond to its hydrogeologic situation. The measured water level is higher than in the main channel; water flows thus toward the latter. The slight shift in high nitrate and dissolved oxygen content and the approximately quarterly shift in seasonal picks indicate more remote infiltration.

Chloride content (Fig. 5) is insensitive to reduction processes and water-sediment interaction, and follows only seasonal changes in the quality of infiltrating water. Time series of chloride content can thus be used for estimating the distance of the infiltration area. Smoothed curves indicate a longer flow distance, as in case of borehole Dkl-7. The considerable difference between the results of water quality in Sounding Site 1 and surface water can be attributed to

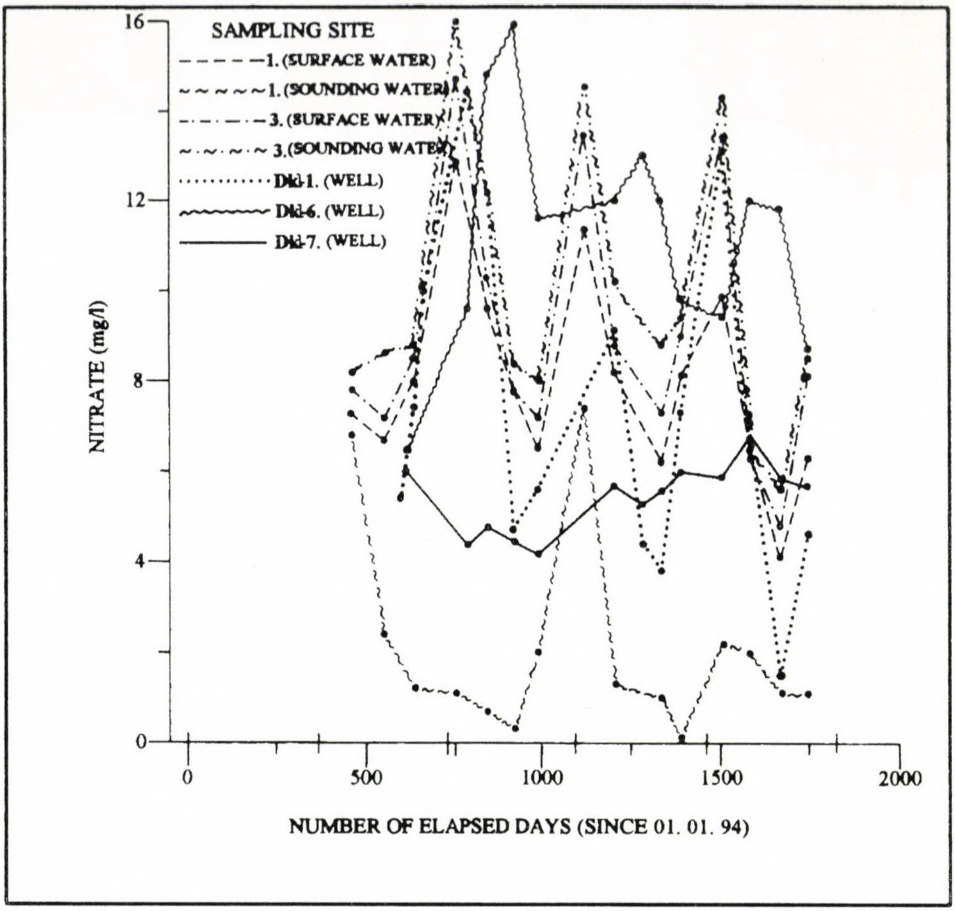

Fig. 3
Time series of changes in nitrate content in sampling sites characterized by different flow position

the same reason. In case of borehole Dkl-6 the already mentioned quarterly shift can also be observed in the time series of chloride content. Seasonal changes can also be revealed in silicic acid content (Fig. 6). However, while nitrate and chloride content maximums occur in winter, the dissolution peak of silicic acid can be observed during summer.

The summarizing overview of iron, manganese and ammonium content is the best tool to describe infiltration conditions and, consequently, the changes in water quality. Results of the analyses between 1994–98 have been summarized in two tables (Tables 2, 3).

In tables we indicated the number of samples (n) and average and median values as well. The average is considerably distorted by extremely high values. It can be compensated through using the median. Data in Table 3 show a slightly decreasing tendency in iron and manganese content of the water infiltrating directly from the channel; moreover, its ammonium content presents a similar character. The infiltrating water contains slightly more dissolved organic matter. Therefore, further dissolution of iron and manganese during the flow in subsurface water could be expected; the chance of further increase in ammonium content can thus be neglected. The area studied by sounding along channels thus provides only a small part of groundwater recharge. The quality of water deriving from more remote sites, directly from the Čunovo-Somorin reservoir, is

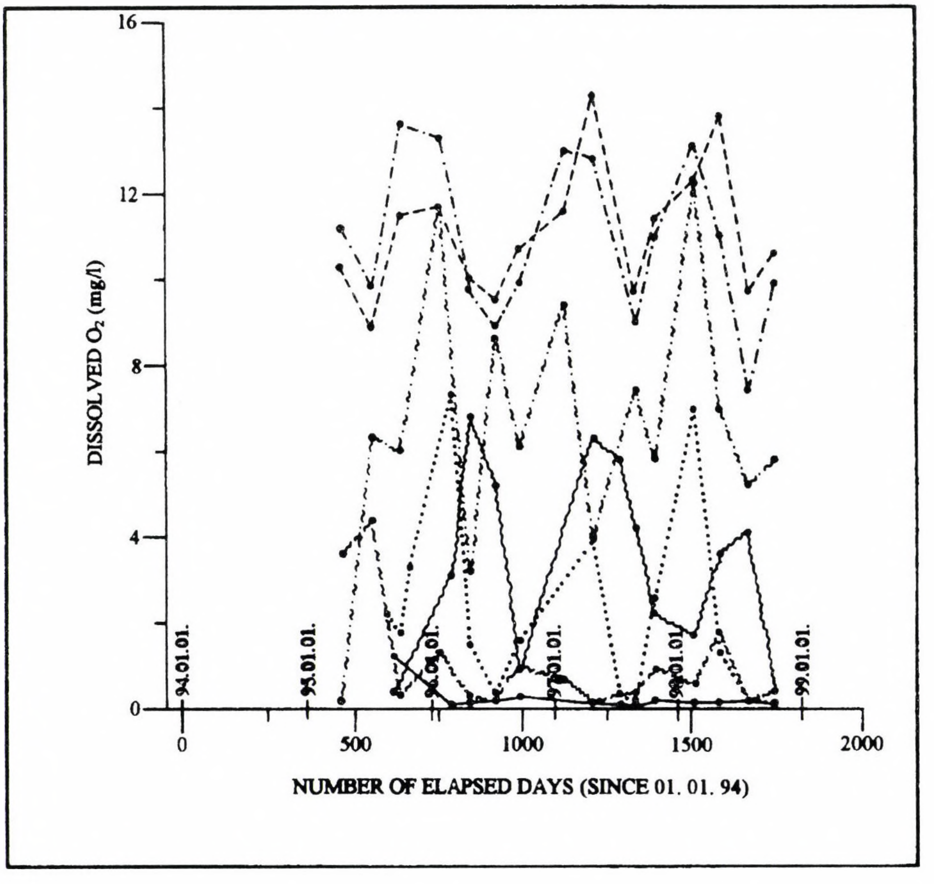

Fig. 4

Time series of changes in dissolved oxygen content in sampling sites characterized by different flow position (see legend in Fig. 3)

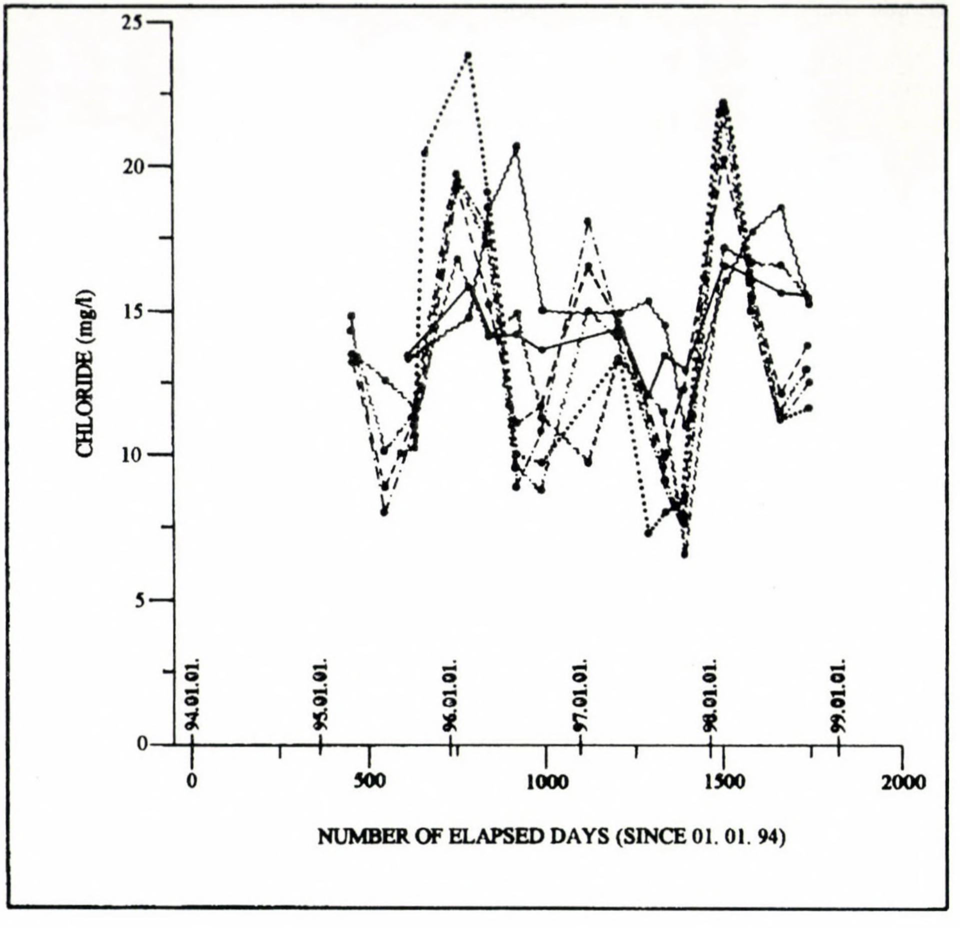

Fig. 5
Time series of changes in chloride content in sampling sites characterized by different flow position (see legend in Fig. 3)

still not known. Extremely high averages of groundwater re-infiltrating in channels measured in 1994 and 1997 can presumably be explained by communal waste pollution.

The regular study of toxic elements (trace components) indicated that – except for arsenic – concentrations approaching health limits have not occurred yet; moreover arsenic (33 μg/l) is also only approaching the limit currently in force (50 μg/l). Arsenic concentration is associated primarily with the geologic conditions of the infiltration area. Arsenic is dissolved from fine-grained channel sediments enriched in organic matter. Its concentration in groundwater will change in the future as a function of the size of screening surfaces involved in groundwater recharge.

Results of hydrogeologic investigations

Following the diversion of the Danube recharge and drainage conditions of subsurface waters in Szigetköz changed considerably. Formerly, the main source of recharge was the Danube with its gravel bed. After diversion this role was transferred to the Čunovo-Somorin reservoir. Later the situation became more complex through the effect of different recharge measures and regulation by the underwater weir. Consequently, the branch system of the active floodplain and protected side, the infiltration canal and the upper reaches of the Mosoni-Danube, as well as the 1 km reach of the main channel immediately upstream of the underwater weir were also involved in groundwater recharge.

Apart from recharge the regulating role of the water level in tapping regions can also be regarded as a decisive factor in groundwater level. The former simple

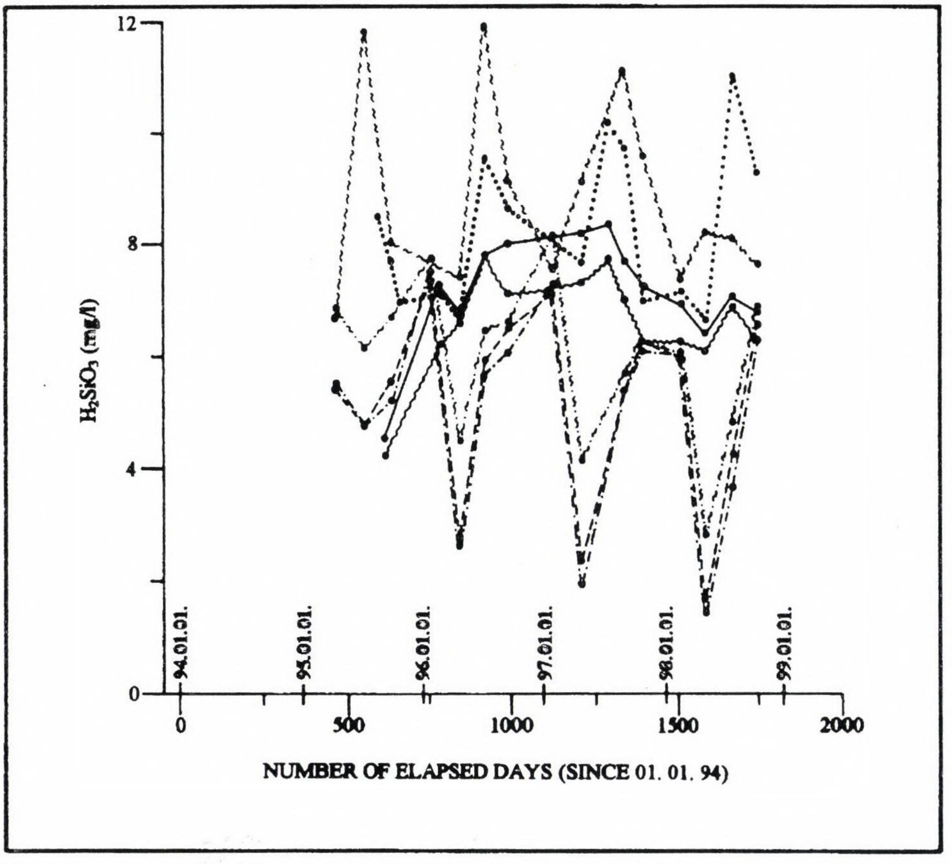

Fig. 6
Time series of changes in silicic acid content in sampling sites with different flow position (see legend in Fig. 3)

Table 2
Iron, manganese and ammonium content of the water percolating through infiltrating reaches measured in soundings (mg/l)

Year	No.	Fe^{++}		Mn^{++}		NH_4^+	
		average	median	average	median	average	median
1994	39	0.64	0.27	0.38	0.16	0.40	0.11
1995	45	0.46	0.19	0.34	0.14	0.23	<0.01
1996	63	0.19	0.11	0.28	0.14	0.26	0.28
1997	54	0.46	0.21	0.24	0.07	0.28	0.20
1998	45	1.16	0.15	0.35	0.07	0.31	0.13

Table 3
Iron, manganese and ammonium content of the water re-infiltrating in the channel in draining reaches measured in soundings and springs (mg/l)

Year	No	Fe^{++}		Mn^{++}		NH_4^+	
		average	median	average	median	average	median
1994	21	1.28	0.40	0.40	0.08	0.50	0.03
1995	30	0.22	0.17	0.35	0.15	0.05	<0.01
1996	50	0.51	0.07	0.29	0.12	0.49	0.24
1997	32	1.18	0.14	0.32	0.03	1.20	0.11
1998	20	0.17	0.04	0.16	0.05	0.15	0.02

picture (i.e. the main draining regions were the lower reaches of the Mosoni-Danube and the Hanság) became more complex here as well, as a result of diversion and construction of the underwater weir (Fig. 7). Downstream reaches of the main channel, the infiltration canal and some other, also downstream reaches of the recharge system, emerged as new draining areas. In this spatially and temporally increasingly sophisticated system the processes can only be appropriately described through implementing high-resolution transient 3-dimensional flow and transport models.

In order to promote mental modeling (describing complex spatial processes) and perform the main trial and error tasks quickly and reasonably, preliminary 2-dimensional permanent flow-and-transport modeling was carried out. For this we used the FLOTRANS software, applying it to a vertical profile whose track presumably followed the direction of subsurface water flow (Fig. 8). The 4400 m-long profile starts in the vicinity of Dunakiliti, traverses the Szigeti-Danube, the main recharging channel at Heléna, the main channel near 1845 km and stops in the central line of the Somorin reservoir; it extends from the surface down to 100 m aBsl.

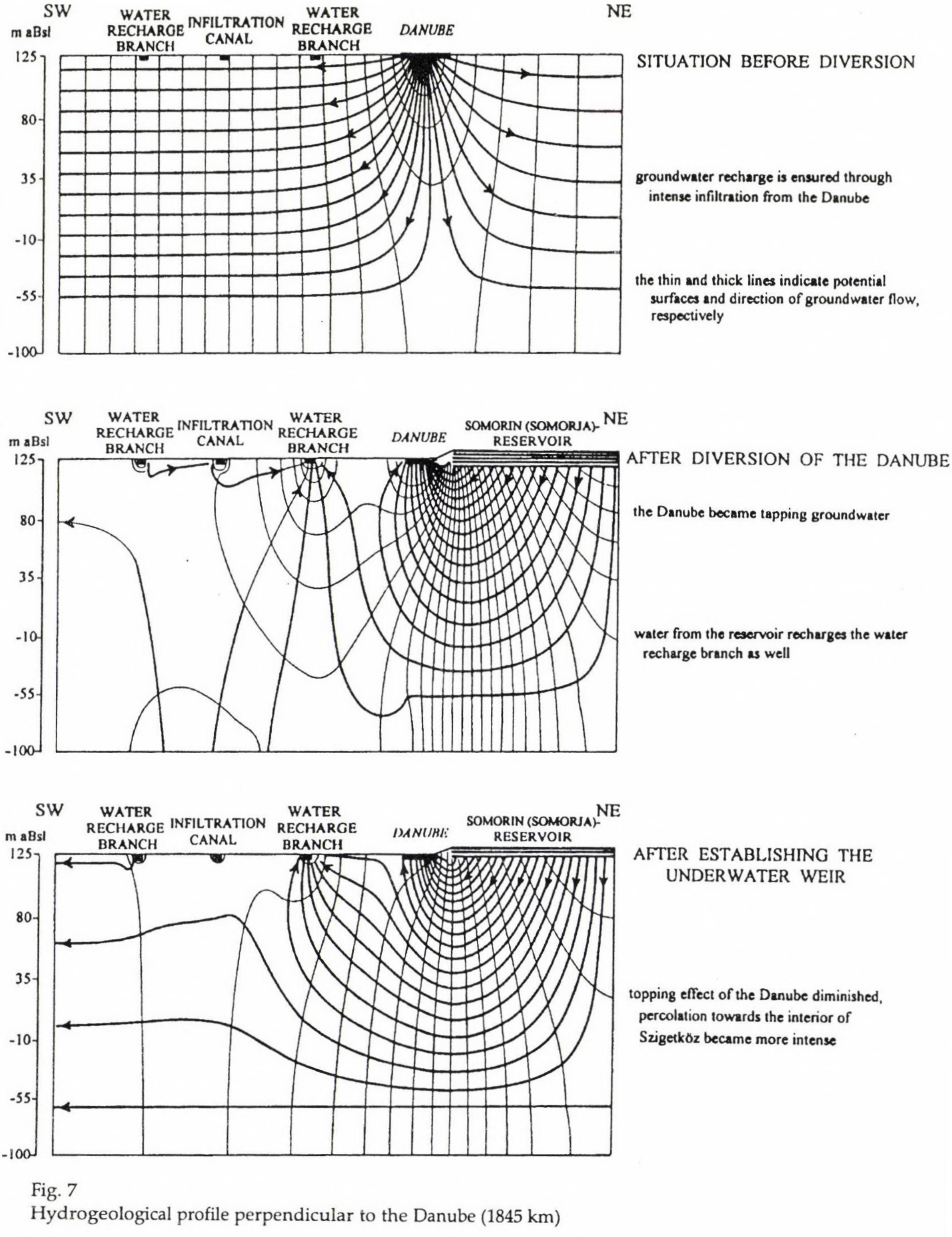

Fig. 7
Hydrogeological profile perpendicular to the Danube (1845 km)

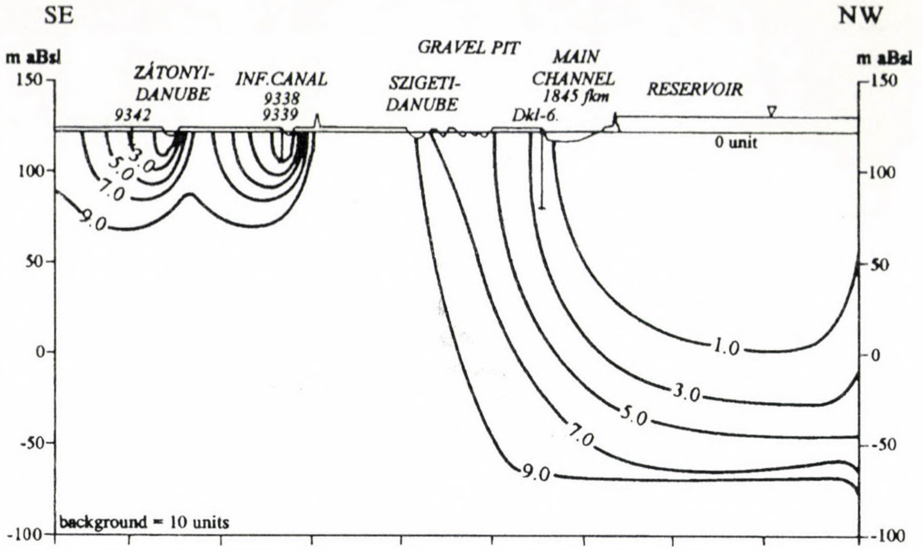

Fig. 8
Result of pollution transport modelling between the Ćunovo reservoir (the Somorin part of the reservoir) and Dunakiliti

Its reaches of constant pressure are represented by the main channel (122.64 m aBsl), the Heléna branch (121.71 m aBsl) and the bordering zone assigned at Dunakiliti (121.6 m aBsl). Recharge in the reservoir is assumed as 0.07 $m^3/m^2/d$, and in the infiltration canal and in Szigeti-Danube it equals 0.02 $m^3/m^2/d$.

The lower 40 m of the profile is represented by sand with a horizontal/vertical permeability coefficient of $k_h/k_v=10/0.5$ m/d. The overlying gravel complex, reaching generally up to groundwater level, is characterized by $k_h/k_v=250/12$ m/d. The silt making up the reservoir base was described as a 5 m-thick, $k_h/k_v=0.5/0.5$ m/d layer (its vertical hydraulic resistance can correspond approximately to that of the 0.5–1-m-thick silt on the reservoir bottom). In the two Hungarian recharge branches a value of $k_h/k_v=0.3/0.3$ m/d was assigned to the silt bed (distributed over a 5-m-thick layer).

Equipotential lines describing the evolved potential space were confirmed by observation wells and sounding sites along the profile as well as by the results of field observations and water level data.

The channel surface providing recharge is different, i.e. richer in fine-grained sediments and organic matter, than the infiltrating surface of the original Danube was.

Changes in water quality, beginning with the new recharge surfaces, were characterized through transport modeling of a fictive, conservative indicator material (in our fictive case this "indicator" was the reductive "nitrate free" water which enters at the bottom of the reservoir. At the same time it was assumed that all the subsurface space has a 10-unit background value). Starting with the constant indicator source, with concentration we were able to trace its temporal and spatial diffusion. It can be stated that during the 4 years which have passed 10% of the indicator could have been traced as far as a distance of 2.5 km. This means that water quality effects deriving from Slovakia could have already spread into Hungary to a considerable degree.

Conclusions

Due to the influence exerted by diversion, filling of dams, water recharge and the effect of the underwater weir channel, reaches ensuring water recharge of groundwater in Szigetköz have been modified. Investigations over the last 5 years provided information of sufficient detail regarding the quality of waters infiltrating from different recharging branches (active floodplain, protected side) – at least as far as inorganic components are concerned.

The results of investigations achieved so far clearly indicate that

1. The in situ study of reaches ensuring overbank screening can be arranged by reasonably implemented soundings and shallow boreholes.
2. A key role should be given to the observation of sounding sites and shallow wells in the monitoring system set up for tracing changes in groundwater of the Szigetköz area.
3. The results acquired so far prove that the quality of infiltrating water in the near-channel zone is determined by the joint effect of interactions between water-sediment-biological conditions.

References

Don, Gy., Kaiser M., Marsi I., Scharek P., Síkhegyi F., Szeiler R., Tullner T., Zsámbok I 1991: A Szigetköz és a kapcsolódó térség földtani viszonyai (Geological setting of Szigetköz and its surroundings) – Manuscript, MÁFI Adattár.

Don, Gy., M. Kaiser, I. Marsi, P. Scharek, F. Síkhegyi, R. Szeiler, T. Tullner, I. Zsámbok 1993: Geological Setting of the Szigetköz – p. 63.+ 14 annexs. - Manuscript MÁFI Library.

Don, Gy., M. Kaiser, P. Molnár, P. Nagy, A. Pentelényi, Á. Rotárné Szalkai, P. Scharek, I. Zsámbok 1995: Hullámtéri észlelőrendszer bővítése és a felszínközeli képződmények szerkezeti elemzése a Szigetközben (Extension of the monitoring system in the active flood-plain and structural analysis of near-surface formations in Szigetköz) – Manuscript MGSZ Adattár, T 17031.

Don, Gy., I. Horváth, M. Kaiser, P. Molnár, P. Nagy, A. Pentelényi, Á. Rotárné Szalkai, P. Scharek, Gy. Tóth, I. Zsámbok 1996: Földtani monitoring hálózat működtetése és az adatok értékelése a Szigetközben (Operation of a geological monitoring network and analysis of recorded data in Szigetköz). – Manuscript MGSz Adattár.

Don, Gy., I. Horváth, P. Scharek, Gy. Tóth 1998: Földtani monitoring hálózat működtetése és az adatok értékelése a Szigetközben (Operation of a geological monitoring network and analysis of recorded data in Szigetköz). – Manuscript MGSZ Adattár, p. 62 T 19066.

Hajósy, A., P. Scharek, L. Tóth, Gy. Tóth 1993: A Szigetköz földtani kutatásai (Geological investigations in Szigetköz). – Magyar Geofizika, 34/2, pp. 86–93.

Horváth, I., P. Molnár, P. Scharek. 1995: Földtani monitoring hálózat fejlesztése és működtetése a Szigetközben (Development of a geological monitoring network and its operation in Szigetköz). – Manuscript MGSZ Adattár, T 17032.

Horváth, I., P. Molnár, P. Scharek, Gy. Tóth 1997: Földtani monitoring hálózat működtetése és az adatok értékelése a Szigetközben (Operation of a geological monitoring network and analysis of recorded data in Szigetköz). – Manuscript MGSz Adattár T 18763.

Janák, E. 1994: A Szigetközben végrehajtott "kárelhárítás" hatásainak bemutatása (Presentation of the effects of damage repair performed in Szigetköz). – Manuscript ÉDUVIZIG, Győr.

Marsi, I., P. Scharek, F. Síkhegyi, T. Tullner 1994: Survey Methodologies for Geological and Geotechnical Cartography of Alluvial Plains – 1st Eoropean Cong. on Reg. Geol. Cart. and Inf. Systems, Bologna, Italy, vol. 5.

Marsi, I., P. Scharek, I. Zsámbok 1994: Talajvízszint és talajvízminőség térinformatikai vizsgálata a Kisalföldön környezete (GIS analysis of groundwater level and quality in Kisalföld [Little Hungarian Plain]). – Kárpát-medence vízkészlete és vizi környezete – Water resources and aquatic environment in the Carpathian Basin I. pp.112–122.

Molnár, P. 1991: A szigetközi Duna-szakasz parti szűrést biztosító mederanyagának aktuálgeológiai értékelése (Actual geological evaluation of in-channel sediments ensuring overbank drainage in the Szigetköz section of Danube) – Manuscript MÁFI Adattár.

Molnár, P. 1994: A szigetközi Duna-szakasz aktuálgeológiai felmérése. – In: Scharek, P. et al.: Beszámoló jelentés az EK szakértői ajánlásaiban megfogalmazott... (Actual geological assessment of the Szigetköz section of Danube) – Manuscript MÁFI Adattár.

Scharek, P., 1998: Geologic Base of Hydrogeological Study in NW Hungary – III. Hidrológiai Konferencia A víz és a vizi környezetvédelem a Duna középső vízgyűjtőjében, Kolozsvár, Vol. I. pp. 221–226

Scharek, P. (szerk.) 1991: Magyarázó a Győr-Észak jelű térképlaphoz (Explanatory text to the map sheet Győr-Észak) – A Kisalföld földtani térképsorozata 1:100 000, Magyar Állami Földtani Intézet, Budapest p.31.

Scharek, P. (szerk.) 1991: Magyarázó a Mosonmagyaróvár jelű térképlaphoz (Explanatory text to the map sheet Mosonmagyaróvár) – A Kisalföld földtani térképsorozata 1:100 000, Magyar Állami Földtani Intézet, Budapest p.35.

Scharek, P., J. Angyal, Gy. Don, I. Horváth, M. Kaiser, P. Molnár, A. Pentelényi, F. Síkhegyi, Gy. Tóth, I. Zsámbok 1994: Az Európai Közösség szakértői ajánlásaiban megfogalmazott hidrogeológiai feladatok elvégzéséhez alapadatok összeállítása és értékelése (Collection and analysis of key data for performing hydrogeological tasks specified in the expert commandations of the European Union) – Manuscript MGSz Adattár: T 16 206.

Scharek, P., I. Horváth, P. Molnár, P. Nagy, Á., Rotárné Szalkai, R. Szeiler, Gy. Tóth, T. Tullner, G. Turczi 1994a: A Szigetköz hidrogeológiai és aktuálgeológiai állapotfelmérése, az adatok térinformatikai feldolgozása (Actual geological and hydrogeological state assessment in Szigetköz and GIS processing of related data). – Manuscript MGSz Adattár: T 16693.

Scharek, P., Gy. Tóth 1997: Geological and Hydrogeological assessment of nature conservation areas – In: Láng, I. et al. (Ed.): Studies on the Environmental State of the Szigetköz after the Diversion of the Danube, pp. 9–12.

Scharek, P., T. Tullner, G. Turczi 1993: GIS as Basic Tool in the Regional and Applied Geological Mapping of the Little Hungarian Plain – EGIS'93, Genoa, Italy, Vol. 2. pp. 1613–1614.

Scharek, P., T. Tullner, G. Turczi 1994b: Die Nutzung geographischer Informationssysteme in der regionalen und angewandten Geologie (The use of Geographical Information Systems (GIS) in regional and applied geology). - Zeitschrift für Angewandte Geologie, 40/2, pp. 87–91.

Scharek, P, T. Tullner, G. Turczi 1995: GIS for Environmental Management in the Little Hungarian Plain (Kisalföld) – Joint European Conference and Exhibition on Geographical Information, The Hague March 26-31, 1995, Vol. 1. pp. 361–367.

Scharek, P., T. Tullner, G. Turczi 1995: Digging deeper: Hungary`s geological survey increases its GIS activity – GIS Europe May 1995, pp. 28–30.

Scharek, P., G. Turczi, T. Tullner 1995: Hungary`s Geological Survey Increases its GIS Activity – Global Link 1995, Vol. 1, No. 2, p. 4.
Scharek, P., I. Zsámbok 1992: A kisalföldi földtani térképezés hidrogeológiai eredményei a Szigetközben (Hydrogeolgical results of the geological mapping of Kisalföld in Szigetköz). - Magyar Hidrológiai. Társaság X. Országos Vándorgyűlése IV, pp. 79–88.
Scharek, P., I. Zsámbok 1997: Hydrogeological Investigation as a Key Aspect in the Geological Study of Alluvial Plains – Second Congress on Regional Geological Cartography and Information Systems, Barcelona Jun. 16–20, 1997, pp. 143–148.

Printed in Hungary
Akadémiai Nyomda, Martonvásár

GUIDELINES FOR AUTHORS

Acta Geologica Hungarica is an English-language quaterly publishing papers on geological topics. Besides papers on outstanding scientific achievements, on the main lines of geological research in Hungary, and on the geology of the Alpine–Carpathian–Dinaric region, reports on workshops of geological research, on major scientific meetings, and on contributions to international research projects will be accepted.

Only original papers will be published and a copy of the Publishing Agreement will be sent to the authors of papers accepted for publication. Manuscripts will be processed only after receiving the signed copy of the agreement.

Manuscripts are to be sent to the Editorial Office for refereeing, editing, in two typewritten copies, on floppy disk with two printed copies, or by E-mail. Manuscripts written by the following word processors will be accepted: MS Word, or ASCII format. Acceptance depends on the opinion of two referees and the decision of the Editorial Board.

Form of manuscripts

The paper complete with abstract, figures, tables, and bibliography should not exceed 25 pages (25 double-spaced lines with 3 cm margins on both sides).

The first page should include:

- the title of the paper (with minuscule letters)
- the full name of the author
- the name of the institution and city where the work was prepared
- an abstract of not more than 200 words
- a list of five to ten key words
- a footnote with the postal address of the author

The SI (System International) should be used for all units of measurements.

References

In text citations the author`s name and the year of the publication between brackets should be given. The reference list should contain the family name, a comma, the abbreviation of the first name, the year of publication, and a colon. This is followed by the title of the paper. Paper titles are followed – after a long hyphen – by periodical title, volume number, and inclusive page numbers. For books the title (English version), the name of the publisher, the place of publication, and the number of pages should be given.

Figures and tables

Figures and tables shuld be referred to in the text. Figures are expected in the size of the final type-area of the quarterly (12.6 x 18.6) or proportionally magnified 20–25% camera ready quality. Figures should be clear line drawings or good quality black-and-white photographic prints. Colour photographs will also be accepted, but the extra cost of reproduction in colour must be borne by the authors. The author`s name and figure number should be indicated on the back of each figure. Tables should be typed on separate sheets with a number.

Proof and reprints

The authors will be sent a set of proofs. Each of the pages should be proofread, signed, and returned to the Editorial Office within a week of receipt. Twenty-five reprints are supplied free of charge, additional reprints may be ordered.

Contents

Acta Geologica Hungarica

VOLUME 43, NUMBER 2, 2000

Akadémiai Kiadó, Budapest

ACTA GEOL. HUNG. AGHUE7 43 (2) 107–222 (2000) HU ISSN 0236–5278

ACTA GEOLOGICA HUNGARICA

A QUARTERLY OF THE HUNGARIAN ACADEMY OF SCIENCES

Acta Geologica Hungarica publishes original studies on geology, crystallography, mineralogy, petrography, geochemistry and paleontology.

Acta Geologica Hungarica is published in yearly volumes of four numbers by

AKADÉMIAI KIADÓ
H-1117 Budapest, Prielle Kornélia u. 4, Hungary
http://www.akkrt.hu

Manuscripts and editorial correspondence should be addressed to the

ACTA GEOLOGICA HUNGARICA

Dr. János Haas
Academical Research Group, Department of Geology, Eötvös Loránd University of Sciences
H-1088 Budapest, Múzeum krt. 4/a, Hungary
Phone/Fax: (36-1) 266 4947
E-mail: haas@ludens.elte.hu

Orders should be addressed to

AKADÉMIAI KIADÓ
H-1519 Budapest, P.O. Box 245, Hungary
Fax: (36-1) 464 8221
E-mail: kiss.s@akkrt.hu

Subscription price for Volume 43 (2000) in 4 issues US$ 180.00, including normal postage, airmail delivery US$ 20.00.

Acta Geologica is abstracted/indexed in Bibliographie des Sciences de la Terre, Chemical Abstracts, GeoRef, Hydro-Index, Mineralogical Abstract

AGeol 43 (2000) 2

Acta Geologica Hungarica, Vol. 43/2, pp. 107–108 (2000)

The Geology of Today – for Tomorrow

Satellite conference of the World Conference on Science 21–24 June, 1999

János Halmai
Geological Institute of Hungary, Budapest

Key words: international conference, report, radioactive waste disposal, protection of subsurface aquifers

This international conference was the last one of a series which commemorated the 150th anniversary of the establishment of the Hungarian Geological Society. The Organizing Committee was given a threefold aim when it was requested to organize this conference: to commemorate the anniversary of the Geological Society, to join the programs of the World Conference on Science (WCS), and thirdly to promote the latest national and international results of scientific research in the selected topics of the meeting. The scientific aim of the conference was to look toward the future. How can geology answer the questions which arise from social and economic developments, resulting from the increased anthropogenic pressures on natural processes? What are the optimal limits for utilizing the natural environment? Where are the limits of the influence exerted by mankind on the environment? Are harmful processes in the environment reversible? Can the natural environment be restored? What is the role of geology in these processes?

Our aims were clearly welcomed by the Hungarian Organizing Committee of the "World Conference on Science" acting under the auspices of UNESCO and of the ICSU (International Council for Science), when our conference was ranked among the satellite conferences. The outstanding importance of the conference was noted by the Hungarian Academy of Sciences (organizer of the WCS). Norbert Kroó, the Secretary-General, welcomed the participants, and Attila Meskó, Deputy Secretary-General of the Academy, was also present at the opening ceremony.

The selected topics of the conference took place under the auspices of the following political and scientific leaders: Attila Chikán, Minister of Economic Affairs, Kálmán Katona, Minister of Transportation, Telecommunication and Water Management, Pál Pepó, Minister of Environmental Protection, József Torgyán, Minister of Agriculture and Country Development, Ferenc Glatz, President of the Hungarian Academy of Sciences, Ernő Mészáros, Head of the

Address: J. Halmai: H-1143 Budapest, Stefánia út 14, Hungary
Received: 14 September, 1999

Department of Earth Sciences of the Hungarian Academy of Sciences, Miklós Varga, Director General of the National Water Authorities, György Vajda, Director General of the National Atomic Energy Agency, István Farkas, Director General of the Hungarian Geological Survey, and György Enyedi, President of the Hungarian National Committee of UNESCO. From the political world Dr. Károly Tamás, Under-secretary of State, participated at the conference, representing Minister József Torgyán and the Ministry of Agriculture and Country Development.

The conference included two selected topics, which dealt with the most important problems of the coming decades: radioactive waste disposal and protection of subsurface aquifers. Nearly 40 papers and 20 posters were presented in the two sessions, which summarized the national and international results of recent research. The conference provided a unique opportunity to present the results of Hungarian research in these topics, results which can also influence the EU integration of Hungary, and help us understand current European research trends, which in itself helps the PR work of the integration process. The work of the two sessions were organized and coordinated by internationally recognized scientists: György Bárdossy and László Rybach, and József Tóth and Eszter Havas Szilágyi respectively. Nearly 90 scientists from 22 countries participated at the conference and the field trip, representing geologic surveys and institutions, universities, academies, ministries, national agencies, the OECD, institutes dealing with radioactive waste disposal and safety assessments, and private companies.

The scientific conclusions of the two sessions are summarized by two internationally recognized scientists, László Rybach (Switzerland) and József Tóth (Canada). These summaries and the entire material of the invited key lecturer are being published in this issue of the Acta Geologica Hungarica. Földtani Közlöny, the journal of the Hungarian Geological Society, will publish several selected papers from the two sessions.

The conference was supported by the Foundation for Hungarian Geology, the Foundation for the Technological Progress of Industry, the Geological Institute of Hungary, the Hungarian Academy of Sciences, the National Atomic Energy Authority, the Paks Nuclear Plant Ltd., Golder Associates Hungary Ltd., Mecsekérc Environmental Protection Ltd., the National Committee of Technological Development and the Public Agency for Radioactive Waste Management.

In addition to the sponsors, as chairman of the Organizing Committee I would like to recognize all the efforts of the previously mentioned scientific organizers, the work of the organizing committee (Károly Brezsnyánszky, Géza Császár, Endre Dudich, Gábor Érdi-Krausz, Gyula Maros, Péter Scharek, Katalin Zimmermann), the field-trip leaders and all those who contributed to the success of the conference.

Acta Geologica Hungarica, Vol. 43/2, pp. 109–112 (2000)

International Satellite Conference "The Geology of Today for Tomorrow"

Ladislaus Rybach
ETH Zürich

József Tóth
University of Alberta, Edmonton

The meeting was organized within the framework of the World Conference of Science (WCS) as an accompanying measure, parallel to numerous other satellite conferences devoted to specific topics. At this occasion the earth sciences concentrated on themes with important future perspectives. Two particular subjects were selected by the organizers as conference topics:

A) Geologic Aspects of Radioactive Waste Disposal
B) Protection of Subsurface Aquifers.

Both subjects are of fundamental importance for the future:

The ongoing production of electricity by nuclear power plants in many countries yields radioactive waste as a problematic byproduct. Its management and disposal are highly controversial issues nowadays; nevertheless solutions which must account for the long half-life of waste components will have to be implemented in the next century.

Subsurface aquifers which provide the water supply for the still growing world population need to be preserved, both in qualitative and in quantitative respect. Groundwater resources are limited, their amount and renewal are increasingly endangered by human activities like forced irrigation; thus, management and protection measures must be developed, tested and implemented to secure sustainable water supply.

The problems of both topics are highly relevant for coming generations and today's scientific community is correspondingly challenged to provide viable solutions which must also be acceptable for concerned people today; thus this Satellite Conference suits well the general theme of WCS, Science and Society.

The Conference took place on 21–22 June in Budapest, followed by a post-conference field trip to the SE Transdanubian Mecsek Mountains to visit and study uranium ore mining and potential waste disposal sites as well as characteristic hydrogeologic features like the Harkány and Tettye springs. The Hungarian Geological Society (which recently celebrated its 150th anniversary) was the conference organizer, with Dr. János Halmai heading the Organizing Committee. Convenors for topic A were Prof. László Rybach (ETH Zurich, Switzerland) and Academician Dr. György Bárdossy, for topic B Prof. József Tóth

Addresses: L. Rybach: Institute of Geophysics ETH Hoenggerberg, 8093 Zurich, Switzerland
J. Tóth: Edmonton, AB., T6G 2E3, Canada
Received: 14 September, 1999

(University of Alberta, Canada) and Eszter Havas-Szilágyi (Ministry of Transport, Communications and Water Management, Budapest). The Conference included a reception in the beautiful historic building of the Hungarian Geological Institute (MÁFI).

The meeting took place under auspices of UNESCO, the ICSU, the Hungarian Academy of Sciences and of several Ministries and high authorities of Hungary and was sponsored by the Foundation for Hungarian Geology, the Foundation for the Technological Progress of Industry, The Geological Institute of Hungary, GOLDER Associates Hungary, the Hungarian Atomic Energy Authority, The MECSEK Ore Environment Ltd., the National Committee for Technological Development, and the Public Agency for Radioactive Waste Management.

The conference was well attended by European and overseas participants from 22 countries. The program included keynote lectures, oral presentations and a poster display. For topic A speakers came mainly from organizations responsible for radioactive waste management and disposal in their respective countries. Besides summarizing the international cooperative programs within the Nuclear Energy Agency of the OECD, numerous national programs were presented which aim at the safe enclosure of the radwaste (i.e. isolation from the biosphere), in repositories at depth in suitable geologic formations like granite, clay or salt. These formations are generally characterized by low permeability and thus prevent deep groundwater flow, which could convey radiotoxic isotopes from the repository to the biosphere. For the characterization of suitable rock formations and the location of favorable disposal sites a wealth of high-tech methods like X-ray fluorescence analysis or 3D seismic reflection surveys are available. The problem remains, regardless how exactly the present-day situation can be evaluated, with the uncertainties in predicting the geologic processes in the future which might have adverse influence on the structure and behavior of the envisaged formations and thus could reduce their isolation capacities.

Several speakers have presented realistic scenarios to cover possible future geologic development which, of course, are highly site-specific. There is general agreement in the scientific community that conservative scenarios should be included and that the uncertainty of the results (the latter usually given as doses to future individuals at the earth's surface, for which national regulatory limits are specified, mostly in mSv/a) should be quantified.

From several presentations at the conference it became evident that the feasibility of radwaste disposal in suitable geologic formations is rather a socio-political than a technical problem. The fact is that the general public exhibits a highly asymmetric and partly irrational risk acceptance/aversion profile. Risk at own will (e.g. smoking, individual mobility) is considered to be smaller than risk "imposed by others" (e.g. mega-technologies like nuclear power plants); individual benefits such as mobile phones are highly welcome by everybody whereas the antennas which emit non-ionizing radiation are welcome nowhere. Similarly there is growing opposition against planned radwaste repositories in deep geologic formations at practically any envisaged location. The democratic rights of local inhabitants, the protest of interest groups, environmentalists, etc., has so far achieved that there is no high-level waste repository in operation in any country of the world. Nevertheless the radwaste exists and new waste is continuously created which must be disposed of, so there is a real problem! As a temporary measure and solution, the waste is now being stored at nuclear power plant sites in many countries. This practice, however, can lead to deficiencies in radiological safety: the power plant sites have been selected on the basis of quite different criteria than those which are applicable to radwaste storage.

Problems also exist with "new concepts" emerging from the above-mentioned concerns and groups. It has been repeatedly suggested that long-term surface storage of radwaste, rigorously controlled over several centuries, should be preferred over the (final) subsurface geologic disposal option. Extreme options advocate the "mausoleum and guardian concept", with proper architectonic and behavioral attributes of the apparently necessary buildings and personnel. Any solution which postpones the final disposal and thus shifts the responsibility (=burden) to future generations violates, however, the concept of sustainability, a key and leading principle of present and future policies. Sustainability calls for "meeting the needs of present generations without compromising the needs of future generations" (Brundtland Commission, 1987) and is thus incompatible with any postponing of actions and responsibilities today to the people of tomorrow. Besides, several speakers emphasized that the future states and possible changes of decisive factors in radwaste disposal can be better predicted than the stability and transformations of future political and social systems which would be responsible for surveillance, safeguard and final disposal.

So we are now in a deadlocked situation, resulting from the suggested controlled, long-term surface storage which violates the sustainability principle on the one hand, and the strong opposition against radwaste transport and nearby geologic disposal on the other. In this situation, viable solutions are urgently needed. The concept of geologic disposal is still considered to be the best option; in this respect technologists such as the representatives of radwaste disposal organizations as well as regulators are in full agreement. This fact must be communicated to the general public.

In the presentations and the following lively discussions there was general consensus at the Conference that involvement of the public is essential and inevitable. Unbiased information about all scenarios which might effect geologic disposal and their possible impacts must be communicated. Consensus and coherence between diverging positions could possibly found by mediation. This could start with a dialog of the involved (and at the beginning conflicting) parties, presenting their views. A credible and well-trained mediator, a neutral referee, can lead the negotiations in bargaining by the opposing parties for benefits and thus finally reach a compromise which serves and satisfies both sides. Successful examples from various countries (Kansas River/USA: industrial gravel dredging from the river bottom vs. recreational activities such as fishing and canoeing; Vienna – St. Pölten motorway in Austria: on surface (planners view) vs. underground (in tunnels; wish of the populace) prove that this is possible even when the starting positions of the participants appear to be intransigent.

Acta Geologica Hungarica, Vol. 43/2, pp. 113–114 (2000)

Report on Section B: "Protection of Subsurface Aquifers" – GTT Conference

József Tóth
Department of Earth and Atmospheric Sciences
University of Alberta, Edmonton

In addition to the "Keynote Lecture" (József Tóth, Canada) and three "Invited Papers" (Emilio Custodio, Spain; T.N. Narasimhan, U.S.A.: Wouter Zijl, The Netherlands), eighteen oral and seven poster presentations were made in the Conference's "Section B" titled: "Protection of Subsurface Aquifers", by participants from eleven countries. Collectively, the various presentations touched upon virtually every aspect of the Section's theme. For an attentive participant it was thus possible to obtain a valuable overview of the entire topic.

The presentations can be divided into three thematic groups, with allowance for some overlap between some papers, due to the broad scope of the main theme. These thematic groups are the following: 1. Illustration of problems; 2. General principles, concepts, strategies; 3. Techniques and methods.

Studies presented in the first thematic group illustrated the diversity and complexity of problems related to aquifer protection very well. Because of these two dominant aspects of the task, it is impossible to develop standard, general, "prefabricated" methods and strategies; every case is a specific problem requiring a specific approach. The case studies illustrated the diversity of the possible problems from the aspects of both area size and technical nature. The discussed areas varied in size from the few hectares of Ukranian municipal waste dumps to the 840,000 km^2 extent of the South American "Botukatu aquifer", with virtually every gradation in between. Representative examples for the varied nature of the presented cases are: groundwater contamination from municipal waste-disposal sites, adverse effects of mine dewatering on thermal springs in a karst area, relation between the quality of riparian well-water and that of its river-water source, chemical and thermal pollution of drinking-water aquifers due to oil-field exploitation by subsurface combustion, response to deep-water production by declining water tables, and reduction or disappearance of wetlands and their aquatic ecology due to production of subsurface water.

The protection of aquifers may become extremely complex in certain cases because of practically unresolvable problems. Examples for such problems are: possible conflicts between drinking- and industrial-water production, on the one hand, and environmental protection, on the other; unclear and/or inaccurate definitions of parameters needed for solution of practical problems; difficulties in

Address: J. Tóth: Edmonton, AB., T6G 2E3, Canada
Received: 14 September, 1999

0236–5278/2000/$ 5.00 © 2000 *Akadémiai Kiadó, Budapest*

characterizing natural conditions, hydraulic parameters of the rock framework, effective boundaries in the subsurface flow domain, and so on; and a lack of standard, i.e., generally applicable methods.

The intended message of the papers in the second thematic group was strikingly similar to that of the first group, although they started out from different thoughts and different examples. The essence of this message was: measures and methods of aquifer protection must be conceived and implemented on the spatial scale of regional drainage basins and at a strategic level, as opposed to the customary approach of local, aquifer-by-aquifer, and tactical type of, problem solving. All seven speakers in this group emphasized, and several exemplified it, that the rock framework is hydraulically continuous. An effect generated in one point of the subsurface environment, whether it be hydraulic as in case of water withdrawal or injection, or chemical as in the case of surface- or subsurface-pollution, may propagate to any other point of the flow domain. The route, rate, and magnitude of propagation is a question only of distance, permeability, and time. For remediation, but even more so for prevention, of problems of both quantity and quality it is necessary to evaluate the geometry of the groundwater flow systems, the location and extent of the recharge- and discharge-areas, the boundaries between adjacent basins, and the natural water balance. Very important is the long-term monitoring of the fluctuations of groundwater-levels and temporal changes in groundwater quality. A new, and for aquifer-protection useful, concept was introduced in a paper on the rigorous mathematical definition and analysis of the "penetration depth" and "spatial- and temporal-scales" of gravity-drive groundwater flow-systems.

According to the "Keynote Lecture", the problem of aquifer protection is fundamentally a hydrogeological problem. Consequently, its solution requires "analytical hydrogeology", based on conceptual understanding and its intelligent implementation (rather than on the blind application of ready-made, "cookbook" techniques), and professional practicians capable of performing it. Ultimately, therefore, the responsibility of solving the problem of aquifer protection rests with the relevant institutions of higher learning.

Thirteen papers were presented in the third thematic group. Most of these papers dealt with geoelectrical and geomagnetic methods used primarily for the detection and estimation of hydrogeologic properties of aquifers. Novel ideas and propositions were the "routine" determination of the transport velocity of contaminants in karst aquifers, and the transformation of the strengths of the Earth's gravity, magnetic, and crustal-stress fields into parameters that would characterize the heterogeneity and dynamics of the rock framework in a hydrogeologically useful way.

The key position of hydrogeology linking the subjects of Sections A and B was underscored by the presence of papers in Section B on regional groundwater flow-modeling related to radioactive waste isolation. Two papers presented stable- and radioactive-isotope methods for evaluation of groundwater flow systems, and three further presentations discussed procedures aimed at the integraton of different methods, or several steps of specific methods.

Acta Geologica Hungarica, Vol. 43/2, pp. 115–134 (2000)

Repositories for high level waste in argillaceous formations – Key geologic questions

Bernard Neerdael, Maria De Craen
Belgian Nuclear Research Centre (SCK•CEN),
Waste and Disposal Department

Research and demonstration studies for the final disposal of high-level and long-lived radioactive waste are performed in several countries. Argillaceous formations, ranging from plastic clays to indurated clay formations or shale, are under consideration for hosting radioactive waste or spent fuel.

Rather detailed characterization programs from underground infrastructures (URL, mine, tunnel) have already been developed for several argillaceous formations such as the Boom Clay (Rupelian) in Belgium, the Opalinus Clay (Aalenian) in Switzerland, the Boda Claystone (Upper Permian) in Hungary and the Tounemire Claystone (Toarcian/Domerian) in France. Other potential formations have been considered and/or are being investigated in Canada, France, Germany, Italy, Japan, the United Kingdom and the United States.

The key geologic questions are addressed and the significance of the values of some parameters and processes on the feasibility and safety aspects of a global repository system is reviewed.

Key words: radioactive waste, disposal, repository, geology, clay, claystone, characterization, safety, feasibility

Introduction

Argillaceous materials are considered all over the world within the framework of waste disposal, either as host formation or as backfill and sealing material ensuring the isolation of waste from the environment for very long periods of time.

Argillaceous formations may vary from plastic clays with high water content to highly compacted shale with very low water content. The more relevant properties of argillaceous materials as host rock with regard to geologic disposal are their low hydraulic conductivity, high retention and ion exchange capacity and favorable geochemical environment. Regarding such applications, other important factors are burial depth and history as well as the fluid/rock interaction.

Gas, water and solutes will always tend to follow paths of least resistance in their way through low-permeability formations. If thick argillaceous media are cut by permeable faults or interconnected fractures, cross-formational flow would be focused along these discontinuities (Lalieux and Horseman 1996). Similar properties, and more especially water uptake, swelling and plasticity also make clay-based materials suitable for backfilling of access galleries, sealing of

Addresses: B. Neerdael, M. De Craen: Boeretang 200, B-2400 Mol, Belgium
Received: 17 November, 1999

disposal galleries/holes or even for surface disposal (cover, filling) of any type of waste.

This paper, however, deals with argillaceous formations used as host rock for the safe disposal either of high-level and long-lived radioactive waste in cases of reprocessing or of spent fuel in case of direct disposal. For this purpose argillaceous formations, ranging from plastic to indurated clay formations, are considered for site characterization, focusing on the mechanical, physico-chemical and hydrological properties, the degree of homogeneity, the detection and role of faults, etc. (Littleboy et al. 1997). For example, indurated clays characterized by very low matrix permeability may present important discontinuities with regard to fluid flow (Horseman and Higgo 1994; Lalieux and Horseman 1996). Site-specific data further require a sound understanding of the basic phenomena, which govern and control the retention and/or mobility of radionuclides through this low to very low-permeability formation. These studies stress the importance of parameters such as clay surface properties, aqueous speciation, the concept of anion exclusion, the diffusion accessible porosity and the role of organic matter.

If many potential clay formations have already been considered and/or are being investigated at surface (outcrops, mapping, 3-D survey) or subsurface (hydraulic testing, core sampling) in Canada, France, Germany, Italy, Japan, the United Kingdom and the United States, more detailed characterization programs have been developed from underground infrastructures (URL, mine, tunnel) for the following formations:

- the Boom Clay (Rupelian) in Belgium;
- the Opalinus Clay (Aalenian) in Switzerland;
- the Boda Claystone (Upper Permian) in Hungary and
- the Tounemire Claystone (Toarcian/Domerian) in France.

These formations are briefly described below within their geologic context and some features of importance in understanding their hydromechanical behavior are highlighted. The paper also addresses generic or specific key geologic questions. One can for example mention the importance of diffusion through the clay matrix, the difficulties in reconciling small and large-scale hydraulic conductivities, the discrepancy between laboratory and field-testing and the role of the excavated disturbed zone. When dealing more specifically with the suitability of indurated clay or claystone, the issue of fluid flow through faults and fractures needs to be understood in order to assess its relevance to repository safety. Depending on the formation considered and the local conditions self-healing of fractures is sometimes noticed; mechanical and chemical phenomena can explain the presence of tight faults at repository depth (Lalieux and Horseman 1996). For most of the questions addressed rock mechanics play a central role, not only regarding constructional aspects and fracturation, but also in connection with hydraulics.

It should further be stressed that the application of hydraulic testing and groundwater sampling to very low permeability formations requires improvement of equipment, test procedures and interpretation methods. In this context, experience can be gained from the people involved in the field of petroleum research.

Repositories for geologic disposal of radioactive waste

The geologic disposal of high-level and long-lived waste is generally based on a multi-barrier concept. Each barrier considered must fulfill a specific role for a well-defined time period in order to provide redundancy in the safety of the entire disposal system and to restrict to some extent the coupling effects to be taken into account. When considering clay as host rock it is generally the main barrier with regard to the critical radionuclides.

The integrity of the host clay must be preserved from disturbances likely to be produced by the repository itself (excavation, heat, radiation, and gas). The large

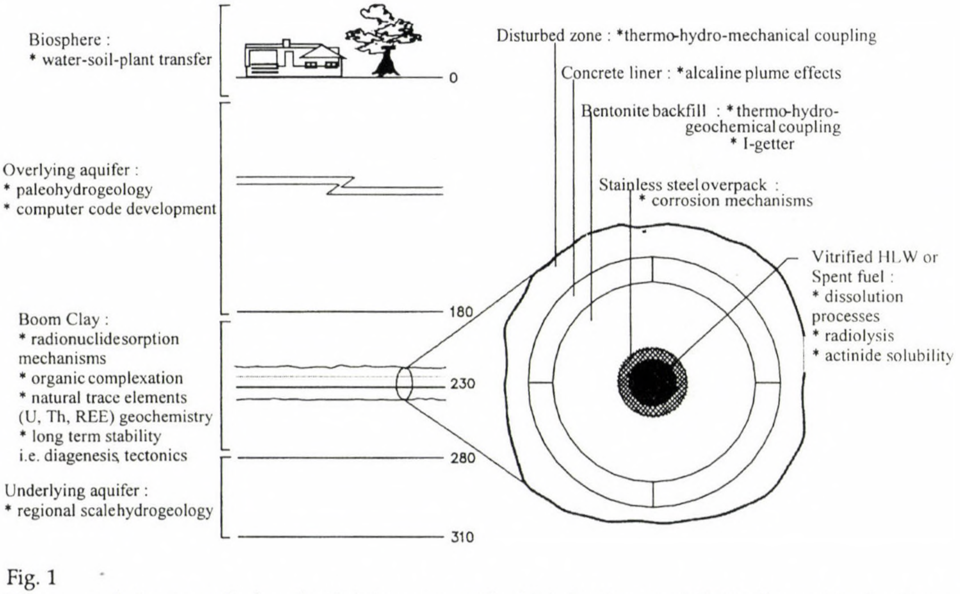

Fig. 1
Key research items applied to the Belgian concept for high level waste (HLW) disposal in the Boom Clay

R&D program associated with these studies not only considers the near field (source term, disposal galleries) but also the geosphere (far field) and the processes taking place in the biosphere (Fig. 1). Ongoing research programs are aimed at demonstrating both the feasibility and the safety of the repository concept and are guided by iterative performance assessments. For demonstration and validation purposes, large-scale integrated experiments must be performed from underground structures in near-real conditions.

With regard to the feasibility of the repository construction key questions mainly deal with geologic structure (layout/concept), soil and rock mechanics (tunneling, lining), hydrogeology (water inflow), rock composition and temperature (operation, depth).

As far as safety is concerned the key issues are related to groundwater flow and radionuclide transport mechanisms, impact of excavated disturbed zone (enhanced hydraulic conductivity), gas effects, effect of alkaline plume on host rock properties, tectonic long-term stability, minimum depth (maximum erosion), and long-term geologic changes.

Referring to the Belgian situation illustrated in Fig. 1 the contribution of the geosphere to repository safety can be summarized in three points:

– Physical protection of the disposal system for long-term periods, providing a better integrity of the engineered barriers and a lower risk of human intrusion;

– Radionuclide retention by sorption and transport limited to matrix diffusion (low hydraulic conductivity and gradients, reducing groundwater chemistry);

– Dilution of contaminated waters in aquifers and surface waters.

Overview of some argillaceous formations and associated key questions

We refer below to the four formations previously mentioned, which can be compared on basis of the information provided in Table I. Depending on the host formation considered and their geologic features specific key questions will be discussed case by case.

Table I
Comparison of selected argillaceous formations

Argillaceous Formation	Age	Water content	Clay minerals	Quartz	Feldspars	Carbonates
Boom Clay	Lower Oligocene (Rupelian) 32 Ma	19–24%	55–65%	20–60%	5–10%	1–5%
Opalinus Clay	Middle Jurassic (Aalenian) 175 Ma	4–12%	40–80%	18–20%	1–3%	5–20%
Tournemire Claystone	Middle Jurassic (Domerian, Toarcian, Aalenian) 180 Ma	1–4%	25–50%	15–20%	0–1.5%	18–54%
Boda Claystone	Middle Permian 230 Ma	?	30–70%	10–50%	10–50%	0–25%

The Boom Clay Formation

Geologic setting

During the Lower Oligocene, an extensive sea (the North Sea) covered large areas of northern Europe. In the deeper part of the North Sea basin, a clay deposit was formed. In Belgium this clay formation is known as the Boom Clay. Sedimentation of the Boom Clay occurred in an open marine shelf environment, 50 to 150 m deep, in a subtropical climate (Vandenberghe and Van Echelpoel 1987).

The Boom Clay Formation is present in northern Belgium (Fig. 2). At Mol the Boom Clay is present beneath SCK•CEN at a depth of 190–293 m. It occurs in a sequence of Tertiary sands and clays (Fig. 3).

Sedimentological characteristics

A detailed sedimentological study by Vandenberghe (1978) indicated that the Boom Clay is characterized by a rather constant chemical and mineralogical composition. Variations in grain size, organic matter, and carbonate content occur and result in the typical layering of the Boom Clay. The variations reflect changes in local tectonics, eustacy and climate and are associated with Milankovitch cyclicity (Van Echelpoel 1991).

Lithostratigraphy

Lithostratigraphically, the Boom Clay can be divided into the Belsele-Waas Member (the lowest and more silty part of the Boom Clay), the Terhagen Member (the least silty part of the Boom Clay), the Putte Member (with high organic matter and low calcareous matter content) and a "transition zone" containing 10 clearly defined silty layers.

Key Geologic Questions

The Boom Clay Formation has been characterized at a rather local scale by a detailed research program, the HADES project, initiated in the late 70s. From what has already been mentioned two specific questions have been raised in the preliminary phases of the project:

– What are the possibilities of digging and lining large-diameter galleries in such a plastic clay at great depth, under high lithostatic pressures, and how will the host clay be affected by construction work?

– How far do we need to analyze the spatial variability of this aquitard (Boom Clay) and of the aquifers when dealing with the regional hydrogeologic modeling work with a view to performance assessment?

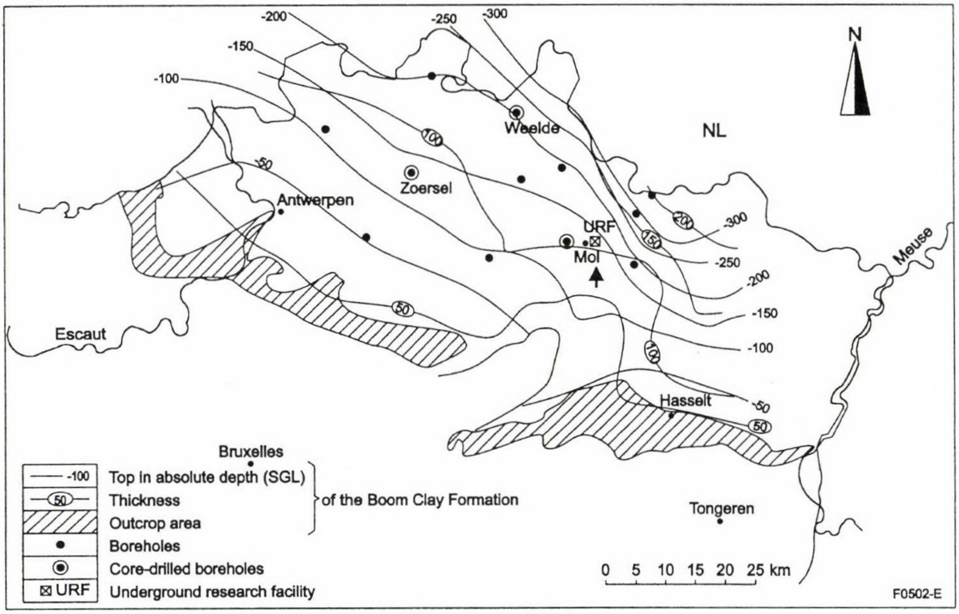

Fig. 2
Outcrop zones of the Boom Clay and location of the Mol-1 borehole. To the north of the outcrops, the Boom Clay is present in the subsurface

The first question was investigated in detail during the construction of the underground research laboratory (URL) which took place in different steps with regard to the mining techniques applied, the diameter considered and the performance of the lining (interaction with clay). The second question has required e.g. the extension of reconnaissance works (seismic survey) and of the piezometer network, including the underlying aquifer. In this context, the difficulties in reconciling small- and large-scale hydraulic conductivities have been taken into account. Providing confidence in long-term safety has also justified launching more recently studies on the paleohydrology of the site.

The Opalinus Clay Formation

Nagra is investigating the Opalinus Clay of northern Switzerland as a potential host rock formation. A site selection program was begun in 1986, which resulted in the selection of a siting region of 500 km². A detailed seismic survey was carried out in 1991/92 in this region and an area of 30 km², showing a tectonically almost undisturbed stratification, has been selected for site characterization with a deep borehole with detailed hydraulic hydrochemical and rock mechanical investigations, accompanied by a 3D seismic survey. In this region, the Opalinus

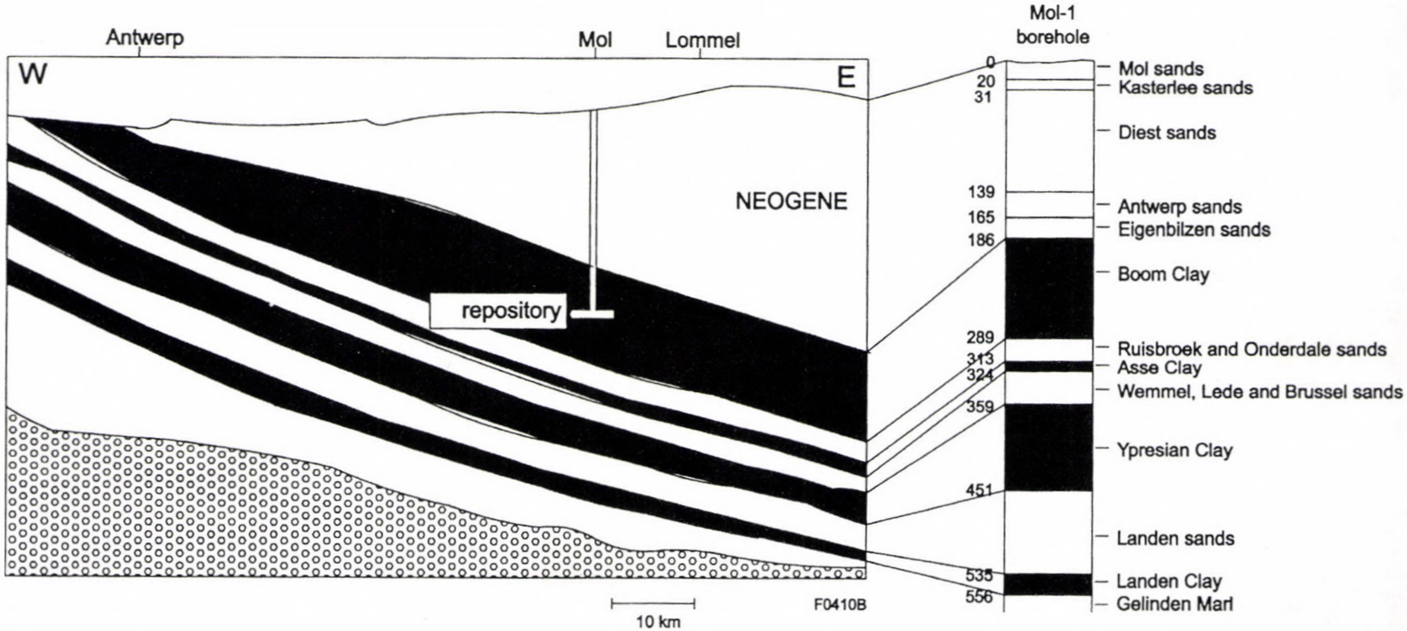

Fig. 3
Geologic section through Tertiary Formations in northern Belgium

Clay occurs as a 110 to 120 m-thick subhorizontal layer with its top at a depth of about 500 m.

In 1995 an international research project started at Mont Terri (Jura) in the Opalinus Clay. This project is under the patronage of the Swiss National Hydrological and Geological Survey. Some key issues to be assessed are groundwater flow mechanism in intact shale and faults, pore water chemistry, excavation-disturbed zone and the evaluation of appropriate investigation techniques (Thury and Bossart 1999).

Geologic setting

The Opalinus Clay was deposited in a very shallow marine environment (between 20 and 50 m) during the Middle Jurassic (Aalenian). A stratigraphic section of the sedimentary sequence of Northern Switzerland is given in Fig. 4 and a geologic section along the Mont Terri tunnel is provided in Fig. 5.

Lithostratigraphy

In the Opalinus Clay three slightly different facies can be distinguished: a shaly facies in the lower half of the sequence, a 15 cm-thick sandy-limy facies in its middle part and a sandy facies interstratified with a shaly facies in the upper part of the sequence. It generally consists of dark gray micaceous shale, partly with thin sandy lenses, limestone concretions or siderite nodules. It is mainly composed of clay minerals (illite, kaolinite, chlorite, illite/smectite mixed layers), quartz and carbonate. Feldspar, pyrite and organic carbon are also present. The water content is in the range of 4 to 12 % (Gautschi 1997).

Specific Key Geologic Question

The Opalinus Clay is a well-consolidated claystone with joints and fault zones. Near the surface, it is relatively permeable due to chemical-mechanical weathering and decompression resulting from erosion of overlaying strata. At greater depths (>100 m) the hydraulic conductivity is relatively low (Gautschi 1997). One of the questions to be addressed was the risk of occurrence of a significant groundwater flow through joints and faults, even at great depth. Subsurface investigations have shown that such an event rarely occurred. Furthermore, at places of water inflow, the swelling of clay minerals often heals fault zones occurring in the rock. As a result of this the rock retains its extremely low permeability (10^{-14} to 10^{-12} m/s). Similar conclusions are inferred from studies on pore water chemistry (relationship composition/residence times). For instance, increasing salinity indicates a transition to a zone of stagnant pore water where diffusion is the dominant migration mechanism (extremely long underground residence times).

The Boda Claystone Formation

The field work in the siting are started in Hungary in 1989 in the western Mecsek Mountains, where an upper Permian albitic claystone, the Boda Aleurolite Formation, was considered to be a suitable geologic host rock. The formation dips beneath a uranium-ore-bearing sandstone formation, which has been exploited for 42 years. Utilizing the facilities and infrastructure of the uranium ore mine, it was possible to explore the formation relatively quickly at the depth of 1,050 m. Despite the large amount of information on the Boda Claystone Formation at this location, some new exploratory tunnels and boreholes drilled after 1993 gave direct access to almost every rock lithology including geologic, hydrogeologic, geochemical and geotechnical features (Ormai et al. 1998a).

The objective of these studies was a preliminary characterization of the Boda Claystone Formation as a potential host rock for a HLW repository.

Geologic setting

Hungary lies in the central part of the Pannonian Basin, surrounded by the Alps, the Carpathians and the Dinarides. The Western Mecsek area consists of Paleozoic and Mesozoic rocks and includes a potential host formation: the Boda Claystone Formation (BCF). The Boda Claystone Formation is a lacustrine deposit set within a sequence of fluvial sandstones, which were deposited in a semi-arid climatic environment (Ormai et al. 1998b). It covers an area of 150 km^2 and is 700 to 900 m thick. However, its structure is quite folded and faulted, mainly as a result of pre-Pliocene tectonic activities (Fig. 6).

Lithostratigraphy

The Boda Claystone contains several stratigraphic members in a vertical section (Fig. 7), without obvious boundaries but with only slightly different properties. In general it is a strongly oxidized, thin and thick-bedded, predominantly reddish brown sedimentary formation. Its chemical composition is quite uniform. It is composed of quartz and feldspar with a high clay content and a significant amount of fine-grained hematite. The claystone has higher quartz content in the upper part of the formation, and the matrix contains up to 10% primary dolomite in layers 1 to 10 cm thick (Ormai et al. 1998a).

The Boda Claystone is highly consolidated and has a very low overall permeability. Faults in the claystone are mostly sealed and filled with calcite, barite, gypsum and clay minerals.

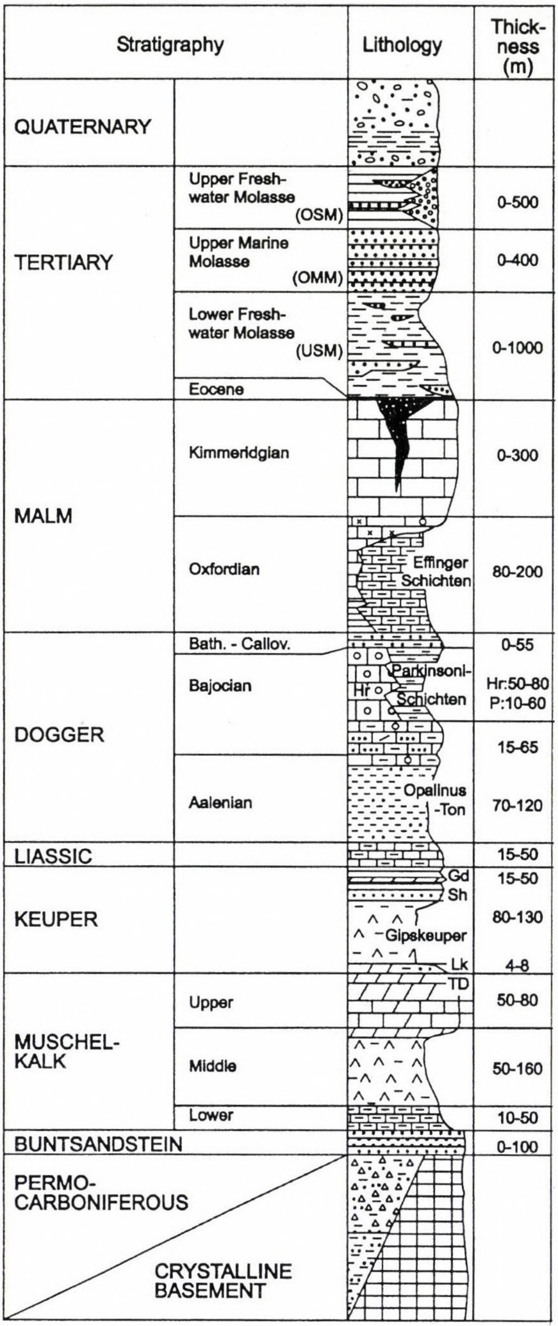

Fig. 4
Stratigraphic section of the sedimentary sequence of Northern Switzerland (Johns et al. 1994)

Lithological description	Hydrogeological characterisation
Moraine, fluvio-glacial gravels and sands, lacustrine clays	Aquifer important for water supply, locally with low permeability beds
Channel sandstones, marls and conglomerates	Various water conducting sandstone channels and layers
Sandstones, glauconitic and bioclastic	Regional aquifer
Channel sandstones and variegated marls	Various water conducting sandstone channels and layers
Micritic limestones, massive to well-bedded	Regional aquifer
Coralline limestone, oolites Alternation of argillaceous limestones and calcareous shales	Effinger Schichten: low permeability Local aquifer in the western Jura ("Rauracian")
Bioclastic limestones, marls Fe-oolite Oolites (Hr), Mudrocks (P)	Parkinsoni-Schichten: low permeability Hr: local aquifer
Sandy bioclastic limestones, shales, Fe-oolite Monotonous sequence of dark grey silty, micaceous clays	Low to very low permeability
Bioclastic limestones, sandy shales Variegated marls, dolomite variegated sandstone	Low permeability rocks with local aquifers
Alternation of shales, nodular and bedded gypsum/anhydrite Satin spar veins	Very low permeability
Dolomite, porous Limestones, bedded	Regional aquifer
Dolomite, laminated Alternation of shales, bedded and massive anhydrite Rock salt Silty mudstones, shales	Very low permeability
Sandstone, porous to well-cemented	Regional aquifer
Permian (Rotliegendes): Red siltstones, sandstones and breccias Carboniferous: sandstones, siltstones bituminous shales, breccias, coal seams Basement: Gneisses with Variscan granite and syenite intrusions	Permo-Carboniferous: water conducting detrital layers Crystalline basement: water conducting faults and fracture zones

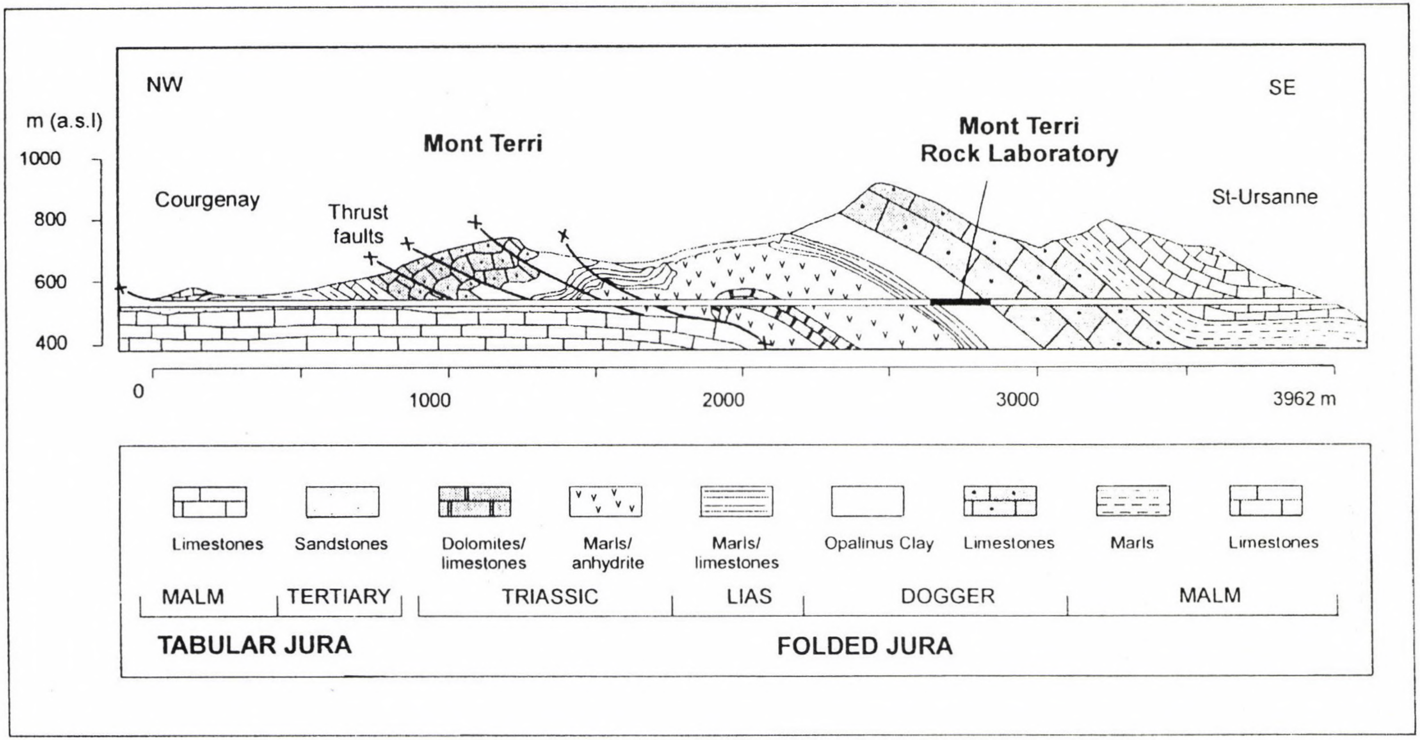

Fig. 5
Geologic section across Mont Terri (Schaeren and Norbert 1989)

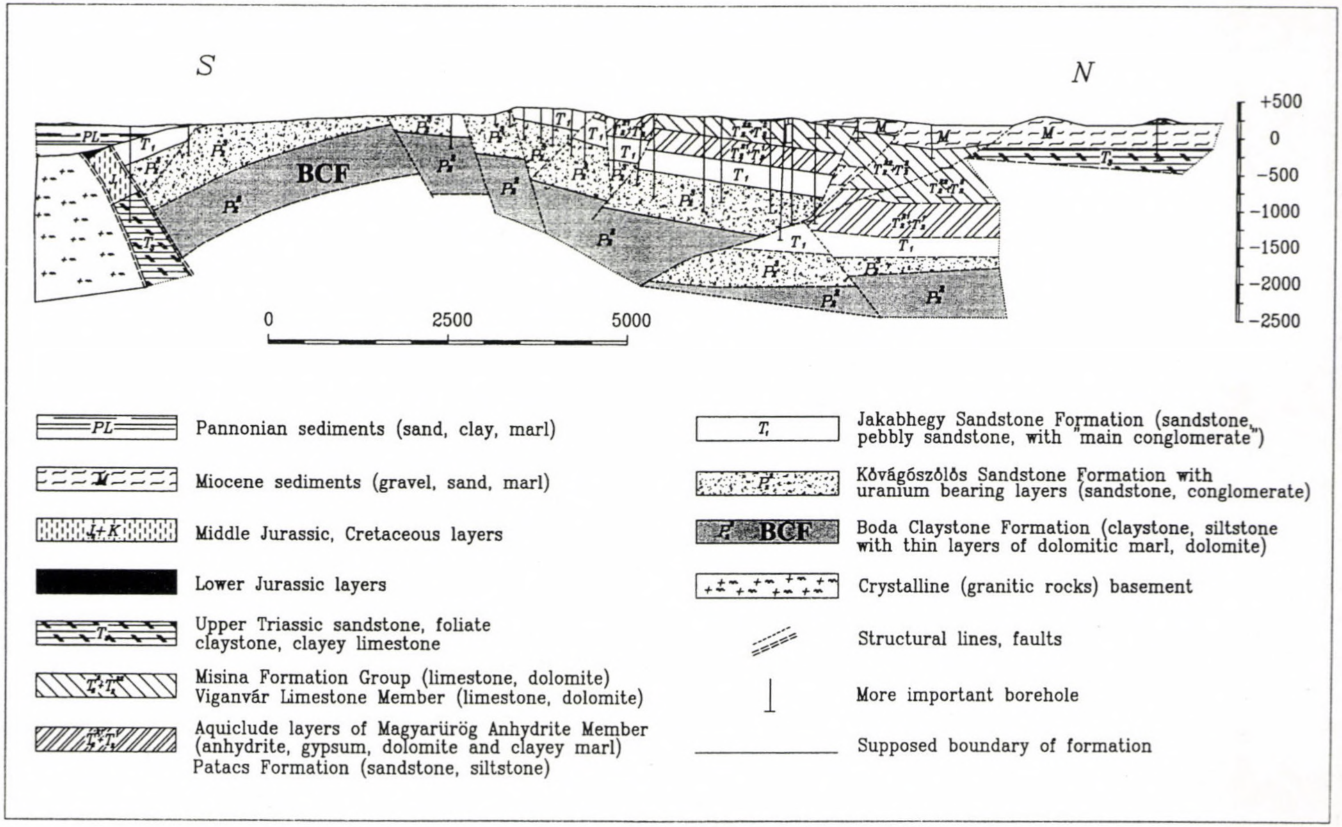

Fig. 6
Geologic cross-section in the western Mecsek Mountains (from Gy. Konrad, and G. Hámos)

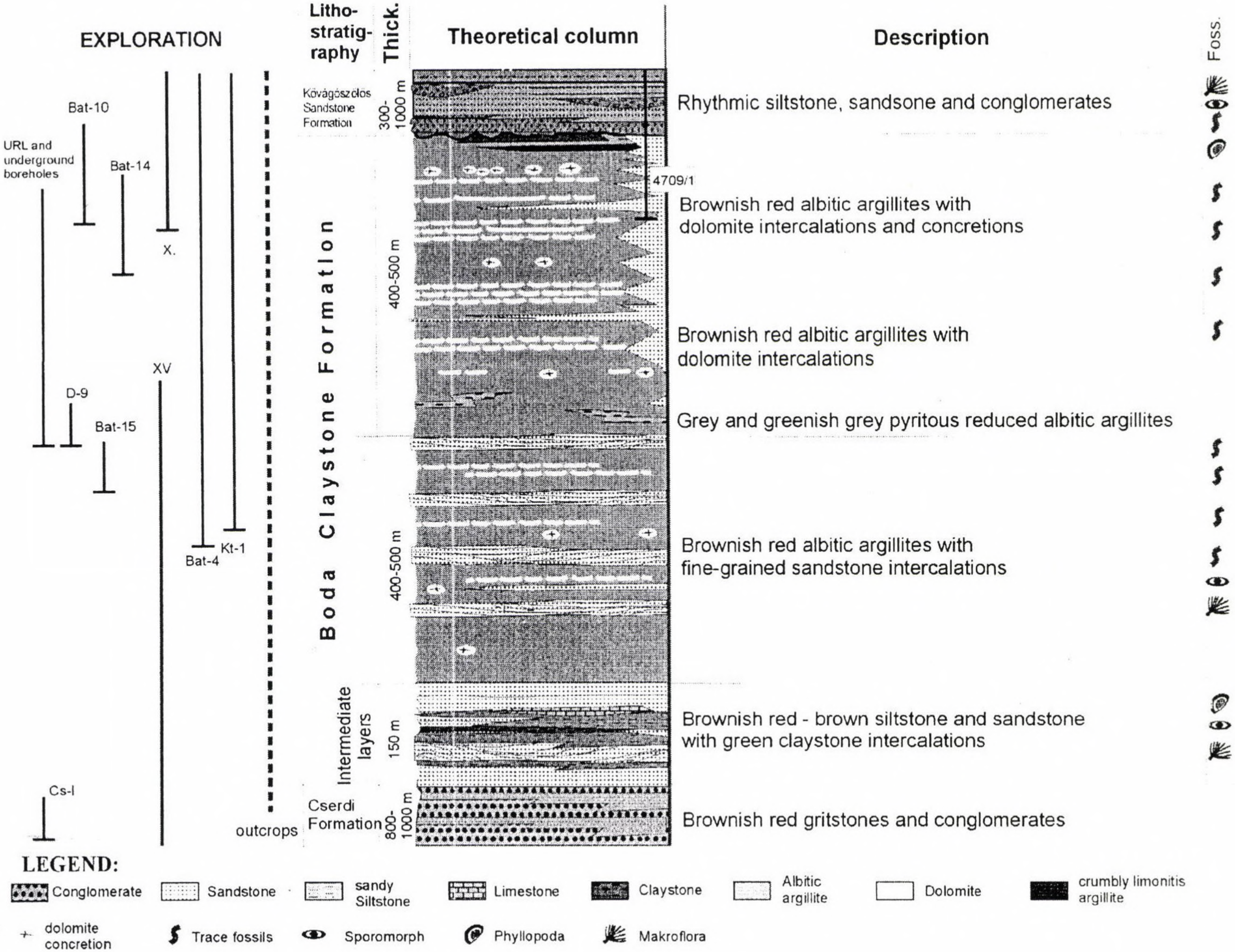

Fig. 7
Stratigraphic section of the Boda Claystone Formation (from Gy. Konrad, and G. Hámos)

Specific Key Questions

The overall information (structure, area, thickness, composition) supports the selection of the Boda Claystone for hosting a HLW repository. However, a question must be raised in this context: is the mining activity and the proximity of natural resource not a site-specific risk to be recognized? To evaluate different potential areas of this large formation, a much more detailed understanding of the lithological, hydrogeologic, geophysical, geochemical and geomechanical conditions of this claystone, adjacent formations and crosscutting faults is required.

The Tournemire Claystone

IPSN (France) is developing *in situ* research programs addressing the confining properties of argillaceous formations. For that purpose, since 1988 the Tournemire tunnel site (Aveyron, France) has been considered for methodological studies only.

Geologic setting

The Tournemire site is located in a Mesozoic marine basin at the southern border of the French Massif Central. The site has been chosen because of its relatively simple geology and because of the presence of a 2 km-long old railway tunnel, which gives a good access to the Toarcian formation. This formation consists of a 250 m-thick indurated Toarcian to Domerian claystone layer, with its top at about 200 m depth. The formation is overlain by 270 m of Bajocian to Bathonian limestone. Cenozoic and post-Cenozoic tectonics have affected the Jurassic formation. A geologic section and stratigraphic column are given in Fig. 8.

Lithostratigraphy

The site of the Tournemire tunnel is located in a sequence of subhorizontal Jurassic sedimentary rocks on a rather large scale consisting of three lithologies:

– upper layer: limestone and dolomite (Upper Aalenian, Bajocian and Bathonian)

– intermediate layer: clayey lithology (Domerian, Toarcian and Lower Aalenian)

– lower layer: limestone and dolomite (Hettangian, Sinemurian and Carixian).

In the Toarcian formation the mineralogy consists of clay minerals (kaolinite, illite-montmorillonite) and mica (40%), of quartz (20%), calcite (20%) and some other phases like dolomite, pyrite, feldspar and siderite (Barbreau and Boisson 1993).

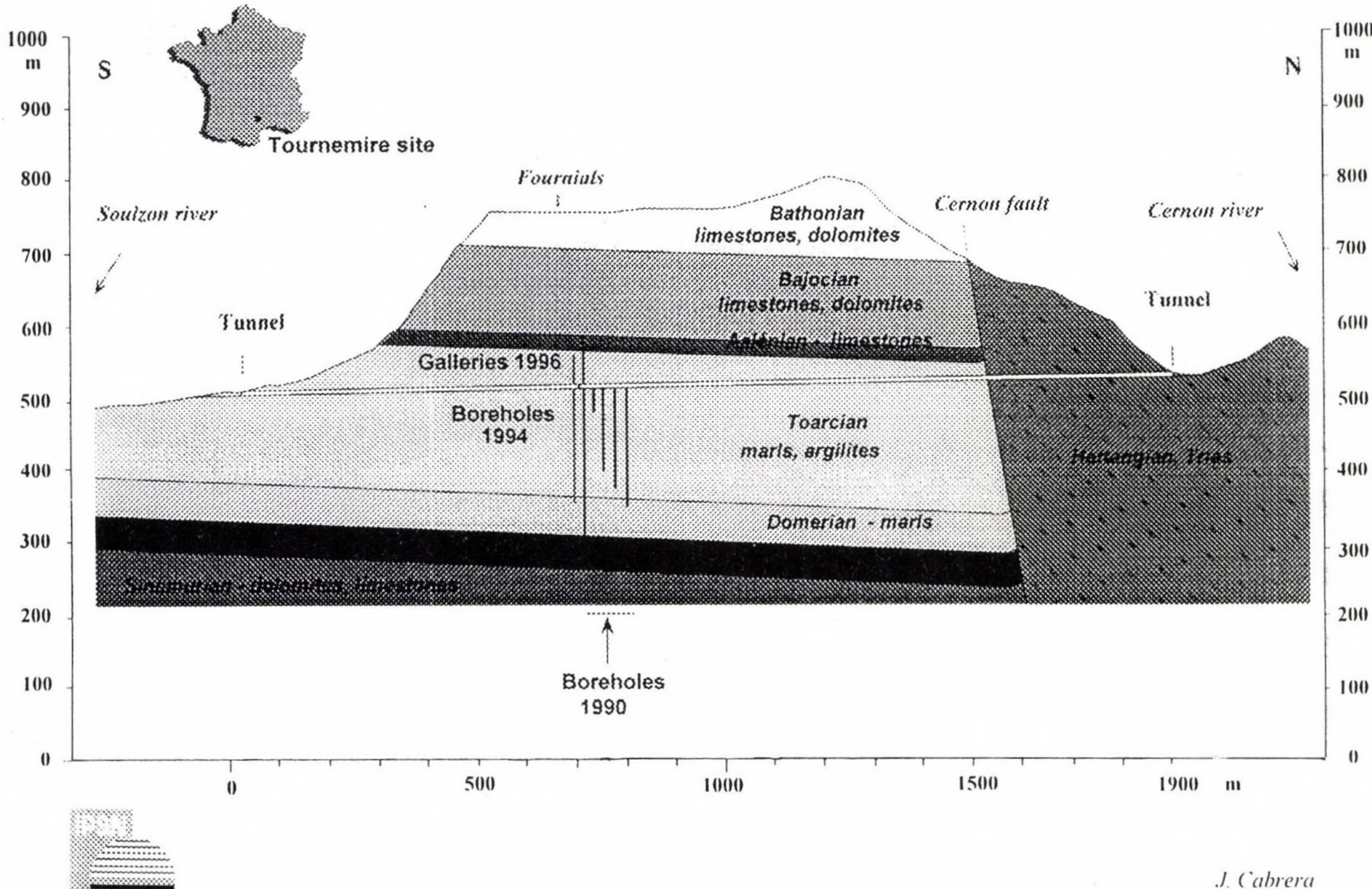

Fig. 8
Geologic cross-section of the Tournemire site (from IPSN)

Specific Key Geologic Question

Because of the very low permeability and porosity, pore water transfer should be of very minor importance and very difficult to detect. However, the existence of faults or fractures should be taken into account, in particular the possible transfers between the aquifers above and below the Toarcian and Domerian argillites. Fracturation analysis of the Tournemire Claystone Formation has been performed by means of 14 boreholes drilled from the tunnel (Boisson et al. 1996, Fig. 9). This study showed the existence of two kinds of planes: planes with different types of calcite filling, and planes without filling. The latter fracturation seems perfectly sealed and impervious to any circulation (Boisson et al. 1996). Pore water circulation within this Jurassic rock mass occurs essentially in the two dolomite/limestone formations, following the N-S fracture network. In contrast, in the intermediate formation any circulation is highly improbable.

The study of the texture, mineralogy and geochemistry of the fracture fillings becomes a priority to better characterize the potential transfer of water through the fractures. Texture, mineralogy, chemical and isotopic contents of the secondary carbonates from the fractured zones have been analyzed in order to determine the origins, ages and chemistry of the initial circulation (Boisson 1996; Boisson et al. 1996; Littleboy et al. 1997). Such information related to the fracture fillings is essential to identify paleocirculation, to classify the successive generations of fractures and to distinguish among them those which might have acted as preferential pathways for water circulation over long distances. The chemical nature of the paleofluids can be determined as well.

Conclusions

The different issues addressed in the previous sections for four potential sites or formations clearly show the direct and indirect impact of geology and geosciences on the feasibility and safety aspects of a repository in argillaceous formations. In particular, rock mechanics are a key factor in determining repository depth. Beside the difficulties and restrictions related to the time scales considered for long-lived waste, the spatial variability observed in nature requires further uncertainty and sensitivity studies.

One way of increasing confidence when assessing the performance of an entire disposal system is of course to have access to reliable and representative field data in near-real conditions for the key parameters. The information gathered from generic sites is therefore as important as the data from potential repository sites, especially when tools, methods and experience are still under development.

The mechanical aspects related to depth, history and lithology are essential for plastic clays where high convergence rates must remain under control without disturbing the surroundings. At the same time the occurrence and the role of fractures and faults in indurated clay formations and shale with regard to water

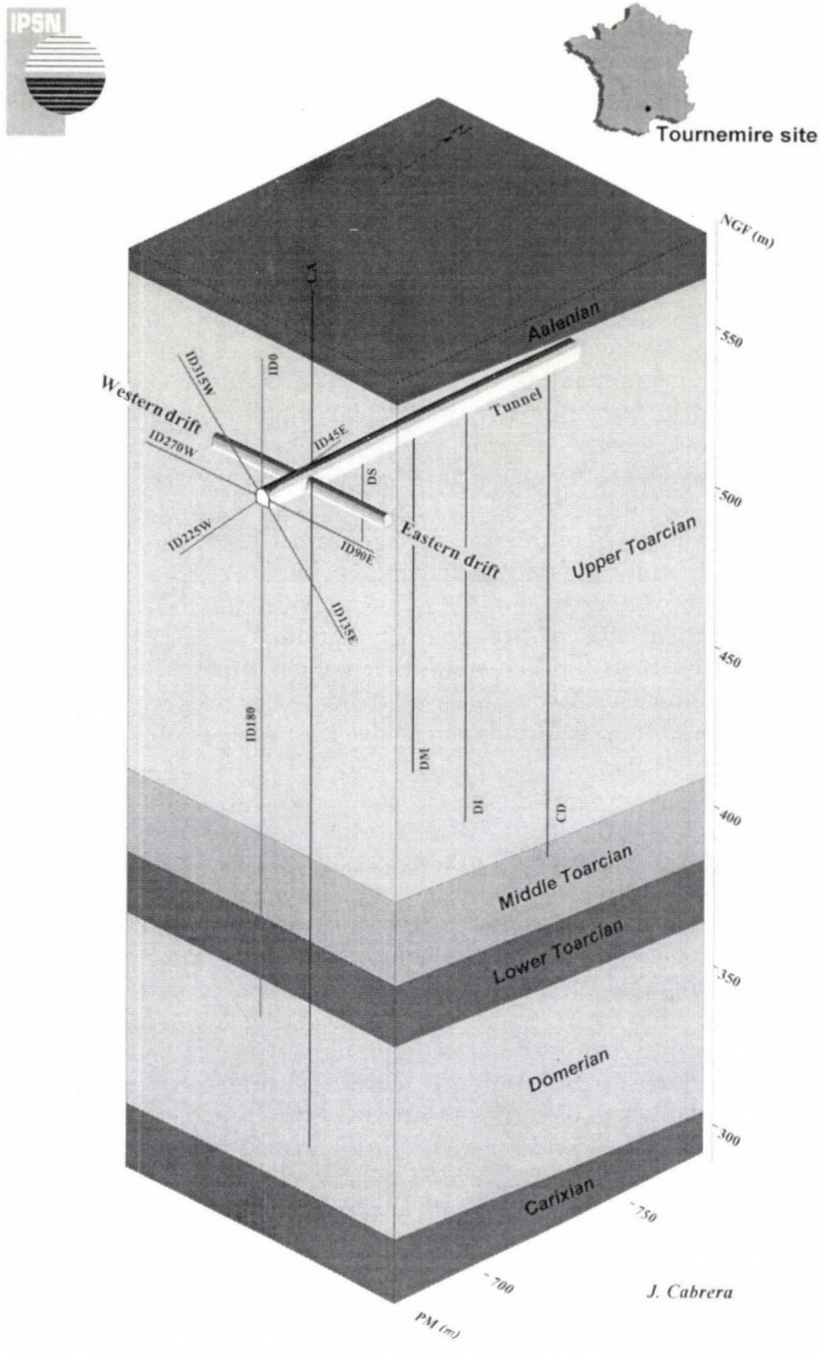

Fig. 9
Geologic block-diagram with borehole and drift locations (from IPSN)

transfer require large research programs and new development, as briefly described for the study on fracture fillings. In addition the nature of such claystone makes any study on water/rock interaction very difficult.

Table II gives an overview of the key geologic questions and illustrates the relationship with the geologic formations discussed in this paper.

Table II
Synoptic summary of geologic key questions

Examples	Boom Clay (Rupelian)	Opalinus Clay (Domerian)	Boda Claystone (Upper Permian)	Tournemire Claystone (Toarcian/Domerian)
Geological key questions	0 not applicable + relevant ++ particularly relevant			
Diffusion through the clay matrix	++	++	+(+)	+(+)
Scale effects for hydraulic conductivities	+	+	+	+
Role of the excavated disturbed zone	++	+	+	++
Fluid flow through faults and fractures	0	+	+	+
Fracture fillings	0	0	+	++
Self-healing of fractures	+	+	0	0
Understanding of tight faults	0	+	++	++
Impact of spatial variability	+	+	+	+

The increasing integration of various types of geoscientific data is needed and currently carried out within national programs to fully comprehend the internal structure and behavior of argillaceous formations. To illustrate this we refer to another paper presented by M. De Craen (also in this volume) dealing with the distribution and mobility of natural U and Th in Boom Clay. Such a multi-disciplinary integration in an international context also contributes to confidence building.

References

Barbreau, A., J-Y. Boisson 1993: Charactérisation d'une formation argileuse, synthèse des principaux resultats obtenus à partir du tunnel de Tournemire. – Rapport d'avancement Nr 1. Contrat CEE-CEA nr. FI 2W-CT 91-0115, 153 p.

Boisson, J-Y. 1996: Transfer Process Studies through a Toarcian Argilite. – Proceedings of the International Congress on Radiation Protection, Vol. 3., Vienna, Austria, April 14–19, 1996.

Boisson, J.-Y., J. Cabrera, L. De Windt 1996: Investigating Faults and Fractures in Argillaceous Toarcian Formation at the IPSN Tournemire Research Site. – In: OECD Proceedings Fluid Flow through Faults and Fractures in Argillaceous Formations, A joint NEA/EC Workshop, Bern, Switzerland, 10–12 June 1996, pp. 207–222.

Gautschi, A. 1997: Hydrogeology of the Opalinus Clay – implications for radionuclide transport. – Nagra bulletin, 31, pp. 24–32.

Horseman, S., J. Higgo 1994: Summary Report on the Workshop on "Determination of Hydraulic and Hydrochemical Characteristics of Argillaceous Rocks". In: Hydraulic and Hydrochemical

Characteristics of Argillaceous Rocks, Proceedings of an International NEA Workshop, Nottingham, United Kingdom, 7–9 June 1994, pp. 7–14.

Johns, R.T., S.G. Vomvoris, S. Löw 1994: Review of Hydraulic Field Tests in the Opalinus Clay of Northern Switzerland. – In: Hydraulic and Hydrochemical Characteristics of Argillaceous Rocks, Proceedings of an International NEA Workshop, Nottingham, United Kingdom, 7–9 June 1994, pp. 167–177.

Lalieux, Ph., S. Horseman 1996: Fluid Flow through Faults and Fractures in Argillaceous Formations – Synthesis of the Workshop. – In: Fluid Flow through Faults and Fractures in Argillaceous Formations, A Joint NEA/EC Workshop, Berne, Switzerland, 10–12 June 1996, pp. 11–30.

Littleboy, A.K., J-Y. Boisson, P. De Canniere, L.Y. Griffauly, A.J. Hooper, F. Plas, J.M. Palut 1997: Site characterisation – Methods and Approaches. Proceedings of the Fourth European Conference on "Management and Disposal of Radioactive Waste", ed. By T. McMenamin, EUR 17543 EN.

Ormai, P., F. Frigyesi, O. Pavlik, Z. Balla, L. Kovács 1998a: Double challenge for Hungary in radwaste management, Paper presented at WM '98 conference at Tucson, USA. – In: Information Package on Boda (Western-Mecsek) Claystone Formation, June 1998.

Ormai, P., F. Frigyesi, I. Benkovics, L. Kovács, J. Csicsák, Gy. Majoros, G. Érdi-Krausz, Gy. Bárdosy 1998b: Hungarian Approach For Final Disposal of High Level Radioactive Waste, Chapter 12 – In: Geological Problems in Radioactive Waste Isolation, ed. By P.A. Whiterspoon, pp. 113–123.

Schaeren, G., J. Norbert 1989: Tunnel du Mont Terri et du Mont Russelin – La traversée des 'roches à risques': marnes et marnes à anhydrite. – In: La traversée du Jura – Les projets de nouveaux tunnels. SIA-Dokumentation D 037. Swiss Society of Engineers and Architects (SIA), Zürich.

Thury, M., P. Bossart 1999: The Mont Terri rock laboratory, a new international research project in a Mesozoic shale formation, in Switzerland. – Engineering Geology, 52, pp. 347–359.

Vandenberghe, N. 1978: Sedimentology of the Boom Clay (Rupelian) in Belgium. – Verhand. Kon. Acad. Wetenschappen België, 40, 147, 137 p.

Vandenberghe, N., E. Van Echelpoel 1987: Field Guide to the Rupelian Stratotype. – Bulletin van de Belgische Vereniging voor Geologie, 96/4, pp. 325–337.

Van Echelpoel, E. 1991: Kwantitatieve Cyclostratigrafie van de Formatie van Boom (Rupeliaan, België) – De Methodologie van het onderzoek van Sedimentaire Cycly via Walshanalyse. Unpublished PhD. K.U.Leuven.

Acta Geologica Hungarica, Vol. 43/2, pp. 135–143 (2000)

Repositories for high level radioactive waste in crystalline rocks, key geologic questions

Timo Äikäs
Posiva Oy, Helsinki, Finland

The key questions for geologic disposal are
- What are we looking for from a suitable geologic environment?
- What is the role of the geologic barrier?
- How good a geologic barrier is needed?

The purpose of final disposal at great depth in a geologic formation is to remove radioactive waste from man's environment and place it out of reach of major disruptive processes. Crystalline bedrock is expected to provide an environment where the rates of natural processes affecting the waste packages and engineered barriers are slow. The basic criteria for siting a deep repository, however, is that the formations considered for final disposal are known to be located in geologically stable areas and preconditions for final disposal are known generally be favorable. This would mean that waste packages, together with their engineered barriers, maintain their integrity and radioactive wastes are isolated permanently from the biosphere. However, can scientific evidence, multidisciplinary and consistent, be collected and analyzed to describe this expected natural evolution of the crystalline environment for the site-specific safety assessment? If this can be successfully done it will have a strong impact on the confidence of the safety case and acceptance of the deep repository.

Key words: radioactive waste management, geologic disposal, spent fuel disposal, site characterization, safety assessment

Introduction

Crystalline bedrock has been the target for intensive investigation into final disposal of high-level nuclear waste since the 1970s. These formations include large areas like the Fennoscandian and Canadian Shield areas, as well as smaller formations of crystalline bedrock beneath sedimentary cover. Common to all formations studied are the structural features – abundance of fracturing and existence of fracture zones. These structural features, together with the groundwater, have received considerable attention in research aiming at safe final disposal in the crystalline environment.

Typical of a disposal concept developed for crystalline bedrock has been the use of metal canisters as the primary engineered barrier. The highly active radioactive waste is packed in canisters. These long-lasting, watertight canisters are intended to prevent radioactive substances from entering the groundwater. The canisters are surrounded by a buffer material, most commonly bentonite clay, which acts as a further barrier to reduce groundwater movement and, in the

Address: T. Äikäs: Posiva Oy, Töölönkatu 15 A, 00100 Helsinki 10, Finland
Received: 14 September, 1999

0236–5278/2000/$ 5.00

event of canister leakage, would keep the radioactive substances from passing onward. The surrounding geosphere is thus one of the many components in a multi-barrier system for final disposal.

This paper is based largely on the experience gained in the research process in Finland aiming at site selection. The program for the siting of a deep repository for final disposal of spent nuclear fuel was already begun in 1983 and is carried out today by Posiva Oy, which continues the work started by Teollisuuden Voima Oy (TVO). The program has progressed in successive interim stages with defined goals (Fig. 1). After an early phase of site identification, five sites were selected in 1987 for preliminary site characterization. Three of these were selected and judged to be best suited for more detailed characterization in 1992. An additional, new site was included into the program based on a separate feasibility study at the beginning of 1997.

Since 1983 several safety assessments, together with technical plans for the facility, have been completed in parallel with the site characterization. Posiva's disposal concept is based on the KBS-3 solution originally developed in Sweden during the early 1980s. During the process of site selection research program, the needs for more detailed consideration of the site-specific properties in safety assessment were increased. The latest safety assessment, TILA-99 (Vieno and Nordman 1999), discusses the site-specific properties of the four candidate sites characterized. Based on the safety assessment and site evaluation all sites can provide a stable environment for safe final disposal.

Posiva submitted an application to the Council of State for a decision in principle, in accordance with the Nuclear Energy Act, in May 1999. In the application the Olkiluoto site in Eurajoki in western Finland (Fig. 1) was nominated as the site to be selected. The decision-making process is underway and will culminate in 2000 when the Government and the Parliament are expected to make their decision.

To begin with

The final disposal concept planned so far has been based on the multi-barrier principle (Fig. 2). In this system the radioactive substances are isolated using a series of independent protective barriers. In this way, if one barrier fails it does not affect the overall barrier function. In this system the geosphere is one of the barriers, together with man-made, engineered barriers.

Many safety cases (SKB-91, TVO-92, Kristallin-I, AECL, SKI-94, TILA-96) together with TILA-99 have shown that the safety-related requirements are probably met by most sites identified and characterized in the crystalline basement areas, which are candidate sites for a deep repository. This experience raises a question: how good the geologic barrier of the selected site will be as a whole? The waste will finally be placed in these bedrock volumes, characterized

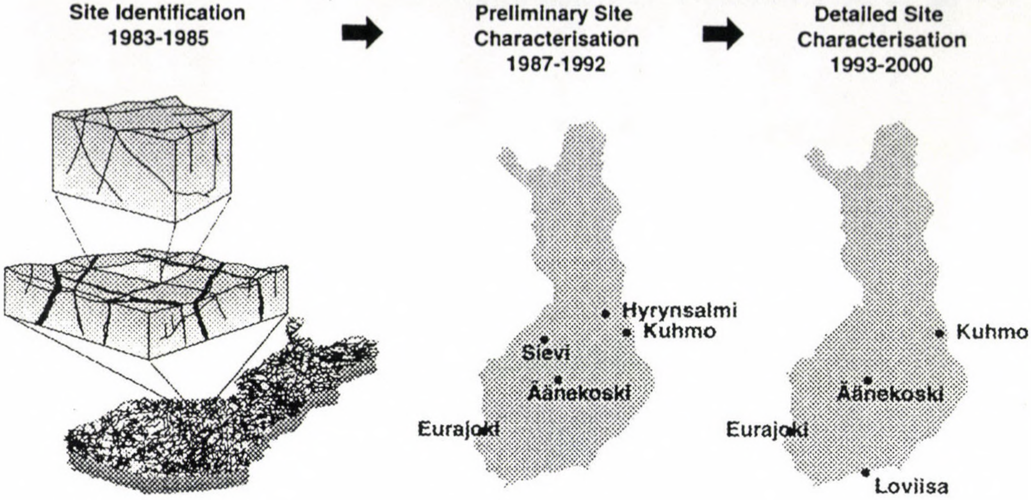

Fig. 1
Site selection research programme aiming at site selection in Finland

in great detail at depth, which are most likely able to provide an effective isolation well into the future.

When judging the importance of crystalline bedrock as a barrier we must begin with the following questions, which then would lead us closer to the key questions in practice:

- what are we looking for from a suitable geologic environment ?
- what is the role of the geologic barrier?
- how good a geologic barrier is needed?

The purpose of final disposal at great depth in a geologic formation is to remove the spent fuel from the human environment and to place it beyond reach of major disruptive processes. The geologic formation is expected to provide an environment where the rates of natural processes affecting the canisters and spent fuel are slow; a thick layer of crystalline bedrock should also provide an adequate shield against a release of radioactive material from the waste itself. The primary function of the bedrock is to provide favorable and sufficiently stable mechanical, chemical and hydrogeologic conditions over long periods of time so that the long-term performance of the engineered barriers is maintained. The bedrock also limits the amount of groundwater coming into contact with buffer material and the containers.

Normally in nuclear technology safety is based on systems built from materials fully characterized and investigated. The behavior of the materials, although not fully understood, can be monitored to maintain a safe operation by making continuous improvements. The main reason for the importance of engineered barriers in a disposal system comes from the fact that at the great depth of the

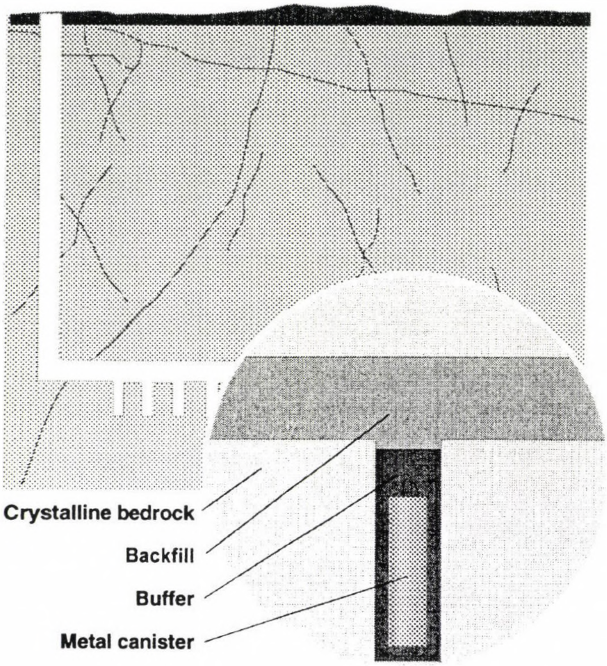

Fig. 2
Multi-barrier principle for final disposal of highly active nuclear wastes in crystalline bedrock

crystalline bedrock practically no technical improvements can be made in terms of the long-term properties of the bedrock. The basic question is how well it is possible to characterize the properties of the bedrock to be used in the repository design and in the site specific safety assessment. Due to the known heterogeneous nature of the geologic environment this question boils down to uncertainties associated with the geosphere, especially in the so-called far field of the repository area. Mainly because this uncertainty a great deal of emphasis in the crystalline environment has been placed on building confidence on the understanding of the near-field of the waste packages in the repository and its interaction with the engineered barrier system.

The main contribution of the geologic barrier of the deep repository to the long-term safety is thus the physical protection of the disposal system as a whole. If something should happen the geologic barrier it should be able to restrict possible radionuclide releases from the repository and through sorption and matrix diffusion be able to retard and retain the radionuclides escaping from the repository into the crystalline rock, so that they do not form a risk to the human environment.

One of the questions is related to the prediction of the future behavior of the crystalline environment together with the complete disposal system over time scales of tens of thousands of years and even longer. The modeling of the degradation of the waste packages, the mobilization of the radionuclides in the groundwater and transport through the geosphere obviously requires careful observations and interpretations of the properties of the crystalline formation, as well as understanding the processes of the natural evolution of the geologic environment. Should this be, however, "realistic" or would the review of a few scenarios suffice?

One scenario, unlikely but still conceivable, can always be defined which leads to activity releases from the repository to the crystalline bedrock. In Scandinavia a post-glacial displacement, for example, is a scenario the probability of which is difficult to judge. In such cases the important question arises how radionuclides will be dissolved from the waste packages and how the groundwater and its possible contaminants will move in fractures of the crystalline bedrock.

What we are looking for from a suitable crystalline environment is that the formations considered for final disposal are known to be located in geologically stable areas and preconditions for final disposal are known generally be favorable. This would mean that waste packages together with their engineered barriers maintain their integrity and radioactive wastes are isolated for a sufficiently long time.

Can scientific evidence, multidisciplinary and consistent, be collected and analyzed to describe the expected natural evolution of the crystalline environment for the site-specific safety assessment? If this can be successfully done it would have a strong impact on the confidence of the safety case and acceptance of the deep repository. The following preferences can be put forward when looking for favorable environment for the repository in crystalline rocks:

- a geologic environment that has evolved only slowly and is currently relatively stable
- a predictable environment, preferably at all scales. This means that homogeneity is preferred in rock types and more homogenous areas are judged to be more amenable to characterization
- low regional and local hydraulic gradients and low hydraulic conductivity of the bedrock are properties desired to ensure low groundwater flow rates and to provide longest possible transport times
- it is evident that the repository should be located away from potential tectonic zones and potential fast geosphere pathways
- in order to minimize the possibility of inadvertent human intrusion the site should consist of common rock types, abundantly available.

How good is good?

Before starting to explore any site or area it is useful to pay attention to the siting criteria. A disposal system based on the multi-barrier principle can be applied to many geologic environments. For this reason it is not useful to develop too detailed requirements on geologic properties. Many "flaws" of a crystalline environment met in characterization can most probably be compensated by engineered solutions.

It is, however, useful to have some guidelines to assist in consideration of a formation or an area to be selected for studies. General criteria for siting were developed in the late 1970s and during 1980s (NEA, 1977; DOE, 1982; IAEA, 1989). In IAEA's "Siting of geological disposal facilities" (IAEA, 1994) some general guidelines on the level of knowledge and key questions have been given.

A general requirement "The geological characteristics of the disposal site shall, as a whole, be favorable for the isolation of the disposed radioactive substances from the environment. An area having a feature that is substantially adverse to safety shall not be selected as the disposal site" (Council of State 1999) forms a basis for the evaluation of a suitable site in Finland at the site selection stage. By favorable characteristics mechanically and chemically stable conditions are meant, in which engineered barriers maintain their performance. The crystalline bedrock itself acts as a barrier by retarding the released radioactive substances and mitigating consequences to an acceptable level. Features substantially adverse to safety can be due to exploitable natural resources, exceptionally high rock stress state, seismic or tectonic anomalies or exceptional values of important groundwater parameters (e.g. redox, oxygen).

The idea of these general requirements is to focus the studies on such formations, which most likely will also maintain their desired geologic properties in the future. Due to natural evolution, to which climatically forced changes also belong, changes may also take place at depth in the crystalline bedrock.

What safety assessments try to tell us

The TILA-96 report (Vieno and Nordman 1996), a continuation and update of the TVO-92 safety analysis (Vieno et al. 1992) confirmed that the planned system for spent fuel disposal fulfils the proposed safety criteria. The most recent safety analysis TILA-99 (Vieno and Nordman 1999) arrives at the same conclusions.

Provided that no major disruptive event hits the repository, initially intact copper canisters preserve their integrity for millions of years and no significant amount of radioactive substances will ever escape from the repository. Impacts of potential canister failures have been analyzed employing conservative assumptions, models and data. Very pessimistic sensitivity and "what if" cases have also been analyzed (Vieno and Nordman 1999). The assumptions in these cases have been even more pessimistic than the conditions assumed in the scenario analysis (Fig. 3). The results show that even in such cases a large number of canisters could be assumed to be initially defective or to "disappear" without the proposed constraints for release rates into the biosphere or dose rates exceeded.

The safety assessment demonstrates that the key phenomena contributing to the performance of the disposal system are (Vieno and Nordman 1999):

– the low flow rate of groundwater at depth

– reducing capacity provided by the material of the container and by the buffer, backfill and the crystalline rock itself
– low dissolution rates of the spent fuel and the cladding material
– low solubilities of radionuclides in the groundwater
– sorption in the buffer, backfill and the crystalline rock
– matrix diffusion in the geosphere.

It is most unlikely that a disruptive event would occur at the selected site and the location where the tunnels have been constructed. It is most likely that at the great depth in a crystalline formation stable geologic conditions will prevail, which makes it possible to implement the final disposal in a planned manner. In this kind of crystalline environment normal evolution will occur slowly and in a predictable manner (Crawford and Wilmot 1998).

The disposal galleries can be fitted between the fracture zones in a rock mass consisting of sparsely fractured rock. Based on the characterization (Anttila et al. 1999a–d) a favorable chemical environment (low oxygen, reducing Eh, neutral – close to neutral pH, low sulfide) is typical for these conditions. The hydraulic conductivity is low, as well as the hydraulic gradient, due to which the turnover of the groundwater in the rock is low. The salinity of the groundwater is not too high (lower than 100 g/l TDS). This would also mean that the key phenomena above would be favorable for long-term safety.

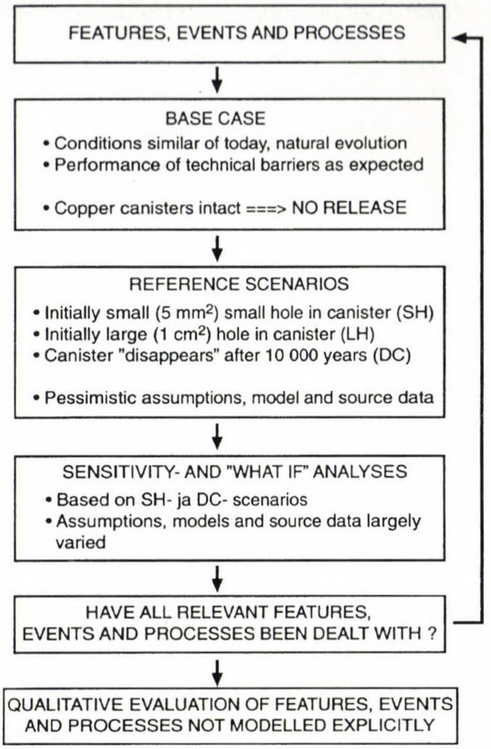

Fig. 3
Scenario structure of TILA-99 safety assessment

The conceptual model uncertainties, especially on the flow and transport in the fractures of the bedrock, must be covered by pessimistic assumptions. One of the main issues is the channeling or fast flowing features, which are suspected to form a network of rapid flowpaths through the geosphere. It is very cumbersome to exclude the possibility for fast flowing features at the site, however, avoiding the fractured zones as much as possible and locating the disposal tunnels in rock sections of high quality and characterizing the canister positions carefully the effects of these features can be minimized.

How does one find the suitable near field?

A lot of attention has been paid to the analysis of groundwater flow and the transport of solutes. In fractured crystalline rocks, however, the problem of fast-flowing features has become a significant uncertainty in the transport analysis. In crystalline rock these features have most often formed by channeled fractures. The fractures can provide, at least in theory, rapid transport pathways for radionuclides. Sure knowledge, however, on their existence and continuity is lacking. The possibilities of studying and modeling the impacts of channeling more realistically can be based on very detailed borehole measurements of flow in fractures. The information obtained in the detailed site characterization (Anttila et al. 1999a–d) suggests that the majority of the sparsely fractured rock mass has a low hydraulic conductivity. This means that the existence of the fast flowing features outside the fracture zones may be sparse but these should be detected and characterized by a representative manner in flow logging.

The heterogeneity makes it difficult to effectively use the barrier properties of the geosphere, due for example to the possibility to rapid pathways. Therefore it is most advantageous to focus the characterization on locating such bedrock volumes in which the near field can provide the required mechanical, chemical and hydrogeologic stability. By careful characterization when excavating the disposal galleries it is possible to evaluate the importance of hydrogeologic features to be met within this volume. Canister positions can then be selected avoiding the risk of placing them next to a significant flowing feature.

The important geologic question is how to delineate such volumes of rock with advantageous near field properties. This question boils down to understanding the structural features of the bedrock and modeling of the characterized site in such a way that suitable bedrock volumes can be identified.

Is constructability important?

Stable geologic environment means provisions for safe disposal but in addition also possibilities to construct the repository by normal methods. The constructability is affected by the rock quality, which means its geotechnical and rock mechanical classification, but also by rock stress and stress/strength ratio. Rock stress has an influence on the depth of the repository. Construction may become difficult under high stress conditions. If rock classification points to very demanding constructability there is an increased need for rock support, reinforcing etc. and may cause some restrictions in using the planned volume. Very demanding constructability may also lead to risk of safety being compromised by insufficient quality in implementation. Therefore the issue of constructability is not only an issue of optimizing the cost of the final disposal. If a repository can be built by normal methods in a planned manner it is also safe.

Question of retrieval?

The Finnish Government made the decision on the safety of the disposal of spent nuclear fuel. The decision contains the principles and general criteria for the final disposal of spent nuclear fuel. According to the decision the planning of the final disposal will be made so that no monitoring of the disposal is required for ensuring long-term safety, but also so that retrievability of the canisters is maintained, to provide for such development of technology that makes this a preferred option.

The key geologic questions have been closely related to long-term isolation of nuclear waste from the biosphere. The decision of the Council of State, however, also raises some new questions considering the possibilities for retrieval.

References

Anttila, P., H. Ahokas, K. Front, H. Hinkkanen, E. Johansson, S. Paulamäki, R. Riekkola, J. Saari, P. Saksa, M. Snellman, L. Wikström, A. Öhberg 1999a: Final disposal of spent fuel in Finnish bedrock – Hästholmen site report. – Helsinki, Posiva Oy. POSIVA 99–08.

Anttila, P., H. Ahokas, K. Front, H. Hinkkanen, E. Johansson, S. Paulamäki, R. Riekkola, J. Saari, P. Saksa, M. Snellman, L. Wikström, A. Öhberg 1999b: Final disposal of spent fuel in Finnish bedrock – Kivetty site report. – Helsinki, Posiva Oy. POSIVA 99–09.

Anttila, P., H. Ahokas, K. Front, H. Hinkkanen, E. Johansson, S. Paulamäki, R. Riekkola, J. Saari, P. Saksa, M. Snellman, L. Wikström, A. Öhberg 1999c: Final disposal of spent fuel in Finnish bedrock – Olkiluoto site report. – Helsinki, Posiva Oy. POSIVA 99–10.

Anttila, P., H. Ahokas, K. Front, H. Hinkkanen, E. Johansson, S. Paulamäki, R. Riekkola, J. Saari, P. Saksa, M. Snellman, L. Wikström, A. Öhberg 1999d: Final disposal of spent fuel in Finnish bedrock – Romuvaara site report. – Helsinki, Posiva Oy. POSIVA 99–11.

Council of State 1999: Council of State's decision on the safety of the final disposal of the spent nuclear fuel 10.11.1983.

Crawford, M.B., R.D. Wilmot 1998: Normal evolution of spent fuel repository at the candidate sites in Finland. – POSIVA 98–15. Posiva Oy. Helsinki.

DOE 1982: National Plan for Siting High-Level Radioactive Waste Repositories and Environmental Assessment. – Public Draft. U.S. Department of Energy.

IAEA 1989a: Guidance and Regulation of Underground Repositories for Disposal of Radioactive Wastes. – Vienna, International Atomic Energy Agency. Safety series No 96.

IAEA 1994: Siting of Geological Disposal Facilities. – Vienna, International Atomic Energy Agency. Safety series No 111-G-4.1.

NEA 1977: Objectives, concepts and strategies for the management of radioactive waste arising from nuclear power programmes. – Nuclear Energy Agency, Organisation for economic co-operation and development (OECD).

Vieno, T., A. Hautojärvi, L. Koskinen, H. Nordman 1992: TVO-92 safety analysis of spent fuel disposal. – Nuclear Waste Commission of Finnish Nuclear Power Companies. Report YJT-92-31E, Helsinki.

Vieno, T., H. Nordman 1996. Interim report on safety assessment of spent fuel disposal TILA-96. – POSIVA-96–17, Posiva Oy, Helsinki.

Vieno, T., H. Nordman 1999. Safety assessment of spent fuel disposal in Hästholmen, Kivetty, Olkiluoto and Romuvaara, TILA-99. – Helsinki, Posiva Oy. POSIVA 99–07.

Acta Geologica Hungarica, Vol. 43/2, pp. 145–155 (2000)

The key to improvements in aquifer protection: Analytical hydrogeology

József Tóth
Department of Earth and Atmospheric Sciences
University of Alberta, Edmonton

The principal objective of aquifer protection is the prevention of contamination of groundwater, over-exploitation of groundwater, and damage to the environment due to abstraction of groundwater. The common methods used to attain this objective are the establishment of protection zones, assessment of groundwater vulnerability, and groundwater management. Unfortunately, all these approaches suffer from several problems even under favorable conditions. Such problems include vague concepts and definitions of factors, processes, and objectives involved; conflicts of interests between production of groundwater, on the one hand, and various aspects of environmental, industrial, and economic concerns, on the other; the impossibility of standardizing procedures of investigation and implementation; inadequacy and/or inaccessibility of relevant data; difficulties in site-specific characterization and modeling of subsurface environments; arbitrary and unnecessarily restrictive protection criteria; lack of qualified professional expertise; and so on. Owing to the number and diversity of the problems impeding the effectiveness of the various aquifer-protection approaches, a meaningful overall improvement of the situation must be sought at the basic, strategic level, rather than in tactical details.

The view is advanced in this paper, therefore, that the key to a general improvement in aquifer protection is analytical hydrogeology. The term "analytical hydrogeology" is used here to denote the modus operandi by which a hydrogeologic problem is tackled. It is defined as hydrogeologic activity based on insight and intuition rather than on knowledge and convention; analytical hydrogeology is characterized by analysis and comprehension of the relevant factors and processes rather than by an uncritical, albeit skillful, application of standard procedures, or "cook-book" hydrogeology.

Specifically, the following points are considered to form the necessary basis of a strategic improvement of aquifer protection: 1. Recognition that aquifer protection is basically a hydrogeologic problem; 2. Recognition that this hydrogeologic problem requires a basin-scale approach both in space and time; 3. Recognition that this approach must include every aspect of hydrogeology (e.g., basinal hydraulics, aquifer and well hydraulics, contaminant hydrogeology), as well as surface water hydrology, meteorology, soil and rock mechanics, and so on; 4. Recognition that the solutions cannot be standardized, i.e., that "analytical hydrogeology" is needed, instead of "cook-book hydrogeology", and finally, and most fundamentally, 5. Encourage and enable universities to develop programs and opportunities for the attraction and education of the bright young minds required for analytical hydrogeology.

Key words: groundwater, contamination, over-exploitation, aquifer protection, analytical hydrogeology

Address: J. Tóth: Edmonton, AB., T6G 2E3, Canada
Received: 14 September, 1999

0236–5278/2000/$ 5.00 © 2000 *Akadémiai Kiadó, Budapest*

Introduction

Geologic formations that can yield groundwater in economic quantities, at sufficient rates, and of suitable quality to satisfy human requirements are called aquifers. A significant portion of the world's population relies on groundwater for its domestic, municipal, agricultural and industrial water uses. According to a report by the U.S. "Federal Coordinating Council for Science, Engineering and Technology (FCCSET, 1989, p. 32), "Approximately 117 million people in the United States get their drinking water from ground-water supplies and 34 of the 100 largest cities in the United States rely completely or partially on ground water." The more than 20 million people of Mexico City are supplied exclusively from aquifers in the Valley of Mexico; more than 70 per cent of public, and almost all private, supplies are derived from groundwater in the Federal Republic of Germany (Schleyer and Milde 1990); and the portion of groundwater of the nation's total consumption exceeds 85 per cent in Hungary. The importance and the scarcity of groundwater in the parched lands of arid and semi-arid regions is common knowledge and needs no illustrative examples.

Due presumably to the undisputed importance of the aquifers and their contents, there is a general consensus among the users, providers and administrators of groundwater resources that they must be protected against the various adverse effects to which they may be exposed or, conversely, which their production may generate. Such problems include the contamination and over-exploitation of groundwater, but also damage to the environment due to abstraction. On the other hand, agreement on methods and techniques of how to protect aquifers is notoriously lacking. As a result, no standard or standardized method of aquifer protection has ever been developed and it is highly doubtful that it ever will.

The lack of agreement on generally effective ways to protect aquifers is understandable in view of the complexity of the problem itself and of the numerous related aspects and ancillary problems involved. Some examples are the diversity of the hydrogeologic environments, the diversity of the tasks to be accomplished, the diversity of the problems caused by groundwater abstraction, that of conflicting interests to be reconciled, the vagueness of several fundamental concepts involved, the non-measurability of some basic parameters, and so on.

My idea of a Keynote Paper is not to discuss details of specific technical solutions, methods of approaches, scientific thoughts or individual case histories in such a huge problem area as aquifer protection; indeed, time and space limitations would not even allow it. Instead, I intend to look at the question at the most fundamental level possible, namely, at the kind of hydrogeology and the kind of hydrogeologists that are needed for the successful protection of aquifers. The basic points in my argument will be that aquifer protection is a hydrogeologic problem and that, consequently, improvement in its effectiveness and efficiency must be sought in improving the type and quality of its practitioners.

The problem

The title of our Session describes the topic to be discussed simply and succinctly: "Protection of Subsurface Aquifers". So let us see first what the dangers are against which aquifers need to be protected, and then what approaches are commonly used to accomplish the task.

The problem may be defined in general as a "Reduction in the availability or sustainable use or usability of a subsurface water source by changes in its quantitative or qualitative aspects, or in environmental conditions, due to any man-induced or natural activity or process." Specifically, such activities or processes may result in i) introduction of contaminants; ii) over-exploitation; and/or iii) undesirable environmental effects.

There are three basic aspects to the problem of introducing contaminants into a subsurface water regime (contaminant is any substance reducing the suitability of water for human use of any purpose, not just for bodily intake), namely: a. the sources of contaminants such as industry, agriculture, and human settlements; b. the types of contaminants as liquid, solid, or vaporous; and c. the place of introduction, whether at or near the land surface, as e.g., the vadose zone, unconfined or water-table aquifer, or deep confined strata. An important sub-group of aspect "c" is the attraction of water of inferior quality into an aquifer by water abstraction, such as "salt coning" (if vertical) or sea/salt-water intrusion (if lateral).

Over-exploitation is commonly regarded in terms of quantity but it may be defined on a quality basis, too. Indeed, salt coning and sea/salt-water intrusion are forms of over-exploitation.

Whereas water in aquifers may be exposed to numerous dangers, its production for human use can also have undesirable environmental effects. Symptoms of such adverse effects include declining groundwater levels, drying of wetlands, reduction or disappearance of spring discharges, influx of contaminants, land subsidence, and so on.

Common approaches to solving the problem

The approaches toward solving "the problem" can, in general, be divided into two basic groups, namely: Preventive and Remedial. In this paper I will discuss the Preventive approaches only because they are more important in the present context and, at the same time, the conclusions are applicable also to the "Remedial" approaches. In addition, the "Remedial" approaches involve prohibitively numerous and diverse techniques to be reviewed meaningfully in a short talk.

The three major types of commonly used and somewhat overlapping Preventive Approaches are:

1. Groundwater Vulnerability Assessment;
2. Groundwater Protection Zones; and
3. Groundwater Management Schemes.

A brief review of the three approaches follows.

Groundwater Vulnerability Assessment

Groundwater vulnerability has been defined (Zaporozec and Vrba 1994, p. xvi) as "...an intrinsic property of the groundwater system that depends on the sensitivity of the system to human and/or natural impacts." It was characterized further (idem, p. xvii) as "Vulnerability of groundwater is a relative, non-measurable, dimensionless property." The principle of vulnerability assessment is the identification of those intrinsic and anthropogenic elements of the natural environment which may contribute to contamination of the groundwater regime (as, for instance: soil, vadose zone, vegetative cover, aquifer, recharge, topography, aquitards, contacts with surface water, land use, population type and density, industrial activity, and so on), then ranking them in importance relative to one another and assigning to them a relative value of hazardousness in the specific local context. Based on the summation of the thus-obtained values of the relative contribution of each of the environmental elements to the sensitivity to contamination for every point of an investigated area, the area can be divided into regions of comparable values of vulnerability. In turn, based on such knowledge of groundwater vulnerability, measures of protection may be designed to regulate the allowable type, amount, and distribution pattern of potential contaminants and water abstraction.

The three main methods of vulnerability assessment are:

i) Hydrogeologic Setting Methods,
ii) Parametric Systems Methods,
iii) Analog and Numerical Models Methods.

All three methods follow the same principle described above. The main difference between them consists of the type, accuracy, and amount of the parameters used which, in turn, depend on their availability, the scale of investigation, and the type and level of expertise involved.

i) The Hydrogeologic Setting Methods describe the parameter sensitivity in relative terms, based on comparisons with vulnerabilities experienced in other areas. Assessment is given only in qualitative terms.

ii) The Parametric System Methods express the sensitivity of selected parameters by numerical values which are processed according to any of the "Matrix System", "Rating System", or "Point-count System", of which a popular prototype is "DRASTIC" (Vrba and Civita 1994 Fig. 10, p. 44).

iii) Analog and Numerical Models Methods are based on functional (mathematical) relations, which are considered to exist between relevant properties of the rock framework and the transport and attenuation of contaminants. The output of these methods (by means of various equations) is a "vulnerability index", "contaminant travel time", "cleaning capacity", and so on.

It requires no deep insight to see that any of these methods rely primarily on the existence, acquisition, judgment (culling), processing and interpretation of hydrogeologic or related data.

Groundwater Protection Zones

The basic principle of protecting a producing aquifer by the method of "Groundwater Protection Zones" is the demarcation of areas of step-wise increasing radial distances around an abstraction facility, with increasingly relaxed control and ban on activities, processes, and installations that are potentially capable of groundwater contamination, as distance from the facility increases. In an ideal, homogeneous, and isotropic rock framework, with the abstraction facility being the only factor inducing water flow, the protection areas are circular and concentric around the facility. The radial distance between the abstraction facility and the boundary of a particular protection zone is determined, in principle, on the basis of the rate and amount of attenuation of potential pollutants permitted in that zone during their travel from the zone's boundary to the withdrawal facility. In practice, with the exception of the nearest, i.e., most protected zone, these distances are established on the basis of hydrogeologic considerations and a pragmatic compromise between the competing interests of the water producers and the various land users.

Commonly, a protected area is divided into three or four zones of differing restrictions. The first zone is immediately surrounding the production well, with a 10–25 m radius. In this zone, pedestrian and vehicular traffic as well as any use of pesticides and manure are prohibited, plus all other restrictions of the more distant zones apply. The outer boundary of the second zone is often determined on the basis of the subsurface travel time needed to eliminate all pathogenic bacteria, viruses, and degradable chemicals. A time limit of 50 days has been considered in Germany to satisfy this criterion (Schleyer and Milde 1990). However, in light of recent research concerning the survival of microbes, questions are raised about the adequacy of this restriction, particularly in fractured aquifers. The distance over which water travels in 50 days to a producing well is dependent on the aquifer's hydraulic properties and the pumping rate and can thus be very variable. Typical items prohibited in this zone are farms, roads, railways, parking lots, cemeteries, sport facilities, waste-water pipes, and bathing in surface water bodies. In addition, all items excluded in the third zone are prohibited also in the second. Prohibitions in the third zone (in Germany: at least two km from the producing well) include: feedlots, open storage and use of pesticides, waste-water treatment, airports, sewage treatment plants, drilling, oil refineries, waste-water injection, and chemical plants.

Groundwater Management Schemes

According to the California State Department of Water Resources (Domenico and Schwartz 1997, p. 139): "Ground water basin management includes planned use of the ground water basin yield, storage space, transmission capability, and water in storage. It includes 1. protection of natural recharge and use of artificial recharge; 2. planned variation in amount and location of pumping over time; 3. use of groundwater storage conjunctively with surface water from local and imported sources; and 4. protection and planned maintenance of groundwater quality."

Shibasaki et al. (1995, p. 43) put the stress on another aspect of basin management, namely, on the area of concern: "In order to ensure a sustained availability of groundwater, the quality and quantity of groundwater should be systematically managed in a whole unit called groundwater basin." They add (p. 45): "A prerequisite for the management of a groundwater basin is to have sufficient knowledge on the natural conditions of groundwater basin, particularly on ... 1) structure of the basin; 2) hydrostratigraphy; and 3) groundwater flow."

These two quotations reveal that protection of the quality and quantity of groundwater is an explicit objective of the "Groundwater Management Schemes", and that this is the only one of the three approaches used which puts the problem of protection into a regional, i.e., basinal, context and links it explicitly to other groundwater related questions. The objective of groundwater management schemes may, therefore, be characterized as an attempt to strike an optimal balance between the utilization and maintenance of available and obtainable groundwater resources (e.g., by artificial recharge, conjunctive use), on the one hand, and economic, environmental and social demands, on the other. The requirements for the accomplishment of this objective are:

i) A thorough and quantitative knowledge of the hydrogeologic conditions of the basin (rock framework, climate, groundwater flow, and groundwater quality);

ii) An accurate knowledge of the amount, rate, and temporal and spatial distribution of groundwater production;

iii) An accurate knowledge of the type, intensity, and temporal and spatial distribution of all potential sources of contaminants;

iv) A purposefully designed monitoring network; and

v) A carefully calibrated and periodically updated groundwater response-model of the basin.

The tacit assumption in the theory of integrated management schemes is that the basin constitutes a thoroughly communicating hydraulic unit, i.e., that the rock framework of the basin is hydraulically continuous – a recognition that requires modern and well educated (rather than trained) hydrogeologists. A fundamental practical requirement of basinal groundwater management is a data bank which contains all existing (i.e., potentially available) information on the rock framework, groundwater quantity and quality, pore pressures and water levels, surface water bodies (lakes and streams), meteorology, land cover and use, and anthropogenic features.

Problems with the common approaches

Regardless of which of the three mentioned approaches are applied, i.e., Groundwater Vulnerability Assessment, Groundwater Protection Zones, and Groundwater Management Schemes, or when in combination, whether they are used in series or parallel, a successful attainment of the objectives is often elusive. It is important to note, however, that the reasons for inadequate results are inherent to the problem itself and cannot be blamed on the methods *per se*.

Some of the most obvious, and damaging, difficulties associated with any, or any combination, of the three approaches include:

i) Some of the basic definitions are vague, imprecise, and qualitative, because of the need for concepts and parameters that cannot be rigorously defined;

ii) Most procedures cannot be generalized and standardized due to the site- and situation-specific nature of each individual case;

iii) Actual field data are never enough to adequately characterize the relevant aspects of the hydrogeologic environment;

iv) Needed information, and even existing data, are usually not available, collected, organized or accessible;

v) The subsurface environment cannot be modeled in sufficient detail to provide reliable answers to the questions related to aquifer protection;

vi) The problem often involves conflicts of interest which are not, cannot be, or should not be solved in favor of aquifer protection;

vii) Protection criteria may be developed without adequate knowledge and/or understanding of the system and factors involved (e.g., survival capacity of microbes, contaminants);

viii) Inherent difficulties may exist in evaluating the appropriate, i.e., the needed, scales of space and time of the problem;

ix) The employed, or available, technical expertise may not have the necessary type or level of specialized education;

x) The key aspects of planning and execution of an investigation, monitoring, and management aimed at aquifer protection require hydrogeologic understanding, insight, and intuition, which are rare commodities, rather than skills and technical know-how, often sought for the task.

The examples below will serve to illustrate some "Problems with the Common Approaches".

i) Poor definitions

a) Concerning the term overexploitation, Custodio (1992, p. 3) writes: "Aquifer and groundwater overexploitation is a relatively new, ambiguous and controversial problem in Hydrogeology. Its definition is difficult due to the many different aspects it involves and the variable perception by different technical and social groups. Overexploitation is commonly referred to as the adverse effect of groundwater exploitation, although a balanced view should also consider the beneficial side."

Further he also makes the points that: (i) the desirability or adversity of the effects is subjective; (ii) exploitation should not be expressed in terms of recharge since recharge cannot possibly be determined; (iii) time lag in water-level reaction to pumping may conceal long-term effects; (iv) abstraction may also result in salt-water upconing or sea-water intrusion at a later date; (v) adverse effects may be real, imagined, or anticipated, and also economic, social, or political.

b) Zaporozec and Vrba (1994, p. xvii) define vulnerability as follows: "Vulnerability is an intrinsic property of the groundwater system that depends on the sensitivity of that system to human and/or natural impact." or, explaining it more closely: "Vulnerability of groundwater is a relative, non-measurable, dimensionless property."

ii) Procedures cannot be standardized

According to Schleyer and Milde (1990, p. 379): "...a successful protection of groundwater for drinking water purposes can only be achieved by carefully assessing all potential sources of contamination and by developing optimal protection strategies including all site-specific criteria.

iv–v) Field data are never enough for sufficiently accurate characterization of the hydrogeologic situation

a) Because of the usual inadequacy of databases, as well as possible later changes in production schedules, "Monitoring related to strict management criteria is the best protection against over-exploitation and should be aquifer or situation specific..." (Lloyd 1992, p. 169).

b) Shibasaki et al. (1995, p. 45) feel that: "... at the present level of the state-of-the-art, a detailed understanding of the aquifer structure and an accurate prediction of contaminant movement in a structure with irregular permeability are very difficult."

vi) Conflicts of interest

a) Lloyd (1992, p. 167) also warns against overly strict restrictions on groundwater abstraction in the name of prevention of over-exploitation, i.e., of aquifer protection; an abstraction policy should be flexible. "In terms of value to the community, abstraction and protection policies that are unnecessarily rigid, may be just as unacceptable as over-exploitation."

b) Schleyer and Milde (1990, p. 382) point out the dilemma that may result from the conflict between the need to protect well-head areas, on the one hand, and the increasing demands for the use of land for other purposes, on the other, in Germany: if all 26,000 well-head protection areas would be designated as such, approximately 11 per cent of Germany's area would come under some degree of ban or restriction of use for any other purpose.

c) Shibasaki et al. (1995, p. 46) also maintain that "Sometimes, even such management plans which may have undesirable objectives from a groundwater basin usage point of view, may be adopted in order to attract industries or public works projects."

ix) The employed expertise may not have the necessary education

a) Llamas (as quoted by Custodio 1992, p. 4) is of the view that some aspects of over-exploitation are due to: "... ill-transposed surface-water hydrology concepts by engineers, planners, and decision makers with poor training in groundwater resources."

Recomendations for solutions

In view of the difficulties of protecting aquifers, as demonstrated above, it appears unproductive to search for a particular measure or procedure, or for a magic wand, to solve the problem. Instead, improvement in the situation should be sought by ensuring that the fundamental aspects of the problem are correctly recognized and appropriately addressed. This view is implied in numerous statements made by foremost researchers and practitioners of the problem of aquifer protection. A few randomly selected quotes suffice to illustrate the point:

Re. Consequences of (over) exploitation of an aquifer.

Custodio (1992, p. 23): "To make an assessment of the consequences of exploitation of an aquifer, and to decide whether it is overexploited under a given set of conditions, it is necessary to have a good and quantitative understanding of the behavior of the aquifer or the aquifer system."

Re. Aquifer contamination.

Fetter (1994, p. 534): "One critical aspect of preventing ground-water pollution is the identification of recharge areas of aquifers. In such areas, protection of the aquifer is vital."

Re. Impossibility to standardize situations and approaches.

Zaporozec (1994, p. 7): "Development of a generally recognized and accepted definition of vulnerability does not imply a standardized approach to vulnerability mapping. Hydrogeological environments are much to diverse to be subjected to a standardized assessment."

Re. Insufficient information.

Schleyer and Milde (1990, p. 388): "It is a prerequisite for the functioning of a groundwater protection system that groundwater resources, their volumes, their drainage areas and in particular, their vulnerability are completely mapped...".

Gilbrich and Zaporozec (1994, p. 1): "... hydrogeological information is essential to the effective protection and management of groundwater quality."

Shibasaki et al. (1995, p. 45): "A prerequisite for the management of a groundwater basin is to have sufficient knowledge on the natural conditions of groundwater basin, particularly on (1) the structure of the groundwater basin which is the container of groundwater, (2) hydrostratigraphic unit which is the basic unit for groundwater flow and its structure, and (3) groundwater flow and its characteristics".

Re. Type of data to be dealt with.

Skinner (1985, p. 126) lists the most important factors that need to be understood in protecting fissured aquifers: "I) magnitude and direction of groundwater flow, II) degree of interaction between water in the fissures and in the intervening rock matrix, III) influence of the unsaturated zone, IV) degree of interaction with surface water systems, V) rock/water reactions within the aquifer."

Summary and conclusion

A synthesis and interpretation of the above, and many other similar, views and cases justify the following summary of the nature and needs of the problem of aquifer protection:

- Basically, it is a hydrogeologic problem.
- It is a problem requiring a basin-scale approach both in space and time.
- The approach may have to make use of every aspect of physical and chemical hydrogeology, plus contaminant transport, surface-water hydrology and meteorology; in addition, it cannot be standardized.
- As a consequence, it needs all-round "analytical hydrogeologists" with emphasis on scientific understanding, intuition, and insight, as opposed to technical skills and know-how.
- The basic strategy to alleviate the problem of aquifer protection is, therefore, the production of "analytical hydrogeologists". Its success depends, ultimately, on the relevant institutions of higher education.

Acknowledgement

I am pleased to acknowledge the helpful comments of my colleague Dr. Carl Mendoza during the preparatory stages of the presentation.

References

Custodio, E. 1992: Hydrogeological and hydrochemical aspects of aquifer overexploitation – In: Simmers, I., F. Villaroya, L.F. Rebollo (Eds): Selected Papers on Aquifer Overexploitation, Vol. 3; 23rd International Congress of the International Association of Hydrogeologists, Puerto de la Cruz, Tenerife, Spain, pp. 3–27.

Domenico, P.A., W. Schwartz 1997: Physical and Chemical Hydrogeology, 2nd edition; John Wiley & Sons, New York, 506 pages.

FCCSET (Federal Coordinating Council for Science, Engineering, and Technology), 1989: The role of science and technology in the management of the nation's ground-water resources – A Report by the Subcommittee on Ground Water, Office of Science and Technology, Washington, D.C., U.S.A.

Fetter, C.W. 1994: Applied Hydrogeology, 3rd edition – Macmillan College Publishing Co., New York, 691 pages.

Lloyd, J.W., 1992: Protective and corrective measures with respect to the over-exploitation of groundwater – In: Simmers, I., F. Villaroya, L.F. Rebollo (Eds): Selected Papers on Aquifer Overexploitation, Vol. 3; 23rd International Congress of the International Association of Hydrogeologists, Puerto de la Cruz, Tenerife, Spain, pp. 176–181.

Gilbrich, W.H., A. Zaporozec, 1994: Introduction, Chapter 1 – In: Vrba, J., A. Zaporozec (Eds): Guidebook on Mapping Groundwater Vulnerability, International Contributions to Hydrogeology Vol. 16; International Association of Hydrogeologists, pp. 1–2.

Schleyer, R., G. Milde, 1990: Well head protection areas for preserving natural drinking water quality – experiences and new developments in the Federal Republic of Germany. – In: Simpson, E.G., J.M. Sharp, Jr. (Eds): Selected Papers on Hydrogeology, Vol. 1; 28th International Geological Congress, Washington, D.C., U.S.A., pp. 379–392.

Shibasaki, T. and Research Group, 1995: Environmental Management of Groundwater Basins, Tokai University Press, Tokyo, 202 pages.

Skinner, A.Ch. 1985: Groundwater protection in fissured rocks, Chapter 4. – In: Matthess, G., S.S.D. Foster, A.Ch. Skinner (Eds): Theoretical Background, Hydrogeology and Practice of Groundwater Protection Zones, International Contributions to Hydrogeology Vol. 6; International Association of Hydrogeologists, pp. 123–143.

Vrba, J., M. Civita 1994: Assessment of groundwater vulnerability, Chapter 5. – In: Vrba, J., A. Zaporozec (Eds): Guidebook on Mapping Groundwater Vulnerability, International Contributions to Hydrogeology Vol. 16; International Association of Hydrogeologists, pp. 31–48.

Zaporozec, A. 1994: Concept of groundwater vulnerability, Chapter 2 – In: Vrba, J., A. Zaporozec (Eds): Guidebook on Mapping Groundwater Vulnerability, International Contributions to Hydrogeology Vol. 16; International Association of Hydrogeologists, p. 7.

Zaporozec, A., J. Vrba 1994: Executive summary. – In: Vrba, J., A. Zaporozec (Eds): Guidebook on Mapping Groundwater Vulnerability, International Contributions to Hydrogeology Vol. 16; International Association of Hydrogeologists, pp. xv–xxiii.

Acta Geologica Hungarica, Vol. 43/2, pp. 157–172 (2000)

Protection of subsurface aquifers: A broader context

T. N. Narasimhan, Jesse Reynolds
Department of Materials Science and Engineering,
Department of Environmental Science, Policy and Management
University of California, Berkeley, CA, USA

Large-scale groundwater extraction for municipal, irrigation, and industrial purposes became widespread throughout the world early in this century with breakthroughs in deep-well pump technology. Accelerated extraction soon led to declines in aquifer productivity, land subsidence, salt-water intrusion, and other adverse impacts. A consensus exists among earth scientists that aquifers are bounded, open systems that constitute the lower part of the hydrologic cycle. They are dynamically linked to the upper part of the hydrologic cycle, comprising the atmosphere and surface water bodies. Whereas surface water bodies respond rapidly to climatic changes, subsurface aquifers respond more slowly over long time periods. In order that we may continue to benefit from groundwater reservoirs into the indefinite future, aquifer management must be linked to management of surface water resources, taking due notice of the differences in the reaction times of surface water and groundwater bodies. An essential foundation to such management is sustained monitoring of the groundwater system and its linkages to the other components of the hydrologic cycle. Experience gained in the development of groundwater resources in the Santa Clara and the San Joaquin Valleys of California provides insights into the technical and human aspects of large-scale integrated development of groundwater resources.

Key words: groundwater, aquifers, hydrologic cycle, protection, scales, integrated management, California

Introduction

On the eve of the 21st century there is a general awareness worldwide that the earth is a finite planet and its natural resources must be managed with great care. Within this overall context the protection of subsurface aquifers from depletion and physical and chemical degradation is a topic of considerable importance. Equally important is the recognition that development of subsurface aquifers for water supply can, in turn, have significant impacts on the greater environment and ecosystems. Thus, it is relevant to simultaneously address both the issue of protecting ecosystems from the effects of aquifer development and that of protecting the aquifer resource itself. The challenge of water management and policy is to balance these impacts so that society may continue to benefit from its groundwater resources for long periods of time.

Addresses: T. N. Narasimhan, J. Reynolds: Department of Materials and Engineering, University of California, Berkeley, CA94720-1760, USA
E-mail: tnnarasimhan@LBL.gov
Received: 4 November, 1999

0236–5278/2000/$ 5.00

In this paper the topic of subsurface aquifer protection is addressed from a generic, philosophical point of view. To give some form and substance to these theoretical concepts, examples of groundwater development are drawn from the state of California. Over the past century and a half California has seen extraordinary developments in water through a combination of its abundant natural resources and its aggressive applications of technology and policy. The experiences that have been gained in California are of great value in providing insights into issues related to aquifer protection in general, regardless of geographic location.

This paper is divided into two parts. The first part on historical background presents observational experience from California to portray issues that are pertinent to subsurface aquifer protection. The second part is devoted to a discussion of scientific concepts relevant to such protection and implications for aquifer management.

Historical background

Although the extraction of groundwater for beneficial use through wells and other structures dates back many thousands of years in Egypt, the excessive removal of water from underground, leading to pronounced deleterious impacts on other components of the environment, is little more than a century old. Extraction of groundwater from considerable depths at a scale large enough to drastically deplete the resource and lead to collateral effects such as land subsidence and salt-water intrusion commenced with the advent of drilling machines during the early part of the 19th century. Between 1850 (when California attained statehood) and 1900 there were numerous artesian belts in sedimentary basins throughout California. Free-flowing artesian wells reaching down to more than 300 meters below the land surface and producing in excess of 3,800 cubic meters per day were common in the Central Valley. Towards the end of the 19th century the drilling of a large number of such wells for irrigation led to a gradual decline in flow rates, accompanied by the lowering of water levels to below the land surface and the subsequent cessation of flow in many wells. The earliest horizontal-shaft centrifugal pumps, operated by steam engines, appeared in California around 1880 (Freeman 1968). These were limited to lifting water from depths less than 10 meters below the land surface. With the construction of the first hydroelectric plant in California in 1893, electric power became available to operate pumps by the early 1900s. Nevertheless, lifting water from depths greater than 10 meters remained a challenge to large-scale groundwater extraction.

A major breakthrough in pump technology, largely driven by the profitability of irrigation, occurred around 1901 when the first multi-stage vertical-shaft turbine pump was designed and tested in Chicago. This design soon underwent major improvements and the first turbine pump for irrigation went into operation in Chino in southern California in 1907 (Freeman 1968). A rapid increase in the use of such pumps throughout California for irrigated agriculture soon followed. In the subsequent decades this new technology contributed to unprecedented overdraft of water in many parts of the state. The nature of the overdraft and consequences are well illustrated by the history of subsurface aquifer development in the Santa Clara and San Joaquin Valleys.

Santa Clara Valley

The Santa Clara Valley is a small, topographically well-defined basin situated at the south end of San Francisco Bay in California (Fig. 1). Renowned worldwide for its prunes, apricots, and other orchard crops in the early twentieth century, this area is now known as the Silicon Valley due to its computer industry. The valley is underlain by over 600 meters of Late Tertiary to Recent sediments, which contain highly productive aquifers down to about 250 meters. Up to the turn of the 20th century a belt of free-flowing wells existed in the lower, northern area of the valley close to the bay. These artesian wells, in addition to pumped wells, supported thriving and rapidly expanding irrigated agriculture. During the 1910s the farmers in the valley began to adopt the turbine pump and increased their ability to lift water from great depths. Within a decade the enormously accelerated withdrawal of groundwater led to rapidly declining water levels and productivity of wells, as shown in Fig. 2. In 1931 a precision survey carried out by the U. S. Coast and Geodetic Survey (Rappleye 1933) revealed that, between 1920 and 1931, an elevation benchmark in the city of San Jose had subsided by about 1.3 meters. A map of the region showing the extent of subsidence during 1935–36 is given in Fig. 3. Based on field data the correlation between land subsidence and groundwater overdraft came to be clearly established. The mechanism of subsidence was soon ascribed to the compaction of soft fine-grained sediments (aquitards) in response to declining water pressure (Meinzer 1937).

The alarming increase in pumping costs resulting from the decline of water levels motivated the farmers of the Santa Clara Valley to commission a study by Fred Tibbetts and Stephen Kieffer, civil engineers, to find means of better managing the water resources of the valley as a whole. Based on intensive data gathering on physiography, geology, climate, surface water runoff, and well inventory, the report (Tibbetts and Kieffer 1921) recommended coordinated water resources management involving storage of winter flood water, artificial recharge, and groundwater extraction. Although these recommendations were only partially implemented thirteen years later, the report largely inspired the subsequent integrated development of surface water and groundwater in the Santa Clara Valley.

By the 1950s the growth of the electronics industry had transformed the valley into a growing metropolitan area. Land-use patterns in the valley began to change steadily from agriculture to urban and suburban. It became clear that the

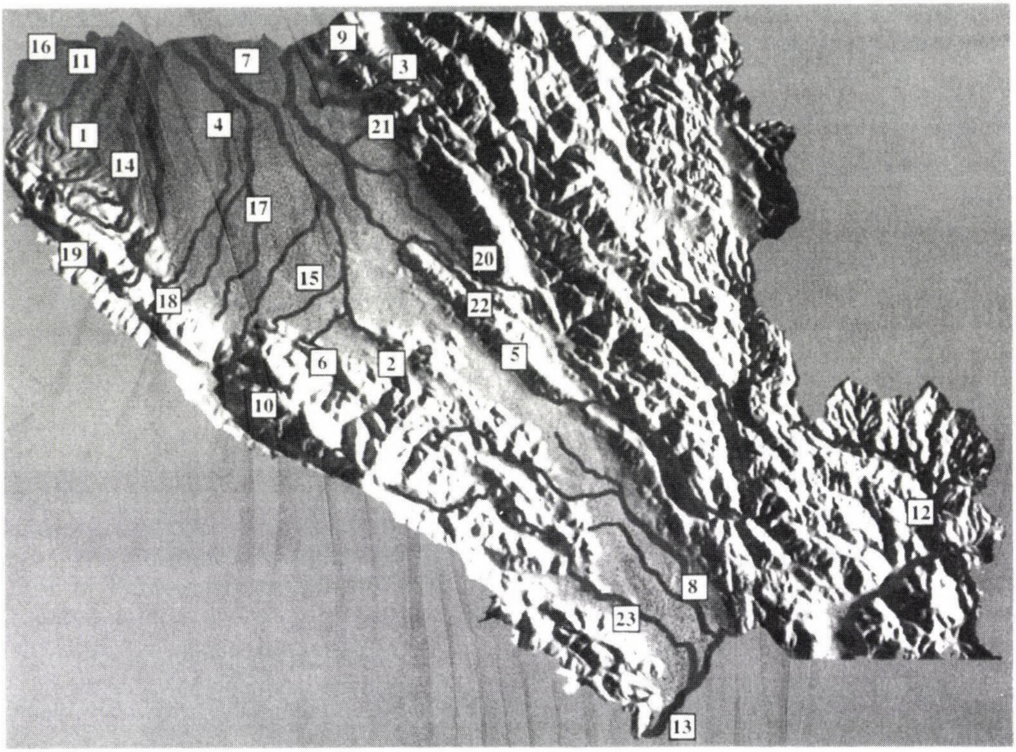

1. Adobe Creek 2. Alamitos Creek 3. Berryessa Creek 4. Calabazas Creek
5. Coyote Creek 6. Guadalupe Creek 7. Guadalupe River 8. Llagas Creek
9. Los Coches Creek 10. Los Gatos Creek 11. Matadero Creek 12. Pacheco Creek
13. Pajaro River 14. Permanente Creek 15. Ross Creek 16. San Francisquito Creek
17. San Tomas Aquino Creek 18. Saratoga Creek 19. Stevens Creek
20. Thompson Creek 21. Upper Penitencia Creek 22. Upper Silver Creek
23. Uvas-Carnadero Creek

Fig. 1
Relief map of Santa Clara Valley, California (From Stream Care Guide for Santa Clara Valley, Santa Clara Valley Water District, circa 1990)

water resources of the local basin alone would be grossly insufficient to support the valley's growing water uses. A decision was made to bring water into the valley from outside.

Currently, water is imported into the valley from the rivers of the Sierra Nevada via three paths: the South Bay Aqueduct of the State Water Project, San Francisco's Hetch Hetchy Aqueduct (both to the northeast), and San Luis Reservoir on the California Aqueduct to the southeast. A map of the modern Santa Clara Valley water system is given in Fig. 4. The current total water used by the valley is approximately 560 million cubic meters per year, or about 1.5 million

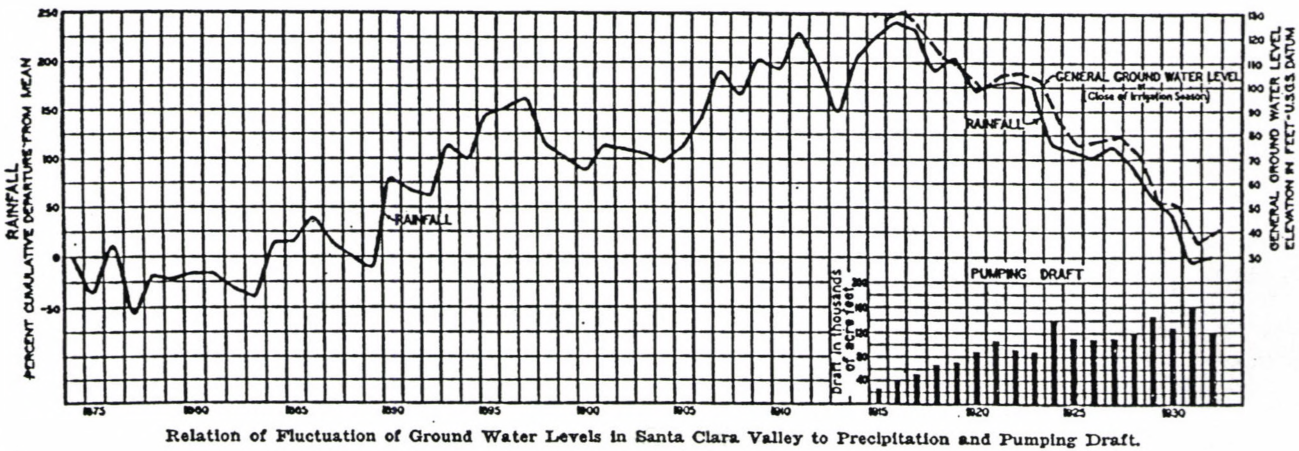

Fig. 2
Decline in water levels and groundwater draft in the Santa Clara Valley following the introduction of deep-well turbine pumps in the 1910`s (From Division of Water Resources 1933)

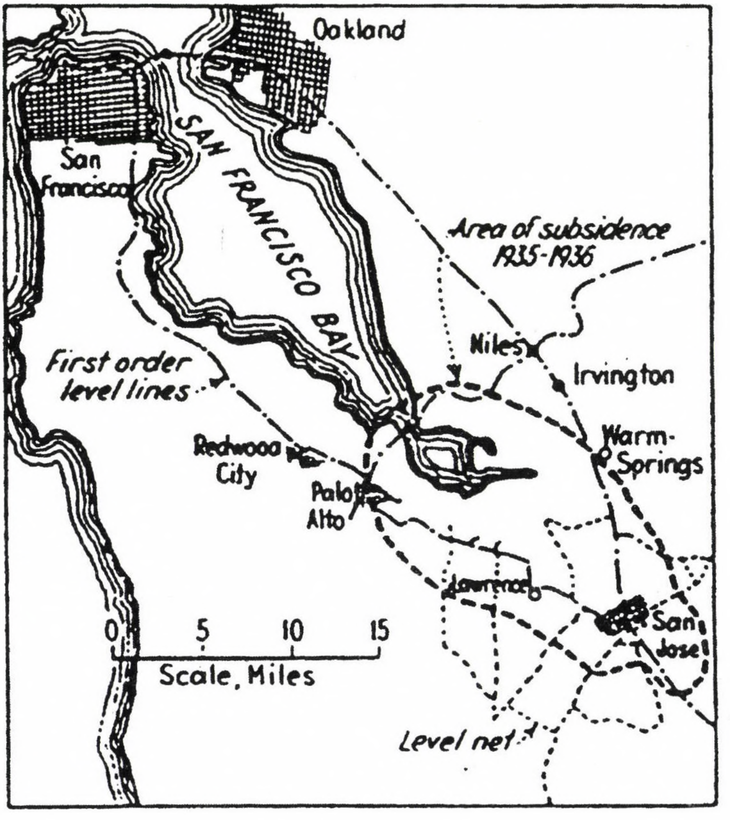

Fig. 3
Land subsidence near San Jose in Santa Clara Valley, California, 1935–36 (From Stohsnet 1937)

cubic meters per day. About half of this is met by imported water. Most of the remainder comes from groundwater, with minor contributions from local surface water. Some wells supplying water for the city of San Jose can produce as much as 9.5 cubic meters of water per minute. Although groundwater pumping could be increased, production is curtailed in wet years and increased during periods of drought. By limiting groundwater withdrawals and artificially recharging the aquifers, land subsidence has been brought under control.

The imported water, surface water reservoirs, and artificial recharge facilities are managed by the Santa Clara Valley Water District, which is overseen by the Santa Clara County government. Private companies and municipalities that pump groundwater under permit and purchase water from the Santa Clara Valley Water District at a wholesale rate carry out the actual distribution of water to communities and end users.

Groundwater recharge, flood control, wastewater reclamation, and public education are all part of the overall management philosophy in the valley. This

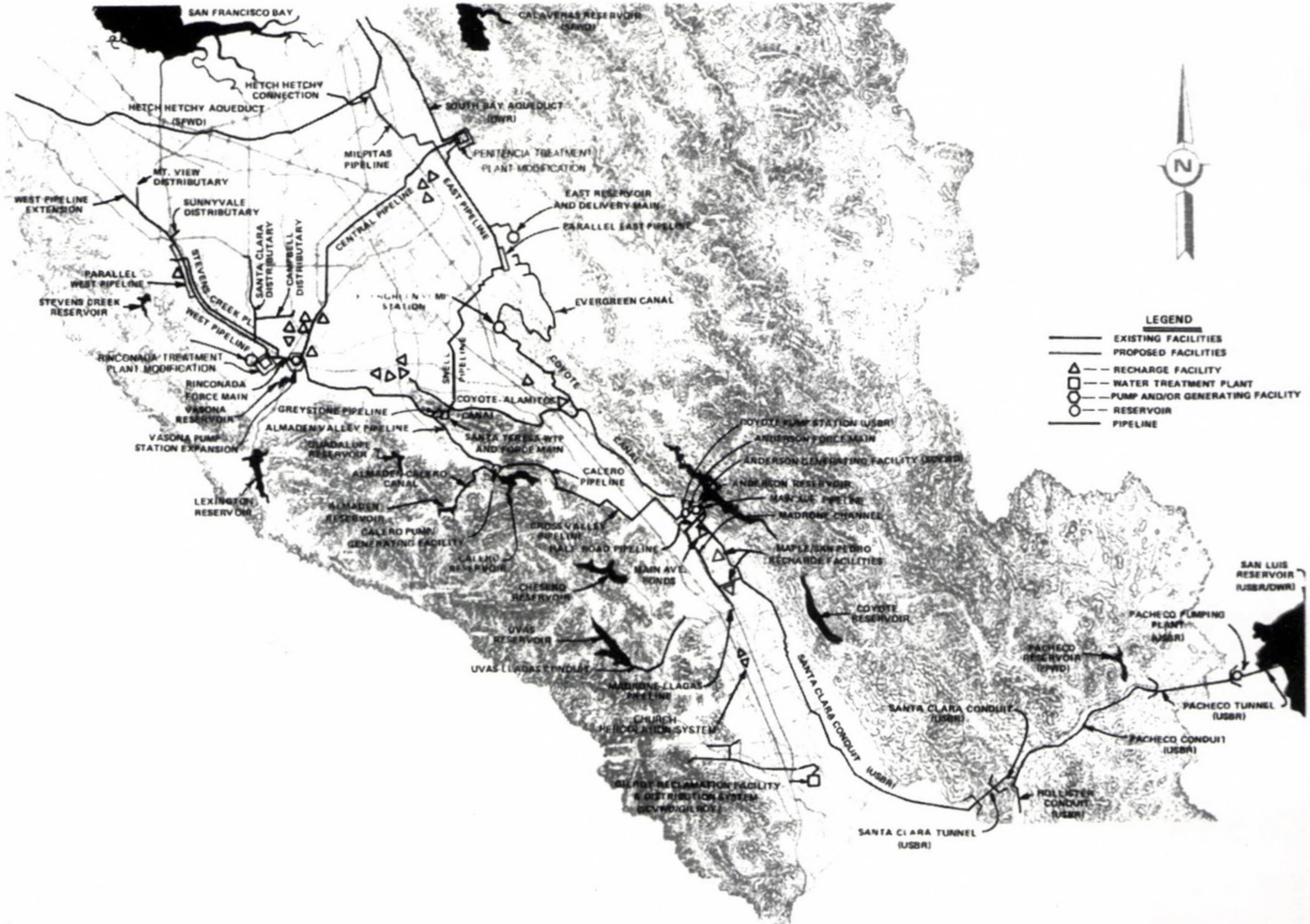

Fig. 4
The Santa Clara Valley water supply system, California (From Discover Water, Santa Clara Valley Water District, 1991)

generally rational approach to integrated management has come into existence, among other reasons, because the unit of management is a self-contained physiographic and groundwater basin and because the local population had the will to judiciously manage its finite resources of water.

San Joaquin Valley

The San Joaquin Valley, the southern half of the Great Central Valley of California, provides an example of how the natural resources infrastructure can be impacted in different ways from water resources development. The San Joaquin Valley is among the most productive agricultural regions of the world. Agriculture in this semi-arid region is sustained by irrigation with water imported from outside the basin and with pumped groundwater. The combination of the aridity, peculiar topography, and geology of this basin have given rise to physical as well as chemical problems that greatly affect the groundwater and soil resources of the valley.

As can be seen in Fig. 5 the Great Central Valley is a prominent intermontane valley about 640 km long and 80 km wide. It is bounded on the east by the Sierra Nevada range and on the west by the Coast Ranges. At the southern extremity of the valley the Sierra Nevada and the Coast Ranges are linked by the Tehachapi Mountains. Due to peculiar sedimentary depositional conditions, the southern third of the San Joaquin Valley is an enclosed inland basin known as the Tulare Basin. The area north of the Tulare Basin is drained by the San Joaquin River, which flows to the north.

Throughout the San Joaquin Valley productive aquifers with high quality water occur within the soft unconsolidated sedimentary formations down to depths of more than 600 meters. During the 19th century a prominent artesian belt of flowing wells occupied the axis of the San Joaquin Valley and the lower parts of the Tulare Basin. This region coincided with swamps, marshes and wetlands, showing that it was the discharge area for regional groundwater flow systems of the intermontane basin. Clearly, regional forces from the Sierra Nevada on the east and the Coast Ranges on the west provided the force that sustained the upward movement of groundwater in the discharge area.

Following the availability of deep-well turbine pumps, the San Joaquin Valley experienced intensive pumping of groundwater for irrigation purposes starting from about 1910. Soon the artesian wells stopped flowing and the artesian belt that occupied several thousand square kilometers disappeared (Fig. 6). Further pumping continued, especially on the western side of the valley, along the foothills of the Coast Ranges where surface water was too scant to support irrigation. By the 1950s the groundwater overdraft resulted in a prominent belt of land subsidence parallel to the Coast Ranges (Fig. 7), exceeding 8 meters at some locations. Groundwater withdrawal clearly could not go on at these excessive rates for long.

Since the 1950s irrigated agriculture in the San Joaquin Valley has benefited greatly from two major multi-purpose water projects, the federal Central Valley Project and the State Water Project. The Delta-Mendota Canal of the Central Valley Project and the California Aqueduct of the State Water Project move immense quantities of water uphill over several hundred kilometers from the basin of the Sacramento River in the north. The importation of this water

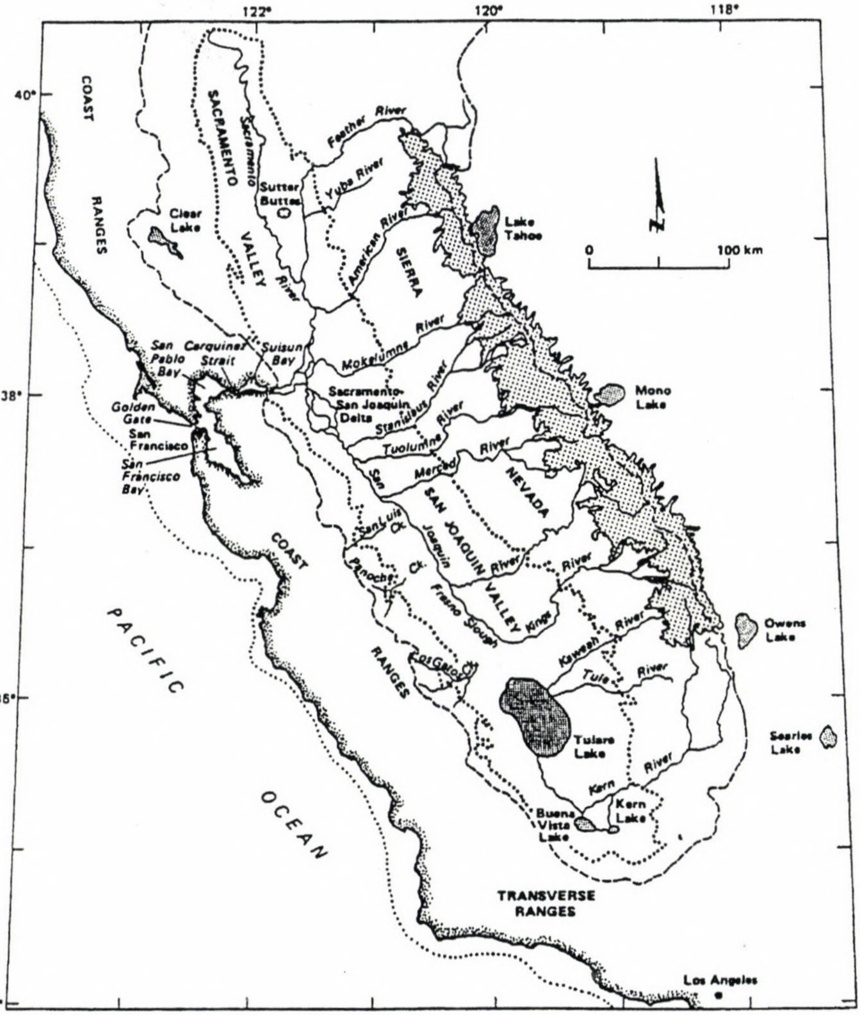

Fig. 5

General map of the Great Central Valley, with the San Joaquin Valley occupying the southern half. Stippled area indicates the Sierra Nevada Range. Dotted line delineates the valley basin (From Erskine et al. 1992)

Fig. 6
A memorial to the artesian belt that once occupied the San Joaquin Valley. It disappeared due to groundwater over draft

significantly helped reduce groundwater withdrawals in the San Joaquin Valley, curtailing subsidence of the land.

Although the importation of large quantities of water from the Sacramento Basin helped to bring more acreage under cultivation and limit land subsidence, it gave rise to more serious problems of groundwater quality. The presence of the artesian belt and wetlands along the axis of the San Joaquin Valley indicates that these discharge areas are dominated by vertical movement of water with very slight horizontal movement. Thus the axis of the valley is naturally vulnerable to gradual accumulation of salts present in the imported water. It has been estimated that between 1985 and 1994 salt was accumulating in the valley at an annual rate of about 800,000 metric tons (Orlob 1991). This excess salt cannot be easily drained out of the valley, both because the natural flows of the San Joaquin River and its tributaries have been drastically curtailed by the construction of

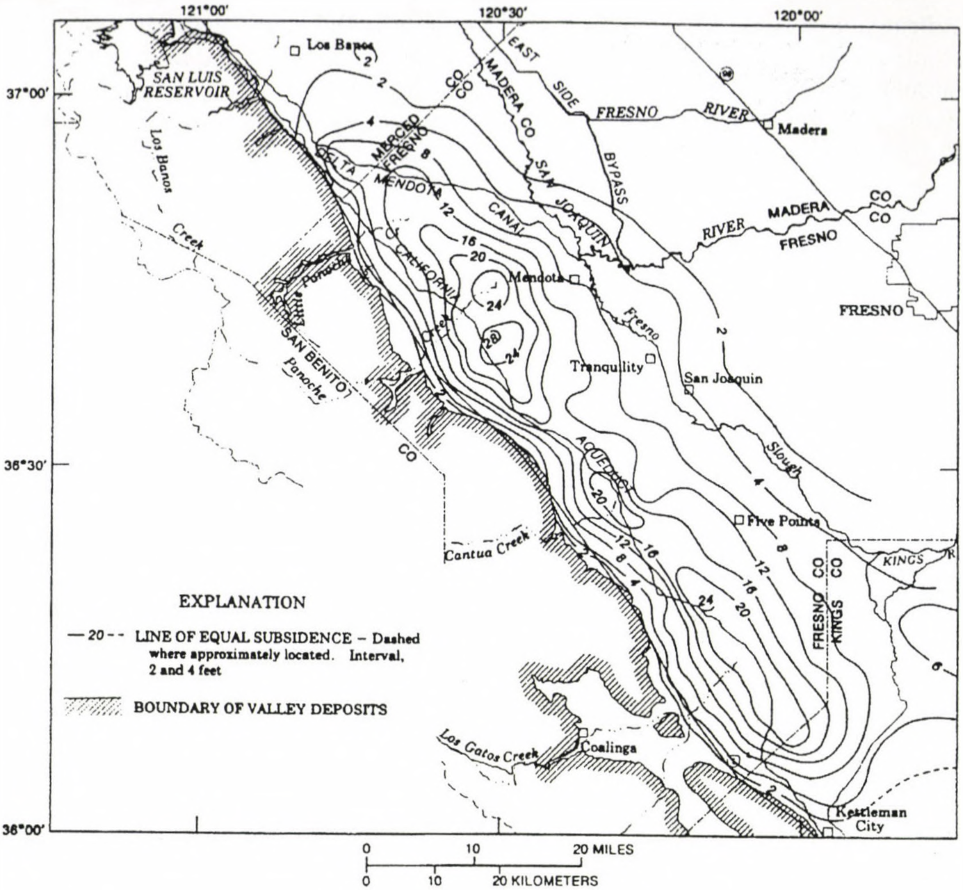

Fig. 7
Land subsidence on the west side of the San Joaquin Valley, 1926–1972 (From Belitz 1990)

many dams, and because horizontal groundwater velocities toward the north are extremely small.

To maintain agricultural productivity under these conditions, farmers have resorted to the use of agricultural drains to remove the excess salts from the root zone and transport them away. However, the salts remain within the San Joaquin Valley because no physically and politically feasible method of exporting the salts into San Francisco Bay or the Pacific Ocean has been developed. In all, over 400,000 hectares of land in the San Joaquin Valley are affected by serious salinity problems and shallow water tables. Furthermore, roughly 2,000 hectares become uncultivable each year because of unacceptable salt accumulation.

At present much remains to be understood about the potential long-term impact of irrigated agriculture and importation of irrigation water on the groundwater resources of the San Joaquin Valley. However, existing information indicates that groundwater and soils are gradually being degraded by the accumulation of salts. Although farmers are able to locally succeed in overcoming salinity through the installation of drains, it is doubtful if modern technology can successfully overcome the enormous forces of the regional groundwater system that ultimately dictate the accumulation of salts in the arid, poorly-drained San Joaquin Valley.

Subsurface aquifer protection

Sustainability and attributes of aquifers

In a general sense subsurface aquifer protection is part of the larger issue of the sustainability of the hydrologic cycle. For our purpose an aquifer is a geologic entity that can produce economic quantities of water. The word economic is significant because it implies a value of water to human society and a dependence of society on the aquifer for its survival and well-being. In this sense of economy and survival society relies on aquifers for domestic and municipal water supplies, agriculture, and industry. As we have seen from the examples of the Santa Clara and San Joaquin Valleys of California, aquifers are vulnerable to physical as well as chemical damage from their development. The goal of modern groundwater resources engineering and policy is to manage aquifers judiciously so that the benefit they bring to society can continue for indefinitely long periods of time. This is essentially the notion of long-term sustainability of aquifers, which provides a basis to define subsurface aquifer protection and to devise means of its implementation.

The wish that aquifers continue to provide benefits to society for long – and even indefinite – periods of time is based on the premise that aquifers are open systems subject to replenishment each year from the upper part of the hydrologic cycle. In addition they also possess the important ability to store and release water. Because of these attributes aquifer systems are rightfully recognized as dynamic groundwater reservoirs. These characteristics of annual replenishment and storage lie at the heart of issues related to subsurface aquifer protection.

The groundwater system has the ability to store a portion of the annual precipitation that infiltrates to the water table. In a simplistic sense an aquifer is sustained if the average quantity of water extracted and naturally discharged annually approximately equals the annual replenishment. However, this approach is inadequate for various reasons. To begin with, annual precipitation is subject to variability on several time scales. Periodic occurrences of several continuous years of below or above normal rainfall are a rule of nature. As a result annual replenishment to the groundwater reservoir is remarkably variable. This is exacerbated by the fact that periods of highest groundwater demand coincide with those of low precipitation and recharge. Second, the ability of subsurface aquifer systems to store water is finite and small. Except for shallow unconfined systems, aquifers and associated aquitards can take into storage infiltrating meteoric water only through their ability to change porosity by very small amounts. Shallow unconfined aquifer systems, on the other hand, can take into storage much larger quantities of water through a change in saturation. Finally, the rate of recharge can be extremely slow, especially for deep aquifers. Because of these attributes, confined aquifers, which lie at greater depths than unconfined ones, are particularly vulnerable to rapid depletion. Unconfined aquifers, despite their larger ability to take water into storage, have limited sustained yields because they generally communicate directly with surface bodies and often contribute to base flow in streams. As a result overdraft of shallow aquifer systems can, in some cases, significantly affect neighboring terrestrial ecosystems through declines in the water table.

Therefore, subsurface aquifer systems can only play the role of dynamic storage reservoirs or buffers that help moderate the effects of uncertain climatic variations. In essence, groundwater storage must be judiciously managed to balance excess water available for recharge during years of above-normal rainfall with satisfying water demands during periods of drought. In the Santa Clara Valley, groundwater is managed in this way by using surplus water for artificial recharge and increasing groundwater extraction during years of surface water deficit. It must be noted, however, that the Santa Clara Valley is presently able to meet its water uses because imports the majority of its water from outside its own surface water and groundwater basins.

Protection of aquifers from overdraft thus entails integrated management of both surface water and groundwater over watersheds and groundwater basins. In regions where aquifer systems at great depth are involved this management becomes challenging because the time lag between annual precipitation cycles and the response of deep aquifer systems is significant.

In the foregoing we have devoted attention to the physical degradation of the productivity of aquifer systems. The chemical degradation of aquifers is a more profound issue in its long-term consequences. Groundwater quality is intimately linked with the chemistry of soils and aquifer materials, and is ultimately controlled by regional groundwater flow patterns. The time scales at which chemical reactions take place are generally larger than those at which water levels and pressures change. As a consequence, once chemically degraded, it is extremely difficult or even impossible to restore water and soil quality. This indeed is the salinity problem in the San Joaquin Valley. The regional flow patterns are such that the only way the problem of salinization can be solved is to export salts out of the valley, a politically impossible task. As agricultural technology the world over increases productivity through the addition of large quantities of fertilizers and pesticides it becomes necessary to visualize the long-term response of regional groundwater systems to these massive inputs. Technology, it appears, is very efficient in solving short-term problems of crop productivity, isolated from potential impacts on other components of the natural system. Experience gained over the past several decades suggests that the time has come to seriously address the long-term consequences to hydrogeologic systems arising from aggressive physical and chemical manipulations of natural resources.

Implications for water management

Aquifers are spatially and temporally complex, interconnected, difficult-to-predict open systems, which are vulnerable to depletion, physical and chemical degradation, and the inducement of secondary environmental consequences. In order to sustain the benefits of aquifers over the long term, hydrogeologists and groundwater managers must expand their scales of consideration, account for uncertainty, and pursue aggressive data-gathering policies.

In the preceding discussion we noted that the hydrologic cycle operates at multiple temporal and spatial scales and is interconnected with adjacent ecosystem components. The shift from simple resource exploitation to sustainable resource use is inherently a process of expanding the scales of concern. Instead of merely locating productive aquifers, pumping groundwater, and resolving disputes, groundwater management must now provide a reliable, sustainable supply of water of a certain quality while preventing and correcting any adverse environmental effects. The emphasis of management must change so that the available resource is utilized in an efficient, sustainable, and equitable manner contributing to the social well-being of the broader community (Das Gupta 1998). In other words the goal must be to sustain natural and social systems instead of a single variable, such as yield.

The logical place to begin to expand considerations is with spatial and temporal scales. Individual aquifers usually cross management and jurisdiction boundaries. Furthermore, real aquifers are not the discrete boxes that managers and modelers may consider them to be. Hydrogeologic processes such as regional groundwater flow and pumping-induced quality degradation are not restricted to single aquifers and often occur over large spatial scales. Clearly a basin-wide approach is an appropriate initial scale of operation. In a similar manner, the temporal scales of groundwater behavior do not conform to human conventions, span a broad range, and include very large scales. Consequently, groundwater managers and engineers must operate at a wide range of spatial and temporal scales that generally do not coincide with convenience.

Aquifer management must also expand its considerations from groundwater *per se* to larger natural and social systems; that is, we must expand our scale of knowledge. It is widely accepted among scholars of water resources that the study and management of groundwater and surface water must be integrated because alterations to one part of the greater hydrologic cycle will affect others. Furthermore, water resource planning should be coordinated with land use and economic planning, such as urban development and human health programs. One approach for this coordination is integrated water management, which is an attempt to formalize and model hydrological, ecological, administrative, social, and economic interrelations (Kuijpers 1993). However, its complexity and institutional barriers have hindered implementation.

Management and modeling of groundwater resources must acknowledge and incorporate uncertainty and complexity (Quinodoz 1998). The first source of uncertainty, incomplete and inaccurate hydrologic characterization, can be reduced but not eliminated through data acquisition. Knowledge of the hydrogeologic system is critical because, as noted above, aquifers have finite and often small storage, and the rate of recharge is slow. The second source of uncertainty is the frequency and magnitude of external events. These are the forcing functions and boundary conditions in hydrogeologic models. Borrowing from ecology, adaptive management offers a framework to address the complexity and uncertainty of future events (Sophocleous et al. 1998).

These sources of uncertainly indicate the need for vigilant monitoring of aquifers. Integrated monitoring of water resources is an issue of infrastructure. The collection of meteorological data and stream discharge data are now readily accepted as part of society's need for basic data on natural resources. Yet the same recognition does not extend to the monitoring of groundwater systems, which need to be monitored over long periods of time. Attitudes of water managers need to change in regard to sustained monitoring of groundwater systems. All levels of government should take an active role in monitoring of resources and data distribution. This allows hydrogeologists and groundwater managers to upgrade their knowledge base of the system attributes, as well as to extrapolate the data for planning. However, we have seen that such planning may be limited to the short term.

This approach of expanding scales while acknowledging uncertainty, and gathering data while remaining flexible, will help prevent aquifer depletion, physical or chemical degradation, and secondary environmental impacts resulting from aquifer utilization. It represents an alternative to simple technological solutions, and addresses the reality of large scale, interconnected systems.

Acknowledgements

Our thanks are due to Ardyth Simmons, Peter Zawislanski, József Tóth and Emilio Custodio for constructive criticisms of the manuscript. This work was supported partly by the Director, Office of Energy Research, Office of Basic Energy Sciences of the U.S. Department of Energy under Contract No. DE-AC03-76SF00098 through the Earth Sciences Division of Ernest Orlando Lawrence Berkeley National Laboratory, partly by the Agricultural Experiment Station of the Division of Agricultural and Natural Resources, University of California and partly by a travel fund from the Committee on Research of the University of California at Berkeley.

References

Belitz, K. 1990: Character and evolution of the groundwater flow system in the central part of the western San Joaquin Valley, California. – Water Supply Paper 2348, U. S. Geological Survey, 28 p.

Das Gupta, A. 1998: Strategic approaches towards sustainable groundwater resources development and management. – Water Resources Journal, 42, pp. 1–7.

Division of Water Resources, State of California. 1933: Santa Clara Investigation, Bulletin 42, 265 p.

Erskine, M., A. Batow, W. Lettis 1992: Field guide to the tectonics of the boundary between the California Coast Ranges and the Great Valley of California. – Amer. Assoc. Petroleum Geol., Pacific Section, Bakersfield.

Freeman, V. 1968: People – Land – Water: Santa Clara Valley and Oxnard Plain, Ventura County, California. – Lorrin L. Morrison, Los Angeles, 227 p.

Kuijpers, C. 1993: Integrated water management in the Netherlands: Myth or practice? – In: A. Biswas (Ed.): Water for Sustainable Development in the Twenty-First Century. – Oxford University Press, Delhi, pp. 116–125.

Meinzer, O. 1937: Land subsidence caused by pumping. – Engineering News Record, 118, 715

Orlob, G.T. 1991: San Joaquin salt balance: Future prospects and possible solutions – In: The Economics and Management of Water and Drainage in Agriculture. – Kluwer Academic Publishers, Boston, pp. 143–168.

Quinodoz, A. 1998: Managing uncertainty in yield estimates. – In: Sophocleous, M. (Ed.): Perspective on Sustainable Development of Water Resources in Kansas. – Kansas Geological Survey Bulletin 239, pp. 200–209.

Rappleye, H. 1933: Recent areal subsidence found in releveling. – Engineering News Record, 110, 845.

Sophocleous, M., R. Buddemeier, R. Buchanan 1998: Evolving sustainability concepts: Modern developments and the Kansas experience. – In: Sophocleous, M. (Ed.): Perspective on Sustainable Development of Water Resources in Kansas. Kansas Geological Survey Bulletin 239, pp. 87–95.

Stohsnet, E.E. 1937: Santa Clara Valley subsidence has now reached 5 feet. – Engineering News Record, 118, 479.

Tibbetts, F., S. Kieffer 1921: Report to Santa Clara Valley. – Water Conservation Committee on Santa Clara Valley Water Conservation Project. Santa Clara Valley Water Conservation Project, San Jose, 243 p.

Acta Geologica Hungarica, Vol. 43/2, pp. 173–202 (2000)

Groundwater-dependent wetlands

Emilio Custodio
Geological Survey of Spain, Madrid

From the biological point of view wetlands are highly productive areas. They are of growing interest not only for wildlife, scenic landscape and recreation, but as a source of income and as a bioreserve. The times when wetlands were considered unhealthy and undesirable areas are fortunately over. However, in Europe and other regions many of them have already been desiccated, often by public initiative. Many wetlands or parts of them depend on groundwater contribution. This means less fluctuating situations than when they depend only on surface water, and physico-chemical characteristics are more stable. Associated vegetation is resistant to drought conditions when there is groundwater available at shallow depth. Not only is groundwater discharge to land surface important, but underground discharge as well, since this plays an important role in the water balance and especially in salinity and solute concentrations of local water. Groundwater-dependent wetlands can vary from small spots to large, elongated areas, from vegetation-rich areas to impoundings of spring water, and they may contain water from fresh to briny and with precipitated salts. Aquifer development may interfere (and often does) with groundwater availability to wetlands. Then there is an environmental conflict. Its solution means a trade-off between development and conservation, which is often a difficult one. This requires compromises by initially very diverse interests, as well as overcoming deeply entrenched myths. Obtaining reliable data and adequate monitoring is a necessary step.

Key words: groundwater, wetlands, impact of development, role of groundwater, quality effects, delayed effects

Introduction

Wetlands are landscape features which can be found in almost all regions of the Earth. Surface areas vary from less than one hectare to many km^2. They are more frequent in flat areas, coastal zones and lowlands, especially if rainfall is relatively important and the terrain is poorly permeable, but they also appear in arid areas, where their relative importance is increased.

Wetlands may develop along valleys, in the central areas of geologic basins, in deltaic areas at places where foothills grade into low permeability flatlands, and in may other situations (Cowardin et al. 1979; González-Bernáldez 1988; Brinson 1993). The Ramsar Convention on wildlife and waterfowl classifies wetlands into marine, estuarine, lacustrine, riparian, paludial and artificial.

Wetlands have been defined as surface features which conform to some of the following conditions:

Address: E. Custodio: Department of Ground Engineering. Pol. Univ. of Catalonia, Gran Capità s/n, Ed. D-2, 08034 Barcelona, Spain. On leave to the Geological Survey of Spain (Instituto Tecnológico Geominero de España), Ríos Rosas, 23, 28003 Madrid, Spain.
Received: 14 September, 1999

a) areas with still water not forming lakes. That is, with a shallow water depth allowing waterfowl to feed and breed at least in a large part of them,
b) areas with a shallow water table which can be used most of the time by plant roots to get water from the aquifer or the capillary fringe,
c) areas in which evapotranspiration is greater than precipitation.

These definitions are not accepted by all scientists and water managers but they are useful to decide what a wetland is.

Wetlands may grade into lakes and into rivers. They can be more or less permanent or seasonal, or even something that fully develops only during and after wet years. Fluctuation is for some wetlands an important characteristic. Generally they contain fresh water, but saline water is found in coastal areas as well as in some continental situations in which salinity may grade from brackish to briny with associated precipitated salts.

Wetlands have been historically – and in some cases they still are – regarded as wasteland and unhealthy areas, a source of malaria and other water-borne diseases, a nuisance to human life and much wanted flatland for cultivation and human establishments. Thus, since old times they have been the subject of destruction by infilling and by drainage. In Europe and other developed regions a large fraction of existing surface area has already been destroyed and irreversibly transformed, up to 80% according to some figures. Regulations fostering this behavior still persist in some countries, especially in developing nations and in tropical areas, where health concerns are still real. Lay people are generally predisposed against wetlands. This is to some extent rooted in legends and myths, and derives from a poor understanding of the environment. In fact large surface areas of wetlands were destroyed and still continue to be in many areas of the world. The situation is being redressed, however, mostly in developed countries, where environmental concern is now part of daily life and where the economic value of wetlands begins to be widely recognized (Llamas et al. 1992; Barbier et al. 1997). Wetland study and evaluation is a current issue in many countries, such as the USA (Adams et al. 1991) and the European Union.

In Spain wetlands are now protected (at least in theory) by the Water Act. The River Basin Water Authorities, in charge of water management, have the duty of inventorying, monitoring and protecting wetlands, with objectives that must be included in the Plans for River Basin's Water Management.

Wetlands are important areas. This is because of the benefits they bring, from the natural, economic, and aesthetic points of view, and which are related to the:
a) very high organic matter production,
b) large diversity of plant and animal species,
c) beneficial effects on the water cycle, since they contribute significantly to regulate variability (e.g., smoothing floods), to retain nutrients, to foster water quality improvement and regularization, and to shape local climate and mitigate its fluctuation,

d) high economic interest for local as well as for downstream population, and also as a growing source of touristic income.

Many wetlands depend on local rainfall plus surface water contribution from a larger area, since they are maintained by river contributions and floods on the alluvial plain and in the flat areas into which they spread, or by contributions from tributaries barred by the main river banks.

Wetlands along the coast may be associated with sea tides, with or without continental contribution. These influences are easily recognized and have been extensively studied from the hydrological and ecological points of view, mostly because they are frequent in the temperate areas of developed countries.

However, groundwater-dependent wetlands are important as well. They present a large variety of patterns, circumstances, salinities (from fresh water to brine) and ecological values, although in many cases they have not been recognized as such until recently, especially when they are a part (often the most permanent one) of larger wetlands in which diverse hydrological circumstances are found.

Publications devoted to groundwater-dependent wetlands and papers focusing on their functioning and characteristics are scarce. A reference publication was edited by Winter and Llamas (1993).

Most examples and results presented hereafter will be taken from experience existing in Spain, which is the country of Western Europe with the largest number of groundwater-dependent wetlands covering a very varied climatic, geomorphologic and geologic range. A first attempt at synthesis was edited by Llamas (1987) and guidelines for restoration were compiled by Montes et al. (1995). The hydrogeologic knowledge is still sketchy.

Two main wetland areas in Spain which combine surface and groundwater-dependent circumstances are the Doñana National and Natural Parks in the SW, and the Las Tablas de Daimiel Natural Park and some other neighboring wetland areas in the Centre. They have been the subject of studies and argument due to the impact of poorly controlled (but to some extent successful) groundwater development for agricultural irrigation, and of some scientifically doubtful restoration undertakings, especially for the second wetland area (Llamas 1988; 1989; 1992). Some background on Doñana can be found in Llamas (1990); Suso and Llamas (1991, 1993); IGME, (1984); Custodio (1995a); Custodio and Palancar (1995); Custodio et al. (1999).

Groundwater-dependent wetlands

Groundwater-dependent wetlands are those in which the source of water is partly, dominantly or exclusively derived from groundwater. The different water contributions increase areal diversity and fluctuation pattern (water depth, surface area, salinity, and chemical conditions), which is important for biodiversity. Groundwater is the more permanent contribution and it secures the existence of permanent habitats, which are essential for a wide range of plants and non-migratory animals. These habitats are often less spectacular to the outsider, hunters, and Nature tourists, since they lack large waterfowl populations. Although they are less known and less protected, in spite of their key ecological and economic role, they are now being rediscovered, due to the large set of interesting aspects they involve.

Groundwater-dependent wetlands include typical ones in which water exists on the land surface and may grade into lagoons, lakes, and river courses. They also include as important features wet meadows and areas in which there is no continuous but patchy water at the surface. In such wetlands vegetation thrives on groundwater since the water table and the capillary fringe are at shallow depths and can be reached by the plants' roots. This vegetation often includes medium to large size trees which in some areas (as in the Doñana area in SW Spain) are called "monte negro" (black forest) in contrast to dominantly smaller-size xerophytic plants called "monte blanco" (white brush).

In other cases, especially in semi-arid and arid climates, the intense evaporation of water at or near the surface locally increases water salinity. This is more conspicuous when there is no surface water outflow and/or discharged groundwater is already rich in dissolved salts due to geologic conditions, such as the existence of soluble salts in the ground, concentration of airborne salts in the scarce groundwater recharge in arid areas (especially in areas which are close to the coast) and the mixing with relict or modern sea water in the ground (Bayó et al. 1996). Saline and brine water wetlands are in many cases highly interesting, as in Fuente de Piedra in SE Spain, which is a resting area for flamingo waterfowl (ITGE, 1998), or in the arid plains of the Monegros in NE Spain (García-Vera, 1994).

Groundwater-dependent wetlands can be classified as groundwater discharge areas corresponding to local, intermediate and regional groundwater flow systems (Tóth 1971, 1972, 1999; Custodio and Llamas 1976, Sect. 24). González-Bernáldez (1992) attempted a first classification from the ecological point of view. A hydrological and geomorphologic classification has been prepared by a group of specialists led by Dr. C. Montes for the Ministry of the Environment of Spain, included in a still unpublished report, which however is being applied by the State and some Regional Administrations. They appear in a large variety of circumstances such as near valley bottoms, in interfluves, in lowlands, in coastal areas and along the shores of large lakes.

Discharge areas generally represent a small part of a groundwater basin and tend to be spotty or elongated, continuous or discontinuous areas. Even in the bottom area of small or large depressions, most groundwater outflow and availability to plants is along strips made up of a vadose zone, since the central part is often occupied by low permeability sediments, which are close to water saturation, and may contain brackish or saline water. However, upward vertical leakage of groundwater through these low-permeability sediments may also play the role of sustaining the wetlands, or of delaying their seasonal dry-up, or of creating local outflows where sediments are discontinuous or more permeable, forming scattered springs ("ullals" and "ojos" in Spain) and sometimes mud and quicksand pits.

As far as the water basin and the aquifer system are concerned, most groundwater-dependent wetlands correspond to some of the lowest areas, although not always. When ground permeability is relatively low and recharge is significant the water table is close to the ground surface everywhere except in the highest areas. Thus even in interfluves and headwater areas, flatlands and depressions may become wetlands. In this case fluctuation may be larger than in regionally depressed areas. In such areas groundwater contribution may be almost constant, independent of seasonal and year to year rainfall (recharge) fluctuation, due to the generally large turnover time of the system (many years to millennia).

Seasonal fluctuation in groundwater-dependent wetlands sometimes seems conspicuous and even the base flow of springs and rivers may disappear. This may not reflect a similar fluctuation of groundwater contribution to the area but the effect of seasonally changing evapotranspiration of the vegetation using groundwater. The total discharged quantity may be constant but the terms into which it is split fluctuate. This is the case of the La Rocina Basin, in the Doñana area (Trick 1998).

Conditions of groundwater-dependent wetlands

Hydrogeologic conditions in groundwater-dependent wetlands change dramatically from one place to another according to recharge area, rate of discharge, regional and local permeability pattern, topography and local sedimentary features around discharge areas. All of them, however, have in common a rather complex three-dimensional pattern of groundwater head potential around and close to the wetland, as well as changing physico-chemical characteristics, including environmental isotopic composition. Their understanding is necessary to explain groundwater behavior and pattern. See Figs 1 and 2 for two examples.

This is often neglected in simplifications. Horizontal, two-dimensional approaches are generally used, which may be enough to reproduce the regional behavior but not the wetland characteristics. It is not rare to consider water table and shallow well data together with some deep borehole water-level elevation information. Sometimes the piezometric levels of some deep, more productive layers, which are obtained from production wells, are the only ones to be considered. In this case the water table elevation may not be represented at all by the piezometric surface. Groundwater–wetland relationships may be greatly distorted. See Figs 3 and 4 for further explanation.

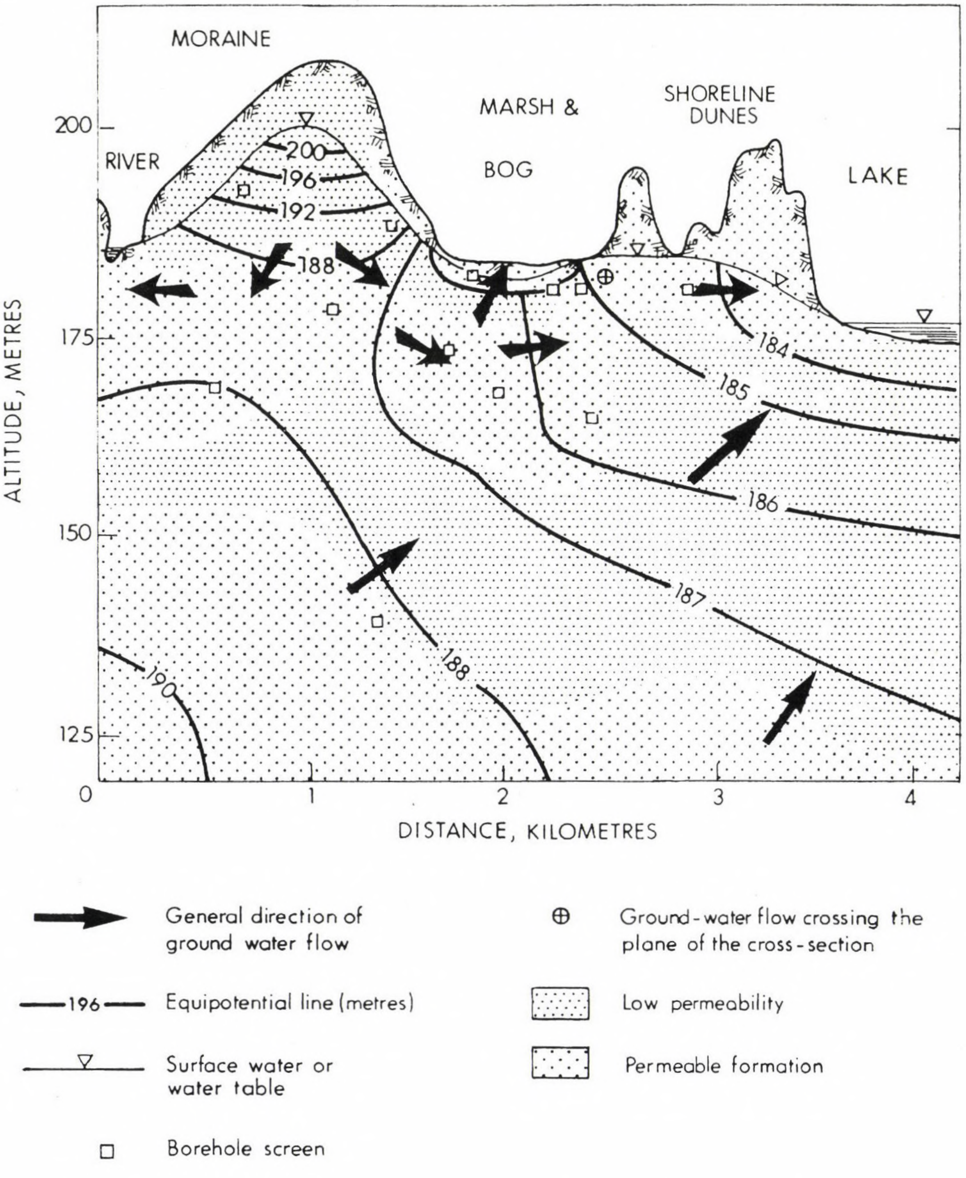

Fig. 1
Three-dimensional flow of groundwater towards Lake Michigan. Groundwater discharge, besides contributing to the lake, feeds an intermediate river and a marsh. Local recharge at the moraine and dune belt and regional groundwater discharge, and the pattern of permeable (dune sand, subtill, bedrock) and low permeability (till) material control the flow pattern (modified from Shedlock et al. 1993)

These types of problems are even more serious when interpreting water chemical and environmental isotope data. Relatively rapid changes in composition can be expected, especially in depth. The pattern of environmental radioactive isotopes show sharp changes from one place to another. If the three-dimensional flow pattern is not considered, data may be misleading and even appear as chaotic and seasonally variable.

The salinity of wetland water depends on the salinity of discharging groundwater, on the contribution of surface water, on local evaporation and transpiration, and on the outflow of salts. This outflow of salts is an important salt balance term (total salinity or a given solute concentration or the isotopic composition) and can be split into several terms:

a) surface water outflow, perennial or seasonal. Generally it can be directly observed,

b) groundwater outflow, perennial or seasonal, depending on wetland water level and groundwater head conditions (Sacks et al. 1992; Novitzki 1982), which is not seen and requires an adequately-designed monitoring network and some seepage studies at the wetland site (Lee 1977; Lewis 1987; Carrera 1997; Hunt et al. 1996),

c) precipitation of some components when the solubility product is overcome due to evaporative concentration, co-precipitation with other solids or changes in pH and/or redox conditions. Some precipitates may be totally or partly re-dissolved in subsequent wet events or trapped with sediments. In some cases, instead of precipitation there occurs mass transfer to the atmosphere, such as happens for nitrogen from reduction or nitrate or carbon dioxide evolved from groundwater,

d) deflation by wind. Generally this is only important in some playa and sabkha-like wetlands; part of the wind-blown salts may be recycled to the wetland after incorporation by rainfall into the aquifer recharge.

Figure 5 shows a cartoon with different simplified conditions of groundwater-dependent wetlands and lagoons, which rely on surface and underground outflow conditions. Figure 6 refers to a chain of wetlands and lagoons in which inflow and outflow change from a wet to a dry period.

Even when the ground does not contribute directly soluble salts, the salinity of groundwater is generally higher than that of local runoff water. This is due to evaporative concentration, the incorporation of hydrolizable minerals after the passage through the soil due to the effect of soil CO_2, and to some extent to the oxidation capacity of dissolved oxygen (oxidation of organic matter, sulphides and nitrogen compounds). Carbonates are easily hydrolizable and given enough time also are many silicates. Silica (such as in siliceous beach and dune sands) does not contribute anions and its own solubility is low at ambient temperatures.

In some areas carbonate (as well as gypsum) dissolution may produce ground collapses, which may extend down to the water table, producing wetlands and lakes. In wetlands and lakes fed by calcium bicarbonate-rich groundwater, the

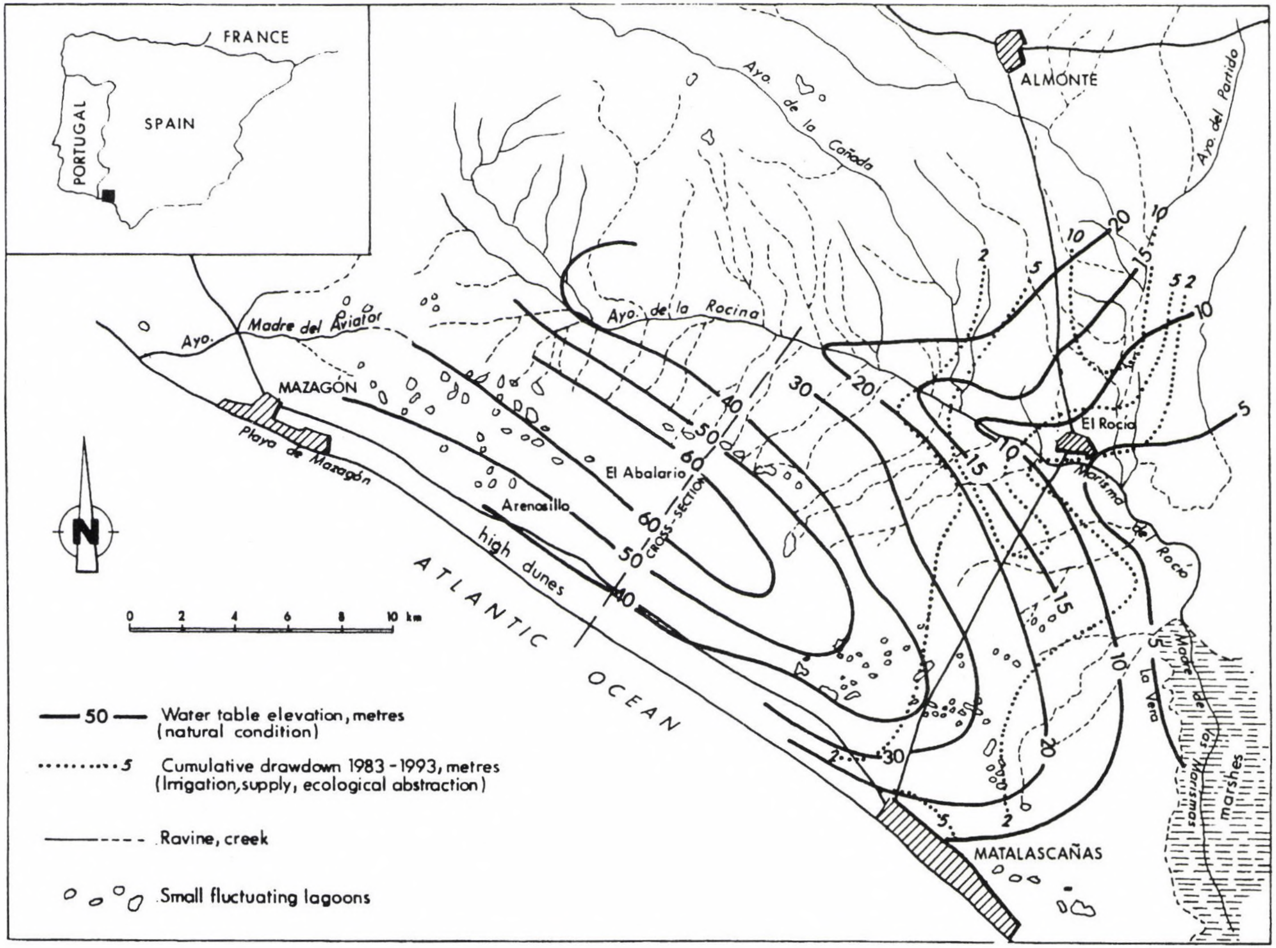
FRANCE
SPAIN
PORTUGAL
ALMONTE
Ayo. de la Cañada
Ayo. del Partido
Ayo. de la Rocina
Ayo. Madre del Aviator
MAZAGÓN
Playa de Mazagón
El Abalario
Arenosillo
high dunes
CROSS-SECTION
El Rocio
Marisma del Rocio
ATLANTIC OCEAN
La Vera
Madre de las Marismas
marshes
MATALASCAÑAS
N
0 2 4 6 8 10 km
50 Water table elevation, metres (natural condition)
5 Cumulative drawdown 1983 - 1993, metres (Irrigation, supply, ecological abstraction)
Ravine, creek
Small fluctuating lagoons

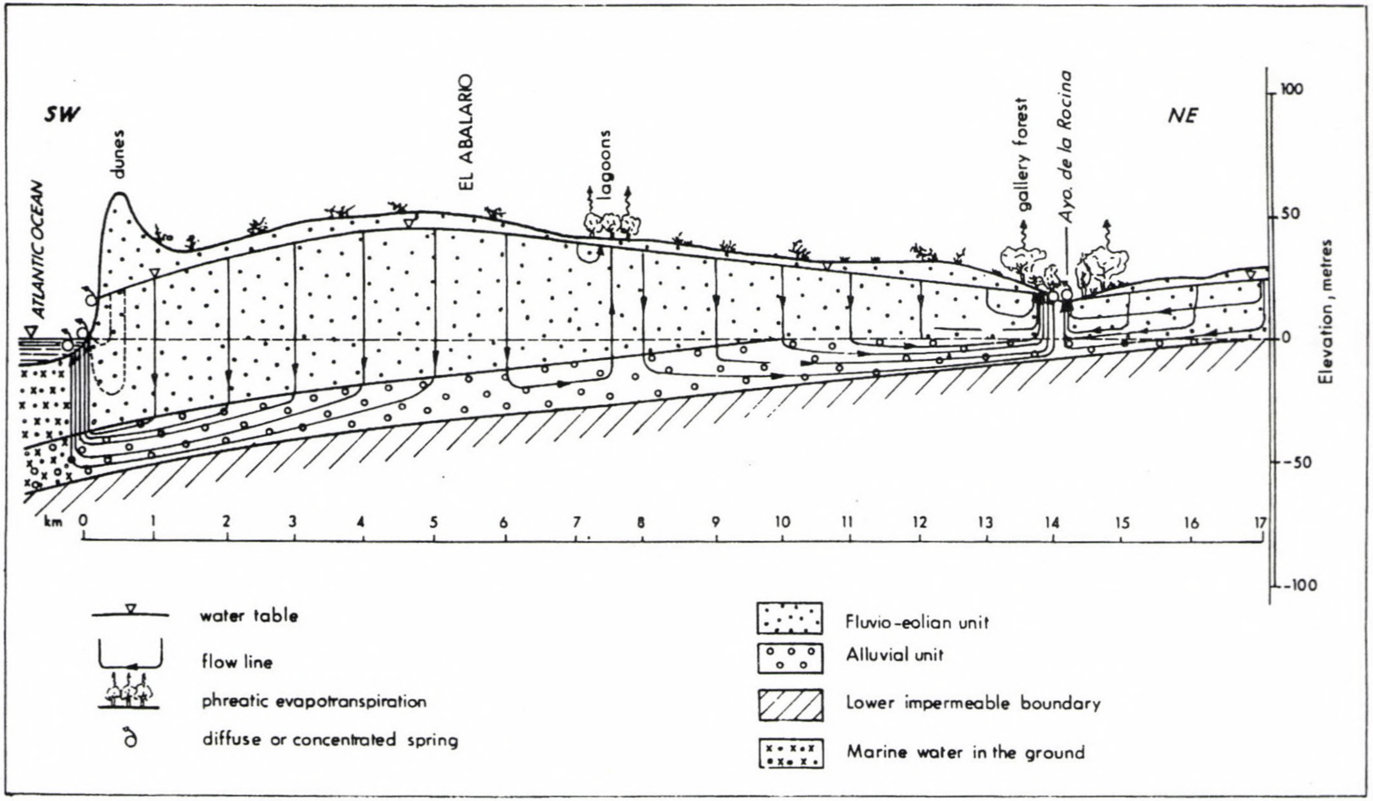

Fig. 2
Schematic representation of the water table elevation of the El Abalario sandy area, to the W of the Doñana wetland area, in SW Spain. The cross-section shows the simplified groundwater flow pattern between La Rocina ravine and the sea. It has a clear three-dimensional pattern due to the existence of a permeable alluvial unit below the sand formation. This last is one to two orders of magnitude less permeable. Equipotencial surfaces are almost horizontal in the sands and close to vertical in the alluvial unit. Beside groundwater discharge at the coast and to the ravine, groundwater sustains the riparian gallery forest and an intermediate area with forest and fluctuating lagoons (after Custodio and Palancar 1995). Model interpretation and chemical and environmental isotope studies confirm these conclusions (Trick et al. 1995; Trick 1998; Iglesias 1999)

loss of CO_2 to the atmosphere and pH changes favors calcium carbonate precipitation. Under favorable water turnover time in the lagoon and biochemical conditions precipitation may be concentrated in the surface water outflow area, thus forming travertine that may partly clog the outlet, and raise the water level in the wetland, lagoon or lake. This is the case of the Lagunas de Ruidera, in Central Spain. This situation differs from the ponding effect

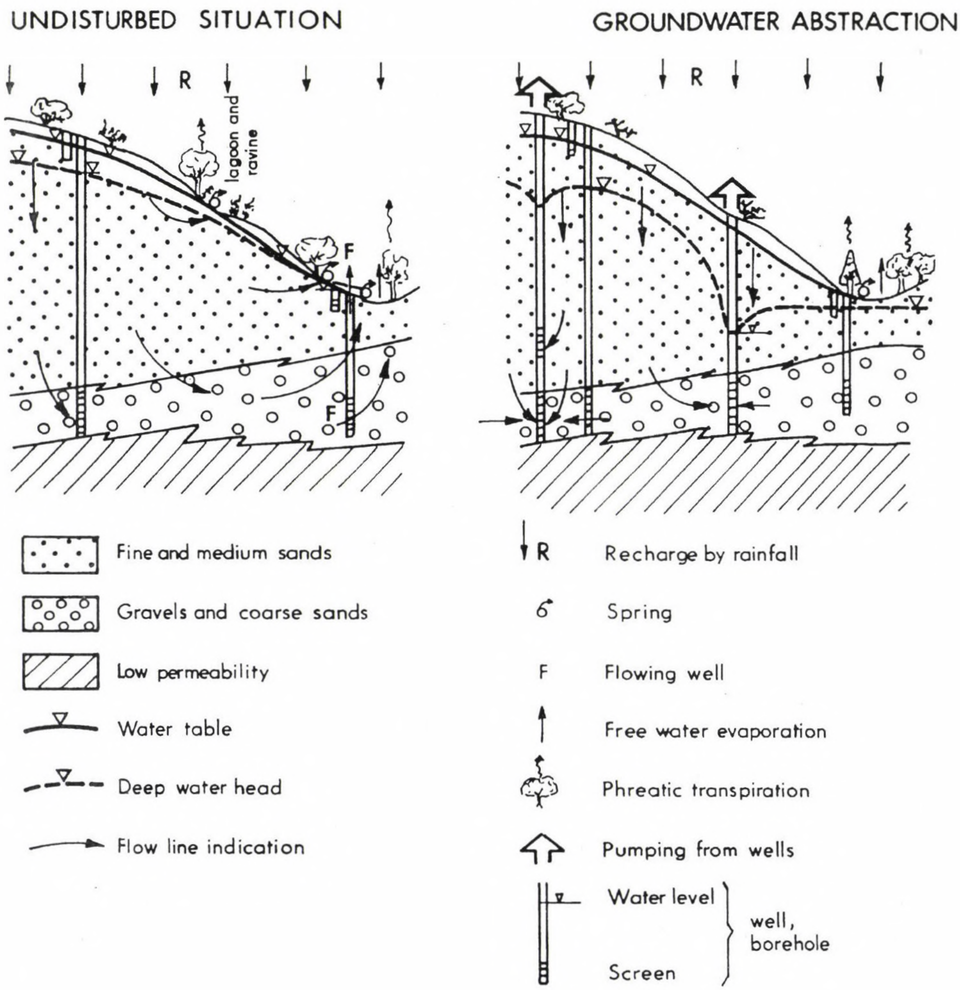

Fig. 3
Idealized cross-sections based on data around the La Rocina ravine from an area close to El Rocío, in Doñana, SW Spain, showing the difference between the water table and the deep water head of the preferentially permeable bottom layer, under undisturbed conditions and with wells abstracting groundwater from the bottom layer

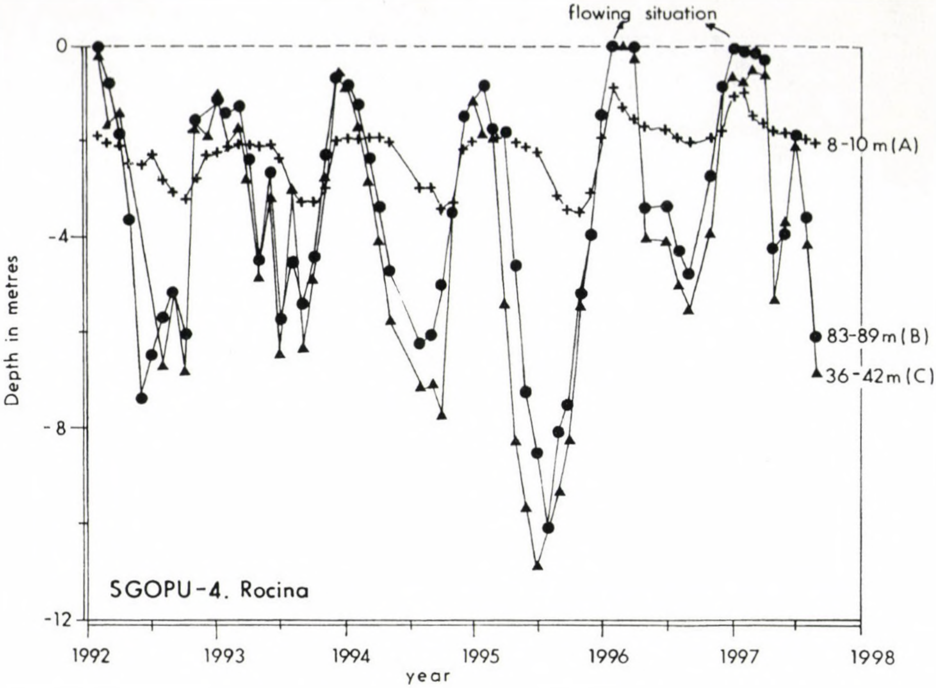

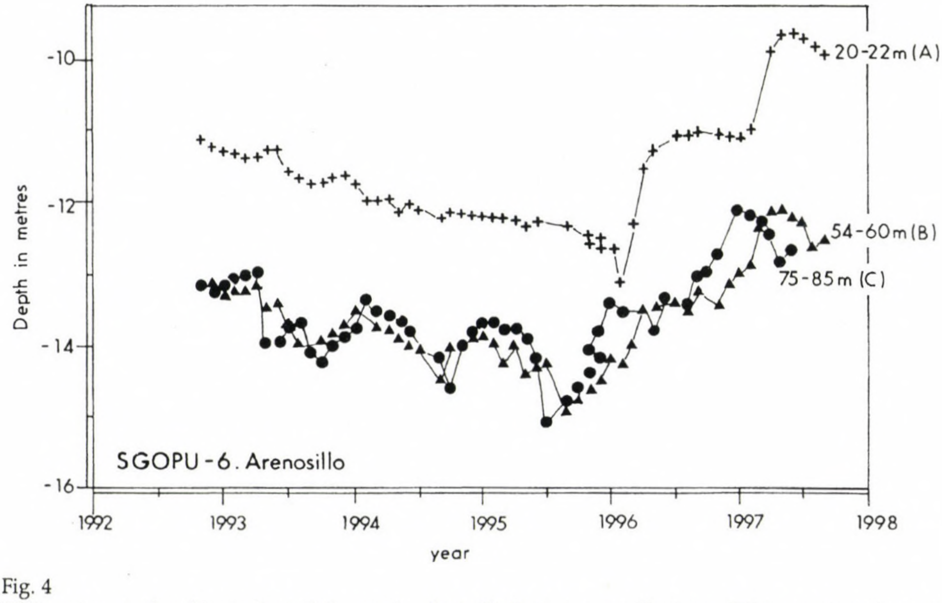

Fig. 4
Different water level records at different depths in El Abalario area, Doñana, SW Spain. See Fig. 2 for the situation. Borehole A represents the water table position and boreholes B and C the water head in the deep, more permeable layers. Note the influence of seasonal deep groundwater development

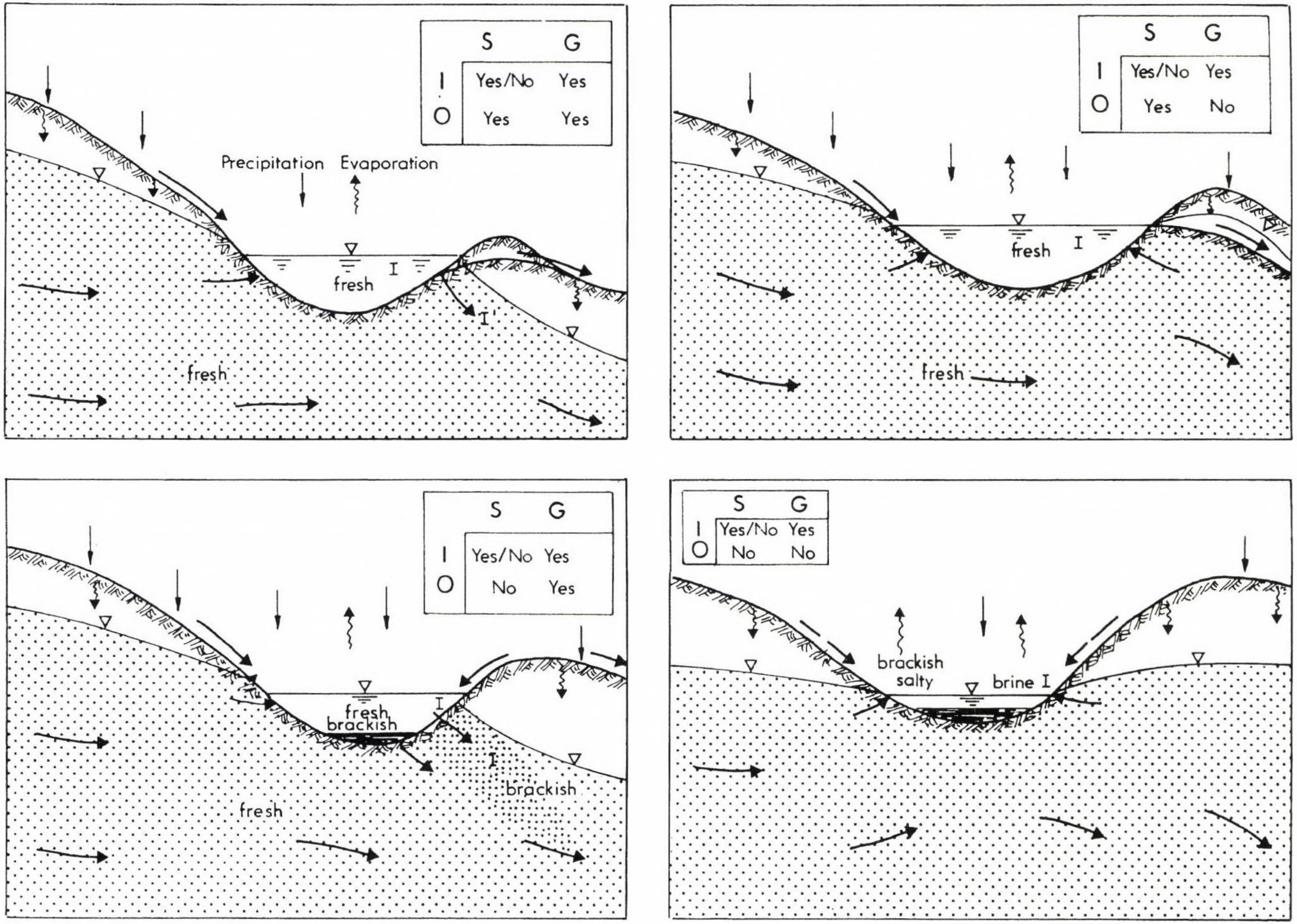

Fig. 5
Cartoons depicting surface water (S) and groundwater (G) inflow (I) and outflow (O) to a wetland, and the salt budget effect on the lagoon and groundwater, assuming that inflow is fresh water. It is assumed that the wetland (or the lagoon) has low permeability bottom sediments that restrict surface-groundwater recharge to the boundaries. "I" means that water has a heavier isotope composition, means water table and water level. The undotted parts below ground level correspond to the unsaturated zone

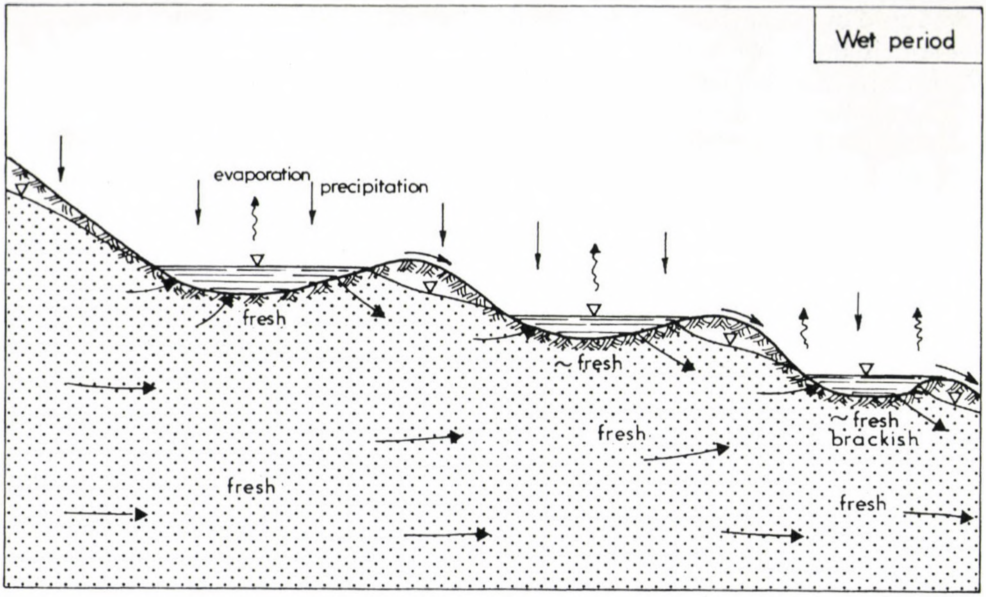

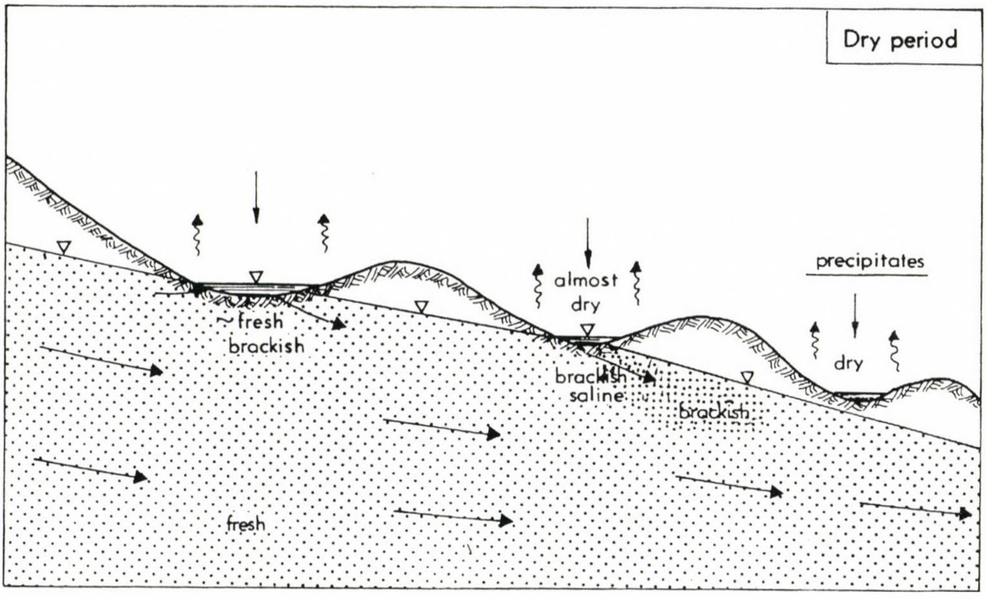

Fig. 6
Cartoon of a series of surface and underground related wetlands and lagoons along a flow path in a wet and in a dry period

produced by tectonics or by obstruction by volcanic outflows or landslides, as can be seen in the Canary Islands, especially in the arid southern Gran Canaria, in the form of oases at the bottom of the deeply-incised creeks (barrancos).

Groundwater salinity in semi-arid environments may be changed if the vegetation cover is changed. This has a delayed but sometimes definitive effect on wetlands and river base flow. An example is the Murray Basin in South Australia (Barnett 1984; Simpson and Herczeg 1991) after eliminating the highly efficient rain water use of eucalyptus forest. This is what probably happened in the arid Monegros area (NE Spain) a few centuries ago, when similarly effective brush forest was destroyed.

As mentioned above, groundwater-dependent wetlands can be found in:

a) areas close to rivers and creeks, in flat lands and alluvial plains, in areas associated with obstructions by landslides or volcanic sediments, and as lateral groundwater discharges from old, elevated terraces,

b) depressions and flats at the foot of slope changes, at dune edges or at inter-dune positions ("corrales" in SW Spain),

c) depressions formed by ground dissolution, such as dolines, poljes and collapse structures, in carbonate rocks but also in gypsum and halite formations. In these karstic features the normal evolution implies a decreasing water table. In this case depressions generally do not reach the water table except if the area is affected by a rise of the regional discharge base level due to tectonics, Holocene sea level rise, obstruction of the river valley, or other effects. Dissolving formations may be shallow or deep ones, acting as a confined aquifer,

d) areas in which spring flow, creeks and rivers are ponded by calcium bicarbonate rich groundwater, which clog and dam the outflow channel by calcium carbonate precipitation, in the form of travertine,

e) areas in which forced, confined aquifer outflow through the confining layers (following tectonic faults or sedimentary discontinuities). In such cases the wetland may form even in elevated areas which are surrounded by highlands where the aquifer recharge is produced (Fig. 7),

f) places where the aquifer flow is forced to discharge due to lateral transmissivity decrease of sedimentary origin or due to coastal sedimentation. Such is the case of aquifers that are bounded laterally or which become confined by recent, low-permeability coastal marine sediments in deltas. It is not rare that discharging water becomes brackish in some areas when there is flow along the fresh groundwater–seawater mixing zone (see Fig. 8).

When the wetland is at the end of an aquifer system its characteristics are rather permanent, the more permanent the larger the system. But there are wetlands receiving only a part of the groundwater flow (the regional discharge being at other place), like an overflow. These show the most large fluctuation and may change dramatically after natural or artificial hydrologic changes (climatic change, vegetal cover modification, and groundwater development).

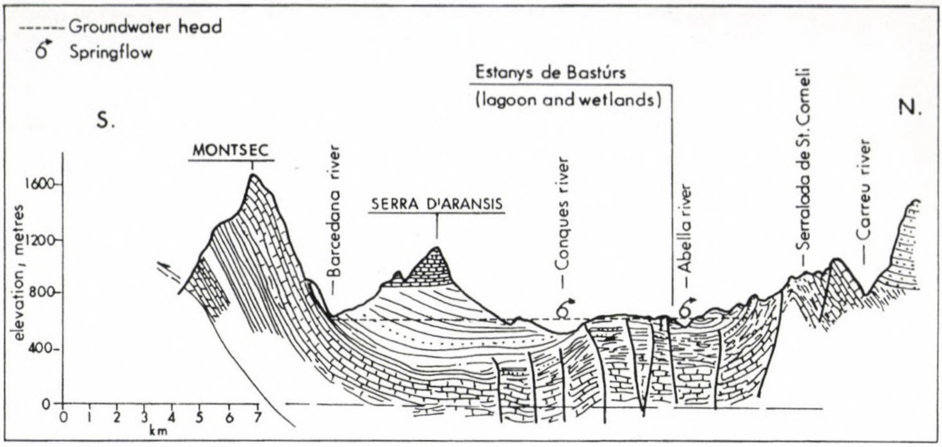

Fig. 7
Basturs lagoon and surrounding wetlands, in central Catalonia, NE Spain (after Pascual 1992). The cross-section shows that they are due to the discharge of a deep limestone aquifer, recharged in the surrounding highlands and discharging to other rivers and artificial reservoirs. Groundwater outflow is through tectonic discontinuities, which connect the deep limestone and sandstone layers with the surface through the marly formations

Groundwater exploitation effects

Aquifers which feed wetlands may also be interesting potential sources for abstracting freshwater. Actually many of them are intensively developed. Groundwater resource development has a clear set of advantages linked to the reliability derived from the associated large water reserve, the generally good chemical and biological water quality, the possibility of direct use as drinking water, the large surface area which allows for direct access from many points (thus avoiding large water transportation networks), the relative security against natural hazards, human failures and criminal actions, and some resilience against rapid, accidental pollution. Groundwater resources and aquifer system characteristics are relatively easy to evaluate, and knowledge improves as development progresses if there is a monitoring network and complementary studies are added. Future behavior can be forecast with some confidence if reasonable future scenarios are used.

However, aquifer development also has negative consequences, most of which can be anticipated if development is carried out rationally. Consequently they are susceptible to correction and economic internalization. These negative consequences are often called problems and/or overexploitation (Custodio 1992, 2000) but are really effects which have not been taken into account beforehand, mostly due to development without adequate knowledge of the aquifer.

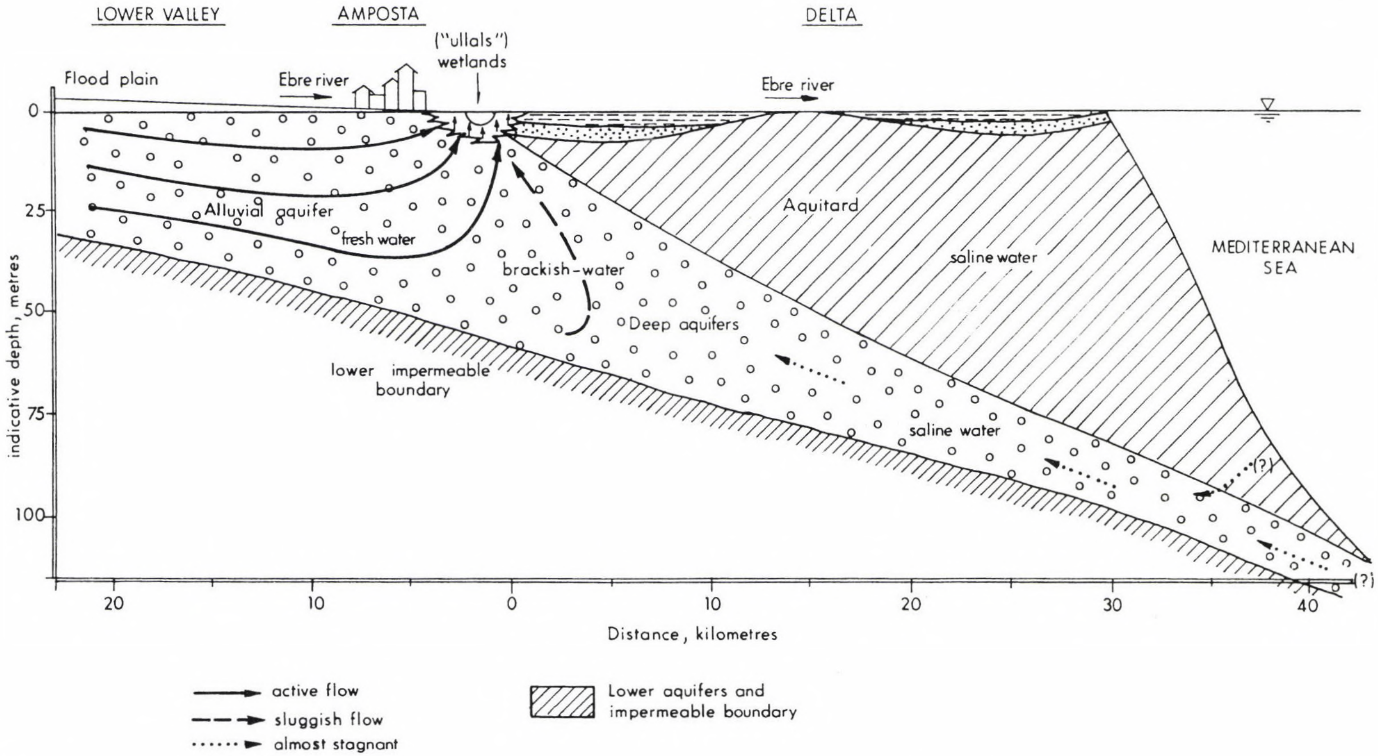

Fig. 8
Schematic representation of groundwater conditions in the lower Ebre river valley and delta, southern Catalonia, NE Spain (after Bayó et al. 1996). Flow of fresh groundwater, recharged at the river terraces and surrounding carbonate mountains, is forced to discharge at the delta apex because the low permeability Holocene sediments confine the Pleistocene aquifer. The higher density of marine water produces a fresh water head at the submarine outcrop of the Pleistocene aquifer, which is higher than the river elevation at the delta apex. This produces a sluggish flow of salt water moving towards the fresh water discharge area in the wetland by means of springs ("ullals"). The result is brackish water by mixing fresh and saline water. Saline water flow is also enhanced by deltaic sediment compaction

Negative groundwater effects refer to the groundwater level drawdown associated to well abstraction, which is hydraulically needed to create the head conditions to convert natural aquifer discharge into well production (see Figs 3, 4 and 9). The associated use of water reserves as water level decrease delays the

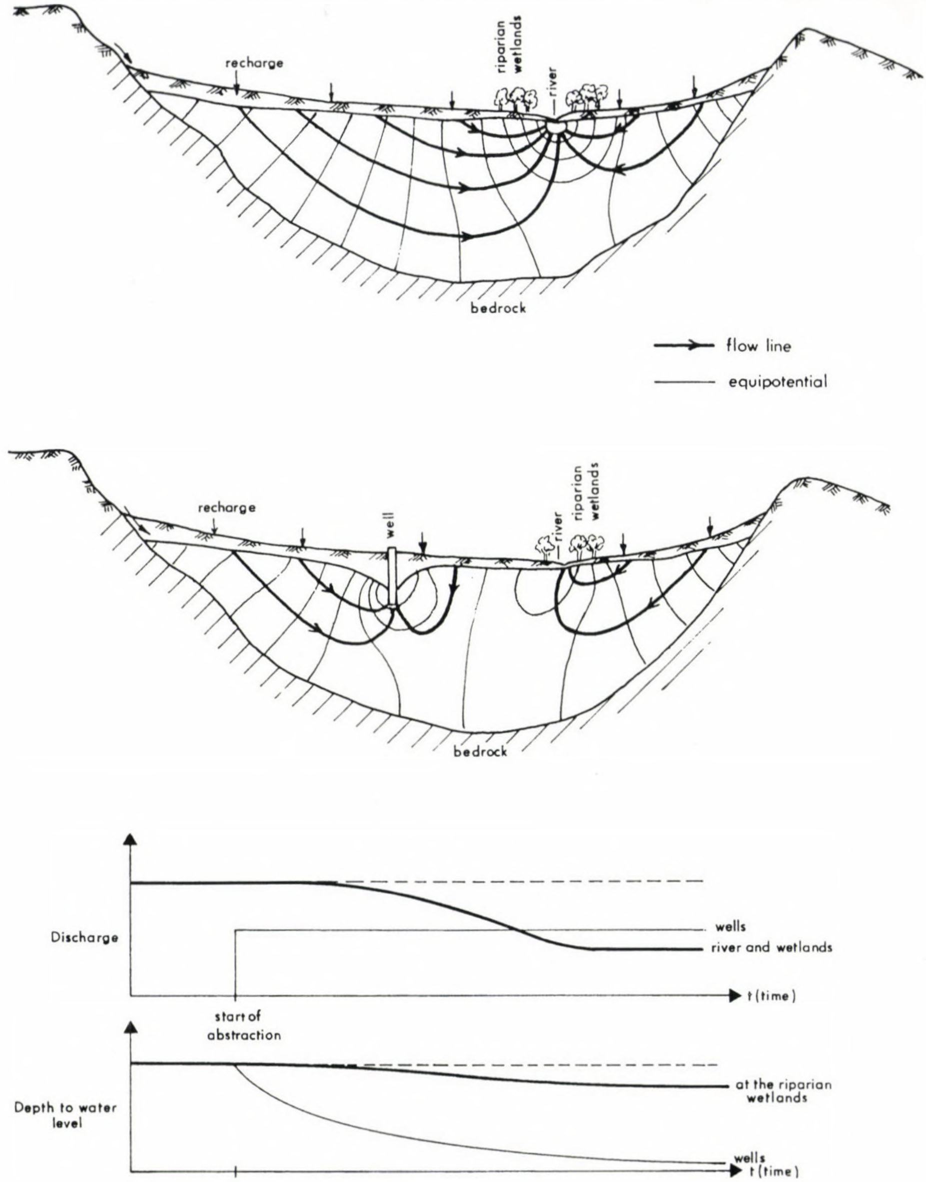

Fig. 9
Effect of groundwater development in the sediments of a river valley or a depression, on riparian wetlands dependent on groundwater

effect from months to millennia, depending on aquifer size and characteristics. The result, however, besides increasing exploitation costs, is the progressive reduction of spring and river base flow and, in general, a decreasing discharge rate at the natural outflow points and surface areas.

Associated to groundwater flow pattern changes, some slow groundwater quality modification may happen due to changes in the water-mixing pattern. This appears when different aquifers and subaquifers are developed at the same time (long screen or multiscreen wells), when different (often poorer) quality groundwater bodies are displaced – recent or relict sea water encroachment in coastal areas is one example – and when surface water infiltration is induced or increased.

Another class of negative consequences is land subsidence due to sediment compaction as pore water pressure decreases, as well as increased collapse rate in karstic areas (carbonates and gypsum), mostly but not exclusively at shallow depths.

The related economic, social and political consequences must be added to these negative technical consequences. The impact on wetlands will be considered below. However, it must be stressed that these negative consequences must be compared with the advantages of groundwater development. Part of the benefits should be applied to compensate physically, economically, and socially for the drawbacks. Often aquifer development, if rationally carried out, has a net economic and social benefit, even if environmental values are affected to some extent. There is a trade-off to be considered between satisfying reasonable human needs and Nature preservation. Not only technical and economical evaluation but also social acceptance and political decisions are needed. This is something not specifically linked to groundwater development, as some argue, mostly to discredit it in order to foster other water resource development projects, which are often more expensive, put a heavy economic burden on the population and may be less environmentally friendly.

From what has been previously explained, the primary impact of groundwater exploitation on wetlands is the decrease of groundwater discharge and the lowering of the water table. This reduces water input to the wetland and in some areas the water table and the capillary fringe are brought down beyond the root depth of plants whose roots cannot follow the deepening of their water source. The result is the reduction of the wetland and phreatophyte surface area. In severe cases they will completely disappear (Fig. 10). All these processes are slow and delayed. The time scale is measured by L2/D, where L is the linear dimension of the affected aquifer and D is hydraulic diffusivity, which is the ratio of

Fig. 10 →
Decline of groundwater contribution to the Las Tablas de Daimiel National Park wetlands, in Central Spain, as a consequence of intensive groundwater development for irrigation. The wetlands are now fed only by surface water and imported water from other river basins. The tail part of the Guadiana river and the main springs ("ojos") feeding it are now dry except for occasional runoff. Some dewatered peatlands may start spontaneous combustion (modified from Llamas 1988, 1989, 1992)

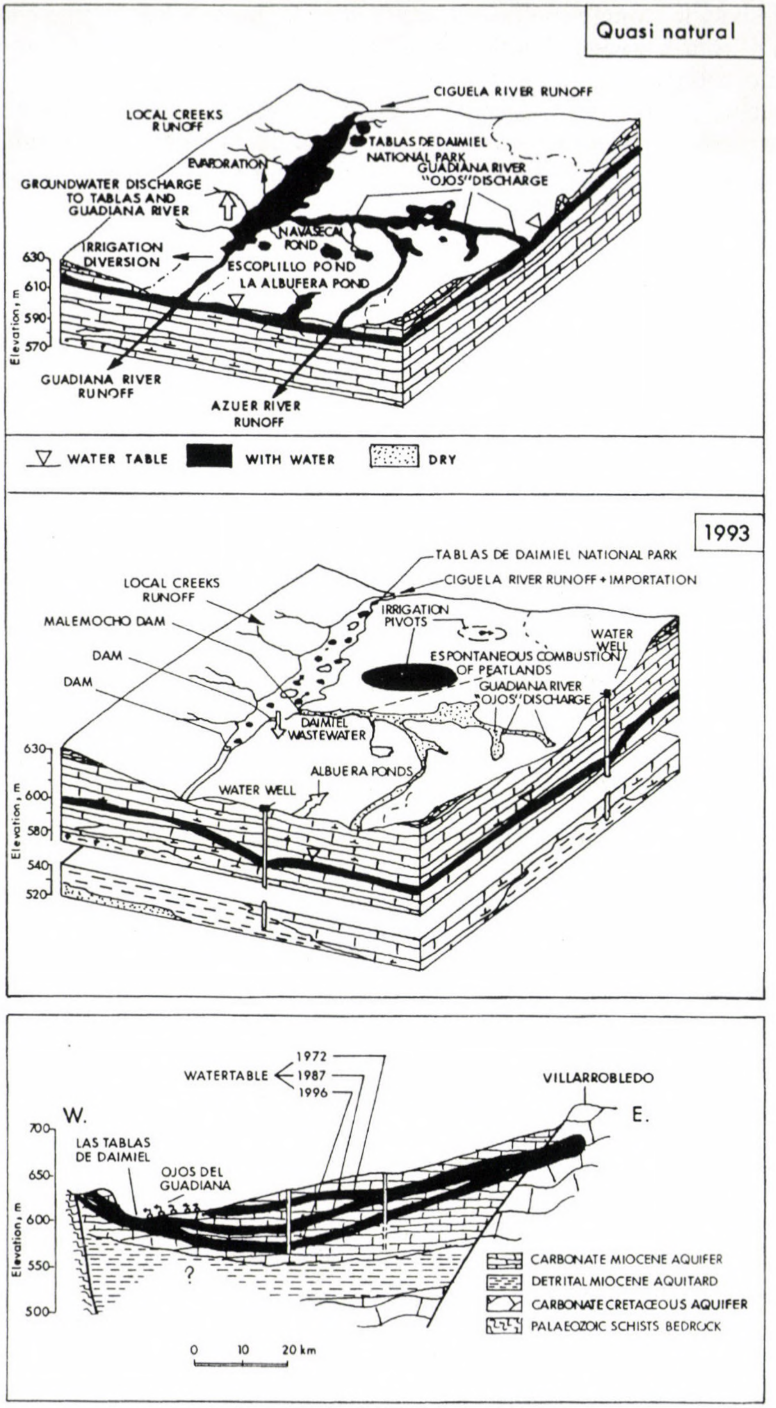
Quasi natural
CIGUELA RIVER RUNOFF
LOCAL CREEKS RUNOFF
TABLAS DE DAIMIEL NATIONAL PARK
EVAPORATION
GUADIANA RIVER "OJOS" DISCHARGE
GROUNDWATER DISCHARGE TO TABLAS AND GUADIANA RIVER
NAVASECA POND
IRRIGATION DIVERSION
ESCOPLILLO POND
LA ALBUFERA POND
GUADIANA RIVER RUNOFF
AZUER RIVER RUNOFF
Elevation, m
WATER TABLE
WITH WATER
DRY
1993
TABLAS DE DAIMIEL NATIONAL PARK
CIGUELA RIVER RUNOFF + IMPORTATION
LOCAL CREEKS RUNOFF
MALEMOCHO DAM
IRRIGATION PIVOTS
DAM
DAM
WATER WELL
ESPONTANEOUS COMBUSTION OF PEATLANDS
GUADIANA RIVER "OJOS" DISCHARGE
DAIMIEL WASTEWATER
ALBUERA PONDS
WATER WELL
WATERTABLE
1972
1987
1996
VILLARROBLEDO
W.
E.
LAS TABLAS DE DAIMIEL
OJOS DEL GUADIANA
CARBONATE MIOCENE AQUIFER
DETRITAL MIOCENE AQUITARD
CARBONATE CRETACEOUS AQUIFER
PALAEOZOIC SCHISTS BEDROCK
0 10 20 km

transmissivity to storage coefficient. When development is less than recharge the evolution comes to stabilization after 0.5 to 2.5 times the indicated value (Custodio 1992).

The actual values of L and D depend on aquifer system structure and heterogeneity, and they may change with time as a larger part of the aquifer system is affected and the confined behavior of some layers evolves toward one close to that of a water table aquifer, as groundwater flow through aquitards extends the influence of groundwater development.

The actual impact of groundwater development is often obscured by natural fluctuation and the generally changing abstraction pattern, compounded by the slow, long-term evolution. Changes may be imperceptible in the near term, even for intensive groundwater development. This makes it impossible to forecast future evolution from the few observations obtained shortly after the start of development, but it is feasible by calculation. One or a few wet years in the rainfall sequence may even change the negative general trend into a positive reaction when monitoring is inadequate and interpretation is carried out without a sound knowledge of hydrogeologic facts.

Deducing impacts from the known behavior of other groundwater-dependent wetlands can only be done if there is real similarity, and this can be only established after a sound hydrogeologic evaluation, which has to go much deeper than the mere similarity of climate, surface area or geology. Calculation is the procedure to be followed, which often has to be based on adequate numerical modeling. This has to be updated and improved as development progresses.

Beside hydraulic changes, water quality changes are just as important, both from the hydrologic and the ecological point of view. Generally water quality changes appear even at a slower pace than the hydraulic ones. Some effects may develop after some relatively long time, when fronts are displaced through some layers. Some of them derive from:

a) changes in the wetland salt balances due to modification of input and evaporative surface area (including that produced by plants). This affects salinity and chemical composition, often in a complex form since outflow may also change,

b) mineralization of sediments of de-watered areas with the help of biochemical reactions supported by oxygen penetration by natural diffusion from the atmosphere or enhanced by plowing when farming activities are carried out in them. This mineralization may incorporate nitrate, sulfates and hardness to recharge water. Redox processes may affect not only organic matter-rich topsoils but also deeper formations. When sediments incorporate precipitated salts they may dissolve,

c) incorporation of contaminants from human activities in the surroundings such as farming, animal raising and urbanization, beside the contribution by recharge surface water. Agrochemicals may be of concern, especially nitrate and possibly pesticides and their metabolites. This last aspect is still poorly known, and degradation and sorption play a dominant role. The transport of phosphorous compounds is delayed in river basins (Weiskel and Howes 1992) but in principle they do not appear a serious threat through the underground path since they tend to be fixed in the ground. But there is still insufficient experience since fixation may be only apparent and the result of very delayed movement. Fixation seems important in carbonate-rich sediments but not as much in pure silica sands, although surface effects are still noticeable in them; the iron oxyhydroxide coatings of sand grains, which are frequent in eolian and fluvio-eolian sediments, may help in phosphorous compounds' retention. Even for conservative contaminants such as chloride and nitrate (in oxidizing ambient conditions) the transport to the wetland may be partly or totally delayed for a long period due to advection, when there are long flow paths. This is the case in Doñana (Custodio 1994; Iglesias 1999).

Chemical changes in a wetland, and especially the increase of nutrients, may have significant effects on vegetation and fauna. Nutrients accumulate slowly, which adds to the delay introduced by the underground transport. When nitrate is the only nutrient reaching the wetland, in addition to being eliminated by some kind of vegetation, it does not necessarily promote the growth of algae typical of eutrophic lakes. At the Ruidera lagoons (Upper Guadiana river basin, Central Spain), in spite of relative high nitrate contents water keeps its transparency and carbonate-associated microorganisms may produce a spectacular green-turquoise color when groundwater contribution dominates. The elimination of nitrate contributed by groundwater seem relatively effective in coastal marshes (Barón et al. 1997; Portnoy et al. 1998; Slater and Capone 1987).

The response of plants to decreasing groundwater availability may also be delayed because they may resist water stress during some periods due to the natural fluctuation. However, a water table drawdown trend means that stress periods become progressively longer. Even if the plant is able to extend its roots downward, it may become less resistant to diseases and external attack, until finally it dies out. This is equivalent to a decreasing rainfall contribution.

Groundwater–wetland relationship study methods

The methods to know, measure, observe and monitor groundwater–wetland relationships under natural conditions and to evaluate and forecast the impact of human activities do not differ from common methods of groundwater study. However there are some specific aspects to be taken into account, beside the regional studies which are always needed:

a) local characteristics may play a dominant role and the nature of sediments in and around the wetland must be considered in detail,

b) even if the wetland is on top of the aquifer, most of the water exchange may be limited to restricted areas,

c) the contributing groundwater basin and the inflow and outflow areas may change with groundwater head fluctuation and changes of the abstraction pattern,

d) mass transport may be controlled by local heterogeneities,

e) groundwater flow and groundwater quality must be known in three dimensions, at least close to the wetland,

f) monitoring and water sampling networks must be designed according to the three-dimensional nature of the flow and quality pattern, and the local characteristics of water exchange between the surface and the ground,

g) the detailed knowledge of the water table and the capillary fringe position is a key issue for the wetland and its surroundings,

h) the values of exchange capacity and sorption characteristics of soils and sediments may be needed to define mass transport,

i) to anticipate and forecast contamination problems, studies and monitoring of the unsaturated zone at selected areas may be needed, as well as to take into account local processes such as how much water repellence of dry sand affects recharge pattern and rate.

The knowledge of aquifer geometry requires some drilling accompanied by geophysical logging, extended by surface geophysical surveys. Methods should be adequate to the objectives and the depths. This is costly and thus restricted for budgetary reasons. Therefore careful planning is needed to get as much useful information as possible with limited budget resources. Surveys and prospection should be combined with monitoring plans and the fieldwork needed to get chemically and isotopically representative samples. In order to get representative samples as soon as possible, the use of drilling fluids and additives must be restricted. Otherwise the disturbance will prove difficult or too expensive to redress.

Monitoring groundwater head and quality often requires tubes screened at different depths. In such cases, nested tubes in a same borehole must be devised. However, in cases in which isolations cannot be guaranteed it is advisable to drill separate boreholes. To get representative samples good isolations of the screens are needed, tubes must be resistant to fissuring and corrosion, and the joints must be waterproof. Electrical conductivity and temperature logs are useful tools to understand water origin and renovation within a borehole (Custodio 1995b, 1999).

The best knowledge is derived when hydraulic and geochemical studies are combined. Evaporation of surface wetland water produces isotopic water changes, which are more sensitive than ion concentration at the early stages. In many cases they can be used as tracers for wetland outflow through the ground. Tritium is still a good environmental tracer to define the flow pattern when turnover time is not too long. Its usefulness can be extended by the tritiumhelium method. Strontium isotope ratio also seems a promising tool (Hunt et al. 1998).

Chemical speciation and reaction computer codes are useful to know groundwater changes and behavior, such as ion exchange, precipitation, dissolution and other reactions, but also simple concentration values and ion ratios are generally readily useful tools if carefully used.

Current behavior, evolution forecasts and the analysis of scenarios for future action (groundwater development, changes in land use and vegetation cover, restoration projects) must be quantified. This can be carried out by well-known groundwater hydraulic methods, even by simple formulae, but complexity and fluctuation favor the use of numerical flow and mass transport simulation models. A large series of useful models are available, but considering the three dimensions may be a major drawback, since they are not prepared for or cannot be run in common computers due to memory capacity problems, and the lack of tools to easily display and analyze the results. In these cases vertical cross-section models may be useful, but flow line convergence or divergence must be taken into account. The radial effect of pumping wells can be incorporated, under some conditions, by introducing corrections based on well hydraulics closed solutions (Trick 1998). Figures 11 and 12 present simulation results for the sandy El Abalario Area, in the Doñana Natural Park, in southwestern Spain.

Representative models, even if crude, are very useful for carrying out sensitivity analyses and thus directing study and monitoring effort to the most influential factors. The analyses of future scenarios are needed to carry out risk assessments of the impact of man's activities and future new conditions, including climatic change.

Unsolved current issues on groundwater-dependent wetlands

The hydrological function of groundwater-dependent wetlands is not sufficiently known, experience is still scarce and complete case studies are lacking. This is a common situation in hydrology when dealing with specific situations, which generally involve a large set of scientific, technical, economical, social and political issues. Scientific and technical issues are generally the best known and the easiest to deal with. This paper refers preferentially to them. The others are much more speculative and involve a large set of non-measurable or difficult-to-measure variables, which also depend on local social perception, regulations and laws, and on a complex network of social and political pressures and objectives. They are mostly licit. But in some cases they may involve obscure interests, which may have little relationship to wetland issues although they use current public sensitivity toward wetlands as an excuse to foster other goals.

Scientific and technical issues, as explained before, besides expanding the basis of knowledge, do not present new specific difficulties that cannot be dealt with existing tools. But some tools are too crude or too sophisticated. How to select

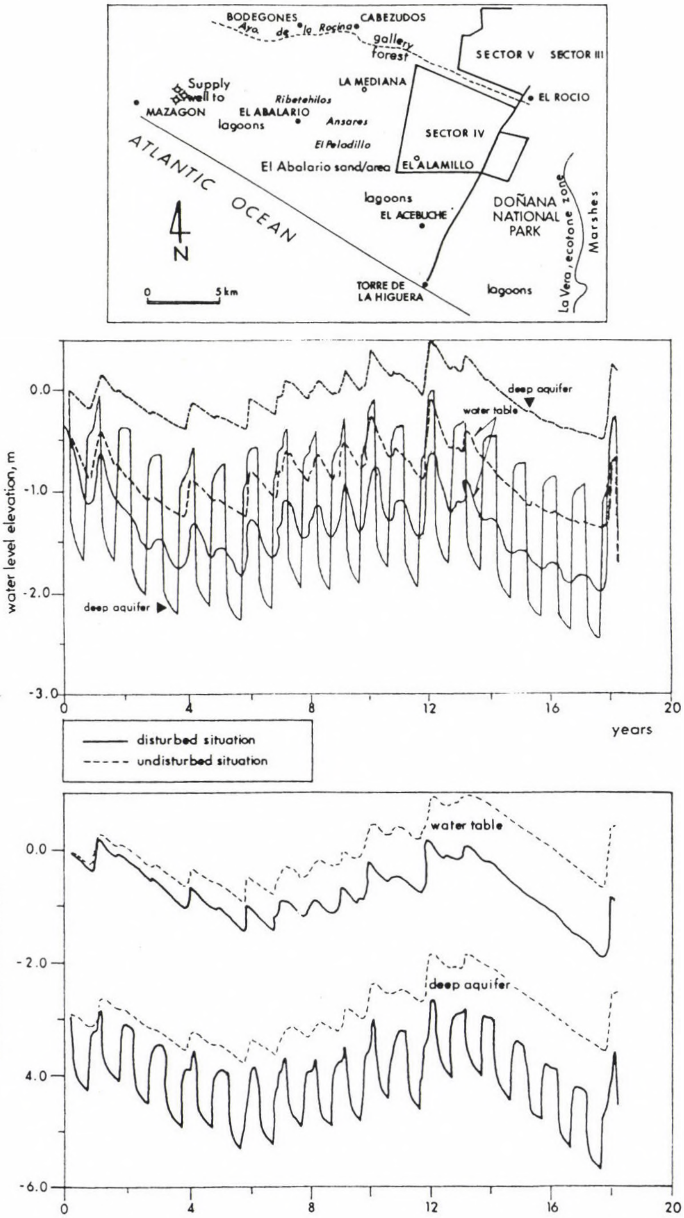

Fig. 11
Simulated effect of groundwater withdrawal from the deep aquifer of El Abalario area, Doñana, SW Spain, after Trick (1998), differentiating the water table from the deep groundwater head. The undisturbed situation is compared to the effect of agricultural abstraction in Sector IV, starting in year 0. Recharge is that calibrated for the 18-year period of data. Other groundwater abstraction is assumed under steady conditions

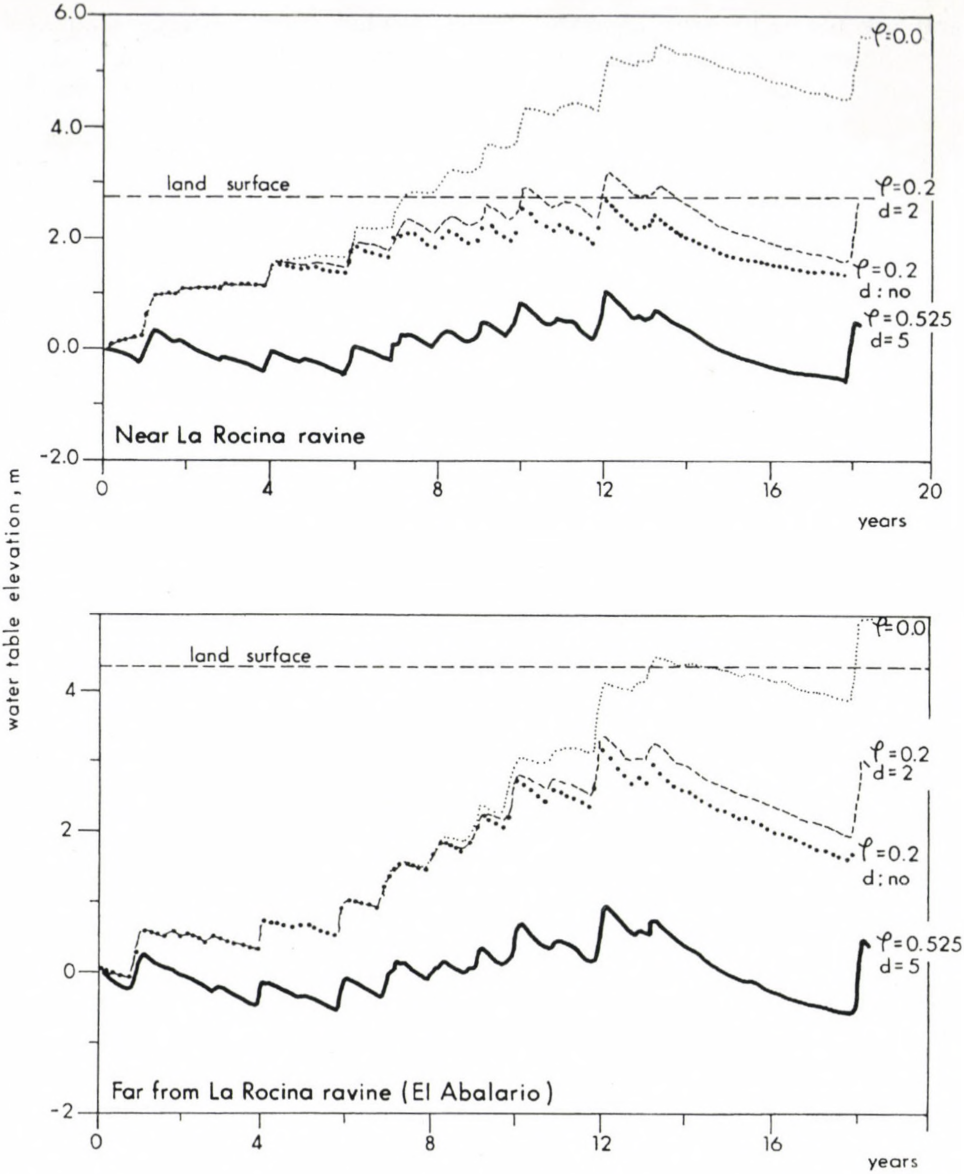

Fig. 12
Simulated effect on water table elevation of land management options in the El Abalario area, Doñana, SW Spain (after Trick 1998). φ is the maximum phreatic evaporation (m a^{-1}); 0,525 is the calibrated situation with eucalyptus plantations; 0.2 is assumed representative of re-established native forest vegetation; 0.0 is after eradication of eucalyptus plantations without new tree cover; d is maximum depth of phreatic evaporation (m); 5 is the value for eucalyptus; 2 is assumed the value for native black forest; "no" means vegetation may adapt to any water table depth

and use the right ones, according to the wanted objectives, is a challenge demanding not only experience, but also wisdom. There is tendency to look for the more complex ones, which demand a large series of data which are mostly unavailable, very expensive and time-consuming, and which are relatively difficult to operate. This is inadequate to make decisions at the right moment and for those who can make them, although there is some pressure by conservationists and biased "scientists" to do so.

Another related issue is how to transform calculations (the significant ones with respect to the problems to be considered) into useful evaluations, forecasts and analyses of scenarios, to make decisions and to help in obtaining agreements among the involved stakeholders.

All this is related to which level of knowledge and monitoring is sufficient to define the problems to be solved and make the adequate decisions. The following list presents a series of economic and social issues, which has political implications, and which are the subject of further research, agreement, and experience:

a) Is a pristine natural situation what is really wanted and needed?

b) How much interference from groundwater development and land use is adequate and bearable, taking into account benefits and social needs?

c) Is it possible and advisable to intervene to maintain an evolving groundwater-dependent wetland as it is today or it was in the past, or it is better leaving Nature to follow its course?

d) Who pays for the lost economic and social benefits which otherwise would be obtained from the now undeveloped groundwater resources, limitations imposed by water quality protection and restrictions to land use due to wetland protection?

e) How to apply fair and equitable limitations to groundwater development and land use to some, while the close neighbors at the other side of an area boundary do not have to support them? Is compensation a solution and by whom and how is it established and carried out?

f) Who pays for the unaccounted side (indirect) effects of groundwater development, groundwater quality changes and wetland value decrease or deterioration?

g) What level of prevention and protection is adequate and enough?

h) How to produce unbiased information for experts, managers and decision-makers, involved people, the public and the mass media?

Conclusion

Groundwater-dependent wetlands, with or without surface water contribution, are important and productive ecosystems characterized by less fluctuation than surface water-dependent ones. Often they are complementary, thus contributing still more diversity and productivity to the wetland. A large diversity of groundwater-dependent wetlands is possible, from small patches to relatively large elongated areas, from fresh water to brine and its associated salt deposits. The underground outlet of many wetlands is also a kind of groundwater-dependent situation which greatly influences water and salt balances. It is a poorly known feature.

Groundwater development of aquifers change hydrodynamic conditions and influence the groundwater quality pattern of related wetlands. Commonly, wetland surface area is decreased and eventually may disappear. The wetland and downstream groundwater may become more saline, although this is often the result of a wide variety of factors. All of these are delayed and slow processes.

An important issue is how to combine wetland preservation and groundwater development. There is a trade-off between some inevitable environmental damage and the desirable benefits from groundwater development. This is not only a scientific and technical issue but also an economic, social and political one, in which not only direct and indirect costs and benefits are to be considered but also many other aspects which are difficult to be reduced to figures easily agreed upon by all concerned. These are the aspects which need more new experience and research, since the scientific and technical ones can be dealt with existing hydrogeologic tools, provided the three-dimensionality of flow and water quality patterns is taken into account, especially near wetlands, where local heterogeneities and sedimentary features may play a dominant role. In any case an adequate degree of knowledge and monitoring needs to be achieved.

Acknowledgements

This paper was prepared after the kind invitation of the Geological Survey of Hungary and the Geological Institute on Hungary, through Doctors Károly Brezsnyánszky and János Halmai. Most of the ideas come from studies carried out at the Department of Ground Engineering of the Polytechical University of Catalonia, Barcelona, where the author is professor, and are especially linked with research projects AMB 92.636 and 95.0372 of the Spanish Interministerial Commission for Science and Technology (CICYT) and project ENV4.CT95.0156 of the European Union Commission. Many of the ideas introduced in the text are the result of many years of discussion and cooperation with Dr. M. Ramón Llamas, member of the Spanish Academy of Sciences and Professor at the Department of Geodymanics at the Complutense University of Madrid, and more recently with Dr. Carlos Montes, Professor at the Department of Ecology of the Autonomous University of Madrid. Much of the work has been carried out by doctoral students in several areas of Spain as well as in Argentina and Uruguay, with the essential, continuous collaboration of Dr. Marisol Manzano in fieldwork and interpretation. Additional knowledge has been incorporated from the experience and knowledge of the Geological Survey of Spain (Instituto

Tecnológico Geominero de España), where the author is temporarily serving as director.

Thanks to the two reviewers, Drs. J. Tóth and W. Zijl, for the suggestions and corrections, as well to Drs. M.R. Llamas and M. Manzano for their comments. The ideas and comments in the text are the author's and are not necessarily shared by any of the mentioned Institutions.

References

Adams, P.R. et al. 1991: Wetland evaluation technique: vol. 1: literature review and evaluation rationale. – U.S. Army Corps of Engineers. Washington D.C. (WES TR WRP-DE-2. Oct. 1991).

Barbier, E.B.; M. Acreman, D. Knowler 1997: Economic evaluation of wetlands: a guide for policy makers and planners. – Ramsar Convention Bureau. Gland, Switzerland, pp. 1–27.

Barnett, S.R. 1984: The management of groundwater induced river salinity due to land clearing in the Murray Basin, southeastern Australia. – Groundwater Management: Quantity and Quality. Intern. Assoc. Hydrological Sciences, Publ. 199, pp. 101–109.

Barón, A., P. Calahorra, E. Custodio, J.A. Fayas, C. González 1997: Saltwater conditions in Sa Pobla area and S'Albufera Natural Park, NE Mallorca Island, Spain. – Proc. XII Salt Water Intrusion Meeting, 1994. University of Cagliary, pp. 243–257.

Bayó, A., E. Custodio, C. Loaso 1996: Las aguas subterráneas en el Delta del Ebro. (Groundwater in the Ebre Delta). – Revista de Obras Públicas. Madrid. 3368, pp. 47–65.

Brinson, M.M. 1993: A hydromorphic classification of wetlands. – U.S. Army Engineer Waterways Experiment Station, Vicksburg, Mississippi, Rep WRP-DE-4.

Carrera, J. 1997: Observación y medidas de la recarga (descarga) a partir de aguas superficiales y conducciones, transferencias y fugas (Observation and measurement of recharge (discharge) from surface water and conduits, transfers and seepages). – La Evaluación de la Recarga a los Acuíferos en la Planificación Hidrológica. Asoc. Intern. Hidrogeólogos. Grupo Español / Instituto Tecnológico Geominero de España. Madrid, pp. 229–245.

Cowardin, L.M., V. Carter, F.C. Golet, E.T. La Roe 1979: Classification of wetlands and deepwater habitats of the United States. – U.S. Fisch and Wildlife Science, Washington D.C.; Publ. FWS/OBS-79/31.

Custodio, E. 1992 Hydrogeological and hydrochemical aspects of aquifer overexploitation. – Selected Papers on Aquifer Overexploitation. Intern. Assoc. of Hydrogeologists. Heise, Hannover, 3, pp. 3–27.

Custodio, E. 1994: Posibles procesos de contaminación agrícola de aguas subterráneas en el área de Doñana, Huelva (Possible agricultural groundwater contamination processes in Doñana area, Huelva). – Análisis y Evolución de la Contaminación de las Aguas Subterráneas en España. Alcalá de Henares. Asoc. Intern. Hidrogeol., Grupo Español, II, pp. 283–308.

Custodio, E. 1995a: El papel de la hidrología en los programas de restauración de humedales en ambientes fluctuantes (The role of hydrology in wetland restauration programmes). – Bases Ecológicas para la Restauración de Humedales en la Cuenca Mediterránea. Consejeria de Medio Ambiente. Junta de Andalucía. Sevilla, pp. 43–60.

Custodio, E. 1995b: The impact of vertical water flow in boreholes: influence on monitoring operations. – Hydrogéologie. Orléans, 3, pp. 3–12.

Custodio, E. 1999: Alteraciones en los registros térmicos por flujo vertical de agua a lo largo de perforaciones (Changes in thermal logs due to vertical water flow along boreholes). – Boletín Geológico y Minero. Madrid, 110 (4), pp. 371–380.

Custodio, E. 2000: The complex concept of overexploited aquifer. Intensive use of Groundwater: Ecological, Technical and Ethical Aspects. – Fundación Marcelino Botín. Madrid, Series A, 2, pp. 1–62.

Custodio, E.; M. R. Llamas 1976; 1983: Hidrología Subterránea (Groundwater Hydrology). Ediciones Omega, Barcelona, 2 vols 2450 p.

Custodio, E., M. Manzano, M. Iglesias, Th. Trick 1999: Las aguas (Water). – Planificación Territorial y Gestión de la Integridad Ecológica del Complejo Palustre del Abalario (Parque Natural del Entorno de Doñana, Huelva). C. Montes, J. Oliver, F. Molina y J. Cobos (Eds.). Agencia del Medio Ambiente. Sevilla. Chap. 6. 4. (in press).

Custodio, E., M. Palancar 1995: Las aguas subterráneas en Doñana (Groundwater in Doñana). – Revista de Obras Públicas. Madrid, 3440, pp. 31–53.

García-Vera, M.A. 1994: Hidrogeología de zonas endorreicas en climas semiáridos: aplicación a los Monegros, Zaragoza (Hydrogeology of closed basins in semiarid climates: application to Monegros, Zaragoza). – Dep. Ground Eng., Pol. Univ. of Catalonia. Barcelona. Doctoral thesis.

González-Bernáldez, F. 1988: Typology of wetlands and evaluation of the resources they represent. Hydrology of Wetlands in Semiarid and Arid Regions. – Agencia del Medio Ambiente. Sevilla, pp. 7–36.

González-Bernáldez, F. 1992: Ecological aspects of wetland/groundwater relationships in Spain. – Limnética. Madrid. 8, pp. 11–26.

Hunt, R.J., Th.D. Bullen, D.P. Krabbenhoft, C. Kendall 1998: Using stable isotopes of water and strontium to investigate the hydrology of a natural and a constructed wetland. – Ground Water, 36/3, pp. 434–443.

Hunt. R.J., D.P. Krabbenhoft, M.P. Anderson 1996: Groundwater inflow measurements in wetlands systems. – Water Res. Research, 32/3, pp. 495–507.

Iglesias, M. 1999: Caracterización hidrogeoquímica del flujo del agua subterránea en El Abalario, Doñana, Huelva. (Hydrogeochemical characterisation of groundwater flow in El Abalario, Doñana, Huelva). – Polytechnical University of Catalonia. Barcelona, Doctoral thesis.

IGME 1984: Hidrogeología del Parque Nacional de Doñana y su entorno (Hydrogeology of the Doñana National Park and its surroundings). – Instituto Geológico y Minero de España. Madrid.

ITGE 1998 Hidrogeología de la reserva natural de la Laguna de Fuente de Piedra, Málaga – (Hydrogeology of the Laguna de Fuente de Piedra lagoon natural reserve, Málaga). – Instituto Tecnológico Geominero de España. Madrid.

Lee, D.R. 1977: A device for measuring seepage flux in lakes and estuaries. Limnol. – Oceanography, 22, pp. 40–147.

Lewis, J.B. 1987: Measurements of groundwater seepage flux onto a coral reef: spatial and temporal variations. Limnol. – Oceanography, 32, pp. 1165–1169.

Llamas, MR. 1987: Bases científicas para la protección de los humedales en España (Scientific basis for wetland protection in Spain). – Real Academía de Ciencias, Madrid, pp. 1–360.

Llamas, M.R. 1988: Conflicts between wetland conservation and groundwater exploitation: two case histories in Spain. – Environmental Geology. 11/3, pp. 241–251.

Llamas, M.R. 1989: Groundwater and wetlands: new constraints in groundwater management: Groundwater Management: Quantity and Quality. – Intern. Assoc. Hydrol. Sciences. Publ., 188, pp. 295–304.

Llamas, M.R. 1990: Geohydrology of the eolian sands of the Doñana National Park (Spain). – Catena Supplement., 18, pp. 145–154.

Llamas, M.R. 1992: Wetlands: an important issue in hydrogeology. Selected Papers on Aquifer Overexploitation. – Intern. Assoc. Hydrogeologists, Heise, Hannover, 3, pp. 69–86.

Llamas, M.R., J. Back, J. Margat 1992: Groundwater use: equilibrium between social benefits and potential environmental cost. – Applied Hydrogeology, Heise, Hannover, 182, pp. 3–14.

Montes, C., J. Oliver, F. Medina, J. Cobos 1995: Bases ecológicas para la restauración de los humedales en la cuenca mediterránea (Ecological basis for wetland restauration in the Mediterranean basin). – Agencia del Medio Ambiente. Sevilla, pp. 1–348.

Novitzki, R.P. 1982: Hydrology of Wisconsin wetlands. U.S. Geological Survey/University of Wisconsin – Extension Geological and Natural History Survey, Madison. Info. Circ 40, pp. 1–22.

Pascual, M. 1992: Hidrogeología básica de las sierras marginales prepirenaicas de la Provincia de Lleida (Basic hydrogeology of the pre-pyrenaic marginal ranges of the Lleida Province). – Hidrogeología y Recursos Hidráulicos, Madrid, 15, pp. 115–129.
Portnoy, J.W.; B.L. Nowicki, C.T. Roman, D.W. Urish 1998. The discharge of nitrate-contaminated groundwater from developed shoreline to marsh-fringed estuary. – Water Res. Research, 34/11, pp. 3095–3104.
Sacks, L.A., J.S. Herman, L.F. Konikow, A.L. Vela 1992: Seasonal dynamics of groundwater-lake interactions at Doñana National Park, Spain. – J. of Hydrology, 136, pp. 123–154.
Shedlock, R.J., D.A. Wilcox, T.A. Thompson, D.A. Cohen 1993: Interaction between groundwater and wetlands, southern shore of Lake Michigan, USA. – J. of Hydrology, 141/1–4, pp. 127–155.
Simpson, H.J., A.L. Herczeg 1991: Salinity and evaporation in the river Murray basin, Australia. – J. of Hydrology, 124, pp. 1–27.
Slater, J.M., D.G. Capone 1987: Denitrification in aquifer soil and nearshore marine sediments influenced by groundwater nitrate. – Appl. Environ. Microbiology, 53, pp. 1292–1297.
Suso, J., M.R. Llamas 1991: Estudio hidrogeológico de la influencia de los bombeos en la zona de El Rocío (Hydrogeological study of pumping influence in the El Rocío area). – Estudios Geológicos, Madrid, 46, pp. 317–345.
Suso, J., M.R. Llamas 1993: Influence of groundwater development of the Doñana National Park ecosystems (Spain). – J. of Hydrology, 141/1–4, pp. 239–270.
Tóth, J. 1971: Groundwater discharge: a common generator of diverse geologic and morphologic phenomena. – Bull. Intern. Assoc. Scientific Hydrology, 16, (1–31), pp. 7–24.
Tóth, J. 1972: Properties and manifestations of regional ground water movement. – Proc. 24th Geological Congress. Montreal, Sect. 11, pp. 153–163.
Tóth, J. 1999: Groundwater as a geologic agent: an overview of the causes, processes, and manifestations. – Hydrogeology Journal, Springer-Verlag: 7/1, pp. 1–14
Trick, Th. 1998: Impacto de las extracciones de agua subterránea en Doñana: aplicación de un modelo numérico con consideración de la variabilidad de la recarga (Groundwater withdrawal effects in Doñana: application of a numerical model taking into account recharge variability). – Polytechnical University of Catalonia. Barcelona. Doctoral thesis.
Trick, Th., E. Custodio, M. Manzano 1995: Actualización del modelo hidrogeológico de la zona de El Abalario, Huelva (Improvements of the hydrogeological model of the El Abalario area, Huelva). – Hidrogeología y Recursos Hidráulicos. Madrid, 19, pp. 661–677.
Weiskel, P.K., B.L. Howes 1992: Differential transport of sewage-derived nitrogen and phosphorous through a coastal watershed. – Environ. Sci. Technology, 26, pp. 352–360.
Winter, T.C., M.R. Llamas (Ed.) 1993: Hydrogeology of wetlands. – J. of Hydrology, 141/1–4, pp. 1–271.

Acta Geologica Hungarica, Vol. 43/2, pp. 203–222 (2000)

Flow systems analysis and homogenization for aquifer protection

Wouter Zijl
Netherlands Institute of Applied Geoscience TNO

Anna Trykozko
Warsaw University of Technology

Flow systems analysis is based primarily on the concept of hierarchical groundwater flow systems. In this approach the topography of the water table is considered as a major factor in the hierarchical nesting of gravity-driven groundwater flow patterns. This results in flow systems of different orders of magnitude in lateral extent and depth of penetration. The 'flow systems concept' turned out to be extremely useful in many application fields. In this paper it will be shown that the concept of flow systems is extremely useful in the analysis of spatial and temporal scales and their mutual relationships. First, the basic equations are briefly introduced at the fine or laboratory scale. Then these equations will be extended to make them applicable at coarser scales, notably regional ones. To this end homogenization techniques will be presented, of which an approximate solution can be found numerically. The combination of the homogenization technique with Tóth's original idea of topography-driven flow systems makes it possible to apply Fourier decompositions of the water table. In this way the different spatial scales of the water table are separated in a natural way, leading to relatively simple expressions for the lateral extensions and penetration depths of the different flow systems. These lateral extensions and depths in turn determine the coarse scale at which the homogenization applies. In addition, this decomposition leads also to the relationship between spatial and temporal scales. The combination of flow systems analysis and homogenization can be made useful for the protection of subsurface aquifers. Arguments are given to show that model reliability may be improved by introducing additional knowledge obtained from flow systems analysis and homogenization. This knowledge will also lead to a better choice of the sizes of the grid cells and of clusters of grid cells, and, most importantly, to a better coarse-scale description of transport phenomena. This, in turn, will improve predictions of the flow paths, residence times and dispersion zone thickness of pollution plumes, both steady and unsteady.

Key words: aquifer protection, flow system, homogenization, scale analysis, transport system

Introduction

Flow systems analysis is primarily based on the concept of hierarchical groundwater flow systems. Tóth (1962, 1963) was the first to introduce this concept. In this approach the topography of the water table, which is strongly related to the topography of the land surface, is considered as a major factor in the hierarchical nesting of gravity-driven groundwater flow patterns. This results in flow systems of different orders of magnitude in lateral extent and depth of

Addresses: W. Zijl: PO Box 80015, NL-3508 TA Utrecht, The Netherlands
e-mail: w.zijl@nitg.tno.nl
A. Trykozko: ul. Nowowiejska 20, PL-00-653 Warsaw, Poland
e-mail: anna.trykozko@is.pw.edu.pl
Received: 14 September, 1999

penetration. The 'flow systems concept' turned out to be extremely useful in many application fields such as, for instance, petroleum exploration (Tóth and Otto 1989; Verweij 1993), geologic storage of radioactive waste (Tóth and Sheng 1996) and aquifer protection (Zijl and Nawalany 1993; Engelen and Kloosterman 1996). In this paper it will be shown that the concept of flow systems is extremely useful in the analysis of spatial and temporal scales and their mutual relationships.

First, the basic equations, Darcy's law and the continuity equation, are briefly introduced at the fine scale. Then these equations will be extended to make them applicable at larger, regional scales. To this end, homogenization techniques will be presented, of which an approximate solution can be found numerically. Here we use the conformal-nodal finite element method (CN-FEM) to find an upper bound, and the mixed-hybrid finite element method (MH-FEM) to find a lower bound. The finite element grid can be refined until the homogenized conductivity is sufficiently accurate. Numerical results will be shown.

A combination of the homogenization technique with Tóth's original idea of topography-driven flow systems makes it possible to apply Fourier decompositions of the water table. In this way the different spatial scales of the water table are separated in a natural way, leading to relatively simple expressions for the lateral extensions and penetration depths of the different flow systems. These lateral extensions and depths in turn determine the coarse scale at which the homogenization applies. In addition, this decomposition also leads to the relationship between spatial and temporal scales.

The combination of flow systems analysis and homogenization can be applied to the protection of subsurface aquifers. At present it is common practice to use numerical groundwater flow models in the design of aquifer protection measures, such as, for instance, the design of hydraulic isolation (Trykozko 1997). Using physical principles, such models form a 'natural' way of combining all sorts of data. Moreover, model construction (data input, etc.) provokes contacts between different disciplines. However, predictions based on such models have not always been reliable. Arguments are given to show that model reliability may be improved by introducing additional knowledge obtained from flow systems analysis and homogenization: knowledge of the lateral extents, the penetration depths and the time scales. This knowledge will also lead to a better choice of the sizes of the grid cells, of clusters of grid cells with equivalent homogeneous conductivities and, most importantly, to a better description of advective and dispersive transport. This, in turn, will improve predictions of the flow paths, residence times and dispersion zone thickness of pollution plumes, both steady and unsteady.

Basic flow equations and parameters on the fine scale

The first basic equation is Darcy's law relating the three components q_i, $i = 1,2,3$, of the flux vector $\vec{q}$ (m.day^{-1}) to the three components $e_j = \partial\phi / \partial x_j$ of the 'driving force' $\vec{e} = -\nabla\phi$ (dbar.m^{-1}), where $\phi = p - \rho\vec{g} \bullet \vec{x}$ (dbar = 10^4 Pa) is the potential, or reduced pressure; p (dbar) is the fluid pressure; ρ (kg.m^{-3}) is the constant fluid density; $\vec{g}$ (on earth $g = |\vec{g}|\ 10^{-3}$ dbar.m^2.kg^{-1}) is the gravitational acceleration, and $\vec{x}$ (m) is the position vector. For fresh water the specific gravity is $\gamma = \rho g = 1$ dbar.m^{-1}. Note that in geohydrological practice 1 dbar = 1 m (water column height), so that $\gamma = \rho g = 1$ disappears from the equations. The most general form of Darcy's law is $\vec{q} = \vec{\vec{k}} \bullet \vec{e}$ or, written in components,

$$q_i = \sum k_{ij} e_j,$$

where $k_{ij} = \kappa_{ij} / \mu$ (m^2.dbar^{-1}.day^{-1}) is the conductivity; κ_{ij} (m^2) represents the nine components of the absolute permeability tensor, and μ (dbar.day) is the fluid viscosity. The absolute permeability is a property of the rock matrix only. In general the conductivity may differ from point to point in the heterogeneous porous formation. On the fine scale the conductivity tensor is symmetric, i.e., $k_{ij} = k_{ji}$ (King et al. 1995).

The second basic equation is the continuity equation. Under the assumption of incompressible flow – i.e., quasi-steady flow – this equation simplifies to $\nabla \cdot \vec{q} = 0$ or, in Cartesian coordinates,

$$\sum_{i=1}^{3} \frac{\partial q_i}{\partial x_i} = 0$$

Upscaling equations and parameters on coarse scales

In many cases the parameters of formations *in situ* are different from the parameters measured in the laboratory on cores. Hence, the lab-scale parameters cannot be used in numerical and analytical models at regional scales. An obvious cause of such a parameter mismatch is heterogeneity at spatial scales that are much smaller than the dimensions of the computational volumes, or cells, in a model. Since present-day and even future computers are too limited to apply numerical models with the extremely large number of cells necessary to represent all the fine scale variability, upscaling is required to find cell-scale parameters, or effective parameters.

In Darcy's law at the fine scale the conductivity varies from 'point' to 'point.' A point scale distribution may be obtained by geologic insight or generated by geostatistical techniques. To obtain cell-scale parameters from spatial point scale parameter distributions, homogenization techniques, or upscaling procedures, must be used.

In an approximation of order zero, the upscaled vertical conductivity is given by the harmonic mean value of the fine-scale conductivities, $K_v = \langle k_v(z)^{-1} \rangle^{-1}$, while the upscaled horizontal conductivity is given by the arithmetic mean value K_h =

$\langle k_h(z) \rangle$. The brackets $\langle \ \rangle$ indicate averaging over the vertical z direction. A first-order correction leads to the following form of the upscaled Darcy's law (Zijl 1996; Rijpsma and Zijl 1998)

$$\begin{pmatrix} \langle q_x \rangle \\ \langle q_y \rangle \\ \langle q_z \rangle \end{pmatrix} = \begin{pmatrix} \langle k \rangle & 0 & M_x \langle k^{-1} \rangle^{-1} \\ 0 & \langle k \rangle & M_y \langle k^{-1} \rangle^{-1} \\ N_x \langle k^{-1} \rangle^{-1} & N_y \langle k^{-1} \rangle^{-1} & \langle k^{-1} \rangle^{-1} \end{pmatrix} \bullet \begin{pmatrix} \langle e_x \rangle \\ \langle e_y \rangle \\ \langle e_z \rangle \end{pmatrix}$$

where the dimensionless coefficients in the off-diagonal components are given by

$$M_i = \left\langle k \int_{z_1}^{z} \frac{\partial k^{-1}}{\partial x_i} dz' \right\rangle - \langle k \rangle \left\langle \int_{z_1}^{z} \frac{\partial k^{-1}}{\partial x_i} dz' \right\rangle$$

$$N_i = \left\langle k^{-1} \int_{z_1}^{z} \frac{\partial k}{\partial x_i} dz' \right\rangle - \langle k^{-1} \rangle \left\langle \int_{z_1}^{z} \frac{\partial k}{\partial x_i} dz' \right\rangle$$

We observe that in first-order accuracy the diagonal terms of the conductivity matrix do not change with respect to their value in the approximation of order zero: the well-known arithmetic and harmonic mean values remain valid. However, in first order the off-diagonal components are non-zero. This result shows that upscaling methods based on repeated application of harmonic and arithmetic mean values – in analogy with the determination of the replacement resistance of network electrical resistances – will yield reasonable results as long as we are not interested in the off-diagonal terms, which influence the flow direction. We can also observe that the upscaled conductivity tensor depends on the boundary conditions at the cell's boundaries. Since in reality there are no boundaries in the subsurface this 'boundary dependence' reflects the fact that upscaled parameters not only depend on the point scale parameter distribution within the cell, but also on the parameter distribution in the neighborhood of the cell. After averaging over the x and y dimensions, the off-diagonal components in the conductivity matrix vanish if the point scale conductivity is periodic and the cell has the dimensions of one or more times the wavelength of the periodicity. However, when there is a trend (a deviation from periodicity), the off-diagonal components will be non-zero and the upscaled conductivity tensor may even be non-symmetric. The stochastic theory of upscaling yields a similar result (Tartakovsky et al. 1999). This result is also in agreement with homogenization theory (Bensoussan et al. 1978), in which it is proved that any periodic fine scale conductivity distribution leads to a symmetric upscaled conductivity tensor.

Homogenization software based on both an upper bound finite element method (CN-FEM) and a lower bound finite element method (MH-FEM) has been developed (Trykozko and Zijl 1999).

Synthetic 2D example using local grid refinement

The two-dimensional periodic fine-scale permeability pattern of this example is shown in Figure 1. The porous medium consists of two different rock types: type 1 has a permeability of $k_1 = 1\ m^2.dbar^{-1}.day^{-1}$, while the permeability of rock type 2 is 100 times smaller, i.e., $k_2 = 0.01\ 1\ m^2.dbar^{-1}.day^{-1}$.

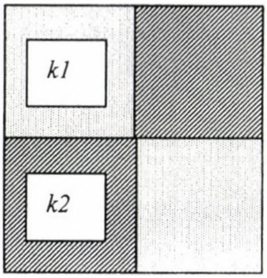

Fig. 1
Periodic structure with singularities

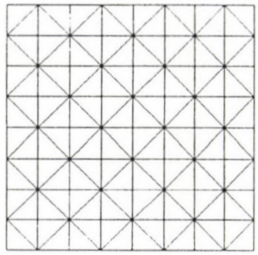

Fig. 2
Uniform triangular FE mesh

For this case the exact homogenized permeability is

$$K = K_{xx} = K_{yy} = \sqrt{k_1\, k_2} \qquad\qquad K_{xy} = K_{yx} = 0$$

As far as the numerical approximations are concerned, large differences in the results obtained with the two methods have been encountered. The values obtained with the CN-FEM on the minimal admissible mesh consisting of 9 nodes are equal to the *arithmetic mean*, whereas the solution obtained with MH-FEM on the same mesh is equal to the *harmonic* mean. This large difference between the two solutions is caused by the presence of the singularity points in the fine-scale mobility reflecting a situation just between disconnected and interconnected channels. One way of decreasing the influence of the singularities on the accuracy of the solution is to refine the computational mesh, thus making the domain of influence of the singularity smaller. Computations were performed for a sequence of *uniformly* refined meshes, of which the triangulation pattern of the mesh is shown in Fig. 2. Figure 3 gives the homogenized values $K = K_{xx} = K_{yy}$ obtained with the two numerical methods plotted as a function of the number of nodes. There is an improvement of the quality of the solution as the mesh becomes finer, though the convergence is slow. Upper and lower bounds hold.

The next step was to apply a non-uniform refinement producing a very fine mesh only in the nearest vicinity of the singularities (Fig. 4). The results are significantly better (Fig. 5) and the convergence to the exact solution is faster than in the uniform case.

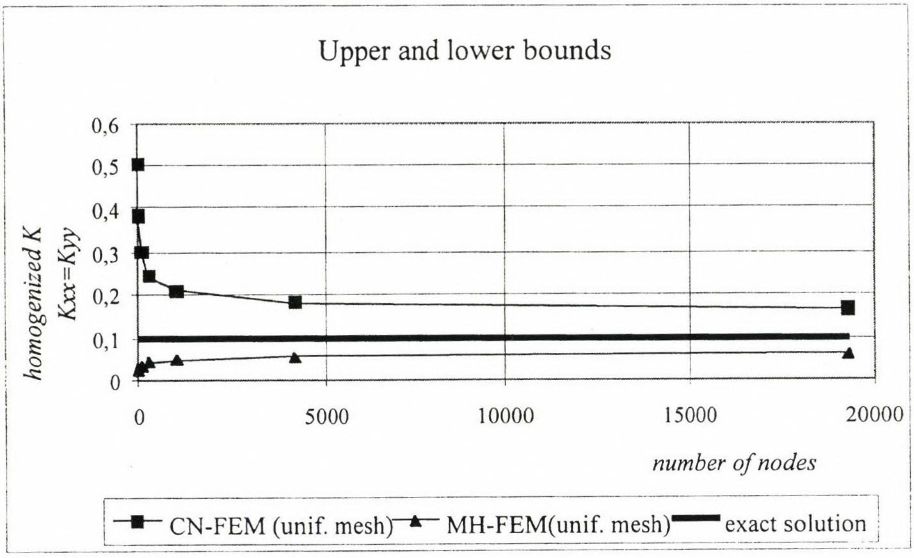

Fig. 3.
Upper and lower bounds for a sequence of uniform meshes

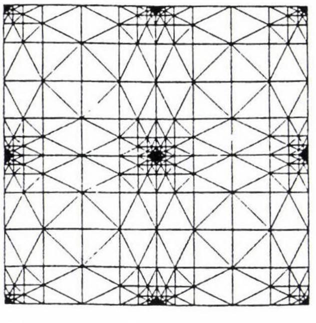

Fig. 4a.
Refinement around singularity points

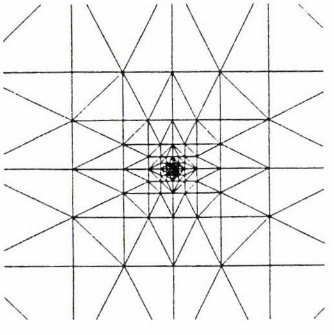

Fig. 4b.
Details of local grid refinement

Field example

The isotropic fine-scale absolute permeability varies from 213.188 mD to 13984.5 mD, cf. Fig. 6 (1 mD = 10^{-15} m^2). Originally, the upscaling domain was divided into 384 hexahedral cells (6×8×8). There are 26 'inactive' cells, which means that the small value of 0.0001 mD has been assigned to the cell's permeability. Each cell is divided into 5 tetrahedral finite elements (Fig. 7).

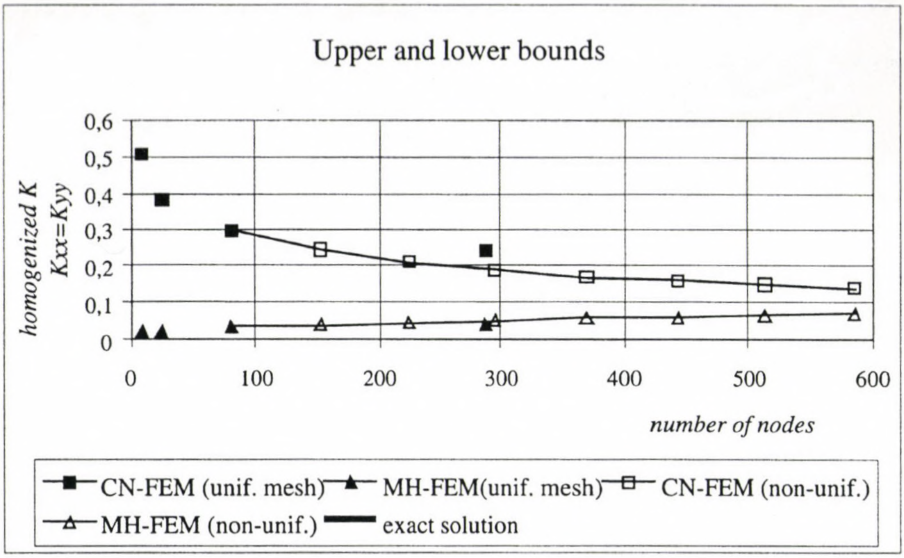

Fig. 5
Upper and lower boundaries for a sequence of non-uniform meshes

The geometry of this example is very anisotropic; the aspect ratio x/z is equal to 6, while the aspect ratio y/z is equal to 25. The characteristics of the two finite element models and the computed upscaled permeabilities are given in Tables 1, 2a and 2b.

Table 1
Original mesh

567 nodes, 1920 elements, 4160 interfaces
CN-FEM: 384 unknowns (nodal pressures)
MH-FEM: 3840 unknowns (interfacial normal fluxeS)

Fig. 6a
Fine-scale permeability distribution

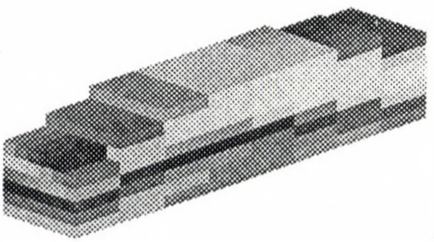

Fig. 6b
Fine-scale permeability distribution with exaggerated vertical dimension

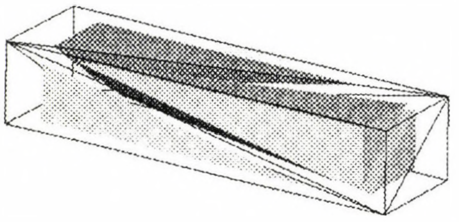

Fig. 7
One hexahedral cell divided in 5 tetrahedra (exaggerated vertical dimension)

Two different upscaling methods are compared: pressure-dissipation averaging – which is the conventional approach to homogenization – and pressure-flux averaging.

The original mesh has been uniformly refined twice; the characteristics of the two finite element models are given in Tables 3 and 4 and are summarized in Figures 8a–g.

Table 2a	Matrix K_{ij} calculated by CN-FEM [mD]		
Pressure-Dissipation averaging (exact symmetry)	0.7481195×10^4	0.2824882×10^3	0.1608522×10^2
		0.7378196×10^4	$-.3967316\times10^2$
			0.2619069×10^4
	Diagonal sum =	$K_{xx}+K_{yy}+K_{zz}$ =	1.7478460×10^4
Pressure-Flux averaging (approximate symmetry)	0.7481552×10^4	0.2824714×10^3	0.1610208×10^2
	0.2824910×10^3	0.7378195×10^4	$-.3967317\times10^2$
	0.1608575×10^2	$-.3967352\times10^2$	0.2619069×10^4
	Diagonal sum =	$K_{xx}+K_{yy}+K_{zz}$ =	1.7478817×10^4

Table 2b	Matrix K_{ij} calculated by MH-FEM [mD]		
Pressure-Dissipation averaging (exact symmetry)	0.7147581×10^4	0.5357514×10^3	0.2795474×10^2
		0.6957348×10^4	$-.3247279\times10^2$
			0.1696884×10^4
	Diagonal sum =	$K_{xx}+K_{yy}+K_{zz}$ =	1.5801813×10^4
Pressure-Flux averaging (approximate symmetry)	0.7147934×10^4	0.5357587×10^3	0.2795624×10^2
	0.5357513×10^3	0.6957345×10^4	$-.3247307\times10^2$
	0.2795459×10^2	$-.3247307\times10^2$	0.1696882×10^4
	Diagonal sum =	$K_{xx}+K_{yy}+K_{zz}$ =	1.5802161×10^4

Table 3
Mesh after first refinement

3757 nodes, 15360 elements, 32000 interfaces.
CN-FEM: 3072 unknowns
MH-FEM: 30720 unknowns (10 times more than CN-FEM)

Table 4
Mesh after second refinement

27225 nodes, 122880 elements, 250880 interfaces.
CN-FEM: 24576 unknowns
MH-FEM: 245760 unknowns

From the above figures we observe that the upper and lower bound properties respectively of CN-FEM and MH-FEM are satisfied for the $K_{xx} + K_{yy} + K_{zz}$ and the sum $K_{xx} + K_{yy} + K_{zz}$, as is required by the 'soft' error estimate. In addition, the upper and lower boundary properties hold for the individual diagonal components K_{xx}, K_{yy} and K_{zz} as well. This may be interpreted as an indication that the principal directions, and hence the directions of the preferential flow paths, are calculated accurately. More details are given by Zijl and Trykozko (2000a, b).

Flow systems related to spatial fourier modes

Spatial scales in the water table and its flow systems

What is considered to be 'regional' and 'local' is largely subjective since it generally depends upon the size of the region being examined. Therefore, it makes sense to speak of a hierarchy of sublocal, local, supralocal, subregional, regional, supraregional, etc. spatial scales. For such a hierarchy of scales, classical trend analysis is not very suitable; therefore we turn to Fourier. The basic

$$h_f(x,y,t) = \int_{-\infty}^{\infty}\int_{-\infty}^{\infty} h_f(x,y,t;\omega_1,\omega_2)\,d\omega_1\omega_2$$

principle of Fourier analysis is that any function of x and y can be represented by a double integral of Fourier modes (Rikitake et al. 1987, pp. 3–19)
where $h_f(x, y, t; \omega_1, \omega_2)$ is one of the Fourier components of the water table $h_f(x, y, t)$; $\omega_1(m^{-1})$ and $\omega_2(m^{-1})$ are the wave number components in the x and y directions respectively and $\lambda = 2\pi\,(\omega_1{}^2 + \omega_2{}^2)^{-1/2}$ (m) is the wavelength. For a water table $h_f(x, y, t)$ defined over a finite domain the integral simplifies to a sum over discrete values of ω_1 and ω_2. Only after separation in Fourier modes do the scales come into play, since each Fourier mode has its own spatial scale λ. Since

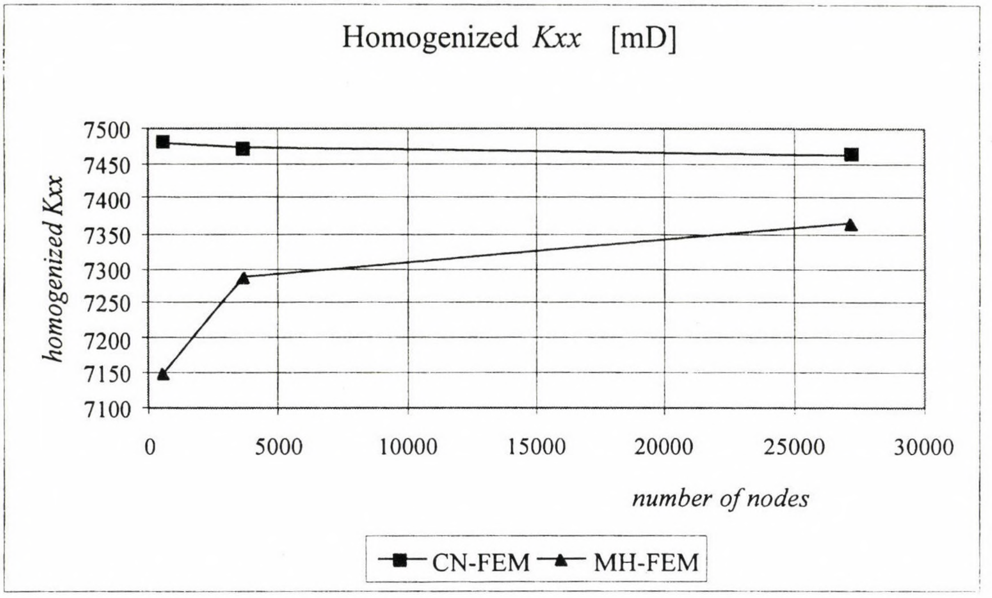

Fig. 8a
Homogenized permeability K_{xx} for a sequence of refined meshes

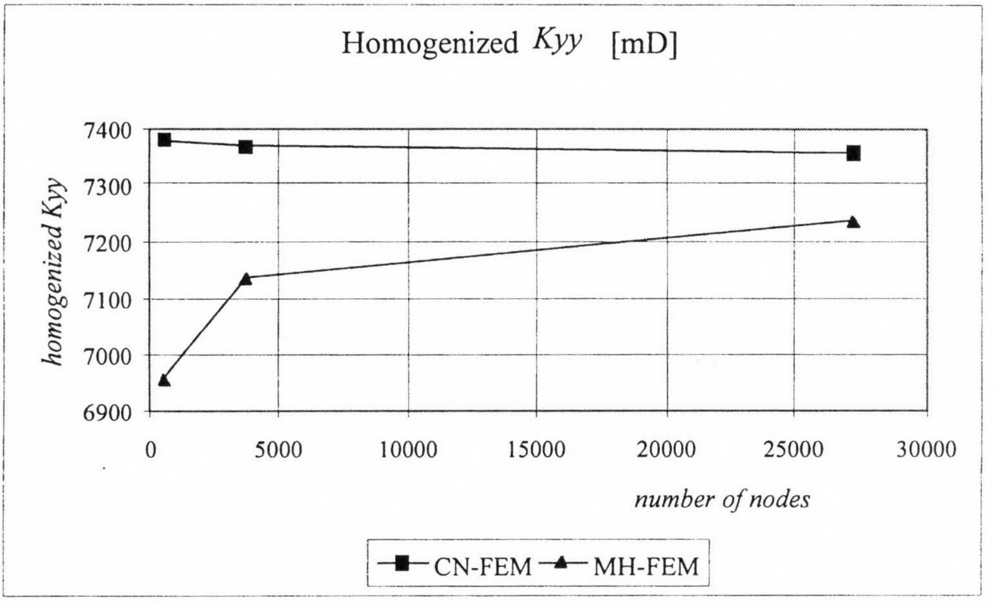

Fig. 8b
Homogenized permeability K_{yy} for a sequence of refined meshes

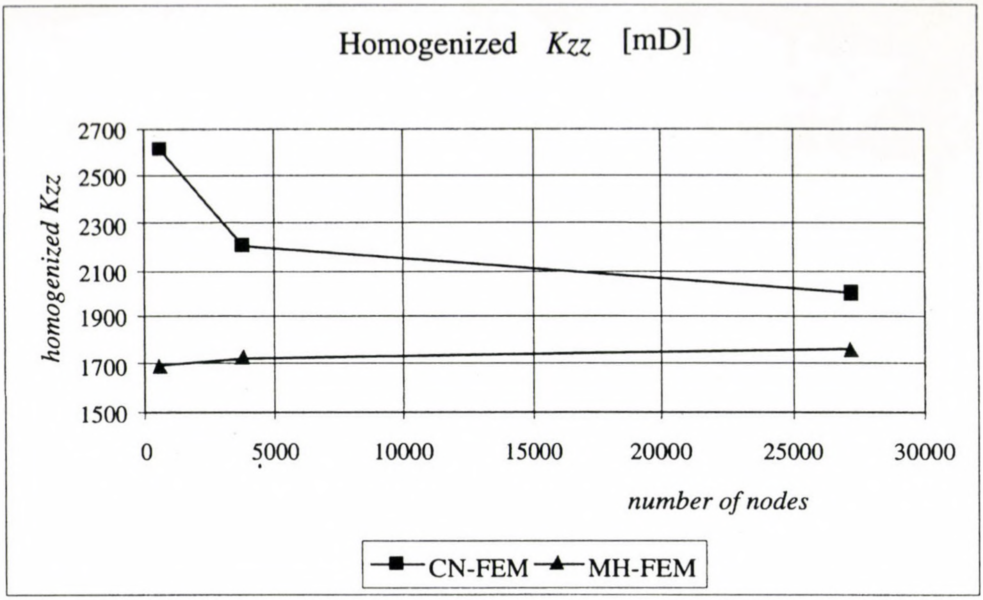

Fig. 8c
Homogenized permeability K_{zz} for a sequence of refined meshes

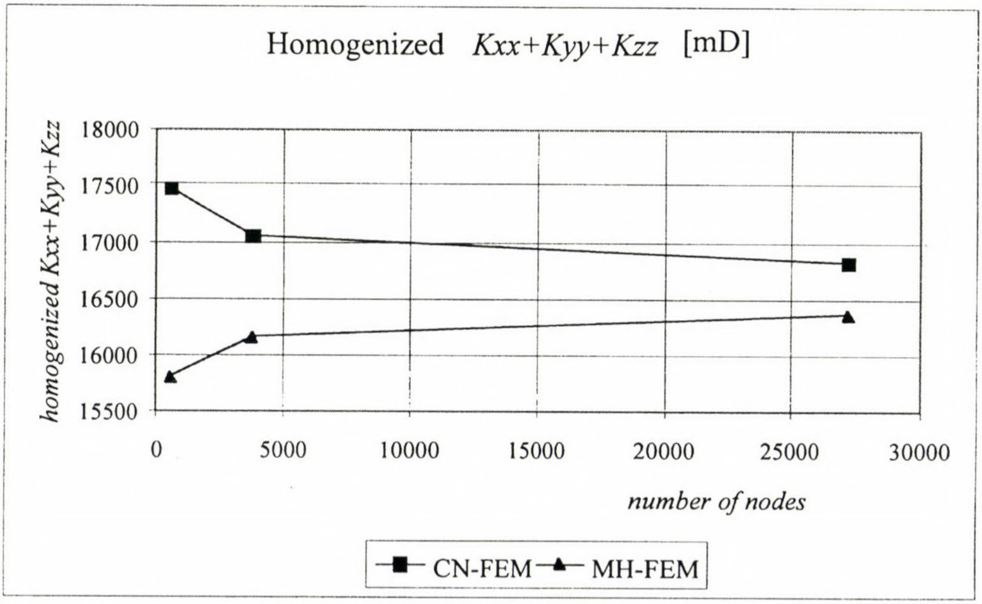

Fig. 8d
Trace $K_{xx} + K_{yy} + K_{zz}$ of homogenized permeabilities for a sequence of refined meshes

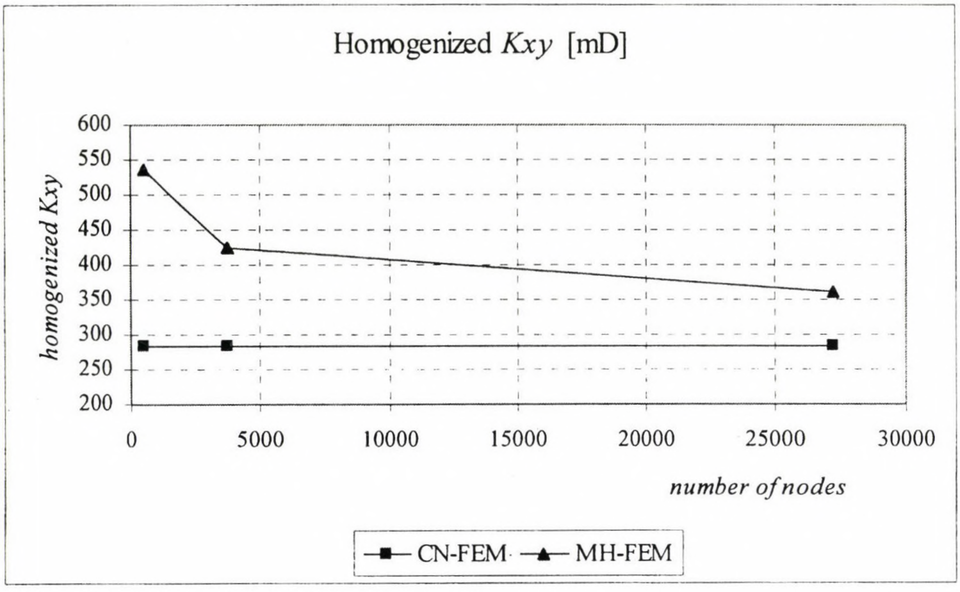

Fig. 8e
Homogenized permeability K_{xy} for a sequence of refined meshes

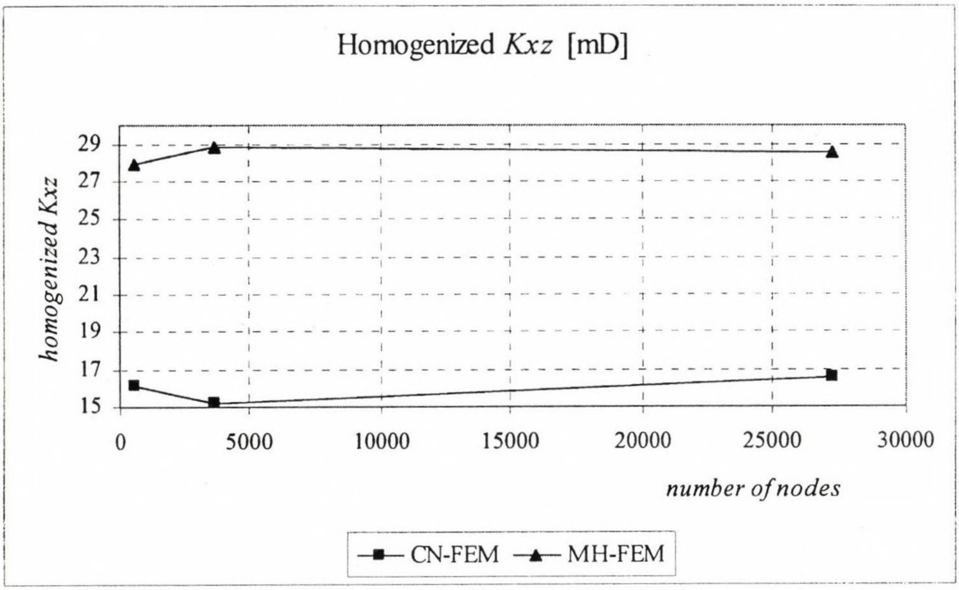

Fig. 8f
Homogenized permeability K_{xz} for a sequence of refined meshes

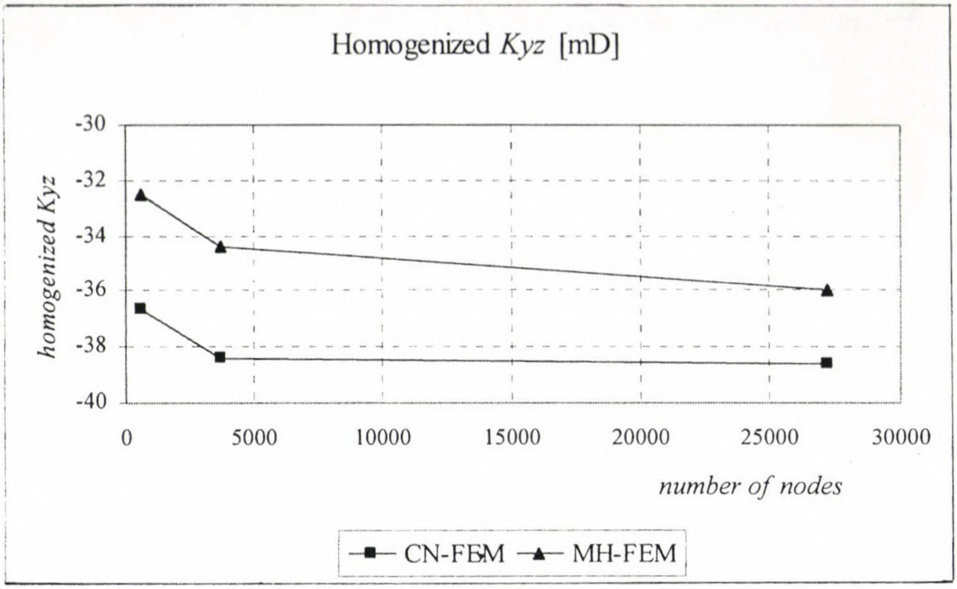

Fig. 8g
Homogenized permeability K_{yz} for a sequence of refined meshes

the groundwater flow problem is linear, the solutions can be determined separately for each Fourier component. Thereafter, all these solutions can be integrated, or summed, over ω_1 and ω_2 to obtain the complete solution.

To obtain qualitative insight in the thoughts underlying flow systems analysis it is useful to consider a homogeneous and anisotropic subsurface. The potential $\phi(x, y, 0, t) = f(x, y, t) = \rho g h_f(x, y, t)$ at the horizontal top plane $z = 0$ represents a projection of the spatial variations of the water table on this plane (Note that on earth $\rho g = 1$ dbar.m^{-1}; therefore, in most textbooks, where 1 dbar = 1 m, gravity drops from the equations). To obtain a clearer picture of one particular Fourier mode and the groundwater flow caused by it, it is preferable to define the following coordinate system in the horizontal plane

$$x' = \frac{\omega_1 x + \omega_2 y}{\sqrt{\omega_1^2 + \omega_2^2}} \qquad\qquad y' = \frac{-\omega_1 x + \omega_2 y}{\sqrt{\omega_1^2 + \omega_2^2}}$$

The $x`y`$ axes are obtained by rotating the original xy axes by an angle, in such a way that $f(x, y, t; \omega_1, \omega_2)$ can be written as a function of only the coordinate $x`$ and the time $t$, independent of the coordinate $y`$

$$f(x', t; \omega) = A(t)\cos(\omega x') + B(t)\sin(\omega x')$$

From the above expressions we find that at the top plane $z = 0$ the horizontal and vertical flux components are given by (replacing $x`$ by x)

$$q_x(x,0,t;\omega) = \omega K_h \left(A(t)\sin(\omega x) - B(t)\cos(\omega x)\right)$$
$$q_z(x,0,t;\omega) = \omega\sqrt{K_h K_v}\left(A(t)\cos(\omega x) + B(t)\sin(\omega x)\right)$$

Furthermore, we find that the magnitudes of the flux components decay exponentially with increasing depth z according to

$$q_i(x,z,t;\omega) = q_i(x,0,t;\omega)\exp(\ -\omega z\sqrt{K_h / K_v}\ )$$

Tóth (1962, 1963) found the solution for the flow field in one cross section (Freeze and Witherspoon 1966, 1967; Domenico 1972, pp. 256–264).

Penetration depths related to lateral spatial scales

At the depth $z = d$ the flux components are given by q_i $(x, z, t; \omega) = q_i$ $(x, 0, t; \omega)$ exp $(-\eta)$ in which $\eta = \sqrt{K_h / K_v}$. If we choose depth d such that $\eta = 1/2\pi$, we find a decrease in magnitude by a factor exp $(-1/2\pi) \approx 0.21$; if we choose d deeper, such that $\eta = \pi$, we find a decrease in magnitude by a factor 0.043; for $\eta = 2/3\ \pi$ we find a decrease in magnitude of approximately 0.01, and for $\eta = 2\pi$ we find a decrease in magnitude of approximately 0.002. Somewhat dependent on the situation, we have a negligibly small vertical flux component for one of these values of η. We do not need to choose an infinite depth; we already get a good approximation of the solution when depth d of the 'impervious' base is chosen in such a way that $\eta = 2\pi$. Therefore, it makes sense to define the penetration depth (Stolwijk et al. 1996)

$$d_p = \lambda\sqrt{K_v / K_h}$$

Indeed, the solution for the flow problem with impervious base at infinite depth is little different from the solution for the flow problem with impervious base at finite depth d_p. The penetration depth d_p defined in this way is therefore dependent on the wavelength λ of the spatial variation in the water table. The choice $\eta = 2\pi$ is not arbitrary, but is based on the fact that a conductivity distribution different from Kv and Kh below d_p does hardly influence the flow, whereas such a conductivity disturbance above d_p influences the flow considerably (Meekes 1997).

Figure 9 shows an illustration of the above-discussed theory. Figure 9a shows the relatively shallow 'impervious' base (i.e., the penetration depth) for the short waves in the water table. Figure 9b shows the deeper 'impervious' base for the long waves in the water table. Since the shallow flow velocities caused by the short waves have a much larger magnitude than the shallow flow velocities caused by the long waves, the shallow streamlines are almost fully determined by the short wavelengths. On the other hand, at depths below the 'impervious' base of the short waves, the flow velocities caused by the long waves are

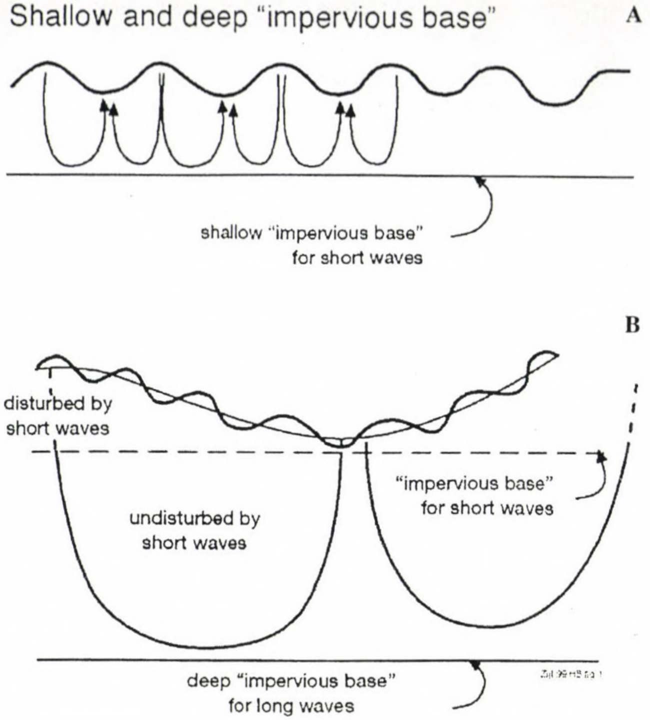

Fig. 9
Penetration depths considered as 'impervious' bases for short and long waves in the water table and the resulting streamline patterns. The upper figure (Fig. 9a) shows the relatively shallow penetration depth for the short waves; the lower figure (Fig. 9b) shows the deeper penetration depth for the long waves

dominant. Hence, the deep streamlines are almost fully determined by the long waves.

Figure 10 shows the superposition of streamlines caused by a long, an intermediate and a short wave in the water table. In Figure 10 it is assumed that these three waves are oriented in such a way that they cause flow in the same cross-section. However, it should be noted that each Fourier component has its own cross-section, which is generally rotated with respect to other cross-sections. The dashed lines indicate streamlines that end at stagnation points (the intersections of two dashed lines) in the flow field.

Of course, the concept of an 'impervious' base is more meaningful in a layered subsurface where aquifers and aquitards alternate. Indeed, in that case the damping factor jumps abruptly in value, and it becomes clear that the 'impervious' base must be at the bottom of an aquifer and at the top of an aquitard. In that case it is also possible to arrive at an exact solution for perfectly layered subsurfaces with piece-wise constant conductivities (Bervoets et al. 1991; Van Veldhuizen et al. 1993). Meekes (1997) has extended the theory for layered

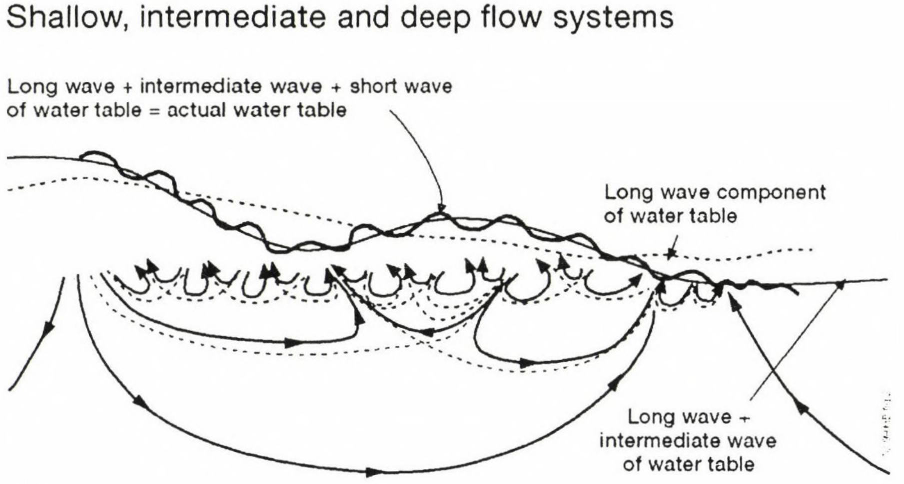

Fig. 10
Superposition of long, intermediate and short waves and the resulting stream line pattern

subsurfaces considerably and he greatly enhanced its applicability in the context of shallow seismic for geohydrological purposes.

The relation between spatial and temporal scales

The supraregional spatial course of the water table is generally associated with the topography of the landscape. Tóth (1962, 1963) first expressed this idea. Since the topography changes only slowly with time, the deep groundwater flow will be almost steady. This can be made more plausible by recognizing that the time dependence of the amplitude of a Fourier mode depends on the wavelength λ of that component. If, as an approximation, the kinematic boundary condition at the water table may be projected on the top plane $z = 0$, and may also be linearized by neglecting the nonlinearities caused by the curvature of the water table, the superposition principle will hold. Consequently, the projected and linearized kinematic boundary condition will also hold for each Fourier mode separately

$$n \frac{\partial h_f(x,t;\omega)}{\partial t} = P(x,t;\omega) - q_z(x,0,t;\omega)$$

where n is the effective porosity, and $P(x,t;\,\omega)$ is the Fourier mode of the 'effective precipitation' $P(x,t)$. The effective precipitation has spatial variability since it includes the effective infiltration at places where surface water occurs (therefore, a better name for $P(x,t)$ would be groundwater replenishment). Now, surface waters like rivers, canals and ditches often have a value of $P(x,t)$ that is controlled by surface water flow in such a way that the water level remains approximately constant in time. Due to this overland flow the effective infiltration, i.e., the values of $P(x, t)$ at the locations where surface water occurs, has completely different values from those of the precipitation minus evaporation found elsewhere. Therefore $P(x, t)$ has spatial variations, which can be decomposed into Fourier modes, in which the wavelengths are determined by the orientation of, and the distances between, the surface waters.

It follows from

$$q_z(x,0,t;\omega) = \omega\sqrt{K_h K_v}\rho g h_f(x,t;\omega)$$

and the kinematic water table condition that

$$n\frac{\partial h_f(x,t;\omega)}{\partial t} = P(x,t;\omega) - \omega\sqrt{K_h K_v}\rho g h_f(x,t;\omega)$$

Let us, for the moment, assume that $P(x,t;\ \omega)$ is constant in time. Then the water table will asymptotically evolve to a steady state

$$h_f(x,t;\omega) = \left(h_f(x,0;\omega) - h(x,t\to\infty;\omega)\right)\exp\left(-\omega\sqrt{K_h K_v}\frac{\rho g}{n}t\right)$$

where $h_f(x, 0;\ \omega)$ is the water table height at $t = 0$ and

$$h_f(x,t\to\infty;\omega) = P(x,t;\omega)/\left(\omega\sqrt{K_h K_v}\rho g\right)$$

is the steady water table height that is asymptotically reached after long time. Hence, the characteristic time is equal to

$$\tau = \frac{n\lambda}{2\pi\sqrt{K_h K_v}\rho g}$$

From the above expression we see that the characteristic time becomes larger as the spatial extent of the variation in water table becomes greater. We also see that gravity plays an important part, whereas in the common geohydrological practice, where $\rho g = 1$, this gravity effect is 'invisible.'

Transport systems

The conventional advection dispersion equation (ADE) generally used by the geohydrological community is given by (Zijl and Nawalany 1993; Bear et al. 1993)

$$n\frac{\partial c}{\partial t} + \vec{q}\bullet\nabla c = \nabla\bullet\left(n\vec{d}\bullet\nabla c + \frac{\alpha_L}{\vec{q}}(\vec{q}\bullet\nabla c)\vec{q} + \frac{\alpha_T}{|\vec{q}|}(\vec{q}\times\nabla c)\times\vec{q}\right)$$

Molecular diffusion is described by the term with the diffusion tensor $\vec{\vec{d}}$ ($m^2.day^{-1}$). Diffusion is a well-understood phenomenon: molecular kinetic theory shows clearly that the solute particles are in random motion that is 'driven' by the thermal random motion of the molecules and ions of the solute-solvent mixture. Random motion leads to the mixing of solute and solvent resulting in a diffusive flux $-n\,\vec{\vec{d}}\,.\nabla c$ on the kinetic scale (a small scale containing many molecules); c (kg.m^{-3}) is the concentration of dissolved matter. Due to the tortuosity of the flow paths in the porous medium the diffusion tensor $\vec{\vec{d}}$ differs somewhat from the diffusion coefficient in clear fluids.

Fluid flow around the grains of the solid matrix, with tortuous flow channels in it, causes a random motion with a larger scale behavior than the thermally induced random motion at the kinetic scale. This 'enhanced diffusion' is generally called mechanical microdispersion. Here we will simply call it 'microdispersion.' In the above equation, the terms with the longitudinal and transversal dispersion lengths, α_L and a_T respectively, represent the microdispersion. The anisotropy is always such that $\alpha_L << \alpha_T$.

At much larger scales, the coarse-scale heterogeneity pattern in the fine-scale conductivity distribution may cause averaged transport that is often treated as a kind of 'enhanced microdispersion' described by the advection–microdispersion equation

$$n\frac{\partial\langle c\rangle}{\partial t}+\nabla\bullet\left(\langle c\rangle\langle\vec{q}\rangle\right)=\nabla\bullet\left(n\vec{\vec{d}}\bullet\nabla\langle c\rangle+\frac{A_L}{|\langle\vec{q}\rangle|}\left(\langle\vec{q}\rangle\bullet\nabla\langle c\rangle\right)\langle\vec{q}\rangle+\frac{A_T}{|\langle\vec{q}\rangle|}\left(\langle\vec{q}\rangle\times\nabla\langle c\rangle\right)\times\langle\vec{q}\rangle\right)$$

In this approach the only difference with microdispersion is that the macrodispersion lengths A_L and A_T are (much) larger than the microdispersion lengths a_L and a_T. However, arguments can be given showing that it is a better approximation to replace in the above equation A_L and A_T with A^*_L and A^*_T respectively

$$\begin{pmatrix}A^*_L\\A^*_T\end{pmatrix}=\begin{pmatrix}\alpha_L\\\alpha_T\end{pmatrix}+\frac{\left|n^2\dfrac{\partial}{\partial t}\left(N\dfrac{\partial\langle c\rangle}{\partial t}+\langle\vec{q}\rangle\bullet\nabla\langle c\rangle\right)\right|}{\left|(n-N)\langle\vec{q}\rangle\bullet\nabla\left(\langle\vec{q}\rangle\bullet\nabla\langle c\rangle\right)\right|}\begin{pmatrix}A_L-\alpha_L\\A_T-\alpha_T\end{pmatrix}$$

where $N<<n$ is a measure of the coarse-scale heterogeneity (Zijl 1999). At time scales when the concentration front is propagating, the transport is unsteady and satisfies approximately the wave equation $n\partial\langle c\rangle/\partial t + \langle\vec{q}\rangle \bullet\nabla\langle c\rangle = 0$; in that case $A^*_L = A_L$ and $A^*_T = A_T$. After long time scales, when the transport has become steady the steady fine-scale advection-dispersion equation has to be upscaled to find the coarse-scale macro-ADE. Steady upscaling hardly influences the dispersion lengths, therefore $A^*_L = \alpha_L$ and $A^*_T = \alpha_T$; i.e., the macrodispersion has become equal to the much smaller microdispersion.

A practical example of flow systems with steady transport conditions is given by hydraulically isolated waste disposal sites, where the polluted water is permanently pumped away by horizontal pumping and injection wells, as is shown in Fig. 11 (Trykozko 1997). The existence of thin mixing zones in steady

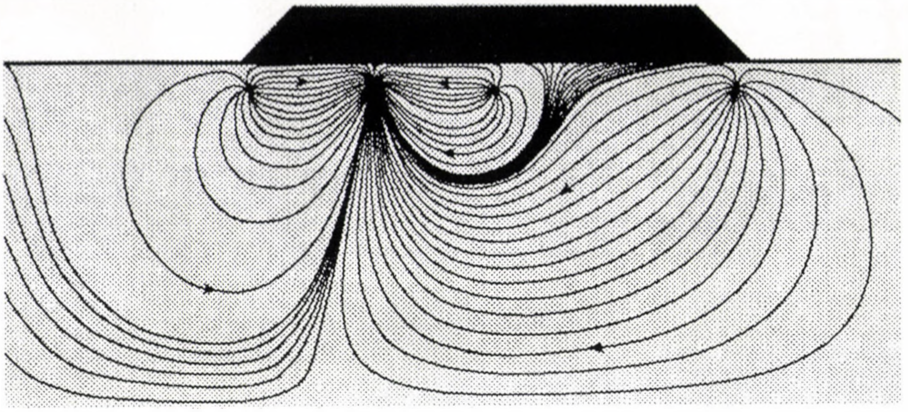

Fig. 11
Waste disposal with horizontal pumping and injection well for hydraulic isolation. Both the groundwater flow and the contaminant transport are steady (after Trykozko 1997)

transport systems may be considered as an additional argument in favor of flow systems analysis.

Summary and conclusion

Flow systems analysis is mainly based on the concept of hierarchical groundwater flow systems (Tóth 1962, 1963; Engelen and Jones 1986; Engelen and Kloosterman 1996), in which the topography of the water table, which is strongly related to the topography of the land surface, turns out to be a major factor in the hierarchical nesting of gravity driven groundwater flow. The flow systems concept distinguishes flowing groundwater bodies with different orders of magnitude in lateral extent and penetration depth. This concept is very useful for the qualitative and quantitative understanding of groundwater flow related phenomena in many application fields, like, for instance, petroleum engineering, geo-environmental engineering and mining. Here it is shown that flow systems analysis is also extremely useful in the analysis of spatial and temporal scales and their mutual relationships.

References

Bear, J., C.F. Tsang, G. de Marsily 1993: Flow and Contaminant Transport in Fractured Rock. – Academic Press, Inc., San Diego.

Bensoussan, A., J.L. Lions, G. Papanicolaou 1978: Asymptotic Analysis for Periodic Structures. – North Holland Publishing Company, Amsterdam.

Bervoets, A.F., W. Zijl, M. van Veldhuizen Nov. 6-8, 1991: Spatial scale analysis of groundwater flow pattern for transport in sedimentary basins. – European Simulation Symposium: Modeling and Control of Water Resources Systems and Global Changes, Gent.

Domenico, P.A. 1972: Concepts and Models in Groundwater Hydrology. – McGraw-Hill Book Comp., New York.
Engelen, G.B., G.P. Jones 1986: Developments in the Analysis of Groundwater Flow Systems. IAHS Publication No. 163.
Engelen, G.B., F.H. Kloosterman 1996: Hydrological Systems Analysis, Methods and Applications. – Kluwer Academic Publishers, Dordrecht.
Freeze, R.A., P.A. Witherspoon 1966: Theoretical analysis of regional groundwater flow I: Analytical and numerical solutions to the mathematical model. – Water Resources Res., 2/1, pp. 641–656.
Freeze, R.A., P.A. Witherspoon 1967: Theoretical analysis of regional groundwater flow II: Effect of water-table configuration and subsurface permeability variation. – Water Resour. Res., 3/2, pp. 623–634.
King, M.J., P.R. King, C.A., McGill, J.K. Williams 1995: Effective properties for flow calculations. – Transp. Porous Media, 20, pp. 169–196.
Meekes, J.A.C. 1997: High Resolution Seismic Reflection Techniques for Subsurface Models in Groundwater Hydrology. – Ph.D. thesis Free University Amsterdam (VUA).
Rijpsma, G., W. Zijl 1998: Upscaling Hooke's law for imperfectly layered rocks. – Mathematical Geology, 30/8, pp. 943–969.
Rikitake, T., R. Sato, Y. Hagiwara 1987: Applied Mathematics for Earth Scientists. – Terra Scientific Publishing Company, Tokyo / D. Reidel Publishing Company, Dordrecht.
Stolwijk, N.H.M., W. Zijl, R. Boekelman 1996: The penetration depth in modeling natural groundwater flow. – Journal of Hydrology, 185, pp. 171–182.
Tartakovsky, D.M., A. Guadagnini, M. Riva 1999: Proceedings of the 5th Annual Conference of the International Association for Mathematical Geology, Trondheim, Norway 6–11th August, pp. 761–766.
Tóth, J., 1962: A theory of groundwater motion in small drainage basins in Central Alberta, Canada. – Journal of Geophysical Research, 67/11, pp. 4375–4387.
Tóth, J., 1963: A theoretical analysis of groundwater flow in small drainage basins. – Journal of Geophysical Research, 68/16, pp. 4795–4812.
Tóth, J., C.J. Otto 1989: Hydrogeology and oil deposits at Pechelbronn-Soultz, Upper Rhine Graben: Ramification for exploration in intramontane basins. – Proc. Int. Symp. on Intramontane Basins: Geology and Resources, Chiang Mai, Thailand, pp. 59–76.
Tóth, J., G. Sheng 1996: Enhancing safety of nuclear waste disposal by exploiting regional groundwater flow: The recharge area concept. – Hydrogeology Journal, 4/1, pp. 4–25.
Trykozko, A. 1997: A numerical model of the hydraulic isolation of waste disposal sites. – Ph.D. thesis Warsaw University of Technology (in Polish).
Trykozko, A., W. Zijl 1999: From fine-scale to coarse-scale permeability by numerical homogenization and volume averaging. – Netherlands Institute of Applied Geoscience, Reports No. 99-4-B, 99-5-B-1, 99-5-B-2, Utrecht / Delft.
Van Veldhuizen, M., A.F. Bervoets, W. Zijl 1993: Dichotomy of a special recurrence relation from the earth sciences. – J. Comput. Appl. Math. 47, pp. 61–66.
Verweij, J.M. 1993: Hydrocarbon Migration Systems Analysis. Developments in Petroleum. – Science, 35, Elsevier, Amsterdam.
Zijl, W. 1996: The symmetry approximation for nonsymmetric permeability tensors and its consequences for mass transport. – Transp. Porous Media, 22, pp. 121–136.
Zijl, W., M. Nawalany 1993: Natural Groundwater Flow. – CRC Press / Lewis Publishers, Boca Raton.
Zijl, W. 1999: Scale aspects of groundwater flow and transport systems. – Hydrogeology Journal, 7, pp. 139–150.
Zijl, W., A Trykozko 2000a: Numerical homogenization of the absolute permeability using the conformal-nodal and the mixed-hybrid finite element method. – Transp. Porous. Media (in press).
Zijl, W., A. Trykozko 2000b: Numerical homogenization of the absolute permeability tensor around wells. – SPE Journal (in press).

GUIDELINES FOR AUTHORS

Acta Geologica Hungarica is an English-language quarterly publishing papers on geological topics. Besides papers on outstanding scientific achievements, on the main lines of geological research in Hungary, and on the geology of the Alpine–Carpathian–Dinaric region, reports on workshops of geological research, on major scientific meetings, and on contributions to international research projects will be accepted.

Only original papers will be published and a copy of the Publishing Agreement will be sent to the authors of papers accepted for publication. Manuscripts will be processed only after receiving the signed copy of the agreement.

Manuscripts are to be sent to the Editorial Office for refereeing, editing, in two typewritten copies, on floppy disk with two printed copies, or by E-mail. Manuscripts written by the following word processors will be accepted: MS Word, or ASCII format. Acceptance depends on the opinion of two referees and the decision of the Editorial Board.

Form of manuscripts

The paper complete with abstract, figures, tables, and bibliography should not exceed 25 pages (25 double-spaced lines with 3 cm margins on both sides).

The first page should include:

- the title of the paper (with minuscule letters)
- the full name of the author
- the name of the institution and city where the work was prepared
- an abstract of not more than 200 words
- a list of five to ten key words
- a footnote with the postal address of the author

The SI (System International) should be used for all units of measurements.

References

In text citations the author`s name and the year of the publication between brackets should be given. The reference list should contain the family name, a comma, the abbreviation of the first name, the year of publication, and a colon. This is followed by the title of the paper. Paper titles are followed – after a long hyphen – by periodical title, volume number, and inclusive page numbers. For books the title (English version), the name of the publisher, the place of publication, and the number of pages should be given.

Figures and tables

Figures and tables should be referred to in the text. Figures are expected in the size of the final type-area of the quarterly (12.6 x 18.6) or proportionally magnified 20–25% camera ready quality. Figures should be clear line drawings or good quality black-and-white photographic prints. Colour photographs will also be accepted, but the extra cost of reproduction in colour must be borne by the authors. The author`s name and figure number should be indicated on the back of each figure. Tables should be typed on separate sheets with a number.

Proof and reprints

The authors will be sent a set of proofs. Each of the pages should be proofread, signed, and returned to the Editorial Office within a week of receipt. Twenty-five reprints are supplied free of charge, additional reprints may be ordered.

Contents

Printed in Hungary
Akadémiai Nyomda, Martonvásár

Acta Geologica Hungarica

VOLUME 43, NUMBER 3, 2000

Akadémiai Kiadó, Budapest

ACTA GEOL. HUNG. AGHUE7 43 (3) 223–347 (2000) HU ISSN 0236–5278

ACTA GEOLOGICA HUNGARICA

A QUARTERLY OF THE HUNGARIAN ACADEMY OF SCIENCES

Acta Geologica Hungarica publishes original studies on geology, crystallography, mineralogy, petrography, geochemistry and paleontology.

Acta Geologica Hungarica is published in yearly volumes of four numbers by

AKADÉMIAI KIADÓ
H-1117 Budapest, Prielle Kornélia u. 4, Hungary
http://www.akkrt.hu

Manuscripts and editorial correspondence should be addressed to the

ACTA GEOLOGICA HUNGARICA

Dr. János Haas
Academical Research Group, Department of Geology, Eötvös Loránd University of Sciences
H-1088 Budapest, Múzeum krt. 4/a, Hungary
Phone/Fax: (36-1) 266 4947
E-mail: haas@ludens.elte.hu

Orders should be addressed to

AKADÉMIAI KIADÓ
H-1519 Budapest, P.O. Box 245, Hungary
Fax: (36-1) 464 8221
E-mail: kiss.s@akkrt.hu

Subscription price for Volume 43 (2000) in 4 issues US$ 180.00, including normal postage, airmail delivery US$ 20.00.

Acta Geologica is abstracted/indexed in Bibliographie des Sciences de la Terre, Chemical Abstracts, GeoRef, Hydro-Index, Mineralogical Abstract

---

AGeol 43 (2000) 3

Tectonostratigraphic terranes of Hungary

Dedicated to Professor Barnabás Géczy
for his 75th birthday

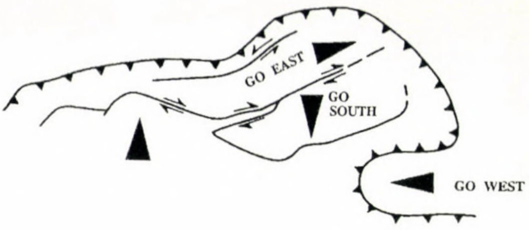

In the last decades, one of the most important results of geologic research work carried out in the Pannonian Region has been the demonstration that the basement of the Pannonian Basin consists of crust fragments of different origin and evolution which only achieved a position close to the present-day one in a late stage of Earth history, immediately prior to the formation of the deep basins. According to the terrane concept these crust fragments may be regarded as terranes. During the last years, within the framework of IGCP Project No. 276 (Palaeozoic Geodynamic Domains and their Alpidic Evolution in the Tethys - Project Leader Prof. D. Papanikolau), a brief definition and description of the structural units (terranes) building up the basement have been carried out according to the given principles, but publication of the detailed definitions and comparative analyses in an international journal has not occurred so far. In the present volume, the terrane definitions compiled by the community of several authors is presented together with the overview of the history of the application of the terrane concept, as well as a brief evaluation of the connections of the terranes.

We dedicated this number of Acta Geologica Hungarica to Professor Barnabás Géczy, who was implicitely the founder of the modern terrane analysis in Hungary in the early 70s, altough the concept itself appeared a few years later in North America.

The size of this paper, covering a wide professional field, extends considerably beyond the usual size of special papers. In this case, the Editorial Board made an exception with regard to the significance of the subject and its character encompassing the entire Pannonian Region in the hope that this decision will meet the acceptance of the readers.

Editorial Board

Acta Geologica Hungarica, Vol. 43/3, pp. 225–328 (2000)

Tectonostratigraphic terranes in the pre-Neogene basement of the Hungarian part of the Pannonian area

Sándor Kovács
Geological Research Group, Hungarian Academy of Sciences, Budapest

János Haas
Geological Research Group, Hungarian Academy of Sciences, Budapest

Géza Császár
Hungarian Geological Institute, Budapest

Tibor Szederkényi
Department of Mineralogy, Petrology, Geochemistry, József Attila University of Sciences, Szeged

György Buda
Department of Mineralogy, Eötvös Loránd University of Sciences, Budapest

András Nagymarosy
Department of Geology, Eötvös Loránd University of Sciences, Budapest

Abstract

The greatest part of the Pre-Neogene basement of the Pannonian Basin is built up by two Alpine megatectonic units, the Pelsonia Composite Terrane in the N, forming the southern part of the ALCAPA Composite Terrane, and the microcontinent-sized Tisia Terrane in the S. They are separated by the Zagreb–Zemplín or Mid-Hungarian Lineament, which likely merges E of the Danube River with the ENE-ward continuation of the Periadriatic–Balaton Lineament. The crustal blocks/terranes of the basement and of the rest of the ALCAPA C.T. form a true orogenic or terrane collage, framed on the E–SE, resp. SW by two deformed, but unbroken Neotethyan continental margin domains: the Median Dacidic (or Bucovino–Getic) – Serbo-Macedonian (i.e. Carpatho–Balkanide) margin on the E and SE and by the South Alpine – Outer Dinaridic (i.e. Adriatic or Apulian) margin on the SW (although the former was partly separated from the European foreland in course of the Late Jurassic – Early Cretaceous by the narrow Outer Dacidic or Civcin–Severin Rift Zone). These two domains enclose the main Neotethyan suture zones of the Axios/Vardar and Maliak–Mirdita–Dinaridic Ophiolite Belt zones, bifurcating in the present setting at the southern margin of the Tisia Terrane.

In the first chapter of the present review a short history of the terrane concept and of the recognition of the heterogeneous block structure of the Pannonian basement is given, followed by some methodology. In the main chapter the major terranes of Hungary (Pelsonia and Tisia, i.e. their Hungarian part) are described, concerning their Variscan and Alpine sedimentary, magmatic, metamorphic and (up to a certain extent) tectonic evolution. Palaeomagnetism is analysed in a separate contribution (Márton, present volume), whereas for a latest review of Mesozoic (especially Jurassic) palaeobiogeography we refer to Vörös (1993). Terranes of the Eastern Alps (Austroalpinia, Penninia) and of the West Carpathians (Veporia, Zemplenia), extending only a small amount into the territory of Hungary, are only briefly characterised, not described in detail.

Addresses: S. Kovács, J. Haas, A. Nagymarosy, Gy. Buda: H-1088 Budapest, Múzeum krt. 4/a, Hungary
T. Szederkényi: H-6722 Szeged, Egyetem u. 2, Hungary
G. Császár: H-1143 Budapest, Stefánia u. 14, Hungary
Received: first version received: July 31, 1998
final version accepted: May 31, 2000

0236–5278/2000/$ 5.00

The ***Pelsonia Composite Terrane*** bounded on the NW and N by the Rába, Hurbanovo–Diósjenő and Lubeník–Margecany Lines, of varying ages and character, includes the following terranes:

– *Bakonyia Terrane*, built up by continental margin-type, mostly very low-grade metamorphosed Variscan and non-metamorphosed Alpine successions. Characteristic are: a thick, Lower Palaeozoic phyllite group, Devonian carbonates (both pelagic and platform-type), mostly platform-type Triassic, with basinal Buchenstein Fm. (containing tuffs) in the Middle Triassic, pelagic Jurassic of mostly Ammonitico Rosso facies. It forms a large, WSW–ENE striking synclinorium, with imbrications on its both flanks. The terrane constituted the floor of the major part of the Hungarian Palaeogene Basin.

– *Zagorje–Mid-Transdanubia Composite Terrane*, bounded on the N by the Periadriatic–Balaton and on the S by the Zagreb–Zemplín Lineaments. It comprises, in a strongly sheared zone, several units in the continuation of the Slovenian and Croatian area (Julian Alps – South Karavanks as well as ophiolite and metamorphosed units of the Dinarides–Vardar Zone).

– *Bükkia Composite Terrane*: it comprises the non- to low-grade metamorphosed, S-vergent folded Bükk Parautochthon Unit with a marine, predominantly carbonate Late Palaeozoic–Early Mesozoic succession, embraced between a Middle Carboniferous Variscan flysch and an Upper Jurassic Eohellenic flysch formation, and the Neotethyan Szarvaskő and Darnó ophiolite complexes, emplaced over the former from the NW (according to present co-ordinates). Up to recent times the marine Palaeozoic Szendrő and Uppony units (in the former also with Middle Carboniferous flysch) had been considered as parts of the "Bükkium" Unit; however, they show an opposite, northerly vergency.

– *Aggtelekia Composite Terrane:* it comprises the non-metamorphosed Aggtelek–Bódva couplet, with a southward thrust and partly folded structure, the former being a predominantly carbonate platform type, whereas the latter a deep-water Triassic succession. In the sole thrust of the former, slices of ophiolites can be found as tectonic inclusions in Upper Permian evaporites (Tornakápolna Unit or Bódva Valley Ophiolite Complex). The very low to low-grade metamorphosed Martonyi (or Torna s.s.) Unit is characterised by Triassic basinal carbonates.

The Alpine ***Tisia Terrane*** in its Hungarian part comprises three Variscan terranes, which form the Pre-Alpine basement of different Alpine zones/nappe systems. They are terminologically separated from the Alpine tectonostratigraphic units. The *Kunságia Terrane* consists of two units. The Mórágy Unit forms the basement of the Alpine Mecsek Zone and is characterised by a Variscan syncollisional granitoid complex, related to the Moldanubian Zone of the Central European Variscides. The Körös Unit forms the Pre-Alpine basement of the Alpine Villány (–Bihor) Zone, and contains both medium-grade metamorphosed rocks and granitoids. The *Békésia Terrane* constitutes the Pre-Alpine basement of the Alpine (Szeged–) Békés–Codru Zone. It also contains medium-grade metamorphosed rocks and in its Battonya Subunit granitoids of different type (West Carpathian or Tatro-Veporic-type). The *(Slavonia–) Dravia Terrane* is also built up by Variscan medium-grade metamorphosed rocks and represents the northern subsurface extension of the of the Papuk–Psunj complexes, occurring at the surface in Croatia. A few occurrences of very low to low grade metamorphosed rocks may be regarded as Pre-Alpine nappe outliers or relics of wrenching zones. During the Late Carboniferous to Late Permian a fault-controlled basin formed above the junction area of the (Slavonia–)Dravia and Kunságia Terranes, in which up to 3,500 m of continental molasse sediments accumulated. Other areas of the Hungarian part of Tisia were exposed to denudation during most of the Late Variscan times.

The base of the Alpine overstep sequence in the Hungarian part of Tisia is constituted by Scythian continental redbeds. However, in its southern zones, outside of the territory of Hungary, marine sedimentation already began in the Scythian. After a marine incursion in the Middle Triassic, separation of the Mecsek and Villány (–Bihor) zones began in the early Late Triassic. The former zone became a rapidly sinking half-graben area, in which up to 4,300 m thick, partly continental, partly marine siliciclastic, resp mixed siliciclastic-carbonate sediments were deposited until the end of Bajocian. On the other hand, the latter area became a swell zone with 0–30 m contemporaneous sedimentation. In the former zone pelagic sedimentation commenced from the Bathonian onward, followed by intense alkaline rift volcanism in the Early Cretaceous. On the other hand, in the latter zone Urgon-type shallow marine deposition prevailed, in the Early Cretaceous, which was overlain by flysch-type deposits in the Albian–Cenomanian.

The comparative analysis of the terranes of the Pelsonia C. T. and of the Tisia T. with the surrounding Alpine (and Fore-Alpine), Carpathian and Dinaridic units/terranes, in terms of both their Variscan and Alpine evolution, reveals the close relationship of the Bakonyia Terrane to the Southern Alps and of the Zagorje–Mid-Transdanubia and Bükkia composite terranes to the Dinarides. Units of the Aggtelekia Composite Terrane show analogies partly to the Juvavicum of the Northern Limestone Alps, but also to the Internal Dinarides and to the Internal Hellenides.

The Variscan basement of the northern part of the Tisia Terrane (Mórágy Unit of the Mecsek Zone) show close relationship to the Moldanubian Zone of the European Variscides, whereas that of the more southern parts to the "Median Crystalline Zone" in sense of Neubauer and von Raumer (1993). In the earlier Mesozoic the (future) terrane was part of the North Tethyan margin, which is also indicated by its anomalously high paleomagnetic latitudes. Cessation of terrigenous input in the Bathonian indicates the separation of the future Tisia Terrane from the European hinterland. Contemporaneously, the character of the fauna also changed from European types to Mediterranean ones. However, a major change in the palaeomagnetic record appears only in the Berriasian (Márton, in the present volume), just before the paroxysm of alkaline rift volcanism in the Mecsek Zone, which shows analogies to that of the Outer West Carpathian Beskides in Poland. From this time on until the end of Early Miocene Tisia moved as an independent terrane.

The most prominent feature of the Pannonian basement for Alpine geology is the Zagreb–Zemplín Lineament (or Zone: Csontos and Nagymarosy 1998), along which the transition from the Dinarides into the Alps has been displaced about 500 km from the NW Dinarides to NE Hungary.

Late Variscan and Neotethyan (P_3–J_3) facies zones of the Pelsonia C. T. reveal its 400–500 km sinistral offset relative to the northerly adjacent main units of the ALCAPA C. T. (Austroalpinia, Tatro-Veporia) and the same dextral offset along the Periadriatic–Balaton, resp. Zagreb–Zemplín lineaments. The sinistral offset must have preceded the Middle–Late Cretaceous nappe stacking, and probably took place synchronously with Neotethyan closure during the Late Jurassic–Early Cretaceous, whereas the dextral offset was the result of the Late Oligocene – Early Miocene eastward escape of the entire ALCAPA C. T. The whole displacement of the composite terrane was the sum of the displacements of its constituent blocks/terranes, moving relative to each other, as well.

The offsets of the Late Variscan and Neotethyan facies zones of the Pelsonia C. T. within the ALCAPA C. T. of higher rank also imply that no Mesozoic (and also no Palaeozoic) palaeotectonic and palaeogeographic reconstruction can be performed in an orthogonal N–S modelling for the North Pannonian–West Carpathian area, as already emphasised by Balla (1988a).

Key words: tectonostratigraphic terranes, Variscan evolution, Alpine evolution, sedimentray evolution, magmatic evolution, tectonometamorphic evolution, terrane analysis, paleogeography, Pannonian basement, Hungary

Application of the terrane concept to the basement of the Pannonian area

Historical review

Short overview of the evolution of the terrane concept

A decade after the advent of the plate tectonic concept (by the late 70s and early 80s) it has become evident that orogenic belts are built up by crustal fragments (or blocks or slivers) showing very different evolutionary history, the agglomeration/accretion of which could neither be explained by the global principles of plate tectonics or by local nappe movements. This new challenge has arisen along the NE Pacific coast through investigations of the North American Cordilleran Chain (cf. Jones et al. 1977; Coney et al. 1980). Such crustal fragments were termed "terranes" and the orogenic belts built of them "orogenic collages" or "terrane collages" (for details see Howell 1989). Palaeontological and facies studies revealed that very different (boreal and tropical) units are juxtaposed here along strike of the mountain range over a distance of 3,000 km, from Nevada to Alaska (cf. Tozer 1982), which was also confirmed by palaeomagnetic investigations (Irving et al. 1980; Monger and Irving 1980). This study series was completed by the first comprehensive terrane map, i.e. the tectonostratigraphic terrane map of the Circum-Pacific region and its explanatory text (Howell et al. 1985).

Although the first applications of the terrane concept were not free of problems and even the term "terrane" already appeared in the early 19th century (see the criticism by Şengör and Dewey 1990), "terranology" really did become a new challenge in geotectonic analysis, e.g. "practical plate tectonics" or "plate tectonics at mapping scale". The application of the concept spread in a few years over many parts of the world (see, for example, the reviews in the volume edited by Dewey et al. 1990) and a second comprehensive terrane map, that of the Circum-Atlantic region (ed. Keppie and Dallmeyer 1990) appeared, with a new definition of the term "terrane" (see below).

For a better understanding of the metamorphic and magmatic evolution of pre-Alpine complexes in the Pannonian basement, the recognition of terranes in the European Variscides (Matte 1986; Ziegler 1986; Franke 1989; Matte et al. 1990) and in the Pre-Alpine basement of the Alps (Frisch and Neubauer 1989; von Raumer and Neubauer 1993) as well as the reconstruction of their evolution were of fundamental importance. Equally important was the recognition that continental terranes found south of the Rheic Ocean suture represent Gondwana-derived continental blocks, rifted away from the northern Gondwana margin following the Pan-African orogeny (cf. Oczlon 1994 and references therein).

The present contribution results from the terrane map programme (co-ordinated by F. Ebner, F. Neubauer and G. Rantitsch) of IGCP Project No. 276 ("Palaeozoic geodynamic domains in the Alpine–Himalayan Tethys and their Alpine evolution", led by D. Papanikolaou, F.P. Sassi and A. Sinha). It is an updated and complemented version of the terrane description of Hungary that appeared in the project volume (Kovács, Szederkényi et al. 1996/1997).

From the "median massif" to the "terrane collage" – recognition of the heterogeneous block structure of the Pannonian basement

Deep hydrocarbon exploration wells reaching the basement of the Pannonian Basin had already provided evidence in the 50s that the isolated pre-Tertiary surface outcrops show a subsurface continuation beneath the Neogene basin fill and have a WSW–ENE striking zonal arrangement. Five pre-Alpine crystalline zones, interpreted in the prevailing autochthonistic concept of that time as "cratogeanticlines" and four zones of Mesozoic sedimentary rocks, interpreted as "cratogeosynclines" and thought to have had their connection to the Tethys somewhere outside of the territory of Hungary, were postulated (Schmidt 1957; Vadász 1961).

The most detailed review of the basement tectonics of Hungary in the "pre-plate tectonic" period was given by Wein (1969), who introduced the "Igal–Bükk eugeosyncline" unit on the basis of marine Permian carbonate sediments and some ophiolites encountered by deep wells in a narrow zone striking between the NW Dinarides and the Bükk Mts. This zone was considered to be the "sea-branch" forming the Dinaridic connection of the Bükk Late Palaeozoic – Early Mesozoic, proved by the thorough comparative analysis by Balogh (1964).

It is a quarter of century ago that, first among Hungarian geologists, Géczy (1972, 1973) pointed out, by means of detailed analysis of Jurassic ammonoid faunas and sedimentary facies, the present inverse position of the Transdanubian Range (=Bakonyia terrane in the present contribution) and Mecsek zones, the former having a typical Mediterranean, and the latter a typical European character. Following Laubscher's (1971) proposal of several 100-km strike-slip displacement along the Periadriatic Lineament, he explained their present position by microplate movements. This pioneer study can eventually be considered to be the first modern comparative terrane analysis in Hungary, although the terrane concept itself only appeared a few years later (see above). Independently, Romanian geologists in those years arrived at a similar conclusion on the basis of Triassic facies zones in the Apuseni Mountains showing a N→S transition from proximal to distal types (Patrulius et al. 1971; Sandulescu 1972; Bleahu 1976; Patrulius 1976; for references see Bleahu et al. 1994).

Analysing the setting and relationships of the major tectonic units of Hungary, Szepesházy (1977) and, reinterpreting his previous review from 1969 in terms of the new plate tectonic concept, Wein (1978) also emphasised that the North Pannonian units (Transdanubian Range, Bükk) with their South Alpine–Dinaridic affinity originated in the South Tethyan region and the South Pannonian units (Mecsek and Villány zones) came from the North Tethyan region. Detailed palaeobiogeographical analysis of Jurassic brachiopod faunas (Vörös 1977, and later works) confirmed Géczy's conclusions based on ammonoids.

On the strength of palaeomagnetic observations Márton and Márton (1978) pointed out that the different positions of the Jurassic palaeomagnetic poles for the Transdanubian Range and the Villány Mts, respectively, are due to large-scale differential movements between the areas north and south of the Zagreb–Zemplín line. They also demonstrated that the Mesozoic segment of the Apparent Polar Wander Path (APW) for the Transdanubian Range is of South Tethyan affinity, but is displaced with respect to the corresponding segment of the African AWP; the displacement was interpreted as being due to Tertiary relative movements between the Transdanubian Range and Africa, manifested in an approximately 35^{0} counter-clockwise rotation of the former relative to the latter (Márton and Márton 1978, 1981, 1983).

Balla (1982) first emphasised the heterogeneous block structure of the Pannonian basement, thus, eventually being built up by a "collage of allochthonous terranes", although not yet using this term. Kázmér and Kovács (1985) proposed the first escape model on the basis of the present distribution of Permian to Palaeogene facies zones, thus explaining the emplacement of the South Alpine–Dinaridic-type Transdanubian Range (=Bakony Unit in that contribution, termed herein as "Bakonyia Terrane") and Bükk units to the north of the Tisza Megaunit (="Tisia Terrane" herein).

Synchronously with the emergence of these new concepts, the great number of hydrocarbon (and partly water) deep exploration wells reaching the basin basement (cf. Bardócz et al. in Bérczi et al. 1981, Fig. 1) and comprehensive geophysical surveys allowed a new synthesis of the Hungarian part of the Pannonian Basin basement resulting in the Pre-Tertiary Geologic Map of Hungary (Fülöp, Dank et al. 1986) and in the Tectonic Map of Hungary (Dank, Fülöp et al. 1990). Besides the units of the Eastern Alps and West Carpathians extending into the territory of Hungary, two major units have been distinguished: the North Pannonian or Pelso Mega-unit (=Pelsonia Composite Terrane herein) and the South Pannonian or Tisza Mega-unit (=Tisia Terrane herein) (cf. Brezsnyánszky and Haas 1986; Fülöp et al. 1987). The terrane subdivision presented herein and in Kovács, Szederkényi et al. 1996/1997 is based on these works.

Fig. 1 →
Tectonic/terrane sketch of the pre-Neogene basement of the Pannonian Basin and its Alpine–Carpathian–Balkanide, resp. Dinaridic–Hellenidic surroundings (compiled after Fülöp 1989, pl. 2; Dimitrijevic 1992; Papanikolaou 1984, pl. I and 1986; Sandulescu 1980, pl. I and 1984, pl. I by Kovács and Koroknai 1996, after Kovács et al. 1996/97, fig. 1). Area framed in white indicates the territory of Hungary

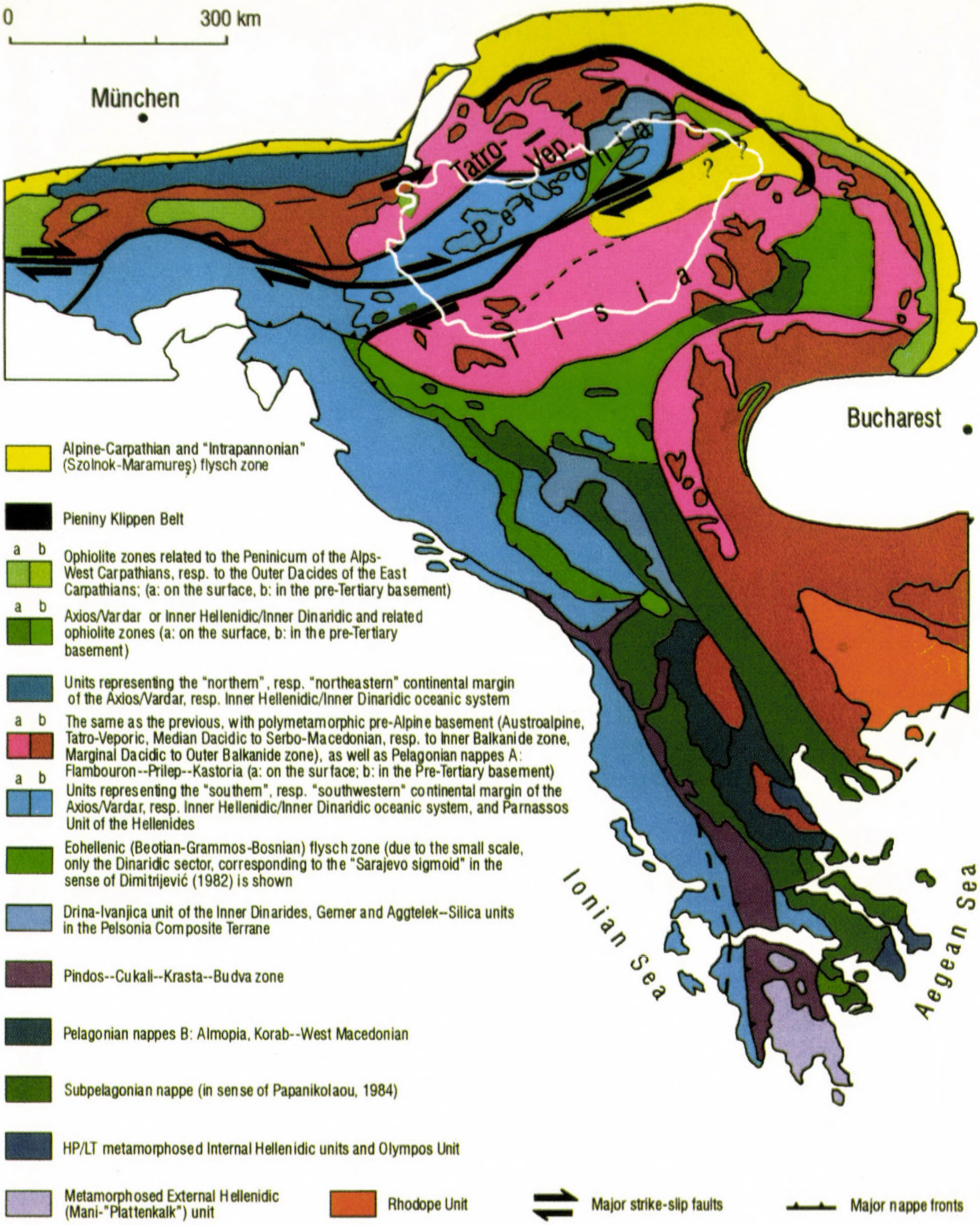
0
300 km
München
Tatro-
Vep.
Pelsonia
Tisia
Bucharest
Ionian Sea
Aegean Sea
Alpine-Carpathian and "Intrapannonian" (Szolnok-Maramureş) flysch zone
Pieniny Klippen Belt
a b
Ophiolite zones related to the Peninicum of the Alps-West Carpathians, resp. to the Outer Dacides of the East Carpathians; (a: on the surface, b: in the pre-Tertiary basement)
a b
Axios/Vardar or Inner Hellenidic/Inner Dinaridic and related ophiolite zones (a: on the surface, b: in the pre-Tertiary basement)
Units representing the "northern", resp. "northeastern" continental margin of the Axios/Vardar, resp. Inner Hellenidic/Inner Dinaridic oceanic system
a b
The same as the previous, with polymetamorphic pre-Alpine basement (Austroalpine, Tatro-Veporic, Median Dacidic to Serbo-Macedonian, resp. to Inner Balkanide zone, Marginal Dacidic to Outer Balkanide zone), as well as Pelagonian nappes A: Flambouron--Prilep--Kastoria (a: on the surface; b: in the Pre-Tertiary basement)
a b
Units representing the "southern", resp. "southwestern" continental margin of the Axios/Vardar, resp. Inner Hellenidic/Inner Dinaridic oceanic system, and Parnassos Unit of the Hellenides
Eohellenic (Beotian-Grammos-Bosnian) flysch zone (due to the small scale, only the Dinaridic sector, corresponding to the "Sarajevo sigmoid" in the sense of Dimitrijević (1982) is shown
Drina-Ivanjica unit of the Inner Dinarides, Gemer and Aggtelek--Silica units in the Pelsonia Composite Terrane
Pindos--Cukali--Krasta--Budva zone
Pelagonian nappes B: Almopia, Korab--West Macedonian
Subpelagonian nappe (in sense of Papanikolaou, 1984)
HP/LT metamorphosed Internal Hellenidic units and Olympos Unit
Metamorphosed External Hellenidic (Mani-"Plattenkalk") unit
Rhodope Unit
Major strike-slip faults
Major nappe fronts

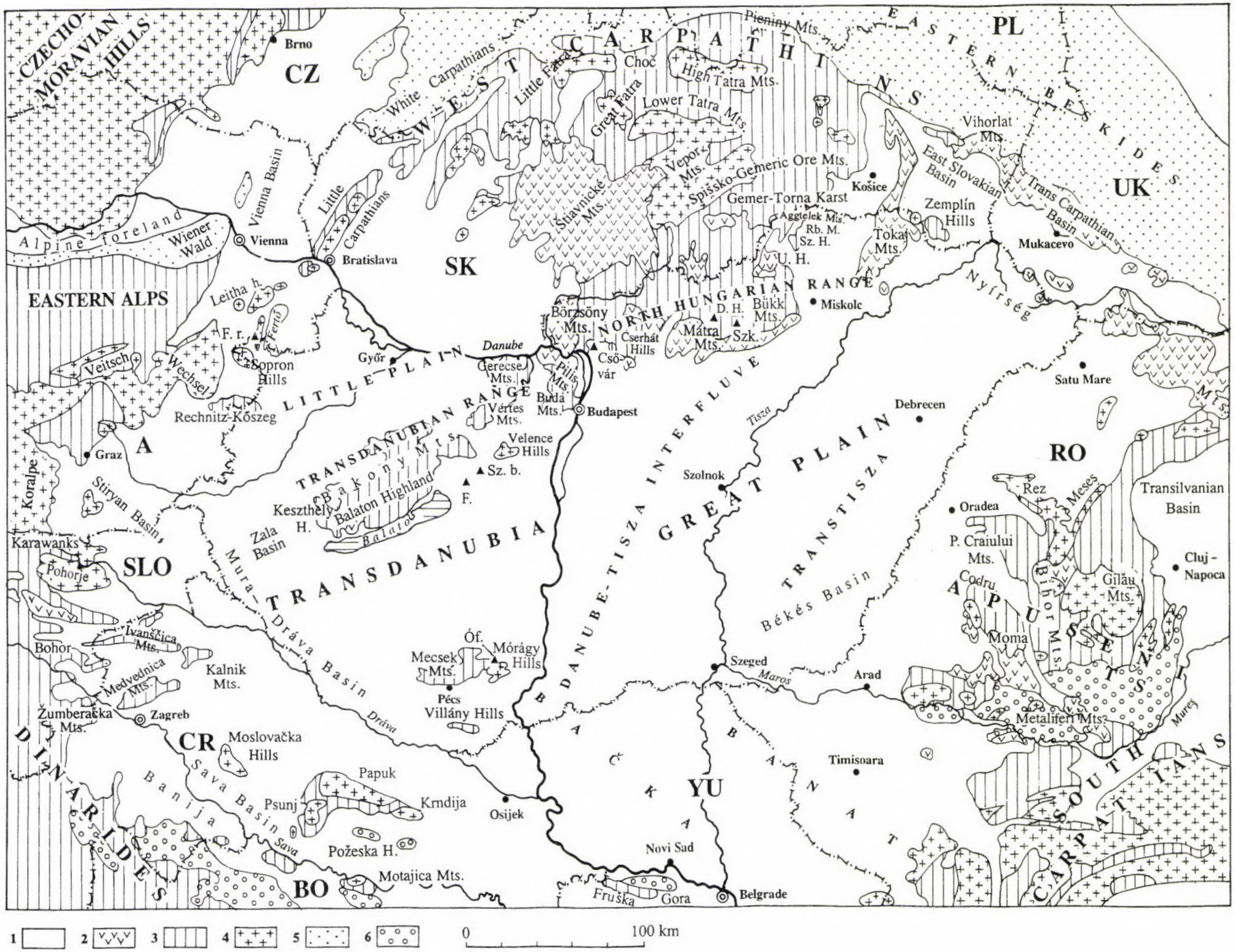

CZECHO-MORAVIAN HILLS
Brno
CZ
PL
UK
SK
A
SLO
CR
BO
YU
RO
EASTERN ALPS
Alpine foreland
Wiener Wald
Vienna
Vienna Basin
Little Carpathians
Bratislava
White Carpathians
WEST CARPATHIANS
Little Fatra
Great Fatra
Choč
High Tatra Mts.
Lower Tatra Mts.
Pieniny Mts.
EASTERN BESKIDES
Vihorlat Mts.
East Slovakian Basin
Trans Carpathian Basin
Zemplín Hills
Tokaj Mts.
Košice
Mukacevo
Štiavnické Mts.
Vepor Mts.
Spišsko-Gemeric Ore Mts.
Gemer-Torna Karst
Aggtelek Mts.
Rb. M.
Sz. H.
U. H.
NORTH HUNGARIAN RANGE
Börzsöny Mts.
Cserhát Hills
Mátra Mts.
D. H.
Bükk Mts.
Szk.
Miskolc
Nyírség
Leitha h.
Fertő
F. r.
Sopron Hills
Veitsch
Wechsel
Rechnitz-Kőszeg
Győr
Danube
LITTLE PLAIN
Gerecse Mts.
Pilis Mts.
Csővár
Buda Mts.
Budapest
Vértes Mts.
Velence Hills
TRANSDANUBIAN RANGE
Bakony Mts.
Balaton Highland
Sz. b.
F.
Keszthely H.
Balaton
Zala Basin
Graz
Koralpe
Styrian Basin
Karawanks
Pohorje
TRANSDANUBIA
Mura-Dráva Basin
Ivanščica Mts.
Bohor
Medvednica Mts.
Kalnik Mts.
Žumberačka Mts.
Zagreb
DINARIDES
Moslovačka Hills
Banija
Sava Basin
Sava
Papuk
Psunj
Krndija
Požeska H.
Motajica Mts.
Mecsek Mts.
Óf.
Mórágy Hills
Pécs
Villány Hills
Dráva
Osijek
DANUBE-TISZA INTERFLUVE
GREAT PLAIN
Tisza
Szolnok
Debrecen
TRANSTISZA
Békés Basin
Szeged
Maros
BAČKA
BANAT
Novi Sad
Fruška Gora
Belgrade
Timisoara
Arad
Satu Mare
Oradea
Rez
Meses
P. Craiului Mts.
Codru
Bihor Mts.
Gilău Mts.
Moma
APUSENI
Metaliferi Mts.
Transilvanian Basin
Cluj - Napoca
Mureş
SOUTH CARPATHIANS
1
2
3
4
5
6
0
100 km

Beside the aforementioned basic works two further fundamental contributions should be mentioned, which greatly promoted the recognition that the basement of the Pannonian Basin is built up by a real terrane collage:

The Slovak geologists Grecula and Varga (1979) described the main fault zones/lineaments of the Inner West Carpathian–North Pannonian area as "main discontinuity zones" (Rába–Rožňava, Balaton–Darnó and Zagreb–Zemplín), i.e. separating very different major geologic units. Although the continuation of the Rába and Balaton lines is seen differently now, these discontinuity zones were presented as what are called now "main terrane boundaries".

Balla (1988a) reconstructed the kinematics of Tertiary block movements in the East Alpine–Carpatho-Pannonian area. He pointed out that, as opposed to the first escape model by Kázmér and Kovács (1985), it was not only the Bakony–Drauzug and Bükk units which moved toward the E; the entire Inner West Carpathian–North Pannonian ensemble took part in this process, which was combined with rotations. Furthermore this ensemble consisted of at least 6–8 different blocks, which moved relative to each other as well. Thus, implicitly, he first recognised the terrane collage in the basement of the Pannonian Basin. Also he called attention to the fact that no Mesozoic palaeogeographic reconstruction could be carried out on the basis of the present distribution of these blocks.

More recently Csontos et al. (1992) presented a model of the accretion and docking of this amalgamated terrane collage ("ALCAPA" terrane, as they called it) to the European platform. Vörös (1993), independently from the ongoing terrane map project of IGCP Project N. 276, also suggested a terrane subdivision of the Mediterranean region, which is strongly taken into account herein, following joint discussions.

Methods

In discriminating and characterising the tectonostratigraphic terranes in the basement of the Pannonian Basin, we followed the definition by Keppie Dallmeyer (1990): "A terrane is redefined as an area characterised by an internal continuity of geology (including stratigraphy, fauna, structure, metamorphism, igneous petrology, metallogeny, geophysical properties, and palaeomagnetic record), that is bounded by faults or melanges representing a trench complex, or a cryptic suture across which neighbouring terranes may have a distinct geological record not explicable by facies changes (i.e. exotic terranes), or may

←Fig. 2

Major geographical objects and geologic occurrences of Hungary and the surrounding area, mentioned in the text. 1. Neogene basins; 2. Tertiary volcanics; 3. Palaeozoic, Mesozoic and Palaeogene sedimentary and slightly metamorphic formations; 4. Metamorphic and granitoid formations; 5. Rhenodanubian-Carpathian flysch; 6. Ophiolite-flysch complexes. Abbreviations: F.r. – Fertőrákos; F. – Füle; Sz.b. – Szabadbattyán; Óf – Ófalu; D.H. – Darnó Hill; Sz.k. – Szarvaskő; Rb.M. – Rudabánya Mts; Sz.H. – Szendrő Hills; U.H. – Uppony Hills

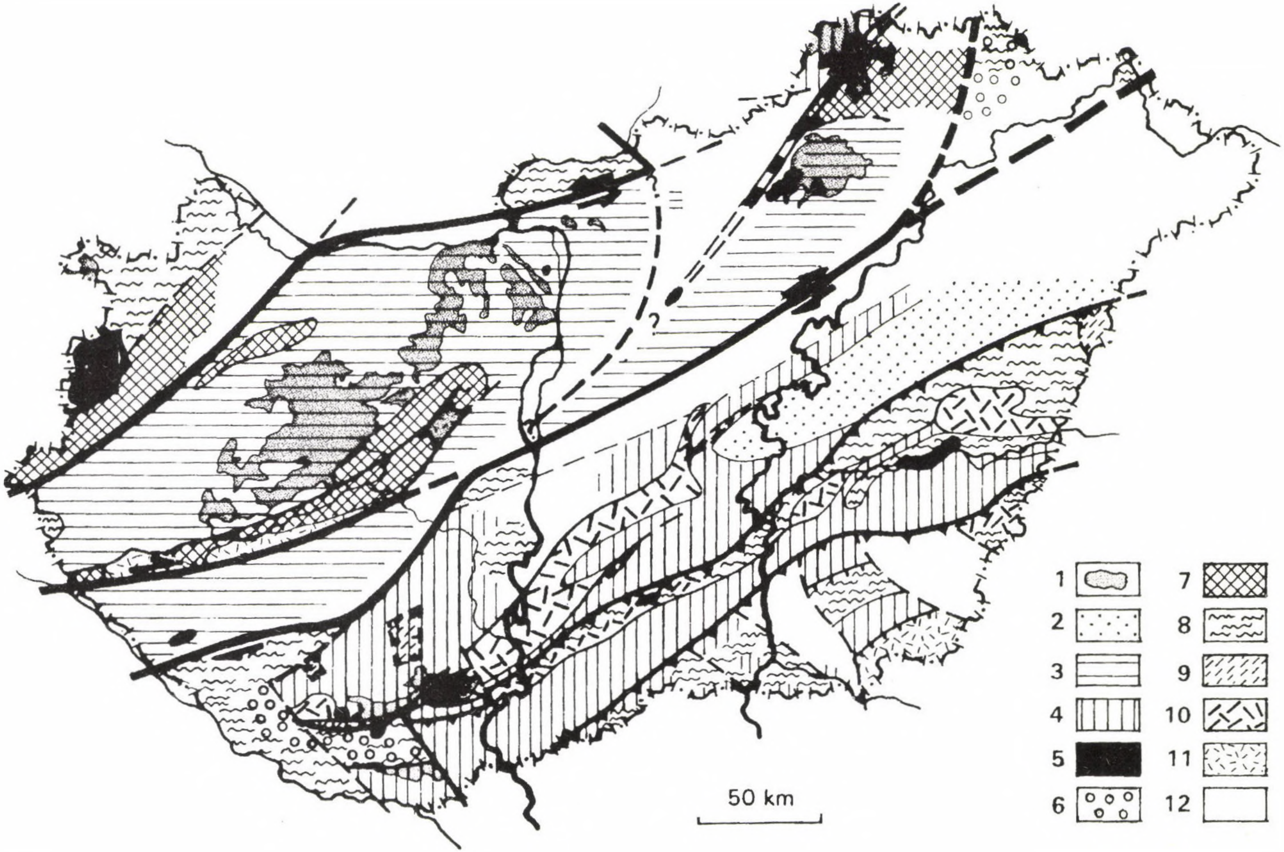
1
2
3
4
5
6
7
8
9
10
11
12
50 km
?

have a similar geological record (i.e. proximal terranes) that may only be distinguished by the presence of the terrane boundary representing telescoped oceanic lithosphere" (e.g. their evolution between two terrane evolutionary events was so much different that it could not be explained by lateral facies transition).

A complex terrane analysis, in correspondence with previously published ones (cf. Howell 1989; Karamata et al. 1996; Sinha 1997 and references therein) should include the following methods of investigation to identify the contrasting evolution of adjacent units and their possible relationships:

– sedimentary evolution (as reflected by stratigraphy)
– magmatic evolution
– metamorphic evolution
– structural evolution/deformational history
– palaeobiogeography
– palaeomagnetic positions.

In our brief analysis, in agreement with the criticism by Hamilton (1990, p. 512), we also attempt a complex evolutionary/genetic approach, instead of a simple, descriptive characterisation. Quantitative palaeobiogeographic analysis of Mesozoic (especially Jurassic) faunas was presented in numerous contributions by Géczy and Vörös; for a most recent review see Vörös (1993) and references therein. Palaeomagnetic analysis is presented in a separate contribution (Márton in the present volume). Research on deformational history (especially ductile) of pre-Tertiary rocks in Hungary, apart from a few exceptions (Balla 1987; Csontos 1988, 1999; Balla and Dudko 1993) is still at the initial stage; therefore our analysis in this important aspect can only be considered a preliminary one.

←Fig. 3

The Terrane Map of Hungary. Scale 1:2 500 000. Base map: "Tectonic Map of Hungary" (Dank et al., 1990), with slight modifications. Legend: 1. Pre-Tertiary rocks on the surface; 2. Flysch Zone; 3. Alpine overstep sequence connected to the southern (South Alpine–Dinaric) shelf of the Axios/Vardar and related Neotethyan oceanic basins; 4. Alpine overstep sequence connected to the northern (East Alpine–Carpathian) shelf of the Axios/Vardar and related Neotethyan oceanic basins; 5. a) Alpine ophiolitic assemblages (Pelsonia and Penninic Composite Terranes), b) Pre-Alpine ultrabasics, eclogites and amphibolites (Tisia Terrane); 6. Post-Variscan, Late Carboniferous overstep sequence with thin anthracite seams (Zemplenicum Terrane and southwestern part of Tisia Terrane); 7. Variscan "overstep"-type (shelf) sequence (with abundant Devonian carbonates, as well as with very low to low-grade Variscan metamorphism in Transdanubia and most probably without Variscan metamorphism in the Bükkium of NE Hungary) (East Alpine units and Pelsonia Composite Terrane); 8. Variscan medium-grade metamorphosed complex; 9. Variscan low to very low-grade metamorphosed, predominantly siliciclastic complex (Tisia Terrane); 10. Syncollisional granitoids (migmatitic complex); 11. Postcollisional granitoids (intrusions); 12. No drilling data on the pre-Neogene basement; *Note*: According to Balla et al. 1987, and Balla and Dudko 1993 the Buzsák Line, located a few km to the S of the Balaton Line, is considered as the southern border of the Transdanubian Range Unit. In this alternative the former line represents the major terrane boundary, which joins the Zagreb–Zemplín (or Mid-Hungarian) Lineament near the Danube River

The terrane collage in the Pannonian domain and in its Alpine–Carpathian–Dinaridic surrounding

The geotectonic interpretation of the pre-Neogene (more exactly: pre-Middle Miocene) basement of the Pannonian Basin has been completely changed in the last quarter century. Increasing geologic (surface and especially borehole) and geophysical data have revealed that the classical "Internide" concept is totally untenable (see above). Instead, it has been recognised that this basement and the immediate Alpine–Carpathian–Dinaridic surrounding of the basin is built up by a collage of allochthonous terranes deriving from different parts of the Tethys, which finally accreted in Late Oligocene–Early Miocene times (cf. Balla 1988a; Csontos et al. 1992).

This terrane collage (see Fig. 1) is bounded to the N and NE by the Pieniny Klippen Belt, to the E and SE by the Mures Ophiolite Belt and the Median Dacides (in the sense of Sandulescu 1980, 1984) of the East and South Carpathians (Bucovino–Getic Terrane according to Kräutner 1996/1997) and on the S and SW by the Inner Dinaridic–Vardar ophiolitic complexes. On the other hand, there is no distinct boundary to the W toward the Eastern Alps, from where the eastward-directed escape of the "North Pannonian–Inner West Carpathian" units, nearly along strike, took place (Balla 1988a; Neubauer and Genser 1990; Ratschbacher et al. 1991; Csontos et al. 1992). The same holds true for the eastern end of the Southern Alps and northwestern end of the Inner Dinarides (c.f. Pamic and Tomljenovic 1998; Haas et al. 1998, 2000).

Table I
The terrane evolutionary events, that can be recognizes in the Pannonian Basement

Q	Neo-Alpine/post-Alpine stage: pull-apart tectonism, formation of the extensional Pannonian Basin (i.e. events recorded within the overall overstep sequence of the "Pannonian terrane collage")
M_2	Docking
$O_3 - M_1$	Amalgamation and accretion
$E_3 - M_1$	Mesoalpine strike-slip dispersion
$J_3 - Cr_2$	Palaeoalpine (+Eohellenic) accretion – nappe stacking
J_2	Penninic (Atlantic) rift dispersion (~180–170 Ma)
T_2	Neotethyan ("Vardar") rift dispersion (~235–230 Ma)
C_{1-2}	Variscan accretion (~360–320 Ma) (Early Variscan or "Caledonian" accretion/suturing: ~440–400 Ma)

Fig. 4 →
Alternative for Fig. 3: the (Gailtal–)Balaton Lineament does not join the Zagreb–Zemplín (or Mid-Hungarian) Lineament, but is considered to continue along the southeastern border of the Late Variscan (lC)–Palaeogene (eTe) Periadriatic magmatic range, the last known representatives of which are the Upper Eocene andesites at Recsk, in the northwestern neighbourhood of Darnó Hill (A detailed description of these volcanics can be found in Varga et al. 1975 and in Csillag et al. 1980, although in these works the relationship with the Periadriatic magmatic range in sense of Bögel 1975, was not yet considered). Kinematically the alternative shown in Fig. 3 is considered to be more likely

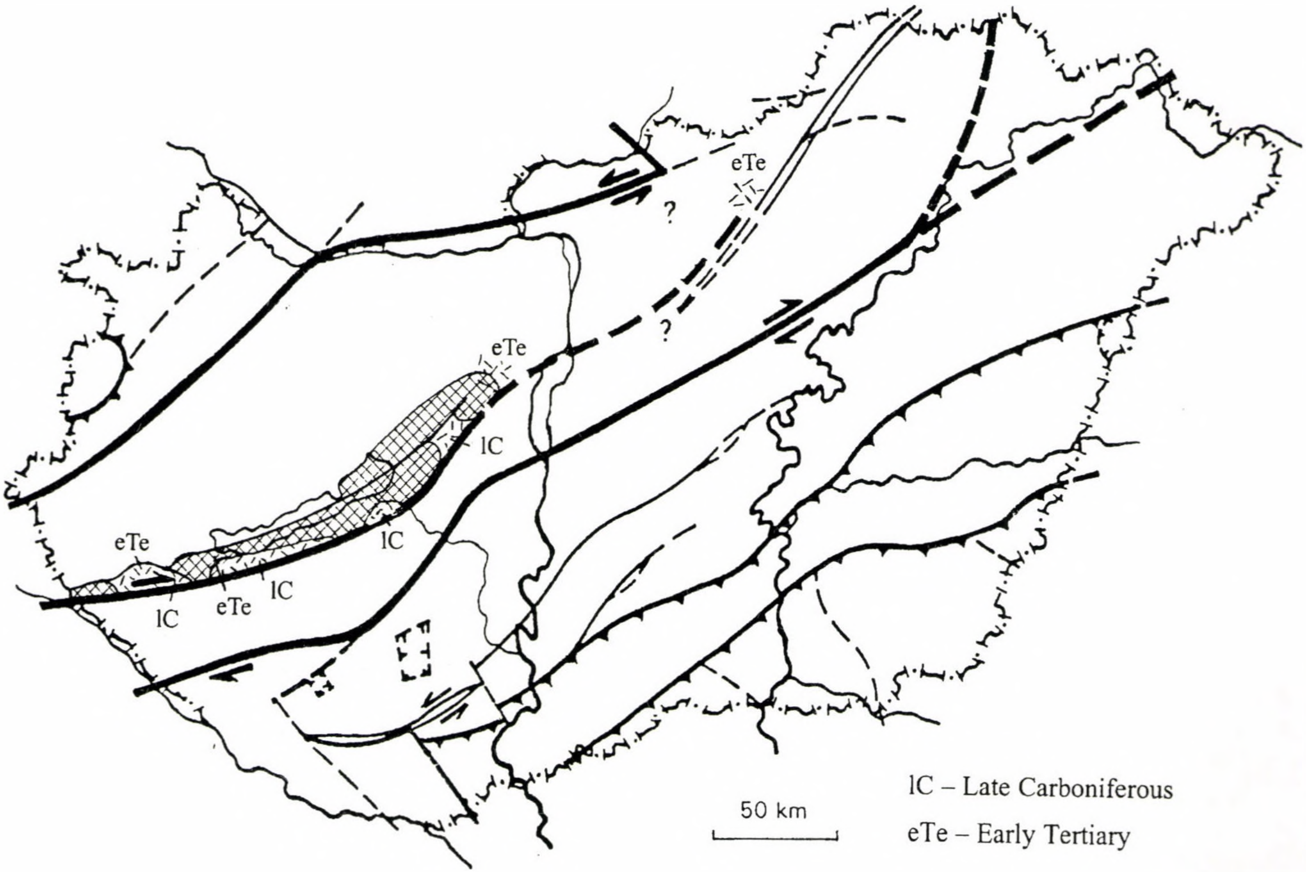
eTe
?
?
eTe
lC
lC
eTe
lC
eTe
lC
50 km
lC – Late Carboniferous
eTe – Early Tertiary

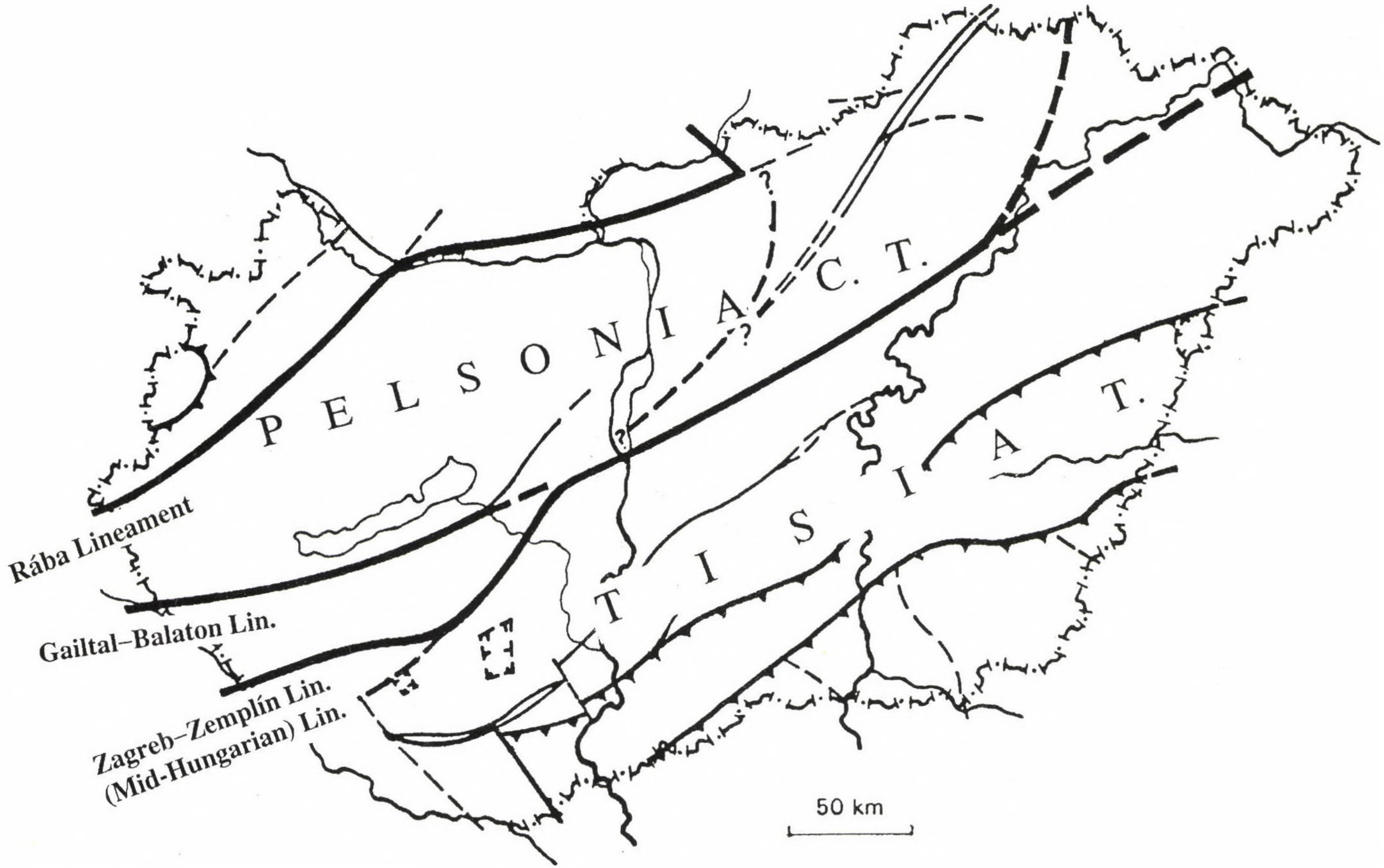

Fig. 5
Major terranes, resp. terrane boundaries in Hungary

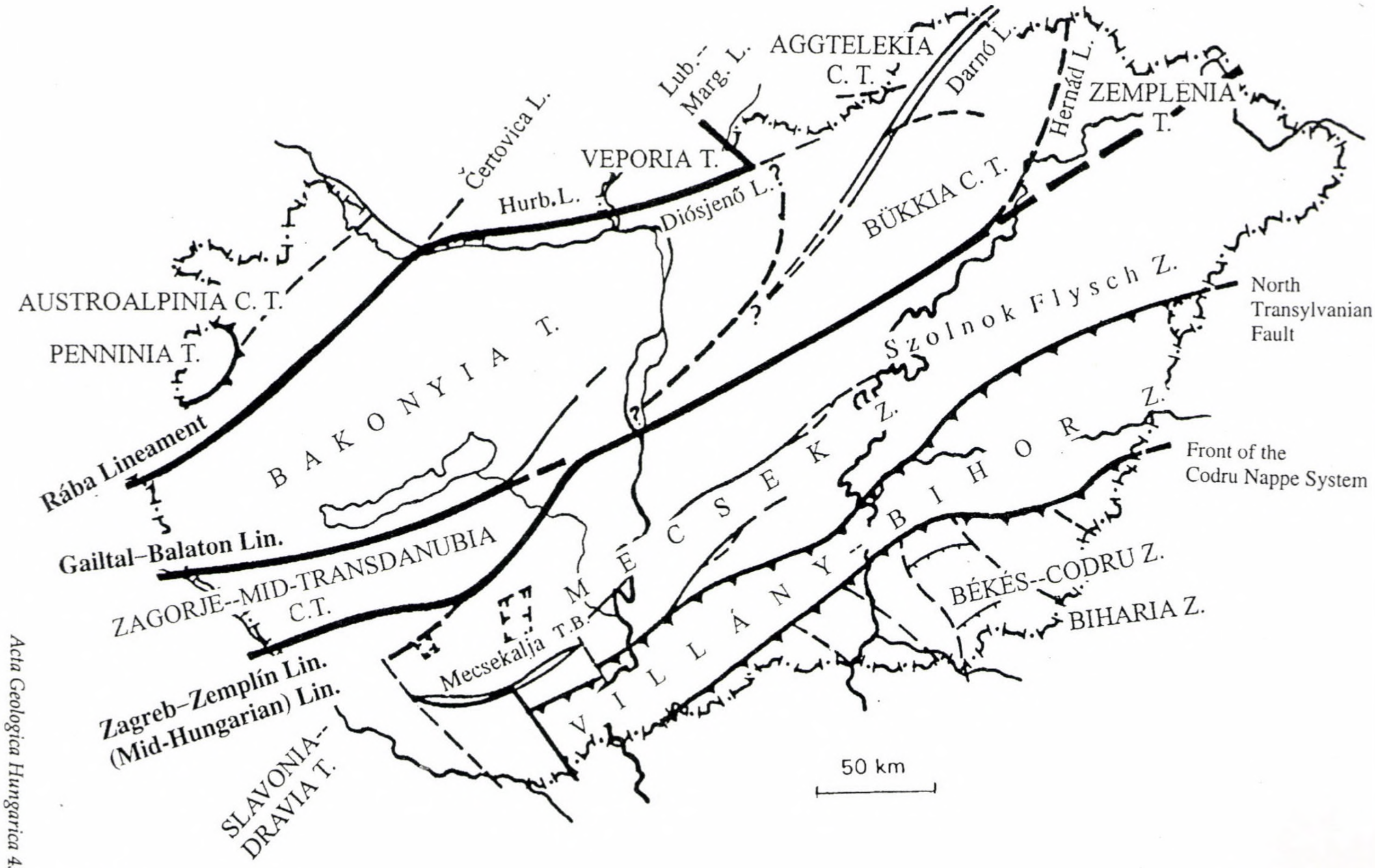

Fig. 6
Smaller terranes or units and tectonic lines of Hungary and of some adjacent areas, described in the text. Hurb. L. – Hurbanovo Line; Lub.–Marg. L.– Lubeník–Margecany Line

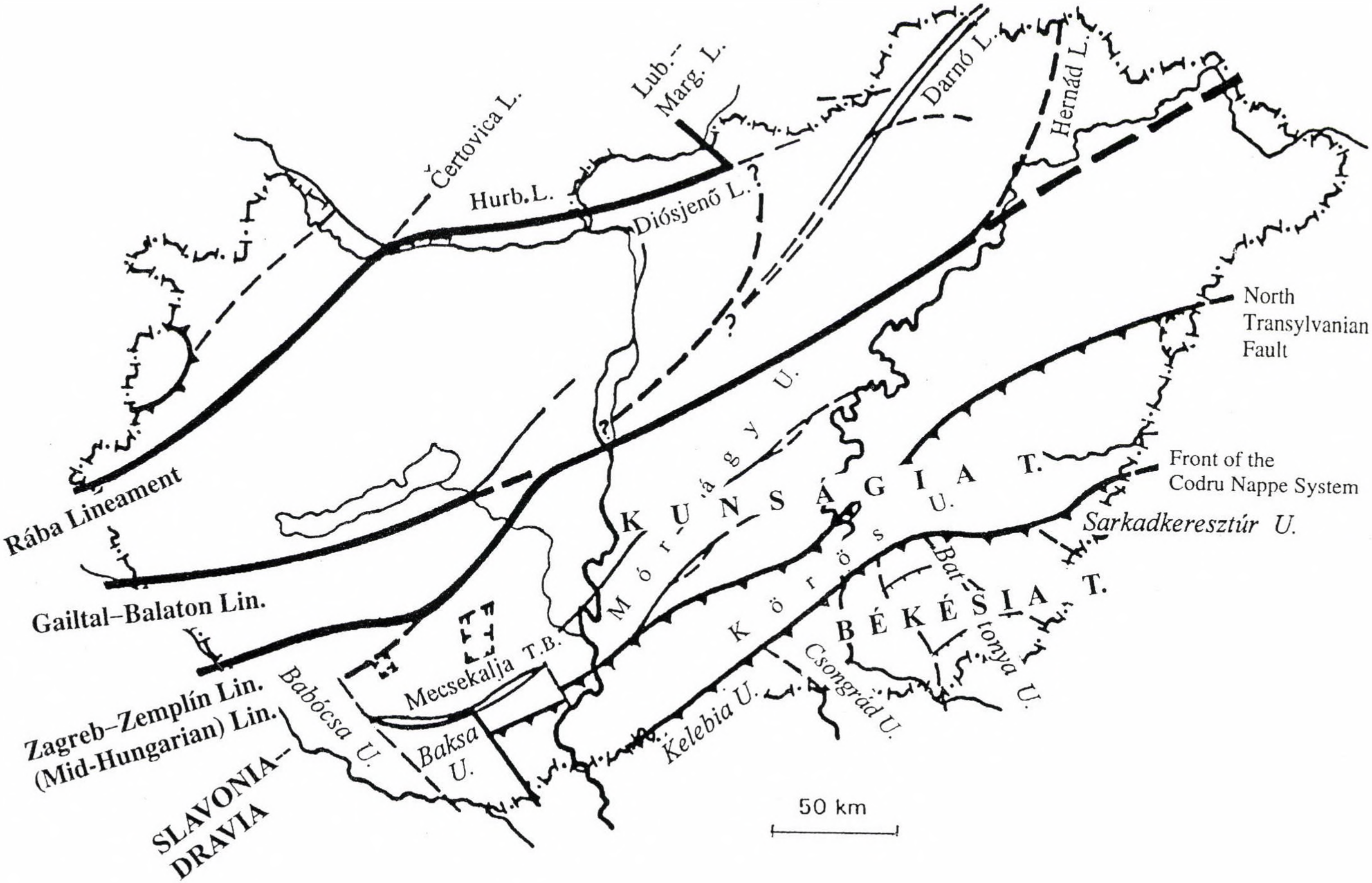

Fig. 7
Variscan terranes and units in the basement of the Alpine Tisia Terrane

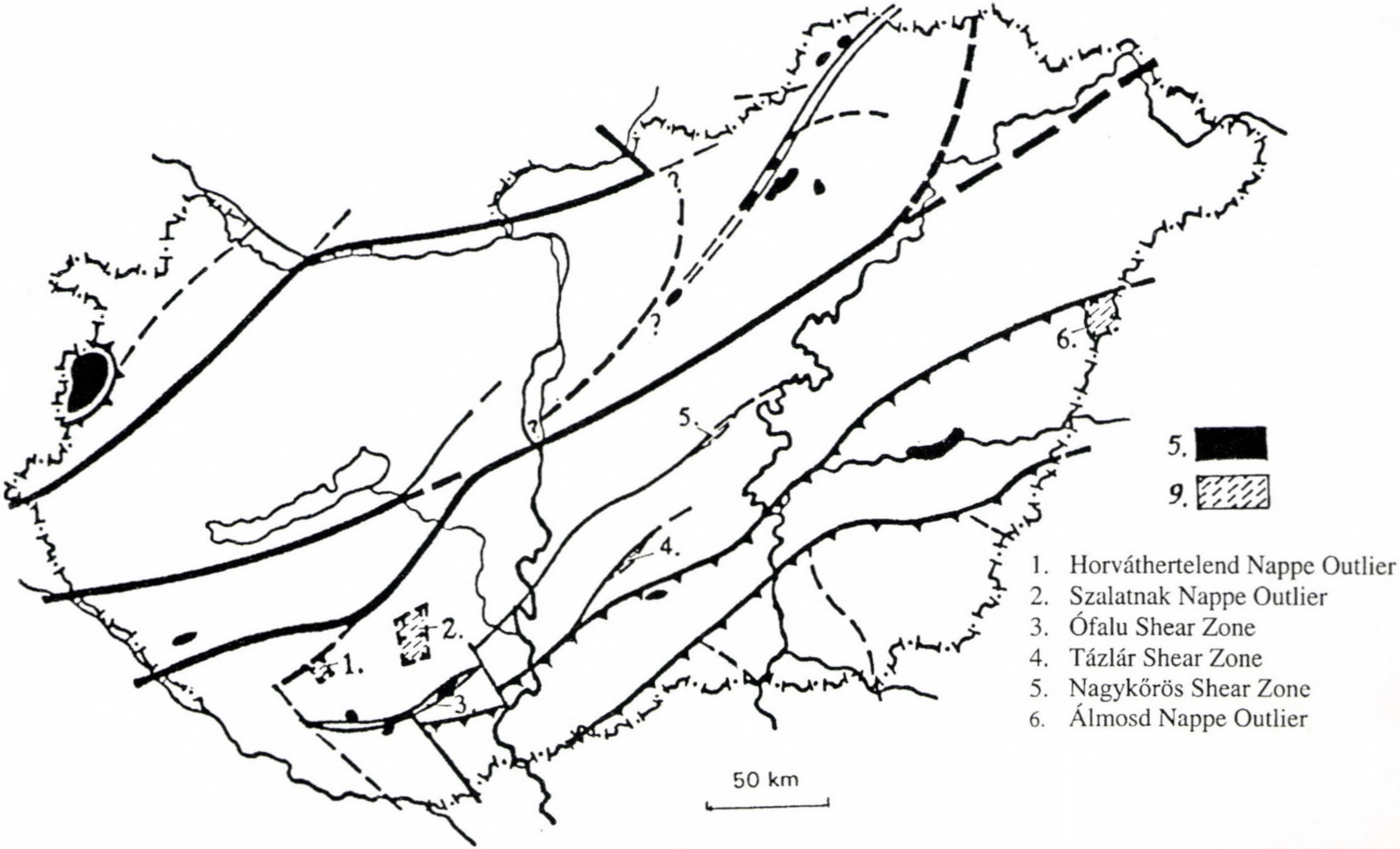

Fig. 8
Smaller pre-Alpine units (described in the text) within the Tisia Terrane. Because of the poor resolution, units marked by symbols Nos 5 and 9. in Fig. 3 are redrawn here

Table II
Tectonostratigraphic terranes/units of the Pannonian basement (Hungarian part)

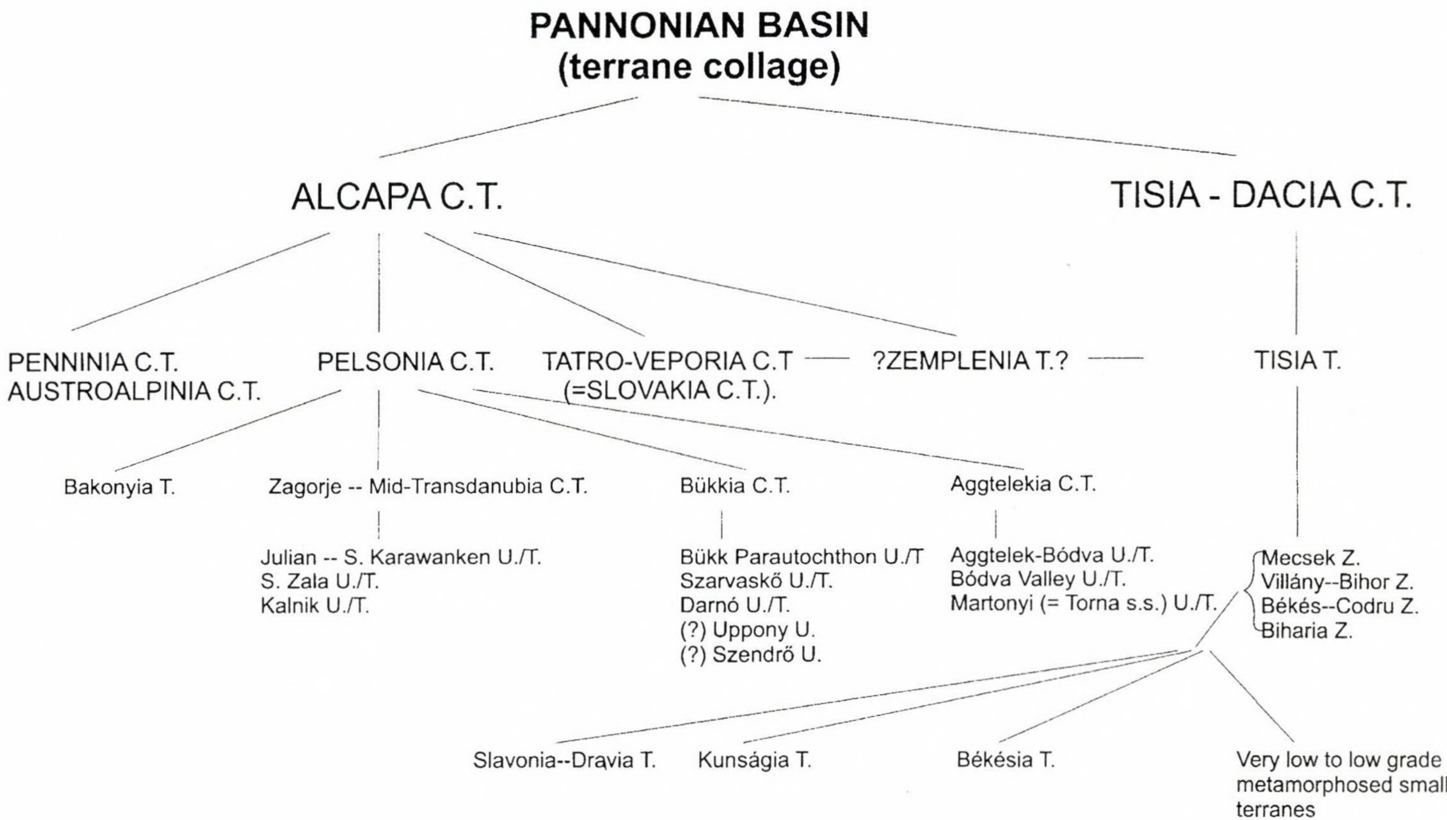

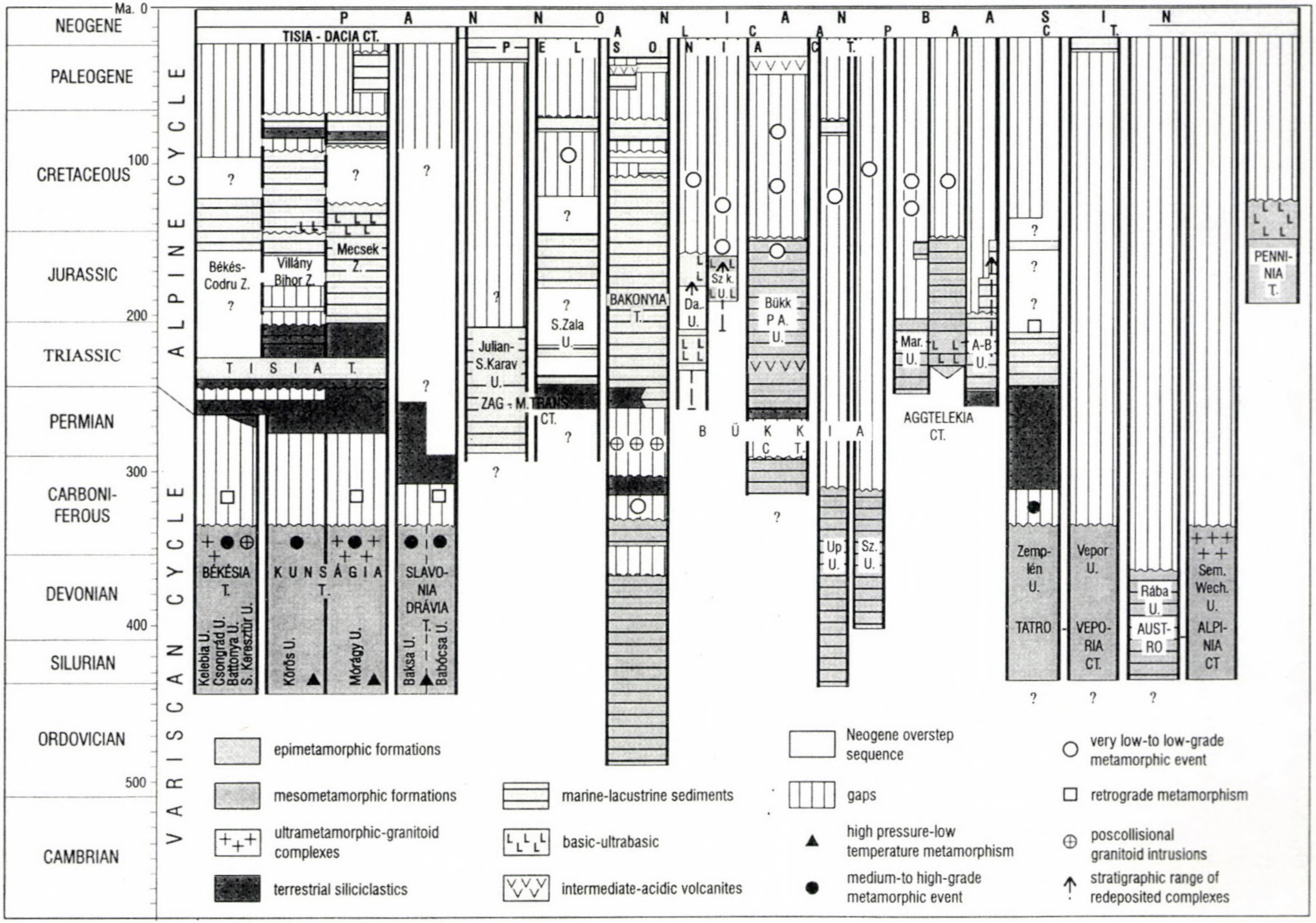

Fig. 9
Stratigraphic scheme and major characteristics of magmatism and metamorphism of the Hungarian structural units/terranes

The Neogene fill of the Pannonian Basin(c.f. Fig. 2) forms the overall overstep sequence of all terranes of the basement. The Pannonian domainis unique in the European Alpides that here, formations and structures related both to the opening and closing of the Neotethyan Ocean (opened from the SE in the Middle Triassic, closed mostly in the Late Jurassic; Robertson and Karamata 1994) and of the Penninic Ocean (opened from the W in the Middle Jurassic, closed in the Middle Cretaceous–Late Cretaceous) overlap each other. This is essentially due to Mesoalpine terrane movements (see in Kázmér and Kovács 1989; however, views on the history of the "Vardar Ocean" s.s. have considerably changed since then; c.f. Karamata et al. 1998, 1999; Pamic et al. 1998).

Thus, the following major Palaeo/Mesoalpine allochthonous (see Figs 3 to 9 for the territory of Hungary) terranes can be distinguished within the Carpatho-Pannonian domain (cf. Fülöp et al. 1987 and Vörös 1993, partly):

– ***Austroalpinia, Penninia;***

– ***Tatro-Veporia Composite Terrane*** (Vozárová and Vozár 1996) (=Slovakia Terrane according to Plašienka 1991), bounded to the North by the Pieniny Klippen Belt and to the South by the Hurbanovo–Lubeník–Margecany Fault (according to Vozárová and Vozár, op. cit., it also includes the Zemplenia or Zemplín Terrane to the NE);

– ***Pelsonia Composite Terrane*** (after the "Pelso Megaunit" introduced by Fülöp et al. 1987), bounded to the NW and N by the Rába–Hurbanovo–Diósjenő–Lubenik–Margecany Fault and to the SE by the Mid-Hungarian (or Zagreb–Zemplín) Lineament;

– ***Tisia Terrane*** (=Tisza Megaunit according to Fülöp et al. 1987), bounded to the South by the Sava fault (i.e. the northern marginal fault of the Sava Depression to the SW) and an as yet unnamed fault in Middle Vojvodina (to the SE, bordering it against the Vardar ophiolite complex; see in Kemenci and Canovic 1988, 1997), to the SE and E by the Mures Ophiolite Belt and to the NNW by the Mid-Hungarian or Zagreb–Zemplín Lineament.

The boundaries of these major terranes/blocks (which, as tectonostratigraphic units, are characterised by an "internal continuity" of geology between two stratigraphic horizons reflecting terrane dispersal or accretionary events) often consist of different segments cutting each other at an angle (like the Rába–Hurbanovo–Diósjenő–Lubenik–Margecany Line), thus being of different nature and partly of different age. Seismic surveys indicate that the major terrane boundaries in Hungary are mostly the expression of young, Neogene movements, either in extensional regimes (like the Rába Line; Tari 1996) or in transpressional ones (like the Mid-Hungarian Line; Csontos and Nagymarosy 1998), which post-date the juxtaposition of different terranes. In other words, in their present form they do not provide an unambiguous explanation for the origin of the large-scale facies offsets recognisable between the Palaeozoic–Mesozoic successions of the crustal blocks they separated. In fact they represent young tectonic features which obliterate older structural elements. Consequently, the significant facies offsets witnessed by the stratigraphy of the presently juxtaposed units/terranes provide indirect evidence for their large-scale lateral displacements.

The Austroalpinia, Tatro-Veporia (or Slovakia) and Pelsonia Terranes moved together during the Late Oligocene–Early Miocene, forming a large, more or less coherent terrane, as shown by their common Late Oligocene–Early Miocene overstepping sequence (ALCAPA Terrane - Csontos et al. 1992). Balla (1982) named this large unit the "North Pannonian Unit" and the Tisia Terrane the "South Pannonian Unit".

Description of the terranes of Hungary

Austroalpinia and Penninia Terranes

Origin of the names: after Vörös (1993), referring to the Austroalpine and Penninic units of the Alps.

In the northwestern part of the country, units of the Eastern Alps extend into the territory of Hungary, as proven by the surface outcrops of the Kőszeg and Sopron Mts., and by numerous wells reaching the basement of the Little Plain basin.

The Kőszeg Mts and their subsurface extension represent the easternmost known occurrence of the South Penninicum, with ophiolites (Koller 1985).

The metamorphic rocks of the Sopron Mts. and their subsurface extension represent the Semmering Unit ("Grobgneis Series") and the crystalline schist of the small hill at Fertőrákos the Wechsel Unit of the Lower Austroalpine Nappe System (Pahr 1991). P–T history of the Sopron metamorphic rocks is given in Török (1996, 1998), Demény et al. (1997) and Draganits (1998).

The low-grade Rába Metamorphic Complex consisting of phyllite, meta-sandstone, basic and intermediary metavolcanics, and dolomite (aligned along the NW side of the Rába Fault) has been considered by most of the authors to be an Upper Austroalpine Unit, related to some types of the Graz Palaeozoic (cf. Árkai et al. 1987; Fülöp 1990). However, doubts recently arose about this affiliation (Balla 1993; Neubauer, pers. comm.), requiring further comparative studies. Nevertheless, this complex undoubtedly represents an eastern extension of the Upper Austroalpine nappe system.

The Rába Fault borders these units of the Eastern Alps in the pre-Neogene basement of the Little Plain against the predominantly South Alpine-type block of the Bakonyia Terrane (Transdanubian Range). Although this fault is unambiguously a major Mesoalpine terrane boundary, its role and character is disputed (for latest summaries see Balla 1993: strike-slip fault; Horváth 1993, Tari 1996: low-angle normal fault). However, its role as low-angle fault in the Miocene (Horváth, op. cit.), in connection with the gravitational collapse taking place in the Eastern Alps (Ratschbacher et al. 1991), does not exclude at all that it acted formerly as an oblique-slip zone.

The overstep sequence covering all these units of the Eastern Alps (e.g. the basin fill of the Little Plain) begins with Middle Miocene.

Veporia Terrane

Origin of the name: after the Veporic Unit or Veporicum of the West Carpathian Mts.

The Inner West Carpathian Tatro-Veporic (or Slovakia) Composite Terrane extends over a small area into the territory of Northern Hungary, as proven by borehole evidence. The medium-grade metamorphic rocks consist of garnet-bearing biotite paragneiss, micaschist and amphibole schist (Fülöp 1990) and correspond to the Kohút Terrane of the South Veporicum (cf. Vozárová and Vozár 1992). For more details we refer to the description by Vozárová and Vozár (1996 1996/1997). In the Hungarian part the Alpine age of the medium-grade metamorphism was proven by Koroknai et al. (in press) with ca. 550 °C and 8 Kbar.

Boundaries: this Veporic unit is bounded to the south by the (Hurbanovo-) Diósjenő Fault and to the east by the southernmost part of the Lubeník–Margecany Fault against the Pelsonia Composite Terrane. The thick Tertiary cover overstepping this boundary begins with Late Oligocene.

Zemplenia Terrane

(after Lelkes-Felvári, in Kovács et al. 1996/1997)

Origin of the name: after the Zemplenic Unit or Zemplenicum of the West Carpathians, as proposed by Vörös (1993).

Boundaries: this terrane in Hungary is bounded by the Hernád Fault to the W, and by the Zagreb–Zemplín Lineament to the SE. The bulk of the terrane is located in the territory of Slovakia, for the description of which we refer to Vozárová and Vozár (1996, 1996/1997 and references therein). The characterisation of the small area extending into Hungary relies on the unpublished investigations of Lelkes-Felvári, as well as on Kisházi and Ivancsics (1988). For a summary of previous results see Fülöp (1994).

The boundaries of the Zemplenia Terrane are covered by an overstepping Middle Miocene sequence. The terrane, based on the similarities of Upper Carboniferous anthracite-bearing molasse sequences, unknown elsewhere in the West Carpathians (Grecula and Együd 1977), was considered by Fülöp et al. (1987) as part of the Tisza Megaunit (= Tisia Terrane). Balla (1988a) suggested its detachment from the SW part of the Tisia Terrane and its incorporation into the eastward escaping "North Pannonian" terrane collage. Similarly to the latter opinion, Haas et al. (1995) saw it as a smaller terrane involved in the escaping Mesoalpine Pelsonia Composite Terrane. On the other hand, Vozárová and Vozár (1996, 1996/1997) consider it as part of the Tatro-Veporic Composite Terrane.

Variscan evolution

Metamorphic evolution

Two main groups can be distinguished within this terrane according to their metamorphic grade: an amphibolite facies complex and a greenschist facies one.

– The amphibolite facies complex is made up of micaschist, gneiss, amphibolite and metagranitoids. As far as the age of their protoliths is concerned no data are available. In Slovak territory values of T=600–700 °C and P=5.5–8.5 Kbar were published by Faryad (1993).

– The greenschist facies complex is made up of phyllite and interlayered acidic metavolcanoclastics. No data for the age of their protoliths is available either.

The greenschist and amphibolite facies rocks occur as pebbles in the Upper Carboniferous conglomerates; their metamorphism is therefore certainly pre-Alpine.

– As far as the radiometric age of the metamorphism is concerned only two data are available from the amphibolite facies rocks: By means of K/Ar method an amphibole age of 312±13 Ma was obtained. This can be interpreted as a Variscan cooling age. A muscovite age of 227±9 Ma from micaschist can be interpreted as a Variscan cooling age rejuvenated by later hydrothermal effects.

– Data for the age of metamorphism in the greenschist facies complex are lacking.

– The Permo-Carboniferous (Late Variscan) sequence displays very low-grade Alpine metamorphic features.

Late Variscan sedimentary and magmatic evolution

These metamorphic complexes are unconformably overlain by a 1,900–2,500 m-thick Carboniferous overstepping sequence (Westphalian C at the base and passing into the Upper Permian upsection). It consists of alluvial, fluviatile and lacustrine conglomerate, siltstone, shale and coal with dolomitic limestone and acidic volcanoclastic intercalations.

Alpine evolution

The Permian is discordantly overlain by Lower Triassic fluviatile redbeds. The Lower Anisian is represented by evaporitic dolomite, which is overlain by dark grey limestone and dolomite of shallow ramp facies, Upper Anisian–Lower Ladinian in age. In a single borehole traces of uppermost Jurassic to lowermost Cretaceous pelagic limestone were encountered.

Pelsonia Composite Terrane

Origin of the name: Fülöp et al. (1987) proposed the name Pelso Unit for the composite unit including the Transdanubian Range, the Mid-Transdanubian and the Bükk Subunits, supposing that they came into juxtaposition before their major displacement in the Palaeogene. The term Pelsonia Terrane was first used by Vörös (1993) but only for the Bakony Unit (Bakonyia Terrane herein).

Boundaries: it is bounded by the Rába–Hurbanovo–Diósjenő Lineament against the Austroalpinia and Tatro-Veporia Composite Terranes. It is in the highest structural position above the Austroalpine crystalline rocks to the NW, and is separated from the Tisia Terrane by the Mid-Hungarian Lineament southeastward.

Subdivision: the Pelsonia Composite Terrane is made up of the following units:
- Bakonyia Terrane;
- Zagorje–Mid-Transdanubia Composite Terrane;
- Bükkia Composite Terrane;
- Aggtelekia Composite Terrane.

Bakonyia Terrane

Origin of the name: in the last decades the name "Transdanubian Central Range" (Fülöp et al. 1987) or "Transdanubian Range" (Balla and Dudko 1989, 1993) Unit has been widely accepted for this terrane; however, Transdanubicum (Tolmann 1987)was also proposed. Kázmér and Kovács (1985) called it Bakony Unit, and Vörös (1993) proposed the name Bakonyia Terrane. We prefer to use this name because it is short and expresses the fact that the largest outcrops can be found in the Bakony Mts.

Boundaries: the Bakonyia Terrane is bounded to the NW by the Rába Line against the Austroalpine units and to the N by the Hurbanovo–Diósjenő Line against the Tatro-Veporic Terrane. To the SE the boundary is the Balaton Line, representing the northeastern continuation of the Periadriatic (Gailtal) Lineament (Haas et al. 2000). The Palaeogene rocks on both sides of the Balaton lineament show considerable offset (Nagymarosy 1990; Csontos et al. 1992), thus proving post-Oligocene activity for this feature. The probable age of the final docking can be between Badenian and Sarmatian. The western boundary of the terrane is close to the Hungarian/Slovenian frontier; however, outliers of the Mesozoic of the Bakonyia Terrane are known above the Middle Austroalpine Murska Sobota Massif (Haas, Mioc, Pamic et al. 2000). Setting and nature of the boundary to the NE against the Bükkia Terrane is not exactly known due to lack of information about the pre-Tertiary basement in that area. In any case Palaeogene rocks overstep the assumed border line and do not show major stratigraphical or facial break at the boundary of the two terranes.

Variscan evolution

Sedimentary and magmatic evolution

The oldest known sequence of the unit is the Balaton Phyllite Group (Lelkes-Felvári 1978; Fülöp 1990), assigned to the Upper Ordovician to Lower Devonian. An exception is represented by Arenigian metasiltstone with achritarchs (Albani et al. 1985) known only from one well. The Balaton Group s.s. consists of quartz phyllite (assigned to the Upper Ordovician), metasiltstone with dark slate and schistose metasandstone containing black lydite, metarhyolite and subordinately metabasalt intercalations (Silurian, as proven by some microfossils) and calcareous metasiltstone, sericite slate, schistose metasandstone with intercalations of andesitic volcaniclastics (assigned to the Lower Devonian). The total thickness is unknown but certainly exceeds 1,000 m. Pelagic limestone with styliolinids and conodonts (Emsian to Frasnian) develop in transition from the above-mentioned calcareous metasiltstone (Fülöp 1990). Shallow-water, crystalline limestone with stromatolitic structures is considered as a coeval carbonate platform deposit ("Middle Devonian" Polgárdi Limestone). To the SW, near the Slovenian border, amphibolite-facies metamorphosed rocks (Fülöp et al. 1986), belonging to the Middle Austroalpine Murska Sobota Massif (Haas, Mioč, Pamic et al. 2000), are known from one well.

According to East Alpine analogies (cf. Ebner et al. 1991) the shallow marine Szabadbattyán Formation (black shale, bituminous, fossiliferous limestone and rare sandstone intercalations) of Late Visean age already represents the marine molasse stage. The next formation, according to age, is the Westfalian or Lower Stephanian terrestrial Füle Conglomerate Fm., with plant remnants.

Aligned to the Balaton Lineament, Upper Carboniferous post-collisional (Buda 1985), peraluminous (Buda 1995) granitoids showing a calc-alkaline granodioritic suite with slight subalkaline characters occur, representing the northeastern continuation of the range of Late Variscan Periadriatic granitoids (in the sense of Bögel 1975). They can be considered as the Late Variscan stitching plutons, with 271–291 Ma K/Ar and 280 Ma Sr/Rb radiometric ages on biotites. North of the western part of the Balaton Lake dacite, assigned to the Lower Permian (Fazekas et al. 1981; Fülöp 1990), is known from boreholes.

Tectonometamorphic evolution

Pre-Late Carboniferous rocks of the unit, as can be seen in the Balaton Highland and Balaton–Velence crystalline ranges at its southeastern margin, bear evidence of a Variscan nappe structure of SE vergency (according to present co-ordinates), with disharmonic and isoclinal folds (Dudko 1988; Dudko and Lelkes-Felvári 1992; Balla and Dudko 1993). They underwent very low grade, in case of the quartz phyllites low-grade (in general greenschist facies, chlorite, maximally biotite isograde) metamorphism (Árkai and Lelkes-Felvári 1987). Locally, close to the Balaton Lineament SW of Lake Balaton, metamorphosed rocks of amphibolite facies were detected (wells Balatonhídvég and Garabonc; Árkai 1987a; Török 1992, 1998), which probably correspond to the "Altkristallin" of the Karavank sector of the Gailtail Lineament (c.f. Schönlaub 1980; Mioc 1998). The age of the deformation and metamorphism is pre-Westfalian (Balla and Dudko, op. cit.).

Alpine evolution

Sedimentary and magmatic evolution

The Alpine evolution of the Bakonyia Terrane was primarily controlled by consecutive, although partly overlapping, opening of ocean branches (Neotethyan and Penninic, respectively) of the Tethys system during the Late Permian to Late Jurassic interval and consecutive and also partially overlapping closure of these basins from the Late Jurassic to the Tertiary.

The earliest, i.e. the Neotethyan passive margin evolutionary cycle commenced in the Late Permian. Upper Permian formations form the overstepping sequence of all Variscan structures and formations. As a result of the Late Permian transgression, a zonal facies pattern came into existence with a definite polarity. A shallow, periodically restricted carbonate ramp with coastal sabkhas was formed to the NE and continental red-beds were deposited in the central and southwestern parts of the Bakonyia Terrane (Majoros 1980, 1983, Haas et al. 1988).

The general facies trend was inherited by the Early Triassic, when as a result of a new transgression a wide ramp came into being. On the ramp fine siliciclastics and carbonates were deposited depending on the fluctuating sea level and the climatic conditions (Broglio Loriga et al. 1992). In the early Middle Triassic, significant decrease in the terrigenous influx led to predominance of the carbonate sedimentation on the ramp. Disintegration of the carbonate ramp began in the Middle Anisian and resulted in the formation of isolated carbonate platforms and intraplatform basins (Budai and Vörös 1992). The rifting continued in the Ladinian. In the deep pelagic basins, cherty limestone (Buchenstein Fm.) accumulated with intercalations of calcalcaline volcaniclastics ("pietra verde") (Harangi et al. 1996). On the coeval platforms thick dolomitised sequences ("Diplopora dolomite" Budaörs Dolomite) were formed. In the middle part of the Carnian, due to an increase in the terrigenous influx, the basins were filled up and an extremely wide and levelled platform emerged by the latest Carnian. In the tectonically calm Late Carnian–Norian a thick platform carbonate series was deposited and the lateral facies relations unambiguously reflect a facies polarity. In the northeastern part of the Bakonyia Terrane intraplatform basin and toe-of-slope facies occur (Haas et al. 1997). They are in intimate relationship with the reefal and oncoidal outer platform facies of the Dachstein Limestone. In the central part of the Bakonyia Terrane the cyclic peritidal-subtidal development of the Dachstein Limestone (dolomite in the lower part of the series) represents the middle platform, whereas the bituminous, thin-bedded Hauptdolomit, appearing in the southwestern part of the Bakonyia Terrane, represents the inner platform facies. In the Late Norian a large extensional basin was formed in the southwestern part of the Bakonyia Terrane, giving rise to deposition of a several hundred metre thick, organic-rich marl succession (Kössen Formation; Haas 1994). In the central and northeastern part of the Bakonyia Terrane platform carbonate deposition continued until the end of the Triassic, and during the latest Triassic highstand interval the platforms even prograded onto the former Kössen Basin. In the southwestern and central part of the Bakonyia Terrane platform evolution also continued in the Hettangian, whereas in the northeastern part (Gerecse Mts.) upbuilding of the platform came to an end in the latest Rhaetian, followed by inundation of the disintegrated blocks of the former platform in the Middle Hettangian. Further northeastward, in the area of the basement blocks east to the Danube, deposition of pelagic cherty limestone continued in the basins, which had already begun to form in the Late Triassic.

Disintegration of the Upper Triassic platforms was an effect of the initiation of the opening of the Ligurian-Penninic oceanic basin in connection with the opening of the Atlantic Ocean.

In the Sinemurian the break-up of the former carbonate platform became even more intense. As a consequence submarine highs and deeper basins were formed and this setting controlled the sedimentation pattern for most of the Jurassic (Galácz and Vörös 1972; Vörös and Galácz 1998; Császár et al. 1998). In the basins continuous successions, mainly red nodular limestone sequences ("Ammonitico Rosso"), and on the highs lacunar ones with a number of gaps, were formed. On the steps and at the toe of fault-controlled slopes, which separated the highs and the basins, and in fissures, scarp breccia and biodetrital grainstone (Hierlatz Limestone) was accumulated. In the Toarcian a significant deepening may have taken place as reflected in the prevalence of the pelagic fossils in the condensed, clayey "Ammonitico Rosso". Local occurrence of black laminated shale and manganese deposits may be considered as an effect of the Early Toarcian anoxic event (Jenkyns et al. 1991). In the Middle Jurassic condensed "Ammonitico Rosso-type limestone prevails in the northeastern part of the Bakonyia Terrane, whereas Bositra limestone shows a westward thickening trend. Maximum deepening of the basins is indicated by the occurrence of radiolarite from the Bajocian to the Oxfordian or locally in the Kimmeridgian. "Ammonitico Rosso"-type Saccocoma limestone characterises the Kimmeridgian to Early Tithonian interval. From the Late Tithonian to the Valanginian "Maiolica"-type cherty limestone, rich in radiolarians and calpionellids, was formed in the southwestern part of the Bakonyia Terrane and condensed Calpionella limestone in its central sector. During the Hauterivian–Barremian interval the basic facies distribution pattern did not change here. Deep-water pelagic basin facies occurred to the SW and shallower facies characterised the central segment of the Bakonyia Terrane.

As opposed to the other parts, in the latest Jurassic–Early Cretaceous interval the Gerecse sector of the Bakonyia Terrane became influenced by the upthrusting accretionary complex of the Neotethys. Due to the compressional movements a foreland basin (trough) and behind it a subaerially exposed high were formed in the late Early Cretaceous (Császár, in press). A large amount of ophiolithic detritus and fragments of intermediate and acidic plutonic and acidic volcanic rocks, probably of magmatic arc origin (Császár and Árgyelán 1994), was transported from the highs into the basin. A basic change also took place in the sedimentation pattern: siliciclastic gravity flow deposits began to form in the Late Berriasian. The general upward coarsening trend of the series indicates progradation of the submarine fans from NNE to SSW (according to present-day co-ordinates) in the Berriasian to Aptian interval (Sztanó 1990).

The subaerial exposure in the middle part of the Bakonyia Terrane was followed by a new transgression in the Middle–Late Aptian that resulted in the formation of shallow marine crinoidal limestone. The structural movements became even more pronounced at the very end of the Aptian, when the characteristic synclinal structure of the Bakonyia Terrane was formed (Császár 1986). The axis of the synclinorium is parallel to the strike of the Bakonyia Terrane, and its limbs are imbricated.

The Aptian tectogenesis led to uplifting in the southwestern and central segments of the terrane. However, its northeastern part remained the depocentre at least until the Albian. In the Early Albian a narrow fringing reef-tract emerged at the margin of the deeper basin and somewhat later a brackish water lagoon was formed behind it. Later on, it was overlain by a rudist platform which was drowned and covered by pelagic marl in the Late Albian (Császár 1986).

Structural movements in the Turonian–Coniacian led to regional uplift and intense denudation. A post-orogenic collapse basin came into existence in the Santonian with elongated depressions and ranges oriented roughly parallel with the strike of the Bakonyia Terrane in its western part. Coal seams and fluvial sediments were deposited in the depressions. Marine inundation reached the Bakonyia Terrane area from the SW during the Santonian. The palaeohighs became flooded in the Campanian leading to establishment of rudistid platforms. They were drowned and covered by pelagic marls in the Late Campanian (Haas 1983).

Another significant tectogenic event at the end of the Cretaceous led to regional uplift and denudation in the Palaeocene to Early Eocene interval. A new transgression commenced in the Middle Eocene from SW to NE.

Lagoonal to bathyal sediments were deposited in the Eocene basin system. In the latest Priabonian–earliest Rupelian the unit emerged and the Palaeogene sequence suffered considerable denudation; in some cases the entire Palaeogene cover has been removed.

Long-term calc-alkaline volcanism occurred in the Zala Basin and Velence Mts, from the Late Lutetian to Late Priabonian. The members of the volcanic chain are arranged along the Balaton–Darnó lineament system. The latest element of the volcanic chain is the Recsk palaeo-volcano in the Mátra Mts (see Bükkium Terrane).

From the Chattian on several minor Oligocene and Miocene marine and continental basins were formed in the area of the Bakonyia Terrane.

Tectonometamorphic evolution

The Bakonyia Terrane was not affected by Alpine metamorphism. The main stages of structural evolution are as follows:

– obduction of the Neotethys oceanic basement and upthrusting of the accretionary complex in the latest Jurassic and Early Cretaceous leading to formation of the Gerecse Basin;

– tectogenesis in the latest Aptian–Early Albian ("Austrian phase") which resulted in the emergence of the folded synclinal structure of the terrane with imbricated limbs;

– tectogenesis (unequal uplift and intense erosion) in the Turonian–Early Coniacian (pre-Gosau phase) and formation of post-orogenic collapse basins in the Santonian;

– tectogenesis (unequal uplift and intense erosion) in the Palaeocene–Early Eocene and genesis of collapse and pull-apart basins in the Eocene.

Zagorje–Mid-Transdanubia Composite Terrane

Origin of the name: the structural unit was defined by Wein (1969) under the name "Igal–Bükk Eugeosyncline". It was named by Fülöp et al. (1987) the "Central Transdanubian" and by Haas et al. (1988) the "Mid-Transdanubian Unit". Since this zone extends into Slovenia and Croatia, mainly in the area of the Hrvatsko Zagorje, according to the agreement with Mioč, Pamić and Tomljenović, we use the name Zagorje–Mid-Transdanubia Composite Terrane in the present paper (see also Pamić 1998). Haas et al. (2000) propose the name Sava Unit for the whole structural zone.

Boundaries: the terrane is actually a strongly sheared narrow zone between the Zagreb–Zemplín or Mid-Hungarian and the Periadriatic (Gailtail)–Balaton Lineaments. The Balaton Line can be unambiguously followed northeastward up to the Velence Hills (Balla and Dudko 1989, 1993). Further to the NE the setting of the lineament is ambiguous; two options are given in Figs 3 and 4.

Pre-Neogene formations of this unit in Hungary are known exclusively from boreholes. The drilled sequences show significant facies differences, suggesting their different origin. The facies relations of these sequences with coeval formations of the Carnic Alps, the South Karavanks, the Sava Folds (= Sava Nappe according to Mioc 1982) and the Dinaridic Ophiolite Belt and/or Vardar Zone indicate the original location of the sheared blocks in the junction area of the Southern Alps and the Dinarides. Metamorphic alteration of some Mesozoic series suggests a nappe structure, which may have formed during the Late Jurassic–Cretaceous compressional stages. Large-scale horizontal displacements in the Tertiary made the structural setting even more complicated.

Subdivisions: based on the evaluation of available core data in Hungary as well as core and outcrop data in Slovenia and Croatia, the following units could be distinguished within the Zagorje – Mid-Transdanubia Composite Terrane (c.f. Haas et al. 2000):

Julian–South Karavank Unit
South Karavank Zone
Julian–Savinja Zone
South Zala Unit
Medvednica Unit
Kalnik Unit.

Among these units the Medvednica and the Kalnik Units are known only from individual boreholes near the frontier of Hungary.

1. Julian–South Karavank Unit

This unit, as defined by Mioč (1995), can be considered as the eastward continuation of the South Alpine range. It is characterised by unmetamorphosed Mesozoic formations, with thick Triassic platform carbonates. Two zones can be distinguished within it:

South Karavank Zone

In a narrow zone (northern subunit) between the Balaton Lineament and the Buzsák Line, running south and parallel to the Balaton Lineament, marine Permian formations were exposed in a few wells. The most complete sequence was traversed in the vicinity of the Slovenian frontier (well Újfalu-1) where the succession begins with a 600 m-thick Lower Permian series. It consists predominantly of fine siliciclastics (grey quartz sandstone and dark grey shale); subordinately, however, fossiliferous, dark grey dolomitic limestone interlayers with fusulinids and lenses of reef talus breccia also occur (Bérczi-Makk and Kochansky-Devidé 1981; Bérczi-Makk et al. 1993). Above the clastic sequence light grey dolomite and dolomitic limestone were exposed. They can be classified into the Upper Permian.

Lithological features and foraminifera association of the Lower Triassic sequence indicate shallow ramp facies with temporal restriction and, mainly in the early part of the Early Triassic, significant terrigenous influx. Anisian is represented by platform carbonates: light grey dolomite, dolomitic marl and limestone rich in foraminifera and algae. The Ladinian series is made up by dark grey siliceous limestone, marl, argillaceous limestone, with radiolaritic tuffite and volcanic tuff interlayers. Facies characteristics of this rock succession indicate basin formation with coeval volcanic activity. In a few boreholes dark grey shale, sandy limestone and limestone were encountered, which could be classed as Carnian in age. The uppermost part of the Triassic sequence is made up of light grey platform dolomite and limestone of remarkable thickness. Based on their foraminifera fauna they can be classified into the Norian–Rhaetian (c.f. Bérczi-Makk et al. 1993).

Julian–Savinja Zone

It is made up of unmetamorphosed, predominantly Triassic sequences with thick platform carbonates. The Savinja and Julian Alps in Slovenia belong to this unit, which can be followed in a zone parallel to the Periadriatic–Balaton Lineament towards Varaždin and Nagykanizsa.

In the territory of Hungary, Permian was reported from a single exploratory well (Tab-1; Fülöp 1991), where Upper Permian oolitic dolomite with characteristic foraminifera and calcareous algae (*Mizzia*) assemblage was found.

A cored well (Igal-7) exposed a complete succession from the topmost part of the Lower Triassic to the Carnian (Haas et al. 1988). In the lowermost part of the sequence, the lithofacies and the fossils indicate peritidal and shallow lagoonal depositional environment. The Anisian is represented by grey brecciated dolomite, dolomitic limestone with dolomitic marl and limestone intercalations and shallow marine foraminifera and calcareous algae. The Ladinian segment of the sequence is made up of grey limestone with Wetterstein-type reefal and near-reef biota. Lower Carnian is represented by light and dark grey limestone with coral and sphinctozoa fragments and pelagic fossils, suggesting platform to foreslope deposition. Some other wells (e.g. Som-1; Haas et al., op. cit.) encountered Upper Carnian–Norian platform carbonates with features akin to those of the Dachstein Limestone.

The most conspicuous and peculiar characteristic of the before-mentioned Triassic sequences is the total lack of volcanics. A similar carbonate platform series without any trace of volcanic activity was reported from the Tara Mountains in West Serbia (Andelković 1976; Pantić et al. 1977), which has been considered as a nappe shed off the Drina–Ivanjica Unit (Dimitrijević and Dimitrijević 1991).

The stratigraphic column of the South Karavank and Julian–Savinja units in the territory of Hungary contains fragments of dislocated Late Palaeogene marine deposits. However, it is not easy to determine whether they belong to the former or the latter unit. Core samples from the wells around Buzsák, Táska, Nagyberény, and Öreglak indicate the presence of an Oligocene series similar both to Carnic Alp (Slovenia), Ravna Gora (Croatia) and Bükk (Hungary) -type Palaeogene (Báldi-Beke 1984; Nagymarosy 1990; Šimunić and Šimunić 1992).

2. *South Zala, Medvednica and Kalnik Units*

In the western part of the Zagorje–Mid-Transdanubian Unit in Hungary (in the South Zala Basin), strongly tectonised Permian to Jurassic sedimentary sequences with deeper water carbonates in the Triassic and pelagic shale in the Jurassic were encountered (Haas et al. 2000). They were generally affected by very low-grade Alpine metamorphism (Árkai et al. 1991).

A key well (Iharosberény-1) traversed limestone of platform and foreslope facies in a remarkable thickness, which was classified into the Ladinian–Carnian. Above the Triassic carbonates brecciated limestone, radiolarite and shale were encountered. The dark grey radiolarite yielded Middle–Upper Jurassic radiolarians (Dosztály 1994).

In the wells Inke-I, and -9, in the neighbourhood of the Mid-Hungarian Lineament, acidic and intermediate metavolcanites, serpentinite, tholeiitic basalt, shallow marine limestone and dark grey radiolarite were encountered. Ladinian (Dosztály 1994) and Carnian (Kozur 1985, in Kozur and Mostler 1994) radiolarians were found in the radiolarite. The extremely mixed rock association of this sequence suggests that it might belong to the tectonised ophiolitic melange complex of the Ivanščica, Medvednica and Kalnik Mts (Kalnik Unit; Pamić 1997).

In the Medvednica Mts the ophiolitic melange (Kalnik Unit) and the Palaeozoic to Triassic complex affected by Early Cretaceous Alpine metamorphism (Medvednica Unit) are unconformably overlain by Senonian conglomerate, sandstone, siltstone, shale and pelagic limestone (Belak et al. 1997).

In Hungary, in the South Zala and Kalnik Units, a few exploratory wells penetrated pelagic shale, which may be classified into the Senonian.

Tectonometamorphic evolution of the composite terrane

Eohellenic to Palaeo-Alpine (Late Jurassic–Cretaceous) compressional tectonics (folding, overthrusting) was connected with low-T metamorphism, whereas the Meso-Alpine tectonophases are characterised by large-scale horizontal displacements.

Considering the grade (temperature) of the regional alterations, different zones were distinguished within the unit, in the region south of Lake Balaton and to the WSW, up to the state border.

In the northwestern zone (South Karavank Unit) the Triassic (near the village of Sávoly) shows only signs of diagenesis. The grades of regional alterations in the "Inner Dinaric type" formations of the northeastern part of the southern zone are variable: diagenetic (borehole Nikla), dynamothermal anchizonal (borehole Öreglak), and low-T contact metamorphic (villages of Buzsák and Újfalu; Árkai et al. 1991).

In the more southwestern part of the southern zone (South Zala and Kalnik Units), epizonal (boreholes Semjénháza, Pat), anchizonal (boreholes Inke, Iharosberény and Bajcsa) and diagenetically altered rocks (boreholes Pátró, Liszó, Murakeresztúr) were distinguished (Árkai et al. 1991). Low to intermediate pressure range is characteristic of the Cretaceous metamorphism. The K-Ar dates of the clay fraction illite-muscovite from slates are 96.7 Ma, and from acidic metavolcanoclastics 93-97 Ma (Árkai et al. 1991). The Mesoalpine tectonophases were connected with local, hydrothermal, mostly retrograde alterations.

In the narrowest, NE-terminating part of the terrane, a Late Priabonian–Early Rupelian neutral volcanism occurred at Újhartyán, Bugyi and Sári villages. The latter two localities can presumably be attributed to the southwestern "tail" of the Bükkia C. T. based upon their Upper Permian stratigraphic record (see below).

Bükkia Composite Terrane

Origin of the name: it was proposed by Vörös (1993); it derives from the Bükk Mts, as well as the "Bükkium" of former authors.

Boundaries: the Bükkia Composite Terrane, forming the southernmost unit of the eastern part of the major Pelsonia Composite Terrane, is bound by the Mid-Hungarian (Zagreb – Zemplín) Lineament against the Mecsek Zone, forming the northernmost zone of the large Tisia Terrane. To the east, against the metamorphic Zemplenia Terrane, the boundary, hidden below the Neogene overstep sequence, seems to be represented by the Hernád Line, probably of strike-slip fault character (Balla 1988). Toward the SW and W, however, the terrane boundary (both its location and character) against the Zagorje – Mid-Transdanubia and Bakonyia Terranes is hidden by the Neogene overstep sequence. To the north the boundary against the Aggtelekia Composite Terrane is partly disputable due to the uncertain affiliations of the Szendrő and Uppony units, and partly uncertain, as the prominent Darnó Fault Zone does not represent a real terrane boundary.

Subdivisions: The composite terrane comprises the following units:

Bükk Parautochton Unit (terrane)

Szarvaskő Ophiolite Complex (disrupted terrane)

Darnó Ophiolite Complex (disrupted terrane)

The metamorphosed, strongly folded Bükk Parautochthon represents the lower plate setting, whereas the intimately related two Neotethyan ophiolite complexes (Szarvaskő and Darnó) are obducted nappes. These units are characterised by southern–southwestern (Dinaridic-type) vergencies.

Units of uncertain structural setting are as follows:

Uppony Unit

Szendrő Unit

These two latter units used to be considered as parts of the "Bükkium", but their affiliation, mainly due their opposite (northern) vergencies, have become uncertain now. However, until their structural relationships are cleared, they will be discussed within this grouping.

1. Bükk Parautochthon Unit (terrane)

Variscan evolution

Sedimentary and magmatic evolution

The oldest known formation of the Bükk Parautochthon (hereafter Bükk PA) is the Middle Carboniferous, flysch-type Szilvásvárad Fm., which both in its facies and pre-metamorphic mineral composition (Árkai 1983) seems to be a partial equivalent of the Szendrő Phyllite of the Szendrő Unit. It is followed by Late Moscowian–Gzhelian fossiliferous limestone and siliciclastics of shallow marine molasse type (Málprogram Fm., corresponding to the Auernig Group of the Carnic Alps; Ebner et al. 1991), with no visible sign of unconformity. The Lower Permian seems to be missing (a probable hiatus); (Filipović et al. 1998).

Tectonometamorphic evolution

Neither Variscan metamorphism nor deformation could be proved up to now in the Bükk PA unit (Árkai 1983; Árkai et al. 1995). Geologic map relationships between the flysch-type Szilvásvárad Formation and the Auernig-type Mályinka Formations (Fülöp 1994, map III: Pelikán, pers. comm.) suggest that, if there was any deformation related to the "Carnic phase" (in the sense of Vai 1975), it did not involve intense thrusting and folding. On the other hand, the Lower Permian seems to be primarily missing, possibly due to a local uplift.

Alpine evolution

Sedimentary and magmatic evolution

The Alpine (Neotethyan) sedimentary cycle started in the Middle Permian, with coastal plain (whitish–greenish, then red-brown sandstones), then sabkha (evaporites) deposits. By the Late Permian shallow marine conditions came into existence, with fossiliferous black limestone ("Bellerophonkalk"). Shallow marine mixed carbonate–siliciclastic sedimentation continued in the Early Triassic on a ramp environment, with a thick (~120 m) oolite horizon at the base. The cessation of the siliciclastic input by the end of the Early Triassic led to the formation of dolomite on the ramp during the Anisian. Dolomite conglomerates with red terrestrial matrix above the dolomite succession indicate local uplift and erosion. A first, island-arc (Szoldán 1990; Kubovics et al. 1990) or early rift-type (Harangi et al. 1996) volcanic event occurred in the Early Ladinian, resulting in 200–300 m-thick andesite lava and pyroclastics. Facies differentiation related to extension began in the Late Ladinian/Early Carnian with the establishment of carbonate platforms and intraplatform basins (the latter is represented by grey, cherty limestone). This regime, with step-by-step drowning of the platforms (Velledits 1998), persisted until the end of the Triassic. A second volcanic event with within-plate type basalts occurred in the basin environments in Late

Ladinian – Early Carnian (Szoldán, op. cit.; Kubovics et al., op. cit.; Harangi et al., op. cit.) The presence of the formerly supposed Middle Carnian siliciclastic "Raibl" event is now highly questionable due to lack of relevant biostratigraphic data (Less, pers. comm.; Velledits 1998).

Biostratigraphic constraints for Early Jurassic to early Middle Jurassic sedimentation are missing at this time; this interval might be partly represented by varicoloured basinal limestones. Bathonian–Callovian varicoloured radiolarites (Dosztály 1994) uniformly cover all older platform and basinal formations (Csontos et al. 1991). Where they occur on the top of platforms, they indicate long hiatus and abrupt subsidence.

Distal, flysch-type, dark grey shales/slates represents the Late Jurassic "Eohellenic flysch stage", with Callovian–Oxfordian black radiolarites and radiolarite breccias in the lowermost part of the formation.

Tectonometamorphic evolution

The Bükk PA was effected by an Eohellenic regional dynamothermal metamorphism (160–120 Ma; although the meaning of the older ages from it is under discussion), the average thermobarometric data of which shows ~350 °C temperature and ~3 Kbar pressure (Árkai 1983; Árkai et al. 1995). However, its intensity, depending on the structural position, is uneven; in parts just exceeding the boundary of diagenesis and metamorphism, in others reaching the epizone, with pressure up to 5 Kbar (Árkai, op. cit.). Contemporaneously with this metamorphic event, km-scale, southward recumbent F_1 folds formed with intense S_2 axial plane foliation (Csontos 1988). Stretching lineation is mostly subparallel to these major F_1 folds axes. F_2 folds – with various fold axis orientations – further deform the first-order F_1 structures (Csontos, op. cit. and 1999; Pelikán, pers. comm.).

A Late Cretaceous (85–95 Ma) metamorphic event can be recognised in the eastern part of the Bükk Mts, which is considered to have been linked with NW–SE trending dextral strike-slip faulting (Csontos 1988; Árkai et al. 1995). In this part of the mountains well-developed mylonites with shear-band structures on steeply dipping F_1 fold limbs were observed (Koroknai, pers. comm.). Arching of previous structures is probably linked to the same event (Csontos, op. cit.).

Upper Eocene limestone at the base of the Tertiary overstep sequence post-dates all metamorphic and ductile deformational events.

2. Szarvaskő Ophiolite Complex (disrupted terrane)

The Szarvaskő Ophiolite Complex is made of by the olistostromal Mónosbél Unit in a lower position and by the Szarvaskő Unit in a higher one, consisting predominantly of mafic magmatic rocks, shale and sandstone (Balla et al. 1983; Csontos 1988; Gulácsy, unpubl. map).

Alpine evolution

Sedimentary and magmatic evolution

The oldest known formation of the Szarvaskő Unit consists of sandstone and shale of probably late Liassic or early Dogger age. In the higher part of the shale sequence, with some black radiolarite, mafic intrusive rocks (gabbro, dolerite) and extrusive rocks (pillow lava) are associated with the sediments. K-Ar ages (~165 Ma on amphiboles, ~166 Ma on whole rocks in average; Árva-Sós et al. 1987; Dosztály and Józsa 1992) point to a Middle Jurassic age of the magmatic rocks, while the radiolarite yielded Bathonian–Callovian radiolarians (Dosztály and Józsa, op. cit.). Geochemical analysis indicates MORB-type character of the magmatic suite, whereas the Ikeda discrimination diagramme points to a back-arc setting (Downes et al. 1990; Harangi et al. 1996).

The *Mónosbél Unit* is built up by a several hundred metre-thick olistostromal complex, with interfingering allodapic ooidal and bioclastic limestone. The ooidal limestone contains the characteristic Middle to Late Jurassic foraminifer species *Protopeneroplis striata* (Bérczi-Makk and Pelikán 1984), whereas the associated black chert yielded Callovian–Oxfordian radiolarians (Dosztály 1994). The olistostromes include, beside slide-blocks of the above-mentioned allodapic limestone, olistoliths of sandstone, radiolarite of Triassic (Ladinian–Carnian) and of Jurassic (Bathonian–Oxfordian) age, rarely also basalt and Triassic limestone (Csontos et al. 1991; Dosztály and Józsa 1992).

Tectonometamorphic evolution

The Szarvaskő Ophiolite Complex can be interpreted as a remnant of a marginal basin, opening up behind an intraoceanic subduction zone (Balla et al. 1984; Harangi et al. 1996; Koller and Aigner-Torres 1999; Csontos 1999). The closure of the basin took place in the Late Jurassic, probably in the Kimmeridgian, and the complex was obducted, as transport directions show, from NW to SE (according to present co-ordinates) onto the Bükk Parautochthon (Csontos 1999), e.g. during the Eohellenic tectogenesis. A low-temperature anchizonal regional metamorphism (Sadek et al. 1996) that followed an intensive ocean-floor hydrothermal metamorphism could be related to this event; however, K-Ar data on white micas show a rather large time range (160 to 120 Ma; Árkai et al. 1995).

3. Darnó Ophiolite Complex (disrupted terrane)

The Darnó Ophiolite Complex is not confined within the Darnó Fault Zone but is thrust onto the NW part of the Szarvaskő Ophiolite Complex in the westernmost part of the Bükk Mts. (Gulácsy, unpubl. mapping) and its sedimentary complex has been encountered by numerous boreholes NW of the Darnó Line s.s. in the Recsk ore area (Zelenka et al. 1983). Within the Darnó Zone it is known from wells in an approximately 90 km long zone from the southwestern margin of the Uppony Hills to Tóalmás, SW of Mátra Mts.

Alpine evolution

Sedimentary and magmatic evolution

As shown by the ongoing new documentation and reassessment of the type wells (Rm-131, -135 and -136) drilled in the Darnó Hill type area (cf. Józsa et al. 1996), the complex consists of two units:

– An upper, magmatic complex of MOR-type pillow and massive basalt (in thickness of up to a few hundreds of metres), with intercalated/imbricated abyssal sediments (in a few m to a few tens of m thickness). The sediments are represented by red radiolarite (yielding alternatively Triassic and Jurassic radiolarians; Dosztály and Józsa 1992; Dosztály 1994), red mudstone and bluish-grey siliceous shale (the latter two only with Jurassic radiolarians; Dosztály, op. cit.). Intrusive rocks (gabbro, microgabbro) are also associated. K-Ar ages on amphiboles and whole rocks show an average value of ~170 Ma (Árva-Sós, in Dosztály and Józsa 1992).

– A lower, proximal toe-of-slope sedimentary complex, showing all transitions between slumping – debris flow – turbidite. Sediments derive mainly from two source areas: a marly-calcareous one (grey, marly limestone and marl) and a pelitic one (dark grey to black shale, bluish-grey siliceous shale). Occasionally debris flows ("micro-olistostromes") deriving from a third source area (indicated by cm to dm-size, grey micaceous sandstone clasts already transported in lithified stage) are also associated. As slide blocks (olistothrymmata) reddish limestone with red chert (containing Ladinian–Carnian radiolarians; Dosztály 1994), resembling the Bódvalenke Limestone of the Bódva Nappe but also associated with amygdaloidal basalts, as well as marine Permian rocks (corresponding to the Szentlélek Formation and Nagyvisnyó Limestone of the Bükk PA) occur.

As deep-water sedimentary rocks NW of the Darnó Fault, in the Recsk ore area, do not seem to represent a different terrane, it can be supposed, that the upper magmatic complex has been eroded there. Serpentinite pebbles in the Miocene Darnó Conglomerate suggest the existence of an uppermost ultrabasic nappe, completely eroded since that time (Sztanó and Józsa 1995).

Upper Eocene andesite in the Recsk area and related granodioritic intrusives (Varga et al. 1976) may be regarded as the northeastern most representatives of the Periadriatic magmatic chain.

Tectonometamorphic evolution

According to present knowledge the Darnó Ophiolite Complex may represent a setting related to initial opening of a Middle Triassic oceanic branch. However, the main oceanisation took place in the Jurassic, behind an intraoceanic subduction zone, as indicated by the presence of ophiolite and arc-related magmatic detritus (B.-Árgyelán and Gulácsy 1997) in the sandstone clasts (olistoliths). The upper magmatic/abyssal sediment complex can be interpreted as a typical accretionary prism and the lower one as a (proximal) trench complex.

Magmatic rocks of the Darnó Ophiolite Complex underwent only ocean floor hydrothermal metamorphism (Árkai 1983; Sadek et al. 1996). On the other hand, K-Ar data around 115 Ma indicate some thermal event in the Middle Cretaceous (Dosztály and Józsa 1992).

The overthrust of the Darnó Ophiolite Complex onto the Szarvaskő one may be related to the emplacement of the latter onto the Bükk PA Unit (Gulácsy, pers. comm.).

Units of uncertain affiliation

Up to the latest years, the Szendrő and Uppony Units had been considered unambiguously by Hungarian geologists as integral constituents of the "Bükkium Unit" (c.f. Árkai 1983) or "Bükkium Terrane" (Kovács et al. 1996/97), especially in the case of the close facial links between the Middle Carboniferous flysch-type Szendrő Phyllite and Szilvásvárad Formations, and disregarding their opposite vergencies. The latest results on their metamorphic evolution (Árkai et al. 1995) and re-consideration of their structural orientation, however, cast doubts on this assignment. Indeed, the Bükk Parautochthon Unit and the related Szarvaskő and Darnó Ophiolite Complexes with their southerly (e.g. southeastern in their present setting, following considerable Tertiary rotations; c.f. Balla 1988a) vergency and unambiguous Dinaric-type development represent Dinaridic elements, whereas the Szendrő and Uppony Units with their northern vergency represent Upper Austroalpine structural settings (c.f. Ebner et al. 1998). As detailed structural studies are still in progress (Koroknai, unpubl.), these two units are described herein in connection with the Bükkia Composite Terrane as "sub-terranes" (indicating their facial links but different structural characteristics), leaving open the possibility to consider them in the future as separate terranes.

4. Uppony Unit

The Uppony Unit is made up of a metamorphosed Palaeozoic series, which is unconformably covered by Upper Cretaceous clastics. The unit is enclosed by the transpressional Darnó Fault Zone. It is divided into two subunits by the Lipóc Fault: the Tapolcsány and Lázbérc Subunits.

Variscan evolution

Sedimentary and magmatic evolution

Tapolcsány Subunit: it is made up quartzite, greywacke (on East Alpine analogies assigned to the base of the Variscan sedimentary cycle, e.g. to the Upper Ordovician) and a several hundred metre-thick, euxinic basinal slate–siliceous slate–lydite sequence (comparable to the Bischofalm Facies of Silurian to Early Carboniferous age in the Carnic Alps – Ebner et al. 1998). The latter includes a Devonian (post-Lochkovian) metabasalt and schalstein horizon of tholeitic composition, within which a volcanic olistostrome occurs with Wenlockian to Lochkovian limestone olistoliths. Another olistostrome with marly–silty matrix, within which Emsian to lower Famennian pelagic limestone olistoliths are found, probably represents the youngest part of the sequence, and therefore already assigned to the flysch stage.

Lázbérc Subunit: it consists of Givetian(?) – Frasnian platform carbonates and pelagic, metatuffitic limestone ("cipollino", Abod Limestone) ranging in age from late Givetian to the Devonian/Carboniferous boundary. The latter contains metabasalt and schalstein bodies of tholeiitic composition. Condensed, thin Tournaisian to Lower Visean flaser limestone (without metatuffitic influence) is followed by an Upper Visean–Lower Baskhirian basinal limestone and shale sequence (Lázbérc Formation; normal alternation without signs of re-sedimentation). Sandy limestone with sandstone and with quartz and lydite pebbles (resembling those of the Mályinka Fm. of Bükk PA) may already represent the Late Carboniferous marine molasse stage.

Tectonometamorphic evolution

No evidence for Variscan metamorphism and deformation exists (Árkai 1983; Árkai et al. 1995).

Alpine evolution

Sedimentary and magmatic evolution

No formations of the Alpine sedimentary cycle older than Late Cretaceous have been preserved. The southerly Tapolcsány Subunit is transgressively covered by Upper Cretaceous (Senonian) post-tectonic, Gosau-type conglomerate. The composition of this conglomerate and that of Lower Miocene one indicate a close relationship with the Mesozoic of the Bódva Nappe of the Rudabánya Mts. On the other hand, there are no common elements with the Lower Miocene conglomerate covering the northern part of the Bükk PA Unit, suggesting that the two units were not juxtaposed before the Middle Miocene (Clifton et al. 1984; Kovács 1992; Pelikán, pers. comm.).

Tectonometamorphic evolution

The Variscan sequences of the unit underwent a Middle Cretaceous anchizonal/epizonal regional dynamothermal metamorphism of 2.5 Kb pressure and 300 °C temperature (Árkai 1983), as indicated by the average K-Ar age data on illites–muscovites (118±14 Ma; Árkai et al. 1995). Ductile deformation attributable to this event resulted in mesoscale to microscale folding with S_1 foliation, which was followed by a subsequent NNW-ward thrusting (Koroknai, unpubl.). The unit is entirely enclosed within the Darnó transpressional zone of Early Miocene age; strike-slip faulting related to this zone was a third deformational event affecting both subunits.

5. Szendrő Unit

Variscan evolution

Sedimentary and magmatic evolution

Abod Subunit: It is made up of (Silurian? –) Lower Devonian euxinic basinal graphitic phyllite, siliceous slate, calcareous phyllite and metasandstone (Irota Fm.), followed by a Middle Devonian limestone–phyllite–metasandstone sequence with coral bioherms (Szendrőlád Limestone) representing a shelf environment with mixed carbonate–siliciclastic sedimentation. Ranging up into the Frasnian, it develops, on the one hand, with transition into a basinal facies with volcanic influence (metatuffitic, "cipollino"-type Abod Limestone, ranging into the Famennian as well), and on the other into a marble of carbonate platform facies.

Rakaca Subunit: It consists of Givetian (?) – Frasnian banded marble of carbonate platform facies and is either overlain by the pelagic Abod Limestone or, with a major hiatus (sediments preserved only in fissure fillings), by thin Upper Visean basinal limestone, or immediately by the Szendrő Phyllite. Carbonate sedimentation resumed in the Late Visean to Early Bashkirian, in form of patch reefs also represented by banded marble, passing laterally into dark basinal limestone, which in turn passes upward into the Szendrő Phyllite of flysch-type (with olistostromes and sandy turbidites).

Tectonometamorphic evolution

No evidence for Variscan metamorphism and deformation has been encountered (Árkai 1983; Árkai et al. 1995).

Alpine evolution

Sedimentary and magmatic evolution

No formations of the Alpine sedimentary cycle have been preserved.

Tectonometamorphic evolution

Variscan formations of the unit were affected by a Middle Cretaceous (108±8 Ma as shown by average K-Ar age data on illites–muscovites; Árkai et al. 1995) epizonal regional dynamothermal metamorphism with 3 Kb pressure and 400 °C temperature (but in some places in the southerly Abod Sub-unit reaching even the biotite isograde, 450 °C; Árkai 1983). Ductile deformation attributable to this event resulted in mesoscale to microscale folding with S_2 foliation, which was followed by NNW-ward thrusting (Koroknai unpubl.).

Aggtelekia Composite Terrane

Origin of the name: it derives from the Aggtelek Mts, referring to the name "Aggtelek – Rudabánya units" of Fülöp et al. (1987) and Brezsnyánszky and Haas (1986).

The terminology applied here is different from that of Kovács et al. (1996/97) because of the chaotic usage of the major tectofacial terms "Silicicum" and "Tornaicum". These are the interpretation and extent of the enlarged "Mega-Silicicum" and "Mega-Tornaicum" of various authors, entirely different from their original sense, as they had been introduced by Kozur and Mock (1973) and Less (1981) in Grill et al. (1984). The same is true for the "Meliata Series", from which the term "Meliaticum", or "Meliata Unit" term derives; various rock assemblages were and are still assigned to this unit. Just as with the well-studied section at the village of Meliata (for the latest description see Kozur et al. 1997, Mock et al. 1998), which lacks ophiolites, it does not define any ophiolite complex either to the N of the Slovak Karst or in the territory of NE Hungary. Therefore, in the present review, to avoid further confusion due to the usage of differently interpreted names, the clearly defined second-order terms by Grill et al. (1984), Less et al. (1987) and Grill (1989) are used, strictly limited to the territory of the Aggtelek–Rudabánya Mts. and to that of Hungary.

Boundaries: both the southern and northern extensions of this composite terrane are disputed, because of uncertainties mentioned at the discussion of the Bükkia Composite Terrane. Toward the east, south and west it dives beneath the Late Oligocene–Early Miocene overstep sequence; however, it certainly does not extend over the Hernád Fault in the east, or possibly it is bounded by the southeastern boundary fault of the Darnó Fault Zone. It certainly does not extend over the junction of the Diósjenő and Lubeník Faults in the west.

Units of the Aggtelekia Terrane are detached from their Variscan basement or represent disrupted oceanic terrane (e.g. the Tornakápolna Terrane).

1. Aggtelek–Bódva nappes (terrane)

Origin of the name: after the Aggtelek and Bódva tectofacies units of Grill et al. (1984), also including the smaller Derenk and Szőlősardó units.

Alpine evolution

Sedimentary and magmatic evolution

The Alpine (Neotethyan) evolutionary cycle began with an Upper Permian sabkha facies (evaporitic sequence). Locally, however, continental redbeds preceding the sabkha stage have also been preserved (Vozárová and Vozár, pers. comm.). Due to the further progression of the Neotethyan transgression a shallow marine ramp environment was formed, first with siliciclastic, then with mixed carbonate-siliciclastic sedimentation ("Werfen megafacies"; Hips 1995). Siliciclastic input ceased by the beginning of the Middle Triassic and a carbonate ramp came into existence, first with euxinic lagoonal (Gutenstein Fm.), then with open lagoonal (Steinalm Fm.) sedimentation.

A drastic change commenced from the Middle Anisian onward, when the initiation of rifting resulted in the disruption of the former uniform carbonate ramp and in a well-expressed facies differentiation. It shows a rapid break-down of the continental margin (at least of the margin of a microcontinent) and subsidence of its blocks to different depths, with a southward-facing rimmed platform margin on the north (Alsóhegy; Kovács 1979; Bérczi-Makk 1996) and a deep basin on the south (Bódva Unit; Grill et al. 1984).

In the eupelagic basin of the Bódva Unit mostly reddish coloured limestone with red chert (Bódvalenke Limestone; Kovács et al. 1989), locally passing into radiolarite, was deposited until the Late Carnian, partly with a few metres-thick horizon of red or brownish grey shale in the Middle Carnian. In the Norian red Hallstatt limestone was deposited, with frequent resedimentation phenomena. The closely related, minor Szőlősardó Unit represented a slope setting until the early Late Carnian, when the Aggtelek Unit (representing up to this time a shelf margin setting – Ladinian–Carnian Wetterstein Fm.) subsided and pelagic Hallstatt limestone was deposited on it. The Derenk Unit, overthrust from the North by the Alsóhegy carbonate platform, is characterised by a peculiar, brecciated Hallstatt Limestone (Derenk Limestone) in the Lower Ladinian to Upper Carnian, without siliciclastics in the Middle Carnian, then by similar Hallstatt and Pötschen limestone as the Aggtelek Unit.

Jurassic formations are known only in the Bódva Unit (Grill 1988). The Telekesvölgy Complex (with tectonic contact, however, to the underlying Triassic) is composed of variegated marl, spotty marl and black, radiolarian-spiculitic, siliceous claystone with Bajocian – Bathonian radiolarians (Dosztály 1994). The Telekesoldal Complex, with sedimentary contact to the Triassic, consists of a claystone-siliceous marl series (with Bathonian radiolarians; Dosztály, op. cit.) and an olistostromal one. Rhyolite, considered to represent a magmatic arc (Kubovics et al.1990; Harangi et al. 1996) is related to this complex.

Tectonometamorphic evolution

Rocks of all the units of the Aggtelek–Bódva nappes remained in the diagenetic zone, i.e. they were not affected by temperature higher than 200 °C. The only exception was encountered in the vicinity of Telekesoldal in the Bódva Unit, which was affected by low temperature anchizonal metamorphism (Árkai and Kovács 1986).

These units from the southern slope of Alsóhegy to the south show southward imbrication. Southward recumbent mesoscale folds occur in the Rudabánya Mts. The age of the movements resulting in this structure is unknown as yet, but it is certainly older than the Early Miocene strike-slip faulting along the Darnó Zone, which cuts them at an angle.

2. Tornakápolna Unit (= Bódva Valley Ophiolite Complex – disrupted terrane)

Origin of the name: after the "Tornakápolna Facies" of Grill et al. (1984); Kovács 1997; Less 1997), applying exclusively to the subsurface ophiolite bodies found in the Bódvavölgy and Galyaság area of the Aggtelek Karst region (Bódvavölgy Ophiolite Formation in Kovács et al. 1989).

Boundaries: the Tornakápolna Terrane represents a typical disrupted terrane formed of ophiolite bodies/slices (serpentinite, gabbro, pillow and massive basalt, subordinately deep-water sedimentary rocks) imbricated into the sole thrust of the Aggtelek Unit.

Alpine evolution

Sedimentary and magmatic evolution

Available age data suggest that the MOR-type magmatic rocks (Réti 1985; Harangi et al. 1996) of the Bódvavölgy Ophiolite Complex are related to a Triassic ocean opening. K-Ar ages on amphiboles from gabbro indicate a Middle Triassic age (233 Ma; Árva-Sós et al. 1987; Dosztály and Józsa 1992).

Sediments of the complex are known only from two horizons of the Tornakápolna-3 borehole. Between 565–569 m a red mudstone–red radiolarite horizon occurs, in sedimentary contact with the pillow basalt and with Middle Triassic (Ladinian) radiolarians (for latest review see Dosztály and Józsa, op. cit.). Between 319–332 m, dark grey to black siliceous shale and sandstone occur between two serpentinite slices. Based on lithological similarities to some parts of the Darnó Complex they are also considered as Jurassic.

Tectonometamorphic evolution

Latest studies on the gabbro (Horváth 1997) indicate that these ophiolite slices underwent two medium-pressure metamorphic events before they had been imbricated into their present non-metamorphic environment at the sole thrust of the Aggtelek Unit. During the first, subduction-related event epidote-blueschist facies conditions were reached, with ~7 Kbar pressure and ~300–350 °C temperature. This was followed by a greenschist facies overprint, with ~4–5 Kbar pressure and ~300 °C temperature. The first event, based on analogies from Slovakia (Faryad, in Horváth, op. cit.) is thought to have taken place during the Late Jurassic, and the second one during the Middle Cretaceous (Horváth, op. cit.). Nevertheless, it should be noted, that these medium-pressure events are not proven in the associated deep water sedimentary rocks.

3. *Martonyi Unit (terrane)*

Origin of the name: Grill (1989) used the name "Martonyi Unit" for the metamorphosed part of Rudabánya Mts.

Boundaries: the actual bounding lines of the unit are the same as those of the Rudabánya Mts: the northwestern, resp. southeastern bounding faults of the Darnó Zone of Early Miocene age. Within these two bounding elements, the metamorphosed units are limited by thrusts, which are evidently younger than the metamorphism, as shown by the section of the Hidvégardó-3 well, which revealed an inverse setting of the metamorphosed unit above a non-metamorphosed, but strongly sheared melange (see below). The unit is detached from its pre-Alpine basement.

Alpine evolution

Sedimentary and magmatic evolution

The oldest known formations are Anisian Gutenstein Dolomite and Steinalm Limestone of carbonate ramp environment. Basinal sedimentation began in the Middle Anisian, when the ramp subsided, and is represented mostly by grey limestone (Szentjánoshegy Limestone; Kovács et al. 1989), without resedimentation phenomena. Monotonous black slate represents the Middle Carnian "Raibl" event. During the Late Carnian and Norian cherty limestone (mostly grey Pötschen Limestone) was deposited. Jurassic formations have not been proven so far.

The only sign of volcanic activity is known in the higher part of the Steinalm Limestone of Esztramos Hill, by some traces of rhyolitic volcanism (Turtegin and Pelikán, unpubl.).

Tectonometamorphic evolution

Rocks of the Martonyi Unit underwent medium-pressure metamorphism of high temperature anchizonal to low-temperature greenschist facies conditions (~7 Kbar, ~300–350 °C; Árkai, in Árkai and Kovács 1986). Tight to isoclinal, upright metre-scale folds, characterising especially the Pötschen Limestone, are thought to be related to this metamorphic event. The Martonyi Unit can be interpreted as occupying a lower plate position during the Late Jurassic subduction. However, only two K-Ar data are known from Carnian slate, which point to a younger event: 129 and 115 Ma, respectively (Balogh et al. 1991). Detailed structural investigations are is progress (Fodor and Koroknai, in prep.).

The Martonyi Unit in its Becskeháza partial nappe (Less 1997) exhibits fine evidence of transported metamorphism in the section of well Hidvégardó-3, where an overturned, horizontally-lying metamorphic sequence is thrust over non-metamorphic tectonic melange (Árkai, in Árkai and Kovács 1986, Fig. 6). This thrust is evidently younger than the above-mentioned metamorphic events.

Tisia Composite Terrane

Origin of the name: this name was introduced to Hungarian earth sciences by Prinz (1914, 1926), who visualised an old "median mass" localised in the place of the later Pannonian Basin, surrounded by Carpathians, Eastern Alps and Dinarides. The Tisia Terrane name derives from Szederkényi (1984). The "Tisia Terrane" as an independent terrane existed from the Late Cretaceous onward (Balla 1986), when its rotation began (or possibly from the late Middle Jurassic?, when it separated from the European margin) to the Early Miocene, and in the territory of Hungary it comprises three large Variscan terranes, covered by a common earliest Alpine (Early Triassic) overstep sequence.

Boundaries: The Tisia Composite Terrane forms the basement of South Hungary, Northeast Croatia, North Serbia and West Transylvania (Romania). It is bounded by the Mid-Hungarian or Zagreb–Zemplín Lineament northwestward, southward by the northern marginal fault of the Sava Depression (Pamic 1998) – Bogojevo–Becej–Lipova Lineament (i.e. the northern border of the Srem–South Backa–Mures Ophiolite Belt), and by the so-called "Somes Lineament" northeastward.

Subdivisions:

The pre-Alpine terranes of Tisia Composite Terrane and units ("sub-terranes") constituting them are as follows (Figs 7, 9, Table II):

- Slavonia-Dravia Terrane
  - Babócsa Unit
  - Baksa Unit
- Kunságia Terrane
  - Mórágy Unit
  - Kőrös Unit
- Békésia Terrane
  - Kelebia Unit
  - Csongrád Unit
  - Battonya Unit
  - Sarkadkeresztúr Unit

In addition to the large terranes listed above, several small units ("outliers" –nappe remnants, tectonic wedges) are also found in the Tisia Composite Terrane(c.f. Fig. 8), which show lithological and metamorphic features totally different from those of the large terranes. They are as follows:

Horváthertelend Unit (terrane)
Szalatnak Unit (terrane)
Ófalu Unit (terrane)
Tázlár Unit (terrane)
Álmosd Unit (terrane)

All these terranes and small "outliers" or "wedges" in the territory of Hungary are covered by a common earliest Alpine overstepping sequence, specifically by the continental redbed-type Jakabhegy Sandstone Formation. The Middle Triassic carbonates (mostly dolomite) show S to N lateral transition (Bleahu et al. 1994). From the early Late Triassic onward a characteristic separation of zones is recorded by the sedimentary successions up to the Early Cretaceous, and although they were thrusted to form nappe zones during the Middle–Late Cretaceous, lateral transition is sometimes recorded. For this reason they do not correspond to the definition of terranes by Keppie and Dallmeyer (see the chapter "Methods"). Consequently, when describing the Alpine evolution, we can speak only about "zones" (Fig. 6), which developed above a part of the European Variscan terrane collage and became detached from there in the Bathonian:

Mecsek Zone (half-graben)
Villány–Bihor Zone (ridge)
Békés–Codru Zone

The "Szolnok Zone" is a Late Cretaceous–Palaeogene flysch zone, which developed above the northeastern part of the Mecsek Zone.

Variscan evolution (general characteristics)

The prevailing rock association of Tisia crystalline rocks is gneiss, micaschist and amphibolite as well as related anatectic granitoids and migmatite, which derived mostly from a psammitic–pelitic type sedimentary sequences (Szederkényi 1984), with several metre-thick mafic lava and/or tuff intercalations. The latter generally show tholeiitic basalt and tuff character (Szederkényi 1983). Based on new geochemical data and discrimination analyses these volcanic rocks represent back-arc basin tholeiite (T-MORB, Tóth M. 1995). In the rock sequences of South Transdanubia and the southern part of the Great Plain some acidic tuff intercalations also occur, showing a presumed continental margin volcanic effect as well.

In the Baksa and Csongrád Units, several metre-thick carbonate (marl, limestone, dolomitic marl, dolomite) interlayers occur in the psammitic-pelitic protoliths. No signs were found for the existence of carbonate layers or lenses in any other units. The age of the protoliths is unknown; supposedly they are Late Proterozoic.

With the exception of not very large sections of the Ófalu and Mórágy Units (Mórágy Hill), all these units are covered by overstep sequences of different ages and they have been encountered in a great number (more than 3,000) of boreholes.

No exact data are available about the existence of pre-Variscan tectonometamorphic events in the Hungarian sector of the Tisia Composite Terrane, but in view of the high level of knowledge about Variscan Europe in general, their existence is rightfully assumed. Proven pre-Mesozoic deformations and metamorphism in the Tisia Composite Terrane (Fig. 10) belong to the Variscan cycle exclusively. Apart from the nappe outliers and tectonic wedges, the metamorphic process may be classed into the following stages (C.f. Szederkényi 1996):

1) High-pressure, relatively low-temperature metamorphism with P=9.5–12 Kb. pressure and 600–560 °C temperature. It was encountered in a few smaller covered occurrences extending along the axis of the Kunságia Terrane (Ravasz-Baranyai 1969; Tóth 1995).

2) Metamorphism characterised by medium-pressure and temperature (Barrow-type) deformation showing P=4–6.5 Kb. pressure and 640–650 °C temperature. This type is predominant in the Kunságia Terrane but could also be detected in the entire area of Tisia Composite Terrane (Szederkényi et al. 1991).

3) Low-pressure and high-temperature metamorphism characterised by P=2–3 Kb. pressure and 680–685 °C temperature is characteristic mainly in the Békésia Terrane, but also occurs in wells at the southern border of the Kunságia Terrane, proceeded by blastomylonitisation. Ages of these metamorphic events: 1) 440–400 Ma Rb/Sr ages by Kovách et al. 1985 (which require further confirmation or rebuttal). 2) 350–330 Ma Rb/Sr ages produced by Svingor and Kovách 1981; Kovách et al. 1985; K/Ar ages measured by Balogh et al. 1983. 3) 330–270 Ma Rb/Sr ages by Svingor and Kovách 1981; Kovách et al. 1985; K/Ar ages by Balogh et al. 1983 (c.f. Fig. 11).

Based on ages, succession of metamorphic events and related deformation characters as well as P-T conditions and existence of special "indicator rocks" (eclogites, blueschists, ultramafics) the following Palaeozoic history may be established in the crystalline rocks of the Hungarian part of the Tisia Terrane (c.f. partly also Árkai et al. 1985; Lelkes-felvári et al. 1996):

1) A conditionally 440–400 Ma-old (Svingor and Kovách 1981) "Caledonian"(?) or rather "Early Variscan" event. Its remnants are preserved in a narrow (5–10 km broad) and poorly explored zone only, located in the axis of Kunságia and Slavonia-Dravia Terranes stretching from Szeghalom (East Hungary) to Görgeteg-Babócsa (South Transdanubia). High-pressure/low-temperature eclogites in the Kőrös area (Szeghalom; Tóth, M. 1995) and SE Transdanubia (Görcsöny; Ravasz-Baranyai 1969) and several obducted serpentinised ultramafic

bodies (Szederkényi 1974; Ghoneim and Szederkényi 1979; Balla 1981), as well as characteristic amphibolite xenolites found in the northern margin of the granite mass of Mórágy Hill (SE Transdanubia), probably indicate a "Caledonian"(?) or rather "Early Variscan" suture.

2) A 350–330 Ma-old (Svingor and Kovách 1981; Kovách et al. 1985; Balogh et al. 1983) Variscan collisional event can be regarded as the culmination of Variscan tectogenesis. During this period the accretion of Variscan Europe took place, including the development of crystalline rock assemblages and related mega-, macro- and microfolding, shearing and blastomylonitisation. Palingenetic granite belts at the axial zones of synclinoria formed during the same period, although the Late Variscan low-pressure and high-temperature effect (late orogenic heating during the 330–270 Ma period) undoubtedly influenced the granitisation as well; also, the younger ages coincide with the ages of Lower Permian rhyolitic volcanism.

3) After the granite genesis, but prior to the Late Carboniferous subsidence, important tectonic events must have taken place. Signs of these events are as follows:

– Nappes of unknown vergency. Remnants of these nappes are the Horváthertelend and Szalatnak outliers.

– A NW–SE striking transcurrent fault bordering the Slavonia–Dravia Terrane eastward,

– Strike-slip faults of ENE–WSW direction (oldest manifestation of the so-called "Mecsekalja Tectonic Belt", as well as the Baja–Tázlár–Túrkeve–Nyírábrány Fracture), which enclose the Ófalu and Tázlár wedges, respectively.

Special characteristics of the individual terranes and units are given below.

Kunságia Terrane

Origin of the name: it is a new name substituting the "Central Hungarian Autochthon" (Szederkényi 1984; Szederkényi et al. 1991) or "Parautochthon Terrane" (Kovács et al. 1996/97; Szederkényi 1996) terms of the previous literature. "Kunság" is the name of a region in the Great Plain, in the underlying basement of which a large part of the terrane is encountered.

Boundaries: the Kunságia Terrane extends over the area located between Middle Hungarian Lineament and Villány–Mecsekalja–Szigetvár fault zone, as well as the northern front of the South Hungarian Nappe Zone (Békésia Terrane). An eastward continuation toward the Apuseni Mts (Romania) can be supposed, but a comprehensive correlation is missing as yet (c.f. Kräutner 1995). In Hungary crystalline rocks of this terrane crop out in the Mecsek Mountains only (west

Fig. 10 →
Variscan metamorphism in Hungary. 1. Very low to low grade; 2. Medium grade; 3. Migmatites, anatectic granites; 4. Occurrences of eclogites

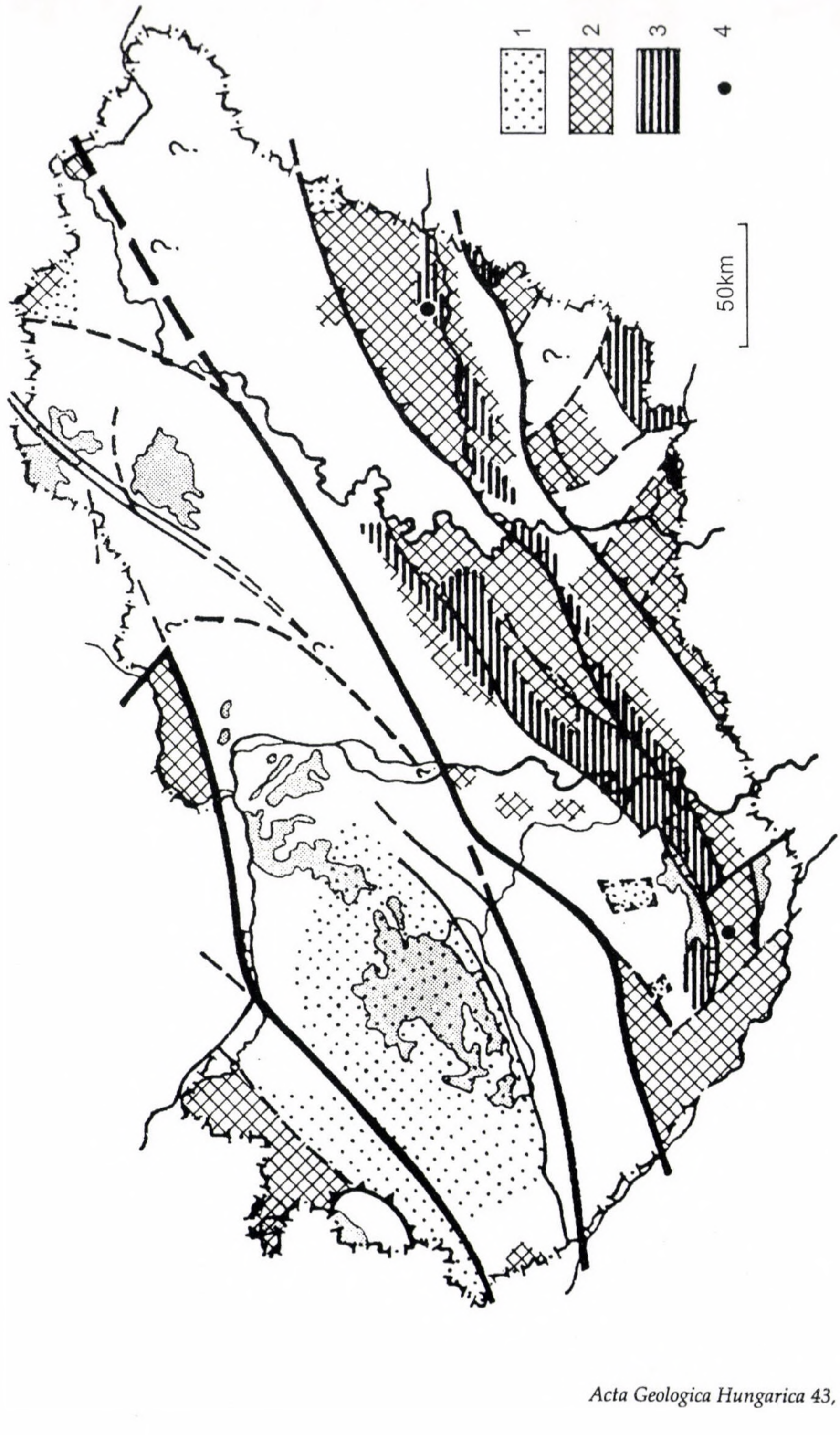
1
2
3
4
50km

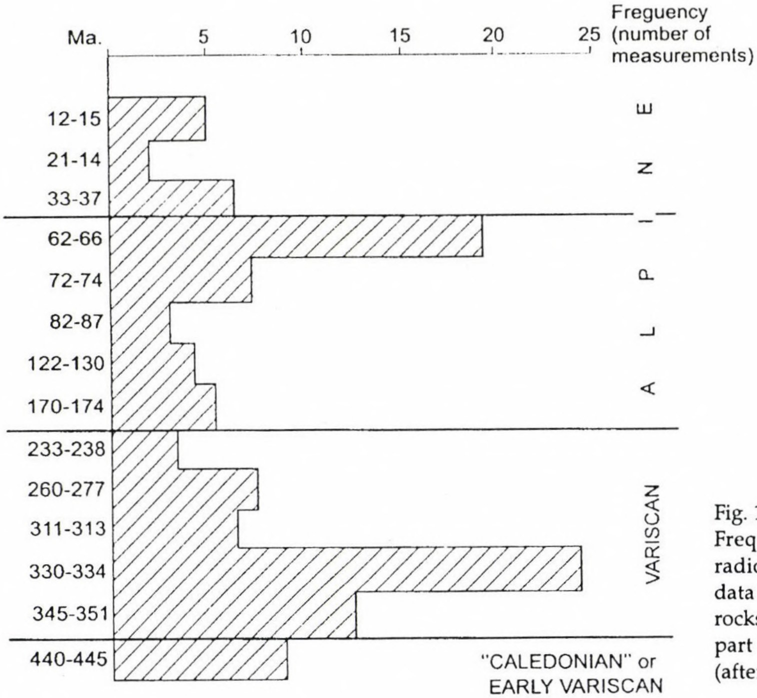

Fig. 11
Frequency diagram of radiometric (K/Ar) age data from metamorphic rocks of the Hungarian part of the Tisia Terrane (after Szederkényi 1996)

Mecsek and Mórágy Hills). "Parautochthonity" of this terrane means that it represents an autochthonous mass in respect to the Békésia Terrane (South Hungarian Nappe Zone); at the same time it shows some not precisely known inner tectonic dislocations.

Sedimentary and magmatic evolution

Basic data on lithology of crystalline rocks of the Kunságia Terrane were presented in the general discussion of the composite terrane. The main difference with the other two terranes is the lack of carbonate rocks. Synsedimentary back-arc basin tholeiite volcanism was also pointed out (Tóth, M. 1995). Lava and tuff are subordinate in the sedimentary sequence; they form smaller lenses interbedded the greywacke-pelite layers. The magmatic rocks show a definite areal distribution; they are located against several smaller sectors located near

Fig. 12 →
Correlation of Variscan granitoids occurring in Hungary and in Central Europe (Buda, 1995; base map after Ellenberger and Tamain 1980, modified). V – Velence Hills (Balaton–Velence crystalline range, Transdanubian Range Unit) ↔ Southern Alps (Periadriatic magmatic range); M – Mórágy (Mecsek–Northern Great Plain Subunit) ↔ Moldanubicum; B – Battonya Subunit (Szeged–Békés–Codru Terrane) ↔ Inner West Carpathians

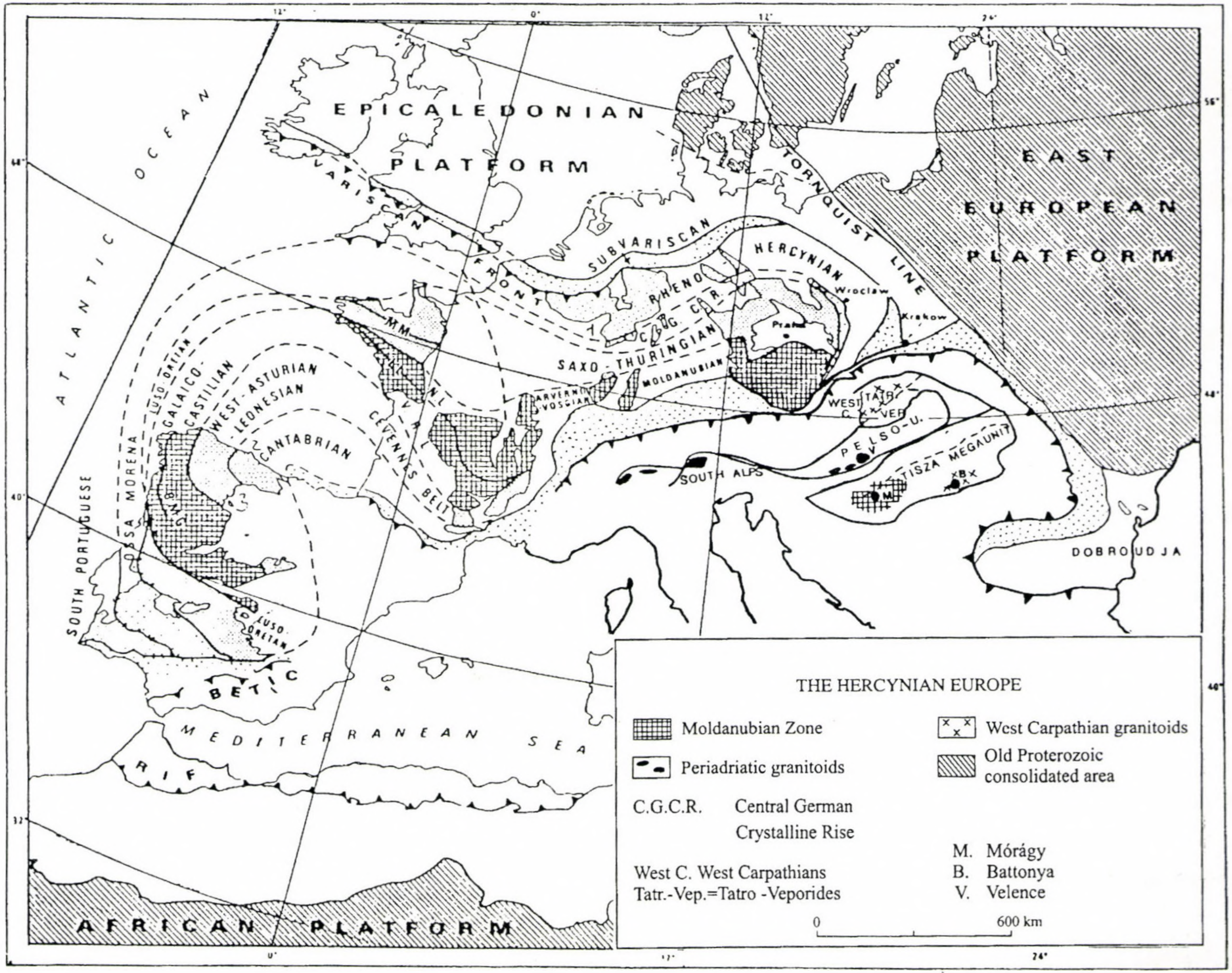
EPICALEDONIAN
PLATFORM
EAST
EUROPEAN
PLATFORM
ATLANTIC
OCEAN
VARISCAN
FRONT
SUBVARISCAN
TORNQUIST
LINE
HERCYNIAN
RHENO
C.G.C.R.
SAXO - THURINGIAN
MOLDANUBIAN
ARVERNO VOSGIAN
MM
CEVENNES BELT
Wroclaw
Krakow
Praha
WEST C.
TATR.
VEP.
PELSO-U.
TISZA MEGAUNIT
SOUTH ALPS
DOBROUDJA
LUSO-ORETIAN
GALAICO-CASTILIAN
WEST-ASTURIAN LEONESIAN
CANTABRIAN
OSSA MORENA
SOUTH PORTUGUESE
LUSO-ORETAN
BETIC
MEDITERRANEAN SEA
RIF
AFRICAN PLATFORM
THE HERCYNIAN EUROPE
Moldanubian Zone
Periadriatic granitoids
C.G.C.R. Central German Crystalline Rise
West C. West Carpathians
Tatr.-Vep.=Tatro -Veporides
West Carpathian granitoids
Old Proterozoic consolidated area
M. Mórágy
B. Battonya
V. Velence
0
600 km

Szeghalom–Szarvas-Szank forming a 5–10 km broad stripe and with a specific high-pressure low-temperature metamorphism.

Tectonometamorphic evolution

The tectonometamorphic evolution of crystalline rocks of the Kunságia Terrane is similar to that described in the general characterisation of the Tisia Terrane. It can be summarised as follows:

– 440–400 Ma-old, high-pressure, low-temperature metamorphism with 9.5–12 Kb pressure and 600–650 °C temperature in supposed outliers or relics of pre-Variscan unit(s).

– 350–330 Ma-old Barrow-type metamorphism and the main granitisation event showing P=4.6–8 Kb pressure and 580–640 °C temperature in all areas of the terrane,

– 330–270 Ma-old low-pressure and high-temperature metamorphism (P=2–3 Kb and 520–685 °C temperature) and subsequent blastomylonitisation in some places at the southern margin of the terrane, as well as completion of the granite magmatism and accompanying Lower Permian rhyolitic volcanism,

– Formation of the Szalatnak and Horváthertelend nappes (outliers) after granite genesis but before Late Carboniferous sedimentation,

– Transcurrent faulting for western delineation of Kunságia Terrane (its age is also pre-Late Carboniferous),

– Generation of two strike-slip faults of ENE–WSW strike, which enclaved the Ófalu and Tázlár Units (terranes) prior to the Late Carboniferous basin formation.

1. Mórágy Unit

Origin of the name: in the earlier literature the name Mecsek–North Plain Unit (e.g. Kovács et al. 1990; Bleahu et al. 1994) was applied. In the present paper a similar name is proposed referring to the Mórágy Complex (Szederkényi 1984; Szederkényi et al. 1991), which constitutes the tectonostratigraphic unit. It forms the pre-Alpine basement of the Alpine Mecsek Zone.

Boundaries: the Mórágy Unit is lithostratigraphically made up of the Mórágy Complex (Szederkényi 1984, 1995). It consists of a granite range (Mórágy–Kecskemét range) accompanied by migmatite–gneiss–micaschist flanks on both sides (c.f. Fig. 10). The most characteristic part of this complex is the granite range itself, represented by S-type granitoids (Buda 1985, 1995).

The granite body forms an approximately 200 km-long and 25–30 km-broad continuous belt, beginning at Szigetvár (South-Transdanubia) and disappearing below the Upper Cretaceous-Palaeogene flysch complex near Szolnok. Its outcrops occur in the Mecsek Mts. (Jantsky 1979).

It is composed of porphyroblastic granite–granodiorite with biotite and/or amphibole-rich xenolites. The latter show 440–400 Ma Rb/Sr ages (Svingor and

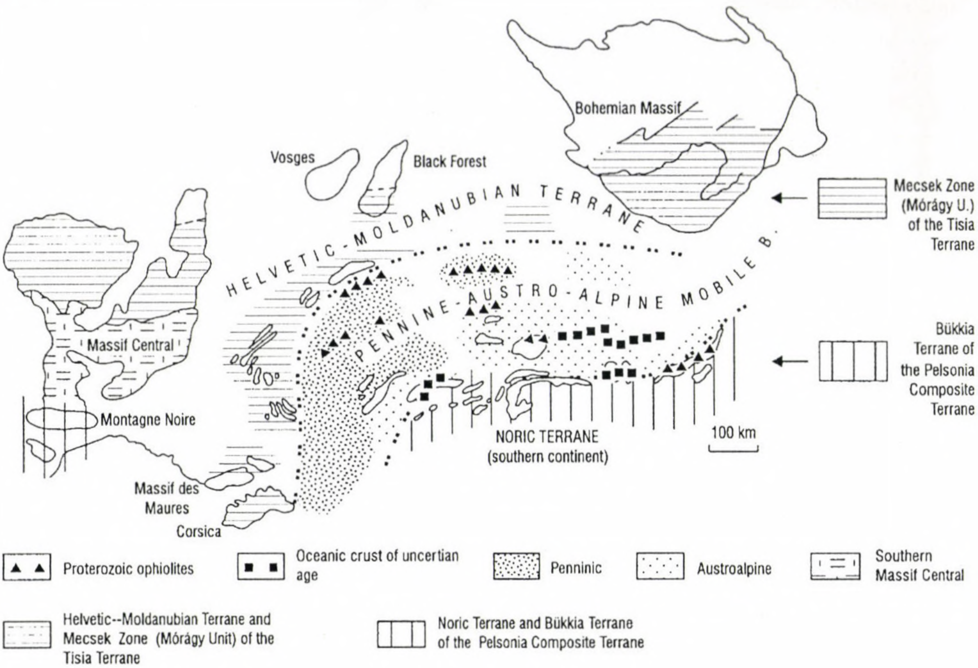

Fig. 13
Setting of the Mecsek Zone of the Tisia Terrane and the Bükkia Terrane in the Variscan European framework (after von Raumer and Neubauer 1993, complemented)

Kovách 1981; Kovách et al. 1985), suggesting a Caledonian/Early Variscan metamorphism, but this assignation requires further confirmation. This granite is a syncollisional, metaluminous, K-rich calc-alkaline one of the monzonitic suite of mixed mantle and crustal origin (Buda 1981, 1985, 1995). The U/Pb age on zircon is 365 Ma, while the K/Ar age on biotite and amphibole is 340–329 Ma (Buda 1995). The rocks are accompanied by crystalline schist showing typical polymetamorphism and forming the limbs of the synclinorium. In the first phase of Variscan metamorphic evolution a Barrow-type event had taken place with P= 6–8 Kb pressure and 580–640 °C temperature (Szederkényi et al. 1991). In the second phase a low-pressure, high-temperature retrogression took place along the Mecsekalja Tectonic Belt and the eastern continuation of the Mecsek Mts (Vajta; Lelkes-Felvári et. al. 1989), producing late kinematic (322 Ma-old) andalusites.

2. *Kőrös Unit*

Origin of the name: in the earlier literature it was named Middle–Plain Unit (Kovács et al. 1990; Kovács et al. 1996/97; Szederkényi 1996). Here a simpler name is proposed, referring to the Kőrös Complex (Szederkényi 1984), which makes up this tectonostratigraphic unit. It forms the pre-Alpine basement of the Alpine "Villány–Bihor" Zone, without the Villány Mts proper (the pre-Alpine basement of which is formed by the Slavonia-Dravia Terrane) and, in the absence of detailed comparative investigations with the surface outcrops in the Apuseni Mts, is understood to apply to the territory of Hungary only.

Boundaries: it is bordered by the Baja–Tázlár–Ebes–Nyírábrány fracture zone to the north and the Békésia Terrane (South Hungarian Nappe Belt) to the south. Its eastern boundary can be found in the Apuseni Mts. (Romania) and the western edge is formed by the Villány–Mecsekalja Fault.

The Kőrös Unit is made up lithostratigraphically of the Kőrös Complex (Szederkényi 1984, 1995). Similarly to the Mórágy Complex, a more than 250 km-long and narrow discontinuous granite range (within a 15–20 km-wide migmatite belt) forms the axial zone of the complex. Within the range five granite bodies, 5–10 km wide and 15–25 km long, occur along the Jánoshalma–Jászszentlászló–Endrőd–Füzesgyarmat–Kőrösszegapáti traverse represented by S- and I-type porphyroblastic biotite granite-granodiorite rocks (Buda 1985, 1995), forming the axis of a synclinorium as well. Similarly to that of Mórágy Complex, this granite-migmatite range is accompanied by medium-grade gneiss–micaschist–amphibolite associations on both flanks of the ENE–WSW striking belt. These crystalline rocks show double-phase progressive metamorphism only (c.f. also Árkai 1987b). Signs of the first uncertain (Caledonian? or earliest Variscan?) phase appear along Szeghalom–Szarvas–Szank–Ófalu–Helesfa traverse in a 5–10 km-broad zone. The second one is a Variscan Barrow-type deformation (medium pressure and temperature conditions and 350–330 Ma Rb/Sr isotope age). The phase marked by appearance of andalusite is missing in the metamorphic history of Kőrös Complex (probably the granite plutonism was less intense in this unit).

3. Wedged-in remnants of older terranes

3a. Szeghalom Amphibolite and Eclogite

In the eastern part of the Kunságia Terrane, in the neighbourhood of Szarvas–Szeghalom, among Barrow-type Variscan metamorphites consisting mainly of amphibolite–amphibole gneiss, older, high-pressure, low and medium-temperature, B or C-type eclogite relics can be found in symplectitised condition (Tóth, M. 1995). Due to a lack of in-depth investigations their tectonic position is unknown; presumably they are in nappe and/or wedge structures, similarly to the other "outliers".

Slavonia–Dravia Terrane

Origin of the name: A joint term for the Dráva Unit of Szederkényi (1984) and the Moslavina–Slavonia Terrane of Pamic et al., introduced according to an agreement with Pamic in 1995.

Boundaries: the Slavonia–Dravia Terrane is located in southeast Transdanubia, extending over the Drava River to Northeast Croatian (i.e. Slavonian) areas southward. It is bordered by the Mid-Hungarian or Zagreb–Zemplín Lineament north-westward and the Villány–Mecsekalja–Szigetvár fracture zone eastward. No outcrops of this terrane are found in Hungarian territory; it crops out in the Papuk and Psunj Mts. (Croatia). A general NW–SE striking of formations is characteristic all over the Slavonia–Dravia Terrane showing unity with the East Croatian crystalline basement.

Sedimentary and magmatic evolution

Characteristics of protoliths of crystalline rocks in the two units of the Slavonia–Dravia Terrane are highly different. The Babócsa Unit metamorphics originated from a simple alternation of greywacke–pelite bands without any carbonate intercalations. Metamorphosed mafic lava and tuffs occur in the metasedimentary sequence only subordinately, in small lenses (T-MORB character; Tóth, M. 1995). On the other hand, the Baksa Unit shows a truly variegated pre-metamorphic rock assemblage, represented mainly by a greywacke-pelite series punctuated by well-developed carbonate members and accompanying thick, T-MORB tholeiite lava intercalations. Limestone, dolomite, marl, dolomitic marl alternating with sandstone–claystone and tholeiitic lava bands form 50–250 m thick members in the monotonous greywacke–pelite mass. Due to the medium and high-grade metamorphism these rocks altered into marble, dolomitic marble and peculiar calc-silicate and amphibolite rocks.

The significant difference existing between the units of the Slavonia–Dravia Terrane would suggest that the Baksa Unit might belong to another terrane (e.g. to the Békésia Terrane). However, a lack of relevant data does not permit solving this problem for the time being.

Tectonometamorphic evolution

The tectonometamorphic characters of crystalline rocks of Slavonia-Dravia Terrane show a slight difference to that of Kunságia Terrane. This difference is manifested primarily in the lack of ultramafic bodies in the crystalline mass of the Kunságia Terrane. The main pre-Late Carboniferous tectonometamorphic events were as follows:

– Formation of eclogites (Görcsöny Eclogite Formation) by Pre-Variscan (Caledonian?) or Early Variscan events (Ravasz-Baranyai 1969);

– Tectonic wedging of obducted serpentinites (Gyód Serpentinite Formation) into the pre-Variscan basement at the beginning of Variscan history;

– 350–330 Ma-old Barrow-type metamorphic event producing undisturbed isogrades and mineral belts up to the sillimanite zone;
– 330–270 Ma-old low-pressure and high temperature metamorphic event at the northern margin of Baksa Unit.

1. Babócsa Unit

Origin of the name: from the Babócsa Complex as a lithostratigraphic unit (Szederkényi 1984, 1996).

Boundaries: it is bordered by the Mid-Hungarian Lineament northwestward and a NW–SE striking transcurrent fault against the Kunságia Terrane, as well as the fault bordering the Villány Mts. westward. It extends southward into Croatian territory. The aerial extension in the Hungarian side exceeds 1,000 km^2.

The Babócsa Unit consists mostly of medium-grade gneiss with subordinate micaschist and amphibolite intercalations, the latter being mylonitised. Apart from an uncertain "Caledonian" datum (Jantsky 1979) two Variscan metamorphic phases were recognised. The first one is represented by a Barrow-type deformation with P=5–10.3 Kb pressure and 540–685 °C temperature, the second one is andalusitic and formed under P=2–3.5 Kb and T=520–600 °C circumstances (Török 1989, 1990).

2. Baksa Unit

Origin of the name: from the Baksa Complex (Szederkényi 1984, 1996).

Boundaries: it forms the crystalline basement of Villány Mts and its northern foreland up to the Mecsek Mts. Its southwestern border is the fault zone (transcurrent fault) between the Kunságia and Slavonia–Dravia Terranes (Kassai 1977).

Petrographically the Baksa Unit consists of a weakly-folded migmatite gneiss–mica schist–marble–dolomitic marble–calc-silicate gneiss association, characterised by a remarkable isograde system showing zones and isogrades from chlorite up to sillimanite, with a southwest progressivity trend (Szederkényi 1976).

The thickness of this complex exceeds 10 km. Two marble and dolomitic marble members, 250 and 25 m thick, are characteristic of the sillimanite zone, accompanied by fairly thick (23–30 m) amphibolite beds. Near the village of Gyód, an obducted (Balla 1983) and partly serpentinised ultramafic body is wedged into this complex (Gyód Serpentinite Formation). North of this body a single eclogite (now symplectite) occurrence (Ravasz-Baranyai 1969) as well as a characteristic high-temperature overprinting with andalusite, were found (Lelkes-Felvári and Sassi 1981), showing at least three phases of polymetamorphism (Árkai 1984).

3. Wedged-in remnants of older terranes

3a. Gyód Serpentinite

Two occurrences of the Gyód Serpentinite (5–6 km long and 600–700 m wide) are known, which are regarded as two lithostratigraphic members: 1) the Helesfa Member consists of a serpentinite and talc-schist assemblage forming a nearly vertical lens-like body wedged into the Variscan granite at the northern border of the Baksa Unit along broad shearing zones, which are filled by talc-rich metamorphics penetrated by numerous metasomatised aplite dikes, not only in the shearing zones but in the serpentinite body as well. This body consists of sheared and completely serpentinised harzburgite showing diapiric structure (Szederkényi 1974, 1977). 2) The Gyód Member is a vertical ultramafic rock body near the northern margin of the Baksa Unit but within it. Its host rock is medium-grade crystalline schist belonging to the Baksa Complex. No traces of shearing are observable; thus the process of serpentinisation is not as advanced as it is in the Helesfa Member. In a narrow central slab a less serpentinised harzburgite zone occurs. According to Balla (1981) both members of the Gyód Serpentinite can be regarded as dismembered fragments of obducted oceanic lithosphere remnants.

3b. Görcsöny Eclogite

This is a poorly investigated formation occurring within the Baksa Complex near its northern margin. It consists of retrograde eclogite, i.e. "symplectite". Its size and extensions are unknown (Ravasz-Baranyai 1969) because it was encountered in a single borehole, represented by one small core sample (well Görcsöny-1). Based on analogies it appears possibly to belong to the group of high-pressure–low-temperature eclogites described by M. Tóth (1995) near Szeghalom (East Hungary).

Békésia Terrane

Origin of the name: It forms the pre-Alpine basement of the Alpine Békés–Codru Zone; however, it is applied only to the Hungarian part of the basement, as detailed comparative investigations with the Codru Terrane in Romania have not yet been carried out. This name substitutes the term "South Hungarian Nappe Zone" (Szederkényi 1984; Szederkényi et al. 1991).

Boundaries: This terrane extends over the area of the southern part of the Great Plain which corresponds to the eastern continuation of the Romanian Codru and Biharia Nappe System into Hungary and Northern Serbia. Its northern border coincides with the northern front of the Late Cretaceous Békés–Codru nappe system ("South Hungarian Nappe Zone"). The western continuation of this terrane is obscure due to lack of relevant tectonic and lithologic evidences. However, based on sporadic data it might be expected south of Mecsek Mts. (Baksa Unit).

Sedimentary and magmatic evolution

The protolith character of crystalline rocks of the Békésia Terrane is fairly variegated and similar to that of the Baksa Unit of the Slavonia–Dravia Terrane. Prevailing protolith was a greywacke–pelitic series, interbedded with 150–200 m-thick carbonate members (mainly at Kiskundorozsma in the Csongrád Unit) with abundant tholeiitic lava and tuff beds (M. Tóth 1995). Limestone, dolomite, marl and dolomitic marl formed these carbonate members which became marble, dolomitic marble and calc-silicate gneiss as an effect of medium-grade metamorphism. They are intercalated in gneiss and schist with amphibolite formed by the same metamorphism.

Tectonometamorphic evolution

Crystalline rocks of the Békésia Terrane show a slightly different tectonometamorphic evolution to that of two previously described terranes. The main differences manifest themselves in the certain absence of a first and hypothetical (440–400 Ma old) phase and a general extension in the third (330–270 Ma old) phase. Alpine contact metamorphism was also pointed out, which was caused by small Late Cretaceous banatitic intrusions along the southern state border (Kunbaja, Kelebia, Ferencszállás, etc.; Szederkényi 1984).

Major tectonometamorphic events are as follows:

– 350–330 Ma-old Barrow-type metamorphism showing 4–6 Kb pressure and 540–585 °C temperature in all areas of the terrane;

– 330–270 Ma-old low-pressure and high-temperature (P=2–3 Kb and T=600–650 °C) phase and following blastomylonitisation on each part of the terrane.

1. Kelebia Unit

Origin of the name: after the Kelebia Complex (Szederkényi 1984, 1996).

Boundaries: it is located in the western part of the Békésia Terrane. The unit is bordered by a nappe boundary northwestward and northward, and the Ásotthalom–Bordány Depression eastward. It extends southward into the Yugoslavian territory. Its southwestern extension is unknown.

The unit of unknown thickness is made up by low and medium-grade, strongly-folded two-micaschists and sometimes by chlorite schist. Marble and Variscan granitoids are missing. The series was affected by Barrow-type Variscan metamorphism.

2. Csongrád Unit (formerly Tisza Complex)

Origin of the name: a new name is proposed in the present paper for this unit, which was earlier called the Tisza Unit (Szederkényi 1984, 1996). We intend to avoid usage of the name Tisza, which has been used in another context (c.f. Tisia Terrane or Tisza Megaunit).

Boundaries: it is bordered by a nappe boundary to the north, the Ásotthalom–Bordány Depression westward and the so-called "Makó Trough" eastward. Its southern border can be found in the Bačka area (Yugoslavia).

100–150 m-thick marble-dolomite and marble members near Kiskundorozsma (Szeged) characterise this unit, as carbonate rocks are unusual in the crystalline basement of the Great Plain. Beside this marble small granite bodies and related migmatites (near Deszk), as well as a medium-grade, slightly folded gneiss–micaschist alternation, are also typical. A 350–330 Ma-old first Variscan (Barrow-type) phase with P=6–8 Kb pressure and 500–570 °C temperature, as well as a 330–270 Ma-old second Variscan one with blastomylonitisation as main metamorphic events, are characteristic.

3. Battonya Unit

Origin of the name: after the Battonya Complex (Szederkényi 1984, 1996).

Boundaries: the unit is actually a 15–25 km long and 10–15 km wide mainly granitic body (stretching over Romania and Yugoslavia). Boundaries are the Makó Trough westward, the Békés Basin eastward and the boundary of the nappe system to the north.

Biotite–muscovite–granodiorite and associated enclaves describe the predominant portion of the deep plutonic body. These are peraluminous rocks of mixed crustal/mantle origin formed at a destructive plate margin (Buda 1995). The granitoids form a more than 150 km-long and relatively narrow continuous range from the Bačka area to the Apuseni Mts. In contrast to the Mórágy Unit the magma of the deep plutonic granite body at Battonya– Mezőhegyes, after in situ melting, moved a little upward during the period of Variscan late kinematic movements (Szepesházy 1969; Szederkényi 1984; Kovách et al. 1985). All deformational and age data are the same as those of Csongrád UNit.

4. Sarkadkeresztúr Unit

Origin of the name: after the Sarkadkeresztúr Complex (Szederkényi 1984, 1996).

Boundaries: it is an isolated, 15 km-long and 5 km-wide uplifted block of the crystalline basement at the eastern side of Békés Basin.

It consists of light-grey diatexite and subordinately porphyroblastic orthoclase-biotite granite. On both sides of the high they are accompanied by a medium-grade gneiss–micaschist–amphibolite association with the same deformational characters and age as the Csongrád Unit (Szederkényi 1984).

Outliers (wedges, nappe remnants; Fig. 8)

1. Szalatnak and Horváthertelend Units (terranes)

The Szalatnak Unit can be found NE of the Eastern Mecsek Mts. It is made up of the Szalatnak Shale Formation, which can be subdivided into three members, two shale members and an 80 m-thick basalt agglomerate member between them. The Mórágy Unit underlies the more than 1,500 m-thick sequence. Thin siliceous shale bands are characteristic for the shale members and several thin anthracite intercalations also occur, mainly in the lower member containing a Llandoverian conodont fauna (Kozur 1984) and graptolite fragments (Oravecz 1964). The whole sequence endured very-low grade metamorphism (prehnite-quartz facies; Szederkényi 1974), which turned into a low-grade one (Árkai et al. 1996) in the lower part of the sequence. This formation extends over a 200 km^2 area. It is covered by Permian and/or Lower Triassic sandstone belonging to the overstep sequence. From a structural point of view the Szalatnak Unit can be regarded as a Late Variscan nappe outlier of unknown vergency. During the Carboniferous (before the nappe movements) a small (about 1 km large) biotite–quartz monzodiorite and quartz monzonite intrusion (Szalatnak Syenite-porphyry Formation) intruded into the lower member, causing a fractured, thin contact aureole. Its Rb/Sr ages are 328–310 Ma (Svingor and Kovách 1981). The geochemical character differs from that of the Mórágy Granite, postulating an intrusion preceding the Carboniferous nappe movements. A similar shale was encountered at the western foreland of the Mecsek Mts. covered by Badenian sediments near Horváthertelend, but it has not been studied yet in detail (Horváthertelend Unit).

2. Ófalu Unit (terrane)

Metagreywacke–phyllite–crystalline limestone and interbedded metabasalt, actinolite–schist, porphyrite and porphyroide form a low-grade metamorphic sequence (Ófalu Phyllite Formation), which is jammed as a wedge into the "Mecsekalja" Tectonic Belt, of 40 km length and more than 2 km width. The weakly folded and tilted (locally vertical) blocks are strongly sheared in general, except a few siliceous shale and crystalline limestone intercalations. They preserved some plant remnants and conodont fragments. Carbonised plant remnants support tissue relics derived from botanically fairly well-developed plants (Kedves and Szederkényi 1996), so a Late Silurian (not older) age of the protoliths can be assumed.

A general Late Palaeozoic (pre-Late Carboniferous) shearing is characteristic in the rocks of this formation, except for the crystalline limestone. Strongest shearing took place at the northern margin of the formation and due to considerable friction heating and related potassium metasomatism, a weak melting also developed in it.

Within the Ófalu Unit near Ófalu a small (12 m wide and about 100 m long), nearly vertical serpentinite body of lherzolite origin (Ghoneim and Szederkényi 1979) is wedged into the metagreywacke along fracture zones. This body can be interpreted as an obducted lower lithosphere remnant (Balla 1981).

3. Tázlár Unit (terrane)

In the central area of the Danube–Tisza interfluve, two rock bodies, about 15 km long and 300 m wide, are wedged into gneisses of the Mórágy Unit within a NE–SW striking fault zone. No more than 300 m of thick, greenish-grey carbonate-phyllite with black graphitic phyllite build up these bodies. Their ages are uncertain; according to Fülöp (1994) they may be Early Palaeozoic or Early Carboniferous.

4. Álmosd Unit (terrane)

A low-grade chlorite schist, two-micaschist and graphite-bearing biotite schist association forms a Late Cretaceous nappe outlier (over an area of about 20 km^2), thrust over the metamorphics of the Kőrös Complex at the Romanian-Hungarian state border. It shows NW vergency and is genetically the same as the low-grade metamorphics of the Békésia Terrane (i.e. it forms a Codru Nappe remnant).

Late Variscan evolution

Non-metamorphosed Late Palaeozoic overstep sequences were deposited variably on different parts of the Tisia Composite Terrane. Each terrane has an individual Upper Palaeozoic sequence but all show a common, molasse character (Fig. 14).

Subsequent to the Variscan tectogenesis, accretion of the Tisia Composite Terrane occurred in several stages. It is reflected in the heterochronity of the overstep sequences, indicating different covering times in the different terranes and units, respectively. The oldest overstep formation is the Late Carboniferous Téseny Sandstone Formation. It overlaps both units of the Slavonia–Dravia Terrane, but is missing in the other terranes.

The next overstep stage is represented by the Lower Permian Korpád Sandstone and/or Gyűrűfű Rhyolite, which appear in every terrane, but they did not form continuous covers above the crystalline basement or the Téseny Sandstone.

The third stage occurred in the Early Triassic and will be discussed later.

Late Carboniferous–Early Permian of the Slavonia–Dravia Terrane

The Late Carboniferous–Early Permian overstep sequence is found in the Slavonia–Dravia Terrane exclusively. The earliest post-orogenic sedimentation event, subsequent to the Carboniferous tectogenic phases, is known in the area of the Slavonia–Dravia Terrane. Above the crystalline basement a coal-bearing Westphalian and Stephanian grey sandstone and clay sequence occurs, grading into Lower Permian redbeds of the Villány Hills (Hetényi et al 1976; Kassai, 1976) According to others (Barabás and Barabás-Stuhl 1998) there is an unconformity between them.

In the area of the Babócsa Unit crystalline basement is overlain by Late Carboniferous molasse in patches (Téseny Sandstone Formation) in the neighbourhood of the villages of Darány, Szulok, and Kálmáncsa (Jámbor 1969).

Crystalline rocks of the Baksa Unit are overlain by a more complete Late Palaeozoic overstep sequence than that of the previous one, but unlike the Mecsek Palaeozoic (where the Téseny Sandstone Formation is missing but a nearly complete Permian succession occurs) it has an incomplete Permian sequence (Barabás-Stuhl 1988). Covered by Lower Triassic redbeds (Jakabhegy Sandstone Formation) the Upper Palaeozoic succession is made up as follows: Upper Carboniferous Téseny Sandstone and Turony Formations, Lower Permian Korpád Sandstone and Gyűrűfű Rhyolite Formations. The thickness of the coal-bearing Carboniferous (Westphalian "C" and Stephanian) formation exceeds 1,500 m, but the overlying Permian redbeds and rhyolite also reach 1,000 m in thickness. The centre of Lower Permian rhyolitic volcanism of SE Transdanubia is located in the northern foreground of the Villány Hills and supposedly the volcanic material extended over from here into the Transdanubian part of the Kőrös Unit and Mecsek part of Mórágy Unit (Fazekas et al. 1981).

Permian overstep in the Kunságia Terrane

Two types of Late Palaeozoic overstep sequences are developed on the Mórágy Unit. They are as follows:

In the area of the Mecsek Mts, 3,200 m-thick Permian molasse overlies the granite and metamorphics of the Mórágy Unit. It is made up of a fairly continuous and undisturbed sequence from the lowermost Permian up to the hiatus existing above the topmost Permian which is covered by Lower Triassic redbeds (Jakabhegy Sandstone Formation). This comprehensively investigated sequence contains five lithostratigraphic units (Fülöp 1994): Korpád Sandstone, Gyűrűfű Rhyolite, Cserdi Conglomerate, Boda Siltstone and Kővágószőlős Sandstone Formations. The Gyűrűfű Rhyolite Formation is a characteristic lava horizon within the Lower Permian sedimentary sequence, which is practically unknown outside of the Mecsek region in the Mórágy Unit.

In other parts of the Mórágy Unit (northern part of the Great Plain and Tolna County), small occurrences of the Lower Permian Korpád Sandstone were en-

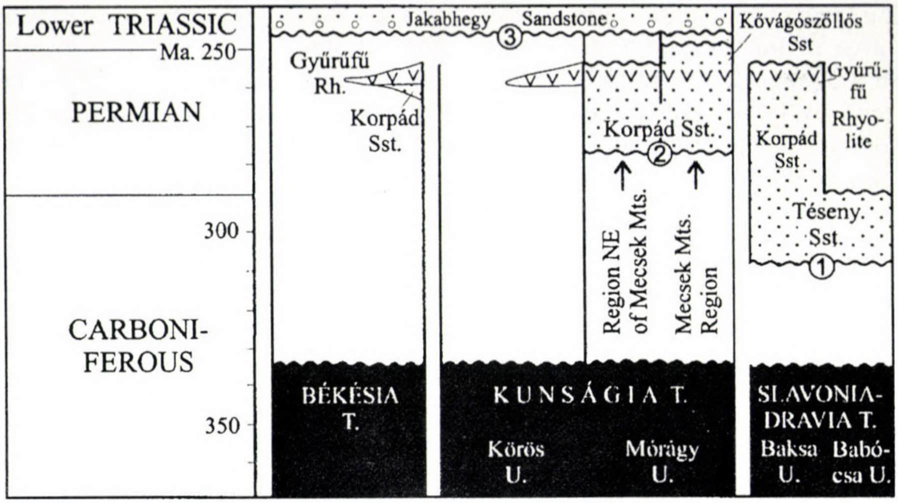

Fig. 14
Late Variscan and earliest Alpine overstep sequences in the Hungarian part of the Tisia Terrane

countered above the crystalline basement (Vajta, Nagykőrös). In a tectonic wedge located in the northeastern continuation of the Mecsekalja Tectonic Belt, presumed Upper Carboniferous molasse was encountered at Nagykőrös.

Apart from a single Lower Permian rhyolite occurrence found on the surface of the crystalline basement near Mélykút no data are available concerning the existence of a Palaeozoic overstep sequence in the Kőrös Unit east of the Danube. West of the Danube, up to the Villány–Szalatnak Fault Zone (eastern boundary of the Slavonia–Dravia Terrane), a characteristic Villány-type Permian sequence can be found, without Upper Carboniferous sandstone (which is widespread in the northern foreground of the Villány Hills beneath the Permian formations). This southwestern segment of the Kőrös Unit is represented by an incomplete Permian sequence akin to that of the Villány Hills (Barabás-Stuhl 1988). The Permian succession is made of by the thin Korpád Sandstone and thin Gyűrűfű Rhyolite. They are covered by Lower Triassic redbeds (Jakabhegy Sandstone).

Permian overstep in the Békésia Terrane

Upper Palaeozoic rocks are very rare in the Békésia Terrane, except for different members of the Gyűrűfű Rhyolite Formation. The oldest known non-metamorphic overstep deposit above the crystalline rocks of the terrane belongs to the Korpád Sandstone Formation. It was found near Tótkomlós (borehole Tótkomlós-1) (Battonya Unit) where a thin sequence of this formation, covered by a Lower Permian rhyolite lava sheet, was deposited onto the erosional surface of the crystalline basement.

The Gyűrűfű Rhyolite is the only widespread non-metamorphic formation in the area of this terrane. It forms numerous isolated lava-sheets, rarely intercalated by ignimbrite or tuff layers, lying on the crystalline basement. These are covered by Lower Triassic redbeds or (if those have been eroded) by Tertiary deposits. The age of volcanism is dated at 248 ± 45 Ma (uncertain age) by the Rb/Sr method carried out on whole rock samples (Kovách and Sviñgor 1973).

Late Variscan tectonic evolution in the SE Transdanubian part of the Tisia Terrane

In SE Transdanubia, in the Mecsek–Villány area, the following Late or post-Variscan events can be partly recognised, and partly supposed, as having taken place after the Variscan orogeny:

– Late Carboniferous strike-slip faulting with a NNW–SSE strike, forming the eastern border of the Late Carboniferous sedimentation area;

– Late Carboniferous strike-slip faulting with ENE–WSW strike, making up the northern border of the Late Carboniferous sedimentation area. It coincides with the southern border of the Mecsekalja Tectonic Belt;

– Middle and Late Permian faulting, coinciding with the northern border of the Mecsekalja Tectonic Belt, forming the border of the Permian sedimentation area southward;

– Permian fault zone of NNW–SSE strike, making up the eastern border of Mecsek Permian sedimentation area, named the "Villány–Szalatnak Deep-fault Zone" (Kassai 1976).

Alpine evolution

Sedimentary and magmatic evolution

The Lower Triassic formations form the overall overstep sequence in the Tisia Terrane. They are made up of continental redbeds (predominantly fluvial facies – Buntsandstein-type Jakabhegy Sandstone Formation) in the Hungarian part of the Tisia. However, in the southernmost zones of the terrane lying outside of Hungary, marine formations appear already in the Scythian (Šikić et al. 1975; Čanović and Kemenci 1988, Kemenci and Čanović 1997; Bleahu et al. 1994). The transgression reached the more northerly parts of the Tisia in the earliest Anisian, when extraordinarily extended tidal flats came into being, the site of deposition of fine siliciclastics. Later on, probably due to the increasing aridity, evaporites and dolomites were formed on the tidal flats (Röt facies). In the subsequent part of the Anisian, a large, storm-affected carbonate ramp was established. On the ramp, Wellenkalk-type carbonates, showing lithology and biofacies akin to those in the Muschelkalk in the Germanic Basin, were deposited (Török 1993, 1998). In the Ladinian a trend of shallowing is detectable both in the Mecsek and Villány Zones, with formation of an extensive dolomite ramp. Definite differentiation of the Mecsek and the Villány Zones commenced in the early part of the Late

Triassic when the Mecsek Half-graben (Nagy, E. 1969, 1971; Szente in Bleahu et al. 1994; Galácz and Vörös, pers. comm.) and the Villány–Bihor Ridge began to form. In the Mecsek Zone a restricted brackish to fresh water lagoon formed, which was followed by delta progradation and establishment of fluvial and lacustrine facies. At the same time a thin sequence of Carpathian Keuper-type siliciclastics, with peritidal dolomite interlayers at their base, was deposited in the Villány Zone. Development and thickness of the Jurassic and Cretaceous of the Mecsek, the Villány-Bihor and the Békés-Codru Zones show even more pronounced differences, and they are separated by Alpine thrust faults (c.f. Fig. 6). However, based on facies transitions, the palaeogeographic relationships of the zones can hardly be questioned. That is why we use the term "facies zone" or "tecto-facies unit" instead of terranes or sub-terranes describing their further Mesozoic history.

Mecsek Zone

The Late Triassic fluviatile-lacustrine sedimentation continued in the Early Liassic, when a thick coal-bearing siliciclastic succession was deposited in lacustrine, deltaic and coastal swamp environments (Gresten facies). The thickness of the coal-bearing formation may reach as much as 1,200 m in the depocentre of the Mecsek Half-graben and several 100 m in the other parts of the Mecsek Zone. From the Sinemurian to the end of the Bajocian grey, bioturbated shale and sandstone ("spotty marl") were deposited in an open marine basin, showing an upward deepening trend. The thickness of the "spotty marl" group may reach 2,500 m in the Mecsek Half-graben. At the end of the Bajocian a basic change took place in the sedimentation: a drastic decrease in the terrigenous input and appearance of the typical Mediterranean lithofacies. The Bathonian to Berriasian interval is represented by a condensed sequence of Ammonitico Rosso-type limestone, cherty radiolarian limestone, siliceous limestone and Calpionella limestone. A significant change could also be recognised in the ammonoid and brachiopod faunas. While the Liassic and Early Dogger faunas show definite European affinity, in the Late Dogger and Malm interval the Mediterranean elements became predominant. In the very long interval from the Carnian to the Bajocian the Mecsek Zone received huge amounts of terrigenous siliciclastic sediments, indicating the proximity of a continental source area (continental hinterland). Therefore, the cessation of terrigenous input is an indicator of the separation of the Tisia Terrane (microcontinent) from the European continent. The rifting continued in the Early Cretaceous, leading to intra-continental rift-related alkaline basalt volcanism (Harangi 1994; Harangi et al. 1996) which extended over a large part of the Mecsek Zone; some traces could even be detected in the Villány–Bihor Zone. The climax of the volcanic activity occurred in the Valanginian–Hauterivian interval but it lasted until the Albian. Intense erosion of the volcanic complex already began in the Late Hauterivian–Barremian interval, when atolls and thick volcaniclastic series were formed containing large amount of shallow marine fossils which were redeposited from the broadened sedimentary zones developed around the volcanic build-ups (Császár and Turnšek 1996).

The marine sedimentation may have been interrupted by the end of the mid-Cretaceous tectonic movements. Due to the Late Turonian–Coniacian tectogenesis and subsequent erosion the Cenomanian–Turonian pelagic siliciclastic series and red shale are preserved as small remnants only.

A new sedimentary cycle commenced in the Santonian–Campanian. Overlying coarse clastics, pelagic Campanian–Maastrichtian red calcareous marl is known in the central part of the Mecsek Zone (Danube–Tisza interfluve) grading northeastward (Szolnok Zone) into grey silty marl and further on into sandstone-dominated sequences ("flysch").

Villány-Bihor Zone

Following the separation of the two zones Carpathian Keuper-type terrestrial sediments were deposited during the Late Triassic on the Villány–Bihor Ridge (0–40 m compared to the up to 600 m of coeval strata in the Mecsek Half-graben). In some areas the entire Carnian– Bathonian interval is missing, while in others Pliensbachian sandy, belemnoid-bearing crinoidal limestone, a few metres thick, may occur (Vörös 1972). A less than one metre-thick Callovian ferruginous, stromatolitic bank, rich in ammonoids belonging mainly to the boreal (or European) province (Géczy 1973, 1984) closes the gap. Oxfordian to Lower Tithonian thick-bedded, light-coloured pelagic limestone represents the Upper Jurassic; then, after a gap represented by bauxite lenses, Valanginian–Lower Albian Urgon-type platform limestone with Dinaridic-type dasycladaceans (Bodrogi et al. 1993) is characteristic of the Hungarian part of the zone (Császár 1992).

Lowermost Cretaceous basaltic volcanics are represented here only by a few sills and dykes, except for the area of Nagybaracska at the Danube, where a small volcano has been identified (Császár et al. 1988). The sequence is terminated by Albian flysch-type formations (Császár and Haas 1984; Császár, unpubl.).

The Late Senonian overstepping sequence consists mainly of marine siliciclastics which may have been deposited in the foreland basins of the Pre-Gosau nappe piles. In the southwestern part of the zone (Danube–Tisza interfluve) Santonian terrestrial basal conglomerate, deposited after the formation of nappe system, is overlain by Campanian bathyal Globotruncana marl which is covered by sandy limestone containing a large amount of redeposited shallow marine bioclasts. Graded sandstone appears in the topmost part of the succession. The entire succession becomes sand and silt-dominated northeastward and thick flysch-type sequences are known in the easternmost part of the Hungarian segment of the zone.

Békés–Codru Zone

Scythian redbeds (Jakabhegy Sandstone Fm.) form the uniform overstepping sequence of all pre-Alpine formations in the Hungarian part of the zone. They are followed by Anisian dark grey dolomite and Ladinian light-coloured platform dolomite, the latter possibly extending partly into the Upper Triassic as well (Bérczi-Makk in Barabás-Stuhl et al. 1993). Red crinoidal limestone represents the Liassic or Dogger. An uppermost Jurassic to lowermost Cretaceous schistose calcareous marl and shale sequence with calpionellids is also characteristic of this zone.

Undisturbed epicontinental Senonian rocks overstepping the nappe front give an upper age limit for the overthrusting of this unit. Small banatite intrusions of the same age also occur (Szederkényi 1984; Szederkényi et al. 1991).

Parallel to the Hungarian state border, in the Békés–Codru Zone several small hypabyssal intrusions and dykes are found related to banatite magmatism located in the Apuseni Mts. and the South Carpathians. This rock association has a dioritic member at Forráskút, a granodioritic one at Ferencszállás and a granitic member at Ferencszállás, Kiszombor and Kunbaja. The 3–6 m thick dyke system and several ten metres-broad intrusions are accompanied by 300–400 m-wide, tourmaline-rich, muscovite schist contact pneumatolitic zones (Szederkényi 1984). The age of intrusions is given in the 62–66 Ma range by K-Ar age determination, carried out by Balogh and Árva Sós (in Szederkényi et al. 1991).

Tectonometamorphic evolution

Based on borehole evidence in Hungary (Pap 1987, 1990) and on surface data in the Apuseni Mts. (Romania; c.f. Ianovici et al. 1976; Bleahu et al. 1981), the following Cretaceous (Palaeoalpine) events can be recognised in the Hungarian part of the Tisia Terrane:

– Albian ("Austrian"; Wein 1967) and Late Turonian–Coniacian ("pre-Gosau") nappe overthrusting of NW vergency; these compressional movements also resulted in the brachyanticline and syncline of the Mecsek Mts and the imbricated structure of the Villány Mts, as well as in the nappe-like overthrusts near the northern margin of the Villány–Bihor Zone (considered formerly to be autochthonous – e.g. boreholes Füzesgyarmat and Sáránd; Pap 1987, 1990; Árkai et al. 1998).

– These nappe movements were probably responsible for the metamorphism and emplacement of a metasandstone-carbonate phyllite unit in the Drava Terrane with a radiometric age 96–98 Ma (Barcs-W area; Árkai 1990).

– Anti-clockwise rotation of the Tisia Terrane took place between Albian and Late Cretaceous, resulting in a N–S oriented position, nearly perpendicular to the original one (Balla 1986).

– Clockwise rotation of the Tisia Terrane, nearly back to its original W–E vergent position, mostly during the Early Miocene (Balla 1986).

In the Early Miocene southward thrusting and folding took place at the northern margin of the Tisia Terrane ("Szolnok (-Maramureş) Flysch Zone" – Balla 1982; Nagymarosy and Báldi-Beke 1993; Nagymarosy 1998).

In the Middle Miocene the formation of the large, pull-apart-type Pannonian Basin began, in which the beginning of sedimentation formed the base of the uniform overstepping sequence of the entire (Carpatho-) Pannonian terrane collage (Horváth and Royden 1981; Royden 1988).

SSE-vergent overthrusting and smaller-scale strike-slip faulting took place along the Mecsekalja Tectonic Belt during the Pannonian and partly even in the Pleistocene.

Relationships

Differences between adjacent terranes (Pelsonia versus Tisia)

In this chapter relationships between the two major terranes (Pelsonia Composite Terrane and Tisia Terrane) in the basement of the Pannonian Basin interior are summarised, based on the regional descriptions presented in the previous chapter. Differences with the East Alpine and West Carpathian terranes/units, extending only partly to the territory of Hungary (e.g. Austroalpinia, Penninia, Veporia, Zemplenia) are not discussed herein.

As could be seen from the characterisation of the terranes in the Pre-Neogene basement of Hungary presented above, the WSW–ENE striking Zagreb–Zemplín or Mid-Hungarian Lineament divides the basement of the Pannonian Basin into two fundamentally different parts, as already emphasised, among others, by Géczy (1972, 1973a, b) and Balla (1982). The latest manifestation of significant geologic activity (large-scale terrane displacement) along this major terrane boundary is marked by the zone of Middle Miocene ignimbrites aligned to it and striking from Zagreb to the Zemplin area, reaching a thickness from 1,000 to 3,000 m (cf. Ravasz .1987 and in Dank and Fülöp et al. 1990).

Along this major terrane boundary the southernmost units/zones of the Pelsonia Composite Terrane and the northernmost zone of the Tisia Terrane, i.e. the Bükk PA Terrane and the Zagorje–Mid-Transdanubia Composite Terrane, as well as the Mecsek Zone, are juxtaposed, showing entirely different Alpine (e.g. pre-Neogene) and pre-Alpine evolution; that is to say that they represent typical "exotic" terranes, being totally unrelated to each other. The main differences between them can be summarised as follows (see Figs 15 to 22, but especially Fig. 21):

1. There is no evidence known for Variscan metamorphism in the units of "Bükkium" in the former sense (cf. Árkai 1983; Árkai et. al. 1995; Kovács et al. 1995), and only very low-grade (in case of quartz-phyllites low-grade) Variscan metamorphism characterises the Bakonyia Terrane (Lelkes-Felvári et al. 1996). Whereas in the mentioned units of the "Bükkium" no Variscan deformation could

be proven either as yet (Csontos 1988), in the Bakonyia Terrane south-vergent nappe-stacking took place (Dudko and Lelkes-Felvári 1992; Balla and Dudko 1993).

On the other hand, in the area of the Alpine Tisia Terrane, although remnants of very low to low-grade metamorphosed terranes are known (probably as nappe-outliers above the Variscan Kunságia Terrane or as tectonic wedges within it), the Mórágy Complex and most probably also the Körös Complex bear evidence of Early Carboniferous (360–340 Ma) Barrow-type metamorphism and associated intense, anatectic, syncollisional granitisation.

2. A fault-controlled basin was formed above the crystalline rocks in the Mecsek–Villány area, i.e. above the junction area of the (Slavonia)–Dravia and Kunságia Terranes, in which 3,000–3,500 m-thick Upper Carboniferous to Upper Permian continental sediments were accumulated. On the other hand, the units of the presently northerly adjacent Zagorje–Mid-Transdanubia CT and Bükkia CT are characterised by marine, predominantly carbonate, Upper Carboniferous-Upper Permian formations, of a maximum of 1,000 m known thickness. This excludes a close palaeogeographic relationship of the two depositional basins in the Late Palaeozoic.

3. As opposed to the continuous Late Permian–Triassic marine sedimentation in the Zagorje–Mid-Transdanubia CT and Bükk PA Terrane, transgression in the area of the Tisia Terrane began only in the Early Triassic in the South (cf. Šikić 1975 in Bleahu et al. 1994; Kemenci and Čanović 1997) and reached the northernmost area, i.e. the Mecsek Zone, only in the earliest Middle Triassic (Barabás-Stuhl 1993; Bleahu et al. 1994).

4. In the Late Triassic, extensional basins (half-grabens) began forming in the area of the Tisia Terrane, leading to the separation of the Mecsek and Villány-Bihor Zones. The Mecsek Half-graben was filled with up to 4,300 m of Carnian to Bajocian sediments, the prevailing terrigenous components of which were derived from a granitoid-metamorphic source area (Nagy, E. 1968, 1971). At the same time, the Villány-Bihor Swell was characterised by major hiatuses, with 0 to a max. few tens of metres sediment thickness, capping Middle Triassic carbonates. Faunas of this time interval clearly belong to the European province (cf. Géczy 1984; Vörös 1993 and references therein) in both zones.

Ophiolitic terranes of the Zagorje-Mid-Transdanubia and Bükkia composite terranes bear witness to an oceanic domain (cf. Harangi et al. 1996; Pamic 1997), although biostratigraphic evidence for the pre-Bathonian time are scarce (Dosztály 1994). On the other hand, the Bakonyia Terrane of the Pelsonia Composite Terrane was part of a subsided continental margin from the Sinemurian onward, with typical Mediterranean facies (mostly "Ammonitico Rosso"-type pelagic sediments) and fauna (cf. Géczy 1984; Vörös 1993 and references therein).

Evidently the terrigenous sediments filling up the Mecsek Half-graben could not be derived either from the terranes of the Pelsonia Composite Terrane (presently located to the north) or from the Middle Triassic carbonate platform of the Villány–Bihor Zone (located to the south), but only from a continental hinterland located to the north at that time. Therefore, in the Early Mesozoic the Mecsek Zone must have been located in the most external Tethyan (or "Peri-Tethyan") zone (cf. Bleahu et al. 1994; Török 1998). Evidences for a prevailingly N to S sediment transport were published by Nagy (1968, 1971), from the Lower Liassic coal-bearing Gresten-type sequence.

5. A major change in the sedimentation of the Mecsek Zone took place in the Bathonian, when the siliciclastic input ceased and "Ammonitico Rosso"-type pelagic sedimentation began with the appearance of Mediterranean faunal elements (Géczy, op. cit.; Vörös, op. cit.; Galácz 1984). This is ample evidence for the separation of the Tisia Terrane from its European Continental hinterland, in connection with the Penninic rifting (although the main rifting phase took place in the earliest Cretaceous, as indicated by the paroxysm of alkaline rift-type basaltic volcanism; Harangi et al. 1996). Separation of the Mecsek and Villány-Bihor Zones persisted throughout the Late Jurassic and Early Cretaceous (with some transitional features, however). Middle Cretaceous synorogenic deposits are represented by Albian flysch-like turbiditic sediments in the Villány Zone (Császár 1992) and by Turonian Puchov-type red marl in the Mecsek region (Balla and Bodrogi 1993).

Meanwhile, the passive margin evolution of the Bakonyia Terrane continued with pelagic sedimentation ("Ammonitico Rosso") until the Middle Tithonian, then with "Maiolica" until the Barremian, with the exception of its northeastern part (Gerecse Mts.), where flysch-type sedimentation with ophiolite detritus began in the Early Cretaceous (Császár and Haas 1984; Császár and B.-Árgyelán 1994). On the other hand, formations of the ophiolitic terranes of the Mid-Transdanubia and Bükkia Composite Terranes bear evidence of Late Jurassic subduction and ophiolite obduction (Eohellenic tectogenesis). The distal flysch-type Upper Jurassic sequence of the Bükk Parautochthon Terrane was evidently related to this event as well, also resulting in the emplacement of the Szarvaskő Ophiolite Complex onto the Bükk PA from the NW to SE (according to present co-ordinates; Csontos 1988, 1999). Therefore, the presently adjacent zones of the Tisia Terrane and Pelsonia Composite Terrane underwent entirely different (or rather opposite) Late Jurassic–Early Cretaceous evolution.

Palaeomagnetic data by Márton were interpreted by Balla (1986) as indicating that the Tisia Terrane did not rotate during the entire Mesozoic before the Albian (and most probably also not during Late Variscan time), i.e. also not after its separation from the European hinterland (or in other words, from the Variscan terrane collage) in the Bathonian. After the Albian it rotated about 90° anticlockwise during the rest of the Cretaceous, then practically back into its original position by the Middle Miocene (Balla, op. cit.).

Fig. 15 →
Upper Permian sedimentary lithofacies in Hungary. 1. Shallow marine carbonates; 2. Evaporites; 3. Continental redbeds; 4. Areas of denudation, overlain by Lower Triassic continental redbeds

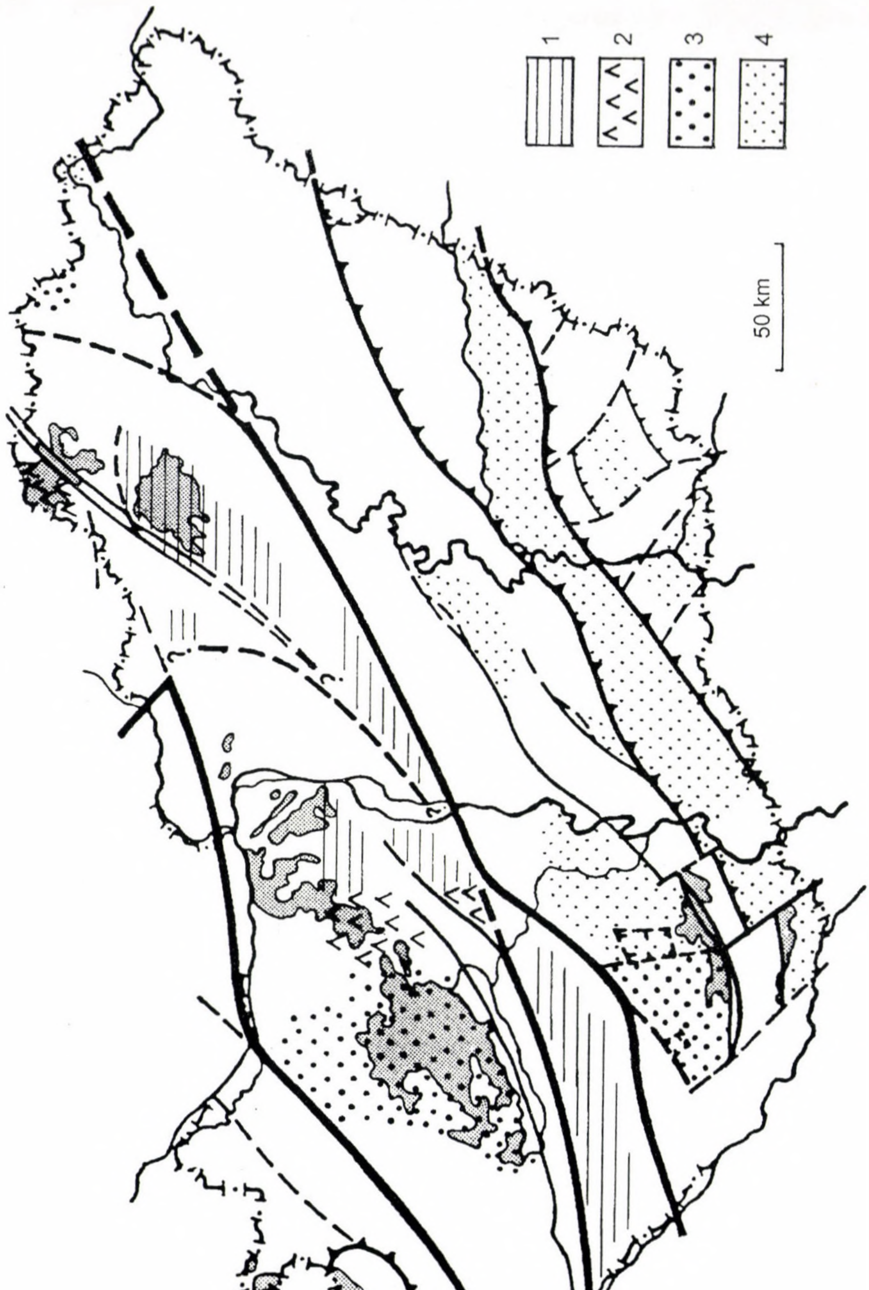
1
2
3
4
50 km

Affinities of the adjoining exotic terranes

Bakonyia Terrane

A number of publications analysing the relationships and original setting of the terrane have appeared since the fundamental recognition by Majoros (1980), who, based on the fitting of Late Permian facies zones of the eastern Southern Alps and of the Transdanubian Range (=Bakonyia Terrane herein), first suggested their original proximity and the 400–500 km dextral displacement of the latter along the Periadriatic (Gailtal)-Balaton Lineament during the Tertiary. The "Mediterranean" (=South Alpine) affinity of the Balaton Phyllite Group (Lelkes-Felvári et al. 1982, 1994) and the analogy of the Szabadbattyán and Nötsch Carboniferous (mostly marine) molasse (Flügel 1990; Ebner et al. 1991; Ebner 1992) support this assignment. The Late Variscan postcollisional granitoids of the Velence Hills are also of South Alpine affinity, e.g. this occurrence represents the (north) easternmost known member of the Late Variscan Periadriatic magmatic chain (Buda 1995, 1996).

Analysis of Late Permian–Triassic (Haas et al. 1995; Haas and Budai 1995) and Jurassic (Vörös and Galácz 1998) facies zones enabled the fitting of the Bakonyia Terrane to the Southern Alps along the Periadriatic Lineament with 10–20 km accuracy, e.g. its southwestern part to the Lombardian Alps, the middle one to the Dolomites and the northeastern one to the Carnic Prealps. At the same time, fitting to the Northern Limestone Alps was possible only within 50–150 km accuracy (mainly because of the very different angle of the zones in this case). It is interesting to note here that palaeomagnetic directions permit moving the Transdanubian Range with the Southern Alps throughout the Mesozoic, but the declination rotation pattern of the Northern Calcareous Alps is incompatible with the first two: in other words, the Northern Calcareous Alps were not moving in co-ordination with the Transdanubian Range and the Southern Alps (Mauritsch and Márton 1995). In general the Permo-Mesozoic succession of the Bakonyia Terrane shows rather South Alpine than North Alpine affinity. It is to be noted, however, that the northward-deepening Ladinian Buchenstein Basin of the Bakonyia Terrane, with definitely more Hallstatt affinity than that of the Southern Alps, was facing a pelagic domain to the north (Budai and Vörös 1992). However, this basin was filled up by up to 1,000 m of siliciclastic-marly sediments in the Carnian (and most probably also the northerly lying pelagic domain, forming the westernmost extension of the Hallstatt Basin), thus giving rise to a uniform carbonate building in the whole area, and also to the S and N of it, in the remainder of the Triassic. Closure of the small oceanic basin located to the north

Fig. 16 →
Upper Triassic (Norian) sedimentary lithofacies in Hungary. 1. Continental ("Keuper" s.l.); 2. Outer shelf lagoonal, partly reefal facies (Dachstein Limestone and Dolomite); 3. Inner shelf lagoonal ("Hauptdolomit" s.s.); 4. Pelagic basins (grey, cherty limestone and Hallstatt Limestone s.s.); 5. Oceanic environments

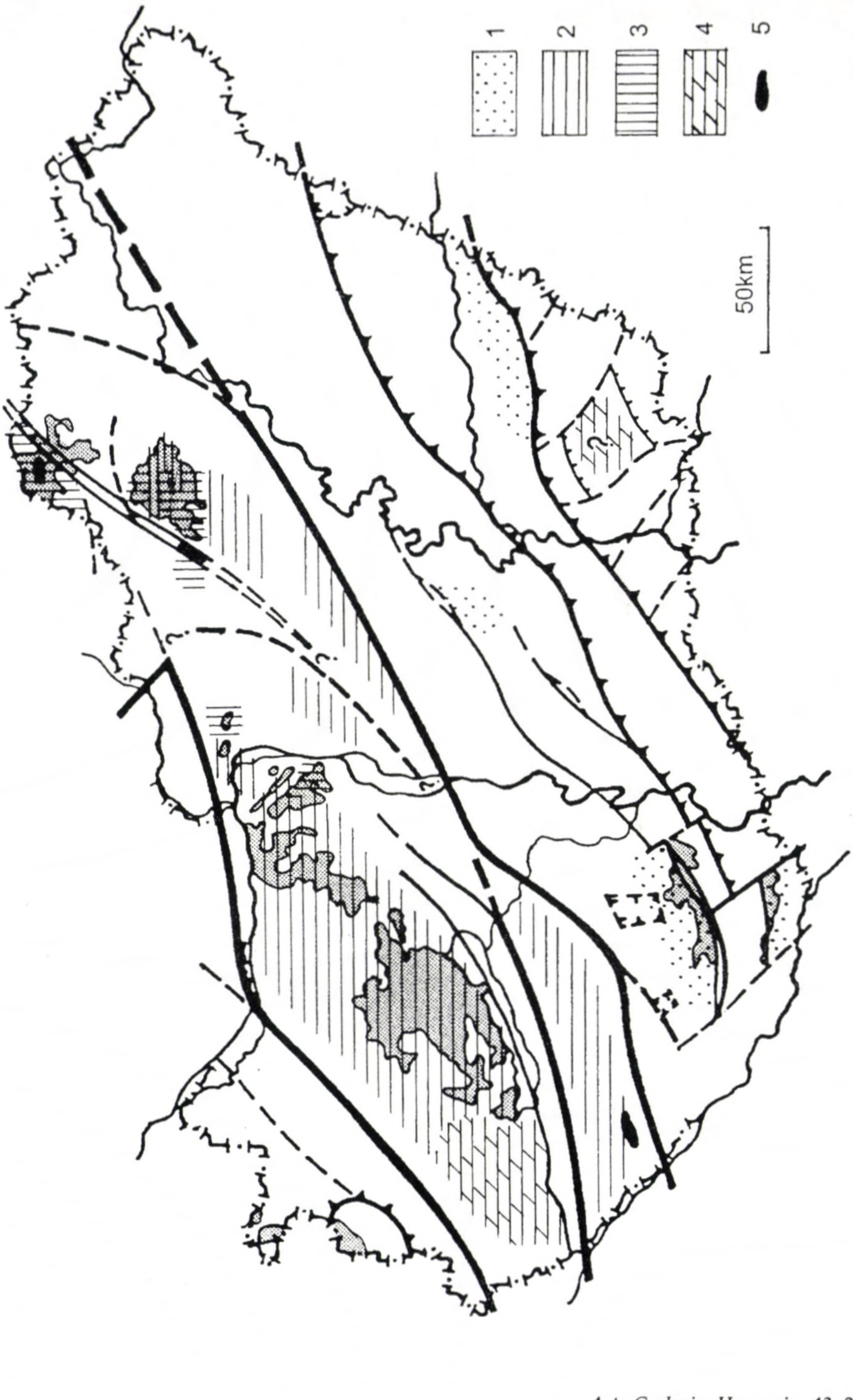
1
2
3
4
5
50km

(probably of its westernmost tip) is recorded in the ophiolite detritus-bearing Lower Cretaceous flysch sequence of the Gerecse Mts. to the NE (Sztanó 1990; Császár and B.-Árgyelán 1994), which was probably located to the south of the Rossfeld Basin of the Northern Limestone Alps.

Senonian formations of the Bakonyia Terrane are rather peculiar. However, they show the closest facies affinity and relation in the benthic fauna assemblage (rudists, foraminifera) with coeval deposits of the Medvednica Mts (Polšak 1981; Haas 1985). Relationships of the shallow marine fossil assemblage with that of the Dinaridic–Apulian platforms were also pointed out (Bignot et al. 1984). Facies relationships may be also assumed with basins of the Southern Gosau belt of the Central Alps. Since flysch-type sedimentation occurred in the Campanian, during maximum extension of the rudist platform in the Transdanubian Range, in Lombardia and also in the Gosau basins of the Northern Calcareous Alps (Wagreich and Faupl 1994), the initiation of considerable displacement of the Bakonyia Terrane from its previous position prior to the Campanian must be assumed.

During the time interval between the Lutetian and the Eggenburgian a series of sedimentary basins was formed in the belt of the Bakonyia Terrane, shifting progressively from the SW to the NE, from the Bakonyia Terrane through Bükkia Terrane up to the Aggtelek Composite Terrane. The continuous transition of Palaeogene rocks from one terrane to the other shows that the amalgamation of these terranes was more or less completed by the Late Palaeogene. In any case the Balaton (and the adjoining Darnó) Lineaments were active also after the Oligocene.

Zagorje-Mid-Transdanubia and Bükkia Composite Terranes

These terranes practically correspond to the "Igal–Bükk eugeosyncline" of Wein (1969), considered at that time to represent a narrow seaway forming a connection between the Bükk Mts. and the NW Dinarides. The necessity of such a connection during the Late Palaeozoic was already recognised by Heritsch (1942, 1944) and Schréter (1943) on the basis of Dinaric-type coral faunas, and was proven by thorough comparative analysis by Balogh (1964 – for earlier references see therein). Several deep wells encountered marine Permian sediments or Mesozoic ophiolites in the zone extending from the Zagorje region (=Croatian Highland) to the Bükk Mts, which formed the basis for Wein (1969) to introduce the above-mentioned "eugeosyncline" (see also in Szepesházy 1977). However, the composite character of the zone is evident; furthermore, from among the

Fig. 17 →
Middle–Upper Liassic sedimentary lithofacies of Hungary. 1. Pelagic environments ("Ammonitico Rosso", Adnet-type limestone); 2. Mixed siliciclastic-carbonatic sedimentation ("Fleckenmergel" or Allgäu-type); 3. Lacunose shallow marine (Villány-type); 4. Gap or ambiguous pelagic carbonates (Bükk-type); 5. Oceanic sediments

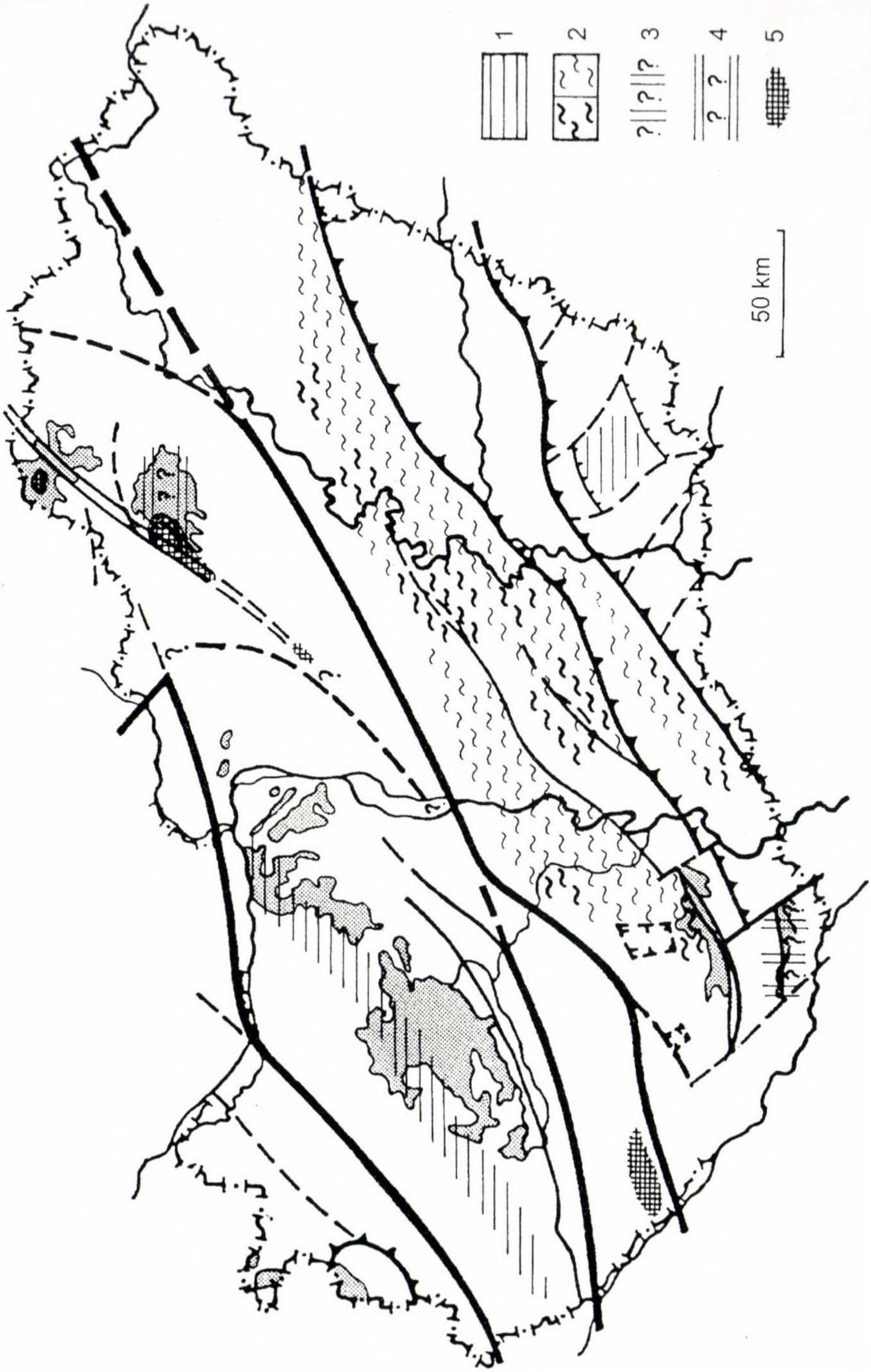
1
2
?||?||? 3
? ? 4
5
50 km

marine Late Permian facies types, it is the Bükk PA Terrane on the far NE extremity, which shows the most distal type.

Units of the Zagorje–Mid-Transdanubia Composite Terrane, in the Hungarian part known only from boreholes (Mid-Transdanubian Unit s.s.) as described in detail in the regional chapter, comprise several units from the South Karavank Unit to the Dinaridic Ophiolite Melange (=Kalnik Unit – Pamic 1997; Haas et al. 1998, 2000). The Medvednica Mts at Zagreb comprises complexes corresponding to the Szendrő Palaeozoic, Bükk Triassic and Szarvaskő Ophiolite Complex in the Bükkia Composite Terrane in NE Hungary (gratefully acknowledged presentation in the field by Pamic, Zagreb; Csontos, pers. comm.). The Szendrő and Uppony Palaeozoic units show a relationship both to the Palaeozoic of Graz and of the Carnic Alps-South Karavank Alps (Ebner et al. 1991, 1998). However, they also show relationships with the Jadar Terrane in the NW Vardar Zone (Filipovic et al. 1998), thus providing evidence that in the Late Palaeozoic, along with the Bükk PA Terrane, they formed a link between the above-mentioned Alpine and Dinaridic units.

From the beginning of the Alpine sedimentary cycle, e.g. from the Middle Permian transgression, until the establishment of a joint stratigraphic record (e.g. until the basal Jurassic), the Jadar and Bükk PA Terranes showed a practically identical evolution (Filipovic et al. 1998). The setting of the Szarvaskő–Darnó ophiolite complexes above the Bükk PA Terrane can be compared with the Maljen ophiolite complex above the Jadar Terrane; although the ultramafic sheet of highest position is missing now in the Bükkia CT, its former presence is indicated by serpentinite pebbles in the Miocene Darnó Conglomerate (c.f. Sztanó and Józsa 1995). Further southward in the Neotethyan ophiolite complexes, the conspicuous analogies between the Darnó and the much larger North Pindos and Othrys ophiolite complexes in the Hellenides are worth mentioning (Migiros et al., in prep.).

The highly sheared and compressed Palaeogene and Lower Miocene fragments in the Mid-Transdanubian-Zagorje zone were involved in Early Miocene tectonic processes, indicating a young, i.e. post-Ottnangian age for the transform fault system of the Balaton and Mid-Hungarian Lineaments (Csontos and Nagymarosy 1998).

Fig. 18 →
Mesozoic magmatic rocks of Hungary. 1. Middle Triassic (mostly Early Ladinian), mainly andesitic rocks (island arc or early rift type?); 2. Middle-Late Triassic (Late Ladinian–Carnian) within-plate type basalts; 3. Middle Triassic-Middle Jurassic Neotethyan ophiolites; 4. Middle Jurassic – Early Cretaceous Penninic ophiolites; 5. (Late Jurassic –) Early Cretaceous alkaline rift type basaltic rocks; 6. Middle or Late Jurassic rhyolites (Mainly after Harangi et al. 1996)

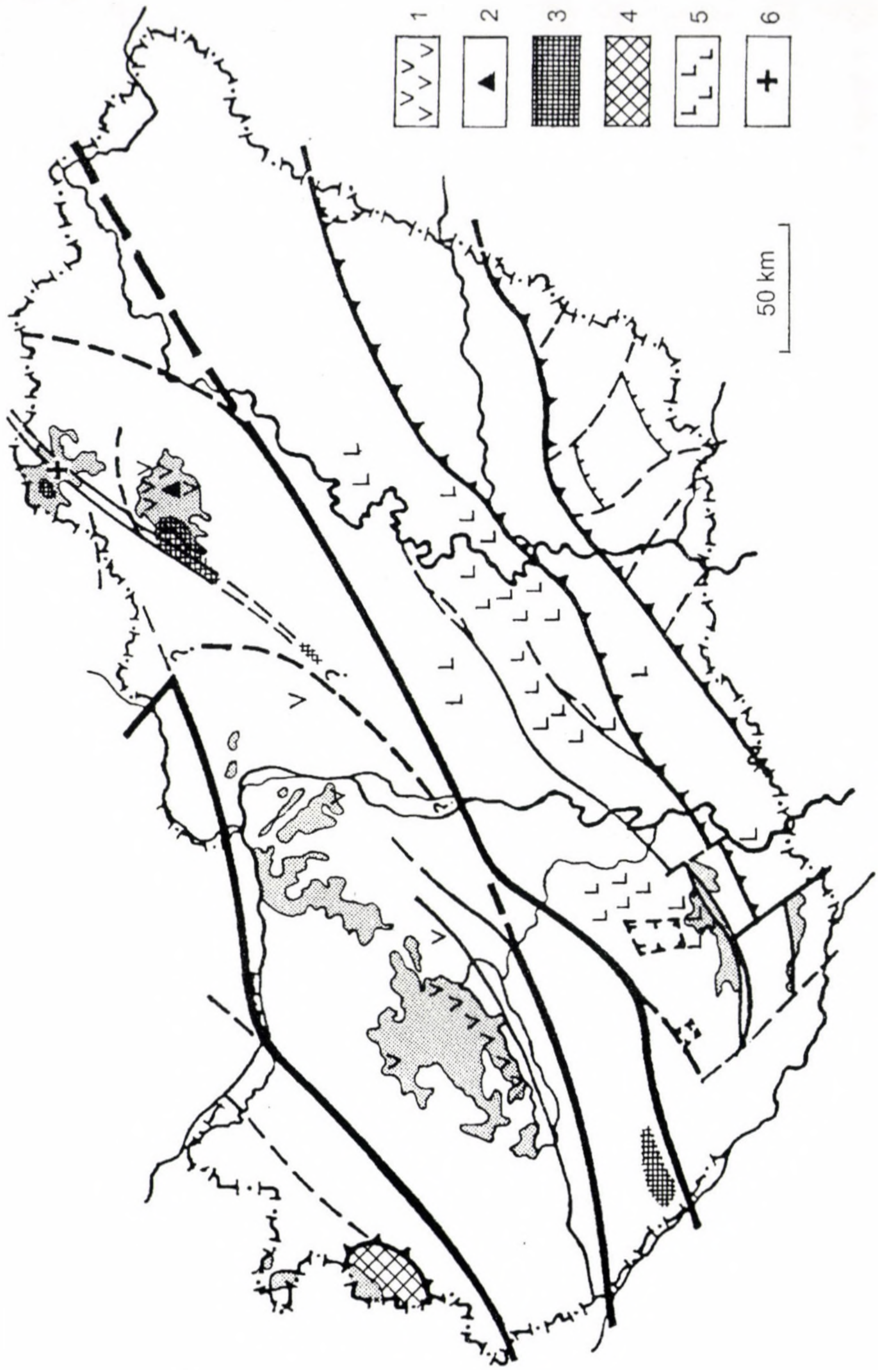
1
2
3
4
5
6
50 km

Aggtelekia Composite Terrane

The Aggtelek Unit with its Hallstatt facies has been considered since Kovács (1980) as an equivalent of the Lower Juvavicum of the Northern Limestone Alps. However, recent structural observations (Schweigl and Neubauer 1997; Plašienka 1997; Vozárová and Vozár 1996) raised the probability of an original symmetric setting on the opposite flanks of an intraoceanic carbonate platform. The Lower Juvavic units are involved in a northward thrust complex beneath the Dachstein carbonate platform of the Upper Juvavicum, whereas the Aggtelek–Bódva units show a southward-deepening tendency into a southward thrust complex (as far as the non-metamorphosed units of the Aggtelek–Rudabánya Mts are concerned; Less et al. 1998). Thus, a palaeogeographic setting analogous to the Drina–Ivanjica Terrane of the Dinarides (cf. Dimitrijević and Dimitrijević 1991; Karamata et al. 1995) can be supposed.

The Bükkia Composite Terrane with its southerly-oriented structure also represents a structurally characteristic exotic, i.e. Dinaridic-type terrane within the North Pannonian–West Carpathian (ALCAPA) terrane collage.

The Bódva Unit with its deep-water, chert-rich development has no equivalent in the known sequences of the Lower Juvavicum. On the other hand, the Bódvalenke-type, reddish cherty limestone is a very common formation in the above-mentioned North Pindos and Othrys complexes (Skourtsis-Coroneou et al. 1995; Migiros et al., in prep.).

The relationships of the Tornakápolna and Martonyi Terranes can be considered in context of those of other terranes in NE Hungary.

Tisia Terrane

As could be seen from the above analysis, the Tisia Terrane with its Variscan and early Alpine evolution represents an entirely exotic, microcontinent-sized block in its present setting within Dinaridic–South Alpine units both to its S and N.

The Variscan evolution of Hungarian crystalline basement reflects several tectono-metamorphic events that occurred between 440 and 315 Ma. The first manifestation of these events was a not yet perfectly proven high-P and low-P metamorphism occurring in a narrow strip of the central, axial part of Hungarian section of the Tisia Composite Terrane, and represented by local eclogite and ultramafic bodies preserved mainly in amphibolite facies rocks.

This high-pressure metamorphism is well recorded and widespread in Variscan Europe, dated between 430 to 400 Ma and is everywhere associated with ultramafic and mafic rocks, probably due to early stage of obduction (Matte 1986). In the absence of up-to-date isotope geochronological investigations no evidence

Fig. 19 →
Alpine metamorphism in Hungary (mainly after Árkai 1991). 1. Very low to low grade; 2. Medium grade; 3. Blueschist facies relics

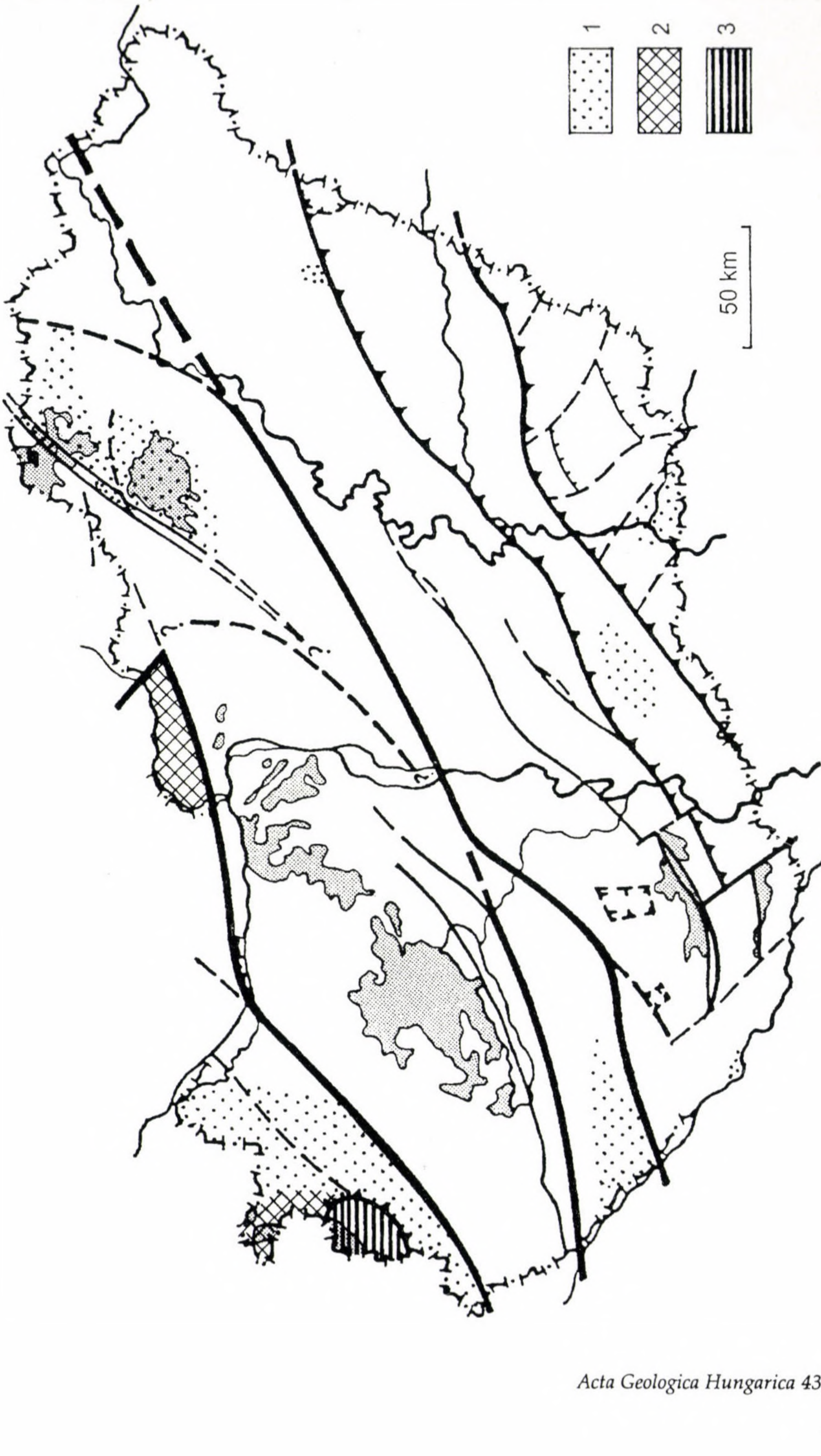
1
2
3
50 km

is available to prove earlier deformations in the crystalline rocks of Hungary. Nevertheless, based on results of research carried out in particular elements of Western and Middle European sections of Variscan Europe (western Spain, northern Portugal, Armorican Massif, Bohemian Massif), there is no reason to assume that such deformations did not occur in the Hungarian crystalline rocks. Since these European Variscan constituents show undoubted Late Precambrian/Early Palaeozoic rifting and subsequent crustal shortening and final collision during the Late Variscan, they represent pieces of the North Gondwana margin (von Raumer and Neubauer 1994), and moreover, the final collision welded them into a single mega-continent together with other large shields, it is entirely reasonable to assume that the Hungarian crystalline rocks underwent a similar Pre-Mesozoic evolution. An important task of Hungarian geology is to find satisfactory methods to demonstrate the reality of this assumption.

Whereas the evolution of the northerly adjacent terranes/zones of the Pelsonia Composite Terrane – with the absence or very low intensity of Variscan metamorphism and with marine development of the Late Palaeozoic – was undoubtedly related to the Noric–Bosnian Terrane, the northernmost zone of the Tisia Terrane, e.g. the Mórágy Unit/Complex of the Kunságia Terrane with its Variscan tectonometamorphic evolution and syncollisional granitisation, shows an unambiguous relationship with the Moldanubian–Helvetic Terrane (cf. Flügel 1990; Neubauer and von Raumer 1993; von Raumer and Neubauer 1993). Therefore, whereas the southernmost zones of the Pelsonia Composite Terrane, according to the polarity of the Variscan tectonometamorphic evolution of the pre-Alpine basement of the Alps (cf. Neubauer 1988), lay in the southern (according to present co-ordinates), most external zone of the Central European Variscides, i.e. in the zone of the Carnic Alps–Dinarides devoid of Variscan granitoids, the northernmost zone of the Tisia Terrane, with its Carboniferous syncollisional granitisation lay in the southern Variscan magmatic arc/collisional zone, i.e. in the continuation of the Helvetic–Moldanubian Zone (Buda 1995, 1996). (This affinity, in terms of the Mesozoic cover sequence, e.g. the Liassic Gresten and overlying "Fleckenmergel" facies, was already emphasised as early as in 1862 by Peters)

Low-grade to non-metamorphic terranes are also present in the Bohemian Variscan terrane collage, as well as in other regions of the southern part of the European Variscan belt (Matte et al. 1990). This can provide an explanation to the presence of such remnants (outliers, wedges) on or within the Kunságia Terrane.

According to Matte (1986), pp. 337–339, the following main tectonometamorphic events can be recognised in the Variscan belt of Europe:

– 430–400 Ma-old early, high-P and low to high-T metamorphism, associated with obduction of mafic and ultramafic rocks;

Fig. 20 →
Alpine flysches in Hungary. 1. Occurrences of flysch deposits (letter symbols indicate the ages)

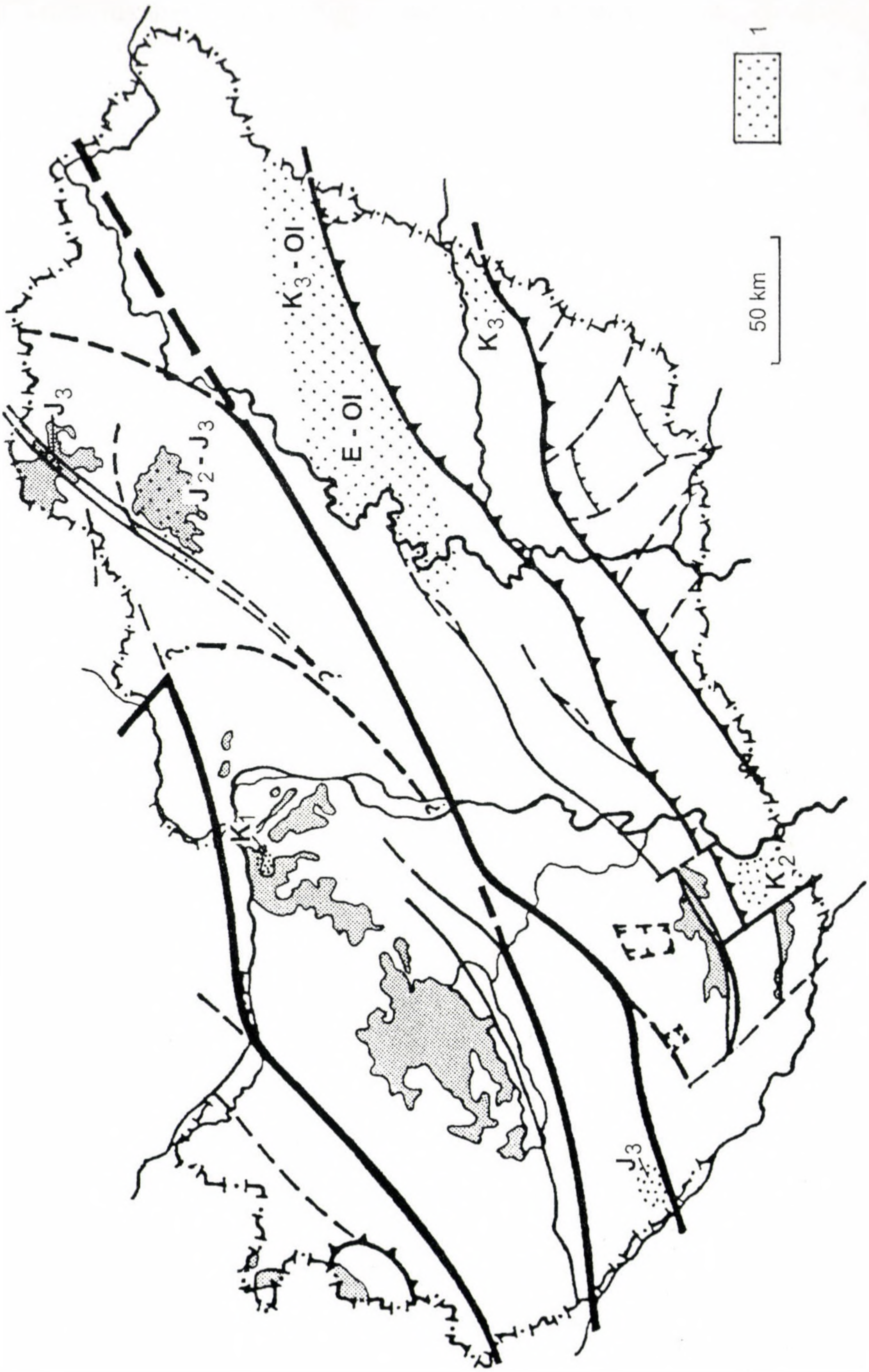
J_3
$J_2 - J_3$
K_1
$K_3 - Ol$
E - Ol
K_3
J_3
K_2
50 km
1

– 380–340 Ma-old Barrowian, intermediate-pressure metamorphism and anatectic granitisation;

– 340–310 Ma-old low-P and high-T metamorphism.

According to the available data these events are fairly well recognisable in the pre-Alpine complexes of the Tisia Terrane (c.f Table III; Szederkényi et al. 1991; Szederkényi 1996; Lelkes-Felvári et al. 1996), i.e. the pre-Alpine evolution of the Tisia Terrane did not represent an exception from the general trend of the European Variscan evolution. Granulitic metamorphism has not yet been proved in the Tisia Terrane. A general Gondwana origin is suggested for sialic complexes/terranes occurring south of the Rheic Ocean suture (cf. Oczlon 1994, for a latest review); however, the "Pan-African memory" has been obliterated in most of the units by the much more intense Variscan metamorphism. Such a situation is highly probable for the pre-Alpine units of the Tisia Terrane, as well (c.f. Neubauer et al. 1994) (Table III).

Apart from the formation of the Late Carboniferous–Late Permian fault-controlled basin in the Mecsek–Villány area (see above), the Variscan orogenic collage from which the future Tisia Terrane was derived did not essentially change until the Middle Jurassic Penninic rifting. Marine sedimentation in the territory of Tisia began in the Scythian in the S (Šikić et al. 1975; Čanović and Kemenci 1988; Bleahu et al. 1994; Kemenci and Čanović 1997) and the transgression had only reached the northernmost Villány–Bihor and Mecsek Zones by the Early Anisian ("Röt" event with evaporites; Török 1993, 1997, 1998; Bleahu et al., op. cit.), when most of epicontinental Europe (e.g. largely that part of the Variscan orogenic collage, which was not involved in the Alpine evolution) also became flooded by the sea. From this time until the Middle Jurassic Penninic rifting the northern zones of the Tisia Terrane (the Villány–Bihor, but especially the Mecsek Zone) showed an evolution corresponding to the most external Tethyan zones, the Mecsek Zone bearing evidence of its immediate proximity to the eastern extension of the "Vindelician Ridge" (which was most probably intermittent), constituting its continental hinterland. This is proved by the predominantly terrigenous sedimentation, by the short marine incursion in the Middle Triassic and by the thick, lower Liassic coal-bearing paralic sequence with its "Fleckenmergel" cover ending with the Bajocian. Separation of the Mecsek Zone from its continental hinterland is indicated by the abrupt cessation of the terrigenous input in the Bathonian, but its final detachment from the former Variscan orogenic collage is best marked by the Early Cretaceous continental rift-

Fig. 21 →

Stratigraphic columns showing the contrasting Late Variscan–Alpine sedimentary and magmatic evolution of the units presently juxtaposed along the Mid-Hungarian Lineament. 1. Continental clastics; 2. Evaporites; 3. Shallow marine carbonates; 4. Basinal/pelagic carbonates; 5. Late Variscan marine molasse; 6. Paralic coal-bearing siliciclastic sequence (Gresten Facies in the Liassic); 7. Marine, mixed siliciclastic--carbonate deposits (Werfen Facies in the Lower Triassic "Fleckenmergel" or Allgäu Facies in the Jurassic); 8. Flysch-type deposits; 9. Pelagic marls; 10. Rhyolites (Lower Permian); 11. Mainly andesites (Middle Triassic); 12. Alkaline rift-type basaltic rocks (Lower Cretaceous, partly Upper Jurassic)

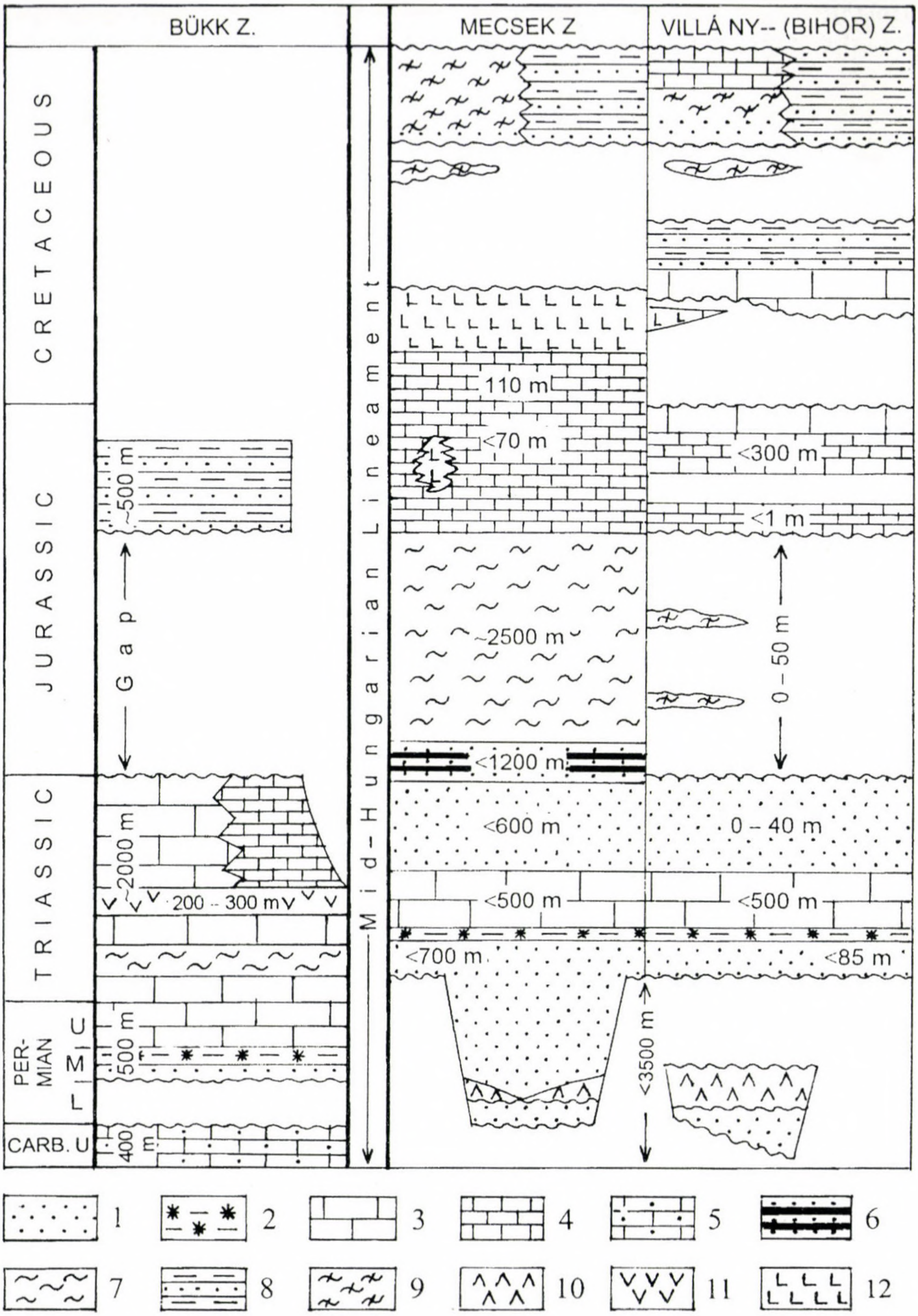
BÜKK Z.
MECSEK Z
VILLÁNY-- (BIHOR) Z.
CRETACEOUS
JURASSIC
TRIASSIC
PERMIAN
U
M
L
CARB. U
Mid-Hungarian Lineament
~500 m
Gap
~2000 m
200 - 300 m
500 m
400 m
110 m
<70 m
~2500 m
<1200 m
<600 m
<500 m
<700 m
<3500 m
<300 m
<1 m
0 - 50 m
0 - 40 m
<500 m
<85 m
1
2
3
4
5
6
7
8
9
10
11
12

Table III
Pre-Alpine metamorphic events recorded in the Tisia Terrane

440–400 Ma:	HP/LT metamorphism, recorded in a narrow, disrupted zone with ultramafics, amphibolites and eclogites (a possible Caledonian suture zone)
350–330 Ma:	Medium pressure Barrow-type metamorphism with kyanite. Syncollisional, anatectic granitization (mainly S-type)
330–320 Ma:	Low pressure metamorphism with andalusite. Postcollisional granitoid intrusions.

type alkaline basaltic magmatism (Harangi 1994 and pers. comm.; Harangi et al. 1996), which already began in the Trans-Tisza segment of the Mecsek Zone in the Late Jurassic (Bérczi-Makk 1986). This magmatism shows close affinity to the contemporaneous teschenitic magmatism of the Beskides (Silesian Zone) of the Polish Carpathians (Harangi, pers. comm.).

Nevertheless, the independent life of the Tisia Terrane with its rotations only began after the Aptian (Balla 1986) and lasted until its final docking into the terrane collage of the Pannonian basement by the Middle Miocene.

Summary – conclusions

– The terrane concept, as developed in other parts of the world (for example in the European Variscides or in the Pre-Alpine basement of the Alps), can readily be applied to the Pannonian basement.

– Comparative analysis of presently adjacent crustal masses (blocks, fragments, slivers) in the Hungarian part of the basement, based mostly on their sedimentary, magmatic and metamorphic evolution, has shown that they represent true "displaced" or "allochth
onous" terranes. They should not be called simply "suspect" terranes of uncertain affiliation, as their original relationships can be fairly well traced. Those presently juxtaposed along the Zagreb–Zemplín or Mid-Hungarian Lineament can be considered as true "exotic" terranes, as they show entirely different Variscan and Alpine evolution and relationships.

– Most of the terranes considered herein represent displaced continental margin blocks/fragments, which are distinguished by their distinct Mesozoic (and partly Palaeozoic) sedimentary successions, the differences between them

Fig. 22 →
Oligocene lithofacies of Hungary. 1. Oligocene marine formations; 2. Oligocene brackish and terrestrial formations; 3. Oligocene marine formations in (partly) flysch facies; 4. Volcano

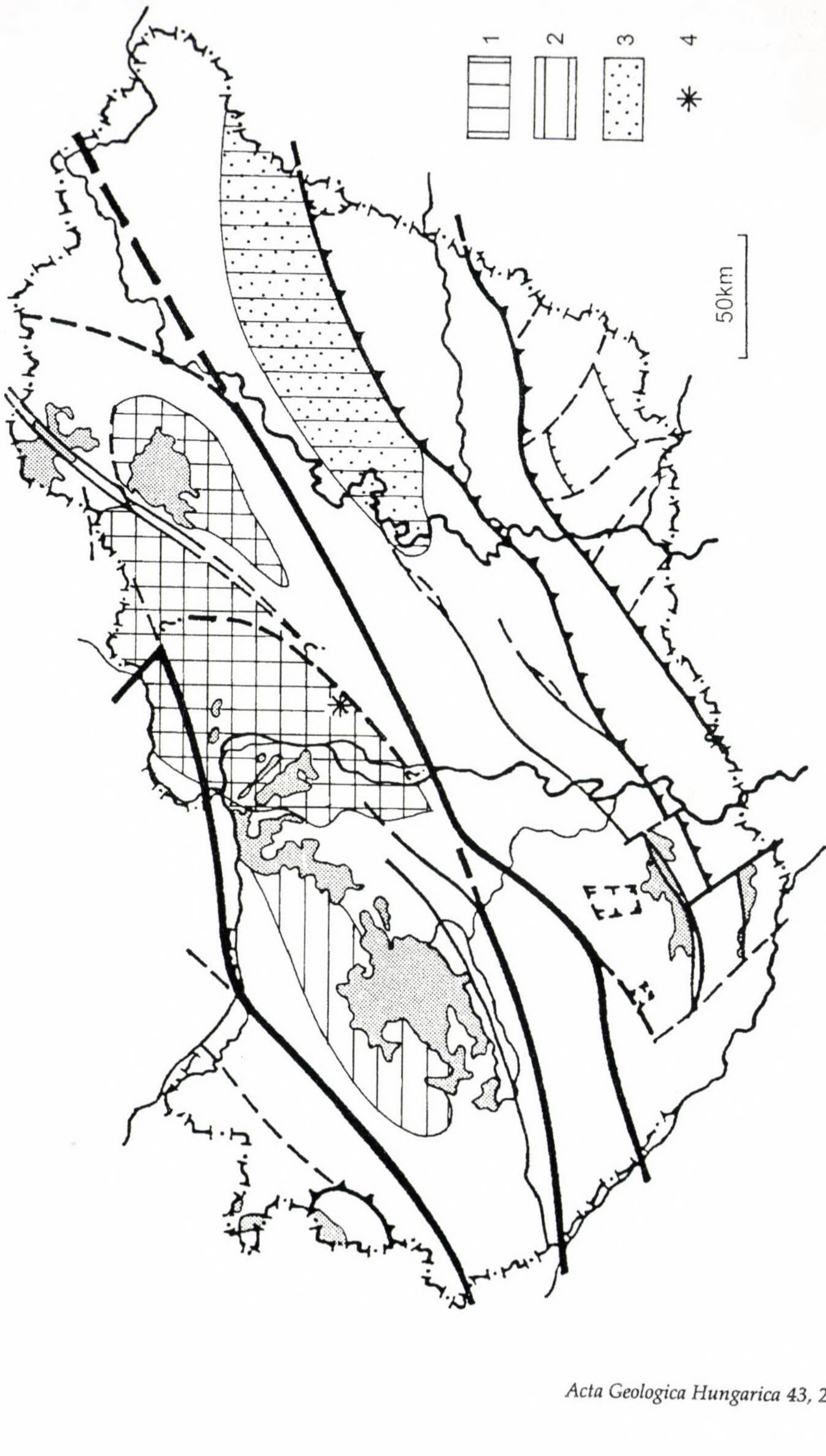
1
2
3
4
50km

being not explainable by lateral facies transition. Although between the Bakonyia and Bükk Parautochthon Terranes a facies transition could be supposed, their different tectonometamorphic evolution precludes considering them as a single terrane.

– Development of the Pannonian basement units can be traced back to the accretion of the European Variscan orogenic collage. However, Pre-Alpine basement complexes of the Tisia and Pelsonia Terranes show relationships opposite to their present N–S setting. This Variscan orogenic collage, in the region where the different Pannonian basement units have derived from, was effected by a Middle Triassic (Neotethyan), then by Middle Jurassic (Penninic) rift dispersion. Amalgamation and accretion of these terranes, resulting in their present setting, took place through multistage dispersion (mainly related to strike-slip faulting) and -accretion processes from the Late Jurassic to the Early Miocene.

– The Pannonian basement can be regarded as a true "terrane collage". Boundaries of its terranes/units are overstepped by Middle Miocene sediments (only the eastern part of the Hurbanovo–Diósjenő Line is covered by Upper Oligocene ones). This fact casts major doubts on Pre-Neogene (and especially Pre-Tertiary) palaeotectonic and palaeogeographic reconstructions based on the present arrangement of these blocks/terranes (see also below).

– The large Tisia Terrane, comprising the entire lithosphere (Posgay et al. 1995), can be regarded as a microcontinent (in sense of Howell 1989). The evolution of its Pre-Alpine metamorphic complexes (Szederkényi et al. 1991; Szederkényi 1996; Lelkes-Felvári et al. 1996) does not show any deviation from the general trend of the European Variscides, which is considered as an orogenic collage accreted during a long-lasting, multistage accretion of Gondwana-derived Pan-African continental blocks and intervening oceanic zones (c.f. Matte 1986, 1991; Matte et al. 1990; Franke 1989). Available geochronological data show a fairly good correlation of metamorphic events (see references cited above).

The Mórágy Complex (Mecsek Zone) of the Tisia Terrane with its syn-collisional, anatectic granitisation and characteristic metamorphic development can be considered as originally forming the continuation of the southern Variscan collisional zone, characterised by the granite range of Massif Central – Vosges – Black Forest – Moldanubicum and Helvetic basement of the western Alps (=Moldanubian Zone in the former literature or Moldanubian–Helvetic Terrane according to von Raumer and Neubauer 1993) (Buda 1995, 1996; see figs 12 and 13 in the present contribution). The more southern parts of the Tisia Terrane could have been in the continuation of the Median Crystalline Zone of the Alps (in the sense of Neubauer and von Raumer 1993). This is supported by the granitoids of the Battonya Unit of the Békésia Terrane, showing affinity to the West Carpathian granitoids (Buda 1995, 1996) (such a setting, however, involves an originally more westerly location of the East Alpine and Tatro-Veporic units, as suggested by Michalík 1994).

Large amounts of siliciclastics were transported into the Mecsek Zone (located in the Early Mesozoic in the most external Tethyan zone) from a northerly adjacent continental hinterland during the Early and Late Triassic and especially during the Early and Middle Jurassic. In this zone a range of half-graben structures developed at the northern foot of the Villány–Bihor Swell, in which up to several 1,000 m of sediments of "Gresten" and "Allgäu" (or "Fleckenmergel")-type were deposited. The future Tisia terrane split off from the Variscan orogenic collage in the Bathonian as shown by sedimentological evidence, but the climax of the rifting was in the Early Cretaceous as shown by the paroxysm of alkaline rift-type magmatism (Harangi 1994; Harangi et al. 1996). Palaeomagnetic evidence shows, however, rotation of the terrane (i.e. when it really behaved as a "terrane", independent from any other unit) at earliest in the Berriasian–Valanginian (Márton, this volume).

– Theories assuming an island setting of the Tisia Terrane during the early Mesozoic (c.f. Trunkó 1996), which would imply filling up the above-mentioned half-graben structures with siliciclastic sediments of granitoid-metamorphic provenance either from the Middle Triassic dolomite platform of the Villány–Bihor Swell, or from the presently northerly adjacent South Alpine–Dinaridic terranes (in which marine carbonate sedimentation has been recorded since the Permian), should be rejected in the light of surface and subsurface geologic data accumulated from the central zones of the Pannonian basement during many decades of geologic research. Models assuming an active margin setting of the Mecsek Zone, facing a northerly adjacent subduction zone during the Late Jurassic–Early Cretaceous (c.f. Froitzheim et al. 1996), should also be rejected on the same grounds.

– As opposed to the Tisia Terrane, the Pelsonia Terrane is a multiple composite terrane, consisting of a larger single terrane (Bakonyia) and three smaller composite terranes (Zagorje–Mid-Transdanubia, Bükkia and Aggtelekia, respectively). In its Hungarian part at least 7–9 smaller terranes of Inner Dinaridic, South Alpine and (in NE Hungary) Upper Austroalpine (but certain Inner Dinaridic relations of the latter are also conspicuous!) can be distinguished. Thus, it represents a real "collage", as first pointed out indirectly by Balla (1988a). These are all crustal fragments, not comprising the entire lithosphere (i.e. they cannot be considered as microcontinents), mostly of continental margin and partly of oceanic origin (even the largest one, the Bakonyia, comprises only the upper parts of the crust; c.f. Tari 1996). Multistage strike-slip faulting resulted mainly in the dispersion of its blocks from their original relationships and amalgamation-accretion into their present setting within the southern part of the large ALCAPA Composite Terrane (Csontos et al. 1992). These movements, also accompanied in the final stage (Early Miocene) by gravitational collapse recorded in the easternmost Alpine–western Pannonian region (Tari, op. cit.), destroyed and dispersed former nappe systems brought about by Eohellenic and Palaeoalpine stackings.

In this context, however, it should be noted that, although on seismic sections the Bakonyia Terrane appears in a "Para-Upper Austroalpine" setting (Tari, op. cit.), during the Late Mesozoic it moved palaeomagnetically in co-ordination with the Southern Alps, considerably differently from the Northern Limestone Alps (Mauritsch and Márton 1995).

A 400–500 km offset of the Palaeozoic and Mesozoic facies zones of the ALCAPA or Pelsonia Composite Terrane was pointed out in respect to those of the Southern Alps–NW Dinarides and to those of the Eastern Alps (Majoros 1980; Ebner et al. 1991, 1998; Haas et al. 1995; Haas and Budai 1995; Vörös and Galácz 1998). Whereas Palaeozoic to Early Cretaceous facies show good correlation with the South Alpine ones, Late Cretaceous facies of the Bakonyia Terrane clearly show that its eastward-directed lateral displacement already began at that time (Császár and Haas, in prep.). This contradicts the simple Tertiary escape model proposed by Kázmér and Kovács (1985; cf. also Haas 1987), which should rather have been understood as displacement of a "collage of blocks" in sense of Balla (1988a), in which the individual blocks moved relative to each other as well. Recent structural geologic investigations in the West Carpathians (Plašienka 1997; Neubauer et al. 1996) provided evidence, however, that the northerly, sinistral offset should have been formed prior the Late Cretaceous nappe stacking. Even in case of some units in NE Hungary (and SE Slovakia) these displacements resulting in the (undoubtedly existing) sinistral offset (i.e. relative to the eastern end of the Eastern Alps) probably began during the Late Jurassic closure of Neotethyan oceanic tract(s), as suggested for the Eastern Alps by Tollmann (1987) and Frank et al. (1987). The dextral offset along the Periadriatic-Balaton lineament system, however, is indeed the result of large-scale Late Oligocene–Miocene strike-slip faulting (c.f. Csontos et al. 1992; Fodor et al. 1998).

– The Pre-Alpine basement units of the Pelsonia Composite Terrane – especially those in NE Hungary, with no proof (or at least up to now without recognisable evidence) of a Variscan tectonometamorphic event – were parts of the southern Variscan foreland, e.g. of the Noric–Bosnian Zone (in sense of Neubauer and von Raumer 1993) or of the Carnic–Dinaridic microplate (in sense of Vai 1995). This is especially valid for units with Carboniferous flysch sediments (Bükk PA and Szendrő Units), which were deposited in the flysch basin, developing above the downwarping "Pre-Apulian" lithosphere due to "loading by incoming thrust sheets of the Median Crystalline Zone" (Neubauer and von Raumer, op. cit.).

– The collage of the Pelsonia Composite Terrane comprises continental margin fragments that were parts of the Adriatic (Apulian) or South Alpine–Dinaridic continental margin of the Neothethyan Ocean, as well as remnants of its tract(s). The uppermost unit of the Aggtelekia CT, the Aggtelek–Bódva Unit, was located at the opposite margin of this tract, or of one of these tracts. In the latter case, it could be the margin of a continental microblock (the Drina–Ivanjica Terrane of the Dinarides in the sense of Dimitrijevic and Dimitrijevic 1991 could be an analogue for such a microblock).

– The collage-like composite character of the Pelsonia Terrane implies that no Pre-Tertiary palaeogeographic and palaeotectonic reconstruction can be carried out in the southern West Carpathian–North Pannonian domain (i.e. south of the Tatric Composite Terrane, in the sense of Vozárová and Vozár 1996) on the basis of the present distribution of these blocks, as was already clearly emphasised by Balla (1988a). Therefore, the probability of models based only upon simple orthogonal opening and likewise orthogonal closing of Early Mesozoic oceanic basin(s), in the traditional "cylindristic" way, disregarding the obvious W to E lateral facies offsets shown by the Palaeozoic and Mesozoic sequences of the Pelsonia CT, is very low, if any.

Acknowledgements

Financial support for the preparation of the present review was provided by the National Research Fund (OTKA), projects No. T 019431 (S. K.), T 4158 and T 017368 (T. Sz.) and T 029797 (J. H.), as well as by the Hungarian Academy of Sciences. Results of the projects, T 23762 (Gy. B.), T 025534 (G. Cs.) and T 029655 (A. N.) are also included herein.

Many years of co-operation with the national terrane map co-ordinators of former IGCP 276 from the surrounding countries, as well as with other colleagues, greatly contributed to understanding the setting and connections of the basement units of Hungary. We have especially benefited from discussions and exchange of views with F. Ebner (Austria), J. Pamić, B. Tomljenović (Croatia), G. Migiros, D. Papanikolaou (Greece), H. G. Kräutner, R. Dimitrescu (Romania), A. Vozárová, J. Vozár (Slovakia), P. Mioč (Slovenia), M. N. and M. D. Dimitrijević, S. Karamata, B. Krstić, I. Filipović (Yugoslavia), P. Árkai, Z. Balla, L. Csontos, S. Józsa, Cs. Péró, E. Rálisch-Felgenhauer, and K. Török (Hungary), which is gratefully acknowledged here.

S. Karamata (Beograd), J. Pamić (Zagreb), A. Vörös and B. Koroknai (Budapest) reviewed the first draft; their critical comments and helpful suggestions greatly improved the paper. K. Szoldán drew the figures; B. Koroknai and L. Fodor computerised Fig. 1; G. Schmiedl and Á. Kriván-Horváth helped in editing the text and Mrs. L. Koi provided technical assistance; all these are sincerely appreciated by the authors. Our special thanks are due to H. M. Lieberman (Houston) for linguistic corrections.

References

Ádám, A. 1985: Electric conductivity increases in the Earth's crust in Transdanubia (W-Hungary). – Acta Geod. Geoph. Mont. Hung., 20/1, pp. 173–182, Budapest.

Aigner-Torres, M., F. Koller 1999: Nature of the magma source of the Szarvasko Complex (NE-Hungary): petrological and geochemical constraints. – Ofioliti, 24/1, pp. 1–12.

Albani, R., Gy. Lelkes-Felvári, M. Tongiorgi 1985: First record of Ordovician (Upper Arenigian, Acritarchs) beds in Bakony Mts., Hungary. – N. Jb. Geol. Paläont., Abh., 170/1, pp. 45–65, Stuttgart.

Andelkovic, M. 1976: Structural yoning of the Inner and Central Dinarides of Yugoslavia. – Ann. Geol. de la Peninssula Balkanique, 40, pp. 1–12.

Árgyelán, G. B. 1996: Geochemical investigations of detrital chrome spinels as a tool to detect an ophiolitic source area (Gerecse Mountains, Hungary). – Acta Geol. Hung., 39/4, pp. 341–368, Budapest.

Árkai, P. 1983: Very low- and low-grade Alpine regional metamorphism of the Paleozoic and Mesozoic formations of the Bükkium, NE-Hungary. – Acta Geol. Hung., 26, pp. 83–10, Budapest.

Árkai, P. 1984: Polymetamorphism of the crystalline basement of the Somogy-Drava Basin (Southwestern Transdanubia, Hungary.). – Acta Miner. Petr. Szeged., 26/2, pp. 129–153, Szeged.

Árkai, P. 1987a: New data on the petrogenesis of metamorphic rocks along the Balaton Lineament, Transdanubia, W-Hungary. – Acta Geol. Hung., 30/3–4, pp. 319–338, Budapest.

Árkai, P. 1987b: Contribution to the knowledge of the polymetamorphic basement of the Great Plain (Pannonian Basin, East Hungary): the environment of the Derecske Depression. – Fragmenta Miner. Palaeont. 13, pp. 7–30, Budapest.

Árkai, P. 1990: Very-low and low-grade metamorphic rocks in the Pre-Tertiary basement of the Drava Basin, SW Hungary. Mineral assemblages, illite "crystallinity", bo data, and problems of geological correlation. - Acta Geol. Hung., 33/1–3, pp. 43–67, Budapest.

Árkai, P. 1991: Alpine regional metamorphism of the different tectonic domains in the Hungarian part of the Pannonian Basin. – In: Baud, A., Thélin, P., Stampfli, G. (Eds): IGCP Project No. 276 "Paleozoic geodynamic domains annd their Alpinic evolution in the Tethys", Newsletter No. 2. Mém. Géol. (Lausanne), N. 10, pp. 5–13.

Árkai, P., Kad. Balogh 1989: The age of metamorphism of the East Alpine type basement, Little Plain, W-Hungary: K-Ar dating of K-white micas from very low and low-grade metamorphic rocks. – Acta Geol. Hung., 32/1–2, pp. 131–147, Budapest.

Árkai, P., Kad. Balogh, I. Dunkl 1995: Timing of low-temperature metamorphism and cooling of the Paleozoic and Mesozoic formations of the Bükkium, innermost Western Carpathians, Hungary. – Geol. Rundsch., 84, pp. 334–344, Stuttgart.

Árkai, P., Z. Horváth, M. Tóth 1987: Regional metamorphism of the East Alpine type Paleozoic basement, Little Plain, W-Hungary: mineral assemblages, illite crystallinity, -b_0 and coal rank data. – Acta Geol. Hung., 30/1–2, pp. 153–175, Budapest.

Árkai, P., S. Kovács 1986: Diagenesis and regional metamorphism of the Mesozoic of Aggtelek-Rudabánya Mts. (Northeast Hungary). – Acta Geol. Hung., 29/3–4, pp. 349–373, Budapest.

Árkai, P., Cs. Lantai, I. Fórizs, Gy. Lelkes-Felvári 1991: Diagenesis and low-temperature metamorphism in a tectonic link between the Dinarides and the Western Carpathians: the basement of the Igal (Central Hungarian) Unit. – Acta Geol. Hung., 34/1–2, pp. 81–100, Budapest.

Árkai, P., Cs. Lantai, Gy. Lelkes-Felvári, G. Nagy 1995: Biotite in a Paleozoic metagreywacke complex, Mecsek Mountains, Hungary: conditions of Low-T metamorphism deduced from illite and chlorite crystallinity, coal rank, white mica geobarometric and microstructural data. – Acta Geol. Hung., 38/4, pp. 293–318, Budapest.

Árkai, P., Gy. Lelkes-Felvári 1987: Very low- and low-grade metamorphic terraines of Hungary. – In. Flügel, H.W., F.P. Sassi, P. Grecula. (Eds): Pre-Variscan and Variscan events in the Alpine-Mediterranean mountain belts. – Miner. slovaca, Monographs, pp. 51–68, Alfa, Bratislava.

Árkai, P., G. Nagy, G. Dobosi 1985: Polymetamorphic evolution of the South Hungarian crystalline basement, Pannonian Basin: geothermic and geobarometric data. – Acta Geol. Hung., 28/3–4, pp. 165–190, Budapest.

Árkai, P., E. Árva-Sós., G. Bagoly-Árgyelán, L. Csontos, L. Dosztály, Z. Gulácsi, P. Horváth, S. Józsa, S. Kovács 1998: Neotethyan oceanic assemblages in NE Hungary: A review of present knowledge.– Carpathian-Balkan Geological Association, XVI. Congress, Vienna, Austria, 1998, Abstract volume, p. 45.

Árva-Sós, E., Kad. Balogh, L. Ravasz-Baranyai, Cs. Ravasz 1987: K/Ar dates of Mesozoic igneous rocks in some areas of Hungary. (In Hung., with English summ.). – M. Áll. Földt. Int. Évi Jel., 1985, pp. 295–307, Budapest.
Árva-Sós, E., S. Józsa 1992: Tectonic apprasial af K-Ar data of Mesozoic ophiolitic mafic rocks of Darnó Hill, Northern Hungary. – Abstract Supplement No. 2 to Terra nova, v. 4, 1992, Graz, Austria.
Bagoly-Árgyelán, G., Z. Gulácsi 1997: Acidic extrusive and plutonic lithic fragments in the silici-clastic sediment of the Darnó and Szarvasko Unit. – Terra Nostra, Sediment '97 Abstracts, p. 3, Heidelberg.
Báldi, T., M. Báldi-Beke 1985: The evolution of the Hungarian Paleogene basins. – Acta Geol. Hung., 28/1–2, pp. 5–28, Budapest.
Báldi-Beke, M. 1984: The nannoplankton of the Transdanubian Paleogene formations. – Geol. Hung., Ser. Palaeont., 43, 307 p, Budapest.
Balla, Z. 1981: Plate tectonic interpretation of the South Transdanubian ultramafics. – Acta Miner.-Petr. Szeged, 25, pp. 3–24, Szeged.
Balla, Z. 1982: Development of the Pannonian basin basement through the Cretaceous–Cenozoic collision: a new synthesis. – Tectonophysics, 88/1, pp. 61–102, Amsterdam.
Balla, Z. 1986: Analysis of the anti-clockwise rotation of the Mecsek Mountains (Southwest Hungary) in the Cretaceous: interpretation of paleomagnetic data in the light of the geology. – Geophys. Transact., 32/2, pp. 147–181, Budapest.
Balla, Z. 1987: Tectonics of the Bükkian (North Hungary) Mesozoic and relations to the West Carpathians and Dinarids. – Acta Geol. Hung., 30/3–4, pp. 257–287, Budapest.
Balla, Z. 1988a: Late Eocene tectonic pattern of the Carpatho-Pannonian region and its bearing on the Mesozoic reconstructions of the Tethys. – Földt. Közl., 118/1, pp. 11–26, Budapest, (in Hung., with English abstr.).
Balla, Z. 1988b: On the origin of the structural pattern of Hungary. – Acta Geol. Hung., 31/1–2, pp. 53–63, Budapest.
Balla, Z. 1993: On the tectonic position of weakly metamorphic rocks in the basement of the Little Hungarian Plain. – Földt. Közl., 123/4, pp. 465–500, Budapest, (in Hung., with English abstr.).
Balla, Z. 1994: Basement tectonics of the Danube Lowlands. – Geol. Carpath., 45/5, pp. 271–281.
Balla, Z., I. Bodrogi 1993: The Vékény Marl Formation of Hungary. – Cretaceous Research, 14, pp. 431–448.
Balla, Z., A. Dudko 1989: Large-scale Tertiary strike-slip recorded in the structure of the Transdanubian Range. – Geophys. Transact., 32/1–2, pp. 3–63, Budapest.
Balla, Z., A. Dudko 1993: Tectonics of the Transdanubian Range. – Excursion guide, ALCAPA Workshop, Sümeg, 1993, pp. 3–24, Budapest.
Balla, Z., D. Hovorka, M. Kuzmin, V. Vinogradov 1983: Mesozoic ophiolites of the Bükk Mountains (North Hungary). – Ofioliti, 8/1, pp. 5–46, Bologna.
Balla, Z., M. Tátrai, A. Dudko 1987: Neotectonics of Mid-Transdanubia on the basis of geological and geophysical data. – M. Áll. Eötvös Loránd Geofiz. Int. Évi Jel., 1986, pp. 74–94, Budapest, (in Hungarian).
Balogh, K. 1964: Die geologischen Bildungen des Bükk-Gebirges. – Ann. Inst. Geol. Hung., 48/2, pp. 245–719, Budapest.
Balogh, K., A. Barabás 1972: The Carboniferous and Permian of Hungary. – Acta Miner. Petr. Szeged, 23, pp. 49–69, Szeged.
Balogh, Kad., E. Árva Sós, Gy. Buda 1983: Chronology of granitoid and metamorphic rocks of Transdanubia (Hungary). – Ann. Inst. Geol. Geofiz., 6, pp. 359–364, Bucuresti.
Balogh, Kad., E. Árva-Sós, Z. Pécskay 1991: Chronological investigation of the Bükkium by K/Ar method. (In Hung.). – Unpubl. research report, ATOMKI, Debrecen.
Balogh, Kad., Á. Kovách 1973: A battonyai kvarcporfir korának meghatározása Rb-Sr módszerrel (Age determination of the Battonya quartzporphiry by Rb-Sr method. – ATOMKI Közl., 15/4, pp. 245–249 (in Hungarian), Debrecen.

Balogh, Kad., Á. Kovách, Z. Pécskay, É. Svingor, P. Árkai 1990: Very low and low-grade metamorphic rocks in the pre-Tertiary basement of the Drava Basin, SW-Hungary. II. K-Ar and Rb-Sr isotope geochronologic data. – Acta Geol. Hung., 33/1–4, pp. 69–78, Budapest.
Barabás-Stuhl, Á. 1993: Palynological reevaluation of Lower Triassic and Lower Anisian formations of Southeast Transdanubia. – Acta Geol. Hung., 36/4, pp. 405–458, Budapest.
Bérczi, I., J. Kókai, V. Dank, A. Somfai 1981: Some New Results for Petroleum Geology Obtained by Hydrocarbon Exploration Wells Drilled in the Hungarian Part of the Pannonian Basin. – Earth Evol. Sci., 3–4, pp. 301–306, Amsterdam.
Bérczi-Makk, A. 1978: Upper Permian marine sediments in the hydrocarbon exploring borehole Sári-2, southeast of Budapest (Hungary). – Földt. Közl., 108/3, pp. 313–327, Budapest, (in Hung., with English summ.).
Bérczi-Makk, A. 1986: Mesozoic formation types of the Great Hungarian Plain. – Acta Geol. Hung., 29/3–4, pp. 261–282, Budapest.
Bérczi-Makk, A., 1993: Békés Unit. – In: Barabás-Stuhl et al.: Lithostratigraphic basic units of Hungary, Triassic, pp. 265–270, Hung. Geol. Inst., Budapest, (in Hungarian).
Bérczi-Makk, A. 1996: Foraminifera of the Triassic formations of Alsó Hill (Northern Hungary). Part 2: Foraminifer assemblage of the Wetterstein Limestone Formation. – Acta Geol. Hung., 39/3, pp. 223–309, Budapest.
Bérczi-Makk, A., B. Cserepes-Meszéna 1985: Geology of the pre-Neogene basement of Nagykőrös (Central Hungary). (In Hung., with English abstr.). – Földt. Közl., 115/3, pp. 249–256, Budapest.
Bérczi-Makk, A., J. Haas, E. Rálisch-Felgenhauer, A. Oravecz-Scheffer 1993: Upper Paleozoic-Mesozoic formations of the Mid-Transdanubian Unit and their relationships. – Acta Geol. Hung., 36/3, pp. 263–296, Budapest.
Bérczi-Makk, A., P. Pelikán 1984: Jurassic rocks from the Bükk Mts.) – M. Áll. Földt. Int. Évi Jel., 1982, pp. 137–167, Budapest, (in Hung., with English summ.).
Bérczi-Makk, A., V. Kochansky-Devidé 1981: Marine Lower and Middle Permian in the oil exploratory well Újfalu-I. (SW-Hungary). – Acta Geol. Hung., 24/1, pp. 117–128, Budapest.
Bignot, G., J. Haas, A. F. Poignant 1984: The limestone with Corallinaceae of the Upper Cretaceous of Sümeg (Transdanubia, Hungary): paleogeographic implications. – Acta Geol. Hung., 27/3-4, pp. 429–440, Budapest.
Bleahu, M. et al. 1994: Triassic facies types, evolution and paleogeographic relations of the Tisza Megaunit. – Acta Geol. Hung., 37/3–4, pp. 187–234, Budapest.
Bleahu, M., S. Bordea, M. Lupu, A. Stefan, D. Patrulius, S. Panin, S. 1981: The structure of the Apuseni Mts. – XII. Congr. Carpatho-Balkan Geol. Assoc., Guide to excursion B3, 107 p., Bucharest.
Bodrogi, I., M.A. Conrad, H. Lobitzer 1993: Lower Cretaceous Dasycladales from the Villány Zone, Southwest Hungary – Biogeographical Significance. – Boll. Soc. Paleont. Ital., Spec. Vol. 1, pp. 59–68, Modena.
Bögel, H. 1975: Zur Literatur über die "Periadriatische Naht". – Verh. Geol. B.-A., 1975/2–3, pp. 163–199, Wien.
Brezsnyánszky, K., J. Haas 1986: Main features of the pre-Tertiary basement of Hungary. – Geol. Carpath., Geol. Zborn., 37/3, pp. 297–303, Bratislava.
Broglio Loriga, C., F. Góczán, J. Haas, K. Lenner, C. Neri, A. Oravecz-Scheffer, R. Posenato, I. Szabó, Á. Tóth-Makk 1990: The Lower Triassic sequences of the Dolomites (Italy), Transdanubian Mid-Mountains (Hungary), their correlation. – Mem. Sci. Geol., 42, pp. 41–103, Padova.
Buda, Gy. 1981: Genesis of the Hungarian granitoid rocks. – Acta Geol. Hung., 24/2–4, pp. 309–318, Budapest.
Buda, Gy. 1985: Variszkuszi korú kollíziós gránitoidok képzodése Magyarország, Ny-i Kárpátok és a Központi Cseh-masszivum gránitoidjainak példáján (Genesis of Variscan collisional granitoids on the example of granitoids of Hungary, West Carpathians and Central Bohemian Massif). – Kand. Diss. MTA Library (in Hungarian).

Buda, Gy. 1995: Correlation of Middle European Variscan granitoids. – Habil. thesis (in Hung.), Budapest.
Buda, Gy. 1996: Correlation of Variscan granitoids occuring in Central Europe. – Acta Miner. -Petr. Szeged, 37, Suppl., p. 24.
Buda, Gy., Gy. Lovas, U. Klötzli, B.L. Cousens 1999: Variscan granitoids of the Mórágy Hills (South Hungary). – Beih. z. Eur. J. Mineral., 11,
Budai, T., A. Vörös 1992: Middle Triassic history of the Balaton Highland: extensional tectonics and basin evolution. – Acta Geol. Hung., 35/3, pp. 237–250, Budapest.
Čanovič, M., R. Kemenci 1988: Mezozoik podine Panonskog basena u Vojvodini (The Mesozoic of the Pannonian Basin in Vojvodina [Yugoslavia]). – 337 p., Matica srpska, Novi Sad, (in Serbo-Croatian, with English summ.).
Clifton, H.E., K. Brezsnyánszky, J. Haas 1984: Lithological characteristics and paleogeographic significance of resedimented conglomerate of Late Cretaceous age in Northern Hungary. – Geophys. Transact., 31/1–3, pp. 131–155, Budapest.
Coney, P.J., D.L. Jones, J.W.H. Monger 1980: Cordilleran suspect terranes. – Nature, 288, pp. 329–333.
Császár G., E. Jocha-Edelényi, J. Knauer, K. Szentgyörgyi 1993: Terrestrial and shallow marine Cretaceous clastics of Hungary. – Cretaceous Research, 14, pp. 307–335, London.
Császár, G. 1992: Urgonian facies of the Tisza Unit. – Acta Geol. Hung., 35/3, pp. 263–285, Budapest.
Császár, G., G. Bagoly-Árgyelán 1994: Stratigraphic and micromineralogic investigation on Cretaceous formations in the Gerecse Mountains, Hungary and their paleogeographic implications. – Cretaceous Research, 15, pp. 417–434, London.
Császár, G., I. Fridel-Matyók, I. Kovács-Bodrogi 1983: Cretaceous rocks drilled at Nagybaracska (S Hungary). – M. Áll. Földt. Int. Évi Jel., 1981, pp. 213–238, Budapest.
Császár, G., J. Haas 1984: The Cretaceous in Hungary: a review. – Acta Geol. Hung., 27/3-4, pp. 417–428, Budapest.
Császár, G in press
Csillag, J., J. Földessy, T. Zelenka, E. Balázs 1980: The plate tectonic setting of the Eocene volcanic belt in the Carpathian Basin. – In: Proc. 17th Assembly of the ESC, pp. 589–599, Budapest.
Csontos, L. 1988: Etude géologique d'unes portion des Carpathes internes: le massif du Bükk (NE de la Hongrie). (Stratigraphie, structures, métamorphism et géodynamique). – Thése de doctorat, Univ. Sci. Techn., Lille Flandres-Artois, 250, 327 p. Lille.
Csontos, L. 1999: Structural outline of the Bükk Mts., N Hungary. – Földt. Közl., 129/4, pp. 611–651, Budapest, (in Hung., with English abstr.).
Csontos, L. 2000: Stratigraphic reevaluation of the Bükk Mts., N Hungary. – Földt. Közl., 130/1, pp. 95–131, Budapest, (in Hung., with English abstr.).
Csontos, L., A. Nagymarosy 1998: The Mid-Hungarian line: a zone of repeated tectonic inversions. – Tectonophysics, 297, pp. 51–71.
Csontos, L., A. Nagymarosy, F. Horváth, M. Kovác, M. 1992: Tertiary evolution of the Intra-Carpathian area: a model. – Tectonophysics, 208, pp. 221–241, Amsterdam.
Dallmeyer, D.R., F. Neubauer, R. Handler, H. Fritz, W. Müller, d. Pana, M. Putis 1996: Tectonothermal evolution of internal Alps and Carpathians: Evidence from 40Ar/39Ar mineral and whole-rock data. – Eclogae Geol. Helv., 89, pp. 203–227.
Dank, V., J. Fülöp et al. 1990: Tectonic map of Hungary. 1:500 000. – Hung. Geol. Inst., Budapest.
Demény, A., D. Sharp., H.R. Pfeiffer 1990: Mg-metasomatism and formation conditions of Mg-chlorite-muscovite-quartzphyllites (leucophyllites) and their relations to Alpine whiteschists. – Contr. Min. Petr., 128, pp. 247–260.
De Wever, P. 1984: Triassic radiolarians from the Darnó area (Hungary). – Acta Geol. Hung., 27/3-4, pp. 295–306, Budapest.
Dewey, J. F., I. G. Gass, G. B Curry, N. B. W. Harris, A. M. C. Sengör (Eds) 1990: Allochthonous terranes. – Phil. Trans. R. Sci. Lond., A 331, pp. 455–647.
Dimitrijević, M.D. 1992: Geological Atlas of Serbia. 1:2 000 000. – Geological Map. Grafimex, Belgrade.

Dimitrijević, M.N., M.D. Dimitrijević 1991: Triassic carbonate platform of the Drina–Ivanjica element (Dinarides). – Acta Geol. Hung., 34/1, pp. 15–44, Budapest.
Dosztály, L. 1994: Mesozoic radiolarian investigations in Northern Hungary. 108 p., unpubl. thesis, (in Hungarian) Budapest.
Dosztály, L., S. Józsa 1992: Geochronological evaluation of Mesozoic formations of Darnó Hill at Recsk on the basis of radiolarians and K-Ar age data. – Acta Geol. Hung., 35/4, pp. 371–393, Budapest.
Dudko, A. 1988: Tectonics of the Balatonfo-Velence area. – Földt. Közl., 118/3, pp. 207–218, Budapest, (in Hung. with English abstr.).
Dudko, A., Gy. Lelkes-Felvári 1992: Variscan tectonics of the Transdanubian Range. – M. Áll. Földt. Int. Évi Jel., 1990, pp. 39–67, Budapest, (in Hung., with English abstr.).
Dumitrica, P., J. Mello 1982: On the age of the Meliata Group and the Silica Nappe radiolarites (localities Držkovce and Bohúnovo, Slovak Karst, CSSR). – Geol. práce, Správy 77, pp. 17–28, Bratislava.
Ebner, F. 1992: Correlation of marine Carboniferous sedimentary units of Slovakia, Hungary and Austria. – In: J. Vozár (Ed.): Western Carpathians, Eastern Alps, Dinarides. Special volume to the problems of the Paleozoic geodynamic domains (IGCP 276). – Dionýz Štúr Inst. geol., Bratislava, pp. 37–47.
Ebner, F., S. Kovács, H.P. Schönlaub. 1991: Das klassische Karbon in Österreich und Ungarn ein Vergleich der sedimentären fossilführenden Vorkommen. – In: Lobitzer, H., G. Császár (Eds): Jubiläumschrift 20 Jahre Geologische Zusammenarbeit Österreich–Ungarn, pp. 263–294, Wien.
Ebner, F., S. Kovács, H.P. Schönlaub 1998: Stratigraphic and facial correlation of the Szendrő-Uppony Paleozoic (NE Hungary) with the Carnic Alps–South Karawanken Mts. and Graz Paleozoic (Southern Alps and Central Eastern Alps); some paleogeographic implications. – Acta Geol. Hung., 41/4, pp. 355–388, Budapest.
Ebner, F., F. Neubauer, G. Rantitsch, G. (Eds) 1996/1997: Terrane Map of the Alpine Himalayan Belt. 1:2 500 000. – In: Papanikolaou, D. (Ed.) IGCP Project No. 276 Terrane Maps and Terrane Descriptions. – Ann. Géol. Pays Helléniq., 37 p.
Ellenberger, F., A.L.G. Tamain 1980: Hercynian Europe. – Episodes, 1980/1, pp. 22–27.
Faryad, S. W. 1993: Geothermo-barometry of metamorphic rocks from the Zemplenicum (Western Carpathians, Slovakia). – Geol. Carpath., 46/2, pp. 193–123.
Fazekas, V., Gy. Majoros, T. Szederkényi 1981: Late Paleozoic subsequent volcanism of Hungary. – IGCP Project No. 5. Newsletter 3, pp. 61–69. Padova.
Fazekas, V., Gy. Majoros, T. Szederkényi 1987: Lower Permian volcanic sequences of Hungary. – Acta Geol. Hung., 30/1, pp. 21–34, Budapest.
Filipovic, I., D. Jovanovic, P. Pelikán, S. Kovács, Gy. Less, M. Sudar 1998: Late Variscan evolution of the Jadar and Bükkium Terranes: A Comparison. – 16th Congress of the Carpathian-Balkan Geological Association, Abstracts, p. 163, Wien.
Flügel, H.W. 1990: Das voralpine Basement im Alpin-Mediterranen Belt. – Überblick and Problematik. – Jb. Geol. B.-A., 133/2, pp. 181–221.
Fodor, L., B. Jelen, E. Márton, D. Skaberne, J. Car, M. Vrabec 1998: Miocene-Pliocene tectonic evolution of the Slovenian Periadriatic fault: Implications for Alpine-Carpathian extrusion models. – Tectonics, 17/5, pp. 690–709.
Frank, W. 1987: Evolution of the Austroalpine elements in the Cretaceous. – In: Flügel, H.W., P. Faupl (Eds): Geodynamics of the Eastern Alps. – pp. 379–406, Deuticke, Vienna.
Franke, W. 1989: Tectonostratigraphic units in the Variscan belt of central Europe. – Geol. Soc. Amer. Spec. Paper 230, pp. 67–90.
Frisch, W., Neubauer, F. 1989: Prealpine terranes and tectonic zoning in the eastern Alps. – Geol. Soc. Amer., Spec. Paper 230, pp. 91–100.
Froitzheim, N., S.M. Schmid, M. Frey 1996: Mesozoic paleogeography and the timing of eclogite-facies metamorphism in the Alps: A working hypothesis. – Ecl. Geol. Helv., 89/1, pp. 81–110.

Fülöp J. 1989: Introduction into the Geology of Hungary. – Akadémiai Kiadó, 246 p., Budapest, (in Hungarian).
Fülöp, J. 1990: Geology of Hungary. Paleozoic I. – MÁFI, 325 p., Budapest, (in Hungarian).
Fülöp J. 1994: Geology of Hungary. Paleozoic II. – Akadémiai Kiadó, 445 p., Budapest, (in Hungarian).
Fülöp, J., K. Brezsnyánszky, J. Haas 1987: The new map of basin basement of Hungary. – Acta Geol. Hung., 30/1–2, pp. 3–20, Budapest.
Fülöp, J., V. Dank et al. 1986: Geological map of Hungary without Cenozoic. 1:500.000. – Hung. Geol. Inst., Budapest.
Galácz, A. 1984: Jurassic of Hungary: a review. – Acta Geol. Hung., 27/3–4, pp. 359–377, Budapest.
Galácz, A., A. Vörös, 1972: Jurassic history of the Bakony Mountains and interpretation of principal lithological phenomena. – Földt. Közl. 102, pp. 122–135, Budapest. (in Hungarian, with English abstract).
Géczy, B. 1972: A júra faunaprovinciák kialakulása és a mediterrán lemeztektonika (The origin of the Jurassic faaunal provinces and the Mediterranean plate tectonics). – MTA X. Oszt. Közl., 5, pp. 297–312, Budapest, (in Hungarian).
Géczy, B. 1973a:The origin of the Jurassic faaunal provinces and the Mediterranean plate tectonics. Ann. Univ. Sci. Budapestinensis, Sect. Geol. 16, pp. 99–114.
Géczy, B. 1973b: Plate tectonics and paleogeography in the East-Mediterranean Mesozoic. – Acta Geol. Hung., 17, pp. 421–428.
Géczy, B. 1984: Provincialism of Jurassic ammonites: examples from Hungarian faunas. – Acta Geol. Hung. 27/3–4, pp. 379–389, Budapest.
Ghanem, M.A.E., L. Ravasz Baranyai 1969: Petrographic study of the crystalline basement rocks, Mecsek Mts., Hungary. – Acta Geol. Hung., 13, pp. 191–219, Budapest.
Grecula, P., K. Együd 1977: Position of the Zemplín Inselberg in the tectonic frame of the Carpathians. – Miner. slovaca, 9/6, pp. 449–462, Spiškà Nová Ves, (In Slovak, with English summ.).
Grecula, P., I. Varga, 1979: Main discontinuity belts on the inner side of the Western Carpathians. – Miner. slovaca, 11/5, pp. 389–404, Spišská Nová Ves.
Grill, J. 1988: Jurassic formations of the Rudabánya Mountains. – M. Áll. Földt. Int. Évi Jel., 1986, pp. 69–103, Budapest, (in Hung., with English abstr.).
Grill, J. 1989: Structural evolution of the Aggtelek–Rudabánya Mountains, NE Hungary. – M. Áll. Földt. Évi Jel., 1987, pp. 411–432, Budapest, (in Hung., with English abstr.).
Grill, J., S. Kovács, Gy. Less, Zs. Réti, L. Róth, I. Szentpétery 1984: Geology and evolution of the Aggtelek-Rudabánya Mountains. – Földt. Kut., 27/4, pp. 49–56, Budapest, (in Hungarian).
Haas, J. 1987: Position of the Transdanubian Central Range structural unit in the Alpine evolution phase. – Acta Geol. Hung., 30/3–4, pp. 243–256, Budapest.
Haas, J. 1993: A "Kösseni medence" kialakulása és fejlődése a Dunántúli-középhegységben (Formation and evolution of the "Kössen Basin" in the Transdanubian Range). – Földt. Közl., 123/1, pp. 9–54, Budapest, (in Hungarian with English abstr.).
Haas, J. 1994: Carnian basin evolution in the Transdanubian Central Range, Hungary. – Zbl. Geol. Paläont. Teil 1 1992 H.11/12, pp. 1233–1252 Stuttgart, Maai 1994. Figs 11.
Haas J., T. Budai 1995: Upper Permian-Triassic facies zones in the Transdanubian Range. – Riv. Ital. di Paleont. e Strat., 101/3, pp. 249–266. Milano.
Haas, J., E. Tardi-Filácz, A. Oravecz-Scheffer, F. Góczán, L. Dosztály 1997: Stratigraphy and sedimentology of an Upper Triassic toe-of-slope and basin succession at Csővár-1, North Hungary – Acta. Geol. Hung., 40/2, pp. 111–177, Budapest.
Haas, J., F. Góczán, A. Oravecz-Scheffer, Á. Barabás-Stuhl, Gy. Majoros, A. Bérczi-Makk 1988: Permian/Triassic boundary in Hungary. – Mem. Soc. Geol. Ital, 34, pp. 221–241, Roma.
Haas, J., S. Kovács, L. Krystyn, R. Lein 1995: Significance of Late Permian–Triassic facies zones in terrane reconstructions in the Alpine–North Pannonian domain. – Tectonophysics, 242/1, pp. 19–40, Amsterdam.

Haas, J., P. Mioč, J. Pamić, B. Tomljenović, P. Árkai, A. Bérczi-Makk, B. Koroknai, S. Kovács, E. Rálisch-Felgenhauer 2000: Complex structural pattern of the Alpine-Dinaridic-Pannonian triple junction. – Int. Journ. Earth Sciences, Abst. Vol. 89/2, pp. 377–389.
Haas, J., E. Rálisch-Felgenhauer, A. Oravecz-Scheffer, E. Nagy, A. Bérczi-Makk 1988: Triassic key sections in the Mid-Transdanubian (Igal) structural zone. – Acta Geol. Hung., 31/1–2, pp. 3–17, Budapest.
Hamilton, W. B. 1990: On terrane analysis. – In: Dewey, J. F. et al. (Eds): Allochthonous terranes. Phil. Trans. R. Soc. Lond., A 331, pp. 511–522.
Harangi, Sz. 1994: Geochemistry and petrogenesis of the Early Cretaceous continental rift-type volcanic rocks of the Mecsek Mountains, South Hungary. – Lithos, 33, pp. 303–321.
Harangi, Sz., Cs. Szabó, S. Józsa, Zs. Szoldán, E. Árva-Sós, M. Balla, I. Kubovics, I. 1996: Mesozoic Igneous Suites in Hungary: Implications for Genesis and Tectonic Setting in the Northwestern Part of Tethys. – Int. Geol. Rev., 38, pp. 336–360.
Hetényi, R., L. Ravasz Baranyai 1976: The anthracitiferous Upper Carboniferous sequence of Baranya, South Hungary, in the light of boreholes Siklósbodony-1 and Bogádmindszent-1. – M. Áll. Földt. Int. Évi Jel. 1973, pp. 323–361, Budapest, (in Hungarian with English abstr.).
Hips, K. 1995: Stratigraphic and facies evaluation of the Lower Triassic formations in the Aggtelek-Rudabánya Mountains, NE Hungary. – Acta Geol. Hung., 39/4, pp. 369–411, Budapest.
Horváth, F., A. Ádám, W.D. Stanley 1986: New geophysical data: evidence for the allochthony of the Transdanubian Central Range. – Rend. Soc. Geol. It., 9, pp. 123–130, Roma.
Horváth, F., L. Royden 1981: Mechanism for the formation of the intra-Carpathian basins: a review. – Earth Evol. Sci., 3/4, pp. 307–316, Amsterdam.
Horváth, P. 1997: High-pressure metamorphism and P-T path of the metabasic rocks in the borehole Komjáti-11, Bódva Valley area, NE Hungary. – Acta Miner., Petr. Szeged., 38, pp. 151–163.
Hovorka, D. 1985: Ultramafic rocks of the Western Carpathians, Czechoslovakia. – GÚDS, 258 p, Bratislava.
Howell, D.G. 1989: Tectonics of Suspect Terranes. – Chapman and Hall, London–New York, 232 p.
Howell, D.G., D.L. Jones, E.R. Schermer 1985: Tectonostratigraphic terranes of the Circum-Pacific region. – In: Howell, D.G. (Ed.): Tectonostratigraphic terranes of the Circum-Pacific region: Houston, Circum-Pacific Council for Energy and Mineral Resources, Earth Sciences Series Number l, pp. 3–30.
Ianovici, V., M. Borcos, M. Bleahu, D. Patrulius, M. Lupu, R. Dimitrescu, H. Savu 1976: Geologia Muntilor Apuseni. – Edit. Acad. Republ. Soc. Romania, 631 p, Bucuresti.
Irving, E. 1977: Drift of the major continental blocks since the Devonian. – Nature, 270, pp. 304–309.
Irving, E. 1979: Paleopoles and paleolatitudes of North America and speculations about displaced terranes. – Canadian Journal Earth Sci., 16, pp. 669–694.
Irving, E., J.W.H. Monger, R.W. Yole 1980: New paleomagnetic evidence for displaced terranes in British Columbia. – In: Strangway, D.W. (Ed.): Continental Crust and Mineral Deposits. – Geol. Assoc. Canada Spec. Pap. 20, pp. 441–456.
Jámbor, Á. 1969: Carboniferous deposits in the area between the Mecsek and Villány Mountains. – M. Áll. Földt. Int. Évi Jel., 1967, pp. 215–221, Budapest, (in Hung., with English abstr.).
Jantsky, B. 1979: Géologie du socle cristalin granitisé de la Montagne Mecsek. – Ann. Inst. Geol. Publ. Hung., 60, 385 p, Budapest.
Jenkyns, H. C. 1991: Impact of Cretaceous sea level rise and anoxic events on the Mesozoic carbonate platform of Yugoslavia. – Am. Assoc. Petrol. Geol. Bull., 75/6, pp. 1007–1017.
Jones, D.L., N.J. Silberling, J. Hillhouse 1977: Wrangellia – a displaced terrane in northwestern North America. – Canadian Journal Earth Sci., 14/11, pp. 2565–2577.
Józsa, S., L. Dosztály, Y. Gulácsi, S. Kovács 1996: Ophiolites of Szarvaskő, Darnó Hill and Bódva Valley. – IGCP 369 Excursion Guide, 16 p, Budapest.
Józsa, S., Sz. Harangi 1998: A review of the petrology and geochemistry of Mesozoic ophioliote complexes in NE Hungary. – Carp.-Balk. Geol. Assoc. XVI. Congress, Vienna, Auustria, 1998. Abstract volume, p. 256.

Karamata, S., N.M. Dimitrijević, M.D. Dimitrijević 1999: Oceanic realms in the central part of the Balkan Peninsula during the Mesozoic. – Slovak Geol. Mag., 5/3, pp. 173–177.

Karamata, S., F. Ebner, B. Krstić. 1996: Terranes – Definition of the Terrane and Importance for Geologic Interpretations. – In: Knezevic, V., B. Krstic (Eds): Terranes of Serbia: The Formation of the Geologic Framework of Serbia and the Adjacent Regions. pp. 23–24, Beograd.

Karamata, S., B. Krstić, M. D. Dimitrijević, M.N. Dimitrijević, V. Knezević, R. Stojanov, I. Filipović 1996/1997: Terranes between the Moesian plate and the Adriatic Sea. – In: Papanikolaou, D. (Ed.): IGCP Project No. 276 Terrane Maps and Terrane Descriptions. – Ann. Géol. Pays Hellénіq., 37, pp. 401–428.

Karamata, S., B. Krstić, M. D. Dimitrijević, V. Knezević, M. N. Dimitrijević, I. Filipović 1994: Terranes between the Adriatic and the Carpatho-Balkan arc. – Bull. T. CVIII. l'Acad Serbe des Sciences et des Arts, Classe des Sciences math. natur., Sci. nat., 35, pp. 47–68.

Kassai, M. 1976: Permische Bildungen im nördliches Vorraum des Villányer Gebirges. – Geol. Hung., Ser. Geol., 17, pp. 11–109, Budapest.

Kázmér, M. 1986: Tectonic units of Hungary: their boundaries and stratigraphy (a bibliographic guide). – Ann. Univ. Sci. Budapest, 26, pp. 45–120, Budapest.

Kázmér, M. 1987: Lower Liassic facies zones in the Bakony unit of Hungary. – Ann. Univ. Sci. Budapest, Sect. Geol., 27, pp. 89–100, Budapest.

Kázmér, M. 1999: Synoptic geology of Hungary – Beih. z. Eur. J. Mineral, 11/2, pp. 1–6.

Kázmér, M., S. Kovács 1985: Permian-Paleogene paleogeography along the eastern part of the Insubric-Periadriatic Lineament system: evidence for continental escape of the Bakony-Drauzug Unit. – Acta Geol. Hung., 28/1–2, pp. 71–84, Budapest.

Kázmér, M., S. Kovács 1989: Triassic and Jurassic Oceanic/Paraoceanic Belts in the Carpathian-Pannonian Region and its surroundings. – In: Sengör, A.M.C. (Ed.): Tectonic Evolution of the Tethyan Region, pp. 77–92, Kluwer Acad. Publ., Dordrecht.

Kedves, M., T. Szederkényi 1997: Coalized plant-remnants from the Ófalu schists, Mecsek Mts., Hungary. – Acta Miner. Petr. Szeged, 39 (in press).

Kemenci, R. 1977: Kristalasti skriljci u paleozoljegu Vojvodine. – Geol. Srbije, Tom. III/2, pp. 237–251, Belgrade.

Kemenci, R., M. Čanović 1997: Geologic setting of the Pre-Tertiary basement in Vojvodina. Part I: The Tisza Mega-unit of North Vojvodina. – Acta Geol. Hung., 40/1, pp. 1–36.

Keppie, J.D., R.D. Dallmeyer 1990: Introduction to terrane analysis and the tectonic map of pre-Mesozoic terranes in Circum-Atlantic Phanerozoic orogens. – Abstracts, IGCP MEETING 233, p. 24. Göttingen.

Kisházi P., J. Ivancsics 1988: Contribution to the petrology of crystalline schists in the Zemplén structure. (In Hung., with English abstr.). – Földt. Közl., 118/2, pp. 109–124, Budapest.

Klötzli, U.S., Gy. Buda, F. Koller 1999: Geochronological evidence for the derivation of the Mecsek Mountains, South Hungary, from Variscan Central Europe. – Beih. z. Eur. J. Mineral., 11/2, p. 126.

Koller, F. 1985: Petrologie und Geochemie der Ophiolite des Pennikums am Alpenostrand. – Jb. Geol. B.-A., 128, 1, p. 83–150.

Kovác, M., A. Nagymarosy, N. Oszczypko, L. Csontos, A. Slaczka, M. Marunteanu, L. Matenco, E. Márton, E. 1999: Palinspastic reconstruction of the Carpathian-Pannonian region during the Miocene. – In: Rakúš, M. (Ed.): Geodynamic development of the Western Carpathians. – Geol. Surv. Slov., Bratislava, 1998, pp. 189–218.

Kováč, M., A. Nagymarosy, J. Soták, K. Sutovská 1993: Late Tertiary paleogeographic evolution of the Western Carpathians. – Tectonophysics, 226, pp. 401–415, Amsterdam.

Kovách, Á., É. Svingor, T. Szederkényi 1985: Rb-Sr dating of basement rocks from the southern foreland of the Mecsek Mountains, Southeastern Transdanubia, Hungary. – Acta Miner. Petr. Szeged, 27, pp. 51–56, Szeged.

Kovács, S. 1979: Geological buildup of the South Gemerian Alsóhegy. – Ősl. Viták, 24, pp. 33–58, Budapest, (in Hung. with English summ.).

Kovács, S. 1980: Paleogeographical significance of the Triassic Hallstatt limestone facies in the North Alpine facies region. (In Hung., with English abstract.) – Földt. Közl., 110/3–4, pp. 360–381, Budapest.

Kovács, S. 1984: North Hungarian Triassic facies types: a review. – Acta Geol. Hung., 27/3–4, pp. 251–264, Budapest.

Kovács, S. 1992: Stratigraphy of the Szendrő-Uppony Paleozoic (Northeastern Hungary). – In: Vozár, J. (Ed.): Western Carpathians, Eastern Alps, Dinarides, Special Volume to Paleozoic Geodynamic Domains, IGCP Project No. 276. pp. 93–108, Dionyz Štúr Geol. Inst., Bratislava.

Kovács, S. 1997: Middle Triassic Rifting and Facies Differentiation in Northeast Hungary. – In: Sinha, A.K., F.P. Sassi, D. Papanikolaou (Eds): Geodynamic Domains in the Alpine-Himalayan Tethys. pp. 375–397, Oxford & IBH Publishing Co. Pvt. Ltd., New Delhi, Calcutta.

Kovács, S. 1998: Events preceding the opening of the Mesozoic Tethys in the East Mediterranean region. – In: Papanikolaou, D. (ed.): IGCP Project No. 276 (Paleozoic geodynamic domains and their alpidic evolution in the Tethys), Newsletter No. 6, Spec. Publ. Geol. Soc. Greece, pp. 122–139, Athens.

Kovács, S., G. Császár, A. Galácz, J. Haas, E. Nagy, A. Vörös 1989: The Tisza Superunit Was Originally part of the Northern (European) Margin of Tethys. – In: Rakúš, M., J. Dercourt, A.E.M. Nairn (Eds): Evolution of the Northern Margin of Tethys, Vol. II. – Mém. Soc. Géol. France, Nouv. Série, 154/II, pp. 81–100.

Kovács, S., Gy. Less, O. Piros, Zs. Réti, L. Róth 1989: Triassic formations of the Aggtelek-Rudabánya Mts. – Acta Geol. Hung., 32/1–2, pp. 31–63, Budapest.

Kovács, S., T. Szederkényi P. Árkai, Gy. Buda, Gy. Lelkes-Felvári, A. Nagymarosy 1996/1997: Explanation to the terrane map Hungary. – In: Papanikolaou, D. (Ed.): IGCP Project No. 276 Terrane Maps and Terrane Descriptions. – Ann. Géol Pays Hellénig., 37, pp. 245–270.

Kozur, H. 1984: Fossilien aus dem Silur von Ungarn (vorläufige Mitteilung). – Radovi Geoinstituta, 17, pp. 163–174, Beograd.

Kozur, H., R. Mock 1997: New paleogeographic and tectonic interpretations in the Slovakian Carpathians and their implications for correlations with the Eastern Alps and other parts of the Western Tethys. Part II: Inner Western Carpathians. – Mineralia Slovaca, 29, pp. 164–209.

Kozur, H., H. Mostler 1994: Anisian to Middle Carnian radiolarian zonation and description of some stratigraphically important radiolarians. – Geol. Paläont. Mitt. Issbruck, Sonderband 3, pp. 39–255.

Kräutner, H. 1996/1997: Alpine and pre-alpine terranes in the Romanian Carpathians and Apuseni Mts. – In: Papanikolaou, D. (Ed.): IGCP Project No. 276 Terrane Maps and Terrane Descriptions. – Ann. Géol Pays Hellénig., 37. pp. 271–330.

Kubovics, I. 1985: Mesozoic magmatism of the Transdanubiaan Mid-Mountains. – Acta Geol. Hung., 28/3–4, pp. 141–164.

Kubovics, I., Cs. Szabó, Sz. Harangi, S. Józsa 1990: Petrology and petrochemistry of Mesozoic magmatic suites in Hungary and adjacent areas an overview. – Acta Geod. Geoph. Mont. Hung., 25/3–4, pp. 345–371, Budapest.

Kurucz, B. 1977: A Pusztaföldvár-Battonya közötti terület medencealjzatának képződményei és hegységszerkezete (Formations and structure of the basin basement of th area between Pusztaföldvár and Battonya). – Ms. Dissertation. Univ. Szeged (in Hungarian).

Laubscher, H.P. 1971: Das Alpen-Dinariden-Problem und die Palinspastic der südlichen Tethys. – Geol. Rundsch., 60, pp. 813–833.

Lelkes-Felvári, Gy. 1978: Petrographische Untersuchung einiger präpermischen Bildungen der Balaton-Line. – Geol. Hung., Ser. Geol., 18, pp. 193–295, Budapest.

Lelkes-Felvári, Gy., C. Mazzoli, D.Visoná 1989: Contrasting mineral assemblages in polymetamorphic rocks from South Transdanubia (Hungary). – Eur. J. Miner., 1, pp. 143–146.

Lelkes-Felvári, Gy., F. P. Sassi, G.B. Vai 1982: Data supporting the Mediterranean affinity of the phyllite sequence from the Bakony Mts. (Hungary). – In: Sassi, F.P., I. Varga (Eds): IGCP Project No. 5 Newsletter, 4, pp. 47–48, Padova–Košice.

Lelkes-Felvári, Gy., F.P. Sassi. 1983: Outlines of the pre-Alpine metamorphisms in Hungary. – In: Karamata, S., F.P. Sassi (Eds): IGCP No.5 Newsletter, 3, pp. 89–99, Padova–Beograd.
Lelkes-Felvári, Gy., F. P. Sassi, G. Zirpoli 1994: Lithostratigraphy and Variscan metamorphism of the Paleozoic sequences in the Bakony Mountainss, Hungary. – Mem. Sci. Geol. 46, pp. 303–312, Padova.
Lelkes-Felvári, Gy., P. Árkai, F.P. Sassi 1996: Main features of the regional metamorphic events in Hungary: A review. – Geol. Carpath., 47/4, pp. 257–270.
Less, Gy. 1997: Földtani felépítés (Geological buildup). – In: Baross, G. (Ed.): Az Aggteleki Nemzeti Park (The Aggtelek National Park). pp. 26–66, Mezőgazda Kiadó, Budapest, (in Hungarian).
Less, Gy., S. Kovács, L. Fodor, Cs. Péró, K. Hips 1998: Geological cross sections through the Aggtelek–Rudabánya Mts., NE Hungary. – 16th Congress Carpatho-Balkan Geol. Assoc., Abstracts, p. 337.
M. Tóth, T. 1995: Retrograde eclogite in the crystalline basement of the Kőrös Unit, Hungary. – Acta. Miner. Petr. Szeged, 36, pp. 117–129, Szeged.
Majoros, Gy. 1980: Problems of Permian sedimentation in the Transdanubian Central Range. A paleogeographic model and some consequences. – Földt. Közl., 110/3–4, pp. 323–341, Budapest, (in Hung., with English summ.).
Majoros, Gy. 1983: Lithostratigraphy of the Permian Formations of the Transdanubian Central Mountains. – Acta Geol. Hung., 26/1–2, pp. 7–20, Budapest.
Maluski, H., P. Rajlich, Ph. Matte 1993: 40Ar-39Ar dating of the Inner Carpathians Variscan basement and Alpine mylonitic overprinting. – Tectonophysics, 223, pp. 313–337, Amsterdam.
Márton, E. 1986: Paleomagnetism of igneous rocks from the Velence Hills and Mecsek Mountains. – Geophysical Transactions, 32, pp. 83–145.
Márton, E. 2000: The Tisza megatectonic unit in the light of paleomagnetic data. – Acta Geol. Hung., (this volume)
Márton, E., P. Márton 1978a: On the difference between the palaeomagnetic poles from the Transdanubian Central Mountains and the Villány Mountains respectively. – Magyar Geofizika, 19/4, pp.129–136, (in Hungarian).
Márton, E., P. Márton 1978b: Tectonic implication of a new palaeomagnetic result from the Jurassic of the Transdanubian Central Mountains. – Tectonophysics, 45,. T1–T6.
Márton, E., P. Márton 1981: Mesozoic paleomagnetism of the Transdanubian Central Mountains and its tectonic implications. – Tectonophysics 72, pp. 129–140.
Márton, E., P. Márton 1983: A refined apparent polar wander curve for the Transdanubian Central Mountains and its bearing on the Mediterranean tectonic history. – Tectonophysics, 98, pp. 43–57.
Márton, E., P. Márton, Gy. Less 1988: Palaeomagnetic evidence of tectonic rotations in the southern margin of the Inner West Carpathians. – Phys. Earth Planet. Int., 52, pp. 256–266, Amsterdam.
Matte, Ph. 1986: Tectonics and plate tectonics model for the Variscan belt of Europe. – Tectonophysics, 126, pp. 329–374.
Matte, Ph. 1991: Accretionary history and crustal evolution of the Variscan belt of Western Europe. – Tectonophysics, 196, pp. 309–337.
Matte, Ph., H. Maluski, P. Rajlich, W. Franke 1990: Terrane boundaries in the Bohemian Massif: Result of large-scale Variscan shearing. – Tectonophysics, 177, pp. 151–170.
Mauritsch, H.J., E. Márton 1995: Escape models of the Alpine-Carpathian-Pannonian region in the light of paleomagnetic observations. – Terra Nova, 7, pp. 44–50.
Michalik, J. 1994: Notes on the Paleogeography and Paleotectonics of the Western Carpathian Area During the Mesozoic. – Mitt. Österr. Geol. Ges., 86, pp. 101–110.
Mioč, P. 1997: Tectonic Structures Along the Periadriatic Lineament in Slovenia. – Geol. Croat., 30/2, pp. 251–260.
Mock, R., M. Sykora, R. Aubrecht, L. Ozvoldová, B. Kronome, P. Reichwalder, J. Jablonsky 1998: Petrology and stratigraphy of the Meliaticum near the Meliata and Jaklovce Villages, Slovakia. – Slovak Geological Magazine, 4/4, pp. 223–261.

Monger, J.W.H., E. Irving 1980: Northward displacement of north central British Columbia. – Nature, 285, pp. 289–294.
Nagy, E. 1968: Triasbildungen des Mecsek Gebirges. –Ann. Inst. Geol. Hung., 51/1, 239 p., Budapest.
Nagy, E. 1969: Paläogeographie. In: Unterlias-Kohlenserie des Mecsek Gebirges (Geologie). – Ann. Inst. Geol. Hung., 51/2, pp. 289–317, Budapest.
Nagy, E. 1971: Der unterliassische schichtenkomplex von Grestener Fazies im Mecsek Gebirge (Ungarn). – Ann. Inst. Geol. Hung., 54/2, pp. 155–159, Budapest.
Nagymarosy, A. 1990: From Tethys to Paratethys, a way of survival. – Acta Geod. Geoph. Mont. Hung., 25/3–4, pp. 373–385.
Nagymarosy, A. 1990: Paleogeographical and paleotectonical outlines of some Intracarpathian Paleogene basins. – Geol. Zborn.Geol. Carpath., 41/3, pp. 259–274, Bratislava.
Nagymarosy, A. 1998: A szolnoki flisöv rétegtani felépítése és ősföldrajzi kapcsolatai (Stratigraphic buildup and paleogeographical connections of the Szolnok flysch belt). – In: Bérczi, I., Á. Jámbor (Ed.): Magyarország geológiai képződményeinek rétegtana (Stratigraphy of the geological formations of Hungary), Mol Rt. és a MÁFI kiadása, Budapest, pp. 389–402 (in Hungarian).
Nagymarosy, A., M. Báldi-Beke 1993: The Szolnok Unit and its probable paleogeographic position. – Tectonophysics, 226, pp. 457–470, Amsterdam.
Neubauer, F. 1988: The Variscan orogeny in the Austroalpine and Southalpine domains of the Eastern Alps. – Schweiz. Mineral. Petrogr. Mitt., 68, pp. 339–349.
Neubauer, F., R.D. Dallmeyer, H. Fritz, P. Reichwalder 1996: Zur Geodynamyik und Kinematik der Meliata-Decke in Westkarpaten und Ostalpen. – 6. Symposium TSK (Tektonik-Struktur-geologie–Kristallingeologie) Salzburg. Eds: Amman, G. R. Handler, W. Kurz, H.P. Steyrer: Erweiterte Kurzfassungen. Wien, Facultas-Univ. Verlag. pp. 300–303.
Neubauer, F., F. Ebner, W. Frisch, F.P. Sassi 1996/1997: Terranes and tectonostratigraphic units in the Alps. – In: Papanikolaou, D. (Ed.): IGCP Project No. 276 Terrane Maps and Terrane Descriptions. – Ann. Géol Pays Helléniq., 37, pp. 211–218.
Neubauer, F., J. Genser 1990: Architektur und Kinematik der östlichen Zentralalpen eine Übersicht. – Mitt. Naturwiss. Steiermark, 120, pp. 203–219, Graz.
Neubauer, F., J.F. Raumer. 1993: The Alpine Basement – Linkage between Variscides and East-Mediterranean Mountain Belts. – In: Raumer J.F., F. Neubauer (Eds): Pre-Mesozoic Geology in the Alps, pp. 641–664, Springer-Verlag.
Oravecz, J. 1964: Silurbildungen in Ungarn und ihre regionalen Beziehungen. – Földt. Közl., 94/1, pp. 3–9, Budapest, (in Hung., with German summ.).
Oczlon, M.S. 1994: North Gondwana origin for exotic Variscan rocks in the Rhenohercynian zone of Germany. – Geol. Rundsch., 83/3, pp. 20–30.
Pahr, A. 1991: Ein Diskussionsbeitrag zur Tektonik des Raumes Alpenostende – Kleine Karpaten – Pannonischen Becken. – In: Lobitzer, H., G. Császár (Eds): Jubiläumsschrift 20. Jahre Geologische Zusammenarbeit Österreich–Ungarn, pp. 297–305, Geol. B.-A., Wien.
Pamić, J. 1997: The northwesternmost outcrops of the Dinaridic ophiolites: A case study of Mt. Kalnik (North Croatia). – Acta Geol. Hung., 40/1, pp. 37–56, Budapest.
Pamić, J. 1998: Crystalline basement of the South Pannonian Basin based on surface and subsurface data. – Nafta, 49/12, pp. 371–390.
Pamić, J., I. Gusić, V. Jelaska 1998: Geodynamic evolution of the Central Dinarides. – Tectonophysics, 297, pp. 251–268.
Pamić, J., V. Jelaska, I. Gusić, K. Šikić, M. Belak, V. Tomić 1996/1997: Tectonostratigraphic units and terranes between the Adratic Sea and the Southern Pannonian Basin. – In: Papanikolaou, D. (Ed.): IGCP Project No. 276 Terrane Maps and Terrane Descriptions. – Ann. Géol. Pays Helléniq., pp. 331–400.
Pamić, J., B. Tomljenović 1998: Basic geologic data from the Croatian part of the Zagorje-Mid-Transdanubian Zone. – Acta Geol. Hung., 41/4, pp. 389–400, Budapest.

Pantic-Prodanovic, S., B. Radosevic 1977: The litostratigraphic characteristics of Triassic sediments of Tara Mountain, Inner Dinarides, Yugoslavia. – In: Proc. of the VI. Colloqium on thee Geology of the Aegean Region. 3, pp. 1159–1167, Athens.

Pantó, G. 1965: A Tokaji-hegység harmadkor előtti képződményei (Pre-Tertiary formations of the Tokaj Mts). – M. Áll. Földt. Int. Évi Jel. 1963, pp. 227–241, Budapest, (in Hungarian).

Pap, S. 1987: Geological results of boreholes below 4500 m depth in East-Hungary. – Alföldi Tanulmányok, 11, pp. 7–43, Békéscsaba, (in Hungarian).

Pap, S. 1990: Upthrusted sequences in the middle part of the territory east of the Tisza. – Spec. Papers Hung. Geol. Inst., 36, Budapest, (in Hungarian).

Papanikolaou, D. J. 1984: Introduction to the Geology of Greece: the Pre-Alpine Units. – In: Field Guide, IGCP Project No. 5 Fieldmeeting in Greece, pp. 3–35, Athens.

Papanikolaou, D. J. 1986: Geology of Greece. 240 p., Athens, (in Greek).

Papanikolaou, D. J. 1989: Are the Medial Crystalline Massifs of the Eastern Mediterranean drifted Gondwanian fragments? – In: Papanikolaou, D. J., F.P. Sassi (Eds): IGCP No. 276 Newsletter, 1, Geol. Soc. Greece, Spec. Publ. 1, pp. 63–90, Athens.

Pelikán, P., L. Dosztály 2000: Jurassic formations of the Bükkzsérc boreholes (SW Bükk Mts., NE Hungary) and their structurtal setting. – Földt. Közl., 130/1, pp. 25–46, Budapest, (in Hung., with English abstr.).

Pešic, L., A. Ramovš, J. Sremac, S. Pantić-Prodanović, I. Filipović, S. Kovács, P. Pelikán 1988: Upper Permian deposits in the Jadar region and their position within the western Paleotethys. – Mem. Soc. Geol. Ital., 34 (1986), pp. 211–219.

Peters, K. 1862: Über den Lias Fünfkirchen. – Sitzungsb. K. Akad. Wiss. Wien, Mat-Nat. Kl., 46, pp. 1–53.

Plašienka, D. 1991: Mesozoic tectonic evolution of the epi-Variscan continental crust of the Central Western Carpathians a tentative model. – Miner. slovaca, 23/5-6, pp. 447–457, Bratislava.

Plašienka, D. 1997: Cretaceous tectonochronology of the Central Western Carpathians, Slovakia. – Geol. Carpath., 48/2, pp. 99–111.

Polšak, A. 1981: Upper Cretaceous biolithic complexes in a subduction zone: examples from the Inner Dinarides, Yugoslavia. – In: Toomey, D. F. (Ed.): European Fossil Reef Models. SEMP Spec. Publ. 30, 447–472.

Posgay, K., K. Szentgyörgyi 1992: A litoszférát harántoló eltolódásos törésrendszer a Pannon medence keleti részén (Strike-slip fault system penetrating the lithosphere in the eastern part of the Pannonian Basin). – Magyar Geofizika, 32/11–2, pp. 1–15. (in Hungarian).

Prinz, Gy. 1914: Magyarország földrajza. A magyar föld és életjelenségeinek leírása (Geography of Hungary). – Budapest.

Prinz, Gy. 1926: Magyarország földrajza. I. Magyarország földjének származása, szerkezete és alakja (Geography of Hungary I. Origin, structure and form of the land of Hungary). – Danubia Könyvkiadó, Pécs, (in Hungarian).

Rálisch-Felgenhauer, E., Á. Török et al. 1993: Mecsek and Villány Mts. – In: Barabás-Stuhl, Á. et al.: Lithostratigraphic units of Hungary. Triassic. pp. 223–264, M. Áll. Földt. Int., Budapest, (in Hungarian).

Ratschbacher, L., W. Frisch, H.G. Linzer, O. Merle 1991: Lateral extrusion in the Eastern Alps. Part 2: Structural analysis. – Tectonics, 10/2, pp. 257–271.

Raumer, J.F. von, F. Neubauer. 1993: Late Precambrian and Paleozoic Evolution of the Alpine Basement – An Overwiew. – In: Raumer, J.F. von, F. Neubauer (Eds): Pre-Mesozoic Geology in the Alps. pp. 625–640, Springer-Verlag.

Ravasz, Cs. 1987: Neogene volcanism in Hungary. – Ann. Inst. Geol. Hung., 70, pp. 275–279.

Ravasz Baranyai, L. 1969: Eclogite from the Mecsek Mountains, Hungary. – Acta Geol. Hung., 13, pp. 315–322, Budapest.

Réti, Zs. 1985: Triassic ophiolite fragments in an evaporitic melange, Northern Hungary. – Ofioliti, 10/2/3, pp. 411–422, Bologna.

Royden, L. 1988: Late Cenozoic tectonics of the Pannonian basin system. – Am. Assoc. Petr. Geol., Mem., 45, pp. 27–48, Tulsa.
Sadek, Gh., P. Árkai, G. Nagy 1996: Alpine polyphase metamorphism of the Szarvaskő complex, Bükk Mountains, Hungary. – Acta Miner. Petr. Szeged, 37, pp. 99–128.
Sandulescu, M. 1980: Analyse géotectonique des chaines alpines alpines situées autour de la Mer Noire occidentale. – Ann. Inst. Geol. Geofiz., 56, pp. 5–54, Bucuresti.
Sandulescu, M. 1984: Geotectonica Romaniei. – Editura Technica, 336 p., Bucuresti.
Schlagintweit, F. 1990: Microfaunistic investigation of Hungaryan Urgonian limestones (Barremian–Albian). – Acta Geol. Hung., 33/1–4, pp. 3–12.
Schmidt, Th., J. Blau, M. Kázmér 1991: Large-scale strike-slip displacement of the Drauzug and Transdanubian Mountains in early Alpine history: evidence from Permo-Mesozoic facies belts. – Tectonophysics, 200, pp. 213–232.
Schweigl, J., F. Neubauer 1997: Structural evolution of the Northern Calcareous Alps: Significance for the Jurassic to Tertiary geodynamics in the Alps. – Ecl. Geol. Helv., 90, pp. 303–323.
Şengör, A. M. C., J. F. Dewey 1990: Terranology: vice or virtue? – In: Dewey, J.F. et al. (Eds): Allochthonous terranes. Phil. Trans. R. Soc. Lond. A 331, pp. 457–477.
Šikić, K., M. Brkić 1975: Donji trijas u Papuku i Krndiji (Lower Triassic of Papuk and Krndija). – Geol. vjesn., 28, pp. 133–141, Zagreb, (in Croatian with English abstr.).
Šikić, K., M. Brkić, A. Šimunić, M. Grimani 1975: Mezozojske Naslage Papuckog gorja (Mesozoic succession of the Papuk Mts). – Radovi Znan. sav. za naftu JAZU, Sekc. Geol. Geof. Geokem., 5, pp. 87–96, (in Croatian with English abstr.).
Sinha, A.K. 1997: The Concept of Terrane and its Application in Himalayan and Adjoining Region. – In: Sinha, A.K., F.P. Sassi, D. Papanikolaou (Eds): Geodynamic Domains in the Alpine-Himalayan Tethys, pp. 1–44.
Skourtsis-Coroneou, V., V. Tselepidis, S. Kovács, L. Dosztály 1995: Traissic pelagic sedimentary evolution in some geotectonic units in Greece and Hungary: a comparison. – Proc. 15th Congress Carpatho-Balkan Geol. Assoc., Geol. Soc. Greece, Spec. Publ. No. 4, pp. 275–281.
Schmidt, E. R. 1957: Geomechanika. – Akadémiai Kiadó.
Šimunic, A., A. Šimunic 1992: Mesozoic of the Hrvatsko Zagorje Area in the southwestern part of the Pannonian Basin (Northwestern Croatia). – Acta Geol. Hung., 35/2, pp. 83–96, Budapest.
Svingor, É., Á. Kovách 1981: Rb-Sr isotopic studies on granodioritic rocks from the Mecsek Mountains, Hungary. – Acta Geol. Hung., 24, pp. 295–307, Budapest.
Szalay, Á. 1977: Metamorphic-granitogenic rocks of the basement complex of the Great Hungarian Plain, Eastern Hungary. – Acta Miner. Petr. Szeged., 23, pp. 46–69, Szeged.
Szederkényi, T. 1974: DK Dunántúl ópaleozóos képződményeinek ritkaelem kutatása (Rare earth element research of the Lower Paleozoic formation of SE Transdanubia). – PhD. Diss. MTA Library, (in Hungarian).
Szederkényi, T. 1974: Paleozoic magmatism and tectogenesis in Southeast Transdanubia. – Acta Geol. Hung., 18, pp. 305–313, Budapest.
Szederkényi, T. 1976: Barrow-type metamorphism in the crystalline basement of Southeast Transdanubia. – Acta Geol. Hung., 13, pp. 27–34, Budapest.
Szederkényi, T. 1977: Geological evolution of South Transdanubia (Hungary) in Paleozoic time. – Acta Miner. Petr. Szeged, 23, pp. 3–14, Szeged.
Szederkényi, T. 1984: Az Alföld kristályos aljzata és földtani kapcsolatai (Crystalline basement and geological relations of the Great Plain). – D.Sc. Thesis. MTA Library, Budapest, (in Hungarian).
Szederkényi, T. 1985: A Bácsalmás-1 sz. fúrás szenon rétegeinek kavicsvizsgálata (Gravel analysis of the Senonian beds of borehole Bácsalmás 1). – Földt. Int. Adattár. (Manuscript, in Hung.)
Szederkényi, T., P. Árkai, Gy. Lelkes-Felvári 1991: Crystalline groundfloor of the Great Hungarian Plain and South Transdanubia, Hungary. – Serb. Acad. Sci. Arts, Nat. Math. Sci., 62/4, pp. 261–272, Beograd.
Szederkényi, T. 1996: Metamorphic formations and their correlation in the Hungarian part of the Tisza Megaunit (Tisa Composite Terrane). – Acta Miner., Petr. Szeged, 37, pp. 143–160.

Szepesházy, K. 1969: Petrographische Angaben zur Kentniss des Battonyaer Granits. – M. Áll. Földt. Int. Évi Jel. 1967, pp. 227–266, Budapest, (in Hung., with German summ.).
Szepesházy, K. 1971: Paleozoic, Archeozoic. (In: Explanation to the Geological map series of Hungary, scale 1:200 000; sheet Kiskunhalas. In Hung.). – M. Áll. Földt. Int., Budapest.
Szepesházy, K. 1972: Die Juragesteine des mittleren Teiles von Tiszántúl auf Grund von Schürfbohrungen auf Erdöl und Erdgas. – M. Áll. Földt. Int. Évi Jel. 1970, pp. 67–78, Budapest, (in Hung., with German summ.).
Szepesházy, K. 1975: Geological setting of the NE-Carpathians and their position in the Carpathian system. – Ált. Földt. Szemle, 8, pp. 25–60, Budapest, (in Hung., with English summ.).
Szepesházy, K. 1977: Mesozoic igneous rocks of the Hungarian Plain. – Földt. Közl., 107/3–4, pp. 384–397, Budapest, (in Hung. with English summ.).
Szoldán, Zs. 1990: Middle Triassic magmatic sequences from different tectonic settings in the Bükk Mts., NE Hungary. – Acta Miner. Petr., 31, pp. 25–42, Szeged.
Sztanó, O. 1990: Submarine fan-channel conglomerate of Lower Cretaceous, Gerecse Mts., Hungary. – N. Jb. Geol. Paläont. Mh., 1990/7, pp. 431–446.
Sztanó, O., S. Józsa 1996: Interaction of basin-margin faults and tidal currents on nearshore sedimentary architecture and composition: a case study from the Early Miocene of northern Hungary. – Tectonophysics, 266, pp. 319–341.
Tari, G. 1996: Neoalpine tectonics of the Danube Basin (NW Pannonian Basin, Hungary). – In: Ziegler, P.A., F. Horváth (Eds): Peri-Tethys Memoir 2: Structure and Prospect of Alpine Basin and Forelands. – Mém. Mus. nat. Hist. nat., 170, pp. 439–454.
Tollmann, A. 1987: Neue Wege in der Ostalpengeologie und die Beziehungen zum Ostmediterran. – Mitt. Österr. geol. Ges., 80, pp. 47–113.
Tozer, E.T. 1982: Marine Triassic Faunas of North America: Their Significance for Assessing Plate and Terrane Movements. – Geol. Rundsch., 71/3, pp. 1077–1104.
Török, Á. 1993: Storm influenced sedimentation in the Hungarian Muschelkalk. – In: Hagdorn, H., Seilacher, A. (Eds): Muschelkalk, Schöntaler Symposium, 1991, Jb. ges. Nat. Württemberg, 2, pp. 133–142, Korb (Goldschneck), Stuttgart.
Török, Á. 1997: Triassic ramp evolution in Southern Hungary and its similarities to the Germano-type Triassic. – Acta Geol. Hung., 40/4, pp. 367–390.
Török, Á. 1998: Controls on development of Mid-Triassic ramps: examples from southern Hungary. – In: Wright, V.P., T.P. Burchette (Eds): Carbonate ramps. Geol. Soc. London, Spec. Publ. 149, pp. 339–367.
Török, K. 1989: Fluid inclusion study of the gneiss from the borehole Nagyatád K-11, SW Transdanubia, Hungary. – Acta Miner. Petr. Szeged., 30, pp. 115–126, Szeged.
Török, K. 1990: New data on the geothermometry and geobarometry of the Somogy–Dráva Basin, SW Transdanubia. – Acta Miner. Petr. Szeged., 31, pp. 13–23.
Török, K. 1992: Cordierite-andalusite-bearing micaschists from the Garabonc-1 borehole, Central Transdanubia, Hungary; Geothermo-barometry and fluid inclusions. – European J. of Miner., 4. pp. 1125–1136.
Török, K. 1994: First record of zinc-bearing spinel and staurolite from the metamorphic basement of W-Hungary. – Földt. Közl., 124/1, pp. 59–67.
Török, K. 1996: High-pressure/low temperature metamorphism of the Kő-hegy gneiss, Sopron (W-Hungary, Eastern Alps); Phengite barometry and fluid inclusions. – European J. of Miner., 8, pp. 917–925.
Török, K. 1998: Magmatic and high-pressure metamorpic development of orthogneisses in the Sopron area, Eastern Alps (W-Hungary). – Neues. Jahrb. für Mineralogie 173, pp. 63–91.
Török, K. 1999: Pre-Alpine development of the andalusite-sillimanite-biotite-schist from the Sopron Mountains (Eastern Alps, W-Hungary). – Acta Geol. Hung., 43/2, pp. 127–160, Budapest.
Trunkó, L. 1996: Geology of Hungary. – Beiträge zur regionalen Geologie der Erde, Bd. 23, 464 p., Gebrüder Borntraeger, Berlin – Stuttgart.

Trümpy, R. 1992: Ostalpen und Westalpen - Verbindendes und Trennendes. - Jb. Geol. B.-A., 135, 4, pp. 875–882.

Vadász, E. 1961: On the problem of the Hungarian median "massif". - Ann. Univ. Sci. Budapestinensis, Sect. Geol. 4, pp. 105–119, Budapest.

Vai, G.B. 1975: Hercynian basin evolution of the Southern Alps. - In: Squyres, C. (Ed.): Geology of Italy, E.S.S.L.A.R., II, pp. 293–298.

Vai, G.B. 1995: Crustal evolution and basement elements in the Italian area: paleogeography and characterization. - Boll. Geofis. Teor. Appl., 36, 141–144, pp. 411–434.

Varga, Gy., E. Csillag-Teplánszky, Zs. Félegyházi 1975: Geology of the Mátra Mountains. - M. Áll. Földt. Int. Évk., 57/1, 575 p., Budapest, (in Hung., with English summ.),

Velledits, F. 2000: Evolution of the area from the Berva Valley to the Hór Valley in the Middle-Upper Triassic. (In Hung., with English abstr.) - Földt. Közl., 130/1, pp. 47–93, Budapest.

Vozárová, A., J. Vozár 1992a: Tornaicum and Meliaticum in borehole Brusník BRU-1, Southern Slovakia. - Acta Geol. Hung., 35/2, pp. 97–116, Budapest.

Vozárová, A., J. Vozár 1992b: Variscan terranes and evolution of Late Paleozoic sedimentary basins - In: Vozár, J. (Ed.): Western Carpathians, Eastern Alps, Dinarides. Special volume to the problems of the Paleozoic geodynamic domains (IGCP 276), pp. 147-154, GÚDS Bratislava.

Vozárová, A., J. Vozár 1996/1997: Terranes of the West Carpathian-North Pannonian domain. - In: Papanikolaou, D. (Ed.): IGCP Project No. 276 Terrane Maps and Terrane Descriptions. - Ann. Géol. Pays Hellénіq., 37, pp. 219–244.

Vörös, A. 1972: Lower and Middle Jurassic formations of the Villány Mountains. - Földt. Közl., 102/1, pp. 12–28, Budapest, (in Hung., with English summ.).

Vörös, A. 1984: Comparison of Jurassic benthonic mollusc and brachiopod faunas of the Transdanubian Mountains (Hungary). - Acta Geol. Hung., 27/3–4, pp. 391–401, Budapest.

Vörös, A. 1988: Conclusions on Brachiopoda. - In: Rakús, M., J. Dercourt, A.E.M. Nairn (Eds): Evolution of the Northern Margin of Tethys. Vol. I. - Mem. Soc. Géol. France, Nouv. Sér. 154, I. pp. 79–83, Paris.

Vörös, A. 1993: Jurassic microplate movements and Brachiopod migrations in the western part of the Tethys. - Palaeogeogr., Palaeoclimatol., Paleoecol., 100, pp. 125–145.

Vörös, A., A. Galácz. 1998: Jurassic Paleogeography of the Transdanubian Central Range (Hungary). - Riv. Ital. Paleont. Strat., 104/1, pp. 69–84.

Wagreich, M., P. Faupl, 1994: Paleogeography and geodynamic evolution of the Gosau Group of the Northern Calcareous Alps (Late Cretaceous, Eastern Alps, Austria). - Palaeogeogr., Palaeoec., Palaeoclimat., 110, pp. 235–254.

Wein, Gy 1967: Tektonik von Südosttransdanubien. - Jb. Geol. B.A. 111, pp. 91–133.

Wein, Gy. 1969: Tectonic review of the Neogene-covered areas of Hungary. - Acta Geol. Hung., 13/1–4, pp. 399–436, Budapest.

Wein, Gy. 1978: Alpine-type tectogenesis of the Carpathian Basin. - M. Áll. Földt. Int. Évi Jel. 1976, pp. 245–256, Budapest, (in Hung., with English abstr.).

Zelenka, T., Cs. Baksa, Z. Balla, J. Földessy, K. Földessy-Járányi 1983: The role of the Darnó Line in the basement structure of Northeastern Hungary. - Geol. Zborn.Geol. Carpath., 34/1, pp. 53–69, Bratislava.

Ziegler, P.A. 1986: Geodynamic model for the Paleozoic crustal consolidation of western and central Europe. - Tectonophysics, 126, pp. 303–328.

Acta Geologica Hungarica, Vol. 43/3, pp. 329–343 (2000)

The Tisza Megatectonic Unit in the light of paleomagnetic data

Emő Márton
Eötvös Loránd Geophysical Institute of Hungary, Paleomagnetic Laboratory, Budapest

The paper deals with the paleomagnetic constraints which are relevant for the definition and tectonic history of the Tisza megatectonic unit.

Concerning the Tertiary, there are sufficient paleomagnetic data to prove that the Tisza megatectonic unit was not a rigid block or microplate. While the eastern part of the Tisza moved in a coordinated manner with the South and East Carpathians, the western part was extremely mobile, as indicated by rotations in opposing directions and of different timings.

Paleomagnetic data bearing on the pre-Tertiary history of the Tisza are confined to the Mecsek–Villány area. These support the stable European origin of the Mecsek and Villány and imply that the geometrical separation from the European margin occurred around 130 Ma.

Key words: Tisza Unit, paleomagnetism

Introduction

The Tisza or Tisza–Dacia megatectonic unit occupies the southwestern half of the Pannonian Basin. In this large unit, however, outcrops of pre-Pannonian rocks are scarce. Thus, the paleomagnetic data presented or reviewed in this paper represent "islands" in the megatectonic unit, such as the Mecsek, Villány, Apuseni, Moslavačka Gora and the Slavonian Mts (Papuk, Krindija Psunj). Nevertheless, there are certain suggestions in connection with the tectonic history of the Tisza that may be tested with the available paleomagnetic data. This paper will deal with the following problems: the stable European origin of the Tisza; the timing of the important events of its tectonic history; and the "rigidity" of the megatectonic unit during the Tertiary. The last problem is relevant to the first two, for it is only in a rigid megatectonic unit where the paleomagnetic data obtained in a restricted area may be interpreted as representing the movements of the entire unit. Therefore, on the basis of quite recently obtained data (Márton and Márton 1999; Márton et al. 1999; Panaiotu 1999) the degree of rigidity will be discussed first.

Address: E. Márton: H-1145 Budapest, Columbus utca 17–23, Hungary
E-mail: h11000mar@ella.hu
Received: 15 October, 1999

The rigidity of the Tisza megatectonic unit in the Tertiary

The source areas of the Tertiary paleomagnetic data in the Tisza–Dacia megatectonic unit are the Mecsek Mts, the Slavonian Mts and the Apuseni Mts (Fig. 1). In the Tertiary of the Mecsek Mts, there are some localities that exhibit counterclockwise, others clockwise and the rest practically no rotation with respect to the stable European reference declination (8°) calculated from data compiled by Besse and Courtillot (1991). In the Slavonian Mts rotations are in a counterclockwise, in the Apuseni Mts in a clockwise direction (Fig. 1).

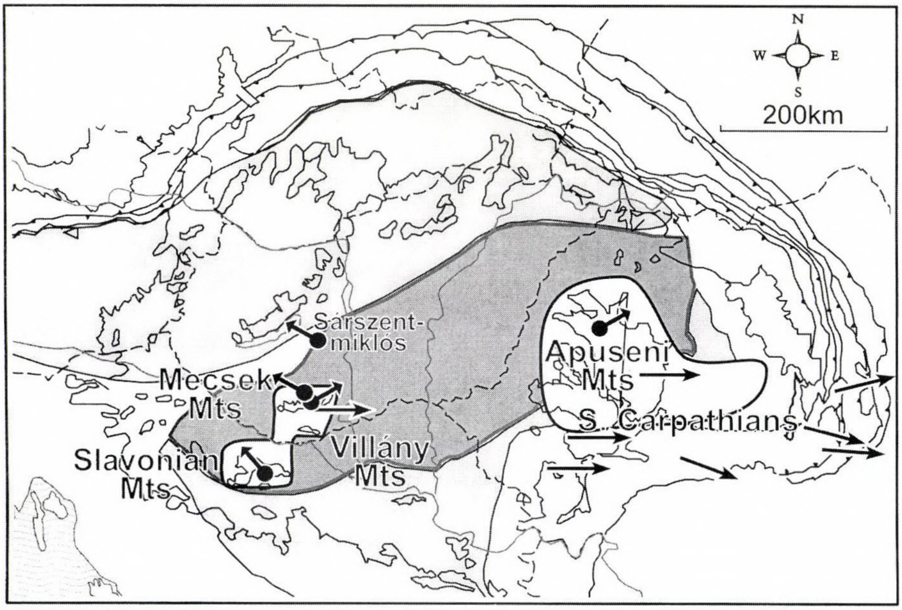

Fig. 1
The source area (study area) of the paleomagnetic data relevant to the tectonic history of the Tisza megatectonic unit. Shorter arrows illustrate the general Neogene rotations described in the text, while longer arrows the general post-Cretaceous net rotations

In the complicated Mecsek Mts (Fig. 2) an average 60° counterclockwise rotation is shown by the Ottnangian ignimbrites, which are aligned with the northern margin of the Neogene sedimentary trough (Fig. 2, localities 11–15). This paleomagnetic direction is remarkably similar to the one obtained for the Sárszentmiklós ignimbrite (Fig. 1), which is situated in the Mid-Hungarian zone. The Badenian sediments of the Neogene sedimentary trough (Fig. 2, localities 6–10) which is north of the main Paleozoic–Mesozoic body of the Mecsek, are not rotated. The rotation observed on the ignimbrites must therefore be of late Ottnangian–Karpatian age. In contrast the declination of the Ottnangian andesite at Komló, (Fig. 2, locality 5), a Karpatian sediment occurrence at Feked

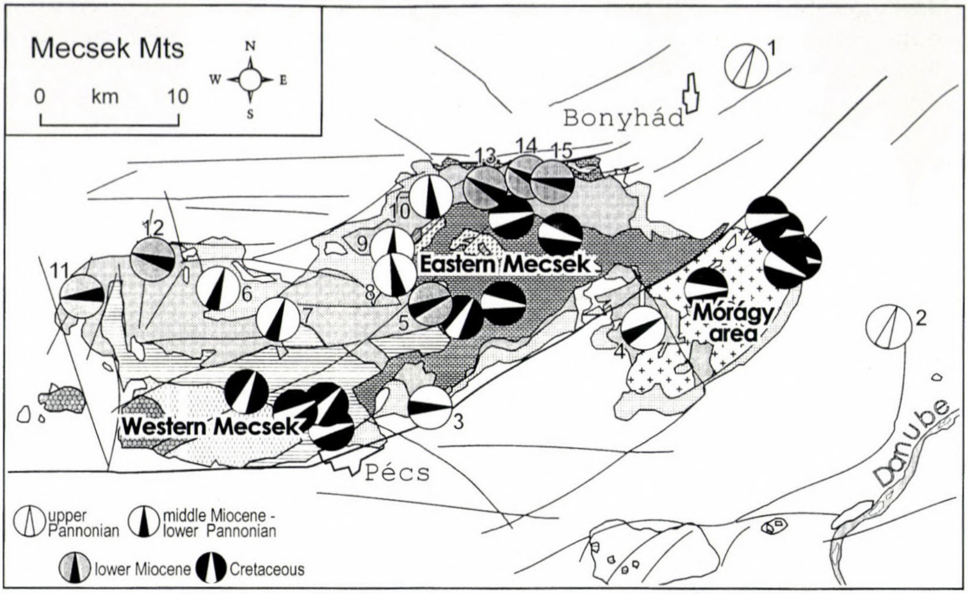

Fig. 2
Mecsek Mts, paleomagnetic declinations obtained from Cretaceous alkali basalts (except lava flows) and Neogene rocks. Arrowheads indicate the location and the directions of the site and locality mean paleomagnetic declinations. Note that the CCW rotations were measured on Ottnangian ignimbrites, and the declinations close to the present north on Badenian and upper Pannonian sediments, respectively

(Fig. 2, locality 4) and a lower Pannonian marl at Danitzpuszta (Fig. 2, locality 3) exhibit rotation to the east (60° – in average). The latter data, with the support of the paleomagnetic directions from Cretaceous alkali basalt sites (Fig. 2, localities without number), permit the conclusion that the main Paleozoic–Mesozoic body of the Mecsek underwent a large clockwise rotation in the Tertiary. However, the exact timing of this rotation is not well constrained by paleomagnetic data. The minimum age of this movement is given by the non-rotated (with respect to stable Europe) declinations of the upper Pannonian sediments around the Mecsek Mts (Fig. 2, localities 1 and 2), but the maximum age is uncertain. Locality 5 and 4 are situated in areas where the Cretaceous alkali basalts also exhibit clockwise rotation; thus, the isolated Tertiary observations are supported by consistent Cretaceous data. Therefore the rotation must be younger than the Karpatian sediment at locality 4. However, the paleomagnetic result for locality 3 is not inferior to that of locality 4, i.e. on a purely paleomagnetic basis we can connect the clockwise Tertiary rotation to the intra-Pannonian compression (Benkovics 1997). Nevertheless, locality 3 is situated very close to the important Mecsekalja tectonic zone; thus, the rotation observed may be the consequence of local tectonics. Microtectonic observations and seismic sections from the Mecsek

Mts suggest that the general Tertiary clockwise rotation must have occurred prior to the Badenian (Csontos et al. in prep). Consequently an intra-Karpatian age of the regional clockwise rotation is more likely than an intra-Pannonian one.

As was already mentioned, the Cretaceous declinations in the Apuseni Mts are also rotated clockwise, with a maximum angle of nearly 90° (Fig. 1). Panaiotu (1999) demonstrated that about 60° of the 90° is due to movements between 14 and 12 Ma. Paleomagnetic data obtained outside of the Apuseni Mts indicate that they were moving in a highly coordinated manner together with the South Carpathians (Patrascu et al. 1990, 1992).

Finally, in the Slavonian Mts, Ottnangian through lower Pannonian rocks show an average 40° counterclockwise rotation, pointing to a post-Lower Pannonian tectonic event as responsible for this phenomenon.

All of the above results suggest that the eastern part of the Tisza megatectonic unit was relatively rigid during the Tertiary, while the western part must have been extremely mobile. In the western part, we observe rotations in opposite directions; if they are in the same direction, then the timing of the movements is not the same. In the Apuseni Mts and in the main Paleozoic–Mesozoic body of the Mecsek the direction and the maximum angle of the rotations are remarkably similar, yet the timing seems to be different.

The stable European origin of the Tisza megatectonic unit

This problem may be discussed by examining the paleomagnetic data from rocks older than Tertiary in the Tisza–Dacia megatectonic unit.

The data set is most complete for the Mecsek and Villány Mts (Fig. 3). It was basically obtained in the eighties, partly in connection with the geologic basic section program, and documented in reports. Since they were never published, the present paper contains information on the quality of the (so far unpublished) results in the form of demagnetization curves (Fig. 4), on the fold test, which

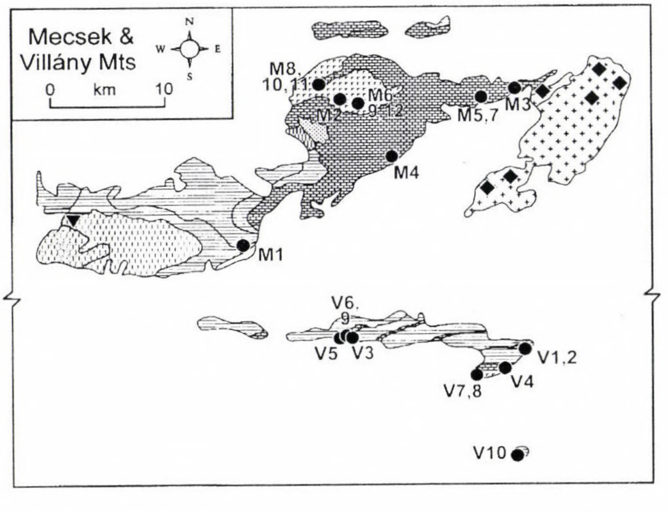

Fig. 3
Pre-Tertiary geologic sketch map of the Mecsek and Villány Mts with the paleomagnetic sampling localities. Diamonds and triangles are for Carboniferous and Permian. V1–V10 and M1–M12 refer to Table I and Table II, respectively

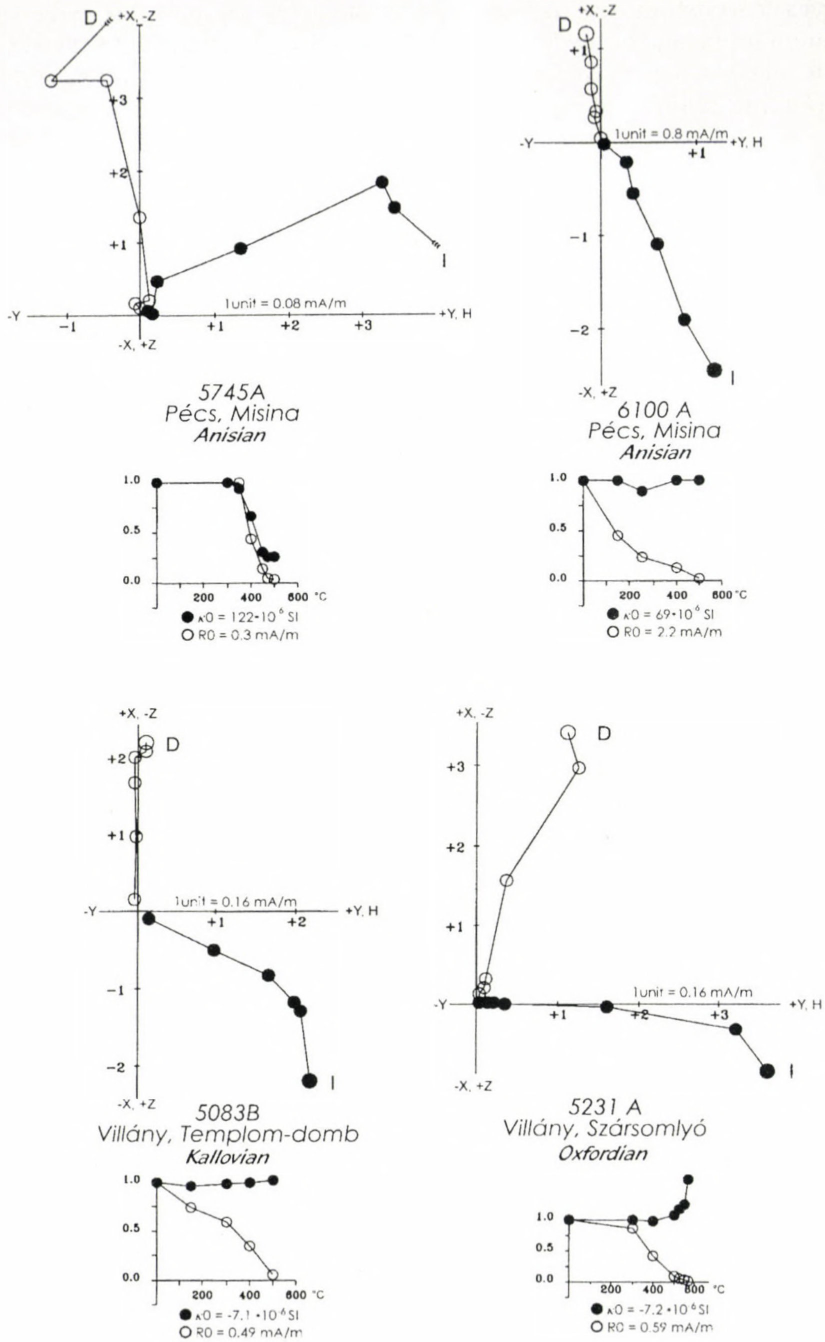

Fig. 4
The behavior of the natural remanent magnetization (NRM) and the susceptibility on demagnetization. Typical modified Zijderveld diagrams (upper diagrams) and normalized susceptibility (dots) and NRM (circles) are shown as a function of the temperature (lower diagrams)

serves to constrain the age of the acquisition of the paleomagnetic signal in relation to the age of the folding (Fig. 5), and the directions with statistical parameters (Tables I–III). The remaining data may be found in Márton and Márton (1969a, 1969b, 1978), Márton (1980, 1986) and in Márton and Elston (1985, 1987).

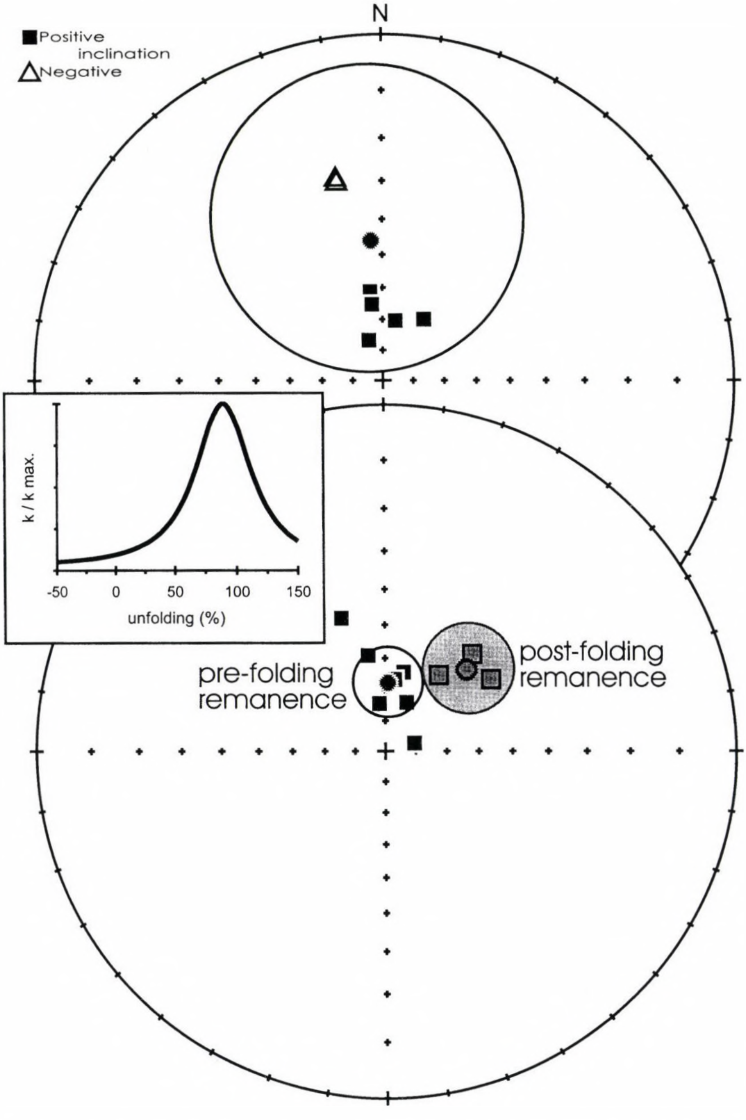

Fig. 5
Pécs, Misina; Anisian limestone. Significant improvement of the statistical parameters for the overall paleomagnetic mean directions on unfolding. The upper one of the stereographic projections shows the site-mean paleomagnetic directions before applying local tilt corrections with the circle of confidence (95% probability level; Fisher 1953), the lower one shows the same after tilt corrections. In the latter, the gray symbols are for the overprint remanence, with a confidence circle for the overall mean direction. The diagram on the left side demonstrates that the best grouping of the paleomagnetic directions is obtained at 90% unfolding

The paleomagnetic record in the Mecsek Mts begins with the Carboniferous, continues with Permian, Anisian, Oxfordian, Tithonian, Berriasian–Hauterivian and ends with the Cretaceous alkali basalts and related rocks. In the Villány, the oldest rocks represented are of Anisian, the youngest of Albian age.

Declinations for rocks older than Cretaceous typically scatter around the present north. The inclinations suggest a considerable northward shift from the Carboniferous to the Anisian (Fig. 6 shows the shift from Permian to Anisian), in accordance with the shift of the large plates. There is, however, a mismatch in timing, for the Mecsek–Villány area seems to have arrived earlier (i.e in the Anisian) to a latitude similar to the present one, while the large plates were still in a more southerly position. The mismatch in timing may be due to the use of different time scales and/or to the incompatibility between smoothed curves characterizing the latitudes of the large plates and the single Anisian stage latitude calculated for the Mecsek–Villány Mts Another possibility is that the magnetization is younger than Anisian, despite the fact that the magnetization is of pre-folding (tilting) age, as Fig. 5 demonstrates. Therefore the alternatives for dating the paleomagnetic signal must be examined.

There are two main events of compression in the Mecsek–Villány area that are thought to be responsible for the folding and tilting. The older one is the late Cretaceous Austrian phase (Wein 1967), the younger one is the intra-Pannonian (Hámor 1970) phase. Though the younger phase had clearly also involved the Mesozoic–Paleozoic sequences, folding and tilting in the pre-Tertiary rocks is basically a Cretaceous event (Benkovics et al. 1997; Konrád, pers. com.)

Carefully analyzing the remanence of the Anisian sediments from the Mecsek Mts, at some sites an overprint component of post-tilting age can be defined (Fig. 5) with a direction which is significantly different from that of the pre-folding magnetization (it has a 15° shallower inclination than that of the pre-folding remanence, and the declination is rotated to the east, i.e. similar to the Cretaceous paleomagnetic vectors). Due to the significant difference between the directions of the pre and post-folding remanence, a Cretaceous age of the pre-folding remanence is unlikely. Remagnetization during the late Miocene, but before the intra Pannonian tectonic phase, is another possibility. This would, however, imply that the folding and tilting is basically intra-Pannonian, which would contradict tectonic observations. Thus, the most likely alternative is that the pre-folding remanence measured on Anisian rocks is indeed of Anisian age, and the reason for the steeper than expected inclination, in addition to the previously described arguments, may be the more northerly position than today of the Mecsek with respect to stable Europe, as Török (1998) postulated.

The post-Triassic paleolatitudes follow the stable European reference curve closely (Fig. 6) except for the one calculated for the re-deposited Berriasian-Valanginian beds of the Mecsek Mts.

Another aspect of the paleomagnetic data relevant to the origin of the Mecsek–Villány area is the declination pattern which is not compatible with those of the

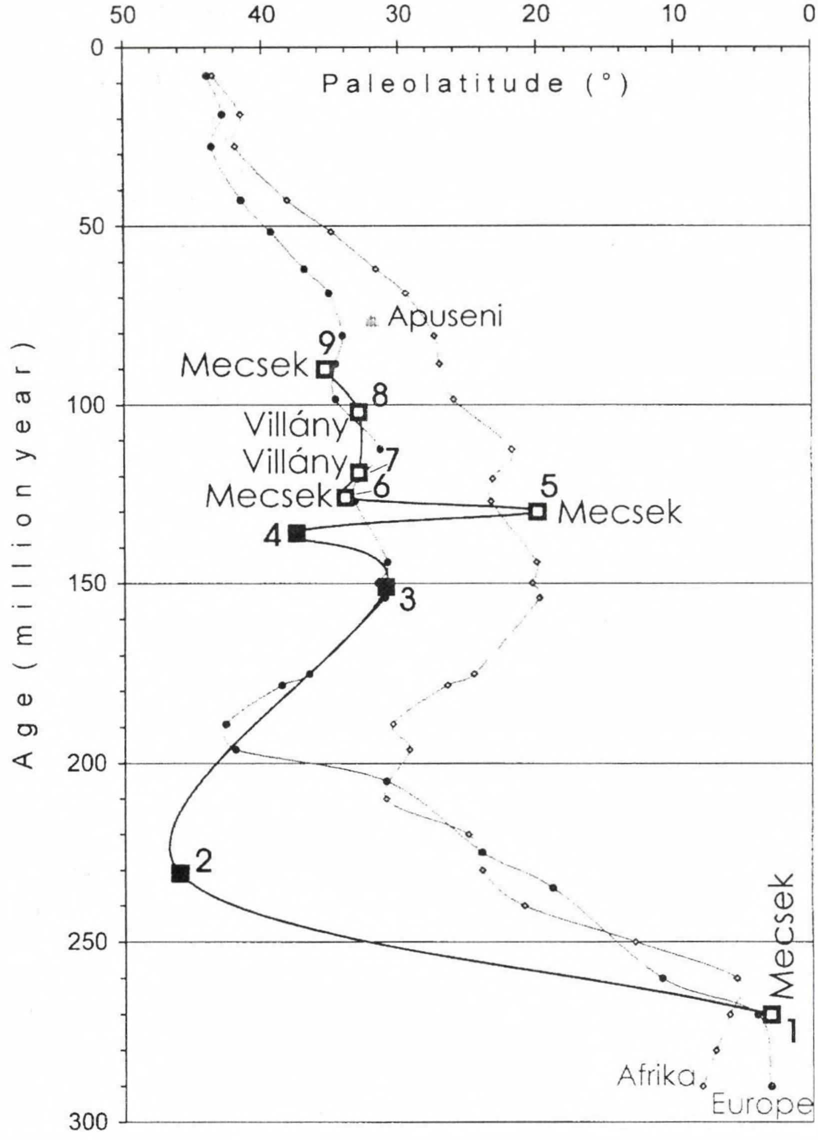

Fig. 6
Paleolatitudes calculated from the paleomagnetic indications observed for the Mecsek and Villány (squares, numbered) and the Apuseni (triangle) Mts in relation to the expected paleolatitudes in a stable European (dots) and an African (diamonds) reference system. Full squares are for combined results for the Mecsek and Villány Mts, empty squares are paleolatitudes for either of the two. Numbers from 1 to 9 refer to Permian (Márton and Elston 1987), Anisian (Table I: M1, Table II: V1), Oxfordian (Table I: M2–M5, Table II: V2–V5), Tithonian-Berriasian (Table I: M6–M8, Table II: V6), Berriasian-Valanginian (Table I: M9, M10), Hauterivian (Table I: M12), Barremian (Table II: V7), Albian (Table II: V8–10), sediments and Cretaceous alkali basalts (Márton 1986), respectively

tectonic units of African origin, such as the Transdanubian Central Range (Márton 1990). Thus, both paleolatitudes and declinations favor the stable European origin of the Mecsek–Villány area over an African origin.

Pre-Tertiary paleomagnetic data from the Apuseni Mts (and the South Carpathians) mostly represent Late Cretaceous igneous rocks exhibiting easterly rotation of about 90° on average (Patrascu et al. 1990, 1992). A series of sediments from Triassic through Cretaceous from the Apuseni Mts shows similar declinations. These data are interpreted as overprint directions imprinted during the late Cretaceous magmatic activity (Surmont et al. 1990). The problem is, however, that the mean inclination for the sedimentary series is steeper by about 30° than the one obtained for the igneous rocks. The second is far too shallow; the first is far too steep to be accommodated between the European and African reference systems. The late Cretaceous paleolatitude for the Apuseni Mts (which is the average paleolatitude calculated from the inclinations of the two datasets – Fig. 6, triangle) is accommodated by the reference systems of the large plates. Nevertheless, the late Cretaceous paleolatitude defined in this manner is quite useless (due to the large scatter in inclinations) in deciding about the European of African affinity of the Apuseni Mts.

As long as the Tisza megatectonic unit could have been conceived as a rigid microplate in the Tertiary, it was possible to extrapolate only the relevant Mesozoic paleomagnetic results from the Mecsek–Villány area to the whole of the mega-unit and speak about its stable European origin. The differential rotations of different timings in the Tertiary, discussed in the previous chapter, invalidate such extrapolation. That is why in the next chapter the discussion will concern the Mecsek–Villány area and not the entire Tisza megatectonic unit.

Separation of the Mecsek–Villány area from stable Europe

In the previous chapter it was demonstrated that the paleolatitudes as well as the declination pattern from the Mecsek–Villány area are basically compatible with a stable European origin. The question is now how closely and how long the European pattern was followed, i.e. the time of separation of the Mecsek–Villány area from stable Europe.

Figure 6 shows that the paleolatitudes for the Mecsek–Villány area suggest that it was close to the stable European margin. There is, however, a swing in the curve around 130 Ma (points 4 and 5), a kind of disturbance, which may be the consequence of an important tectonic process.

The declinations scatter around the present north until the end of the Jurassic. Again, at about 130 Ma "anomalous declinations" appear. The source rocks of the out-of-pattern inclinations and declinations are resedimented limestone beds, which occur in two sections (Mészkemence-völgy and Kisújbánya) with different tilts. The paleomagnetic vectors from the resedimented beds cluster significantly better after tilt correction than before it (Table III; combination of data M9 and

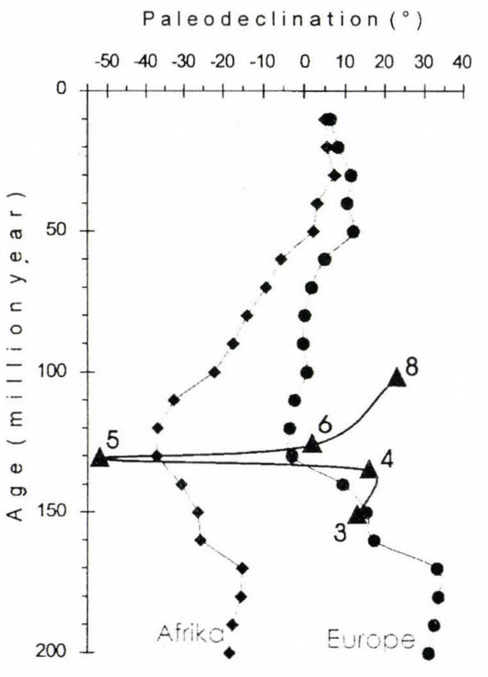

Fig. 7
The time of geometrical separation of the Mecsek–Villány area from the stable European margin suggested by paleomagnetic data. Expected paleodeclinations (Besse and Courtillot 1991) for latitude 47.3°, longitude 19.5°. Numbers to 3–8 are same as for Fig. 6

M10 from Table I), which indicates that we are dealing with a remanence of pre-tilting age, i.e. very likely a primary remanence acquired during re-sedimentation. The "anomalous directions" may be of tectonic significance due to the facts that the two sections are several kilometers apart, that remanence directions are fairly well grouped in each section and, most importantly, that they respond positively to tilt correction. In other words, they may indicate the separation from the stable European margin.

The age of the sediments below the resedimented strata is very well constrained. Thus, we can date the separation of the Mecsek–Villány area from the stable European margin as having occurred at about 130 Ma (Figs 6 and 7).

In the declination curve of Fig. 7 the change from low easterly to westerly (negative) declination is sudden (Fig. 7, points 4 and 5), while a similar trend shown by the declinations expected in a stable European frame (from higher easterly to near-zero declinations) is smooth. Since the stable European reference curve is smoothed and averaged, it is difficult to tell if the change in declination from near zero to westerly in the Mecsek is still a more or less coordinated rotation with Europe, or basically an independent one. In either case, however, by correction for the first rotation about 130 Ma ago, the older than Berriasian declinations will become easterly, as would be expected in a stable European reference system.

The second rotation, i.e. the one which brings the declination for the Mecsek first close to, then beyond the stable European reference curve, on the clockwise rotated side (Fig. 7, points 5, 6, 8) must have been independent, and relatively slow. Its angle well exceeds 90° and may be connected to the subduction closing the Vardar Ocean.

Table I
Locality mean paleomagnetic results from the Mesozoic of the Mecsek Mts

	Locality	n/N	D°	I°	k	α_{95}°	Dc°	Ic°	k	α_{95}°
M 1	Pécs, Misina Anisian	48/7	355	+46	3	41	1	+66	28	11
M 2	Csengőhegy Oxfordian (Bath-Callovian)	25/7	18	+59	17	15	11	+53	17	15
M 3	Ófalu Oxfordian	7/2	35	+54	30	11	349	+39	29	12
M 4	Pécsvárad Oxfordian	7/2	11	+76	18	19	356	+37	18	19
M 5	Apátvarasd Oxfordian	10/2	66	+44	40	8	21	+46	40	8
M 6	Márévár valley Tithonian	5/1	38	+38	88	8	6	+52	88	8
M 7	Apátvarasd Tithonian/Berriasian	12/2	86	+47	19	10	37	+66	19	10
M 8	Mészkemence-völgy Berriasian	35/9	40	+63	30	9	350	+40	35	9
M 9	Kisújbánya Berriasian	15/5	302	+28	36	13	305	+37	41	12
M 10	Mészkemence-völgy Valanginian	18/6	284	+84	31	12	311	+36	43	10
M 11	Mészkemence-völgy Hauterivian	9/2	67	+56	15	14	4	+25	15	14
M 12	Kisújbánya Hauterivian	7/2	6	+58	75	7	2	+44	75	7

1, 2, 8, 9, 10 statistics based on sites; 3, 4, 5, 6, 7, 11, 12 statistics based on samples; 9, 10 resedimented strata; 11 interpreted as overprint due to the closeness of an alkali basalt intrusive body

Key: n/N: number of samples/sites
D/I: mean declination, inclination before DC, IC the same after tilt correction
k, α_{95}: statistical parameters (Fisher 1953)

Table II
Locality mean paleomagnetic results from the Mesozoic of the Villány Mts

	Locality	n/N	D°	I°	k	α_{95}°	Dc°	Ic°	k	α_{95}°
V 1	Villány Templomdomb Anisian	6/1	2	+23	120	6	10	+74	120	6
V 2	Villányi Templomdomb Oxfordian	18/5	6	+27	100	8	50	+68	111	7
V 3	Máriagyüd Oxfordian	6/1	6	+36	91	7	19	+58	91	7
V 4	Szársomlyó Oxfordian	26/5	14	-14	32	14	25	+55	30	14
V 5	Harkány-Siklós road junction Oxfordian	5/1	3	+27	64	10	10	+57	64	10
V 6	Vízügyi bánya Tithonian	7/1	12	+41	155	5	40	+68	155	5
V 7	Szársomlyó Barremian	13/3	25	-6	214	8	46	+57	56	17
V 8	Szársomlyó Albian	4/1	22	+27	33	16	42	+76	33	16
V 9	Vízügyi bánya Albian	16/4	5	+35	68	11	36	+69	68	11
V 10	Beremend Albian	15/4	29	+50	19	21	29	+50	19	21

2, 4, 7, 9, 10 statistics based on sites; 1, 3, 5, 6, 8 statistics based on samples.

Key: same as for Table I.

Table III
Overall-mean paleomagnetic results for different stages for the Mecsek, for the Villány and (wherever applicable) for both

Locality	D°	I°	k	α_{95}°	D_c°	I_c°	k	α_{95}°	unfolding	paleomagnetic pole		paleo-
									%	lat	lon	latitude
Mecsek *Anisian* based on 4 localities	355	+46	3	41	0	+64	33	11	90	88	199	45
Villány *Oxfordian* based on 4 localities	7	+19	13	27	21	+58	70	11	94	72	131	39
Eastern Mecsek *Oxfordian* based on 4 localities	39	+60	19	21	10	+50	48	13	73	72	170	32
Villány and Eastern Mecsek *Oxfordian* based on 8 localities	18	+41	7	22	13	+50	59	7	74	71	164	31
Eastern Mecsek *Tithonian-Berriasian* based on 3 localities	55	+52	14	34	16	+56	20	28	78	74	146	36
Villány and Eastern Mecsek *Tithonian* based on 4 localities	42	+50	12	28	24	+57	29	17	64	70	130	37
Mecsek *Berriasian-Valanginian* based on 11 samples, 2 localities	117	-60	6	20	127	-37	49	7	98	40	276	21
Villány *Albian* based on 3 localities, 9 sampling sites	18	+38	28	23	23	+53	227	8	53	68	143	33

Paleolatitudes are calculated for lat.: 47.3°, lon.: 19.5°.

Key: same as for Table I. The "unfolding" column indicates the degree of unfolding in percent, where the statistical parameters are the best for the given group of samples, sites or localities. The higher the percentage, the better the result from the viewpoint of purely prefolding age of the remanence

The estimated time of the separation of the Mecsek–Villány area from the stable European margin based on paleomagnetic data is somewhat younger than the one estimated from paleontological data (Vörös 1993). The difference, however, is easily explained by the fact that the paleomagnetic data reflect the time of the geometrical separation, while the differentiation of the fauna can start when rifting is still at an early stage.

Acknowledgement

This work was partially supported by an OTKA (Hungarian Research Fund) grant (No. T 017008).

References

Benkovics, L. 1997: Etude structurale et géodynamique des Monts Buda, Mecsek et Villány (Hongrie). – These Présentée à l'université des sciences et technologies de Lille. Docteur de l'université en géologie et géochemie sédimentaires. 230 p.

Benkovics, L., J-L. Mansy, L. Csontos, F. Bergerat 1997: Folding in the Abaliget road cut (Mecsek Mts). – Acta Geol. Hung., 40, pp. 425–440.

Besse, J., V. Courtillot 1991: Revised and Synthetic Apparent Polar Wander Paths of the African, Eurasian, North American and Indian Plates, and True Polar Wander Since 200 Ma. – J. of Geophys. Res., 96, B3, pp. 4029–4050.

Fisher, R. 1953: Dispersion on a sphere. – Proc. R. Soc. London, Ser. A., 217, pp. 295–305.

Hámor, G. 1970: Miocene of eastern Mecsek Mts. – MÁFI Évk., 53, 484 p.

Márton, E. 1980: Multicomponent remanent magnetization of migmatites, Mórágy area, SW Hungary. – Earth and Planet. Sci. Letters, 47. pp. 102–112.

Márton, E. 1986: Paleomagnetism of igneous rocks from the Velence Hills and Mecsek Mountains. – Geophys. Transactions, 32, pp. 83–45.

Márton, E. 1990: Kinematics of the principal tectonic units of Hungary from paleomagnetic observations. – Acta Geod. Geoph. Mont. Hung., 25/3–4, pp. 387–397.

Márton, E., D.P. Elston 1985: Structural rotations from paleomagnetic directions of some Permo-Triassic redbeds, Hungary. – Geophys. Transactions, 31, pp. 217–230.

Márton, E., D.P. Elston 1987: Tectonic rotations south of the Bohemian Massif from palaeomagnetic directions of Permian red beds in Hungary. – Tectonophysics, 139, pp. 43–51.

Márton-Szalay, E., P. Márton 1978: On the difference between the palaeomagnetic poles from the Transdanubian Central Mountains and the Villány Mountains respectively (in Hungarian). – Magyar Geofizika, 19/4, pp. 129–136.

Márton, E., P. Márton 1999: Tectonic aspects of a paleomagnetic study in the Neogene of the Mecsek Mountains. – Geophys. Transactions, 42, pp. 159–180.

Márton, E., D. Pavelic, B. Tomljenovic, J. Pamic, P. Márton 1999: First paleomagnetic results on Tertiary rocks from the Slavonian mountains in the southern Pannonian basin, Croatia. – Geologica Carpathica, 50, pp. 273–279.

Márton, P., E. Márton-Szalay 1969a: Palaeomagnetic investigation of magmatic rocks from the Mecsek Mountains, Southern Hungary. – Ann. Univ. Sci. Budapestinensis de Rolando Eötvös nom., Sect. Geol., 12, 1968, pp. 67–80.

Márton, P., E. Márton-Szalay 1969b: Palaeomagnetism and tectonics in the Eastern Mecsek Mountains (in Hungarian). – Magyar Geofizika, 10/5, pp. 216–220.

Panaiotu, C. 1999: Paleomagnetic studies in Romania: Tectonophysics implications. – PhD. Thesis University of Bucharest.

Patrascu, St., M. Bleahu, C. Panaiotu 1990: Tectonic implications of paleomagnetic research into Upper Cretaceous magmatic rocks in the Apuseni Mountains, Romania. – Tectonophysics, 180, pp. 309–322.

Patrascu, St., M. Bleahu, C. Panaiotu, C.E. Panaiotu 1992: The paleomagnetism of the Upper Cretaceous magnetic rocks in the Banat area of South Carpathians: tectonic implications. – Tectonophysics, 213, pp. 341–352.

Surmont, M., M. Sandulescu, S. Bordea 1990: Mise en évidence d'une réaimantation fin crétacée des séries mésozoiques de l'unité de Bihor (Monts Apuseni, Roumanie) et da sa rotation horaire ultérieure. – C. R. Acad. Sci. Paris, t.310, Série II, pp. 213–219.

Török, Á. 1998: Controls on development of Mid-Triassic ramps: examples from southern Hungary. – In: Wright, V.P., T.P. Burchette (Eds): Carbonate Ramps. Geological Society London, Special Publications, 149, pp. 339–367.

Vörös, A. 1993: Jurassic microplate movements and brachioid migrations in the western part of the Tethys. – Paleogeogr., Paleoclim., Paleoecol., 100, pp. 125–145.

Wein, Gy. 1967: Tectonics of southeast Transdanubia (in Hungarian). – Földtani Közlöny, 47, pp. 371–395.

Acta Geologica Hungarica, Vol. 43/3, p. 345 (2000)

Conference report

"The Earth Sciences on the Evolution of the Carpathian Basin. Past and Present Trends. Variety in Unity." – HUNGEO-2000

The Fifth Meeting of Hungarian Goescientists took place on August 15–19, 2000. For this occasion (Millenium of the Christian Hungarian State) a total of 135 geoscientists from 11 European countries and from the USA gathered at the campus of P. Pázmány Catholic University at Piliscsaba (24 km NW of Budapest). The European countries represented were Austria, France, Germany, Hungary, the Netherlands, Romania, Slovakia, Sweden, Switzerland, Ukraine, and Yugoslavia.

The meeting was organized by the Hungarian Geological Society, in co-operation with the scientific societies of Cartography, Geodesy and Remote Sensing, Geography, Geophysics, Karst Research and Speleology, and Meteorology, under the auspices of the Hungarian Academy of Sciences, several Ministries and other high instances. (About the four previous meetings see vol. 42/3, pp. 347–348, of Acta Geol. Hung.; these took place in Budapest (1996), Csíkszereda/Miercurea Ciuc, Romania (1997), Budapest (1998), and in eastern Slovakia and Transcarpathian Ukraine (1999).

Invited top scientists of the host country delivered 11 keynote lectures. In six sections (Cartography, Geography, Geology, Geophysics, Meteorology, and Education) altogether 38 talks were given and 21 posters were presented.

Two one-day excursions visited (A) Gödöllő (former royal hunting castle), Hollókő village (World Cultural Heritage site), Ipolytarnóc (Lower Miocene sandstone with abundant footprints of mammals and birds covered and preserved by rhyolite tuff) and (B) Esztergom (XI-XII. c. royal castle, cathedral), Tata (Geopark), Vértesszőlős (fossil man site) and Tatabánya (open-air museum of coal mining).

A Volume of Abstracts and a Field Guide were printed and distributed to the participants.

The Commission of HUNGEOTOP (Hungarian Geoscientists' Scientific and Educational Program) was renewed for a second four-year term (until 2004).

The next (6th) meeting is scheduled to take place in the West Hungarian University in the town of Sopron, with excursions to Austria (mainly Burgenland), in August 2002 (not 2001).

For further information please contact
Hungarian Geological Society (MFT), H-1027 Budapest, Fő utca 68., I/102.
Phone/Fax: (36/1) 201 9129, E-mail: mail.mft@mtesz.hu

Endre Dudich

Akadémiai Kiadó, Budapest

Acta Geologica Hungarica, Vol. 43/3, p. 347 (2000)

Book review

Landform evolution studies in Hungary
Studies in Geography in Hungary, 30
Edited by Márton Pécsi

Akadémiai Kiadó, Budapest, 216 pages

The volume was dedicated to the 150th anniversary of the Hungarian Geological Society and the 125th anniversary of the Geographical Society. Forty-four authors (geologists and geomorphologists) participated, writing the different chapters. Mr. Márton Pécsi, regular member of the Hungarian Academy of Sciences co-ordinated the work of the authors as editor-in-chief.

The volume offers a general outlook and review on geomorphological researches in Hungary performed during the last decades, furthermore it contains ideas and proposals for the future. The study and the protection of the environment became a subject of top priority in recent days. The authors discuss this problem as well, from the special point of view of geomorphology. New methods of geomorphological mapping are presented, such as environmental typological maps. Problematic questions are also discussed, like the dating of landforms.

An introduction, written by M. Pécsi outlines the history and the background of geomorphological research in Hungary. The volume contains four main chapters. In the first one the working theories concerning the landform evaluation in Hungary are presented. This is the longest chapter of the book, with seven contributions. In the second chapter the main geomorphic processes are discussed; it also comprises seven contributions. The third chapter is entitled "Surveying the relief and landforms". Here the methods of geomorphological mapping and the classification of relief types are discussed. Problems of social and economic importance are reviewed as well, such as flood control, boreholes and mining in relationship geomorphological research.

The final chapter of the volume contains the scientific biography and the major publications of the most prominent Hungarian geologists and geographers, who participated in the study of landform evolution in Hungary. This chapter gives an excellent review of the professional life and main achievements of these outstanding scientists.

The volume contains an extremely rich list of references over 50 pages. A subject index helps the reader to find topics of his/her special interest. The book ends with a set of coloured photographs showing books published in Hungary on geomorphologic and geologic topics. The volume is recommended to geographers and geologists with an interest for the present situation and the major achievements of geomorphological research in Hungary.

George Bárdossy

Printed in Hungary
Akadémiai Nyomda, Martonvásár

GUIDELINES FOR AUTHORS

Acta Geologica Hungarica is an English-language quarterly publishing papers on geological topics. Besides papers on outstanding scientific achievements, on the main lines of geological research in Hungary, and on the geology of the Alpine–Carpathian–Dinaric region, reports on workshops of geological research, on major scientific meetings, and on contributions to international research projects will be accepted.

Only original papers will be published and a copy of the Publishing Agreement will be sent to the authors of papers accepted for publication. Manuscripts will be processed only after receiving the signed copy of the agreement.

Manuscripts are to be sent to the Editorial Office for refereeing, editing, in two typewritten copies, on floppy disk with two printed copies, or by E-mail. Manuscripts written by the following word processors will be accepted: MS Word, or ASCII format. Acceptance depends on the opinion of two referees and the decision of the Editorial Board.

Form of manuscripts

The paper complete with abstract, figures, tables, and bibliography should not exceed 25 pages (25 double-spaced lines with 3 cm margins on both sides).

The first page should include:

- the title of the paper (with minuscule letters)
- the full name of the author
- the name of the institution and city where the work was prepared
- an abstract of not more than 200 words
- a list of five to ten key words
- a footnote with the postal address of the author

The SI (System International) should be used for all units of measurements.

References

In text citations the author`s name and the year of the publication between brackets should be given. The reference list should contain the family name, a comma, the abbreviation of the first name, the year of publication, and a colon. This is followed by the title of the paper. Paper titles are followed – after a long hyphen – by periodical title, volume number, and inclusive page numbers. For books the title (English version), the name of the publisher, the place of publication, and the number of pages should be given.

Figures and tables

Figures and tables should be referred to in the text. Figures are expected in the size of the final type-area of the quarterly (12.6 x 18.6) or proportionally magnified 20–25% camera ready quality. Figures should be clear line drawings or good quality black-and-white photographic prints. Colour photographs will also be accepted, but the extra cost of reproduction in colour must be borne by the authors. The author`s name and figure number should be indicated on the back of each figure. Tables should be typed on separate sheets with a number.

Proof and reprints

The authors will be sent a set of proofs. Each of the pages should be proofread, signed, and returned to the Editorial Office within a week of receipt. Twenty-five reprints are supplied free of charge, additional reprints may be ordered.

Contents

Acta Geologica Hungarica

17.

VOLUME 43, NUMBER 4, 2000

Akadémiai Kiadó, Budapest

ACTA GEOL. HUNG. AGHUE7 43 (4) 349–501 (2000) HU ISSN 0236–5278

ACTA GEOLOGICA HUNGARICA

A QUARTERLY OF THE HUNGARIAN ACADEMY OF SCIENCES

Acta Geologica Hungarica publishes original studies on geology, crystallography, mineralogy, petrography, geochemistry and paleontology.

Acta Geologica Hungarica is published in yearly volumes of four numbers by

AKADÉMIAI KIADÓ
H-1117 Budapest, Prielle Kornélia u. 4, Hungary
http://www.akkrt.hu

Manuscripts and editorial correspondence should be addressed to the

ACTA GEOLOGICA HUNGARICA

Dr. János Haas
Academical Research Group, Department of Geology, Eötvös Loránd University of Sciences
H-1088 Budapest, Múzeum krt. 4/a, Hungary
Phone/Fax: (36-1) 266 4947
E-mail: haas@ludens.elte.hu

Orders should be addressed to

AKADÉMIAI KIADÓ
H-1519 Budapest, P.O. Box 245, Hungary
Fax: (36-1) 464 8221
E-mail: kiss.s@akkrt.hu

Subscription price for Volume 43 (2000) in 4 issues US$ 180.00, including normal postage, airmail delivery US$ 20.00.

Acta Geologica is abstracted/indexed in Bibliographie des Sciences de la Terre, Chemical Abstracts, GeoRef, Hydro-Index, Mineralogical Abstract

AGeol 43 (2000) 4

Acta Geologica Hungarica, Vol. 43/4, pp. 349–350 (2000)

Professor Ernő Nemecz's scientific career

Professor Ernő Nemecz was born in Losonc in 1920. He finished his studies in 1943 at the Péter Pázmány University (Budapest), receiving a diploma as a teacher in natural geography and chemistry. He obtained his doctorate degree in geology in 1944 at the same university. In 1973 he became a member of the Hungarian Academy of Sciences. He is presently Professor Emeritus of the Department of Earth and Environmental Sciences of the University of Veszprém. At the same time he is an honorary member of the Societé de Géographie (Paris, France). In 1942 Professor Nemecz held a research assistance position in the Department of Mineralogy at the József Nádor Technical and Economical Science University. In 1949 he joined the Veszprém University of Chemical Engineering and he set up the Department of Mineralogy. In 1953 he accepted an appointment as Dean at the University of Veszprém and between 1971 and 1980 he served as Rector of the University.

Prof. Nemecz's interest covers a wide spectrum of geology and geochemistry. His major research field includes the characterization of natural Hungarian zeolite minerals, namely clinoptilolite and mordenite, investigations of clay minerals, and application of X-ray powder diffraction and fluorescence spectrometry to the identification and quantitative determination of crystalline materials. He has worked on the determination and aging of the mineral components of soils sampled at different depth. Among his books, Clay Minerals (1981) was published in English, and the other four in Hungarian. His advanced book Agyagásványok (1973) is well known to students, geologists and scientists in Hungary. He has published several papers and has given lectures in Europe.

His career has brought him numerous awards. These include the Gold Medal for Excellent Work (1964, 1974), Award of the Hungarian Academy, for his research work in the field of mineralogy (1969), State Award (1982), and Award of Pro Universitate Vespremienses (1982).

He has been an active member in the Department of Earth Sciences of the Hungarian Academy of Sciences since 1973. He served as Chairman between 1985 and 1990 and member of the Presidium (1976–1990). He was an active

0236–5278/2000/$ 5.00 © 2000 *Akadémiai Kiadó, Budapest*

founding member of the Regional Committee of the Hungarian Academy of Sciences at Veszprém and served as Chairman of the Committee between 1975–1980. For 6 years he accepted the position as the President of the Hungarian Geological Society (1966–1972) and played a major role in the development and integration of the domestic earth sciences.

Along with his personal research achievements, which were fundamental in many respects, Professor Nemecz's major contributions to science have been in the areas of teaching geology, crystallography and earth resources as scientific disciplines. He has been lecturing on graduate and post-graduate courses since 1949 having shown interest, understanding and enthusiasm to his students.

József Hlavay

Acta Geologica Hungarica, Vol. 43/4, pp. 351–378 (2000)

Composition, diagenetic and post-diagenetic alterations of a possible radioactive waste repository site: the Boda Albitic Claystone Formation, southern Hungary

Péter Árkai
Laboratory for Geochemical Research
Hungarian Academy of Sciences

Kadosa Balogh
Institute of Nuclear Research
Hungarian Academy of Sciences

Attila Demény, István Fórizs,
Géza Nagy
Laboratory for Geochemical Research
Hungarian Academy of Sciences

Zoltán Máthé
Mecsek Ore Environment Company

In southern Hungary a thick Upper Permian claystone formation has been selected as a possible repository of high-level nuclear waste. Detailed petrographic and geochemical characterizations of the formation are given, using the results of microscopic observations, X-ray diffractometric modal and phyllosilicate crystallinity, X-ray fluorescence major element bulk chemical, K-Ar isotope geochronologic and stable C, O and H isotope ratio analyses. On the basis of peculiar bulk chemistries and modal compositions characterized by extremely high, authigenic albite, low quartz, high hematite and moderate carbonate contents, the formation is considered to have been deposited in a shallow-water lacustrine environment, under semi-arid to arid climatic conditions and highly alkaline, strongly oxidative hydrological ones. Illite and chlorite crystallinity as well as vitrinite reflectance data point to late or deep diagenesis (max. 200–250 °C) that – according to the K-Ar ages of the <2 μm grain-size fraction K-white micas – culminated in the Lower Jurassic. Post-diagenetic fracturing caused by repeated brittle deformations of the rigid rock mass is a common phenomenon. In the most frequent fault gouges phyllosilicate retrogression (i.e. chlorite alteration, smectite and mixed-layered clay mineral formation, etc.) occurs. K-Ar ages show that these processes proceeded under disequilibrium conditions. C and O isotope compositions of whole rock carbonates indicate sedimentary origin, while whole rock carbonates with high $\delta^{13}C$ and variable $\delta^{18}O$ values suggest pervasive diagenesis. Ubiquitous fracture fillings are grouped into calcite-, baryte+quartz- and anhydrite-dominated veins, the barytic one with traces of sulfidic mineralizations. The combined H-C-O isotopic study of fissure-filling carbonates and fluid inclusions suggests three fluid generations acting in fractures, namely: magmatic fluid and meteoric waters related to warm and cold climates, respectively. A significant effect of recent meteoric water in fracture fillings is unlikely.

Key words: Permian claystone, modal composition, illite crystallinity, chlorite crystallinity, diagenesis, K-Ar dating, stable isotope geochemistry, fracture fillings, Hungary, radioactive waste repository

Addresses: P. Árkai: H-1112 Budapest, Budaörsi út 45, Hungary. E-mail: arkai@sparc.core.hu
A. Demény, I. Fórizs, G. Nagy: H-1112 Budapest, Budaörsi út 45, Hungary
K. Balogh: H-4001 Debrecen, Bem tér 18/c, Hungary
Z. Máthé: H-7633 Pécs, Esztergár L. út 19, Hungary
Received: 15 May, 2000

Introduction

Thick, fine clastic (pelitic-silty) formations with low porosity and permeability are generally considered as ideal geologic objects for isolating hazardous materials. Therefore, such formations are intensively studied for long-life storing of radioactive waste worldwide. The present paper summarizes the results of extensive petrographic, mineralogical, major element and stable isotope (O, C, H) geochemical investigations carried out on a 700–900 m thick, rather homogeneous Upper Permian claystone series found in the western part of the Mecsek Mountains, southern Hungary. Special attention is paid to the unusual modal and chemical compositions of the claystone that are attributed to peculiar depositional and diagenetic conditions. These characteristics, together with diagenetic transformations and post-diagenetic changes (which were connected mainly with repeated brittle deformations of the rock mass), are the main factors that control the hydrological and mechanical properties of the claystone selected as a possible repository of high-level nuclear waste in Hungary.

Geologic outline

The Boda Albitic Claystone Formation (abbreviated in the following as BACF) is located in the Mecsek Mountains, southern Transdanubia, Hungary (Fig. 1). According to recent plate tectonic reconstructions the pre-Tertiary basement of the Carpathian or Pannonian Basin is built up by different blocks (microplates) that originated from various parts of the Tethys, as well as of neighboring areas. Thus, the Tisza Unit (also known as the Tisia Composite Terrane; see Kovács et al. 1996–97), in the central part of which the investigated BACF is found, represents a fragment of the northern (stable European) border of the Tethys detached from the continent during the Middle Jurassic and moved to its present position by horizontal microplate displacements, mainly during the meso-Alpine tectonophases (Géczy 1973; Kovács 1982; Kázmér and Kovács 1985; Kovács et al. 1996–97). The easternmost part of the Mecsek Mountains (Mórágy Hills) is built up by Variscan granitoids and metamorphic rocks. The Eastern Mecsek Mountains consist of a huge syncline containing a thick, continuous Mesozoic series ranging from the Lower Triassic up to the Lower Cretaceous. In contrast the thick, mostly clastic sedimentary formations of Lower Permian to Upper Triassic age in the Western Mecsek Mountains form a large-scale perianticlinal structure (Fig. 2). For a detailed geologic description of the area the authors refer to Fülöp (1994) who summarized the relevant, partly published, mostly unpublished works of Barabás, Barabás-Stuhl, Jámbor, Fazekas, Vincze and Wéber and Barabás and Barabás-Stuhl (1998).

The present study focuses on the Upper Permian BACF that forms a distinct part of the terrestrial – fluvial – lagoonal Permian sedimentary sequence. It consists of a continuous, conformable sedimentary transition, characterized by repetitions of strata between the 700–900 m thick BACF and the footwall Cserd

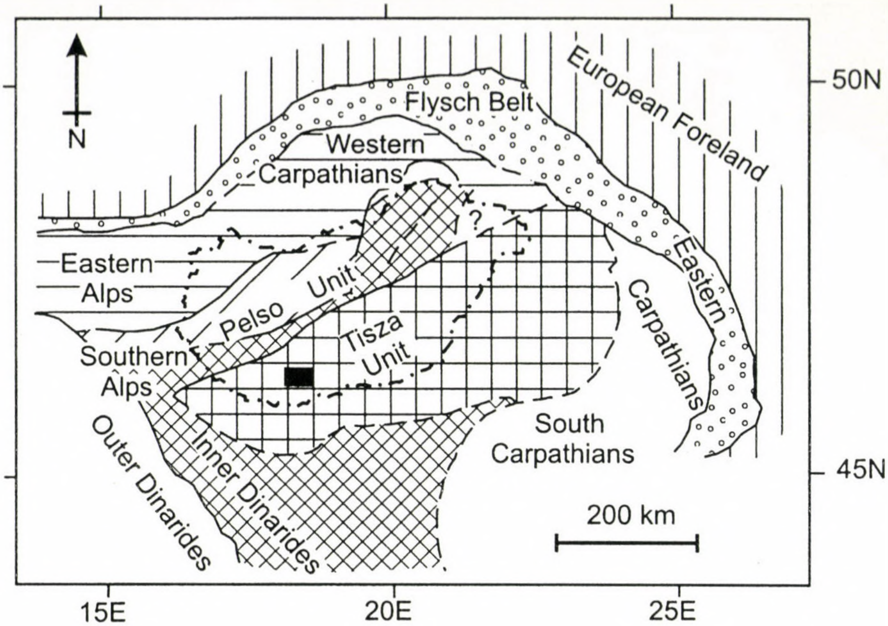

Fig. 1
Location of the area (filled rectangle) within the Alpine-Carpathian-Dinaridic framework

Conglomerate Formation, while the boundary with the hangingwall Kővágószőlős Sandstone Formation, which represents the beginning of a new sedimentary cycle, is also conformable but rather sharp. The BACF itself consists of reddish brown albitic claystone, siltstone, sandstone, and brownish-gray dolomite marl with rare gray or green claystone intercalations. On the basis of the proportions of these rock types, the BACF is subdivided into three parts. These are (from the bottom upwards): (a) ~ 150 m thick "transitional" sandstone with green claystone intercalations; (b) 350–450 m-thick, reddish-brown albitic, silty claystone, in which intercalations of "albitolite" (a sedimentary rock with >50% albite, rich in hematite, clay and carbonate minerals), parallel and cross-bedded muscovitic siltstone and sandstone with albitic and calcitic matrix and albitic dolomite also occur; (c) 400–500 m-thick, reddish-brown, albitic, silty claystone with dolomite intercalations displaying desiccation cracks. In the uppermost, transitional part of this zone, dark brown, strongly limonitic claystone layers are also found. These uppermost layers also contain dolomite as concretions, and are free of albite. Layering, thick-bedded development and spaced cleavage can be observed throughout the formation.

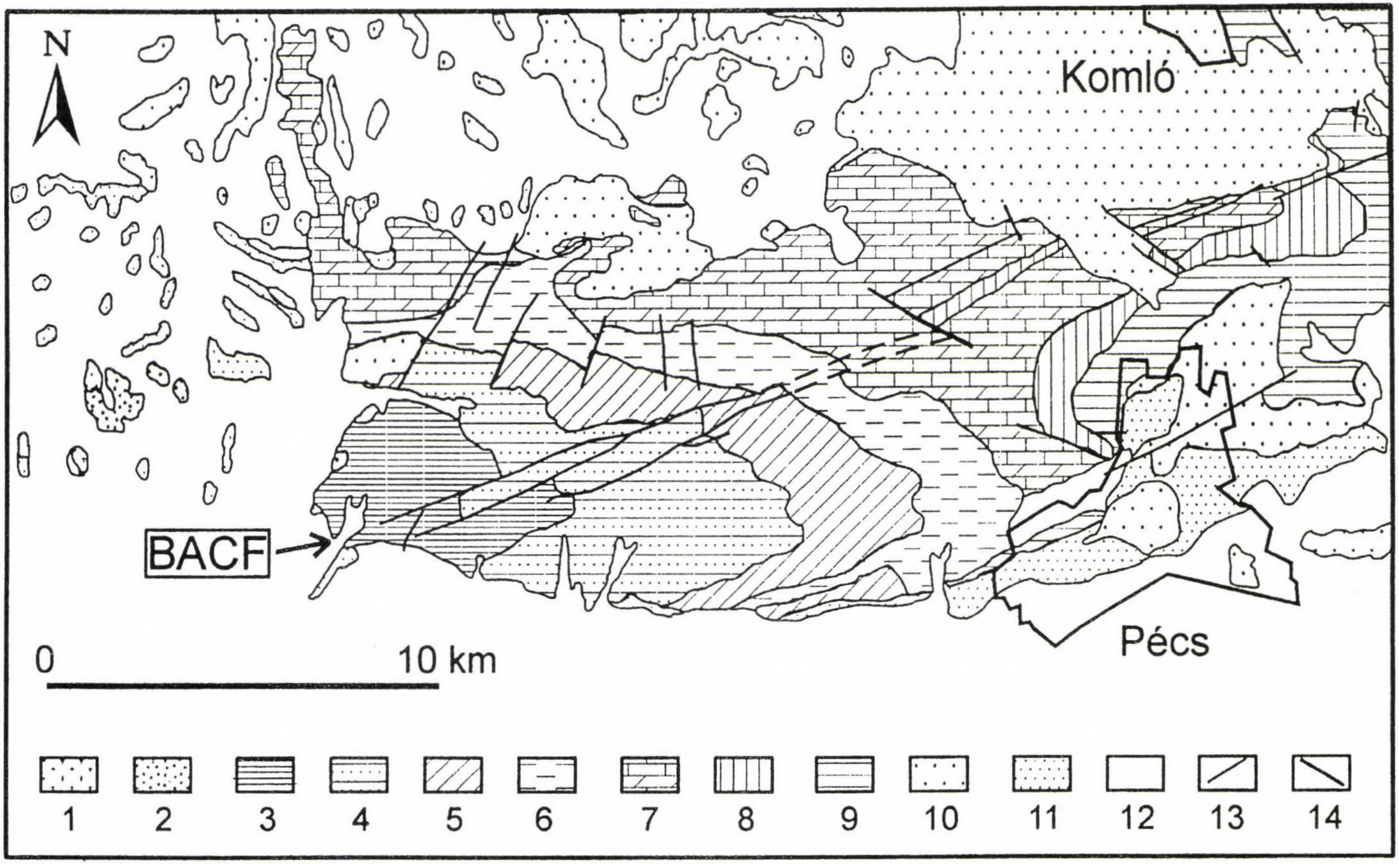

Fig. 2

Geologic map of the Western Mecsek Mountains after Forgó et al. (1966), modified. Legend: 1. Variscan granitoids; 2. Lower Permian sandstone and conglomerate; 3. Upper Permian Boda Albitic Claystone Formation (BACF); 4. Upper Permian sandstone; 5. Lower Triassic sandstone; 6. Middle Triassic sandstone, marl, limestone and anhydrite; 7. Middle-Upper Triassic limestone, dolomite; 8. Upper Triassic sandstone; 9. Jurassic formations; 10. Miocene formations; 11. Pliocene formations; 12. Quaternary; 13. main fault; 14. town boundary

Methods

Field and petrographic microscopic observations were used to determine rock types and microstructural features with special attention to the distinction of inherited (detrital), authigenic (diagenetic) and post-diagenetic (fissure-filling) features and minerals. *Vitrinite reflectance* (R_{random}) characteristic of finely disseminated and coalified organic matter were measured to determine thermal maturity as described by Árkai (1983).

Qualitative modal compositions of the rocks studied were determined by X-ray powder diffraction (XRD), while *semiquantitative modal composition* was estimated by combined application of XRD, thermic, bulk rock major element analytical methods, following the technique elaborated by Bárdossy (1966, 1968). For determining *diagenetic* – incipient metamorphic *grades*, XRD-measured phyllosilicate crystallinity parameters were applied. The procedure of preparing <2 μm grain-size fraction samples was similar to that used by Kübler (1968), as described by Árkai et al. (1996, 1997). The procedures and instrumental conditions applied in the XRD work were the same as used and described in detail by Árkai et al. (1997). The actual boundary ranges of illite crystallinity [IC, i.e., the full-width-at-half-maximum (FWHM) of the first, 10-Å basal reflection of illite-muscovite] and chlorite crystallinity indices [i.e., the FWHM values of the first (14-Å) and second (7-Å) basal reflections of chlorite indicated as ChC (001) and ChC (002)] of the present paper, which correspond to Kübler's original anchizone, are 0.284–0.435°, 0.309–0.390° and 0.284–0.348$\Delta°2\Theta$, respectively (see also Árkai et al. 1995b). All of these boundary values refer to air-dried (AD) mounts. A detailed description of *K-Ar dating* applied to illite-muscovite-rich <2 μm and <0.4 μm grain-size fraction samples is presented in Árkai et al. (1995a).

Bulk rock major element chemical compositions were determined by X-ray fluorescence spectrometry using ARL 8410-131 and 8420 type devices. The FeO, CO_2 and H_2O contents were analyzed by conventional wet chemical methods. *Chemical compositions of* selected (mostly fissure-filling) *minerals* were determined by a JEOL JXCA-733 type electron microprobe (EMP). The description of instrumental and measuring conditions including standard errors are given in Árkai and Nagy (1994) and Árkai and Sadek Ghabrial (1997).

Stable isotope compositions of carbonates and inclusion fluids were determined using the conventional acid digestion (McCrea 1950) and decrepitation–Zn-reduction (Vennemann and O'Neil 1993; Demény 1995) methods. D/H, $^{13}C/^{12}C$ and $^{18}O/^{16}O$ ratios were measured in H_2 and CO_2 gases using a Finnigan MAT delta S mass spectrometer. The isotope compositions are expressed in the conventional δ value [$\delta=(R_{sa}/R_{st}-1)\times1000$, where R_{sa} and R_{st} are the isotope ratios in sample and standard, respectively] as ‰. The reproducibilities of $\delta^{13}C$, $\delta^{18}O$ and δD values are better than ±0.2 ‰ and ±3 ‰, respectively.

Results

Bulk rock chemistry

Figure 3 displays the frequency distributions of major elements expressed in weight-% of their oxides. Fifty-seven analyses from main rock types of the BACF were included in these histograms. The number of analyses is roughly proportional with the volumetric amounts of each rock type within the BACF. Statistical parameters (mean, median, mode and standard deviation) are also given in Fig. 3.

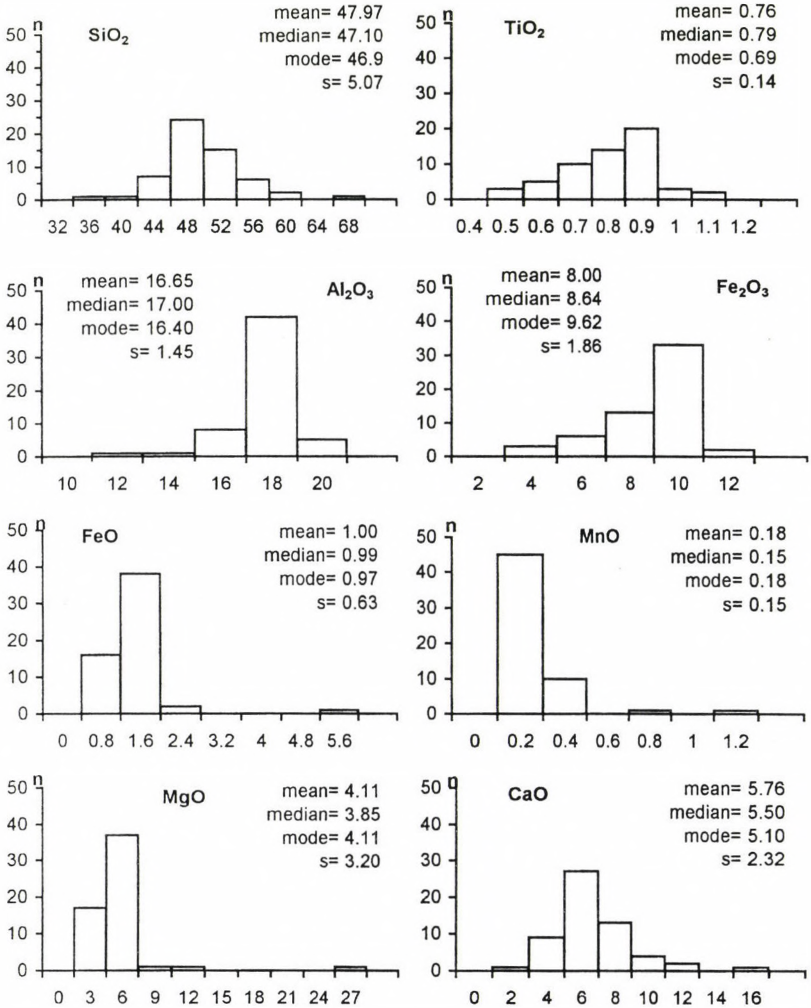

Fig. 3
Frequency distributions of major chemical components in the rocks of the BACF (weight-%, n=57)

The SiO_2 content varies strongly between 32.90 and 66.10%, displaying a one-maximum, positively skewed, flat distribution. In contrast, the range of Al_2O_3 contents is relatively narrow (10.30–19.83%), and their distribution is negatively skewed. High Fe_2O_3 % (2.39–10.62%) with strong, negative skewing and relatively low FeO contents (0.14–1.77%; in one sample: 4.88%) are characteristic features of the BACF. MgO varies between 0.07 and 9.20% with a single outlier value of 25.38%. CaO contents range between 1.59 and 11.00%, with a single outlier of 15.70%, and shows normal distribution, similarly to Na_2O (which ranges between 1.48 and 7.17%) and to the loss of ignition without CO_2 (that is practically ±equal to H_2O), the latter occurring between 0.14 and 6.78%. The distribution of K_2O is negatively skewed and its values scatter between 0.79 and 6.00%. CO_2 varies strongly, while TiO_2, MnO and P_2O_5 change within narrow ranges.

Modal composition

As shown in Figs 4 and 5, the largest scatter is found in the plagioclase (albite) content (12 to 59 w%). XRD and EMP analyses proved that the plagioclase is pure

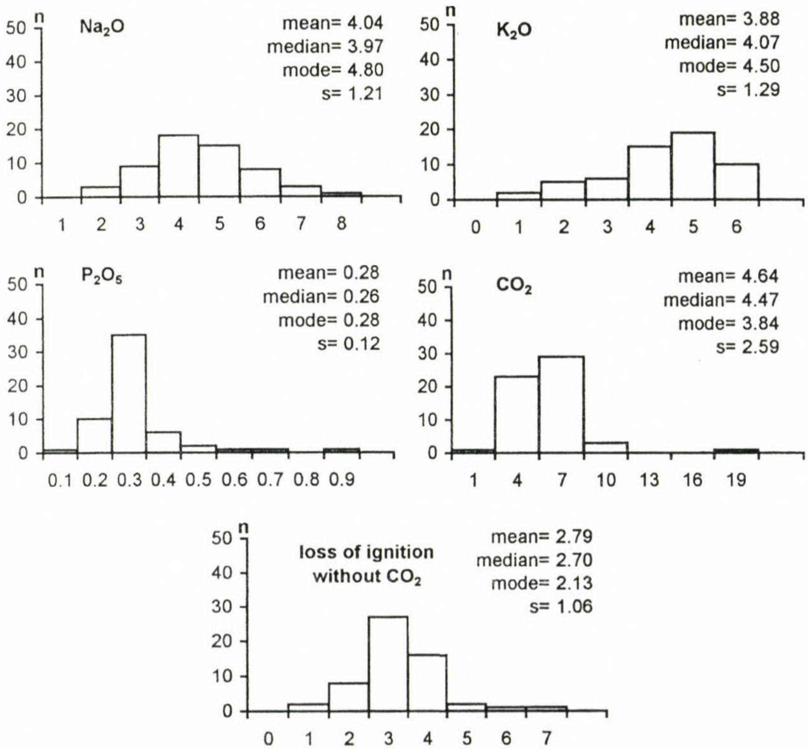

Fig. 3 cont.

albite with ordered (low-temperature) structure indicating its authigenic origin. Its frequency distribution is near to normal type. As compared to albite, the amount of K-feldspar is subordinate, <5%, mostly <1%. Most of its grains are of detrital origin. However, authigenic K-feldspar associated with albite also occurs. Quartz varies between 2 and 33%, its unimodal distribution is positively skewed.

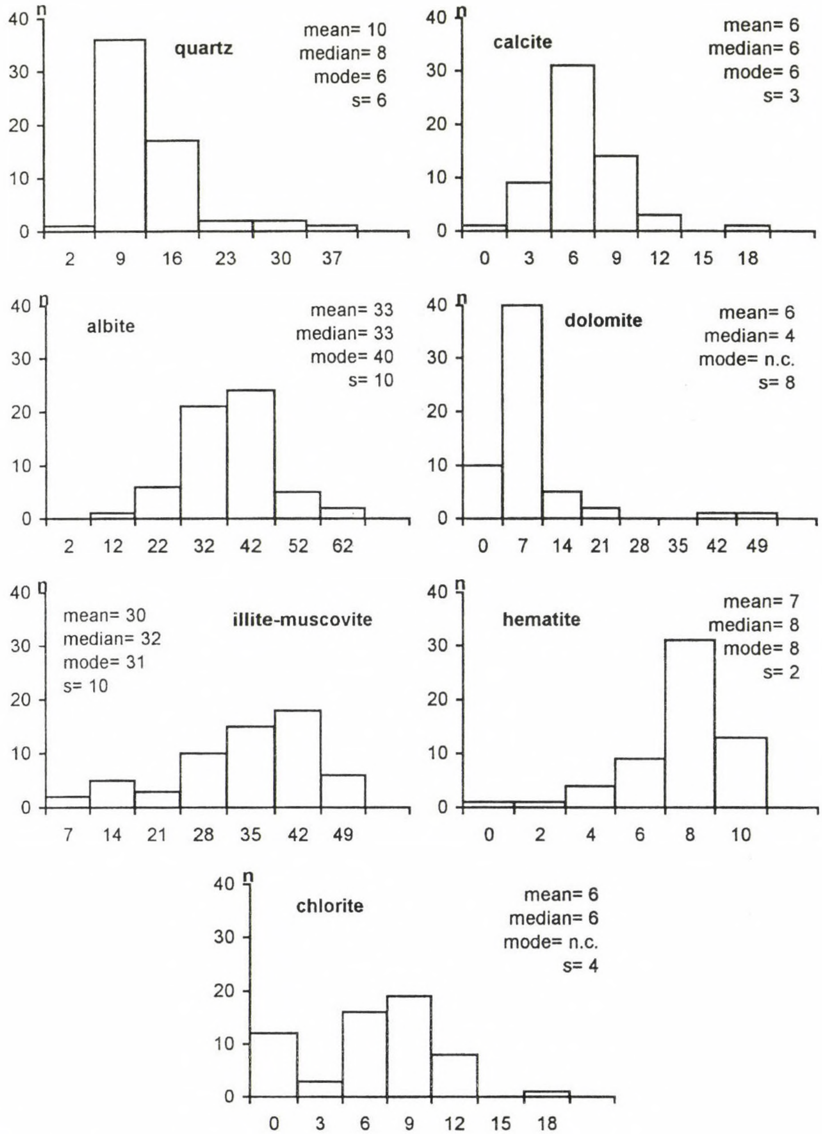

Fig. 4
Frequency distributions of the rock-forming minerals (weight-%, n=59)

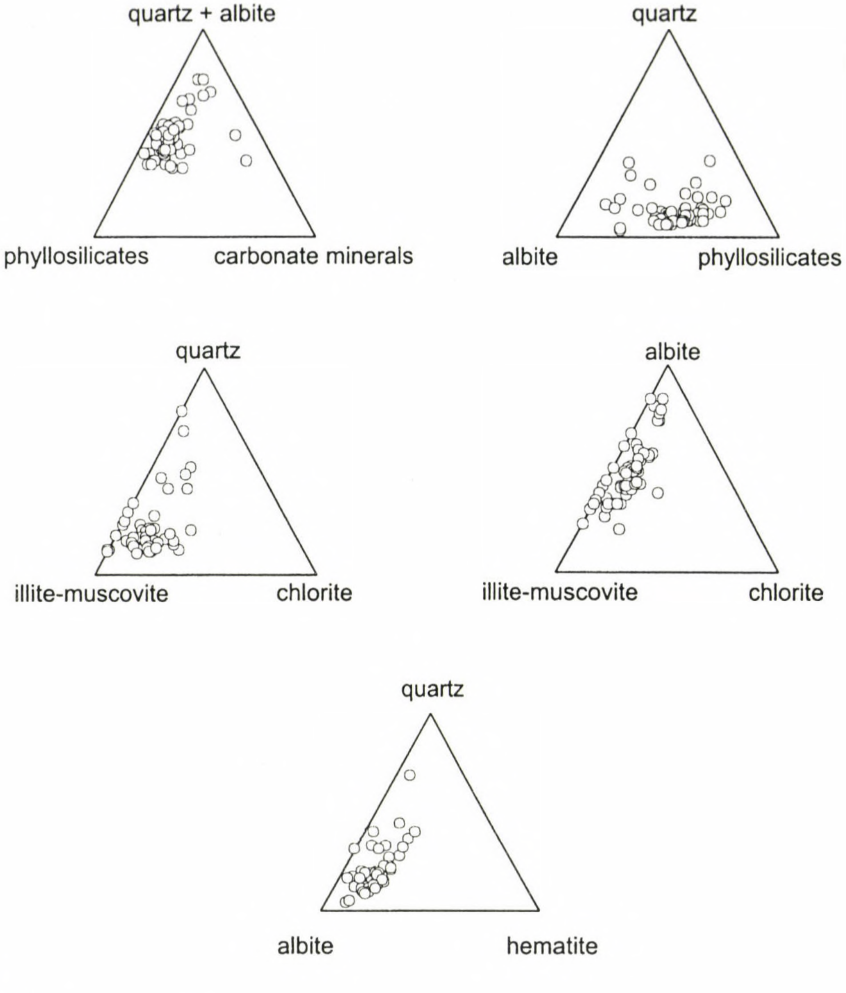

Fig. 5
Ternary plots of modal compositions

Illite-muscovite and chlorite are the most common phyllosilicates, the former always being predominant. In samples representative of the main rock mass devoid of post-diagenetic changes, illite-muscovite and chlorite may only contain expandable mixed-layers in minor quantities, as no significant changes due to ethylene glycol-solvation, either in shape or in intensity ratios of the basal reflections, could be observed. Other clay minerals such as chlorite/smectite, illite/smectite mixed-layers, vermiculite, smectite and kaolinite are rare and occur only sporadically. Negative skewing is characteristic of the distribution of illite-muscovite whose amounts range between 7 and 45%. The distribution of chlorite

Table 1
Statistical parameters of the phyllosilicate crystallinity indices expressed in $\Delta°2\Theta$ units

samples	IC			ChC (001)			ChC (002)		
	all	fresh	tectonized	all	fresh	tectonized	all	fresh	tectonized
Mean	0.448	0.432	0.511	0.459	0.477	0.366	0.372	0.372	0.377
Standard error	0.010	0.009	0.022	0.022	0.025	0.013	0.004	0.005	0.010
Median	0.444	0.428	0.481	0.403	0.417	0.369	0.373	0.372	0.376
Mode	0.434	0.434	#N/A	0.403	0.403	#N/A	0.363	0.418	#N/A
Standard deviation	0.078	0.068	0.083	0.125	0.128	0.029	0.034	0.034	0.030
Sample variance	0.006	0.005	0.007	0.016	0.016	0.001	0.001	0.001	0.001
Kurtosis	1.593	-0.114	2.512	1.051	0.474	-1.171	-0.528	-0.633	1.412
Skewness	0.717	0.234	1.541	1.398	1.230	0.381	-0.077	-0.083	-0.288
Range	0.432	0.311	0.312	0.473	0.459	0.069	0.138	0.138	0.109
Minimum	0.296	0.296	0.416	0.325	0.339	0.337	0.293	0.293	0.320
Maximum	0.728	0.607	0.728	0.798	0.798	0.406	0.431	0.431	0.429
Count	67	53	14	32	27	5	59	50	9
Confidence level (95%)	0.019	0.018	0.044	0.043	0.048	0.025	0.009	0.010	0.020

is rather irregular: 12 samples out of the total of 59 do not contain chlorite. In the main part of the samples chlorite contents vary between 2 and 18%, and are mostly below 10%. Disregarding the carbonate-rich intercalations, the majority of the rocks contain calcite and dolomite in quantities between 5 and 10%. Although the mean values of calcite and dolomite are the same, their distributions are rather irregular. The amount of calcite usually exceeds that of dolomite, although rocks with dolomite>calcite and dolomite>> calcite relations are also abundant. Siderite occurs only sporadically and always in subordinate (<5%) quantities. Hematite is a common rock-forming mineral of the BACF. Its quantity ranges generally between 5 and 10%.

In the <2μm grain-size fraction samples, enrichment of phyllosilicates and decrease in quantities of the other rock-forming minerals were observed. In these so-called clay fraction samples illite-muscovite is the predominant phase, although the amount of chlorite can also be significant. Enrichments of other clay minerals were observed only in a few samples.

Phyllosilicate crystallinity

Statistical parameters of IC and ChC values calculated for fresh rocks, fracture fillings and all the investigated sample populations are listed in Table 1. As shown in Fig. 6a

IC values fall partly in the anchizone, partly in the diagenetic IC zone in the sense of Kübler (1968, 1990). Both the mean and median values correspond to the high-temperature part of the diagenetic zone (also called late or deep diagenetic zone), and similarly to the mode, are very near to the low-temperature boundary of the anchizone.

The distribution of ChC (001) indices (Fig. 6b) is similar to that of the IC. Mean, median and mode values of ChC (001), similarly to those of ChC (002) in Fig. 6c correspond to the late or deep diagenetic zone as determined for pelitic rocks by Árkai et al. (1995b). The significantly larger scatter and positive skewing of ChC (001) values as compared with those of ChC (002) are related to the presence of expandable mixed-layers that modify the shape of the 14-Å reflection, but have practically no effects on the second-order (7-Å) one.

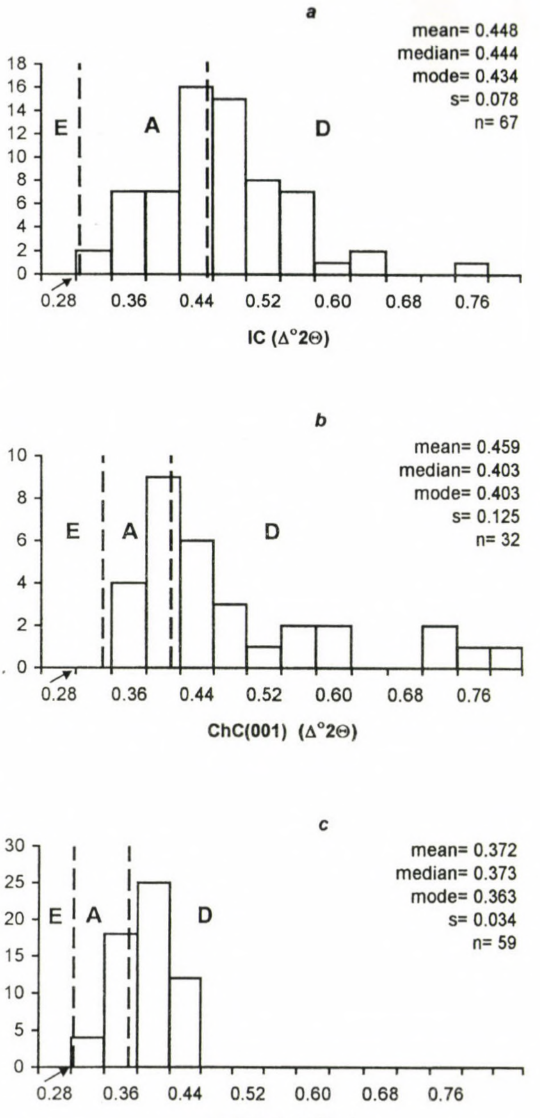

Fig. 6.
Histograms of the illite (a) and chlorite (b and c) crystallinity indices with statistical parameters of the distributions. E – epizone; A – anchizone; D – diagenetic zone in the sense of Kübler (1968, 1990)

Vitrinite reflectance

The BACF contains a single, thin (1–2 m thick), strongly reductive pelitic interlayer. The histogram and statistical parameters of the vitrinite reflectance values of the dispersed coalified particles are displayed in Fig. 7.

K-Ar isotope geochronologic data

Table 2 contains the K-Ar analytical data and the calculated age values obtained from the illite-muscovite-rich, <2 μm grain-size fraction samples also used for IC and ChC measurements. The ages range from 76 to 215 Ma,

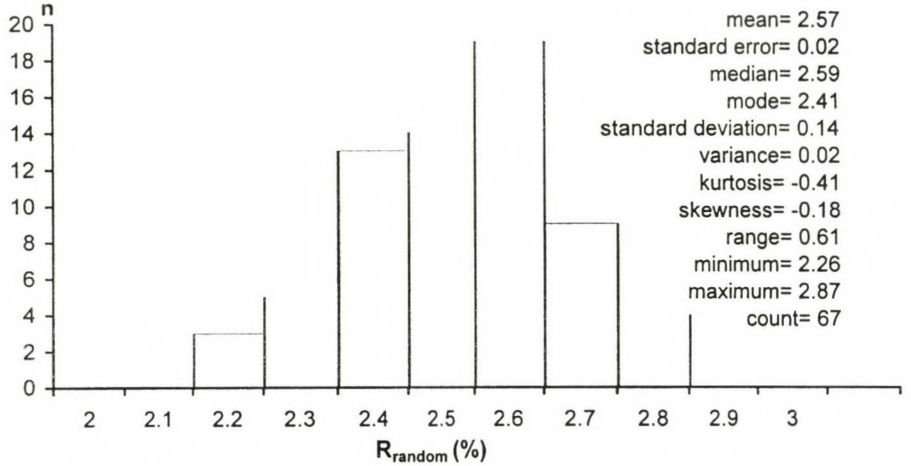

Fig. 7
Frequency distribution of vitrinite reflectance (R_{random}) data measured in a thin reductive layer (sample from borehole Bat-4 851.5 m)

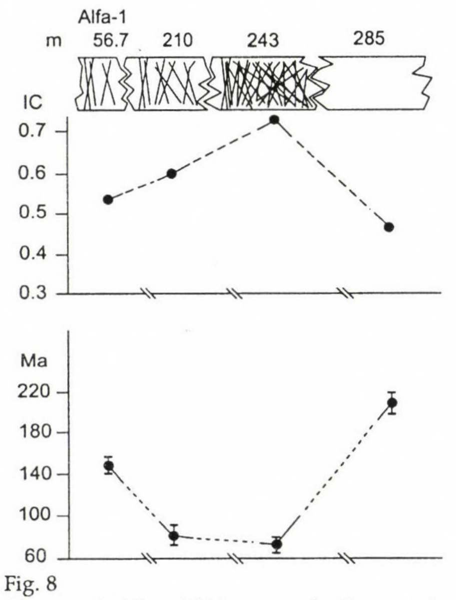

Fig. 8
Changes in IC and K-Ar ages of <2 μm grain-size illite-muscovite in function of post-diagenetic fracturing and related clay mineral retrogression in tunnel Alfa-1. IC values in $\Delta°2\Theta$ units

showing correlation with the tectonic characteristics of the rocks (Table 2) and illite crystallinity indices (Figs 8, 9 and 10).

EMP data

Owing to the very fine grain-size of the rocks studied, EMP analyses could only be performed on the fissure-filling minerals. On the basis of microscopic observations, XRD and EMP data, the following types of fissure fillings have been distinguished:

– Calcite-rich fissure fillings with quartz, barite and dolomite in small quantities.

– Barite-quartz veins with calcite as a general component (tunnel Alfa-1, boreholes Gamma-2, Delta-11). Additionally, dolomite, albite, chlorite, anhydrite and Cu-sulfides (chalcopyrite, bornite and covelline) were

Table 2
Illite crystallinity (IC) and K-Ar age data of the illite-muscovite-rich <2 μm fraction samples

Sample	IC ($\Delta°2\Theta$)	K (%)	^{40}Ar (rad) ($10^{-5}cm^3/g$)	^{40}Ar (rad) %	Age (Ma)±σ	Remarks
Bat-4. 907.6 m	0.495	4.46	3.556	93.3	194.5±7.4	fresh
Bat-4. 811.5 m	0.591	5.26	2.833	90.4	133.5±5.1	tectonized
Bat-5. 848.0 m	0.488	3.64	3.075	86.1	205.0±7.8	fresh
Bat-5. 751.0 m	0.416	2.86	2.157	89.3	184.2±7.0	tectonized
VII 1928.0 m	0.444	2.60	3.037	88.8	191.2±7.3	fresh
XIV 2035.6 m	0.559	4.07	2.900	92.5	179.3±6.8	fresh
Alfa-1. 285.0 m	0.468	3.47	2.989	91.9	209.1±7.9	fresh
Alfa-1. 243.0 m	0.728	5.24	1.586	80.5	76.3±2.9	tectonized
Alfa-1. 210.0 m	0.609	5.82	1.846	86.2	79.9±3.0	tectonized
Alfa-1. 56.7 m	0.535	5.84	3.398	92.9	143.9±5.5	tectonized
Alfa-1. 378.4 m	0.499	3.42	2.491	43.4	178.7±8.0	strongly tectonized material from a fracture zone
Alfa-1. 378.4 m	0.422	3.90	3.183	22.4	198.8±13.3	0.5 m from the fracture zone
Alfa-1. 378.4 m	0.388	3.36	2.658	64.8	193.0±7.6	1 m from the fracture zone (right)
Alfa-1. 378.4 m	0.418	3.69	2.843	62.8	188.2±7.5	wall of the fracture zone
Alfa-1. 378.4 m	0.428	3.81	2.870	88.8	184.8±7.0	1 m from the fracture zone (right)
Alfa-1. 346.0 m	0.438	3.32	2.479	65.5	182.6±7.2	strongly tectonized material from a fracture zone
Alfa-1. 346.0 m	0.472	3.78	2.822	77.5	182.6±7.0	lower wall of the fracture zone
Alfa-1. 346.0 m	0.401	3.55	2.993	59.6	205.0±8.3	0–20 cm from the lower wall
Alfa-1. 346.0 m	0.386	2.64	2.226	27.5	205.0±11.8	1 m from the lower wall
Alfa-1. 346.0 m	0.358	2.77	2.382	80.7	208.9±8.0	40 cm from the upper wall
Delta-10. 36.0 m	0.419	4.06	3.057	90.0	184.0±6.9	fresh wall-rock of a tectonized rock
Delta-10. 38.4 m	0.457	4.99	3.831	95.1	187.4±7.0	upper part of a tectonized zone
Delta-10. 44.8 m	0.447	4.50	3.700	92.4	200.0±7.5	middle part of a tectonized zone
Delta-10. 57.8 m	0.470	5.03	3.339	75.5	163.2±6.3	lower part of a tectonized zone
Delta-10. 63.6 m	0.383	3.30	2.579	90.0	190.6±7.2	fresh wall-rock of a tectonized rock
Delta-5. 168.7 m	0.414	3.27	2.914	92.8	215.8±8.1	fresh rock near to a fracture
Delta-5. 167.0 m	0.485	4.24	3.546	91.8	203.3±7.7	tectonized zone
Delta-7. 51.0 m	0.406	3.74	3.137	92.4	203.8±7.7	fresh wall-rock of a tectonized zone
Delta-7. 79.8 m	0.524	4.21	2.939	90.5	171.2±6.5	strongly tectonized zone
Delta-7. 85.4 m	0.476	5.61	3.021	95.3	133.5±5.0	tectonized zone

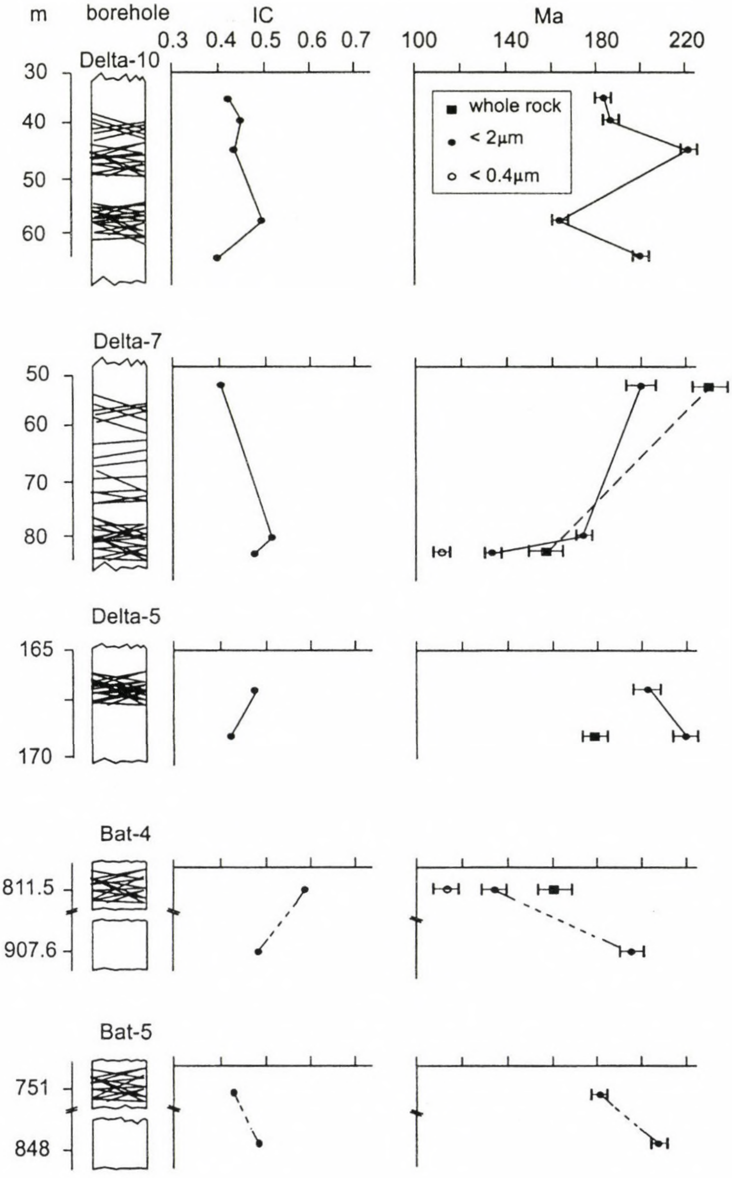

Fig. 9
Variations in IC (Δ°2Θ) and K-white mica K-Ar ages in borehole profiles crosscutting unaltered and fractured (fault gouge) zones

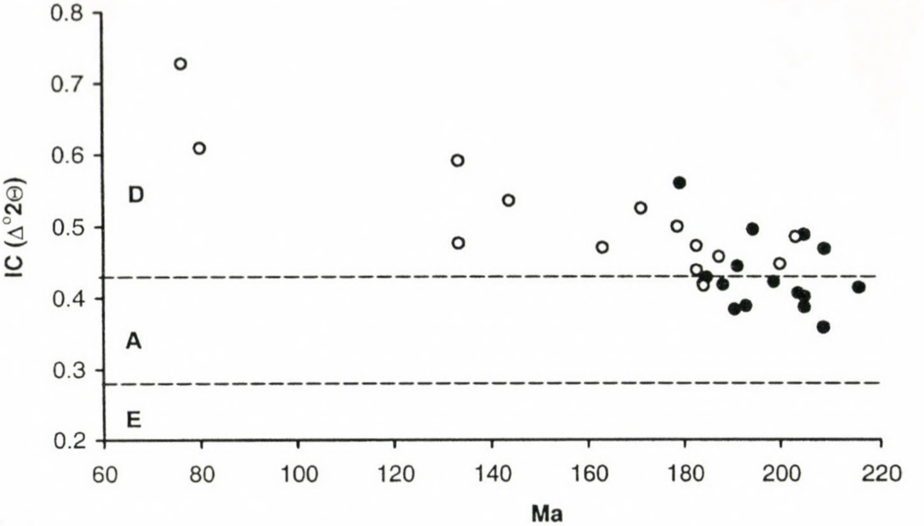

Fig. 10
IC vs. K-Ar ages of the <2 μm grain-size fraction illite-muscovite-rich samples. Filled circles: fresh, unaltered rocks, open circles: fractured, fault gouge rock samples. E – epizone; A – anchizone; D – diagenetic zone

Table 3
Chemical compositions of chlorite and albite from fissure fillings in sample from borehole Delta-11 31.0 m (EMP data)

	Chlorite			Albite
SiO_2	27.53	26.94	26.83	67.17
TiO_2	0.06	0.06	0.02	0.00
Al_2O_3	18.56	18.47	18.51	20.00
FeO*	22.26	23.01	22.09	0.25
MnO	0.01	0.03	0.05	0.01
MgO	18.28	17.41	18.07	0.00
CaO	0.02	0.10	0.04	0.17
Na_2O	0.00	0.02	0.01	11.43
K_2O	0.00	0.01	0.05	0.07
total	**86.72**	**86.05**	**85.67**	**99.10**
	number of cations on the basis o			
		28 O		8 O
Si	5.76	5.72	5.69	2.97
Al^{IV}	2.24	2.29	2.31	1.04
Al^{VI}	2.34	2.33	2.32	-
Ti	0.01	0.01	0.00	0.00
Fe^{2+}*	3.90	4.08	3.92	0.01
Mn	0.00	0.01	0.01	0.00
Mg	5.70	5.51	5.72	0.00
Ca	0.00	0.02	0.01	0.00
Na	0.00	0.01	0.00	0.97
K	0.00	0.00	0.01	0.00
total	**19.95**	**19.98**	**19.99**	**4.99**

*: total Fe calculated as FeO and F^{2+}, respectively

identified by EMP. Using the nomenclature of Foster (1962), the chlorite is of brunsvigite composition (Table 3).

– Quartz-free veinlets of Mn-bearing calcite , with subordinate amounts of pyrite, galenite, chalcopyrite, Fe-rich sphalerite and chlorite (borehole Bat-4 1195.7 m) and 3–4 mm thin veinlets of calcite with barite, pyrite, albite and chlorite (borehole XV 412.1 m);

– Anhydrite-dominated veins with calcite, albite and rarely Sr-rich barite (lower parts of boreholes Bat-4 and -5). In these veinlets albite always forms a thin zone between the rock matrix and the anhydrite vein.

Stable H, C and O isotopic data

The $\delta^{13}C$ and $\delta^{18}O$ data are listed in Table 4. Whole rock carbonates have high $\delta^{13}C$ and $\delta^{18}O$ values, close to the ranges of marine sedimentary carbonate, whereas the carbonates collected from surficial rocks have isotopic compositions similar to the

Table 4
Stable hydrogen, carbon and oxygen isotope compositions ($\delta^{13}C$ relative to V-PDB, δD and $\delta^{18}O$ relative to V-SMOW as ‰ and iclusion H_2O contents (as ppm) in carbonates and inclusion fluids)

Locality	$\delta^{13}C$	$\delta^{18}O$	H_2O	δD
veins				
Alfa-1. 447.0 m	-5.5	16.4	1090	-79
Alfa-1. 213.0 m	-4.4	16.4	780	-71
Alfa-1. 244.5 m	-4.3	16.4	800	-72
Alfa-1. 250.0 m	-4.6	16.0	570	-65
Alfa-1. 260.3 m	-4.8	16.1	970	-73
Alfa-1. 256.5 m	-4.6	15.9	260	-51
Alfa-1. 278.0 m	-4.3	15.9	1330	-72
Alfa-1/2. 12.0–13.0 m	-4.2	15.8	1210	-75
Alfa-1. 232.0 m	-3.3	16.1	300	-71
Alfa-1/9. M-236	-5.2	15.9		
Alfa-1. 244.5 m	-3.4	15.7	370	-87
Alfa-1. 258.0 m	-5.7	16.2	1000	-80
Alfa-1 301.4–303.3 m	-3.8	16.4	1870	-71
Alfa-1. 378.4m	-3.9	15.3		
Alfa-1. 443.0m	-3.8	15.6	2600	-77
Alfa-1. 444.0–445.5m	-2.6	17.7	3600	-75
Alfa-1. 461.0–461.5 m	-3.3	14.3		
Bat-4. 1188.5 m	-5.3	15.7		
Bat-4. 913.8 m	-4.7	15.9		
Bat-4. 720.6 m	-0.2	18.5		
Bat-4. 632.5 m	-0.9	16.9		
Bat-10. 77.9 m	-2.3	17.5		
Bat-12. 44.4 m	-9.8	21.9		
Bat-13. 38.3 m	-9.3	21.6		
Bat-14. 84.0 m	-2.6	19.6	300	-87
Gamma-2. 279.5 m	-4.4	14.8		
Gamma-3. 88.3 m	-5.0	15.8	940	-85
Gamma-3. 136.5 m	-4.5	15.9		
Gamma-3. 167.3 m	-4.2	16.8		
Gamma-3. 197.6 m	-4.2	16.7		
Gamma-4. 17.0–17.05 m	-3.2	15.8		
Gamma-4. 112.4–112.5 m	-0.2	15.6		
Delta-2. 13.0 m	-5.3	16.4		
Delta-2. 55.0 m	-3.7	16.7		
Delta-3. 149.6 m	-3.5	16.9		
Delta-3. 156.3–156.4 m	-4.1	15.8		
Delta-3. 164.2 m	-5.1	18.0		
Delta-3. 174.2 m	-4.7	16.5	2640	-68
Delta-3. 182.1 m	-5.1	15.7		
Delta-3. 183.3–183.4 m	-4.3	16.7		
Delta-3. 184.25–184.35 m	-5.1	15.3	530	-90
Delta-4. 8.3 m	-2.6	15.0		
Delta-4. 54.2 m	-5.3	16.0		
Delta-4. 70.0–70.1 m	-4.8	13.9	480	-74
Delta-5. 162.6 m	-3.3	14.2		
Delta-5. 165.1 m	-4.7	15.7		
Delta-5. 165.6 m	-3.7	14.5		

Table 4
(cont.)

Locality	$\delta^{13}C$	$\delta^{18}O$	H_2O	δD
veins				
Delta-7. 15.65 m	-4.5	15.8		
Delta-7. 18.6 m	-3.7	16.6		
Delta-7. 21.3 m	-4.5	15.6	320	-75
Delta-7. 50.5 m	-4.6	15.5		
Delta-11. 17.1 m	-4.6	16.7		
Delta-11. 18.6 m	-5.2	15.4		
Delta-11. 66.0 m	-5.9	17.9		
4709-1. 1889.5 m	-3.5	15.0	690	-42
4709-1. 1986.4 m	-3.4	14.4	680	-52
4709-1. 1995.5 m	-3.3	14.4		
S-36. 13.0 m	-10.7	22.6		
K-124. 74.0 m	-9.5	22.2		

Whole rocks

locality	Rock type	$\delta^{13}C$	$\delta^{18}O$
Bat-14. 23.4 m	claystone	-8.1	21.9
Bat-14. 24.7 m	claystone	-2.1	21.2
Bat-14. 25.9 m	claystone	-2.6	20.9
Bat-14. 28.4 m	claystone	-1.5	20.9
Bat-14. 59.2 m	claystone	-0.1	19.9
Bat-14. 94.8 m	claystone	-0.4	25.7
Delta-3. 10.1–10.2 m	dolomite	-0.7	30.6
Delta-3. 69.4–69.5 m	albitolite	-1.1	24.3
Delta-5. 146.8–147.02 m	claystone with albite vugs	-2.7	21.4
Delta-5. 154.6 m	claystone with albite vugs	-2.4	23.4
Delta-5. 180.15 m	claystone with albite vugs	-1.7	28.1
K75. 3.0 m	claystone	-3.0	17.3

ranges of soil carbonates (Sacket and Moore 1966; Fritz et al. 1989; Alpers et al. 1990) and dissolved carbonate in local shallow groundwaters (Demény et al. 1996). The $\delta^{13}C$ and $\delta^{18}O$ values of calcite veins fall into relatively narrow ranges (–6 to –2 ‰ and 13 to 19 ‰, respectively). Fluid inclusion contents of calcite veins – represented by H_2O content – usually scatter between 250 and 1000 ppm; however, some of the veins have significantly higher H_2O contents (up to 3600 ppm; Table 4). The δD values of inclusion fluids show a large and irregular scatter from –90 to –42 ‰ (Table 4).

Discussion

Sedimentary and diagenetic conditions

The BACF series differs from the average shale (see e.g. Pettijohn 1975) in significantly lower SiO_2, somewhat lower FeO, significantly higher Fe_2O_3, Na_2O, and somewhat higher MgO and CaO contents. Considering also the CO_2 values, the higher CaO and MgO values can be unequivocally attributed to the elevated carbonate (calcite and dolomite) content of the BACF compared to the shale average. Based on the stable isotope compositions these carbonate-rich layers are of sedimentary origin (Fig. 11). These deviations explain the low quartz, extremely high albite and high hematite contents of the rocks in question. Taking rock textures, the low amounts of K-feldspar and quartz and the chemical and crystal structural features of albite into account, a potential detritic origin of this feldspar should be ruled out. Instead, authigenic, syn- and post-sedimentary chemical precipitation may have been the main mechanism of albite formation. During the diagenetic and partly also the post-diagenetic processes, small-scale migration and local accumulation of albite together with calcite, barite, anhydrite and sulfide minerals in the rather homogeneous matrix can be considered a common phenomenon. Diagenesis is suggested to be responsible for the $\delta^{18}O$

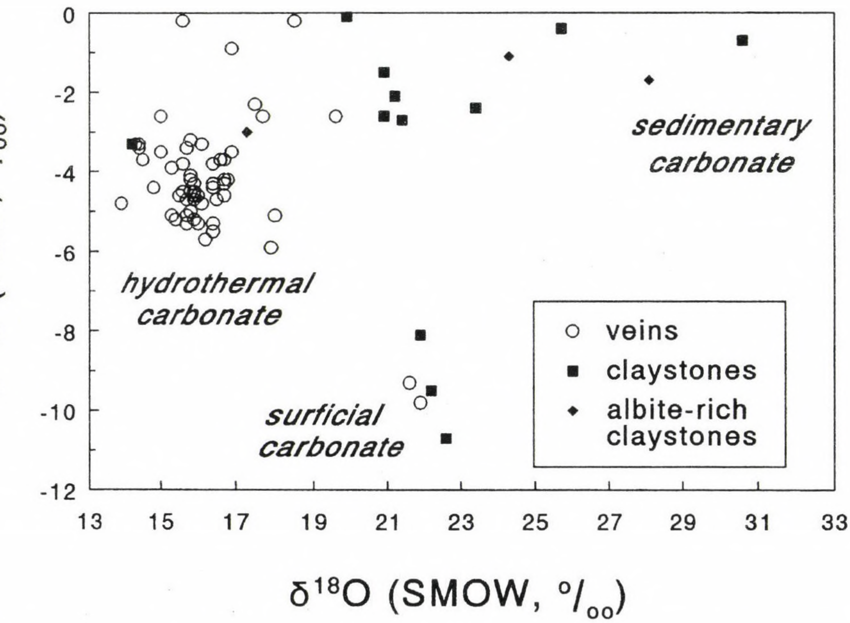

Fig. 11
Stable carbon and oxygen isotope compositions of carbonates in the Boda Albitic Claystone Formation

decrease in whole rock carbonates with high $\delta^{13}C$ values (Fig. 11). Whole rock carbonates of albite-rich rocks show both high and low $\delta^{18}O$ values (Fig. 11), thus supporting the authigenic-diagenetic albite formation. Except for a thin reductive interlayer, the sedimentation and diagenesis of the BACF took place in highly oxidative circumstances, as evidenced by the high hematite content. The sedimentary deposition conditions may have been similar to that observed for alkaline lake sediments (e.g. Poroda and Behr 1988; Eugster and Hardie 1975; Rowlands et al. 1980; Manega and Biena 1987). In this sedimentary model a so-called starving alkaline sedimentary basin characterized by high (8–10) pH, highly alkaline waters and strongly oxidative conditions was formed due to a dry climate and the large distance between the basin and the eroding area. In this basin shallow-water lacustrine conditions frequently alternated with desiccation intervals (see also Fülöp 1994).

The illite-muscovite + chlorite phyllosilicate assemblage is in agreement with the IC and ChC averages, all demonstrating late or deep diagenetic conditions, close to the diagenetic zone/anchizone boundary. As can be seen in Figs 6a-c, the scatters of the phyllosilicate values are rather large. Therefore, statistical parameters of the fresh rock samples (main rock mass) and of the post-diagenetically altered ones were calculated separately (Table 1). The differences in their IC and ChC (001) averages explain the positive skewing of their distributions and the tectonized (fault gouge) materials showing mostly higher absolute values (lower apparent grade).

The chemical, physical and various geologic factors that may affect IC were reviewed by Frey (1987). As demonstrated by Árkai (1983), well-crystallized, detrital K-white micas may also be present in the <2 μm fraction samples, often seriously influencing the interpretation of IC. Judging from the rare occurrence of coarse-grained detrital muscovite and chlorite and subordinate proportion of detrital quartz and plagioclase, the effect of detrital phyllosilicates on crystallinity indices causing a shift to lower IC and ChC values (i.e., higher apparent grades) may not be serious, although this may cause scatter of indices toward the anchizone.

Phyllosilicate crystallinity values as empirical indicators of diagenetic – incipient metamorphic zones express only relative differences in reaction progress of phyllosilicate aggradation processes and cannot be used as mineralogical thermometers (for recent reviews see Merriman and Peacor 1999 and Merriman and Frey 1999). However, the boundary between the diagenetic IC zone and anchizone may be put between about 200 and 250 °C, as supported by results of fluid inclusion and stable isotope thermometric comparative studies (for reviews see Kisch 1987; Merriman and Frey 1999). Therefore, a 200–250 °C maximal burial diagenetic temperature can be estimated for the BACF.

Although the correlation between IC and coal rank (vitrinite reflectance) is influenced by numerous factors (see Kisch 1987), and no overall valid quantitative relation exists so far, the R_{random} value obtained in the reductive interlayer of the BACF supports the conclusion drawn from the late-diagenetic alteration from the phyllosilicate crystallinity parameters. Kübler et al. (1979) correlated the boundary between diagenesis and anchizone with R_{random} values of 2.6–2.8%. According to Kisch (1987) this boundary is associated with coal ranks ranging between 2.3 and 3.1% R_{random} in various terrains.

The average K-Ar age of the illite-muscovite-rich, <2 μm grain-size fraction samples calculated from the data of Table 2 is 197.3 Ma (s=10.6, n=16). The data range between 215.8 and 179.3 Ma. As the estimated maximum burial temperature is somewhat lower than or equal to the closure temperature range of the <2 μm-size illite muscovite (260±20 °C during 10±5Ma; Hunziker et al. 1986), this age can be regarded characteristic for the main phase of illite-muscovite formation or recrystallization, suggesting that the diagenetic illite formation culminated in the Lower Jurassic (Liassic), most probably due to the regionally enhanced thermal conditions preceding the Jurassic breakup of the Variscan continental crust in central Europe, from which the Tisza Unit was detached during the Jurassic. The large regional extent and importance of the Liassic hydrothermal activity in Western Europe were documented earlier by Clauer et al. (1996).

Post-diagenetic alterations

The BACF series repeatedly experienced brittle tectonic deformations after the Permian, resulting in the formation of various fracture systems. In the most common type of faulting, fractures are filled with tectonically crushed, loose, brecciated rock material. In the majority of fault gouges modal changes are associated with IC (and ChC) variations and a variable decrease of apparent (mixed) K-Ar ages of the <2 μm grain-size fraction samples appears. Table 2 and Figs 8 and 9 provide examples of changes observed in cross-sections in boreholes and tunnels. In detailed sections of tunnel Alfa-1 at 346 m and 378.4 m (see Table 2) approaching fracture zones, increased IC values (increasing illite-muscovite degradation) are accompanied by decreased chlorite contents and the appearance of disordered chlorite/smectite mixed-layer clay mineral and even discrete smectite, as well as a moderate decrease of K-Ar ages of <2 μm illite-muscovite. In a longer section of tunnel Alfa-1 (Fig. 8) drastic changes in IC values and K-Ar ages were demonstrated: IC increases, K-Ar ages and chlorite contents decrease from fresh, compact zones to strongly tectonized ones. In boreholes various patterns appear (Fig. 9). In borehole Delta-10 IC slightly increases (in one case illite/smectite also appears) and chlorite content decreases in the crushed zones compared to the unaltered, fresh rocks. K-Ar ages of the <2 μm illite-muscovite fraction show only fluctuation and do not seem to be related to fracturing. In boreholes Delta-7, Delta-5 and Bat-4 IC increases and K-Ar ages decrease with increasing fracturing, whereas in a section of borehole Bat-5 opposite trends are observed.

In summary, restricted fluid infiltration and migration caused modal changes (decrease of chlorite content, appearance of chlorite/smectite, illite/smectite mixed-layered clay minerals and even discrete smectite) and degradation of illite-muscovite (increase of IC) in fault gauges. The increase in IC may be related to increasing amounts of smectitic mixed-layers, i.e., to decreasing interlayer charge of the mica-like structure. Partial mobilization of the interlayer potassium and its radioactive daughter product from the mica-like structure may result in partial rejuvenation of illite-muscovite, producing variations in K-Ar ages from about 216 to 76 Ma in the <2 μm fraction. The differences in K-Ar ages between the <2 μm and <0.4 μm fractions demonstrated in Figure 9 show that the smaller the grain-size, the larger the rejuvenating effect might be.

Figure 10 shows the relation between IC and K-Ar ages. As the degradational reaction process of illite-muscovite proceeds K-Ar ages decrease. As these changes appear to be continuous (no distinct age or IC averages can be determined for the tectonized materials), one can conclude that the fault-related retrogression has not reached an equilibrium state. Instead, the varying IC data from the fault gouges represent transitional states, while the K-Ar ages can be considered as mixed ages between the age of the main phase of diagenesis (Lower Jurassic) and the age(s) of brittle deformation-related mineralogical transformations. On the basis of clay-mineral degradation described in fault gouges the chemical effects of infiltration by relatively cold and dilute hydrous fluids should be taken into consideration. In addition to illite-muscovite retrogression, neoformation of poorly crystallized illite during fluid migration might contribute considerably to the IC and K-Ar variations described above.

Calcite veins in the rocks of the BACF represent an important indication of past fluid migration. In general, carbon isotope fractionation between precipitated calcite and dissolved C is not significant (see compilation in Friedman and O'Neil 1977); thus the $\delta^{13}C$ value of calcite would reflect the origin of the dissolved C. Marine carbonate sediments have $\delta^{13}C$ values around 0‰, whereas organic matter is much more ^{12}C-enriched with $\delta^{13}C$ values around –25‰ (Hoefs 1973). Oxidation of organic matter thus produces ^{12}C-enriched CO_2. The third source for hydrothermal solutions is magmatic fluid. The primary carbon isotope composition of the mantle is about –7‰; degassing of such magma would produce CO_2 with d13C values around –4‰ (Javoy et al. 1978; Mattey 1991). These data show that dissolved carbon in hydrothermal fluid with a $\delta^{13}C$ value of –5‰ might derive either from a magmatic source or from mixing of organic-derived CO_2 and dissolved sedimentary carbonate.

For a proper interpretation of $\delta^{18}O$ values of hydrothermal carbonates another factor should be taken into consideration. Since in the case of calcite precipitating from water most. of the oxygen is in the form of H_2O, the oxygen isotope composition of the calcite is determined by both temperature and fluid composition. The temperature dependence of calcite-water oxygen isotope fractionation was given by Friedman and O'Neil (1977) who recalculated the original equation of O'Neil et al. (1969). Using their equation, the measured $\delta^{18}O$ value of calcite and formation temperature inferred from independent methods the oxygen isotope composition of the fluid can be calculated. Due to the difference in formation temperature and $\delta^{18}O$ (fluid) values marine carbonates are the most ^{18}O-enriched, whereas hydrothermal carbonates (with a higher formation temperature) or surficial carbonate (with lower $\delta^{18}O_{water}$ value) have lower $\delta^{18}O$ values.

Further important information on the fluid under study can be obtained by measuring hydrogen isotope compositions. Since carbonate minerals do not contain hydrogen, the H_2O-bearing fluid inclusions trapped in the calcite represent the fluid – and its hydrogen isotope composition – from which the calcite was precipitated. Later influences on the fluid inclusions – such as leakage – might deteriorate this representativity. Waters of different origin show systematic δD and $\delta^{18}O$ distributions (see Sheppard 1986); thus, the δD and $\delta^{18}O$ values measured and calculated, respectively, might indicate the origin of the fluid. Therefore, combined use of H, C, and O isotope determinations can decrease the uncertainties of the interpretation of the individual isotope compositions and provide useful information on fluid origin.

X-ray diffractometric and electron microprobe investigations showed three main types of fracture fillings: calcite-dominated veins, barite-quartz veins and anhydrite-dominated veins. Stable C and O isotope compositions of calcites were measured in the former two types; the anhydrite-dominated veins do not contain appropriate amounts of carbonate. The $\delta^{13}C$ and $\delta^{18}O$ data are plotted in Fig. 11 and lead to the following observations: the majority of veins have $\delta^{13}C$ and $\delta^{18}O$ values around –4‰ and 16.5‰, respectively, forming a separate $\delta^{13}C$–$\delta^{18}O$ group; some veins have high $\delta^{13}C$ values characteristic for sedimentary carbonate; veins collected from near-surface rocks have very low $\delta^{13}C$, similar to that of soil carbonate. The origin of carbonate-forming fluids can be assessed using measured and calculated isotopic compositions. The large scatter of δD values of fluid inclusion waters can be attributed to fluid mixing or to multiple fluid migrations. Some of the veins have a much higher inclusion content than the majority of the fillings (Fig. 12), that might indicate higher amounts of fluid flowing in the fractures or the absence of later tectonic reworking. The presence of sulfide minerals in the barite-quartz veins point to the possibility of magmatic fluid migration, which could also produce the high amounts of fluid in these fractures. The $\delta^{13}C$–δD plot (Fig. 13) does not reveal distinct groups; however, the distribution of data indicates mixing of three fluids or their products precipitated in the fractures.

Fluid inclusion microthermometric data (K. Török, unpublished results) suggest that the majority of calcite veins were deposited at ~70 °C, whereas the barite-quartz veins might have been formed at higher temperature (~150 °C). Using these formation temperatures and the fractionation equation of O'Neil et al. (1969) re-calibrated by Friedman and O'Neil (1977), the oxygen isotope

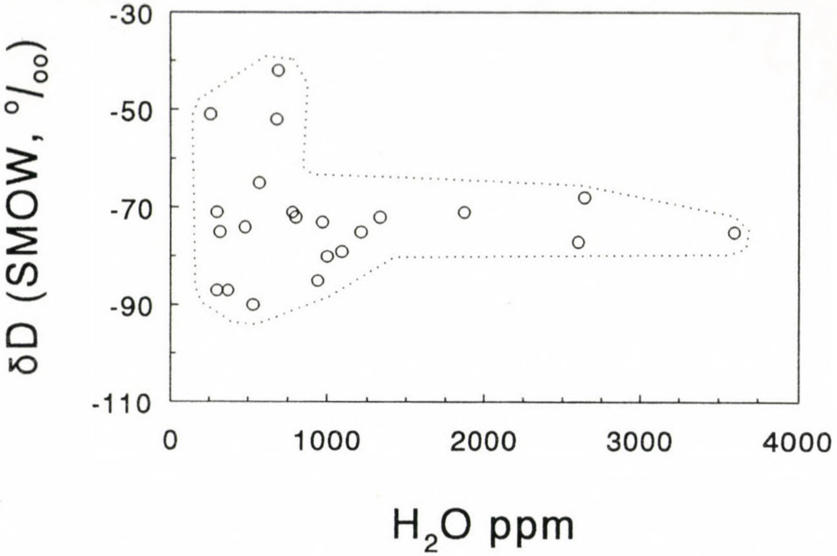

Fig. 12
Stable hydrogen isotope compositions of fluid inclusion water vs. water contents in calcite veins in the Boda Claystone Formation

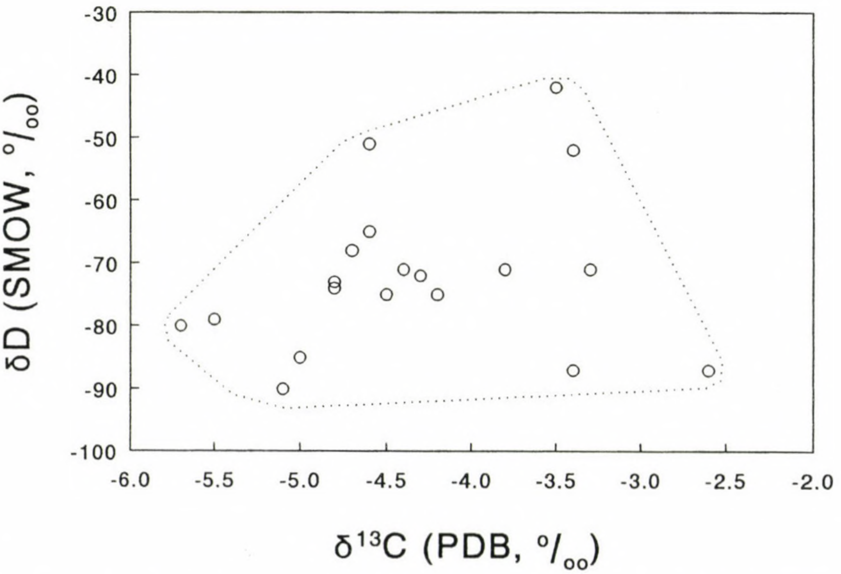

Fig. 13
Stable hydrogen vs. carbon isotope compositions of inclusion water and host calcite in fissure filling veins in the Boda Claystone Formation

compositions of fluids in equilibrium with calcites have been calculated and plotted in Fig. 14. The data show systematic distributions. The barite-quartz veins plot close to the magmatic water's field, whereas the other data indicate mixing of two fluids or their precipitation products. The fluid with high δD (up to –42 ‰) plots close to the meteoric water line suggesting a meteoric water origin related to a warm climate. The δD value of the other end-member of the mixing process is similar to that of the Hungarian formation waters of Pleistocene age (Deák 1995, unpubl. rep.; see also Fig. 13), with, however, a higher oxygen isotope composition. If the Pleistocene meteoric water origin is accepted, this fluid must have migrated to greater depths in order to experience such a significant positive

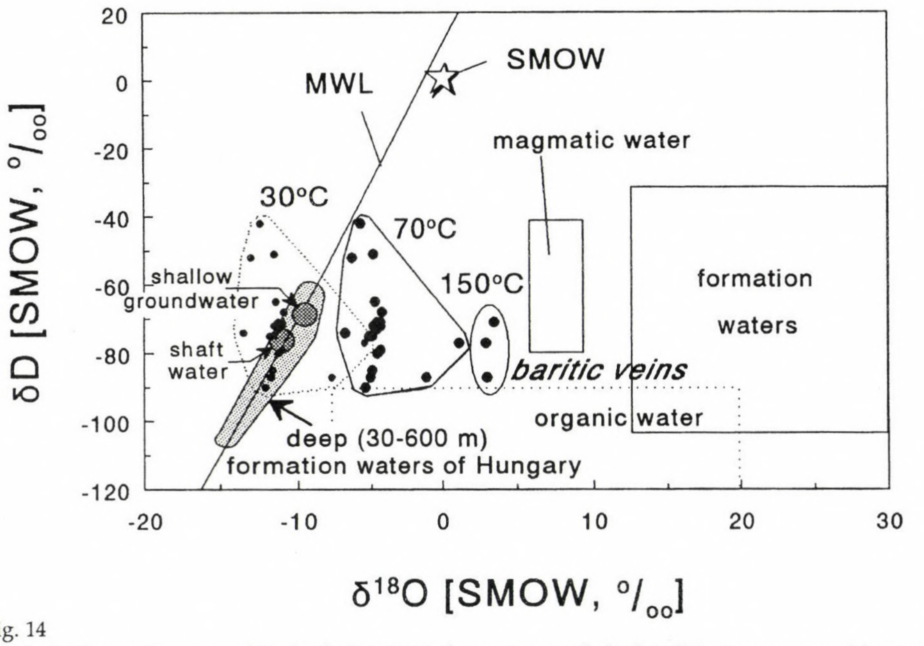

Fig. 14
Stable hydrogen (measured in inclusion waters) vs. oxygen (calculated) isotope compositions of waters in equilibrium with fissure filling calcites. See also text. Ranges of water types are from Sheppard (1986), shallow groundwater and shaft water compositions are from Demény et al. (1996), deep formation water compositions are from Deák (1995, unpublished report)

$\delta^{18}O$ shift during isotope exchange with ^{18}O-enriched sedimentary rocks. Another explanation would be given assuming lower formation temperatures in case of calcites formed from low-δD fluid. Decreasing the formation temperature to about 30 °C would place the low-δD fluid on the meteoric water line. In this case the data points would fall close to the composition of water collected in the

Table 5
K-Ar dates measured in whole rock samples and their various grain-size fractions

Sample	Rock, fraction	IC (Δ°2Θ)	K(%)	^{40}Ar (rad) ($10^{-5}cm^3/g$)	^{40}Ar (rad) %	Age (Ma)±s	Remarks
Delta-7. 51.0 m	whole rock		2.51	2.355	84.1	226.5±8.6	fresh wall-rock of a tectonized zone
	<2 µm	0.406	3.74	3.137	92.4	203.8±7.7	
Delta-7. 85.4 m	whole rock		4.43	3.486	82.5	191.8±7.6	tectonized zone
	<2 µm	0.476	5.61	3.021	95.3	133.5±5.0	
	<0.4 µm		6.58	2.732	47.5	103.8±4.4	
Delta-5. 168.7 m	whole rock		2.74	2.001	69.3	178.7±7.0	fresh rock near to a fracture
	<2 µm	0.414	3.27	2.914	92.8	215.8±8.1	
Bat-4. 811.5 m	whole rock		4.06	2.5825	75.5	156.6±6.0	tectonized
	<2 µm	0.591	5.26	2.833	90.4	133.5±5.1	
	<0.4 µm		6.20	2.744	81.5	110.3±4.1	

shaft and of present-day shallow groundwater (Fig. 14). However, no indication of such low formation temperature has yet been encountered, and would be difficult to reconcile with the present-day rock temperature (~50 °C).

One of the most important observations is that no significant migration of present-day surficial water occurred in the fractures that would cause $\delta^{13}C$–$\delta^{18}O$ shifts in the calcite toward the field of surficial carbonates, although two veins among the 55 with $\delta^{13}C$ values above –6‰ show slight shifts toward surficial compositions (Fig. 11).

Conclusions

The unusual bulk rock major element and modal compositions of the Upper Permian Boda Albitic Claystone Formation (low quartz, high albite, considerable hematite and carbonate contents) are explained by peculiar paleogeographic and paleoclimatic circumstances during sedimentation in a shallow-water lacustrine intramountain basin with highly alkaline and oxidative waters alternating with drying-up periods in semi-arid to arid conditions.

On the basis of illite and chlorite crystallinity indices, vitrinite reflectance and K-Ar ages, this formation suffered late or deep diagenetic alterations (reaching maximally 200–250 °C) that culminated in the Lower Jurassic. In the main rock mass phyllosilicates are represented by illite-muscovite and chlorite, the former always being predominant.

Both minerals contain only minor swelling, mixed-layered impurities. Whole rock carbonates have high C and O isotope compositions that prove sedimentary carbonate formation. Whole rock carbonates with high $\delta^{13}C$, but very variable $\delta^{18}O$ values, indicate extensive diagenesis.

Because of the brittle mechanical behavior of the rocks, tectonic deformations caused repeated fracturing. In the post-diagenetic fault gouges restricted migration of low-temperature fluids resulted in retrogression of phyllosilicates, i.e., in transformation of chlorite, formation of swelling mixed-layers and smectite, degradation of illite-muscovite and/or neoformation of poorly crystallized illite. The latter two processes are expressed by IC increase and inequilibrium resetting of K-white mica K-Ar ages.

In addition to fault gouges, three types of fissure fillings, namely calcite-, baryte+quartz- and anhydrite-dominated veins (the barytic one with sulfidic mineralization) could be distinguished. The combined application of H, C and O isotope compositions suggests three fluid generations: magmatic fluid that produced barite-quartz veins at ~150 °C, and meteoric waters related to warm and cold climate conditions that produced calcite veins at ~70 °C.

Isotopic compositions characteristic of surficial carbonate is observed only in surface-derived rocks, although some fracture filling calcites show slight shifts toward surficial compositions. Considering the present data set, a significant effect of recent meteoric water in fracture fillings is unlikely.

Acknowledgements

The present work was initiated and financially supported, and its publication permitted, by the Mecsek Ore Environment Co. The phyllosilicate crystallinity and stable isotope studies also form parts of projects Nos. T-022773 and T-014968 financed by the Hungarian Scientific Research Fund (OTKA), Budapest.

References

Alpers, C.N., D.L. Dettman, K.C. Lohmann, D. Brabec 1990: Stable isotopes of carbon dioxide in soil gas over massive sulfide mineralization at Crandon, Wisconsin. – Journal of Geochemical Exploration, 38, pp. 69–86.

Árkai, P. 1983: Very low- and low-grade Alpine regional metamorphism of the Paleozoic and Mesozoic formations of the Bükkium, NE-Hungary. – Acta Geol. Hung., 26, pp. 83–101.

Árkai, P., K. Balogh, I. Dunkl 1995a: Timing of low-temperature metamorphism and cooling of the Paleozoic and Mesozoic formations of the Bükkium, innermost Western Carpathians, Hungary. – Geologische Rundschau, 84, pp. 334–344.

Árkai, P., K. Balogh, M. Frey 1997: The effects of tectonic strain on crystallinity, apparent mean crystallite size and lattice strain of phyllosilicates in low-temperature metamorphic rocks. – Schweiz. Mineral. Petrogr., Mitt. 77, pp. 27–40.

Árkai, P., R.J. Merriman, B. Roberts, D.R. Peacor, M. Tóth 1996: Crystallinity, crystallite size and lattice strain of illite-muscovite and chlorite: comparison of XRD and TEM data for diagenetic to epizonal pelites. – Eur. J. Mineral., 8, pp. 1119–1137.

Árkai, P., G. Nagy 1994: Tectonic and magmatic effects on amphibole chemistry in mylonitized amphibolites and amphibole-bearing enclaves associated with granitoid rocks, Mecsek Mountains, Hungary. – Acta Geol. Hung., 37, pp. 235–268.

Árkai, P., D. Sadek Ghabrial 1997: Chlorite crystallinity as an indicator of metamorphic grade of low-temperature meta-igneous rocks: a case study from the Bükk Mountains, northeast Hungary. – Clay Minerals, 32, pp. 205–222.

Árkai, P., F.P. Sassi, R. Sassi 1995b: Simultaneous measurements of chlorite and illite crystallinity: a more reliable tool for monitoring low- to very low-grade metamorphisms in metapelites. A case study from the Southern Alps (NE Italy). – Eur. J. Mineral., 7, pp. 1115–1128.

Barabás, A. 1955: Permian formations of the Mecsek Mountains. – C.Sc. thesis, Budapest (in Hungarian).

Barabás, A., Á. Barabás-Stuhl 1998: Stratigraphy of the Permian formations in the Mecsek Mountains and its surroundings. – In: Stratigraphy of geological formations of Hungary. Mol Plc. and Hung. Geol. Institute, Budapest, pp. 187–215 (in Hungarian).

Bárdossy, Gy. 1966: X-ray diffractometric study of the modal composition of bauxites. – Kohászati Lapok, 8, pp. 355–363 (in Hungarian).

Bárdossy, Gy. 1968: A method for quantitative modal analysis of bauxites and laterites with X-ray diffractometry. – Litol. Polezn. Iskop., 6, 125–139 (in Russian).

Clauer, N., H. Zwingmann, S. Chaudhuri 1996: Isotopic (K-Ar and oxygen) constraints on the extent and importance of the Liassic hydrothermal activity in western Europe. – Clay Minerals, 31, pp. 301–318.

Demény, A. 1995: H isotope fractionation due to hydrogen-zinc reactions and its implications on D/H analysis of water samples. – Chemical Geology, 121, pp. 19–25.

Demény, A., I. Fórizs, Z. Máthé 1996: A preliminary stable isotope study on a potential radioactive waste repository site in the Mecsek Mountains, Southern Hungary. – Rapid Communications in Mass Spectrometry, 10, pp. 1415–1417.

Eugster, H.P., L.A. Hardie 1975: Sedimentation in an ancient playa-lake complex: The Wilkins Peak Member of the Green River Formation of Wyoming. – Geol. Soc. Amer. Bull., 86, pp. 319–334.

Fazekas, V. 1987: Modal composition of the Permian and Lower Triassic formations of the Mecsek Mountains. – Földt. Közl., 117, pp. 11–30 (in Hungarian).

Forgó, L., L. Moldvay, P. Stefanovits, Gy. Wein 1966: Maps and explanatory text to the geological map series of Hungary in scale 1:200000, L-34-XIII, Pécs. – Hungarian Geological Institute, Budapest (in Hungarian).

Frey, M. 1987: Very low-grade metamorphism of clastic sedimentary rocks. – In: Frey, M. (Ed.): Low Temperature Metamorphism, Blackie, Glasgow, pp. 9–58.

Foster, M.D. 1962: Interpretation of the composition and a classification of the chlorites. – U.S. Geol. Surv. Prof. Paper, 414-A, pp. 1–33.

Friedman, I., J.R. O'Neil 1977: Compilation of stable isotope fractionation factors of geochemical interest. – In: Data of Geochemistry 6, Geol. Surv. Prof. Paper 440-KK.

Fritz, P., J.-Ch. Fontes, S.K. Frape, D. Louvat, J.-L. Michelot, W. Balderer 1989: The isotope geochemistry of carbon in groundwater at Stripa. – Geochimica et Cosmochimica Acta, 53, pp. 1765–1775.

Fülöp, J. 1994: Geology of Hungary. Paleozoic, II. – Akadémiai Kiadó, Budapest (in Hungarian).

Géczy, B. 1973: The origin of the Jurassic faunal provinces and the Mediterranean plate tectonics. – Ann. Univ. Sci. Budapest. R. Eötvös Nom. Sect. Geol., 16, pp. 99-114.

Hoefs, J. 1973: Stable Isotope Geochemistry. – Springer, Berlin, Heidelberg.

Hunziker, J., M. Frey, N. Clauer, R.D. Dallmeyer, H. Friedrichsen, W. Flehmig, K. Hochstrasser, P. Roggwiller, H. Schwander 1986: The evolution of illite to muscovite: mineralogical and isotopic data from the Glarus Alps, Switzerland. – Contrib. Mineral. Petrol., 92, pp. 157–180,

Javoy, M., F. Pineau, I. Iiyama 1978: Experimental determination of the isotopic fractionation between gaseous CO_2 and carbon dissolved in tholeiitic magma. – Contrib. Mineral. Petrol., 67, pp. 35–39.

Kázmér, M., S. Kovács 1985: Permian–Paleogene paleogeography along the Eastern part of the Insubric–Periadriatic lineament system: evidence for the continental escape of the Bakony–Drauzug Unit. – Acta. Geol. Hung., 28, pp. 71–84.
Kisch, H.J. 1987: Correlation between indicators of very low-grade metamorphism. – In: Frey, M. (Ed.): Low Temperature Metamorphism. Blackie, Glasgow, pp. 227–300.
Kovács, S. 1982: Problems of the "Pannonian Median Massif" and the plate tectonic concept. Contributions based on the distribution of Late Paleozoic–Early Mesozoic isopic zones. – Geol. Rundschau, 71, pp. 617–640.
Kovács, S., T. Szederkényi, P. Árkai, Gy. Buda, Gy. Lelkes-Felvári, A. Nagymarosi 1996–1997: Explanation to the terrane map of Hungary. – Annales Géol. Des Pays Helléniques, 37, pp. 271–330.
Kübler, B. 1968: Evaluation quantitative du métamorphisme par la cristallinité de l'illite. – Bull. Centre Rech. Pau — S.N.P.A. 2, pp. 385–397.
Kübler, B. 1990: "Cristallinité" de l'illite et mixed-layers: brève révision. – Schweiz. Mineral. Petrogr., Mitt. 70, pp. 89–93.
Kübler, B., J.-L. Pittion, Y. Heroux, J. Charollais, M. Weidmann 1979: Sur le pouvoir reflecteur de la vitrinite dans quelques roches du Jura, de la Molasse et des Nappes préalpines, helvétiques et penniques. – Eclogae geol. Helv., 72, pp. 343–373.
Manega, P.C., S. Biena 1987: Modern sediments of Lake Natron, Tanzania. – Sci. Géol. Bull., 40, pp. 83–95.
Mattey, 1991: Carbon dioxide solubility and carbon isotope fractionation in basaltic melt. – Geochimica Cosmochimica Acta, 55, pp. 3467–3473.
McCrea, J.M. 1950: On the isotopic chemistry of carbonates and a paleotemperature scale. – The Journal of Chemical Physics, 18, pp. 849–857.
Merriman, R.J., M. Frey 1999: Patterns of very low-grade metamorphism in metapelitic rocks. – In: Frey, M., D. Robinson (Eds): Low-Grade Metamorphism. Blackwell Science, Oxford, pp. 61–107.
Merriman, R.J., D.R. Peacor 1999: Very low-grade metapelites: mineralogy, microfabrics and measuring reaction progress. – In: Frey, M., D. Robinson (Eds): Low-Grade Metamorphism. Blackwell Science, Oxford, pp. 10–60.
O'Neil, J.R., R.N. Clayton, T.K. Mayeda 1969: Oxygen isotope fractionation in divalent metal carbonates. – The Journal of Chemical Physics, 51, pp. 5547–5558.
Pettijohn, F.J. 1975: Sedimentary rocks. 3rd Ed. – Harper and Row, New York, p. 628.
Poroda, H., H.J. Behr 1988: Setting and sedimentary facies of late Proterozoic alkali lake (playa) deposits in the southern Damara Belt of Namibia. – Sedimentary Geology, 58, pp. 171–194.
Rowlands, N.J., P.G. Blight, D.M. Jarvis, C.C. Van der Borch 1980: Sabkhas and playa environments in late Proterozoic grabens, Willouran Ranges, South Australia. – J. Geol. Soc. Australia, 27, pp. 55–68.
Sackett, W.M., W.S. Moore 1966: Isotopic variations of dissolved inorganic carbon. – Chem. Geol., 1, pp. 323–328.
Sheppard, S.M.F. 1986: Characterization and isotopic variations in natural waters. – In: Valley, J.W., H.P. Jr. Taylor, J.R. O'Neil (Eds): Stable isotopes in high temperature geological processes. – Reviews in Mineralogy, 16, pp. 165–184.
Vennemann, T.W., J.R. O'Neil2 1993: A simple and inexpensive method of hydrogen isotope and water analyses of minerals and rocks based on zinc reagent. – Chem. Geol. (Isot. Geosci. Sect.), 103, pp. 227–234.

Acta Geologica Hungarica, Vol. 43/4, pp. 379–404 (2000)

Formation of minerals in loess and soils

Márton Pécsi
Geographical Research Institute,
Research Centre for Earth Sciences,
Hungarian Academy of Sciences

Ernő Nemecz, Zsuzsanna Hartyáni,
Tímea Horváth
University of Veszprém
Department of Earth and Environmental Science

A recurring problem of the theories of loess formation is the origin of quartz grains of 10–50 mm size, which make up the bulk of loess material. Literature on loess abounds in simplifications claiming that nowadays hardly anyone questions the theory of eolian origin. Such formulations are due to erroneous terminology and should be considered as a result of the vulgarization of the concept of loess.

According to a long-debated theory by Berg loess was a product of soil formation. His concept has attracted both supporters and ardent opponents. At any rate, recent theories of loess formation should count with the process of loessification (diagenesis).

We attempt to explain the formation of 10–50 μm particle size and minerals in relation with pedogenesis. We undertook a series of detailed granulometric mineralogical and chemical investigations of soils having formed on loess as parent material and of paleosols buried in typical loess. We found that granulometry both in the soils formed on loess and in paleosols displays a typical double maxima (in 5 μm and 20–45 μm). At the same time, quartz as the main mineral component of loess (60–65 m/m%) shows enrichment in the 20–45 μm particle size interval as well. A repeated occurrence of this phenomenon made the clearing up of the problem an actual necessity.

After joint meetings and field trips the conclusion was arrived at that the weathering of the main mineral components of loess (quartz, feldspar and mica) into coarse silt grains probably took place predominantly during steppe soil formation. Certainly this circumstance stimulated the formation of the characteristic loess fabric as well as that of loess-paleosol granulometry, mineral and chemical composition.

Key words: concept of loess, genesis of loess, loessification as a product of week steppe soil development, the distribution of particle size, minerals in loess, paleosols, recent steppe soils nearly identical

Introduction

Among characteristic features of loesses a specific grain size distribution is usually the first thing to be mentioned. However, it is also the general case that granulometric curves of certain loess-like sediments show striking similarities with those of the typical loesses. In many cases no substantial difference can be observed between the grain size of loesses and that of loess-like deposits.

Nevertheless the systematization, classification and terminology used for the lithological characterization of loesses are often based on granulometry (e.g. Mihályiné Lányi 1953; Szilárd 1983, 1985; Pécsi 1993).

Addresses: M. Pécsi: H-1112 Budapest, Budaörsi út 43–45, Hungary
E. Nemecz, Zs. Hartyáni, T. Horváth: H-8201 Veszprém, P. O. Box 158, Hungary
Received: 27 March, 2000

An important prerequisite for the classification of loesses according to their origin is the knowledge of the circumstances of loess formation which has been a subject to academic debates for more than a hundred years (Smalley 1980; Hahn 1977). Generally four main groups of factors affecting loessification are distinguished:

– the way and place where the particles were formed (1),
– the mode of material transport (2),
– the process of accumulation of particles (3),
– the role of diagenesis, i.e. of weathering in the place of accumulation (4).

The origin of the coarse silt fraction (10–50 μm) predominant in loess has been explained by frost shattering, physical weathering caused by insolation, glacier grinding, or by the presence of fine-grained fluviatile and lacustrine sediments. Desert sands are also often claimed as the source.

From the scientific point of view the issue of the origin of loess and loess-like deposits comes to the fore. Several concepts have been proposed:

– A most frequent and simple explanation for grain size distribution, transport and the characteristic sorting of typical loess is provided by wind action. A specific relative position of particles without orientation is derived from atmospheric deposition and accumulation. Another argument is the occurrence of loess mantling landforms in different settings and configurations. According to this concept of eolian origin, transport and deposition of mineral material of typical loess are airborne phenomena.

– According to another group of explanations the mineral weight of loess, and especially of its derivatives, have undergone multiple means of transportation processes (for details see Pécsi and Richter 1996, 5. 1–5, Chapter 4).

On the issue of explanations for the origin of loess Berg (1916, 1953) and Pécsi (1991) considered it important to emphasize that the sedimented material is not yet loess, i.e. it is not the loess which accumulates but its mineral weight. *The ideal conditions for loessification are provided by soil horizons of semi-arid steppes and open woodlands (in some places warm and dry steppes) and during Pleistocene periglacials in those of cold steppes and open woodlands; they form the megazones of loess formation.*

There have been explanations given concerning loess formation emphasizing the predominant role played by the geographical environment, i.e. by the loess megazone, in the soils of which organic and non-organic processes play a more important part than any other transportation or accumulation processes (von Richthofen 1877, I. 2. P. 78; Berg 1916; Pyaskovskii 1946; Kriger 1965; Pécsi 1968, 1987).

Since loess was recognized and separated from other unconsolidated deposits and was named in the early 19th century (von Leonhard 1823/24), a number of concepts and theories have been born and opinions on the matter are divided. In general it can be stated that explanations concerning the genesis of loess, similar to the concepts of loess, are legion, due to the occurrence of loesses in several regions, and to the many varieties of loess. The majority of nearly one hundred interpretations of loess deal with the different processes of transport, sorting and accumulation of its material and only a small part is devoted to the complex environmental-geochemical processes of diagenesis.

The origin of silt-size particles of quartz-feldspar in huge quantity as a fundamental problem

A recurring problem of the theories of loess formation is the origin of quartz grains of 10–50 mm size which make up the bulk of loess material. For the adherents of the theory on "warm" loess, quartz grains originate from the dust of deserts transported by storms and accumulated in areas beyond the desert zone. Some experts hold frost action under cold climates responsible for the creation of silt in amounts large enough to account for loess formation. Others emphasize glacier grinding that decreased rock detritus to silt size; the resulting sediment was accumulated by meltwater in fluvioglacial deposits. Some scientists express the opinion that silt-size particles can also be found in sufficient amounts in river load. According to them silt fraction is transported by rivers from the clastic material accumulated in the high mountain zones and is deposited over the flood plain during floods. Some attribute this process to the transportation and accumulation of fluvioglacial material.

Those representing the "soil formation concept" explain characteristic particle size distribution in loess partly by frost shattering and biochemical comminution and partly by in situ soil formation. According to this theory coarser grains undergo shattering in the course of frost action and soil formation, while clay particles coagulate and aggregate into loess (coarse silt) fraction.

According to Pécsi (1967) the mechanism leading to the formation of coarse silt size can be polygenetic, while others assume a single dominant process. In the view of Smalley (1975) quartz grains underwent multiple processes of transportation until their ultimate accumulation and might have originated from different source areas. However, they all emphasize the prominent role of glaciers as Tutkowskii (1900) did earlier. They consider loess a fine clastic sediment and in their definition three main factors are considered:

1. Formation of coarse silt particles,
2. Eolian accumulation of these grains, and
3. A complicated process including multiple transport and accumulation, with repeated redeposition.

Literature on loess abounds in simplifications claiming that nowadays hardly anyone questions the theory of eolian origin. Such formulations are due to erroneous terminology and should be considered as a result of the vulgarization of the concept of loess.

According to a long debated theory by Berg (1916) loess was a product of soil formation. Along loess sections traces of pedogenesis are recognizable in most cases; they can be weaker or stronger (the latter in the case of fossil soils). In the present study the above concept will be supported and confirmed by more recent methods and the results of laboratory analyses.

Berg's theory cannot be used to explain the fairly thick loess-paleosol series, with several buried soils. After pedogenesis, sedimentation of material must take place on the newly developed surface, which subsequently undergoes loessification, then turning into paleosol.

According to Berg, however, the relationship between loess and parent material is similar to that between parent rock and soil. In order to turn parent rock into soil there must be soil formation, and to turn the unconsolidated deposit into loess there must be loessification. According to Berg the mineral material of loess can be accumulated by different processes but fine clastic skeletal soil can develop in situ through eluvial comminution.

The working hypothesis of Berg – loess is a product of soil formation – still exerts a strong influence on explanations concerning the origin of loess. His concept has attracted both supporters and ardent opponents. In any case, recent theories of loess formation should count on the process of loessification (diagenesis).

According to the polygenetic theory of loess formation particle size could have been shaped and the bulk of loess been accumulated in several different ways. The sedimentation of mineral material could have taken place by temporally and spatially repeated eolian, derasional[1], fluvial, fluvioglacial, eluvial, or pedogenetic processes. In these processes zonal and partly local environmental ecological factors, pedogenetic and geochemical phenomena played a major role.

An attempt to explain the formation of 10–50 μm particle size and minerals in relation to pedogenesis

– A widely distributed type of loess within the Carpathian Basin is lowland loess, one of the varieties which are the so-called *infusion loesses*, the grain size and loess fabric which Pécsi (1982) explained by the formation of steppe soil and not by the mode of sedimentation. Studies of several loess profiles (brickyards) in the Great Hungarian Plain enabled the present authors to arrive at the conclusion that the widespread 'infusion' loess blanket over the plain can be classified in terms of loess silt. As a result of meadow soil and chernozem soil formation it has acquired a loess structure (fabric) by diagenesis to a depth of 1.5–2 m (Pécsi 1982, p. 145).

Below steppe soils at a depth of 1.5–2 m, fine, stratified sandy silt occurs, having turned into loess-like sediment through diagenesis. This was facilitated by hollows of burrowing animals and carbonate accumulation in the course of steppe soil formation (Pécsi 1993, p. 259).

– Recently Nemecz and Hartyáni (1995) and Nemecz et al. (2000) undertook a series of detailed, granulometric and mineralogical investigations of soils having formed on loess as parent material and of paleosols buried in typical loess. They found that granulometry both in the soils formed on loess and in paleosols displays a typical double maxima (in <5 μm and 20–45 μm fractions; Figs 1A, B,

[1] derasion: mass movements, slope wash, all kind of solifluction

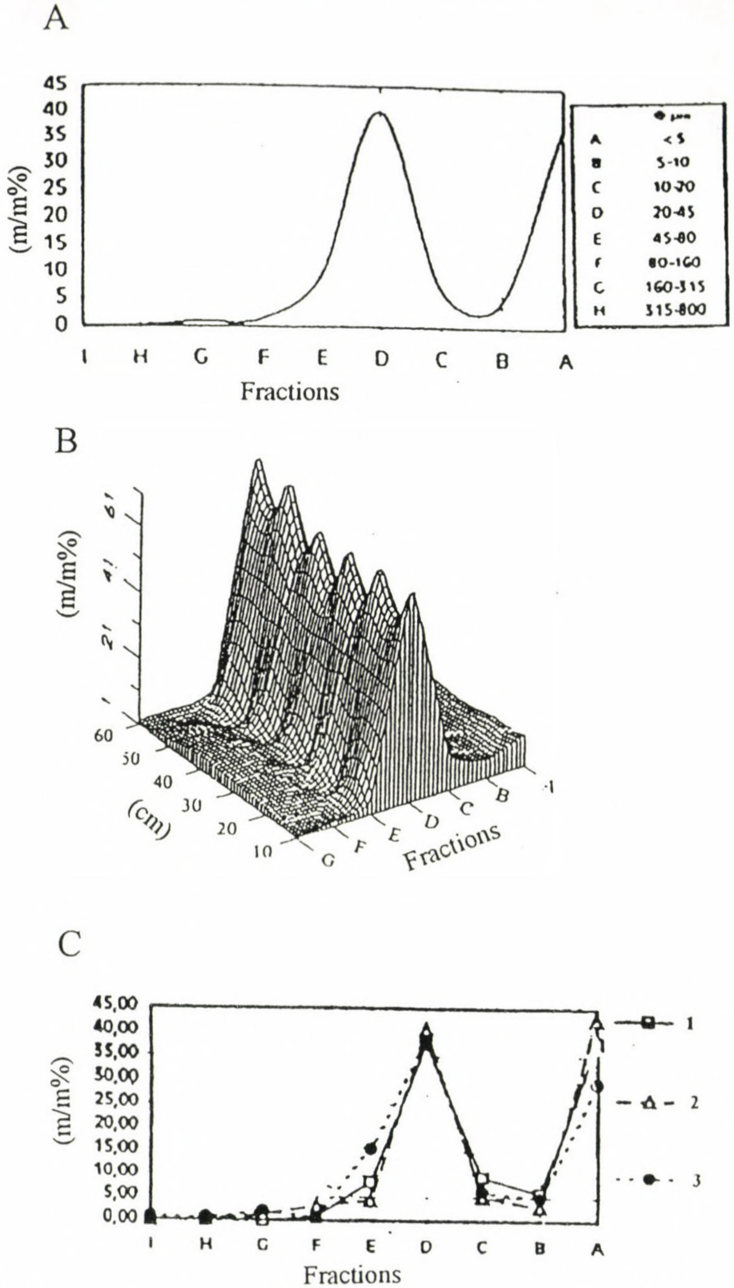

Fig. 1
Particle-size distribution of loess-paleosol formations in Hungary (after Nemecz and Hartyáni 1995). A. Average grain size distribution curve of 16 Hungarian soils. B. quartz grain size distribution curve in MB1 paleosol at Paks; C. Average grain size distribution curves of loesses (1), paleosols (2) and recent soils (3)

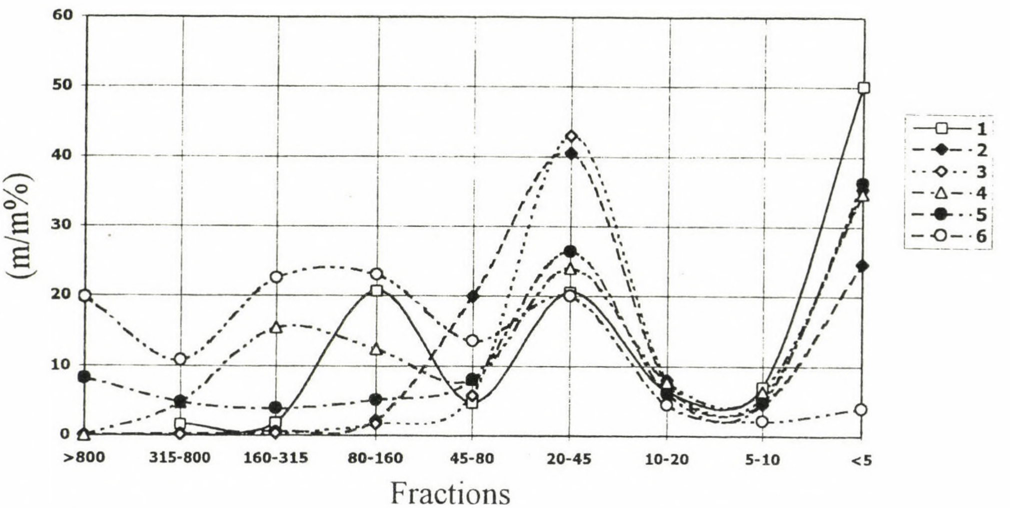

Fig. 2
Granulometric distribution of different sediments and soils (after E. Nemecz et al. 2000). 1. particles transported and sedimented by fluvial and eolian processes (Sahara dust settled at Budapest 1997; the suspended load carried by the Danube at Surány at MWL; fine silt samples deposited by the Danube at Budapest, Csepel Island; fine silt on the bottom of Lake Balaton from four different localities); 2. loesses; 3. paleosols in loess; 4. mainly meadow and steppe soils; 5. recent soils on magmatic rocks (granite, andesite, basalt, rhyolite); 6. artificial pressed objects (hydrostatic pression: 20 t cm^{-2} 60 s^{-1}) (glass, granite, basalt, andesite, monocrystal quartz, microcline, calcite, garnet)

C). At the same time, quartz as the main mineral component of loess (60–65 m/m%) shows enrichment in the 20–45 μm particle size interval as well (Fig. 3). A repeated occurrence of this phenomenon made the clearing up of the problem a necessary task.

Following joint meetings and field trips the conclusion was reached that the weathering of the main mineral components of loess (quartz, feldspar and mica) into coarse silt grains probably took place predominantly during steppe soil formation (Figs 4–6). Certainly this circumstance stimulated the formation of the characteristic loess fabric as well as that of loess-paleosol granulometry and mineral composition.

Research methods

Samples were collected from the cleaned walls of loess-paleosol exposures at 10-cm depth intervals. From each sample 170 g dry mass was taken for preparing a 15 m/m% suspension using de-ionized water (for fraction <2 μm it was ca. 5 m/m%). Through moderate peptization the samples were fractionated by sieving the averaged samples into the fractions shown in Table 1. The <45 μm size fractions were sieved in an ultrasonic bath with laser beam-made sieves.

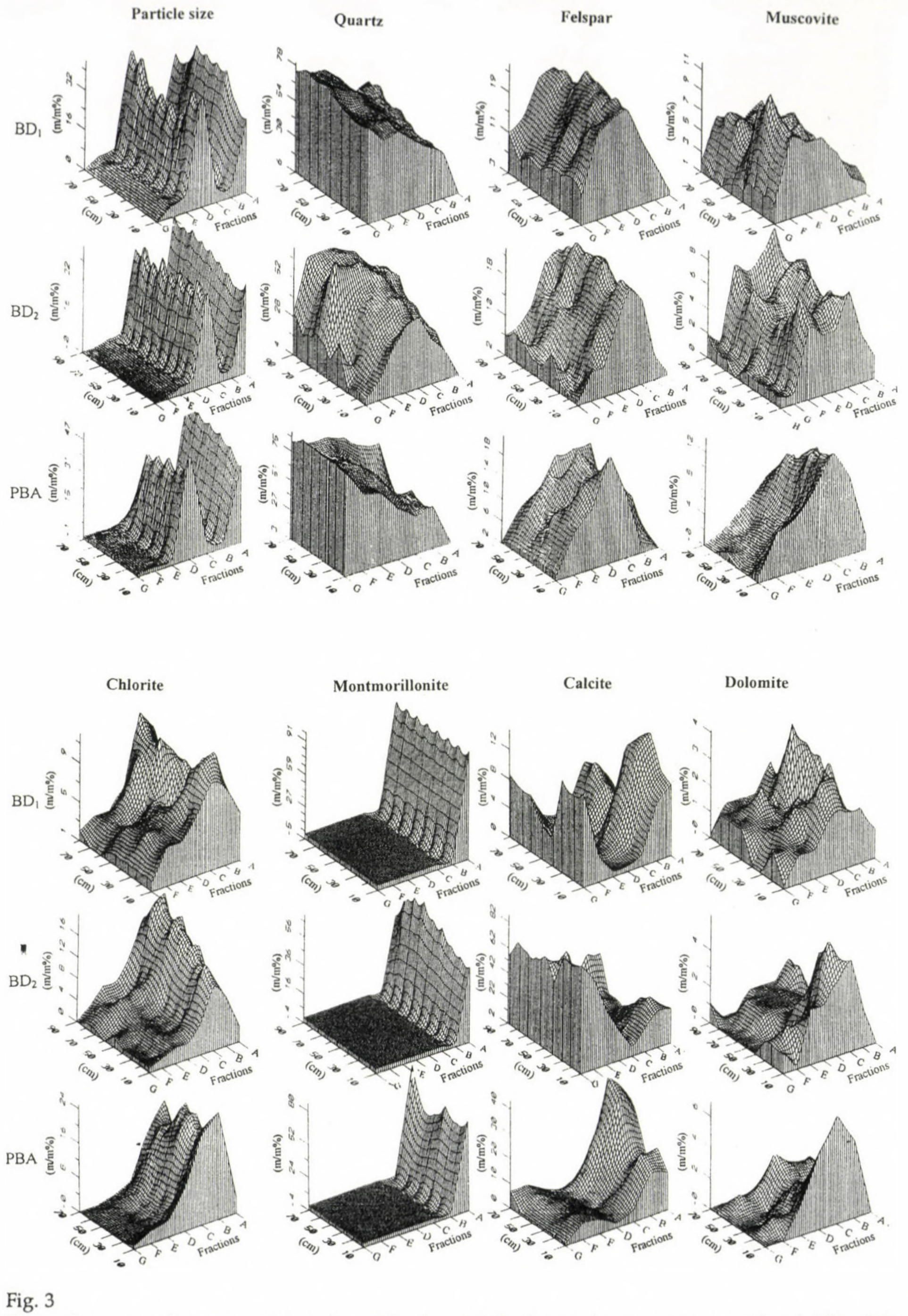

Fig. 3
Three-dimensional representation of particle size distribution and mineral composition inBD_1, BD_2 (in Basaharc, and PBA (Paks, brickyard section) of paleosol samples (X axis the depth, Y axis the fraction, see Fig 1A) (Nemecz et al. 2000)

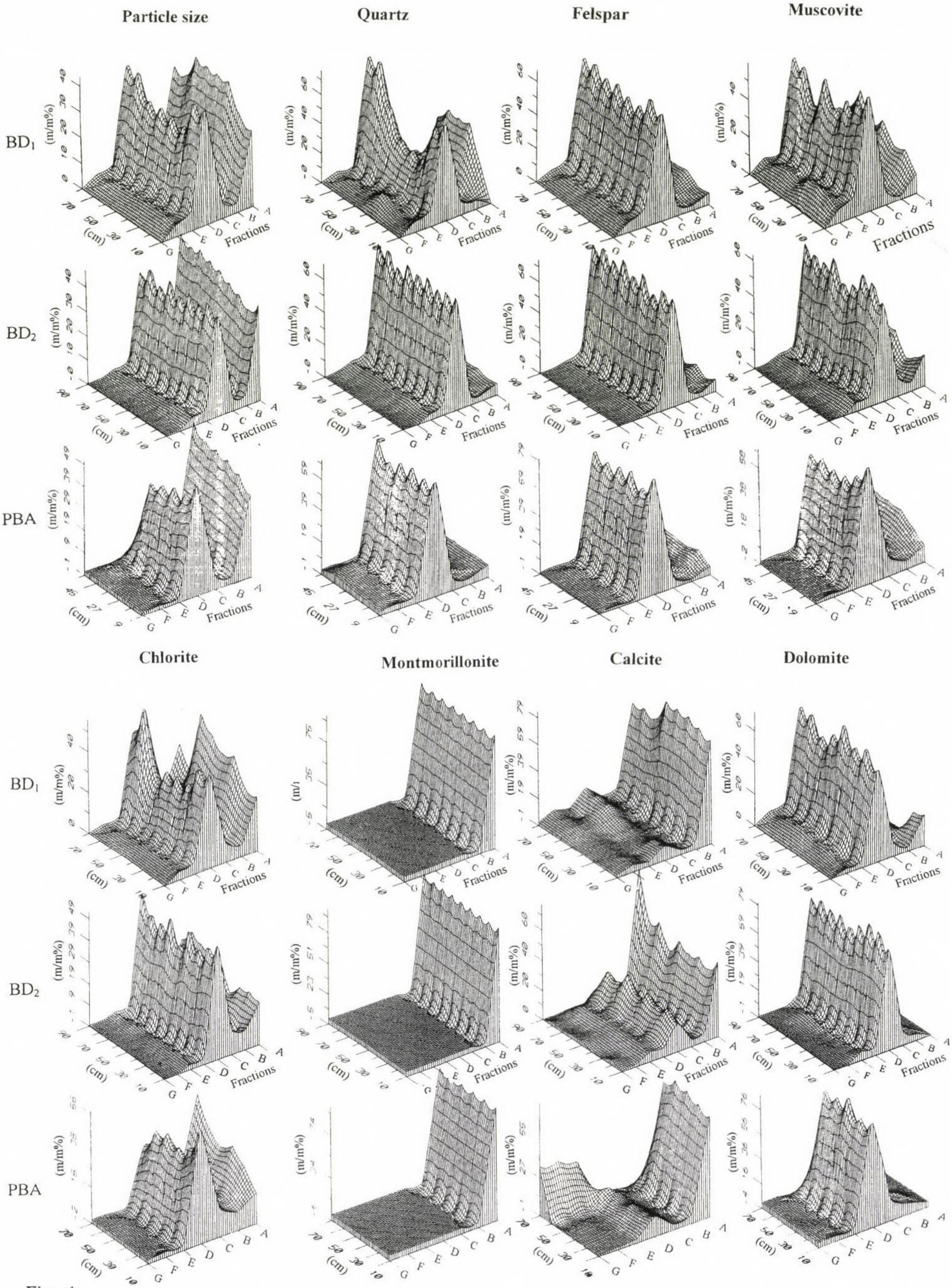

Fig. 4
Three-dimensional representation of individual distribution[1] (ID) of minerals in the BD_1, BD_2 and PBA paleosols (Nemecz et al. 2000)

[1] Individual distribution of a mineral (ID) is the distribution of any minerals among particle size fractions taking in account the relative amount of a mineral in the particle size distribution of the whole sample

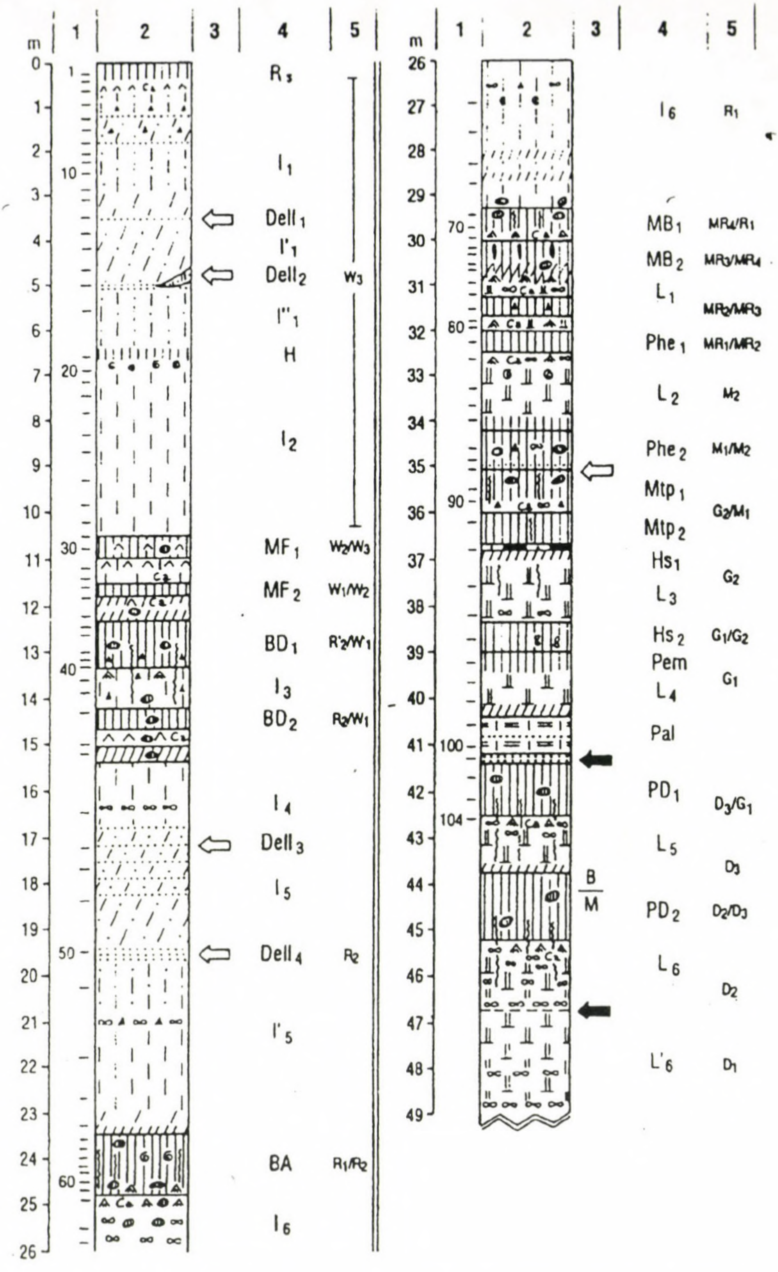

Fig. 5
The loess-paleosol sequence at Paks its lithostratigraphic and chronological subdivision (Pécsi et al. 1995. Loess InForm No 3. p. 65). 1. number of samples; 2. lithostratigraphy; 3. erosional and minor derasional gaps (white arrows), stronger erosional gaps (black arrows); 4. lithological and pedological indices; 5. presumable chronological subdivision; B/M = Brunhes/Matuyama boundary (ca 0.75 Ma)

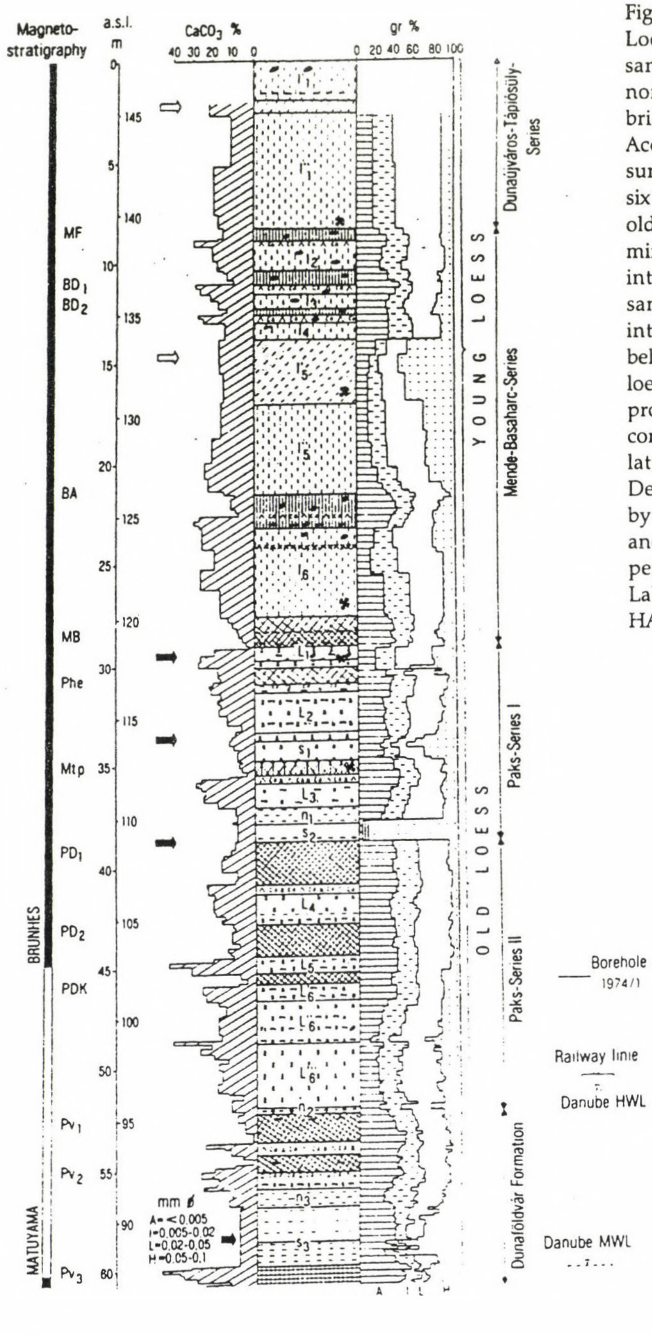

Fig. 6

Loess-paleosol sequence with sand intercalations in the northern section of the Paks brickyard (after Pécsi 1993). According to the detailed survey of 1971, 14 buried soils, six young loess layers (l_1–l_6), 7–8 old loess pockets (L_1–L_6), 2–3 minor and 3 significant sand intercalations (S_1–S_3), 3 silty sand (clayey fine sand) interbeddings (n_1–n_3) and, below the paleosols and in old loess (in some cases without soil profile) horizons of carbonate concretions, calcareous accumulation (in 14–15 cases) occur. Detailed magnetostratigraphy by M.A. Pevzner. Lithological and paleopedological analyses performed in the Soil Laboratory of Geogr. Res. Inst. HAS

To obtain quantitative mineral and chemical composition of fractions, samples were analyzed by X-ray diffraction (Philips PW 1710 diffractometer), X-Ray Fluorescence Spectrometry (Philips PW 2404 spectrometer), and DTA, TG. In some cases a complete chemical analysis was performed. The lower limit of disclosure – slightly fluctuating by minerals – was about 1 m/m %. The results were plotted in three-dimensional diagrams, where depth from the soil surface in multiples of 10 cm were shown along axis X, grain size fractions along Y, and the percentage of minerals belonging to points xy along Z (Fig. 1B, 3, 4, 5, 10, 12).

Results of granulometric analyses

Based on the results obtained through the above-outlined methods of investigations it could be established that the recent zonal soils, i.e. chernozems, which formed on the loesses of Hungary had the following grain size distribution: clay content (fraction A = <5 μm): ca. 28 m/m%, coarse silt (fraction D = 20–45 μm): ca. 34 m/m%.

Coarse and fine silt fractions (B+C+D+E) together represent about 67 m/m% (Table 1, Mv1). Meadow soils formed on the so-called infusion loesses show a substantially different granulometry. On the lower terraces and higher flood plains over the Great Hungarian Plain there are waterlogged areas where in meadow chernozems or salt-affected meadow soils fraction A constitutes nearly 50 m/m%, while the dominant (coarse) silt fraction represents a mere 21.2 m/m% and a combined percentage of silts (B+C+D+E = 41 m/m%) comes close to that of clay (Table 1, Rs me 1). In typical young loess coarse silt is the consistently dominant fraction with ca 43 m/m%, clay representing ca. 24 m/m% and the former two together with silt fractions (B to E = 5–80 m) making up 75 m/m% (Table 1, Mv3).

Forest steppe paleosols intercalated in young loess show remarkably similar grain size composition. Coarse silt is predominant with ca. 40 m/m% slightly exceeded by clay with 42 m/m%. Silt fractions altogether (B through E) represent 53 m/m% (Table 1, Mv4). Average values for the dominant fractions of old loesses differ only slightly from the typical ones of the young loess (Table 1, Mv5).

Paleosols enclosed in old loesses of the Paks brickyard section gave 38 m/m% for D and 40 m/m% for A, with almost no variations from the paleosols intercalated in young loesses (Table 1, Mv6). A lower percentage of the clay fraction to be found consistently in paleosols of old loess compared with the soils intercalated in young loesses, indicating drier paleoecological conditions, which are also shown by a frequent occurrence of levels of carbonate concretions and of typical chestnut paleosols.

To sum up: the above data suggest that granulometric composition of loess and paleosols result primarily from paleoclimate and catena conditions. In the course of granulometric investigations of Hungarian loesses – in accordance with the data obtained from international literature – a dominance of clay and silt

Table 1
Particle size distribution of loess-paleosol formations selected from Hungarian occurrences (After investigations and analytical methods by E. Nemecz et al. 2000)

	corse sand			f.sand	corse silt		fine silt		clay	silt	silt+fs	
ϕ (μm)	>800	315-800	160-315	80-160	45-80	20-45	10-20	5-10	<5	5-45	5-80	Remarks
Symbol of fractions	I	H	G	F	E	D	C	B	A	B+C+D	B - E	
	Samples of recent chernozem soils on young loess											Rs chr
Paks	0,65	0,6	1,93	6,7	24,75	35,3	4,27	3,74	22	43,31	68,06	1
Bátaapáti			0,01	0,7	6,44	41,4	8,17	6,12	36,6	55,69	62,13	2
Dunaújváros		0,5	0,4	1,3	24,6	25,5	13,7	5,1	28,9	44,3	68,9	3
Albertirsa				3,4	21,6	33,6	12	4,9	24,3	50,5	72,1	4
Average			***0,8***	***3,0***	***19,3***	***34,0***	***9,5***	***5,0***	***28,0***	***48,5***	***67.8***	Mv_1
	Samples of recent medow soils on infusion loess											Rs me
Abony salt effected		0,12	0,7	2,45	11,92	21,2	3,95	4,05	55,6	29,2	41,12	1
Infus.loess bedroc	0,05	0,32	0,82	3,37	15,79	26.5	7,67	5,49	40	39,66	55,45	2
	Samples of young loesses at Paks (l_2 - l_6)											⊗
Paks (l_2) 9,8 - 9,9 m		0,01	0,04	0,82	23,76	44,9	7,5	3,98	19	56,38	80,14	up.:MF_1
Paks (l_3) 13,8 - 13	0,05	0,05	0,43	2,17	21,01	31,41	6,76	4,76	33,37	42,93	66,11	be.:BD_1
Paks (l_4) 15,5 - 15	0,05	0,18	1,31	5,39	18,78	42,1	6,01	4,22	21,9	52,33	71,11	be.:BD_2
Paks (l_5) 23 -23,1	0,03	0,8	0,87	2,51	14,07	49,2	7,76	4,19	20,06	61,15	81,21	up.:BA
Paks (l_6) 27,5 - 27	0,02	0,12	0,12	0,68	17,52	46,5	6,58	4,64	23,83	57,72	75,24	be.:BA
average	***0,0***	***0,2***	***0,6***	***2,3***	***19,0***	***42,8***	***6,9***	***4,4***	***23,6***	***54,1***	***74,8***	Mv_3
	Samples of paleosols in lower part of young loess											
Basaharc BD_1 13,4 m			0,36	4,36	6,71	36,8	4,09	3,16	44,5	44,05	50,76	forest
Basaharc BD_2 18,5 m		0,23	0,44	2,7	4,42	41,8	5,17	3,33	41,8	50,3	54,72	steppe
Paks BD_2 14,4 m			2,3	4,23	4,83	40,8	5,28	2,67	39,4	48,75	53,58	paleo-
Paks BA24,2-24,3 m			1,36	2,71	2,98	42,2	4,52	2,74	43,9	49,46	52,44	sols
average			***1,1***	***3,5***	***4,7***	***40,4***	***4,8***	***3,0***	***42,4***	***48,1***	***52,9***	Mv_4
	Samples of old loesses at Paks (Hungary) (L_2 - L_5)											⊗
Paks (L_2) 33,5 m	0,17	0,07	0,28	1,01	15,61	40,34	10,98	5,29	26,26	56,61	72,22	be.:Phe
Paks (L_3) 38,1 m	0,16	0,19	0,31	1,13	24,25	38,25	6,36	4,7	24,65	49,31	73,56	be.:Mbp_2
Paks (L_4) 40.1 m	0,01	0,19	1,49	3,49	24,53	30,63	7,81	4,53	27,32	42,97	67,5	be.:Pem
Paks (L_5) 42,4 m	0,06	0,07	0,04	0,78	9,75	43,32	8,90	5,66	31,42	57,88	67,63	be.:PD_1
average	***0,1***	***0,1***	***0,5***	***1,6***	***18,5***	***38,1***	***8,5***	***5,0***	***27,4***	***51,7***	***70,2***	Mv_5
	Samples of paleosols in old loesess at Paks (Hungary)											
Paks MB_2 30,5 m			1,23	1,7	2,41	40,8	6,22	3,16	43,50	50,18	52,59	chesnut-
Paks PD_1 42,2 m	0,03	0,05	0,05	0,6	7,11	35,07	9,52	6,97	40,6	51,56	58,67	like
Paks PD_2 43,8 m	0,03	0,04	0,04	0,64	6,67	37,76	11,88	6,01	36,93	55,65	62,32	paleo-
Paks PD_2 44,6 m	0,08	0,05	0,05	0,94	10,43	35,37	7,81	5,41	39,86	48,59	59,02	sols
Paks PD_2 45,15	0,14	0,04	0,05	0,56	7,45	37,45	8,15	5,99	40,24	51,59	59,04	
average	***0,1***	***0,0***	***0,3***	***0,9***	***6,8***	***37,3***	***8,7***	***5,5***	***40,2***	***51,5***	***58,3***	Mv_6

Abbreviations
be.: Phe = belowe Phe
up.: BA = upper BA paleosol

⊗
Paks profile in Hungary usually occur at least 6 young loess (l_1 - l_6) and at least 6 - 8 old loess units (L_1 - L_6 L_6'' - L_6'''
Rs chr = recent chernozem
Rs me = recent medow soil
$Mv_{1...6}$ = main values

fractions was established. Through a finer selection of grain size (<5, 5–10, 10–20, 20–45, 45–80, 80–160, 160–315 μm) further relevant characteristics were recognized.

The fraction between 20 and 45 μm plays a more important part than the clay fraction and not only in loess but in soils formed on other rocks. To illustrate this Fig. 2 is presented to emphasize the role of the 20–45 μm fraction predominant in various soils, rocks and minerals that were exposed to mechanical pressure and underwent physical comminution. This type of granulometry is highly similar to those of loesses and interbedded paleosols.

– Both in loesses of different age and distribution as well as in soils a dominance of <5 μm (ca. 25 m/m %) and 20–45 μm (ca. 40 m/m %) fractions could be determined. In the same loess sections clay fraction tends to increase during soil formation (up to 35 wm/m %); however, not at the expense of the 20–45 m fraction (Figs 7A, B) but through reducing of the amount of 45–160 μm fraction (cf. Mv4 and Mv6). All this (with other phenomena) indicates the high resistance of the 20–45 μm fraction to weathering and to its dominant role in clastic sediments and soils.

– This is an indication of the silt fraction being typical not only of loess but also generally of decomposing minerals in the course of weathering; the paramount question is what kind of mechanism leads to a further enrichment of this fraction in loess.

Analyses of mineral transformation processes in loesses and paleosols

– Typical loesses and paleosols from internationally known key sections in Hungary (those at Paks and Basaharc) were investigated;

– To introduce 'infusion' loess of the Great Hungarian Plain the brickyard section at Abony was chosen;

– Sandy loess formed on the alluvial plain is represented by an exposure at Újfehértó (near Nyíregyháza NW of Hungary);

– The results of representative granulometric analyses are presented in Table 1.

Typical loess and paleosols at Paks: mineralogical distribution by soil horizons

The loess exposure at Paks is located within a moderately dry (ca. 500 mm annual precipitation) steppe region along the Middle Danube Basin, in the Great Hungarian Plain. The recent soil is typical chernozem. The loess section contains 12–14 intercalated paleosols.

In the upper part of the section dark colored steppe soils (chernozems) are recognized (MF_1, MF_2, PBD_1, PBD_2, PBA, PMB_1), while in the lower part warm steppe soils (ochre red chestnut soils: Phe_1, Phe_2, PD_1, PD_2), a polygenetic forest steppe soil (MB_2) and double meadow soils (Mtp_1, Mtp_2, developed under strong hydromorphic impact) are found (Figs 5 and 6). Below the typical loess-paleosol

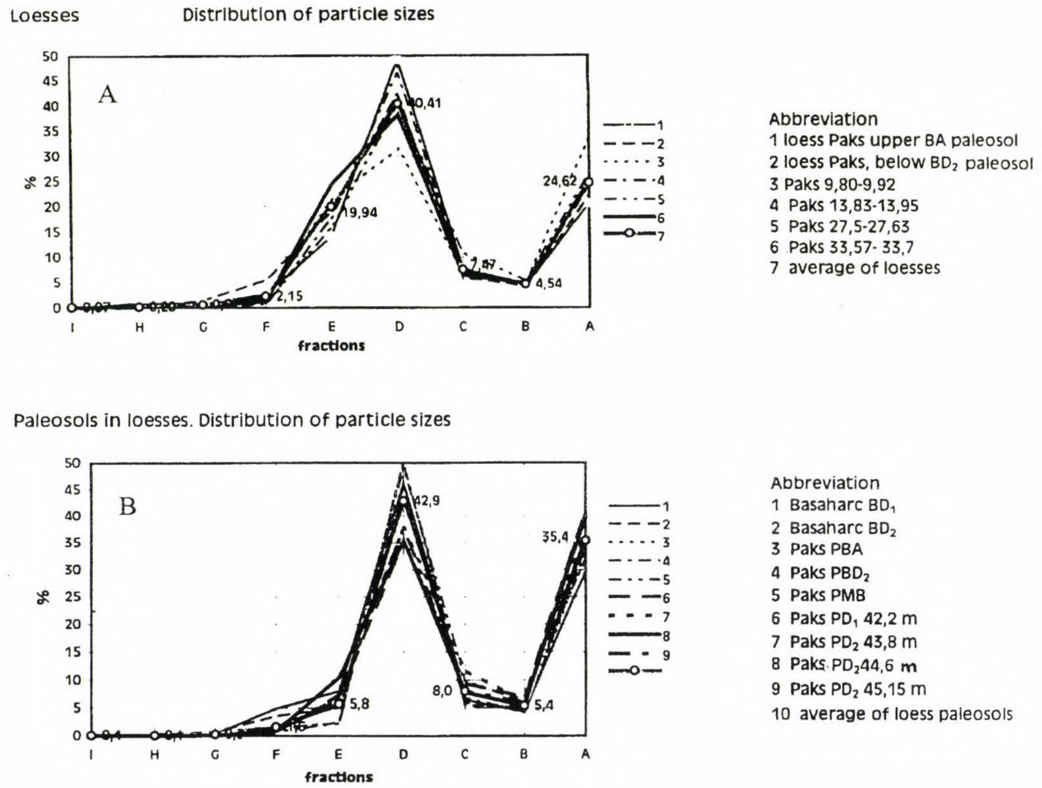

Fig. 7
Granulometric curves of selected stratotype layers in key sections of Paks and Basaharc. A. Particle size distribution curve of some characteristic loess layers within the Paks section (see Fig. 6). B. Comparative granulometric curve of stratotype paleosols from the Basaharc and Paks brickyard sections. For abbreviations of paleosols and stratigraphic position of loess layers see Figs 5 and 6

series red clay soils and variegated sandy clay layers occur, overlying the Upper Miocene (Pannonian) formations (Fig. 6).

Grain size distribution and mineral composition of the dark colored soils in the upper part of the section can be derived from diagrams BD_1, BD_2, PBA (Fig. 3). Diagrams BD_1 and BD_2, PBA (Fig. 4) indicate the Basaharc key section probably developed in a more humid environment than the Paks one, as is reflected by a higher clay content of BD_2.

A characteristic feature of these soils is that fraction D (20–45 μm) amounts to 40.5 m/m %, which is very close to that of fraction A (<5 μm – 42.6 m/m %). The individual distribution (ID) of the minerals proper by depth and grain size categories (Fig. 4) shows an arrangement as a result of soil formation (quartz, feldspars, dolomite and montmorillonite as fractions with a single maxima exception of quartz BD_1); calcite, and chlorite form double maxima as a function of granulometry and soil depth.

The average values of the dominant fractions of old loesses hardly differ from those of the young ones (Table 1, Mv3, Mv5).

At Paks the clay content of paleosols (PD_1, PD_2) intercalated in old loesses (Fig. 5, Table 1) is somewhat lower (36–40 m/m %) than in Paks BA (PBA) and Paks MB_2 (PMB_2) paleosols in the lowermost part of the upper series (43.9 and 43.5 m/m %, resp.); a similar difference is shown by fraction D, (Mv1, Mv6) (Table 1). These variations probably point to the formation of the older paleosols in somewhat drier and warmer climatic conditions.

In the old loesses (Table 1) fraction A averages 27 m/m% while coarse silt (D = 20–45 μm) shows a significantly higher (38 m/m %) presence. Concerning the distribution of minerals proper by soil depth and granulometry, old loess differs from paleosols only in the amount of calcite and dolomite, with a slight double maxima of these minerals toward deeper horizons (Fig. 5). Both along the old and young loess sections investigated there, traces of intense and weaker soil formation processes could be observed in paleosols and loess pockets respectively, with the rearrangement of particles, minerals and trace elements.

The mineral composition and trace elements of the Paks l_6 loess

In the Paks brickyard section horizon l_6 is a typical loess formation (Figs. 6 through 8). Apart from the amorphous phase it contains nine minerals with a frequency of occurrence higher than 1 m/m% (Fig. 8A). Particle size distribution is characterized by a high amount of fractions <5 μm (ca. 25 m/m %) and that of 20–45 μm (ca. 47 m/m %). Decomposing minerals are represented in the <5 μm fraction with 5 m/m% as a maximum, while only the ratio of authigenic minerals (montmorillonite and calcite) exceeds that of the fraction itself.

It is very instructive to interpret Fig. 8B (showing the individual distribution of minerals). Here each mineral shows enrichment in the 20–45 μm fraction as compared with the neighboring fractions. This means that not quartz but rather feldspars and dolomite have their highest occurrence in this fraction.

Among trace elements Zr and Sr are dominant, which was not shown in Fig. 8C due to problems with representation. A similar behavior of Pb and Zn (with an even higher content) is remarkable and characterized by increasing amounts in the <5 μm and 80–160 μm fractions.

When granulometric conditions are also taken into consideration in the distribution of trace elements (Fig. 8D) it can be observed that an overwhelming part thereof also accounts for the <5 μm and 20–45 μm fractions. However, most

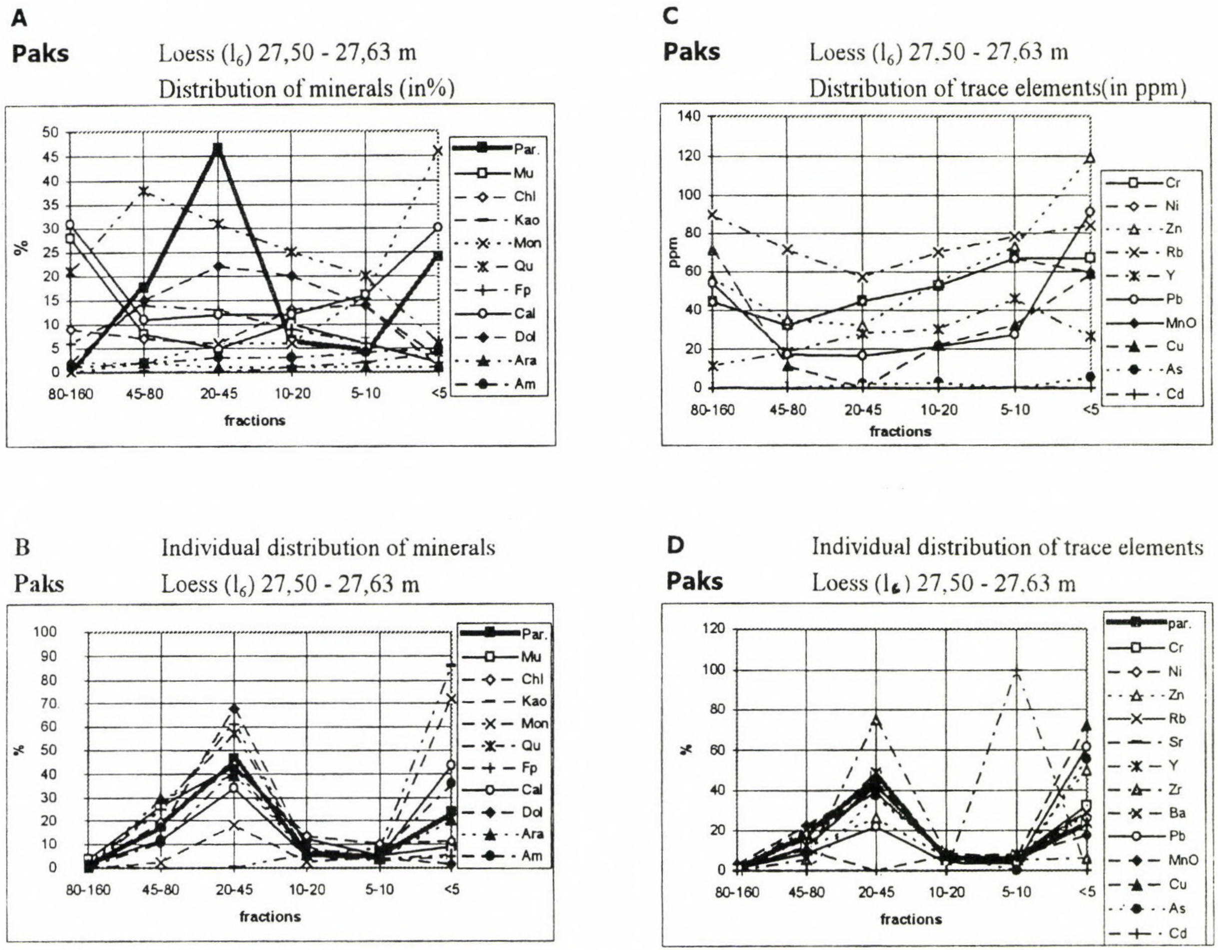

Fig. 8

Mineralogical analysis of the l6 loess horizon at the Paks brickyard section (after Nemecz et al. 1999). A. m/m percentage distribution of minerals; B. distribution of minerals concerning the wt. % of fractions; C. distribution of trace elements (in ppm); D. distribution of trace elements concerning the wt. % of fractions of the trace elements here show the highest enrichment in the clay fraction (<5 μm), apparently due to a stronger adsorption of ions by phyllosilicates.

Alluvial plain, 'infusion' loess

In the brickyard section at Abony the recent soil is salt-affected meadow chernozem, developed on 'infusion' loess. The grain size distribution and mineralogical composition of the latter are shown on diagrams of Figs (9, 10, and Table 1.

The grain size distribution of the recent soil found at Abony and also the distribution of the dominant mineral components (quartz, feldspars, muscovite, chlorite, montmorillonite etc.) by fractions and along the soil section may have developed during soil formation. This assumption is also supported by distribution of trace elements by fractions and by soil depth (some results of the analysis of samples taken every 10 cm were omitted).

The percentage of montmorillonite shows a consistent diminishing parallel to grain size growth and also a partial aggregation of this mineral into coarser particles. Quartz is dominant in each of the fractions (except for that of <5 μm) and its amount grows with the enlargement of grains. Calcite forms a double peak with minimum in the coarse silt fraction (20–80 μm), except for the carbonate accumulation horizon of the soil. These intrinsic changes can be deduced from the rearrangement of minerals along the soil profile. It should be emphasized that salt-affected meadow chernozem soils developed on infusion loess are periodically waterlogged.

Alluvial-infusion-loess formed by recent meadow chernozem

The qualitative distribution of minerals is similar to that in the Paks loess but kaolinite is missing and in the alkalic meadow clay the dominant mineral is montmorillonite. The fractions, however, show substantial differences as far as their quantitative distribution is concerned. The soil is dominated by the <5 μm fraction (55 m/m %), while the 20–45 μm fraction only accounts for 24 m/m% (Figs 9A, B, C, D). All this corresponds to a general observation that in the course of soil formation on loess, the amount of clay fraction tends to increase considerably. For the sake of comparison with the uppermost 10 cm layer of the soil, the distribution of minerals within the lowermost 90–100 cm layer is also presented. A striking feature is that, owing to a weaker intensity of soil formation, the ratio of the 45–80 μm fraction is on the increase in the lower horizon. In the <5 μm fraction montmorillonite, micas, chlorite, calcite and amorphous material are over-represented in comparison with the particle size average, thus indicating an authigenic origin of these minerals (Fig. 9B).

Concerning trace elements an opposite behavior of Pb and Zn is conspicuous as compared with the phenomena found in loess. Since this is a recent soil, lead

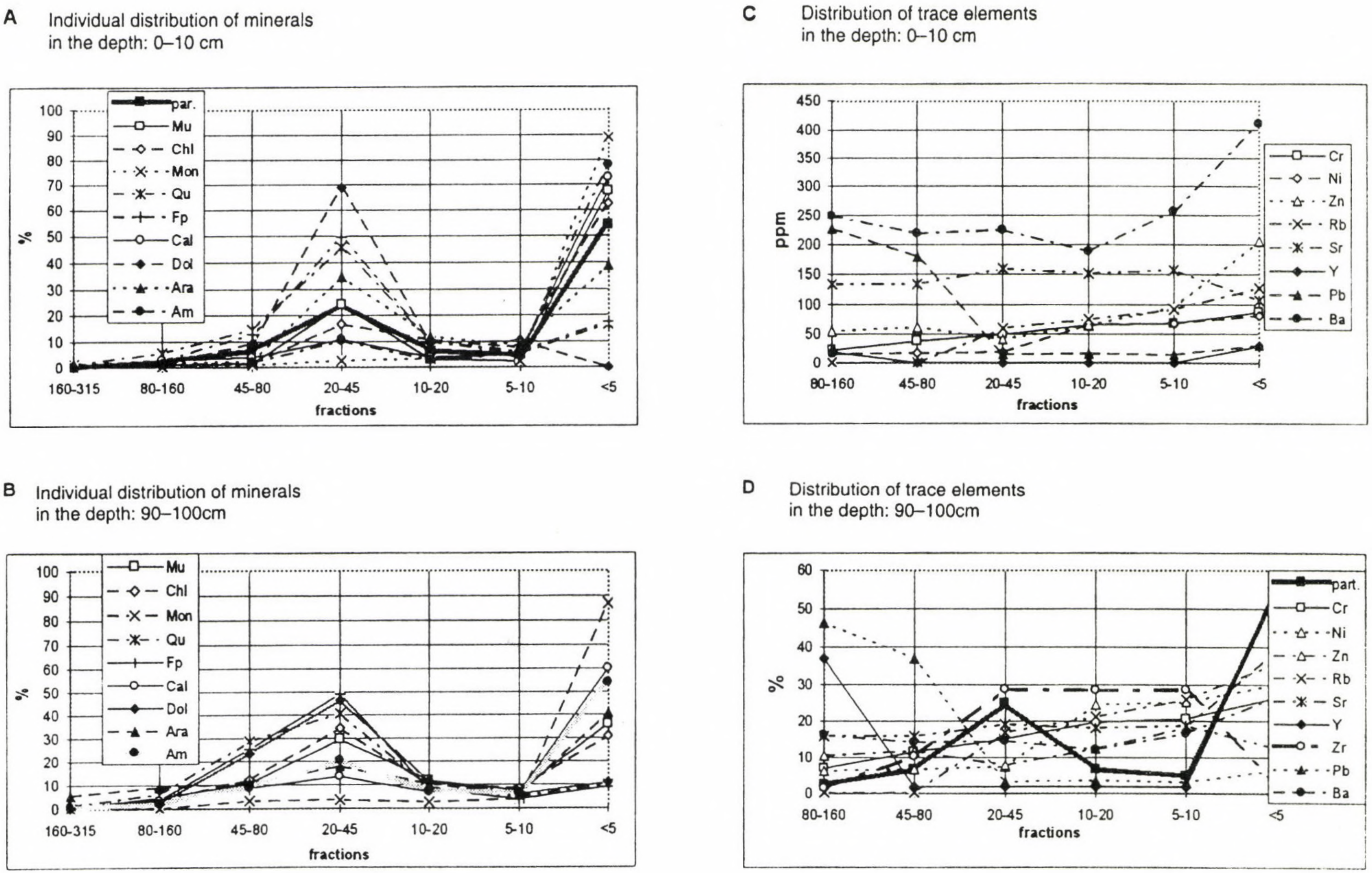

Fig. 9
Mineralogical analyses of 'infusion loess' and salt affected meadow chernozem developed on it. Abony brickyard.A. individual distribution of minerals in the soil, depth 0–10 cm. B. in loess 90–100 cm. C. distribution of trace elements (in ppm). D. individual distribution of trace elements, part = particle size

shows abnormally high values in the 45–160 μm fractions, then in finer grain-size fractions drops to those found in loess. Zn has a peak in the <5 μm fraction, i.e. opposite to Pb, but its amount also exceeds that occurring in loesses. Most of Zr falls between 5–45 μm, obviously due to its confinement to the mineral zircon. An overwhelming quantity of Ni and Cr is bound adsorptionally within the <5 μm fraction (Fig. 9C).

The striking difference concerning the distribution of trace elements between loess and loess soil is that while the distribution of trace elements in loess is closely linked to the two most frequent fractions, the picture is significantly different in soil (Fig. 9D).

Chernozem and sandy loess on a sandy alluvial fan

Of the three regions with sandy loess surface in Hungary a young (Quaternary) alluvial fan of the Tisza River and its tributaries has formed in the Nyírség region, the southern part of which is covered by a sandy loess blanket in a thickness of several meters. This type of surface with sandy loess formed on the underlying sand by the chernozem soil development NW of the Hungarian Great Plain at Újfehértó (Photo I). The grain size distribution and mineralogy of the uppermost 1.5 m horizon of soil are shown (Figs 10 and 11).

Affected by soil formation, coarse particles become finer toward the soil surface, with a simultaneous and considerable diminishment of minerals (quartz, feldspars, muscovite), while muscovite, chlorite and montmorillonite only show a slight decrease only in the <5 μm fraction.

In the Újfehértó soil profile (Fig. 11) the percentage *oxides of main elements* (Al_2O_3, Fe_2O_3, MgO, K_2O) show a slight growth with depth, or they remain unchanged. The content of Al_2O_3, Fe_2O_3, CaO, K_2O is much higher toward the finer grain size fractions, while SiO_2 and MgO dominate fractions coarser than 20 μm (Fig 12).

The individual distribution of *main elements* in the soil *by fractions represents* the rearrangement and transformation having taken place in soils (Fig. 10). For instance, SiO_2 closely follows changes in granulometry and percentage mineral distribution of quartz proper, increasing with depth. An impact is caused by soil formation and characterized by double maxima in most of the oxides of main elements (Al_2O_3, TiO_2, CaO, K_2O, and, partly in case of Fe_2O_3), while the peak of MgO and Na_2O occurs in the coarse fraction.

The percentage distribution of trace elements among fractions (Fig. 13C, D) shows increase with depth, similar to grain size.

It is noteworthy that in the case of chernozem soils, which developed on sandy loess and sand, *enrichment of trace elements* can be observed not only in the clay fraction (A) but also in coarse silt (E) and fine and medium sand (F = 80–160 μm) (Figs 13A–D), but in steppe soils formed on loess the main mineral components and trace elements are predominant in fraction D.

A major part of trace elements follows the distribution of particle size and main elements; on the other hand each of them (with the exception of Zr) is dissolved out of minerals and absorbed in ionic form in the <5 μm fraction.

The carbonate accumulation horizon of (CCa) has formed below 2.6 m, and the soil horizon cemented by lime with root remnants and hollows of burrowing animals can be observed at a depth of 1.6–2.0 m (Photo I). The concentration of trace elements in the chernozem at Újfehértó shows considerable differences from PAAS values only for Ba and Sr (there is significantly less of these elements measured compared with the standard). In contrast, the concentration of Zr slightly exceeds PAAS (Fig. 14).

Photo I
Chernozem, sandy loess and sand exposure at Újfehértó, NW Hungary (Photo M. Pécsi). 1. slightly sandy chernozem; 2. sandy loess; 3. sandy loess enriched by carbonats; 4. fluvial sand (sandy alluvial fan)

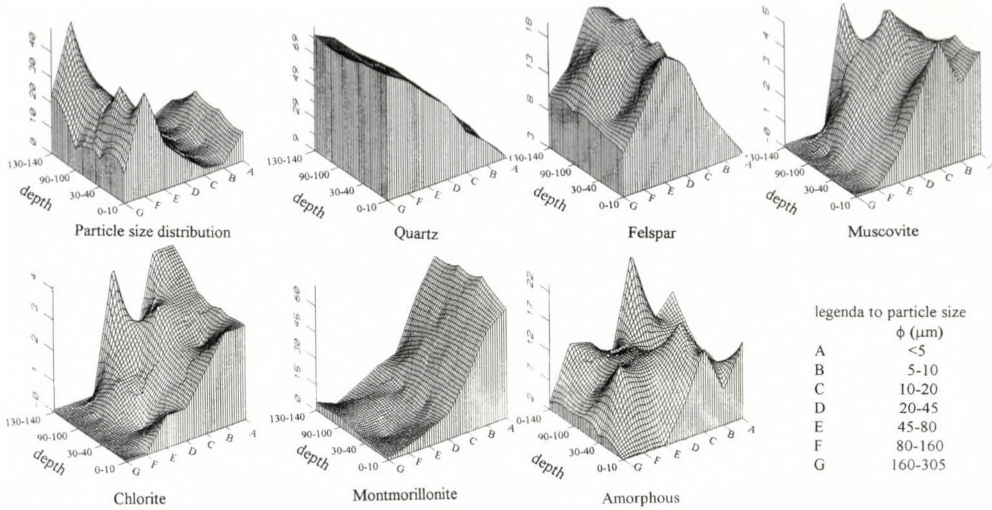

Fig. 10
Particle size distribution and mineralogical composition in a chernozem developed on sandy loess at Újfehértó (a sand quarry exposure located in northeastern Hungary)

Conclusion

The briefly outlined research methods make it possible to recognize that during pedogenesis processes of mineral formation, modification of minerals and particle size take place in loess, paleosols and recent soils, changing with soil depth. Main minerals predominant in loess and paleosols such as quartz, feldspars, micas, dolomite, and chlorite occur mainly in the coarse silt fraction (10–50 μm), while clay minerals show prevalence in the <5 μm fraction. The two groups make up a characteristic double maxima by particle size.

Results obtained using this new method of granulometric mineralogical and chemical analyses seems to support an earlier hypothesis (or perhaps to confirm it), that grain size distribution in loesses, paleosols and at least in recent steppe soils is related to loessification and soil formation processes rather than to some actions of exogenous accumulation.

Acknowledgement

This work was supported by FKFP 0606/ 1997 and the Hungarian Research Fund (OTKA) T026423, T025703. We are grateful to L. Merényi and J. Szauer for their active help in the present work.

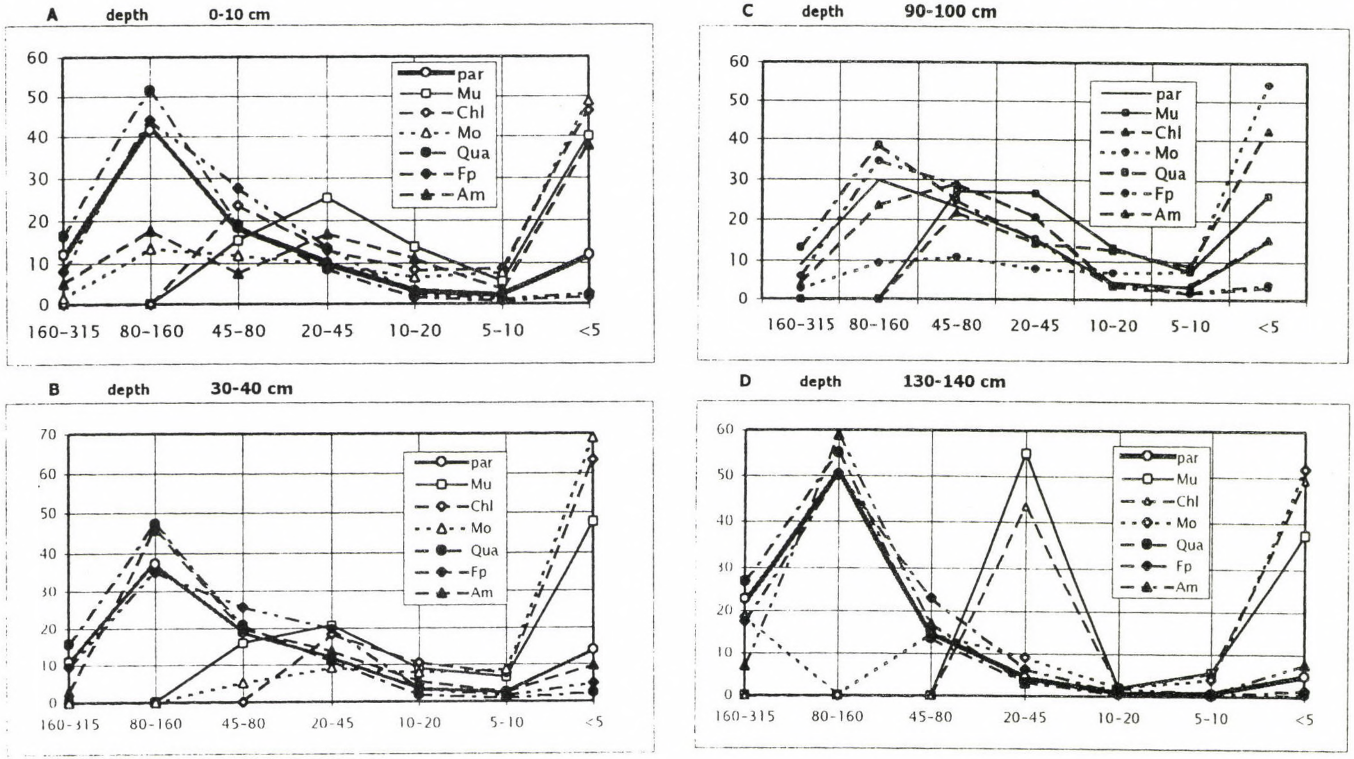

Fig. 11

Particle size and individual distribution of minerals in the soil profile at Újfehértó in the depths: A. 0–10, B. 30–40, C. 90–100 and D. 130–140 cm. X – fractions of particle sizes (μm), Y – m/m% of minerals, Par – particle, Mu – muscovite, Chl – chlorite, Mo – montmorillonite, Qua – quartzite, Fp – Feldspar, Am – amorphous

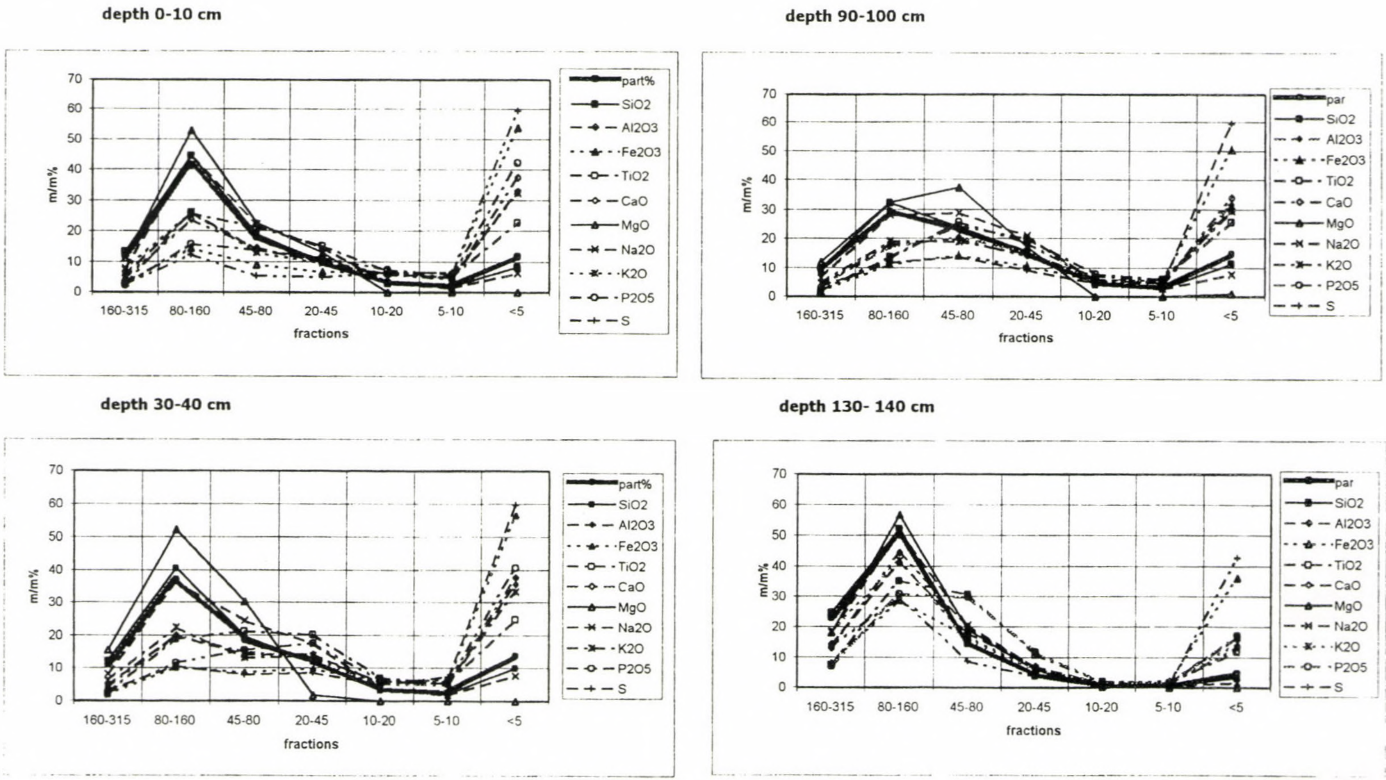

Fig. 12
Particle size and individual distribution of oxides in the soil profile at Újfehértó in depth: A. 0–10, B. 30–40, C. 90–100, D. 130–140 cm

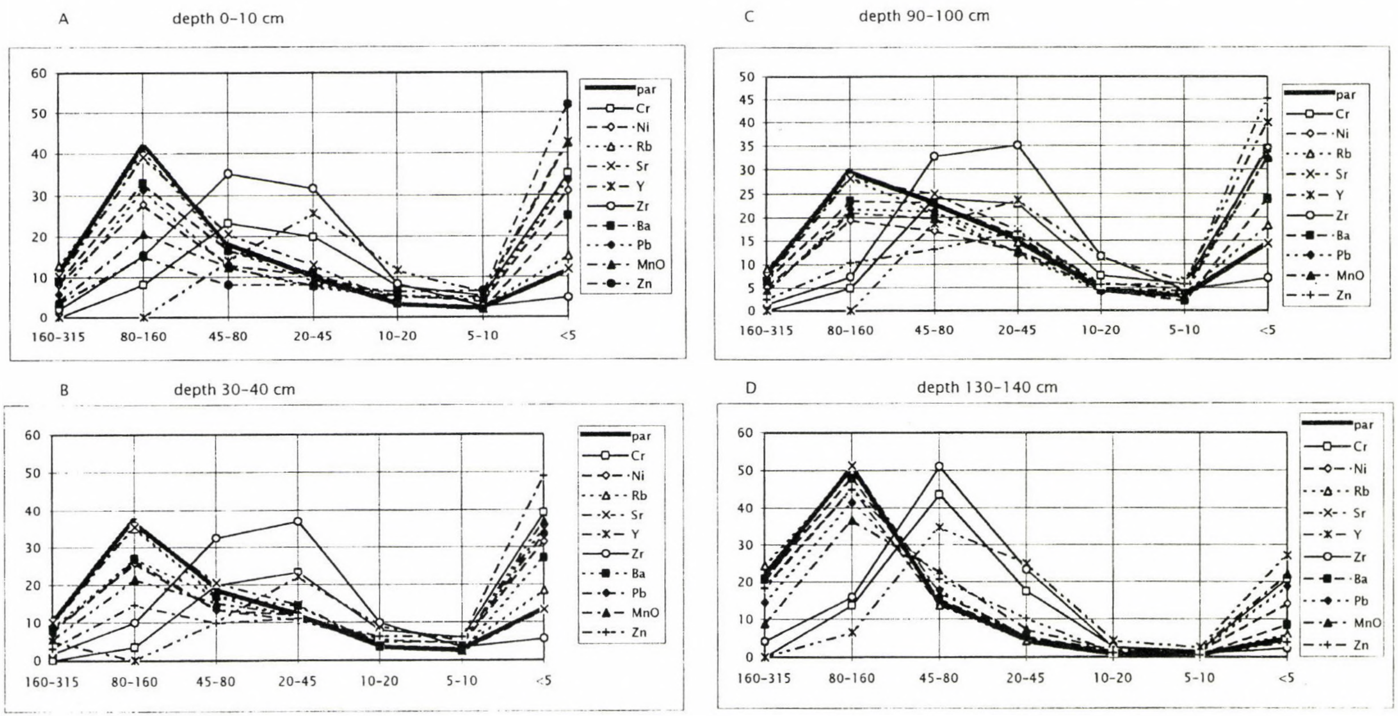

Fig. 13
Particle size and individual distribution of trace elements in soil profile at Újfehértó in the depth: A. 0–10, B. 30–40, C. 90–100, D. 130–140 cm. X – fractions of particle sizes (μm), Y – relative quantity of trace element (%)

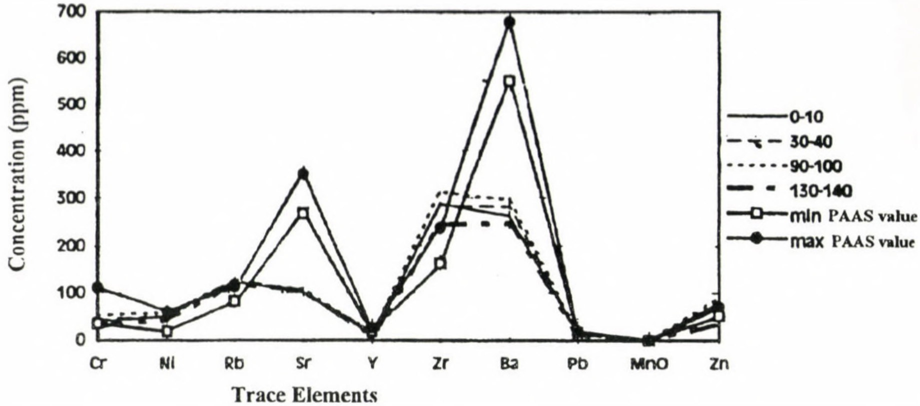

Fig. 14
Concentration of trace elements in the chernozem at Újfehértó between 0–140 cm, showing considerable differences from PAAS values only for Ba and Sr (there is significantly less of these elements measured compared with the standard). In contrast, the concentration of Zr slightly exceeds PAAS

References

Berg, L.S. 1916: The origin of loess. – Communications of the Russian Geographical Foundations, Vol. 11, pp. 579–646.

Berg, L.Sz. 1953: Az éghajlat és élet (Climate and life). – Akadémiai Kiadó, Budapest. 510 p.

Hahn, Gy. 1977: A magyarországi löszök litológiája, genetikája, geomorfológiai és kronológiai tagolása (Lithology, genesis, geomorphological and chronological subdivision of the loesses in Hungary). – Földrajzi Értesítő, 26/1, pp. 1–28.

Kriger, N.I. 1965: Lyoss, jego svojstva i svyaz s geograficheskoj sredoj (Loess, its characteristics and relation to the geographical environment). – Nauka, Moscow. 296 p.

Leonhard, K.C. von 1823/24: Charakteristik der Felsarten (Characteristics of rock types).– 3 Bde. Heidelberg (J. Engelmann). 772 p.

Mihályiné Lányi, I. 1953: A magyarországi löszváltozatok és egyéb hulló porképződmények osztályozása (Classification of loess varieties and other formations of airborne dust in Hungary). – In: Alföldi Kongresszus. 1952. szept. 26–28. Akadémiai Kiadó, Budapest. pp. 1–15.

Nemecz, E., Csikós-Hartyáni, Zs. 1995: Processes in soils and paleosols. A new method for the study of weathering. – GeoJournal, 36/2–3. pp. 139–142.

Nemecz, E., M. Pécsi, Zs. Hartyáni, T. Horváth 2000: The origin of the silt size quartz grains and minerals in loess. – Quaternary International 68–71, pp. 199–208.

Pécsi, M. 1967: A löszfeltárások üledékeinek genetikai osztályozása a Kárpát-medencében (Genetic classification of sediments in loess profiles in the Carpathian Basin). – Földrajzi Értesítő 16. pp. 1–9. (Summary in Russian: Geneticheskaja klassifikaciya otlozhenij lessovykh obnazhenij v Karpatskom bassejne.)

Pécsi, M. 1968: Loess. – In: Encyclopaedia of Geomorphology. New York, Reinhold Book Corporation. pp. 674–678.
Pécsi, M. 1982: The most typical loess profiles in Hungary. – In: Pécsi, M. (Ed.): Quaternary Studies in Hungary. Budapest, Geogr. Res. Inst. Hung. Acad. of Sci. (Theory–methodology–practice, 24). pp. 145–170.
Pécsi, M. 1987: International Loess Symposium in China, Xian, Shaanxi Province, October 5–16, 1985. – GeoJournal, 14/4, pp. 435–445.
Pécsi, M. 1991: Problems of loess chronology. – GeoJournal, 24/2. pp. 143–150.
Pécsi, M. 1993: Negyedkor és löszkutatás (Quaternary and Loess Research). – Akadémiai Kiadó, Budapest. (Theory–methodology–practice, 54) 375 p.
Pécsi, M. 1997: Lösz- és őstalajsorozatok és a negyedidőszaki ősföldrajzi változások kutatásainak elvi-módszertani kérdései (Theoretical and methodological problems of studies on loess-paleosol sequences and paleoclimatic changes). – Fülöp J. emlékkönyv. Akadémiai Kiadó, Budapest. pp. 263–279.
Pécsi, M., F. Heller, F. Schweitzer, J. Balogh, M. Balogh, J. Havas 1995: A new loess-paleosol sequence of Paks in Hungary. – In: Pécsi, M., F. Schweitzer (Ed.): Concept of loess, loess-paleosol stratigraphy. Budapest, Geogr. Researc Inst. Hung. Acad. of Sci. pp. 63–78.
Pécsi, M., G. Richter 1996: Löss. Herrkunft–Gliederung–Landschaften (Loess. Genesis – Subdivision – Landscapes). – Zeitschrift für Geomorphologie, N.F. Supplementband, 98, 391 p.
Pécsi, M., A.A. Velichko (Eds): 1995: Loess-Paleosol and Paleoclimatic Investigations: Principles, Methods and Criteria. GeoJournal, 36/2–3, 294 p.
Pyaskovskii, B.V. 1946: Loess as a Deep Soil Formation – Pochvovedenie, N 1. pp. 686–696.
von Richthofen, F. 1877–85: China: Ergebnisse eigner Reisen und darauf gegründeter Studien (China: Results of own travels and studies based thereupon) (5 vols). – Dietrich Reimer, Berlin.
Smalley, I.J. 1975 (Ed.): Loess Lithology and genesis. – Stroudsburg, Dowden, Hutchinson and Ross, 430 p.
Smalley, I.J. 1980: Loess. A partial bibliography. – Geo Abstracts Ltd., Norwich. 103 p.
Szilárd, J. 1983: Dunántúli és Duna–Tisza-közi löszfeltárások új szempontú litológiai értékelése és tipizálása (Lithological evaluation and typification of loess profiles in Transdanubia and on the Danube–Tisza Interfluve from a new perspective). – Földrajzi Értesítő, 32/1. pp. 109–167.
Szilárd, J. 1985: A new lithological evaluation and typology of loess exposures in Transdanubia and on the Danube–Tisza interfluve. – In: Pécsi, M. (Ed.): Loess and Quaternary. – Chinese and Hungarian case studies. Akadémiai Kiadó, Budapest. pp. 111–118.
Tutkowskii, P.A. 1900: M. Paul Tutkowskii on the origin of loess. Scottish Geographical Magazine 16.

Acta Geologica Hungarica, Vol. 43/4, pp. 405–429 (2000)

Origin and environmental significance of clay minerals in the Lower Jurassic formations of the Mecsek Mts, Hungary

Béla Raucsik, László Merényi
University of Veszprém
Department of Earth and Environmental Sciences

Lower Jurassic open marine sequences (consisting of an alternation of carbonate-rich and carbonate-poor layers of different lithologies) of the Mecsek Mountains (Tisia Terrane) record climatic and eustatic changes of the sedimentary basin and alterations during diagenesis. Mineral assemblages of 81 samples were determined by X-ray diffraction.

Sedimentation seems to be controlled, in part, by eustatic factors. Shelf progradation with intensive turbidite sedimentation and deposition of coarser-grained sediments are characteristic during the Late Pliensbachian in the Mecsek Mountains. Distribution of clay minerals could be closely related to eustatic driving forces.

The clay mineralogical composition of examined Lower Jurassic sedimentary rocks can be characterized by the dominance of kaolinite, illite, and illite/smectite mixed-layer minerals, which indicate humid climate and intensive weathering in the source area. The dominance of kaolinite and illite can be explained by 1) the relatively proximal depositional realm (Lower Pliensbachian grey calcareous marls, Pécsvárad); 2) redeposition of kaolinite and illite from nearshore areas by turbidity currents (Upper Pliensbachian turbidites, Kopasz Hill and Farkas Ravine); 3) more humid climate and intensive continental weathering relative to the former period, which could be connected to stabilization of upwelling and shelf anoxia (Lower Toarcian black shale, Réka Valley).

Mixed-layer illite/smectite minerals seem to be of pedogenic origin. They could have been carried into the basin from a relatively distant source area by eolian transport. Differences between types of mixed-layer illite/smectites can be explained by different heating levels during burial diagenesis. 70–75% smectite in mixed-layer structures with S=0 or S=1 type of interstratification indicates 50 (–100)°C temperature during diagenesis for samples of Farkas Ravine. The rest of the examined Pliensbachian samples seems to be heated at 130 (–150)°C, as suggested by their 30–40% expandability with S=1 or S=2 type of ordering. A 45% smectite content with S=1 type ordered structure of mixed-layer phases of Lower Toarcian black shale suggests about 100°C heating during burial.

Key words: Lower Jurassic, hemipelagic sequences, turbidites, clay mineralogy, diagenesis, Mecsek Mountains, paleoenvironment, X-ray diffraction, eustatic sea-level changes

Introduction

Jurassic formations are exposed in the eastern part of the Mecsek Mountains. These formations form a mostly marine sequence. In the Jurassic the area was part of Tethys and participated in its evolution. Differentiation of the carbonate shelf into half-graben structures and submarine plateaus started during the Late

Addresses: B. Raucsik, L. Merényi: H-8201 Veszprém, P. O. Box 158, Hungary
Received: 27 March, 2000

Triassic (Nagy 1969). At the end of the Ladinian, the sedimentation on the outer zones of the European shelf became siliciclastic due to more intensive continental erosion related to eustatic sea level lowstand and/or climatic changes. The earliest Lower Jurassic in the Mecsek Mountains is characterized by a continental and shallow marine siliciclastic sequence containing arkose and black coal (Gresten facies). In the upper part of Sinemurian this facies was converted into a hemipelagic/pelagic one with mixed siliciclastic-carbonate lithologies, in accordance with effects of eustatic sea level rise and intensive subsidence. Upsection, hemipelagic bioturbated marl and calcareous shale are intercalated by calcareous and mixed calcareous-siliciclastic turbidites. This sedimentation was the most prominent during the Pliensbachian. In the Early Toarcian (with decreasing abundance of turbidites) hemipelagic marl sedimentation became dominant again. This intensively bioturbated hemipelagic/pelagic marl facies is characteristic of the northern (European) margin of the Tethys (Allgäu facies) (Haas 1994).

The causes of the appearance of the very frequent turbidite beds within the Lower Jurassic hemipelagic marl succession are still unknown. Organic-rich horizons appear in many horizons within the Pliensbachian and Toarcian parts of the sequence. Dulai et al. (1992) applied the model of Jenkyns (1985) to explain deposition of the Lower Toarcian shale. Pliensbachian organic-rich lithologies of the Mecsek Mountains have not been compared to the better-known Toarcian black shale; causal relations to eustatic and climatic effects were not been investigated. Consequently, the Pliensbachian successions are good candidates for detailed analysis to examine the origin of event stratification.

Many authors applied clay mineral assemblage studies to determine the role of climatic and eustatic effects in the evolution of a given basin (Biscaye 1965; Chamley 1967; Chamley and Debrabant 1984; Pacey 1984; Singer 1984; Gygi and Persoz 1986; Hallam et al. 1991; Egger et al. 1997). Sections located near the villages of Pécsvárad, Óbánya and Mecseknádasd were selected for analysis to examine the origin of these Jurassic formations and its possible connection with the distribution of clay minerals (Figs 1 and 2).

Geologic setting

Stratigraphically, the studied profiles represent a Pliensbachian–Lower Toarcian succession belonging to three lithostratigraphic units: the Hosszúhetény Calcareous Marl Formation, the Mecseknádasd Sandstone Formation and the Óbánya Aleurolite Formation (Császár 1997). During fieldwork and collection of the samples biostratigraphically important macrofauna were found in two sequences (Kopasz Hill and Farkas Ravine; Mecseknádasd Sandstone Formation): the ammonites *Amaltheus* sp. indicate Late Pliensbachian age (Galácz 1999, pers. comm.). No index fossil were found in the Pécsvárad (abandoned quarry) and Réka Valley sections. However, paleontological data suggest an Early

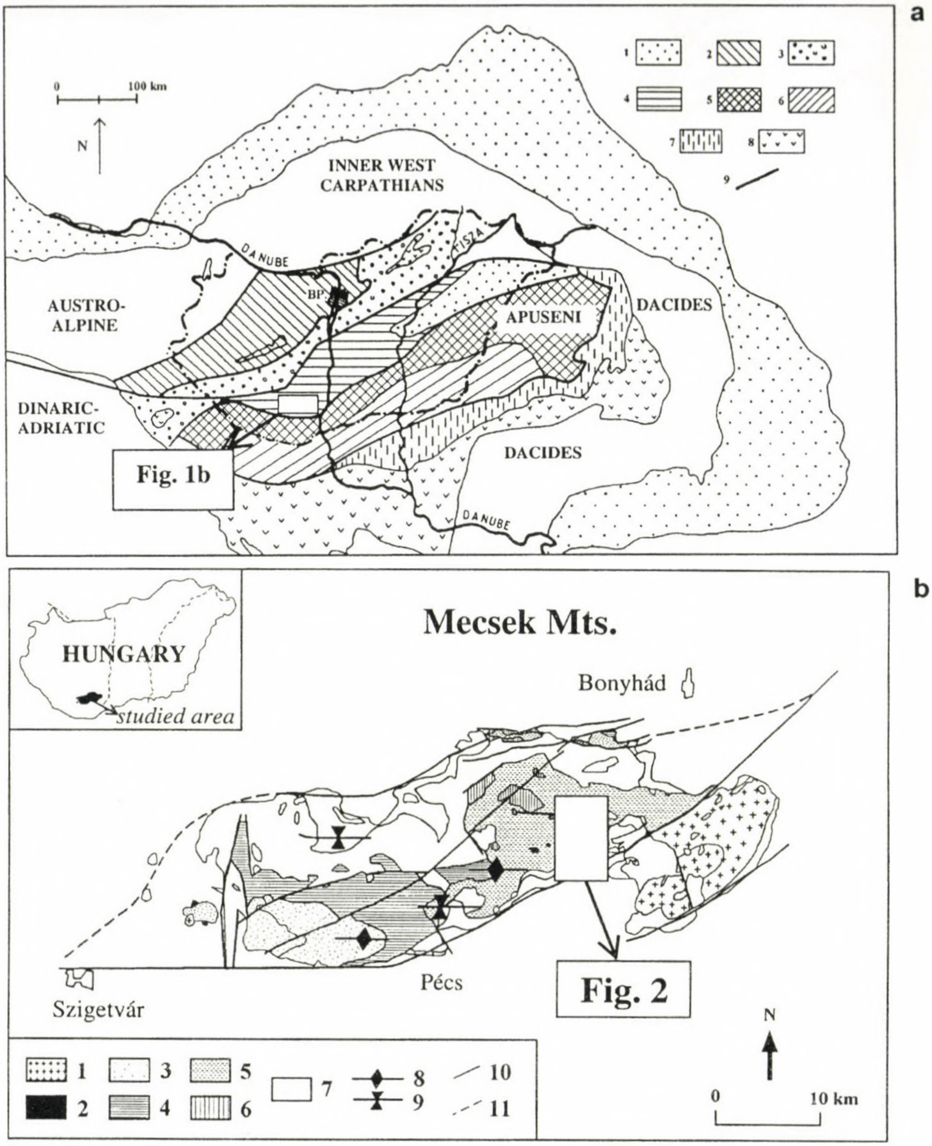

Fig. 1

a) The location of Mecsek Mountains in the Mesozoic tectonofacies units of Hungary, modified after Török (1997a). 1. Foredeep and flysch units; 2. Transdanubian and Drauzug units; 3. Bükk and Inner Dinaric unit; 4. Mecsek unit; 5. Villány-Bihor unit; 6. Papuk-Lower Codru unit; 7. N. Backa-Upper Codru, Persani unit; 8. Oceanic nappes (Vardar, Meliata, Mures and Olt); 9. Boundaries of tectonofacial units.

b) Geological map of the Mecsek Mountains, simplified after Török (1997b). 1. Carboniferous granite; 2. Permian rhyolite; 3. Permian; 4. Triassic; 5. Jurassic; 6. Cretaceous; 7. Post-Cretaceous; 8. anticline; 9. syncline; 10. fault; 11. fault supposed.

Pliensbachian age for the former outcrop (Hetényi 1966) and an Early Toarcian one for the latter (Dulai et al. 1992).

Three sections were studied (Fig. 2):

Pécsvárad (abandoned quarry);

Kopasz Hill, exposed to the west of Mecseknádasd. This section is divided into two subsections:

Kopasz Hill I, where a continuous section of Mecseknádasd Sandstone Formation was examined, and

Kopasz Hill II, located near the former outcrop. This subsection was not examined in detail, only 11 organic-rich shale samples were collected;

Farkas Ravine, exposed to the northwest of Óbánya.

Four black shale samples were collected to compare with their Pliensbachian counterparts from the classic outcrop of the Lower Toarcian Óbánya Aleurolite Formation in the Réka Valley.

Lithology

Pécsvárad (abandoned quarry)

According to Hetényi (1966) this sequence belongs to the Lower Pliensbachian part of the Hosszúhetény Calcareous Marl Formation. Fifteen samples were collected from the undisturbed and almost unweathered parts of the outcrop. The section consists of massive black and dark-grey calcareous marl and limestone with decimeter-scale bed thicknesses. The rocks show a very fine grain size indicated by conchoidal fractures. All the layers seem to contain some organic matter (indicated by intensive bituminous odour after being hit with a hammer) but diffuse spots (bioturbation?) on weathered rock surface are abundant. These rocks have 0.12–0.64 percent total organic carbon (TOC) content (Raucsik et al. 2000). Current-indicating sedimentary structures were not identified. Macrofaunal elements are represented by some belemnite rostra and small brachiopod shells.

Sedimentation was controlled by low-energy hemipelagic processes. The sediment was deposited below the storm wave base in a deep shelf margin, as indicated by micritic, microsparitic matrix and pervasive bioturbation. Bioclastic packstone texture is characteristic. The most abundant allochems are sponge spiculae, echinoid fragments, thin-shelled bivalves, brachiopod shells and foraminifera. Calcite-filled molds without any inner structure are very abundant. The latter microfauna elements seem to be recrystallized radiolarians and/or calcisphaerae. Several quartz and muscovite silt grains (up to 0.1 mm diameter) appear.

Kopasz Hill

This succession belongs to the Mecseknádasd Sandstone Formation. Rocks consisting of marly lithologies with turbidite intercalations are exposed by a deep ravine. The turbidites are mostly mixed carbonate-siliciclastic rock types with 20–60 centimeter bed thickness showing atypical Bouma-sequences. Normal and cross lamination, gradation, sharp base of layers are very common. Channel structures and bottom marks are rarely found. Silicification is characteristic, with a few layers almost completely silicified. The most frequent biogenic components

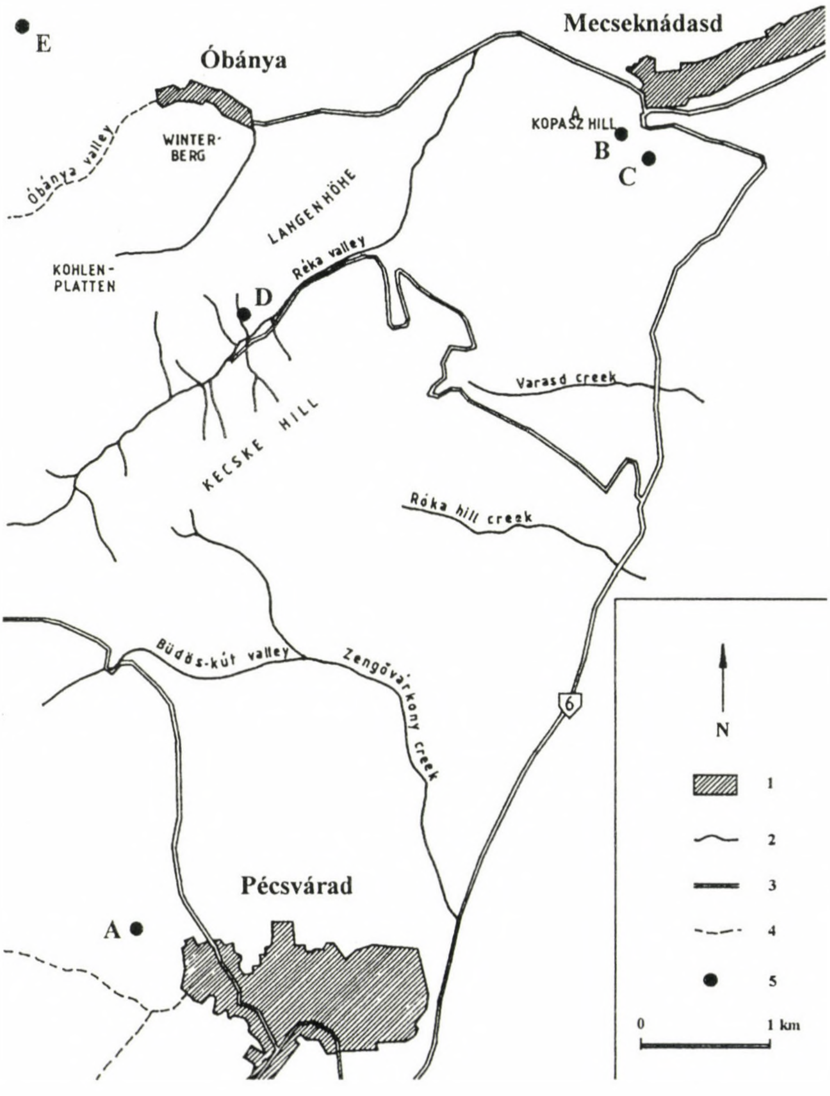

Fig. 2
Location map of the examined sections. 1. villages; 2. creek; 3. road; 4. path; 5. sampled outcrops. A: Pécsvárad, abandoned quarry, B: Kopasz Hill II; C: Kopasz Hill I; D: Réka Valley; E: Farkas Ravine

of turbidites are echinoderms, sponge spiculae and brachiopod fragments. Nodosariid-type foraminifera and ostracods were found rarely. Among the terrigenous components silt- and sand-sized quartz, feldspar, muscovite and a few (metamorphic and recrystallized volcanic?) rock fragments (up to 1 mm diameter) are characteristic.

In some cases, above graded turbidite layers, 20–30 centimeter thick, grey to brownish grey, or dark-grey, homogeneous, massive, fine-grained marl beds appear. A part of this type of marl shows slump structures on polished surface. Another part is laminated in thin section. Bioturbation or gradation does not appear. Shelf-derived elements (parallel-oriented sponge spiculae, small echinoid fragments) with silt-sized, unrounded quartz and muscovite grains, are the most prominent components. Some of the massive dark marl beds have up to 1% TOC. This sediment can be interpreted as a fine-grained turbidite deposited from a very low-density current, or from the fine-grained tail of a normal-density turbidite (Piper E1 division; Heath and Mullins 1984; Piper and Stow 1991).

The 'normal' background sedimentation is represented by some decimeter-thick marl beds, which can be easily split into 2–3 centimeter-thick parts parallel to the layering. In many cases, they are laminated, with dark grey color. Generally, TOC values fluctuate about 0.1–0.2% but some samples from the sections Kopasz Hill I and II have 0.3 to 1% of total organic matter. Other marly background sediment layers (whose TOC contents are less than 0.1%) show distinct bioturbation. In thin section, spotted marl beds show bioclastic wackestone texture with abundant micritic matrix. The dominant faunal elements are pelagic: recrystallized radiolarians and filaments. Some sponge spiculae and echinoderm fragments appear as well. Terrigenous quartz grains (0.01– 0.05 mm in diameter) are abundant.

Farkas Ravine

This sequence consists of the same rock types as the Kopasz Hill section and also belongs to the Mecseknádasd Sandstone Formation. There are differences between the two successions: turbidites are more frequent in Kopasz Hill than in Farkas Ravine. Consequently, the hemipelagic marl interbeds are thinner in Kopasz Hill. Bioturbation of the massive hemipelagic spotted marl and calcareous marl beds is more distinct in the Farkas Ravine section.

Réka Valley

Early Toarcian black shale exposed in this outcrop belongs to the Óbánya Aleurolite Formation. Their macroscopic and microfacies characterization is presented according to Dulai et al. (1992). The color of the shale is black or dark brown. Average thickness of laminae is 3 to 4 mm, but at places it disintegrates into very fine (0.2–0.3 mm thin) laminae. Their surface is usually flat. On the fracture surfaces, many mica flakes can be observed. In thin section, the texture shows preferred orientation parallel to the laminae. The main terrigenous constituents are angular quartz and muscovite grains. The contact between the pelitic and sandy laminae is always sharp.

The black shale beds were intercalated by hard, brittle turbiditic sandstone layers. The thickness of these turbiditic beds varies between 1 and 40 centimeters. The size of the grains is between 0.2 and 0.5 mm. Graded bedding is apparent in thin section. The grains are made of angular quartz and silicified echinoderm fragments.

In essence, the studied profiles represent deep shelf margin to intra -shelf basin facies. Normal hemipelagic sedimentation characterized by settling of grains through the water-column was interrupted by turbidite events. Basin floor oxygenation seems to have been variable.

Methods

The X-ray measurements were carried out at the Department of Earth and Environmental Sciences of the University of Veszprém. The clay fraction under 2 mm was separated by sedimentation after dissolution of $CaCO_3$ by 10% acetic acid and ultrasonic deflocculation. X-ray diffraction analysis of clay minerals was performed on oriented specimens made by the smear-on-glass method. Two X-ray diagrams were performed on each sample of clay fraction: one under natural conditions, one after saturation with ethylene glycol. Calcite-free bulk samples

Table 1
Instrumental parameters of XRD measurements

Type:	Philips PW 1710
Generator:	PW 1730/10
Goniometer:	PW 1050/70
X-ray source:	CuK_α
Tube current:	40 mA
Tube voltage:	50 kV
Slit system:	1°-1°
Monochromator:	graphite single crystal
Velocity of goniometer:	0.035°/s
Detector:	proportional counter

were measured on disoriented specimens. Table 1 shows instrumental parameters of the measurements.

Clay minerals were identified primarily by the position of their basal reflections. Specific values were used for characterization of clay mineral types. For estimation of values of illite/smectite ratio in mixed-layer structures and for estimating the ordering of interstratification the standard methods of Srodon (1980, 1984) and Watanabe (1981) were used. The relative abundance of clay minerals was determined by the peak area ratio of the 001/001 reflection of mixed-layer illite/smectite and the 001 reflection of illite and kaolinite after glycolation. Peak areas of mixed-layer illite/smectites were corrected by factors published by Rischák and Viczián (1974). Mixed-layer phases close to pure illite were corrected by multiplying by a factor 2, while those close to smectite were multiplied by a factor 0.5. Peak area of discrete illite was corrected in a similar manner by a factor of 2. Kaolinite has factor of 1.

Results

The mineralogical composition of the calcite-free samples is dominated by quartz, various types of phyllosilicates and titanium dioxides. Feldspars (K-feldspar, in some cases K-feldspar and albite) occur mainly in the turbidites and in a few hemipelagic background sediment samples. Amongst the iron-rich mineral species pyrite and goethite were found. Pyrite appears in background sediments but goethite can be found in all the examined rock types.

According to thin section analyses, quartz, feldspars and muscovite are of terrigenous origin. Some diagenetic silica (mainly in coarse-grained rock types such as turbidites) contributes to the total mass of quartz. Rutile seems to be a terrigenous heavy mineral component. Főzy et al. (1985) have published the same observation on the Mecseknádasd Sandstone Formation. Weathering of Ti-bearing silicates and ilmenite, subsequent transportation and reprecipitation of Ti within a sedimentary basin may cause the appearance of anatase (Frederickson 1948). Pyrite is probably diagenetic. Goethite generally occurs in the examined samples. The most reasonable cause of its existence is that it is a weathering product of other iron minerals (e.g. pyrite). A terrigenous origin of the goethite in the examined samples does not seem to be probable. In further research other methods (for example electron microscopy) are necessary to solve this problem.

Semi-quantitative clay mineralogical compositions of the <2 mm fraction are shown in Tables 2–4. Figs 3, 4 and 5 show typical XRD patterns of the <2 mm fraction of the examined rock types. Each diagram in Figs 3, 4 and 5 contains two diffraction patterns: air-dried samples are indicated by 'a', ethylene glycol-treated samples are indicated by 'b'.

Muscovite, illite, kaolinite and mixed-layer illite/smectites of various degree of expandability are always the dominant clay minerals. Illite is generally of good crystallinity (values of the Kübler index determined on ethylene glycol-treated samples vary between 0.3–0.6°2Θ). Intermediate stages of the transition from smectite to illite clearly appear on the XRD diagrams of most samples where illite/smectite mixed-layers with various proportions of both component layers can be observed.

Table 2
Semi-quantitative clay mineralogical composition of the <2 μm fraction of redeposited sediments

Number of samples	Rock types	Kaolinite (~%)	Muscovite± illite (~%)	Illite/smectite (~%)
KHD-2	mix. turb. s.	-	98	tr
KHD-6a	mix. turb. s.	34	44	22
KHD-6b	mix. turb. s.	46	45	9
KHD-15	mix. turb. s.	15	83	tr
KHD-23	mix. turb. s.	19	79	tr
KHD-25	mix. turb. s.	28	63	9
KHD-48a	mix. turb. s.	38	58	4
KHD-48b	mix. turb. s.	52	37	11
KHD-50	mix. turb. s.	55	43	tr
KHD-62	mix. turb. s.	40	56	4
KHD-63a	mix. turb. s.	59	39	tr
KHD-83a	mix. turb. s.	27	62	11
KHD-88	mix. turb. s.	31	47	tr
KHD-89	mix. turb. s.	14	84	tr
average$_{KHD}$		*35*	*60*	*<9*
FA-2a	mix. turb. s.	-	82	18
FA-2c	mix. turb. s.	-	42	58
FA-4b	mix. turb. s.	11	53	36
FA-6b	mix. turb. s.	12	55	33
FA-57*	mix. turb. s.	-	100	-
FA-68	mix. turb. s.	16	48	36
average$_{FA}$		*<13*	*63*	*36*
average$_{MTS}$		***31***	***61***	***<21***
KHD-33	mud turb.	30	68	tr
KHD-49	mud turb.	12	86	tr
KHD-53	mud turb.	16	82	tr
KHD-66a	mud turb.	12	86	tr
average$_{MT}$		***17***	***81***	***tr***

*: siliciclastic turbidite; mix. turb. s.: mixed turbiditic sandstone (MTS); mud turb.: mud turbidite (MT); tr: trace amount. Abbreviations of the outcrops: KHD: Kopasz Hill I (Upper Pliensbachian Mecseknádasd Sandstone Formation); FA: Farkas Ravine (Upper Pliensbachian Mecseknádasd Sandstone Formation)

Tables 5–7 show the results of measurements on mixed-layer structures. The $\Delta 2\Theta_1$ values are expressed by Watanabe's (1981) terminology. However, in case of many samples their $\Delta 2\Theta_1$ values cannot be precisely determined and fixed on Watanabe's diagram, due to the low amount of the illite/smectite mixed-layer phases. For the determination of illite content and ordering, another standard

Table 3
Semi-quantitative clay mineralogical composition of the <2 μm fraction of background sediments

Number of samples	Rock types	Kaolinite (~%)	Muscovite± illite (~%)	Illite-smectite (~%)
KHD-12	spotted marl	5	93	tr
KHD-34	spotted marl	10	88	tr
KHD-54	spotted marl	14	84	tr
KHD-111	spotted marl	-	98	tr
KHD-120	spotted marl	7	91	tr
average$_{KHD}$		*9*	*91*	*tr*
FA-3b	spotted marl	19	47	34
FA-8	spotted marl	17	65	18
FA-37	spotted marl	23	63	14
FA-49	spotted marl	19	62	19
FA-59	spotted marl	23	53	24
FA-62	spotted marl	16	54	30
FA-66	spotted marl	19	67	14
average$_{FA}$		*19*	*59*	*22*
average$_{SM}$		***16***	***72***	***<22***
KHD-5	calc. shale	tr	98	tr
KHD-24	calc. shale	18	80	tr
KHD-35	calc. shale	9	89	tr
KHD-66b	calc. shale	16	82	tr
average$_{KHD}$		*<14*	*87*	*tr*
FA-7	calc. shale	36	46	18
FA-34	calc. shale	19	54	37
FA-36	calc. shale	20	64	16
FA-39	calc. shale	18	55	27
FA-42	calc. shale	12	56	32
FA-69	calc. shale	27	58	15
FA-71	calc. shale	12	58	30
FA-74	calc. shale	tr	42	58
average$_{FA}$		*<21*	*54*	*29*
average$_{CS}$		***<19***	***79***	***<29***

SM: spotted marl; calc. shale: calcareous shale (CS); tr: trace amount.
Abbreviations of the outcrops: KHD: Kopasz Hill I (Upper Pliensbachian Mecseknádasd Sandstone Formation); FA: Farkas Ravine (Upper Pliensbachian Mecseknádasd Sandstone Formation)

method published by Srodon (1980, 1984) was applied. If a reflection occurred between 5.3° and 8.7°2Θ in the diffraction pattern of an ethylene glycol-solvated illite/smectite, the examined illite/smectite was considered as an interstratification ordered to some degree (Srodon 1980). Many samples do not show precisely detectable peaks after glycol-saturation because of low amount of mixed-layer

Table 4
Semi-quantitative clay mineralogical composition of the <2 μm fraction of bituminous rock types.

Number of samples	Rock types	Kaolinite (~%)	Muscovite± illite (~%)	Illite-smectite (~%)
PV-1	d.grey c.marl	33	65	tr
PV-2	d.grey c.marl	28	70	tr
PV-3	d.grey c.marl	32	66	tr
PV-4	d.grey c.marl	24	74	tr
PV-5	d.grey c.marl	25	73	tr
PV-6	d.grey c.marl	36	62	tr
PV-7	d.grey c.marl	45	53	tr
PV-8	d.grey c.marl	37	61	tr
PV-9	d.grey c.marl	39	59	tr
PV-10	d.grey c.marl	27	71	tr
PV-11	d.grey c.marl	47	51	tr
PV-12	d.grey c.marl	39	59	tr
PV-13	d.grey c.marl	33	65	tr
PV-14	d.grey c.marl	32	66	tr
PV-15	d.grey c.marl	41	57	tr
average$_{PV}$		*35*	*63*	*tr*
KHD-10	black shale	-	98	tr
KHD-11	black shale	13	85	tr
KHD-26	black shale	18	80	tr
average$_{KH\,I}$		*15*	*88*	*tr*
FA-3a	black shale	28	49	23
average$_{FA}$		*28*	*49*	*23*
K-1	black shale	-	98	tr
K-2	black shale	13	85	tr
K-3	black shale	9	89	tr
K-4	black shale	4	94	tr
K-5	black shale	6	92	tr
K-6	black shale	7	91	tr
K-7	black shale	11	87	tr
K-8	black shale	8	90	tr
K-9	black shale	-	98	tr
K-10	black shale	-	98	tr
K-11	black shale	6	92	tr
average$_{KH\,II}$		*8*	*89*	*tr*
R-1	black shale	39	59	tr
R-2	black shale	41	57	tr
R-3	black shale	56	42	tr
R-4	black shale	57	41	tr
average$_{RV}$		*48*	*50*	*tr*
average$_{BIT}$		***28***	***73***	***tr***

d.grey c.marl: dark grey calcareous marl; BIT: bituminous rocks; tr: trace amount.
Abbreviations of the outcrops: PV: Pécsvárad (Lower Pliensbachian Hosszúhetény Calcareous Marl Formation); KHD and KH I: Kopasz Hill I (Upper Pliensbachian Mecseknádasd Sandstone Formation); FA: Farkas Ravine (Upper Pliensbachian Mecseknádasd Sandstone Formation); K: Kopasz Hill II (Upper Pliensbachian Mecseknádasd Sandstone Formation); R and RV: Réka Valley (Lower Toarcian Óbánya Aleurolite Formation)

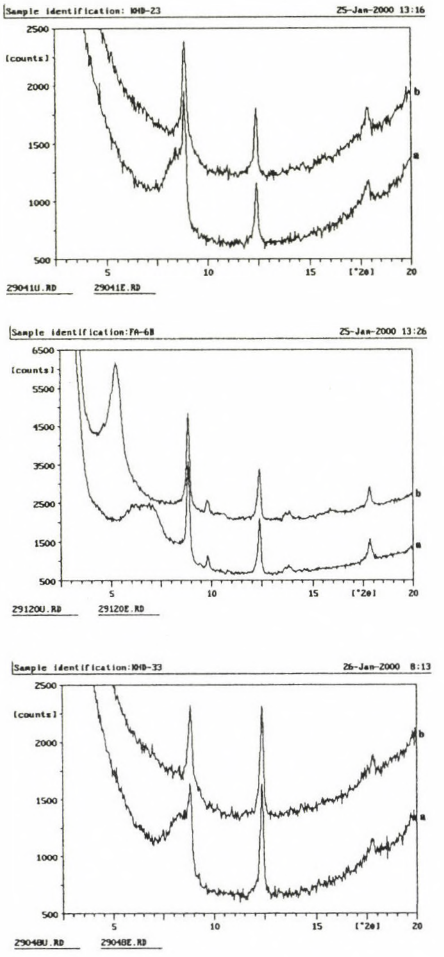

Fig. 3
Typical XRD patterns of the <2 μm fraction of the redeposited sediments. A: mixed turbidite sandstone (sample KHD-23, section Kopasz Hill I); B: mixed turbidite sandstone (sample FA-6B, section Farkas Ravine); C: mud turbidite (sample KHD-33, section Kopasz Hill I)

phases. Degree of ordering of these samples cannot be determined, but the high amount of illite component was suggested by peak position before glycolation: there are peaks very close to the illite position. Positions of these peaks are collected in Tables 5–7. Expandability indexed by '1' and the degree of ordering are calculated by peak position between 5–8.2°2Θ according to Srodon (1984). Expandability indexed by '2' is calculated after $\Delta 2\Theta_1$ values (sensu Watanabe, 1981). Degree of ordering is expressed by using 'Reichweite' values ('S').

Mixed-layer illite/smectites of the samples of Farkas Ravine differ from other examined Pliensbachian illite /smectite minerals in expandability and ordering. About 70–75% expandability was detected with S=0 or S=1 type ordering in the case of the samples of Farkas Ravine, both in sandstones and marls. Samples from other Pliensbachian outcrops are characterized by a lower degree of expandability (30–40%) and S=1 or S=2 type interstratification. The four measured Lower Toarcian black shale samples show about 45% smectite in expandable phase with S=1 type ordering (see Tables 5–7).

An obvious difference can be found in the relative abundance of kaolinite (see Tables 2–4): 1. the Lower Toarcian Réka Valley samples have significantly the highest amounts of kaolinite (average of 48 %); 2. amongst the Pliensbachian samples of mixed turbidite sandstones and the Lower Pliensbachian dark-grey calcareous marl samples of Pécsvárad, there is higher amount of this clay mineral

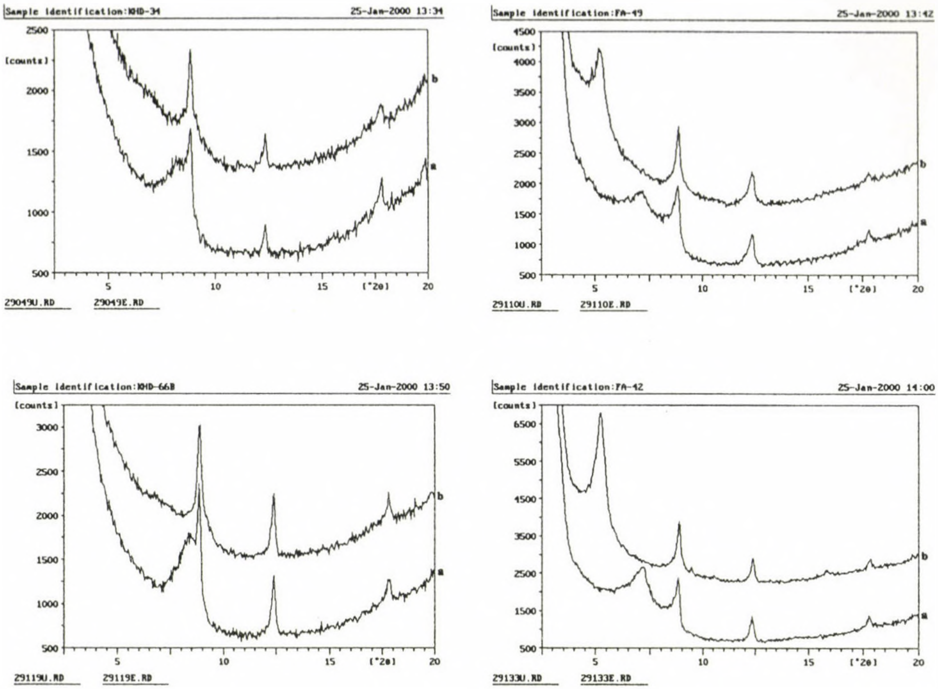

Fig. 4
Typical XRD patterns of the <2 μm fraction of the background sediments. A: spotted marl (sample KHD-34, section Kopasz Hill I); B: spotted marl (sample FA-49, section Farkas Ravine); C: calcareous shale (sample KHD-66B, section Kopasz Hill I); D: calcareous shale (sample FA-42, section Farkas Ravine)

(averages of 31% and 35%, respectively) than in the background sediments of the Mecseknádasd Sandstone Formation.

Discussion

Clay minerals as indicators of environment and diagenesis

In most regions of the world ocean, clay detrital assemblages reflect the combined influences of land petrography and continental climate (Biscaye 1965). The common clay minerals, as environmental indicators requiring a discussion here, are kaolinite, mixed-layer illite/smectite and illite.

In recent deep-sea sediments, kaolinite tends to increase in relative abundance in regions of tropical continental weathering (Biscaye 1965). The strong increase

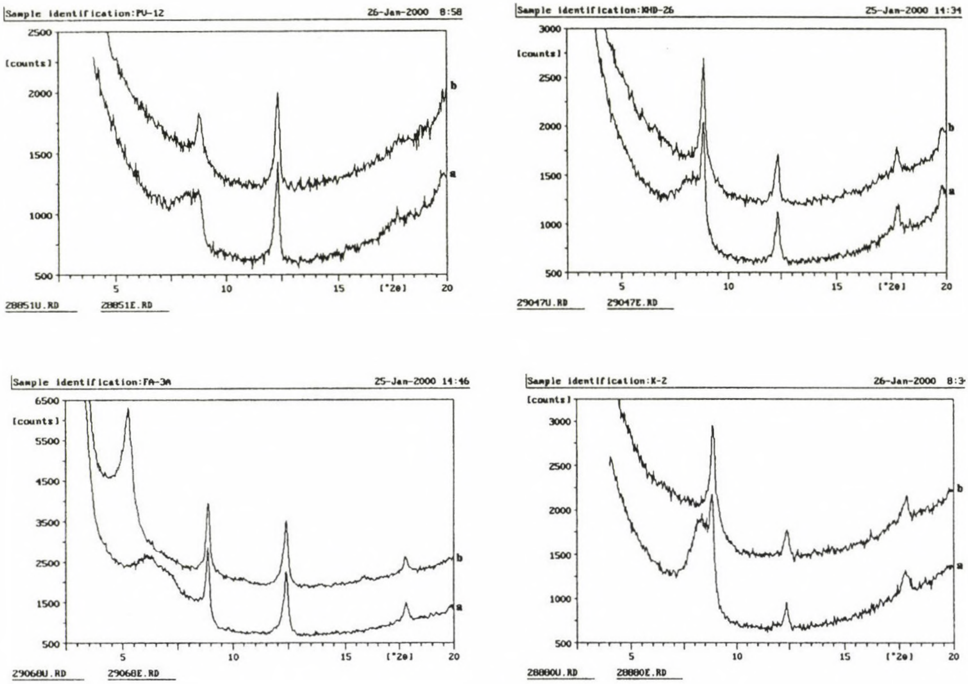

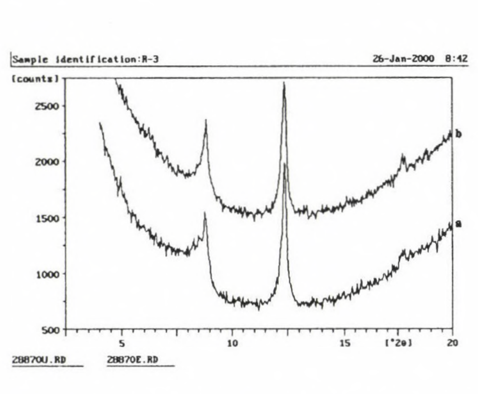

Fig. 5
Typical XRD patterns of the <2 μm fraction of the organic-rich sediments. A: grey calcareous marl (sample PV-12, section Pécsvárad, abandoned quarry); B: black shale (sample KHD-26, section Kopasz Hill I); C: black shale (sample FA-3A, section Farkas Ravine); D: black shale (sample K-2, section Kopasz Hill II); E: black shale (sample R-3, section Réka Valley)

in kaolinite (together with goethite, gibbsite) is thought to reflect intensive weathering and soil production on the source area (Chamley 1989).

Mixed-layer illite/smectite minerals have long been believed to be formed in diagenetic environments through the transformation of smectite (Hower 1981). A detrital origin of smectitic minerals has been proposed for many locations. Numerous mineralogical and chemical studies of smectitic minerals suggested that smectites from most Mesozoic sediments were mainly soil-derived minerals (Chamley 1989). Smectite and illite/smectite mixed layers form recently under a variety of climates; the most important type appears to be the one in which a pronounced dry season alternates with a less pronounced wet season (Singer 1984). It is noteworthy that an eolian origin of smectitic minerals has been suggested for Jurassic and Cretaceous sediments (Lever and McCave 1983; Hallam 1984) in which calculation of mass accumulation rates suggested that smectitic minerals were deposited almost entirely from the background concentration of tropospheric dust (Kimblin 1992). Evidence does exist that mixed-layer illite/smectites may form in a weathering environment through the leaching and degradation of a precursor illite (Chamley 1967, 1989). Robinson and Wright (1987) have suggested that some mixed-layer illite/smectite could be produced from smectite during pedogenesis. It should be noted that smectite may be volcanogenic in origin, being derived directly from the weathering and/or halmyrolysis of volcanic rocks. In this case, however, distinctive accessory minerals should occur, such as biotite, sphene, cristobalite, zeolites and, rarely, relict glass shards (Pacey 1984; Çelik et al. 1999). The main question which arises from this hypothesis is that volcanic debris is very rarely recognized in common sediments and would have to have been supplied in huge quantities to justify the very large amount of smectite identified (Chamley 1989; Deconinck and Chamley 1995). Neoformation of smectites in the host sediment during periods of low sedimentation rate is a theory supported by many authors (Jeans 1968, 1978; Steinberg et al. 1987; Thiry and Jacquin 1993).

The occurrence of discrete illite in sediments probably has no particular climatic significance (Hallam et al. 1991), but Singer (1984, 1988) claims that illite exhibiting high crystallinity signifies formation in either cold or dry conditions with minimum hydrolyzation.

Clay mineral segregation by differential settling is a common phenomenon on certain continental margins characterized by a simple influx from river to ocean. As early diagenesis does not seem (from available data) to account for such a strong differentiation, one may expect that clay sorting was reinforced both by a hydrolyzing climate providing abundant kaolinite and smectite to the sea, and by sudden variations of turbulence between shelf and basin environments. The mechanisms responsible for clay changes recorded on continental margins appear to be dominated by grain-size sorting. The influence of direct and rapid subvertical sinking of clay aggregates on sedimentation should not be overestimated, since horizontal transport and resuspension of individual particles and aggregates occur widely in the ocean, under the action of surface, deep and bottom currents (Chamley 1989). Kaolinite tends to increase in abundance in nearshore facies, probably reflecting its coarse-grained nature and its strong tendency to flocculate compared to most other clays. Clay sorting usually determines the farther transportation of smectite and fibrous clays relative to most other clay species. There is evidence that abundance of smectitic minerals in marine sediments depends partly on eustatic sea-level changes. Landmass surface is reduced because of the highstand of the sea level. This could

Table 5
Parameters of mixed-layer illite/smectite minerals of the <2 μm fraction of redeposited sediments

Number of samples	Rock types	Position of 001/001 before glyc. (°2Θ)	Positions after glyc. (°2Θ)	$\Delta 2\Theta_1$	Expand.$_1$ (%)	Expand.$_2$ (%)	"S" value
KHD-2	mix. turb. s.	-	-	-	-	-	-
KHD-6a	mix. turb. s.	~7.7-8.6	-	-	-	-	-
KHD-6b	mix. turb. s.	~8.1-8.3	-	-	-	-	-
KHD-15	mix. turb. s.	~8.6	~6.9, 9.2	2.3	20-40	20-30	1 or 2
KHD-23	mix. turb. s.	~8.5	~6.6, 9.2	2.6	25-50	28-38	1 or 2
KHD-25	mix. turb. s.	~8.2-8.4	-	-	-	-	-
KHD-48a	mix. turb. s.	~8.4-8.6	~6.9, 9.3	2.4	20-40	23-33	1 or 2
KHD-48b	mix. turb. s.	~8.1-8.5	-	-	-	-	-
KHD-50	mix. turb. s.	-	-	-	-	-	-
KHD-62	mix. turb. s.	-	-	-	-	-	-
KHD-63a	mix. turb. s.	~7.7-8.5	-	-	-	-	-
KHD-83a	mix. turb. s.	~7.7-8.2	-	-	-	-	-
KHD-88	mix. turb. s.	~8.2-8.5	~6.7, 9.2	2.5	25-50	25-35	1 or 2
KHD-89	mix. turb. s.	~8.3-8.5	~6.5, 9.2	2.7	25-50	30-39	1 or 2
average$_{KHD}$		***~8.1-8.5***	***~6.7, 9.2***	***2.5***	***25-50***	***25-35***	***1 or 2***
FA-2a	mix. turb. s.	~6.9-7.6	-	-	-	-	-
FA-2c	mix. turb. s.	~5.9-7.2	~5.3, 9.8	4.5	>40	75	0 or 1
FA-4b	mix. turb. s.	~7.0-7.4	~5.3, 9.7	4.4	>40	73	0 or 1
FA-6b	mix. turb. s.	~6.0-7.1	~5.3, 9.8	4.5	>40	75	0 or 1
FA-57*	mix. turb. s.	-	-	-	-	-	-
FA-68	mix. turb. s.	~5.8-6.0	~5.4, 9.8	4.4	>40	73	0 or 1
average$_{FA}$		***~6.3-7.0***	***~5.3-9.8***	***4.5***	***>40***	***74***	***0 or 1***
KHD-33	mud turb.	~8.2-8.5	~6.6, 9.2	2.6	25-50	28-37	1 or 2
KHD-49	mud turb.	~8.1-8.5	~6.5, 9.3	2.8	25-50	35	1
KHD-53	mud turb.	~7.9-8.4	~6.4, 9.2	2.8	30-55	35	1
KHD-66a	mud turb.	~8.1-8.3	~6.3, 9.2	2.9	30-60	38	1
average$_{MT}$		***~8.1-8.4***	***~6.4, 9.2***	***2.8***	***30-55***	***35***	***1***

*: siliciclastic turbidite; mix. turb. s.: mixed turbidite sandstone; mud turb.: mud turbidite; glyc.: glycolation; expand.: expandability. Other abbreviations see Table 2

have been responsible for the weak detrital input in the deep sea and relatively higher amount of smectitic minerals in the clay fraction. Eustatic sea-level falls tend to reduce the distance from terrigenous sources of any marine basin. A large part of illite, chlorite and kaolinite therefore tends to be carried into the more distal part of the trough compared to the situation of high sea-level stand (Deconinck and Chamley 1995).

Another complication concerns diagenesis. The distribution of mixed-layer minerals in the present day oceans have strong geographic controls. This indicates continental sources rather than in situ diagenetic origin (Biscaye 1965). Under conditions of increased temperature due to burial, smectite tends to turn into to illite via intermediate stages of mixed-layer minerals (Reynolds and

Table 6
Parameters of mixed-layer illite/smectite minerals of the <2 μm fraction of background sediments

Number of samples	Rock types	Position of 001/001 before glyc. (°2Θ)	Positions after glyc. (°2Θ)	$\Delta 2\Theta_1$	Expand.$_1$ (%)	Expand.$_2$ (%)	"S" value
KHD-12	spotted marl	~8.3-8.4	~7.0, 9.3	2.3	20-30	20-30	1 or 2
KHD-34	spotted marl	~8.0-8.5	~6.3, 9.5	3.2	30-60	52	1
KHD-54	spotted marl	~7.3-8.0	~6.6, 9.1	2.5	25-50	25-35	1 or 2
KHD-111	spotted marl	~8.3-8.5	~6.6, 9.2	2.6	25-50	28-38	1 or 2
KHD-120	spotted marl	~8.3-8.5	~6.6, 9.4	2.8	25-50	35	1
average$_{KHD}$		***~8.0-8.4***	***~6.6, 9.3***	***2.7***	***25-50***	***30-39***	***1 or 2***
FA-3b	spotted marl	~6.0-6.2	~5.3, 9.8	4.5	>40	75	0 or 1
FA-8	spotted marl	~6.2-7.2	~5.2, 9.7	4.5	>40	75	0 or 1
FA-37	spotted marl	~5.6-6.4	~5.2, 9.5	4.3	>40	72	1
FA-49	spotted marl	~6.8-7.3	~5.2, 9.8	4.6	>40	76	0 or 1
FA-59	spotted marl	~5.4-7.4	~5.2, 9.5	4.3	>40	72	1
FA-62	spotted marl	~5.9-6.3	~5.2, 9.5	4.3	>40	72	1
FA-66	spotted marl	~5.8-7.2	~5.2, 9.5	4.3	>40	72	1
average$_{FA}$		***~6.0-6.9***	***~5.2, 9.6***	***4.4***	***>40***	***73***	***0 or 1***
KHD-5	calc. shale	~8.2-8.6	~6.5, 9.4	2.9	25-50	38	1
KHD-24	calc. shale	~8.3-8.6	~7.0, 9.5	2.5	20-30	25-35	1 or 2
KHD-35	calc. shale	~8.2-8.5	~6.8, 9.5	2.7	25-45	30-39	1 or 2
KHD-66b	calc. shale	~8.3-8.4	~6.8, 9.4	2.6	25-45	28-37	1 or 2
average$_{KHD}$		***~8.3-8.5***	***~6.8, 9.5***	***2.7***	***25-45***	***30-39***	***1 or 2***
FA-7	calc. shale	~7.0-7.2	~5.3, 10.0	4.7	>40	55-79	0 or 1
FA-34	calc. shale	~6.9-7.1	~5.3, 9.5	4.2	>40	70	1
FA-36	calc. shale	~7.1-7.3	~5.3, 9.5	4.2	>40	70	1
FA-39	calc. shale	~5.7-7.2	~5.3, 9.7	4.4	>40	73	0 or 1
FA-42	calc. shale	~7.1-7.2	~5.3, 9.5	4.2	>40	70	1
FA-69	calc. shale	~5.8-7.5	~5.3, 9.5	4.2	>40	70	1
FA-71	calc. shale	~5.8-7.2	~5.2, 9.8	4.6	>40	76	0 or 1
FA-74	calc. shale	~7.0-7.2	~5.2, 10.3	5.1	>40	92	0
average$_{FA}$		***~6.6-7.2***	***~5.3, 9.7***	***4.4***	***>40***	***73***	***0 or 1***

calc. shale: calcareous shale. Other abbreviations see Table 3

Hower 1970; Hower et al. 1976; Srodon et al. 1990; Veblen et al. 1990). Viczián (1994), Hillier et al. (1995), Elliott and Matisoff (1996) and Altaner and Ylagan (1997) have reviewed the application of the smectite-to-illite series as geothermometer. According to their results the intensity of the smectite to illite transition depends on the variables time (Pytte and Reynolds 1989), temperature, K^+ availability, K^+ concentration in the pore water during diagenesis (Huang et al. 1993) and activation energy.

Application of the clay mineral proxy to the Lower Jurassic of Mecsek Mts

Paleoclimate simulations using three-dimensional general circulation models for greenhouse Earth (such as during Jurassic) have been created by many authors. Parrish et al. (1982), Hallam (1984), Kutzbach and Gallimore (1989),

Table 7
Parameters of mixed-layer illite/smectite minerals of the <2 μm fraction of bituminous rock types

Number of samples	Rock types	Position of 001/001 before glyc. (°2Θ)	Positions after glyc. (°2Θ)	$\Delta 2\Theta_1$	Expand.$_1$ (%)	Expand.$_2$ (%)	"S" value
PV-1	d.grey c.marl	~7.2-8.7	~6.7, 9.5	2.8	25-50	35	1
PV-2	d.grey c.marl	~8.0-8.4	~6.5, 9.6	3.1	25-50	45	1
PV-3	d.grey c.marl	~8.0-8.4	~6.3, 9.2	2.9	30-60	38	1
PV-4	d.grey c.marl	-	-	-	-	-	-
PV-5	d.grey c.marl	~7.9-8.7	~6.5, 9.4	2.9	25-50	38	1
PV-6	d.grey c.marl	~7.6-8.5	-	-	-	-	-
PV-7	d.grey c.marl	~7.2-8.4	-	-	-	-	-
PV-8	d.grey c.marl	~7.6-8.6	~7.0, 9.2	2.2	20-30	18-29	1 or 2
PV-9	d.grey c.marl	~7.6-8.5	-	-	-	-	-
PV-10	d.grey c.marl	~7.8-8.5	~6.5, 9.4	2.9	25-50	38	1
PV-11	d.grey c.marl	-	-	-	-	-	-
PV-12	d.grey c.marl	~8.1-8.5	~6.2, 9.3	3.1	30-60	45	1
PV-13	d.grey c.marl	~7.7-8.4	~6.1, 9.4	3.3	35-70	50	1
PV-14	d.grey c.marl	~8.1-8.6	~6.2, 9.3	3.1	30-60	45	1
PV-15	d.grey c.marl	~8.0-8.5	~6.1, 9.4	3.3	35-70	50	1
average$_{PV}$		***~7,8-8.5***	***~6.4, 9.40***	***3.0***	***30-60***	***41***	***1***
KHD-10	black shale	~8.3-8.6	~6.2, 9.4	3.2	30-60	48	1
KHD-11	black shale	~8.1-8.4	~6.5, 9.3	2.8	25-50	35	1
KHD-26	black shale	~7.8-8.5	~6.6, 9.5	2.9	25-50	38	1
average$_{KH\ I}$		***~8.1-8.5***	***~6.4, 9.4***	***3.0***	***30-60***	***41***	***1***
FA-3a	black shale	~6.0-7.3	~5.2, 9.7	4.5	>40	75	1
average$_{FR}$		***~6.0-7.3***	***~5.2, 9.7***	***4.5***	***>40***	***75***	***1***
K-1	black shale	~8.2-8.6	~7.0, 9.2	2.2	20-30	18-29	1 or 2
K-2	black shale	~8.2-8.6	~6.1, 9.4	3.3	35-70	50	1
K-3	black shale	~8.2-8.7	~6.7, 9.3	2.6	25-50	28-37	1 or 2
K-4	black shale	~8.2-8.5	~6.8, 9.4	2.6	25-45	28-37	1 or 2
K-5	black shale	~7.8-8.6	~6.7, 9.4	2.7	25-50	30-39	1 or 2
K-6	black shale	~8.1-8.6	~6.1, 9.2	3.1	35-70	45	1
K-7	black shale	~8.1-8.6	~6.8, 9.4	2.6	25-45	28-37	1 or 2
K-8	black shale	~8.2-8.6	~6.5, 9.5	3.0	25-50	41	1
K-9	black shale	~7.8-8.5	~6.6, 9.5	2.9	25-50	38	1
K-10	black shale	~8.1-8.5	~6.3, 9.4	3.1	30-60	45	1
K-11	black shale	~8.2-8.6	~6.5, 9.5	3.0	25-50	41	1
average$_{KH\ II}$		***~8.1-8.6***	***~6.6, 9.4***	***2.8***	***25-50***	***35***	***1***
R-1	black shale	~7.2-8.5	~6.0, 9.4	3.4	35-65	53	1
R-2	black shale	~7.6-8.5	~6.2, 9.3	3.1	30-60	45	1
R-3	black shale	~7.2-8.7	~6.3, 9.4	3.1	30-60	45	1
R-4	black shale	~7.0-8.5	~6.2, 9.2	3.0	30-60	41	1
average$_{RV}$		***~7.3-8.6***	***~6.2, 9.3***	***3.1***	***30-60***	***45***	***1***

d.grey c.marl: dark grey calcareous marl. Other abbreviations see Table 4

Chandler et al. (1992) and Weissert and Mohr (1996) are in agreement that both modeling and empirical research suggest that zonal winds were probably much less important on the Jurassic supercontinent than monsoonal winds. Three major features of the simulated Jurassic climate include the following: 1) Global warming, compared to the present; 2) Decreases in albedo; 3) High rainfall rates associated primarily with monsoons that originated over the warm Tethys Ocean.

Generally the occurrence of kaolinite, illite and illite/smectite can be observed in the samples of Lower Jurassic formations of Mecsek Mountains. The abundance of kaolinite indicates humid climate, intensive leaching, weathering and soil production on the source area.

A part of the mixed-layer illite/smectite minerals could have been carried in the basin originally as pedogenic smectites from a relatively distant source area. Based on suggestions of other authors (Deconinck and Chamley 1995) eolian transport of smectite cannot be excluded. Relative abundance and expandability (70–75%) of mixed-layer phases of the Pliensbachian from the Farkas Ravine seem to be higher, and their degree of ordering is lower (S=0 or S=1) than those of the same mineral collected from other Pliensbachian locations (30–40%, S=1 or S=2, respectively), unrelated to rock type (see Tables 5–7). The examined Lower Toarcian black shale samples from Réka valley show about 45% smectite in expandable phase with S=1 type ordering. The differences between relative amount and type of mixed-layer illite/smectites can be explained by different diagenetic heating. In the northern part of the Eastern Mecsek syncline, the Jurassic succession is much thinner (~1000 m) than in the southern part (~3000 m). This tendency of thicknesses is valid for the sediments younger than Pliensbachian (Haas 1994). Therefore heating of the Pliensbachian rocks deposited in the southern part of the basin could have been more intensive during burial.

Hower (1981) and Viczián (1994) have presented temperature trend lines calculated from illite/smectite interstratifications. Part of these diagrams, corresponding to 70–75% smectite in mixed layer, indicates 50–100 °C heating temperature during burial diagenesis for samples of Farkas Ravine. The same diagrams suggest 130–150 °C maximum burial temperature for the other Pliensbachian samples. Considering the long duration of the diagenetic heating effect, the lower limits of these temperature intervals seem to be rather more probable. Lower Toarcian black shale from Réka Valley seems to have been heated at about 100 °C. Viczián (1990) suggested that illite contents in the mixed-layer phases of the Hettangian to Sinemurian Mecsek Coal and the Vasas Marl Formations are 70–80%. This higher illite contents and higher degree of ordering are due to deeper burial and a higher degree of heating of illite/smectites, in accordance with the deeper stratigraphic position of these two formations.

The highest amounts of kaolinite were found: 1. in the Lower Pliensbachian bioturbated, dark grey calcareous marl of Pécsvárad; 2. in the sandy turbidite beds of the Late Pliensbachian Mecseknádasd Sandstone Formation (Kopasz Hill, Farkas Ravine) and 3. in the black shale of the Early Toarcian Óbánya Aleurolite Formation (Réka Valley). According to our opinion, in the first case (Pécsvárad) the occurrence of kaolinite and illite can be accounted for by a relatively proximal settling in a deep, outer shelf environment. In the second case (Kopasz Hill, Farkas Ravine) redeposition of kaolinite and illite from proximal areas by turbidity currents seems to be an evident explanation. However, some authigenic kaolinite cannot be excluded because of the occurrence of feldspars in turbiditic sandstone. A very high amount of kaolinite was found in the black shale samples of the Óbánya Aleurolite Formation, deposited in periodically anoxic deep shelf facies. Anoxic water mass could have spread over the shelf during transgression and black shale appeared at the same time (Dulai et al. 1992). Examined samples are "pure" hemipelagic sediments; thin turbidite intercalations were not collected and measured. Therefore the abundant occurrence of kaolinite in the examined black shale cannot be explained by resedimentation from nearshore areas. According to our opinion, intensive continental weathering and freshwater runoff would be connected with stabilization of upwelling. This climatic effect would have been favorable to increasing kaolinite input. As far as the Mecsek Mountains are concerned, Noske-Fazekas and Nagy-Melles in Nagy (1969) and Viczián (1987) reported relatively high amounts of kaolinite and illite in the formations deposited during the Hettangian to Aalenian interval. Upsection kaolinite is replaced by smectite and from the Bajocian illite+smectite association becomes dominant. Our results on clay mineral assemblage of Pliensbachian and Lower Toarcian sedimentary rocks are in accordance with these data.

Sedimentation seems to have been controlled in part by eustatic forces. According to Hallam (1988) and Haq et al. (1987) relative sea-level stagnation and subsequent relative lowstand prevailed during late Early and Late Pliensbachian. Shelf progradation with intensive turbidite sedimentation, deposition of coarser-grained sediments relative to the Upper Sinemurian-Lower Pliensbachian are characteristic during the same interval in the Mecsek Mountains. Higher amounts of kaolinite and illite in the clay fraction could be related to this eustatic factor. Sea-level lowstand and high sedimentation rate could have been unfavorable to smectite neoformation.

In comparison with the Pliensbachian hemipelagic background sediments, the highest amount of kaolinite was found in the Lower Toarcian black shale. During deposition of this organic-rich sediment the sea level rose very rapidly (Haq et al. 1987); thus, lowstand progradation cannot explain the preferred occurrence of this mineral. A more humid climate relative to the Pliensbachian could be a relevant explanation for the appearance of kaolinite. Assuming the above-mentioned conditions, eustatic sea-level fall-related lowstand progradation and increased sedimentation rate seem to be more probable driving forces on sedimentation of turbidites and organic-rich sediments of the Mecseknádasd Sandstone Formation.

The abundance of kaolinite can be influenced by diagenetic alteration to illite. According to Velde (1965), Huang and Otten (1985), Chermak and Rimstidt (1990), and Huang (1992, 1993) the rate of this reaction depends on pH and temperature of the system. The reaction begins at 180–190 °C and becomes very rapid at 300 °C (at 0.5 kbar pressure). Composition of arising illite depends on temperature: illite formed from kaolinite at low temperature (~200 °C) contains few expandable layers; therefore, its behavior is very similar to the illite/smectite mixed-layer phases of low smectite component. On the other hand, illite generated from kaolinite at relatively high temperature (~300 °C) shows the X-ray diffraction characteristics of muscovite. Maximum burial temperature about 130 °C estimated by illite proportion and ordering of mixed-layer illite/smectite minerals seems to exclude kaolinite-to-illite transformation in the Pliensbachian succession of the Mecsek Mountains.

Conclusions

Clay mineralogical composition of the examined Lower Jurassic sedimentary rocks is characterized by the dominance of kaolinite, illite and illite/smectite mixed-layer minerals. Differences in the relative abundances of these phases seem to depend 1. on the sampling locations and 2. on the rock types.

1. Mixed-layer illite/smectites of the samples of Farkas Ravine differ from other examined Pliensbachian samples. 70–75% smectite was detected with S=0 or S=1-type interstratification in the samples of Farkas Ravine. Mixed-layer illite/smectites from other Pliensbachian outcrops are characterized by lower expandability (30–40%) and S=1 or S=2-type interstratification. Lower Toarcian black shale samples show about 45% smectite with S=1-type ordering.

The differences can be explained by different heating during burial diagenesis. Mixed-layer structures indicate 50–100 °C heating temperature during diagenesis for samples of Farkas Ravine, lower values being more probable. The other examined Pliensbachian samples seem to have been heated at 130 °C. Lower Toarcian black shale from Réka Valley was heated at about 100 °C.

2. A difference can be observed in the relative abundance of kaolinite. The black shale samples of Réka Valley have very high amounts of kaolinite. Pliensbachian mixed turbiditic sandstones and dark-grey calcareous marls of Pécsvárad are rich in kaolinite, too. Kopasz Hill samples have generally lower amounts of kaolinite (except the for turbiditic sandstone samples).

High kaolinite contents indicate humid climate and intensive weathering in the source area. Occurrence of kaolinite and illite can be explained in particular by

a) the relatively proximal depositional realm (Lower Pliensbachian grey calcareous marls, Pécsvárad);

b) redeposition of kaolinite and illite from relatively nearshore areas by turbidity currents (Upper Pliensbachian turbidites, Kopasz Hill and Farkas Ravine);

c) authigenic formation of kaolinite from feldspars in turbiditic sandstones;

d) more intensive continental weathering and freshwater runoff relative to former periods connected to stabilization of upwelling and shelf anoxia (Lower Toarcian black shale, Réka Valley).

3. Mixed-layer illite/smectite minerals of the examined samples seem to be pedogenic. They could have been carried from pedologic blankets of a relatively distant source area by eolian transport into the basin.

Acknowledgement

The authors thank Professor József Hlavay, Head of the Department for financial support of measurements. György Barkó, Balázs Tolnai and Andrea Varga are acknowledged for their help in sampling and in fieldwork. We are grateful to András Galácz and István Viczián for the evaluation of the data and for their constructive advice.

References

Altaner, S., R. F. Ylagan 1997: Comparison of structural models of mixed-layer illite/smectite and reaction mechanisms of smectite illitization. – Clays and Clay Mins., 45/4, pp. 517–533.

Biscaye, P. E. 1965: Mineralogy and sedimentation of recent deep-sea clay in the Atlantic Ocean and adjacent seas and oceans. – Geol. Soc. Am. Bull., 76, pp. 803–832.

Çelik, M., N. Karakaya, A. Temel 1999: Clay minerals in hydrothermally altered volcanic rocks, Eastern Pontides, Turkey. – Clays and Clay Mins., 47/6, pp. 708–717.

Chamley, H. 1967: Possibilités d'utilisation de la cristallinité d'un minéral argileux (illite) comme temoin climatique dans les sediments recents (Possibilities of utilisation of the crystallinity of a clay mineral (illite) as climatic evidence in Recent sediments). – C. R. Acad. Sci., 265, pp. 184–187 (in French).

Chamley, H. 1989: Clay Sedimentology. 623 p. Springer Verlag, Berlin, Heidelberg, New York.

Chamley, H., P. Debrabant 1984: Paleoenvironmental history of the North Atlantic region from mineralogical and geochemical data. – Sedim. Geol., 40, pp. 151–167.

Chandler, M. A., D. Rind, R. Ruedy 1992: Pangean climate during the Early Jurassic: GCM simulations and the sedimentary record of paleoclimate. – Geol. Soc. Am. Bull., 104, pp. 543–559.

Chermak, J. A., J. D. Rimstidt 1990: The hydrothermal transformation of kaolinite to muscovite/illite. – Geochim. Cosmochim. Acta, 54, pp. 2979–2990.

Császár, G. (Ed.) 1997: Basic lithostratigraphic units of Hungary. – Stratigraphic units of Hungary, Budapest.

Deconinck, J. F., H. Chamley 1995: Diversity of smectite origins in Late Cretaceous sediments: example of chalks from Northern France. – Clay Mins., 30, pp. 365–379.

Dulai, A., Zs. Suba, A. Szarka 1992: Toarci (alsójura) szervesanyagdús fekete pala a mecseki Réka-völgyben [Toarcian (Lower Jurassic) organic-rich black shale in the Réka Valley (Mecsek Hills, Hungary)]. – Földt. Közl., 122/1, pp. 67–87 (in Hungarian).

Egger, H., M. Bichler, I. Draxler, M. Homayoun, H. J. Huber, E. C. Kirchner, P. Klein, R. Surenian 1997: Mudturbidites, Black Shales and Bentonites from Paleocene/Eocene Boundary: the Anthering Formation of the Rhenodanubian Flysch (Austria). – Jb. Geol. B.-A., 140/1, pp. 29–45.

Elliott, W. C., G. Matisoff 1996: Evaluation of kinetic models for the smectite to illite transformation. – Clays and Clay Mins., 44/1, pp. 77–87.

Főzy, I., Cs. Lantai, K. Schlemmer 1985: A Pliensbachian-Lower Cretaceous profile at Zobákpuszta, Mecsek Mts., Hungary. – Ann. Univ. Sci. Budapest, Sect. Geol., 25, pp. 97–115.

Frederickson, A. F. 1948: Mode of occurrence of titanium and zirconium in laterites. – Am. Mineral., 33, pp. 374.

Gygi, R. A., F. Persoz 1986: Mineralostratigraphy, litho- and biostratigraphy combined in correlation of the Oxfordian (Late Jurassic) formations of the Swiss Jura range. – Ecl. geol. Helv., 79/2, pp. 385–454.

Haas, J. 1994: Magyarország geológiája – Mezozóikum (Geology of Hungary – Mesozoic) – Lecture notes. Eötvös Loránd University of Sciences Budapest p. 199. (in Hungarian).

Hallam, A. 1984: Continental humid and arid zones during the Jurassic and Cretaceous. – Palaeogeography, Palaeoclimatology, Palaeoecology, 47, pp. 195–223.

Hallam, A. 1988: Reevaluation of Jurassic eustasy in the light of new data and the revised Exxon curve. – In: Wilgus, C. K., B. J. Hastings, H. Posammentier (Eds): Sea level changes: an integrated approach. – Soc. Econ. Paleont. Miner. Spec. Publ., 42, pp. 261–273.

Hallam, A., J. A. Grose, A. H. Ruffell 1991: Palaeoclimatic significance of changes in clay mineralogy across the Jurassic–Cretaceous boundary in England and France. – Palaeogeography, Palaeoclimatology, Palaeoecology, 81, pp. 173–187.

Haq, B. U., J. Hardenbol, P. R. Vail 1987: Chronology of fluctuating sea levels since the Triassic. – Science, 235, pp. 1156–1167.

Heath, K. C., H. T. Mullins 1984: Open-ocean off-bank transport of fine-grained carbonate sediment in the northern Bahamas. – In: D. A. V. Stow, Piper, D. J. W. (Eds): Fine-grained sediments: deep-water processes and facies. – Geol. Soc. Lond. Spec. Publ., 14, pp. 199–208.

Hetényi, R. 1966: A mecseki középső-liász tagolása (Subdivision of Middle Liassic of Mecsek Mountains) – Ann. Report Hung. Geol. Inst. for 1964, pp. 23–29 (in Hungarian).

Hillier, S., J. Mátyás, A. Matter, G. Vasseur, 1995: Illite/smectite diagenesis and its variable correlation with vitrinite reflectance in the Pannonian Basin. – Clays and Clay Mins., 43/2, pp. 174–183.

Hower, J. 1981: Shale Diagenesis. – In: Longstaffe, F. J. (Ed.): Clays and the resource geologist. – Min. Ass. Can. Short Course Hdbk., 7, pp. 60–80.

Hower, J., E. V. Eslinger, M. E. Hower, E. A. Perry 1976: The mechanism of burial metamorphism of argillaceous sediment: 1. Mineralogical and chemical evidence. – Geol. Soc. Amer. Bull., 87, pp. 725–737.

Huang, W. L. 1992: Illitic clay formation during experimental diagenesis of arkoses. – In: Houseknecht, D.W., E. D. Pittman (Eds): Origin, Diagenesis, and Petrophysics of Clay Minerals in Sandstones. SEPM Spec. Publ., 47, pp. 49–63.

Huang, W. L. 1993: The formation of illitic clays from kaolinite in KOH solution from 225°C to 350°C. – Clays and Clay Mins., 41/6, pp. 645–654.

Huang, W. L., G. A. Otten 1985: Kinetics of K-mica and K-natrolite formation as a function of temperature. – In: Program and Abstracts, 2nd International Symposium on Hydrothermal Reactions, University Park, Pennsylvania. pp. 34.

Huang, W. L., J. M. Longo, D. R. Pevear 1993: An experimentally derived kinetic model for smectite-to-illite conversion and its use as a geothermometer. – Clays and Clay Mins., 41, pp. 162–177.

Jeans, C. V. 1968: The origin of montmorillonite of the European chalk with special reference to the Lower Chalk of England. – Clay Miner., 7, pp. 311–329.

Jeans, C. V. 1978: Silicifications and associated clay assemblages in the Cretaceous marine sediments of southern England. – Clay Miner., 13, pp. 101–126.

Jenkyns, H. C. 1985: The Early Toarcian and Cenomanian-Turonian anoxic events in Europe: comparisons and contrasts. – Geologische Rundschau, 74, pp. 505–518.

Kimblin, R. T. 1992: The origin of clay minerals in the Coniacian Chalk of London. – Clay. Miner., 27, pp. 389–392.

Kutzbach, J. E., R. G. Gallimore 1989: Pangean climates: megamonsoons of the megacontinent. – Jour. of Geophys. Research, 94, pp. 3341–3357.

Lever, A., I. N. McCave 1983: Eolian components in Cretaceous and Tertiary North Atlantic sediments. – J. Sed. Petr., 53, pp. 811–832.

Nagy, E. 1969: A Mecsek hegység alsóliász kőszénösszlete. Földtan (Lower Liassic coal formation of the Mecsek Mountains. Geology) – Annales of Hung. Geol. Inst., 51/2, pp. 245–971 (in Hungarian).

Pacey, N. R. 1984: Bentonites in the Chalk of central eastern England and their relation to the opening of the northeast Atlantic. – Earth Planet. Sci. Lett., 67, pp. 48–60.

Parrish, J. T., A. M. Ziegler, C. R. Scotese 1982: Rainfall patterns and the distribution of coals and evaporites in the Mesozoic and Cenozoic. – Palaeogeography, Palaeoclimatology, Palaeoecology, 40, pp. 67–101.

Piper, D. J. W., D. A. V. Stow 1991: Fine-grained turbidites. – In: Einsele, G., W. Ricken, A. Seilacher (Eds): Cycles and Events in Stratigraphy. Springer Verlag, Berlin, Heidelberg, New York. pp. 360–376.

Pytte, A. M., R. C. Reynolds 1989: The thermal transformation of smectite to illite. – In: Naeser, N. D., T. H. McCulloh (Eds): Thermal history of sedimentary basins: Methods and case histories. Springer Verlag, Berlin, Heidelberg, New York. pp. 133–140.

Raucsik, B., B. Tolnai, T. Horváth, V. Szilágyi, M. Hetényi 2000: Geochemistry of Lower Jurassic organic-rich sediments from the Mecsek Mountains, Southern Hungary. – Goldschmidt 2000 An International Conference for Geochemistry, Sept. 3–8, Oxford, UK. Journal of Conference Abstracts, 5, 2, pp. 829.

Reijmer, J. J. G., W. G. H. Z. Ten Kate, A. Sprenger, W. Schlager 1991: Calciturbidite composition related to exposure and flooding of a carbonate platform. – Sedimentology, 38, pp. 1059–1074.

Reynolds, Jr., R. C., J. Hower 1970: The nature of interlayering in mixed-layer illite-montmorillonite. – Clays and Clay Mins., 18, pp. 25–36.

Rischák, G., I. Viczián 1974: Mineralogical factors determining the intensity of basal reflections of clay minerals. – Annual Report of Hung. Geol. Inst. for 1972, pp. 229–256 (in Hungarian).

Robinson, D., V. P. Wright 1987: Ordered illite-smectite and kaolinite-smectite: pedogenic minerals in a Lower Carboniferous paleosol sequence, South Wales. – Clay Miner., 22, pp. 109–118.

Singer, A. 1984: The paleoclimatic interpretation of clay minerals in sediments – a review. – Earth Sci. Rev., 21, pp. 251–293.

Singer, A. 1988: Illite in aridic soils, desert dusts and desert loess. – Sediment. Geol., 59, pp. 251–259.

Srodon, J. 1980: Precise identification of illite/smectite interstratifications by X-ray powder diffraction. – Clays and Clay Mins., 28/6, pp. 401–411.

Srodon, J. 1984: X-ray powder diffraction identification of illitic materials. – Clays and Clay Mins., 32, pp. 337–349.

Srodon, J., C. Andreoli, F. Elsass, M. Robert 1990: Direct high-resolution transmission electron microscopic measurement of expandability of mixed-layer illite/smectite in bentonite rock. – Clays and Clay Mins., 38, pp. 373–379.

Steinberg, M., T. Holtzapffel, M. Rautureau 1987: Characterization of overgrowth structures formed around individual clay particles during early diagenesis. – Clays Clay Mins., 35, pp. 189–195.

Thiry, M., T. Jacquin 1993: Clay mineral distribution related to rift activity, sea-level changes and paleoceanography in the Cretaceous of the Atlantic ocean. – Clay Miner., 28, pp. 61–84.

Török, Á. 1997a: Dolomitization and karst-related dedolomitization of Muschelkalk carbonates, in South Hungary. – Acta Geol. Hung., 40/4, pp. 441–462.

Török, Á. 1997b: Triassic ramp evolution in Southern Hungary and its similarities to the Germano-type Triassic. – Acta Geol. Hung., 40/4, pp. 367–390.

Veblen, D. R., G. D. Guthrie, K. J. T. Livi, R. C. Reynolds 1990: High-resolution transmission electron microscopy and electron diffraction of mixed-layer illite/smectite: Experimental results. – Clays and Clay Mins., 38, pp. 1–13.

Velde, B. 1965: Experimental determination of muscovite polymorph stabilities. – Amer. Mineral., 50, pp. 436–449.

Viczián, I. 1987: Agyagásványok Magyarország üledékes kőzeteiben (Clay minerals in sedimentary rocks of Hungary). – D.Sc. Thesis, Budapest. p. 205 (in Hungarian).

Viczián, I. 1990: Jelentés a Máza-26. sz. mélyfúrás liász anyagán végzett ásványtani vizsgálatokról. – MÁFI Adattár. Leltári szám 577/32. (Report of the mineralogical examinations taken on the material of part belongs to the Liassic of the borehole Máza Nb. 26. Manuscript report. Dataset of the Hungarian Geological Institute) (in Hungarian).

Viczián, I. 1994: A szmektit-illit átalakulás függése a hőmérséklettől. (Smectite-illite geothermometry) – Földtani Közlöny, 124/3, pp. 367–379 (in Hungarian with English abstract).

Watanabe, T. 1981: Identification of illite/montmorillonite interstratifications by X-ray powder diffraction. – J. Min. Soc. Japan Spec. Issue, 15, pp. 32–41.

Weissert, H., H. Mohr 1996: Late Jurassic and its impact on carbon cycling. – Palaeogeography, Palaeoclimatology, Palaeoecology, 122, pp. 27–43.

Acta Geologica Hungarica, Vol. 43/4, pp. 431–445 (2000)

Mineralogical and chemical investigation of soil formed on basaltic bentonite at Egyházaskesző, Transdanubia, Hungary

Zsuzsanna Hartyáni, Ildikó Pécsi, László Merényi

University of Veszprém, Department of Earth and Environmental Sciences

Sándor Szabó, Judit Szauer, Virág Szilágyi

University of Veszprém, Department of Earth and Environmental Sciences

In Veszprém University soils have been investigated genetically for many years following the guidelines of Prof. Nemecz, to whom this paper is dedicated. We investigated mainly the weathering processes. Formerly, soils formed on different parent rocks were investigated. In this paper soil formed on basaltic bentonite, superposed on a volcanic crater (Egyházaskesző, Hungary) was measured with two X-ray techniques (X-ray diffraction and X-ray fluorescence spectrometry) and with thermal analytical methods. A new dynamic method of investigation was used. Mineralogical features and chemical composition (main components and trace elements like ^{25}Mn, ^{28}Ni, ^{30}Zn, ^{37}Rb, ^{38}Sr, ^{39}Y, ^{40}Zr, ^{56}Ba, ^{82}Pb) were considered not only as a function of depth but also as a function of grain size. Crystalline phases identified were illite/montmorillonite, muscovite, chlorite, quartz and feldspar. At depths of 70–80 cm, as well as 80–90 cm, high amounts of calcite were found. On the top of the soil layers, at depths of 0–10 cm and at the bottom, gypsum is present. Applying the dynamic method we confirmed the original theory that the grain-size distribution of a soil mineral (the shape of the 3-dimensional distribution pattern) provides information about the genesis of the mineral. In soils formed on basaltic bentonite, quartz, muscovite and feldspar are interpreted to be decomposing minerals, and montmorillonite, chlorite, calcite and gypsum as authigenic phases.

Trace elements are mainly concentrated in the smallest grain-size fraction, absorbed on the surface of clay minerals or built into the interlayer spaces. This is also an explanation for the high efficiency of alginite and basaltic bentonite as soil-improving raw material in Hungary.

Key words: soil, minerals, weathering, X-ray spectrometry, X-ray diffractometry, basaltic bentonite

Introduction

At the former Department of Mineralogy (today Department of Earth and Environmental Sciences), under the leadership of Prof. Nemecz, the authors investigated different types of Hungarian raw materials, mainly clay minerals (Nemecz 1973). One of these raw materials was basaltic bentonite. At the very beginning of the 80s we collected samples from one of the boreholes at Várkesző (Olaszi 1996). The main aim of that research was to find a mineralogical raw material for industrial application. All of the samples under examination were collected from outcrops of the mines of Egyházaskesző, Várkesző, Gérce and Pula

Addresses: Zs. Hartyáni, I. Pécsi, S. Szabó, J. Szauer, L. Merényi, V. Szilágyi: H-8201 Veszprém, P. O. Box 158, Hungary, E-mail: csikosne@almos.vein.hu
Received: 03 July, 2000

0236–5278/2000/$ 5.00 © 2000 *Akadémiai Kiadó, Budapest*

(Transdanubia, Hungary). X-ray analysis (XRD) was chosen as the first step of the research work, and depending on the results of other analytical methods like XRFS, micromineralogical examinations and thermal analyses were applied. Other authors (Barna and Földvári 1992, 1996) also used the thermoanalytical method for identifying crystalline phases in basaltic bentonite samples from this area. Juhász (1989) carried out detailed mineralogical and technological studies. All these authors identified iron-rich beidellite (=montmorillonite) in the smectite phase of bentonite.

In Egyházaskesző the 8 m-thick bentonite clay, of green color and low $CaCO_3$ content, occurred as a part of a 13 m-long profile perpendicular to the wall of the mine. The clay mineral content here was 70%. Below bentonitic clay, a bentonite bed of brown and gray colors appeared, with 90–95% clay mineral content. For comparison the high-quality bentonite in the Tokaj Mountains contains only 60–70% montmorillonite. Beside the montmorillonite and beidellite as main components feldspars, quartz, calcite, hematite, clinozoisite, piemontite, andradite, Mg-almandine, grossularite, dravite, rutile, ilmenite and pseudobrookite were identified (Olaszi 1996).

The results were in good agreement with the statements of Solti and Viczián (Solti 1985, 1996; Viczián 1996). Solti underlined that bentonite found in Egyházaskesző is completely different from other bentonites discovered and mined in Hungary so far. The difference is due primarily to the extremely high trace element content throughout the section.

As emphasized by Jenny (1941) the unique characteristic of the soil lies in the organization of its constituents and properties into horizons that are related to the present-day surface and that change vertically with depth. Soil profiles vary in make-up within wide limits according to their genetic and geographic environment (Hindrich et al. 1985; Bohn et al. 1979). The parent material contributes to the raw material of the soil and is therefore a factor controlling the nature of the resultant soil (Webb and Rose 1979; Berrow 1988; Follett and McHardy 1965). Continuing the research of Nemecz (Nemecz and Hartyáni 1991, 1995) in the field of growth mechanism of minerals, there are some very important publications in the field of genetic interpretation of sample size distribution of fine grained minerals (Altaner and Ylagan 1997; Cuadros and Altaner 1998; Eberl et al. 1998). At the very beginning of our research the weathering process of soils formed on different types of parent material were investigated. Soils from Mátraháza (parent material is andesite), loess paleosol from Basaharc, and soil from Pákozd (parent material is granite) can be mentioned as examples (Nemecz and Hartyáni 1995; Pécsi et al. 2000).

Materials and Methods

Local Geology

During the past 20 years numerous volcanic craters filled with raw materials such as alginite and basaltic bentonite (Pula, Gérce, Várkesző, Egyházaskesző) have been uncovered by the geologists and geophysicists of the Hungarian Geological Institute and the Loránd Eötvös Geophysical Institute (Solti 1996).

Between the villages Egyházaskesző and Várkesző they have succeeded in outlining minor reserves of alginite overlain by a bentonite deposit of medium-sized extent. These deposits fill volcanic craters formed by the Late Pannonian basalt volcanism (Bence et al. 1977). The occurrence of high-quality basaltic bentonite at Egyházaskesző, representing the hanging wall of the alginite beds, can be regarded as a general example of the deposition in maar craters (Solti 1996; Solti et al. 1988). The boreholes drilled in the area explored this maar sediment sequence. Below the soil layer down to 10.1 m, there is a limy bentonite bed containing basaltic tuff debris; between 10.1 and 37.0 m occurs a bentonite bed of high montmorillonite content, free of lime, and at the depth of 39–90 m alginite, basaltic tuffite and basaltic tuff beds are encountered. Above the sediments the thickness of brown forest soil formed on basaltic bentonite is only 90 cm. The soil samples we investigated were taken in the vicinity of borehole Ekt.5 at Egyházaskesző.

Soil samples

The grain-size distribution and mineralogical content of brown forest soil samples (Stefanovics 1975; Szendrei 1994, 1998) formed on basaltic bentonite in Egyházaskesző were analyzed. The soil formed on basaltic bentonite overlying a deposit of alginite is particularly interesting because alginite and basaltic bentonite are registered as soil-improving mineral raw materials in Hungary. The parent material itself is an excellent soil-conditioning agent (Solti and Csirik 1996).

Dynamic method for investigation of soils

Our goal was to apply a method that is appropriate to characterize the weathering processes not only from a mineralogical but also a geochemical perspective. This is the first time that the so-called dynamic method is used for evaluation the results from a geochemical point of view (trace element analysis). Originally the method was developed to characterize the weathering processes from a mineralogical perspective (Nemecz and Hartyáni 1995).

The basic principle of the dynamic method is that the grain-size distribution of a mineral is characteristic of the weathering process acting on the mineral. As a result of chemical weathering the relative abundance of the mineral decreases in the smaller-size ranges. The reason for this is that small grains dissolve more rapidly than large grains due to the large specific surface area of the small particles. This method assumes the opposite trend for the size distributions of authigenic soil minerals.

To apply this method the mineralogical and chemical composition of various soil-size fractions were determined. Sampling the area we obtained 9 soil samples at 10 cm intervals and then fractionated by sieving the averaged samples into the following (A, B, C, D, E F, G, H) 8 grain-size fractions:

A: 315–800 μm	D: 45–80 μm	G: 5–10 μm
B: 160–315 μm	E: 20–45 μm	H: <5 μm.
C: 80–160 μm	F: 10–20 μm	

The <45 μm size fractions were sieved in an ultrasonic bath with laser beam-made sieves. In that way we obtained altogether 72 samples. Analysis of mineralogical and chemical composition for 7 main components and 9 trace elements were performed for all soil fractions. In some cases, when it was important, we performed thermogravimetric measurements as well (for evaluation of the results we handled more than 1500 data).

The mineralogical and chemical compositions of fractions A to H were determined quantitatively and plotted in three dimensions (Figs 1 and 2). X-axis: depth from the soil surface in multiples of 10 cm; Y-axis: A to H grain size fractions (μm); Z-axis: the amount of the measured parameter (m/m% or ppm). In the 3-dimensional diagrams each point of the enveloping surface represents the relative amount of a mineral or chemical compound (m/m% or ppm) in a certain grain size fraction and at a given soil depth.

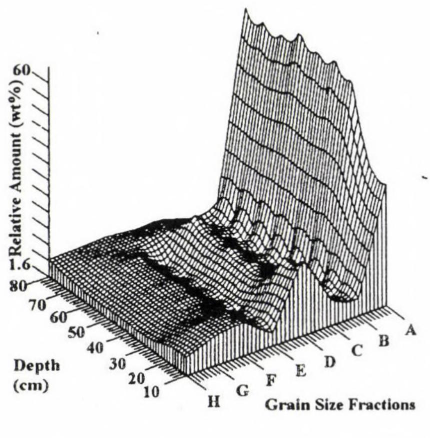

a) grain size distribution of the whole sample

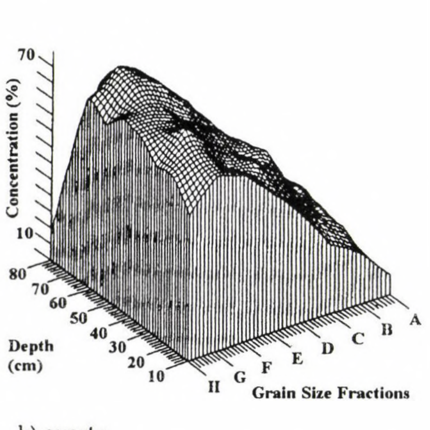

b) quartz

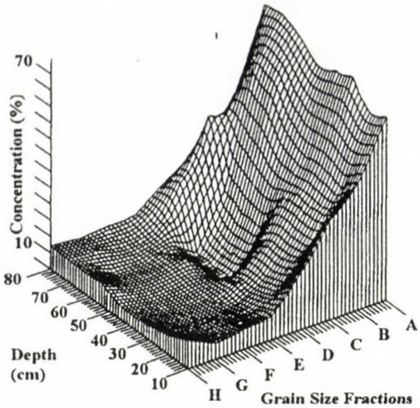

c) montmorillonite

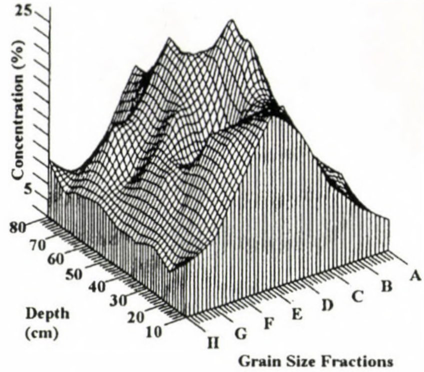

d) feldspars

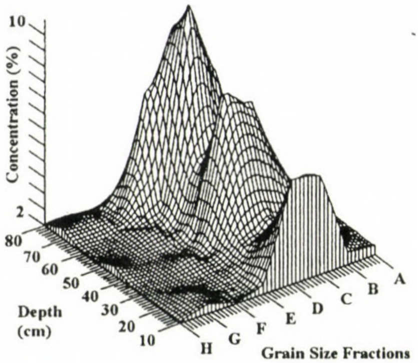

e) chlorite

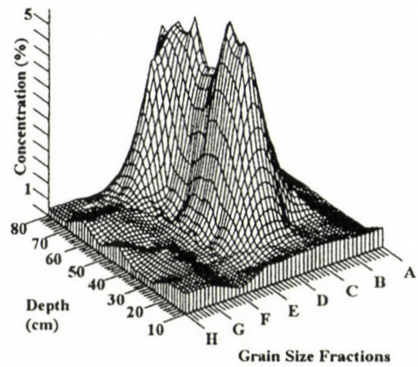

f) muscovite

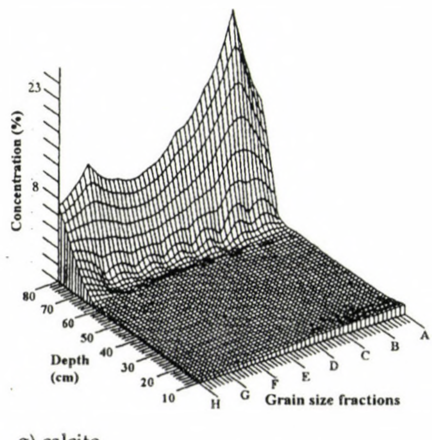

g) calcite

Fig. 1
Particle size distribution versus depth diagram and distribution of identified minerals of the soil formed on basaltic bentonite, as a function of depth and grain-size fractions

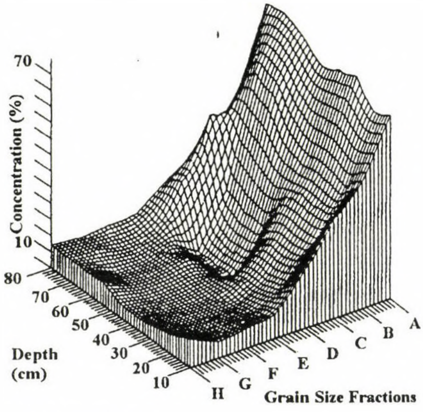

a) montmorillonite

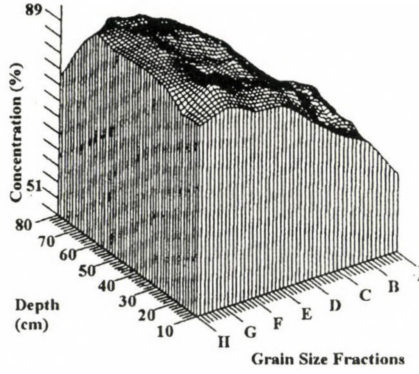

b) SiO_2

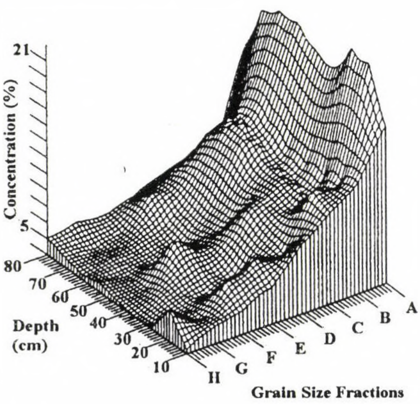

c) Al_2O_3

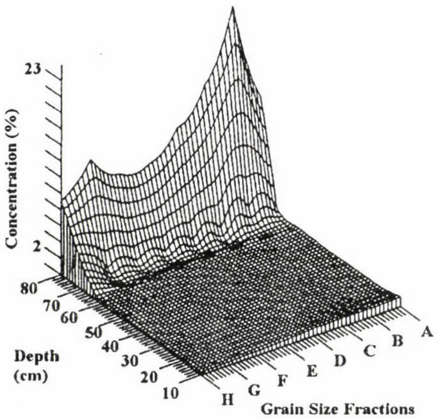

d) CaO

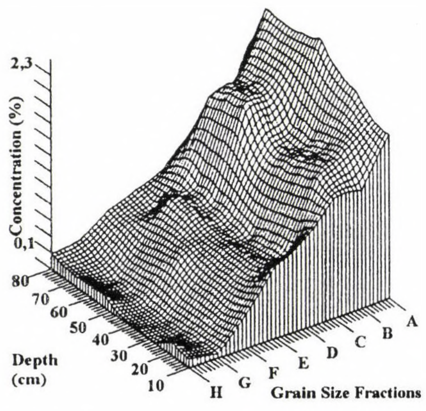

e) TiO_2

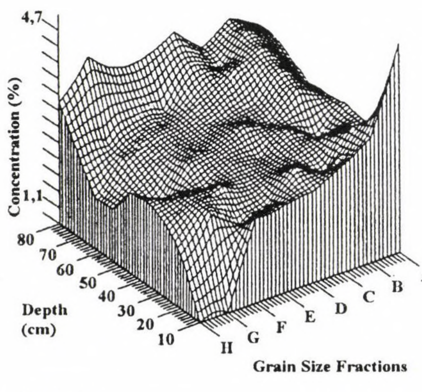

f) MgO

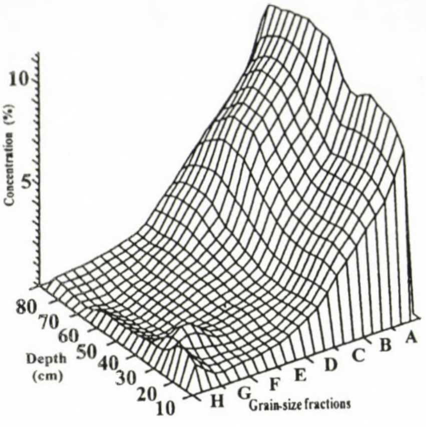

g) Fe_2O_3

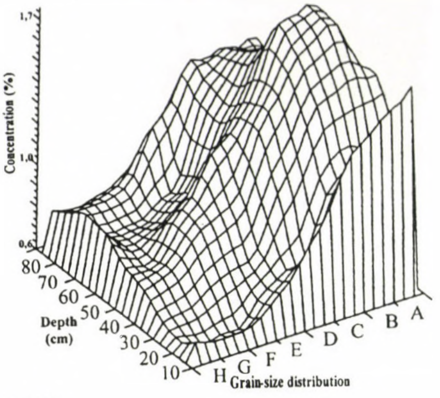

h) K_2O

Fig. 2a–h
Distribution of some major elements of the soil as a function of grain-size fractions and depth

Organic compounds of the samples were removed by H_2O_2 treatment because only the inorganic parts of the soil were investigated (Farmer and Mitchell 1965; Raab 1988).

Analytical methods

X-ray diffraction (XRD)

Determination of mineral composition of the samples separated in particle size fractions was made by means of X-ray diffraction (Raab 1988). The instrument used was a PHILIPS PW 1710-type X-ray diffractometer (X-ray: CuKα/λ=1,542ÅT, 50 KV, 50 mA, slit: 1°/1°, monochromator: graphite). Crystalline phases of concentration higher than 1–5 rel. % were identified qualitatively and having chosen some characteristic reflections (Table 3) the phases were determined semi-quantitatively as well.

X-Ray Fluorescence Spectrometry (XRFS)

For quantifying the chemical composition of the soil fractions, XRFS analysis was performed using a Philips PW 1410/20 wavelength dispersive spectrometer (Tube 3 kW Cr anode, 50 kV, 50 mA). In cases of some trace elements (Pb, Zn, etc.) a brand-new PHILIPS PW 2404 spectrometer (1999) was applied for validation the measurements made earlier (tube: 4 kW Rh, max 60 kV). Major elements (MgO, Al_2O_3, SiO_2, K_2O, CaO, TiO_2 and Fe_2O_3) were determined on fused beads of samples mixed with lithium tetraborate. The double dilution method of Tertian (Tertian 1968) was applied (ratio sample/flux 1:10 and 1:20) for elimination of the matrix effect. Trace elements measured were Zr, Rb, Sr, Zn, Ni, Y, Ba, Pb and Mn.

They were analyzed on pressed powder pellets (Zsolnay et al. 1984). Each soil fraction was pulverized in a RETCH mill to 5 μm grain size. 1.6 g of each soil sample was weighed and 0.4 g boric acid was added. Both materials were homogenized in a rubbing mortar with abs. ethanol added. Scattered radiation was used for matrix correction (Reynolds 1967; DeLong and McCollough 1973; Wilband 1975). Reproducibility is better than 2%. In the case of major elements the accuracy of the measurements, as determined by using international soil standards, is 0.8–1.5 rel. % and around 5–8 rel. % for trace elements.

Measuring parameters of XRFS measurements for trace elements can be seen in Table 1 and for major elements in Table 2.

Results and discussion

Mineralogical composition and grain size distribution of soil

As mentioned before the basic principle of the dynamic method (Nemecz and Hartyáni 1995) is that the size distribution of a mineral is characteristic of the weathering process acting upon the mineral. Before knowing anything of the mineralogical composition of the soil one of the most important data is the mass distribution of grain size (Table 4). The particle-size distribution diagram can be

Table 1
Measuring parameters of trace elements measured with XRF as pressed powders

Element	Line	λ [A]	2Θ	X-tal	Detector	Collimator
^{25}Mn	Kα	2.102	92.43	LiF(200)	scintillation+flow	fine
^{28}Ni	Kα	1.658	48.61	LiF(200)	scintillation+flow	fine
^{30}Zn	Kα	1.435	41.74	LiF(200)	scintillation+flow	fine
^{37}Rb	Kα	0.926	26.58	LiF(200)	scintillation+flow	fine
^{38}Sr	Kα	0.875	25.09	LiF(200)	scintillation+flow	fine
^{39}Y	Kβ	0.740	21.17	LiF(200)	scintillation+flow	fine
^{40}Zr	Kβ	0.701	20.04	LiF(200)	scintillation+flow	fine
^{56}Ba	Kα	0.385	10.97	LiF(200)	scintillation+flow	fine
^{82}Pb	Lα	1.175	33.92	LiF(200)	scintillation+flow	fine

Table 2
Measuring parameters of major components measured with XRF as fused discs

Major component	Line	λ [Å]	2Θ	X-tal	Detector	Collimator
MgO	^{12}Mg Kα	9.889	136.76	ADP	flow	course
Al_2O_3	^{13}Al Kα	8.337	145.31	PE	flow	course
SiO_2	^{14}Si Kα	7.125	109.26	PE	flow	course
K_2O	^{19}K Kα	3.741	50.69	PE	flow	course
CaO	^{20}Ca Kα	3.358	113.14	LiF(200)	flow	fine
TiO_2	^{22}Ti Kβ	2.748	86.16	LiF(200)	flow	fine
Fe_2O_3	^{26}Fe Kβ	1.936	57.51	LiF(200)	flow	fine

Table 3
Diffraction lines (Bragg angle and Miller Indexes) for quantifying the minerals in the soil

Mineral	Bragg angle (2θ)	(hkl)
Muscovite	8,9°	(001)
Gypsum	11,6°	(020)
Chlorite	12,5°	(002)
Montmorillonite	19,9°	(110)
Quartz	26,6°	(101)
Feldspar (albite)	28,0°	(002)
Calcite	29,4°	(104)

seen on Fig. 1a. On all diagrams a continuous three-dimensional distribution shape obtained from the discrete analytical data can be seen.

Using the XRD method in all of the soil samples we identified the following crystalline phases: montmorillonite, muscovite, kaolinite, chlorite, quartz, and feldspar (mainly albite). At depths of 70–80 cm, and at 80–90 cm, a large amount of calcite was found. At the top of the soil layers, at depths of 0–10 cm and on the bottom of the soil layer, at depths of 80–90 cm, gypsum was present. All of the soil fractions contained a more or less amorphous phase as well.

Table 4
Particle size distribution of the soil

Depth	Mass distribution of grain size (m/m%)							
[cm]	<5 μm	5–10 μm	10–20 μm	20–45 μm	45–80 μm	80–160 μm	160–315μm	315–800 μm
0–10	34.89	5.38	7.75	21.73	3.98	9.77	8.83	5.57
10–20	37.48	5.74	7.13	19.25	4.84	9.37	8.52	5.34
20–30	57.77	4.46	4.87	11.15	3.10	7.27	5.97	3.28
30–40	60.00	3.51	4.55	11.12	2.86	6.94	5.74	2.93
40–50	58.57	3.64	4.26	11.84	2.67	7.42	5.98	3.11
50–60	60.71	3.58	4.19	11.34	1.90	7.19	5.91	2.88
60–70	56.33	4.39	4.27	13.85	1.59	7.48	6.18	3.01
70–80	56.31	4.26	4.43	7.66	6.78	5.98	6.32	3.92
80–90	56.64	4.66	2.73	5.30	5.20	6.21	5.75	5.43

Regarding the line-shape of the diffractograms it appeared that the soil contained mixed-layer illite/montmorillonite clay minerals as well. Due to its low occurrence this type of clay mineral was not quantified. As was mentioned before the type of smectite mineral in basaltic bentonite samples was identified as Fe-rich beidellite (Juhász 1989; Viczián 1996). However, in the following part of this paper we mention the smectite clay minerals simply as montmorillonite in the general sense of the term (Hendricks et al. 1940). It was also not easy to identify the exact type of feldspars (Na, K or Ca-feldspar). In almost all grain-size fractions they were identified as albite Na-feldspar (28.0 2Θ) with traces of microcline K-feldspar. The quantity of feldspars in the smallest and in the largest grain-size fractions was relatively low (2–5%). The ratio between these types of feldspar in the smallest particle-size fractions was approx. 1:5 to albite and in the largest grain-size fraction the ratio was 1:1. There were also some difficulties in distinguishing between chlorite and kaolinite. As a result it has been found that

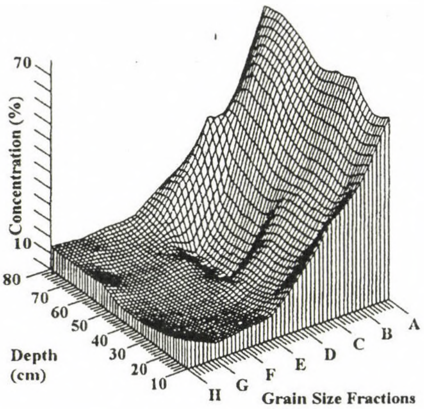

a) montmorillonite

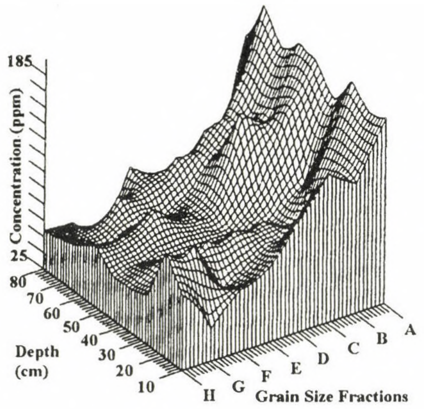

b) Y

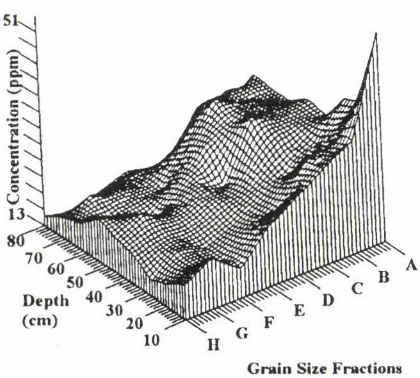

c) Rb

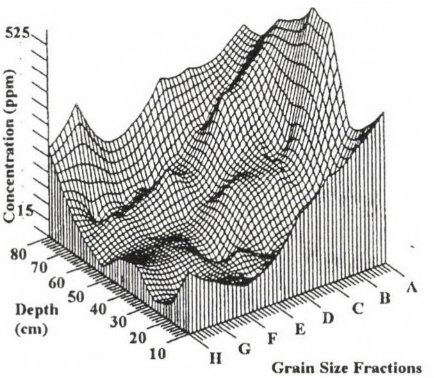

d) Ni

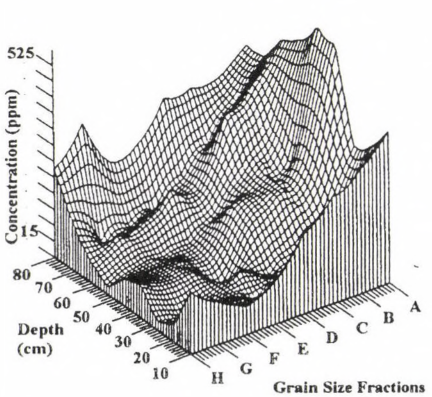

e) Zn

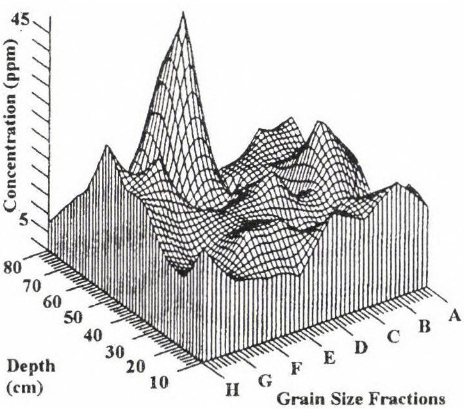

f) Pb

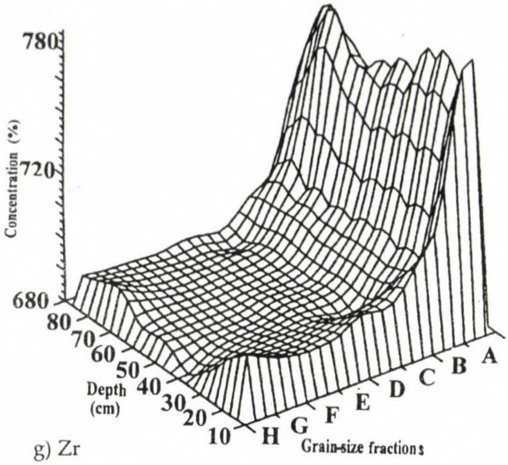

g) Zr

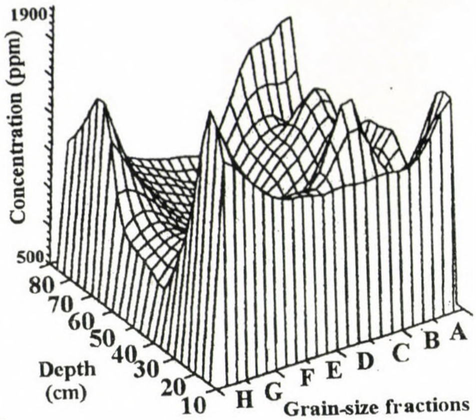

h) Ba

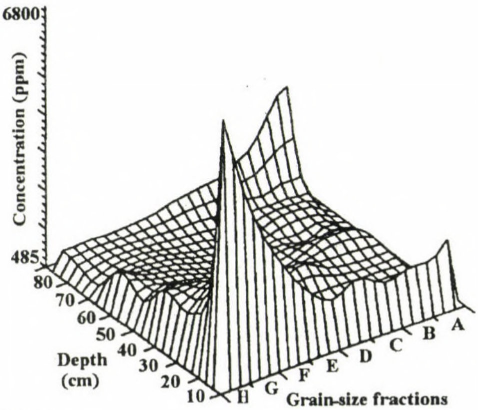

Fig. 3 a–i
Distribution of some trace elements of the soil as a function of grain-size fractions and depth

i) Mn

kaolinite was present only in traces, mainly in the smallest grain-size fractions. Intensive diffracted lines without any interference were chosen for semi-quantifying the minerals. The Bragg angle and the (hkl) Miller indexes of the used lines are shown in Table 3.

The mineralogical compositions of fractions A to H determined semi-quantitatively were plotted in three dimensions. Results of the mineral distribution of the soil are compiled in the series of Figs 1b–g.

Major and trace elements

The concentration of major chemical components and trace elements in individual grain-size fractions taken from 0–10 cm depth is shown in Tables 5 and 6 as an example. Data for major and trace elements plotted as a function of depth

Table 5
Concentration of main components of soil collected from 0-10 cm depth (the concentrations relates of ignited samples at 1000 °C)

Oxides	Concentration of major components in different grain size fractions [m/m%]							
	5μm	5–10 μm	10–20 μm	20–45 μm	45–80 μm	80–160 μm	160–315 μm	315–800 μm
MgO	4.36	2.58	2.21	1.88	1.81	1.76	0.53	0.38
Al_2O_3	20.38	15.13	12.88	10.41	6.71	5.25	4.63	3.05
SiO_2	60,.68	70.70	74.81	80.37	86.56	87.32	90.74	88.56
K_2O	1.77	1.63	1.46	1.10	0.84	0.74	0.74	0.79
CaO	1.70	1.44	1.45	1.26	0.81	0.57	0.40	0.31
TiO_2	1.81	1.34	1.36	1.06	0.88	0.49	0.18	0.22
Fe_2O_3	9.79	6.18	4.82	2.93	2.14	1.81	1.31	2.64

All the results are concerned for ignited soil fractions at 1000 °C

and grain-size fractions can be seen in Figs 2 and 3. The distribution diagram of montmorillonite is shown in Figs 2a and 3a for comparison.

Conclusions

1. We can draw the first important conclusion in relation of the grain-size distribution. Representing graphically the distribution of masses according to particle-size domains (Fig. 1a) we obtained a curve with two peaks. The position of the first peak (60% of the whole mass) is in the grain size fraction $< 5\ \mu m$ (containing montmorillonite as the main constituent). The second peak (with approx. 22%) is at the size class of 45–80 μm of particles (containing feldspars + muscovite + chlorite).

2. The mineral composition of particle classes is heterogeneous; the individual minerals are not distributed among the fractions proportionally, but have maxima in some fractions, while in other fractions they can be missing.

Table 6
Concentration of trace elements in the soil fractions from 0-10 cm depth

Element	Concentration of trace elements in different grain size fractions [ppm]							
	5μm	5–10μm	10–20μm	20–45μm	45–80μm	80–160 μm	160–315 μm	315–800 μm
^{25}Mn	4176	2674	2098	1702	1386	1631	1995	8094
^{28}Ni	146	100	93	73	64	56	43	64
^{30}Zn	386	275	235	163	83	62	87	134
^{37}Rb	308	153	133	101	73	49	69	61
^{38}Sr	334	209	230	186	145	108	87	103
^{39}Y	162	100	108	73	43	36	19	50
^{40}Zr	403	360	707	452	408	142	111	162
^{56}Ba	1970	2109	2538	2229	1509	1434	1198	1892
^{82}Pb	23	28	22	23	10	12	14	26

Considering montmorillonite (Fig. 1c), one can observe that the relative quantity of the mineral increases with decreasing particle size. Such a pattern of distribution can come into existence only if the minerals mentioned are grown in-situ (authigenic). This is the case of in-situ formation of gypsum and chlorite (Fig. 1e) as well. The distribution of the calcite formed from soil solution also indicates in-situ mineral formation. Calcite was present only at the deepest layers, at 70–80 cm and 80–90 cm depth. No dolomite was present in the soil samples at all. In fact the parent material and the whole maar crater is carbonate-poor.

3. In the case of quartz (Fig. 1b) the quantity decreases with decreasing particle size, which is the consequence of decomposition of these minerals under given geologic conditions. Some of the quartz content should have come from other sources because the average quartz content of bentonite at Egyházaskesző was only 10–15%. The rapid decomposition of feldspars is a known phenomenon. It shows a typical decomposing character (Fig. 1d), but only below 30–40 cm depth.

4. Regarding the distribution of major elements of the soil it is not surprising that Al_2O_3 (Fig. 2c) and TiO_2 (Fig. 2e) follow the shape of montmorillonite. This is the case in the distribution of Fe_2O_3 as well (Fig. 2g). In the soil fractions no Ti-minerals were identified. The close identity of the concentration profile of these elements proves that Fe and Ti substitute Al in the lattice of montmorillonite. The SiO_2 content in the whole soil profile is mainly present as quartz (see Figs 1b and 2b). The CaO distribution is in good agreement with the calcite precipitation in the lower layers of the soil. There are only traces of calcite in the upper layers, while between 80–90 cm the concentration is above 20% (Fig 1g). This is in good agreement with the chemical analysis (Fig 2d).

5. Based on investigations of trace elements of the soil divided into grain-size fractions it was shown that distribution of individual elements according to fractions depends on the particle-size distribution. It was found that most of the measured trace elements: Zr, Y, Ni, Zn, Rb (Figs 3g, 3b, 3d and 3c) are mainly concentrated in the smallest grain-size fraction, so they are bound to montmorillonite or they are built into the interlayer spaces. From the agricultural point of view this is a very important conclusion because the mobility of these species is very high. It is also an explanation for the agricultural exploitation of alginite and basaltic bentonite. In the case of some trace elements, precipitation and dissolution processes follow each other. Two pairs of elements could have been paired according to their behavior. While one of them dissolves, the other precipitates at the same depth. These pairs of elements are Zr-Rb, Ni-Y, Sr-Zn, and Ba-Pb. In the fractions of larger grain-size fractions the quantity of quartz grows, yet this phase has no role in binding trace elements. Here the trace elements bound to feldspars are of more importance. Sequential extraction methods will shed light upon the open questions.

Acknowledgements

This paper is dedicated to Prof. Ernő Nemecz who has been the Teacher of the authors in many aspects of science and life.

The authors are indebted to Timea Horváth for her help in preparing the figures.

This work was supported by grant FKFP 0606/ 1997 and by the Hungarian Research Fund (OTKA) grant T026423.

References

Altaner, S. P., R.F. Ylagan 1997: Comparison of structural models of mixed-layer illite/smectite and reaction mechanism of smectite illitization. – Clays Clay min. 45/4, pp. 517–533.

Barna, Zs., M. Földvári 1992: Basalt bentonites of W. Hungary. Thermoanalytical measurements (abstract). – 12th Conf. Clay Min. Petr., Bratislava, 1992. Book of Abstracts 8.

Barna, Zs., M. Földvári 1996: Thermoanalytical examinations of basaltic bentonites. – :Olajpala, alginit, bazaltbentonit kutatása és hasznosítása 1987–1993. Research and application of oil shale, alginite and basaltic bentonite), Alginit Alapítvány, (Alginite Foundation), Budapest. pp. 77–80.

Bence, G., Á. Jámbor, Z. Partényi 1977: A Várkesző Malomsok környéki Alginit- (olajpala-) és bentonitkutatások eredményei (Exploration of alginite /oil-shale/ and bentonite deposits between Várkesző and Malomsok). – MÁFI Évi Jel. 1977, pp. 257–267.

Berrow, M.L. 1988: Sampling of Soils and Plants for Trace Element Analysis. – Anal.proc., 25/4, pp. 116–118.

Bohn, H., Mc Neal, B., G.A. O'Connor 1979: Soil Chemistry – John Wiley Sons New York, pp. 131–177.

Cuadros, J., S. Altaner 1998: Characterization of mixed-layer illite-smectite from bentonites using microscopic, chemical, and X-ray methods: Constraints on the smectite-to-illite transformation mechanism. – Am. Min., 83/7–8, pp. 762–744.

DeLong, S.E., D.B. McCullough 1973: Compton - scattered Tungs X-ray a Measure of Mass Absorption Coefficients in Rocks. – The Amer. Min., 58, pp. 1073–1075.

Eberl, D.D., V.A. Drits, J. Srodon 1998: Deducing growth mechanisms for minerals from the shapes of crystal size distributions. – Am. J. Sci., 298/6, pp. 499–533.

Farmer, W.J., B.D. Mitchell 1965: Clay Minerals. – Analytical Procedures, 7, pp. 42–45.

Follett, A.C., W.J. McHardy 1965: Chemical dissolution techniques in the study of soil clays. – Clay Minerals, 6, pp. 23–43.

Hindrich, L.B., B.L. Mcneal, G.O. O'Connor 1985: Talajkémia (Soil chemistry). Budapest, 3/1, pp. 92–113.

Hendricks, S.B., R.A. Nelson 1940: Hydration mechanism of the clay mineral montmorillonite saturated with various cations. – Journ. Am. Ceram. Soc., 62, pp. 1457–1464.

Jenny, H.I.G. 1941: Factors in soil formation. – McGraw-Hill, London ? p.

Juhász, Z. 1989: A várkeszői bentonittípus technológiai tulajdonságai. – Földt. Kut., 32/4, pp. 65–70.

Nemecz, E. 1973: Clay Minerals. – Akadémiai kiadó, Budapest. pp. 61–62.

Nemecz E., Zs. Csikós-Hartyáni 1991: A novel method for studying weathering in soils. – OTKA Report, Veszprém.

Nemecz, E., Zs. Csikós-Hartyáni 1995: Processes in soils and paleosoils: A new method for the study of weathering. – Geo Journal, 36, 2/3, pp. 139–142.

Olaszi, V. 1996: A bazaltbentonitok ásványtani vizsgálata (Mineralogical examination of the basaltic bentonite,) – Olajpala, alginit, bazaltbentonit kutatása és hasznosítása 1987–1993. (Research and application of oil shale, alginite and basaltic bentonite1987–1993), Alginit Alapítvány, (Alginite Foundation), Budapest. pp. 67–70.

Pécsi, M., E. Nemecz, Zs. Hartyáni, T. Horváth 2000: The origin of the silt size quartz grains and minerals in loess. – Quaternary Int., pp. 68–71, 199–208.
Raab, G.A. 1988: Semiquantitative Analysis by X-ray Powder diffraction of the <2 mm and < 0,002 mm fractions of soil – Power Diffraction. 3/3, pp. 144–152.
Reynolds, R.C. 1967: Estimation of mass absorption coefficients by Compton scattering. – The Amer. Min., 52, pp. 1493–1497.
Solti, G. 1985: A pedological study of alginitic bentonite from Egyházaskesző. – Földtani Kutatás, 28/1–2, pp. 95–111.
Solti, G. 1996: Historical Review and perspective of the research work on oil shales and basaltic bentonites) – Olajpala, alginit, bazaltbentonit kutatása és hasznosítása 1987–1993. (Research and application of oil-shale, alginite and basaltic bentonite 1987–1993), Alginit Alapítvány, (Alginite Foundation), Budapest. pp. 22–23.
Solti, G., Gy. Csirik 1996: The Geology of the bentonite of Egyhazaskesző and Magyargencs – Olajpala, alginit, bazaltbentonit kutatása és hasznosítása 1987–1993. (Research and application of oil shale, alginite and basaltic bentonite1987–1993.), Alginit Alapítvány, (Alginite Foundation), Budapest. pp. 103–105.
Solti, G., Gy. Csirik, G. Rischak 1988: Összefoglaló földtani, készletszámítási és anyagvizsgálati jelentés az egyházaskeszői bentonit- alginit-telepek elő és felderítő szintű kutatásáról (Summary report on the geological, inventory and analytical investigations of bentonite-alginite deposites based on preliminary and recovery test). – MÁFI Évi Jel. 1988, pp. 257–267 Budapest.
Szendrei, G. 1994: Talajásványtan. – Módszertani Közlemények 1 Talajásványtan, MÁFI Budapest
Szendrei, G. 2000: Talajtan. – Eötvös kiadó, Budapest
Stefanovics, P. 1975: Talajtan. Mezőgazdasági Kiadó Budapest, pp. 44–58.
Tertian, R. 1968: Double dilution method in XRFS analysis. – Spectrohimica Acta, 23, pp. 305–321.
Tertian, R. 1968: Double dilution method. – C.R. Acad. Sc. Paris, 266, pp. 617–619.
Viczián, I. 1996: A Kisalföldi olajpala és bazalt-bentonit ásványtani összetétele (Mineralogical composition of the oil shales and basaltic bentonites of the Little Hungarian Plain) – Olajpala, alginit, bazaltbentonit kutatása és hasznosítása 1987–1993. (Research and application of oil-shale, alginite and basaltic bentonite1987–1993), Alginit Alapítvány, (Alginite Foundation), Budapest pp. 72–76.
Webb, J.S., A.W. Rose 1979: Geochemistry in mineral exploration. – Academic Press, 7, pp. 149–153.
Wilband, J.T. 1975: Rapid Method for background Corrections in trace Element Analysis by X-ray Fluorescence Analysis – The Amer. Min., 60, pp. 320–323.
Zsolnay, I.M., J.M. Brauer, S.A. Sajka 1984: X-ray fluorescence determination of trace elements in soil. – Anal. Chim. Acta, 162, pp. 423–426.

Acta Geologica Hungarica, Vol. 43/4, pp. 447–461 (2000)

Advanced methods of thermal analysis in the investigation of clay minerals

Mária Földvári
Geological Institute of Hungary, Budapest

In this paper, the application of the new techniques and principles of thermal analysis to the characterization of clay minerals is presented. The Derivatograph-Pc equipment, beside the recording of the classical DTA and TG curves, is suitable for the calculation of the second derivatives of primary curves and the estimated kinetic parameters from the non-isothermal TG and DTG curves. Beside dynamic thermal analytical measurements, examinations can be carried out with isothermal or quasi-isothermal heating programs. By using the corrected thermal decomposition temperature the measured data become more characteristic and comparable. Using these methods the thermal analysis is suitable not only for the identification, but also for the deeper recognition of the nature, the structure and the specific properties of clay minerals.

Key words: thermal analysis, clay minerals, reaction kinetics, second derivative of thermal curves, "Quasi-isothermal" thermal analysis, corrected decomposition temperature

Introduction

Thermal analysis plays a specific role in the identification and quantitative determination of mineral components of rocks. The most widespread methods used for the investigation of minerals (inclusive of clay minerals) are differential thermal analysis (DTA) and thermogravimetry (TG), as well as (especially in the ceramic industry) thermodilatometry (TD) (Schomburg and Störr 1984). Both differential thermal analysis and thermogravimetry methods are useful in identification. They should be able, besides providing qualitative data, also to give quantitative, or at least semiquantitative, information, with the thermogravimetric method being more accurate than that of differential thermal analysis.

The classical thermoanalytical methods in the last decades were developed with new principles and measurement techniques. Hungarian specialists played a leading role in these methodology and instrument developments The different generations of the derivatograph well reflect this (Paulik et al. 1958; Paulik and Paulik 1971; Paulik and Paulik 1971, 1972, 1973, and 1986; Paulik et al. 1982–1984). The derivatograph-Pc, the microcomputer-operated latest type of these systems, summarizes the advantages. It can be used for the simultaneous recording of thermogravimetric, derivative thermogravimetric, thermogastitrimetric, differential thermoanalytical and thermodilatometric curves. The second

Address: M. Földvári: H-1143 Budapest, Stefánia út 14, Hungary
Received: 27 March, 2000

derivatives of primary curves (DDTG, DDTA etc.) can also be produced with the microprocessor. Beside dynamic thermal analytical measurements, examinations can be carried out with isothermal or quasi-isothermal heating programs (Paulik et al. 1987), when the heating in the investigated temperature interval is self-regulated (Q–TG, Q–DTA etc.). The software of the equipment calculates the estimated kinetic parameters from the non-isothermal TG and DTG curves as a function of time (Arnold et al. 1987). The new possibilities are useful for the investigation of geologic samples as well (Földvári 1990).

Thermal reactions of clay minerals

Clay minerals are the most intensively investigated group of silicates by thermal analysis. This paper contains some practical examples of the above-mentioned methods used for the examination of clay minerals. The main thermal reactions of clay minerals are dehydration, dehydroxylation and different kinds of phase transition at high temperature. The dehydration process gives information about of interlayer space, the dehydroxylation process about the octahedral sheet and both about the order of the structure. The high temperature endothermic–exothermic inversion represents the transition of the structure to an amorphous state through decomposition and crystallization of new phases (e.g. cristobalite, mullite, olivine, spinel, enstatite, and others)

Dehydration

Dehydration is the removal of water molecules bound to the external surface (so-called sticking water) and in the internal spaces of the structure by van der Waals forces. This water may appear because the net negative charge of the crystal-forming layer complex can be balanced by exchangeable cations and by water molecules. The reason for the negative charge of the structure is the tetrahedral and octahedral cation substitution. Thus, Si is partially replaced by Al and sometimes Fe^{3+} in the tetrahedral sheet, and Al atoms of the octahedral sheet are partially replaced by Mg or Fe^{2+}. In certain trioctahedral clay minerals the charge due to ionic substitutions in the octahedral sheet may be positive, the total charge of the silicate layer, however, is always negative.

Beside the charge of the structure, the amount of water on the external surface depends on the structure of the atomic planes. The oxygen plane and the hydroxyl plane have different wettability properties. When the hydroxyl plane is on the external surface of the clay mineral (TO minerals), it does not form hydrogen bonds with adsorbed water molecules. The oxygen plane, however, may form hydrogen bounds with water molecules, when it is located on the external surface – that is, the hydrophilicity increases with decreasing Si-O-Si angle of the siloxane (Si-O-Si) group.

Water adsorption also occurs on the edge surfaces. The exposed functional groups are very active because their valences are not as completely compensated as they were in the interior of the crystal. The surface properties depend greatly upon the exposed atoms. The charges may be balanced by the adsorption of cations or anions. Adsorption of water on this surface takes place via three mechanisms (Yariv 1992) and the adsorbed water can be divided into three zones (Yariv and Cross 1979): dissociative chemisorption, hydration of exchangeable ions (A_m zone) and hydrogen bonding between the water molecules and exposed hydroxyls or oxygen atoms (A_b zone). The third B_{bm} zone serves as a bridge between the two other zones.

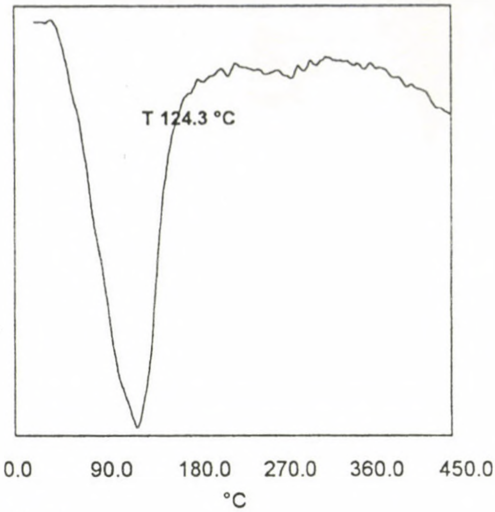

Fig. 1
DTG curve of natural montmorillonite, Magyargencs borehole-7, Hungary

The interlayer space of certain clay minerals may contain free water molecules and water adsorbed directly to the active sites or in the second or third layer between the two parallel silicate sheets, bordered by oxygen planes of siloxane groups. In the interlayer space, the exchangeable compensating cation is surrounded by a co-sphere due to the electrostatic interaction between the cation and water molecules. In the co-sphere the organization of water molecules differs from that in the remainder of the interlayer space. Accordingly, three zones may be distinguished in the interlayer space, zones A_o, A_m and B_{om}, respectively (Yariv and Cross 1979). Two zones contain ordered water; the third is a disordered zone (B_{om}) separating the zones A_o and A_m. The structure of the interlayer water depends upon the nature of the oxygen planes, which border the interlayer space on one hand, and, upon the other, on the nature of the exchangeable cations located in the interlayer space. The nature of the oxygen plane depends on the charge of the silicate layer and on whether the charge results from tetrahedral or octahedral substitution. The size of zone A_m decreases with increasing ionic size and increases with increasing ionic charge.

The binding energy of all kinds of adsorbed water is low (1–25 kjoule/mol). Due to the comparatively weak bond, the water can escape at relatively low temperatures. Under traditional conditions of thermoanalytical investigations the adsorbed water can be removed at 40–180 °C and in most cases can form a single peak in the DTA and DTG curves (Fig. 1). Sometimes the water species adsorbed in different positions on the external surfaces and edge may be recognized on the low temperature side of the peak (Fig. 2). In this low temperature interval the escape of the "quarry-sap" water of low-binding energy may be observed (Fig. 3). Somewhat higher is the binding energy of water molecules coordinated around the cations (Fig. 3; peak at 201 and 204 °C). The hydration energy is also closely connected to the charge and radius of the cation. The higher the hydration energy, the higher the temperature of the water loss. The elimination of water linked to cations and that of other forms of water in the interlayer space is distinguished in the DTA and DTG curves when the hydration energy of the cation is sufficiently high (Mg, Mn, Ca, Cu, Li, etc.). Fig. 3 shows a DTG curve of natural Ca-montmorillonite with a peak maximum at 201 and 204 °C and Fig. 4 a Mn saturated montmorillonite with a peak maximum at 258 °C. The estimation of water loss linked to the interlayer bivalent cations with lower hydration energy (Ba, Hg, Cd, Ag, etc.) is possible by means of the second derivative of the TG curve (DDTG curve; Fig. 5, Földvári et al. 1998). In

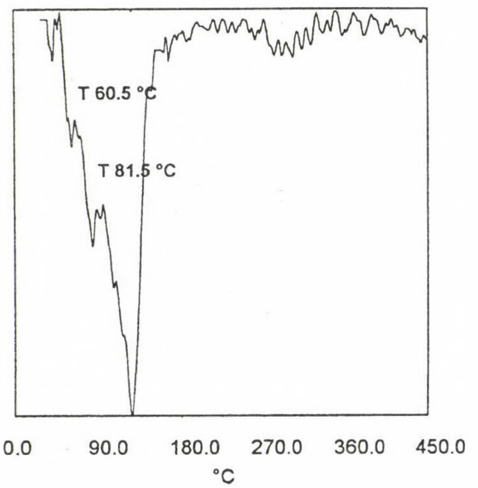

Fig. 2
DTG curve of natural montmorillonite, Stejera, Romania

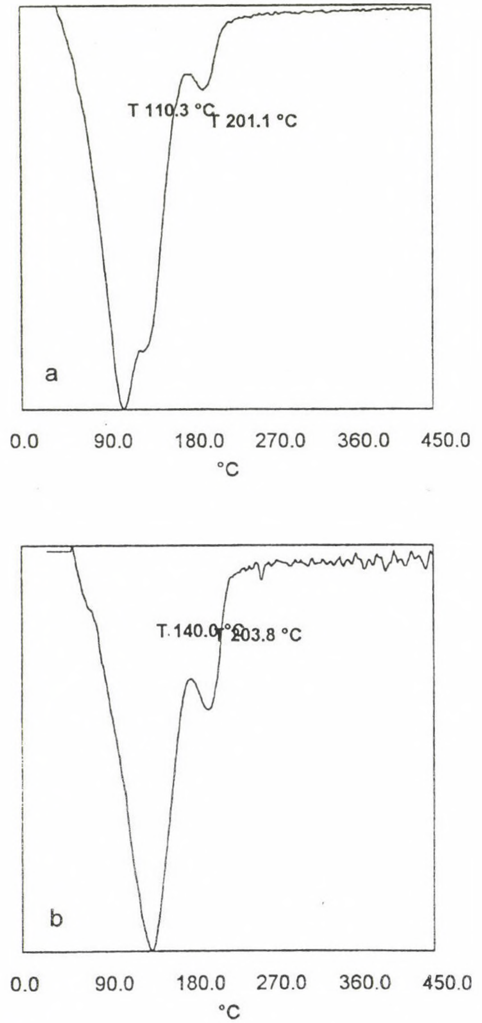

Fig. 3.
DTG curve of natural montmorillonite, Buru, Romania: a) "quarry-sap" state. b) in air-dried state after five months

the case of monovalent ions (due to their large size and low electric charge) the hydration zone of the exchangeable cation and the binding energy are small, and therefore this water is invisible even after the second derivation (Fig. 6). By using the second derivative of curves the water types bound with different low energies are often visible separately (Fig. 7).

Dehydroxylation

The water escaping in the course of thermal dehydroxylation is an integral part of the structure which it influences. It is not present in molecular form in the structure; therefore the mechanism of the thermal dehydroxylation, like the thermal dissociation process, consists of two phases:

1. Formation of the escaping components (ionic → molecular form) – in the case of hydroxides: proton accommodation (for carbonates, sulfates, etc.: oxygen rejection)
2. Loss of decomposition product.

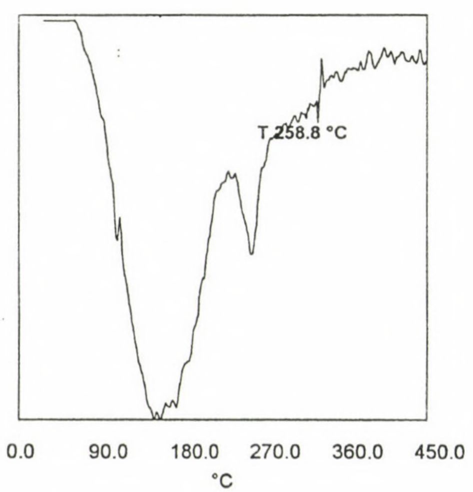

Fig. 4
DTG curve of montmorillonite, Istenmezeje, Hungary after Mn saturation with $Mn(ClO_4)_2$

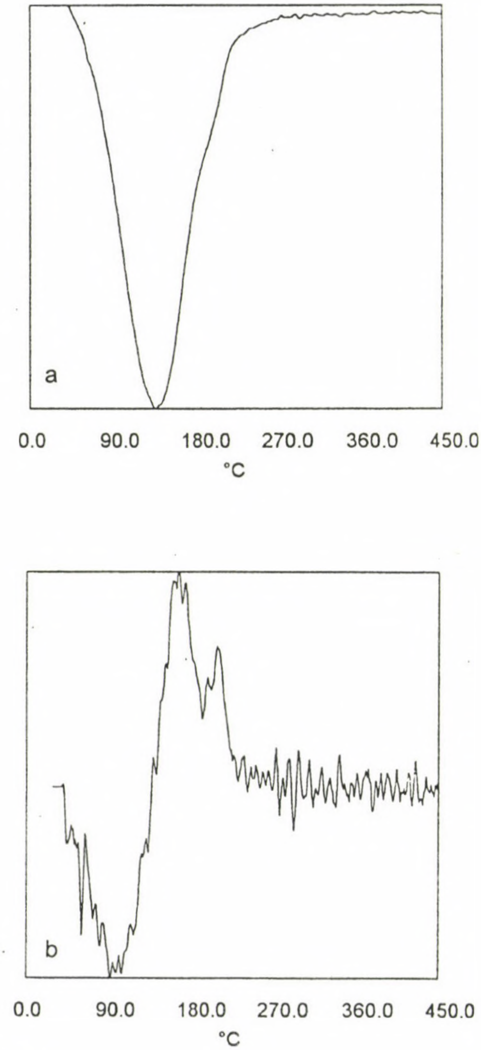

Fig. 5
a) DTG and b) DDTG curve of montmorillonite, Istenmezeje, Hungary after Hg saturation with $HgCl_2$

In the case of dehydroxylation, because of the much stronger ionic or covalent bonds in the structure, the process is influenced by structure of the lattice and by the nature of the compound, modifying the conditions of the thermodynamic phase equilibrium. Among these factors bonding strength should be mentioned first.

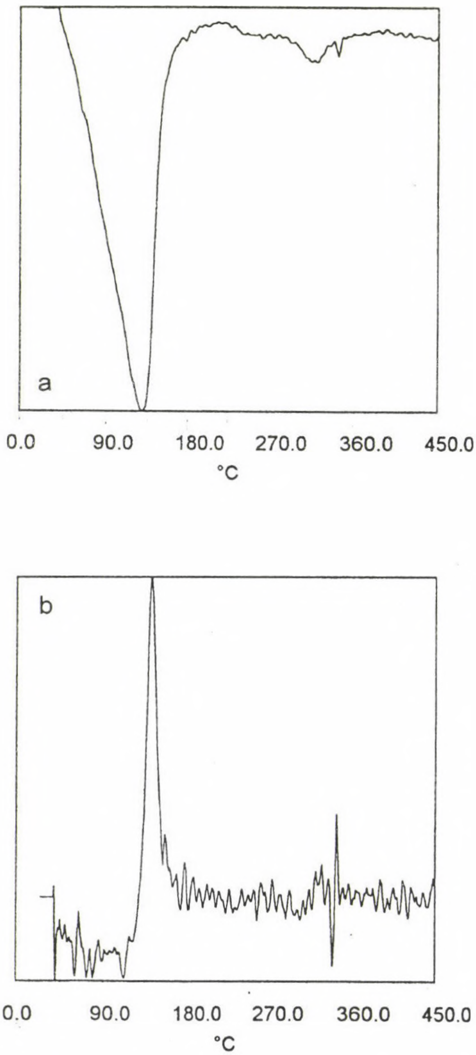

Fig. 6
a) DTG and b) DDTG curve of montmorillonite, Buru, Romania after Na saturation with NaCl

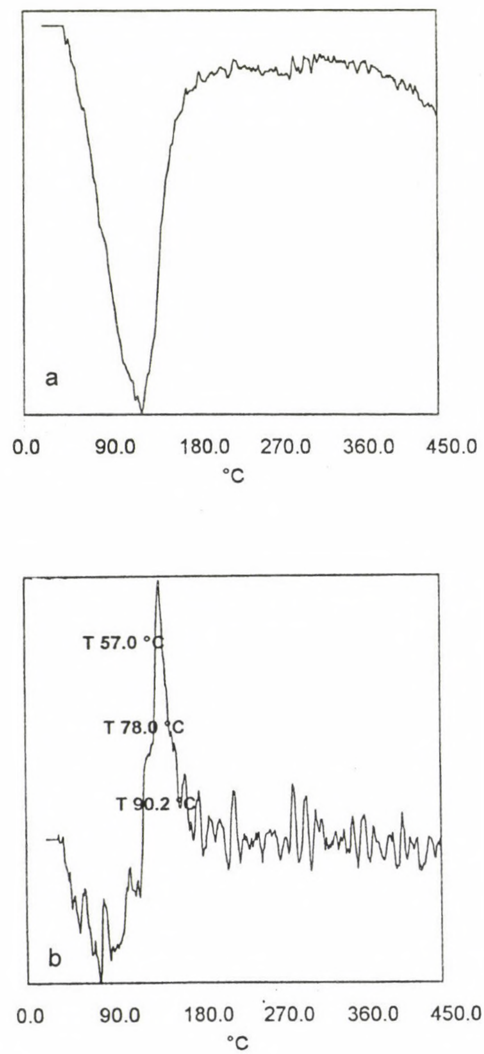

Fig. 7
a) DTG and b) DDTG curve of natural montmorillonite, Magyargencs borehole-7, Hungary

The decomposition temperature of a given bond is also determined by the structure of the lattice. The phenomenon is jointly resulted by several factors. On one hand part of the structure not directly participating in the bond has an indirect impact on the bond strength and the stability of the structure. The possibility of the necessary diffusion in the course of the decomposition process is also influenced by the structure. In the case of hydroxides the diffusion takes place in both stages of the decomposition (proton migration to form water molecules from the individual OH groups and removal of water). For molecule development with oxygen rejection, of course, the process will occur in an in-place manner; therefore diffusion plays a role only in the removal of the escaping component from the crystal lattice. In the case of hydroxides the structure may determine the number and distance of OH-groups yielding water during thermal dissociation, and their position within the lattice structure may influence the decomposition temperature as well. Dehydroxylation processes of phyllosilicates well reflect their structural differences. The fact that a majority of the OH-groups are found on the surface of the layers for 1:1 phyllosilicates, but within the layer complex for 2:1 phyllosilicates, is also reflected by the thermal curves of phyllosilicates. The third factor influencing the decomposition temperature is the ability of the residual structure to transform. This is because the accommodation of oxygen generally requires that the residual structure should change the co-ordination number, which is only feasible at a certain temperature.

The dehydroxylation process is essentially of isothermal character (see portlandite, Fig. 8). The more complicated lattice structure is expressed not only by the shift of the reaction to higher temperatures, but also by the fact that the process of the reaction will be increasingly farther away from the zero-order isothermal character (see böhmite, kaolinite, pyrophyllite; Fig. 8) (Földvári et al. 1988).

Based on what has been discussed above the dehydroxylation of two types of clay minerals will be presented.

Dehydroxylation of kaolinite group minerals

In the structure, or more exactly in the octahedral sheet of kaolinite, cation substitution is subordinate. The main factor which influences the process of dehydroxylation is the order of the structure, which well reflects the geologic processes (genesis, alteration, etc.).

Various instrumental analytical methods – including some thermoanalytical methods – have been used for the determination of the polytype modifications, crystallinity and the degree of ordering of kaolinite group minerals. Table 1 summarizes the most important thermoanalytical data based on the approximately two hundred kaolinite samples carried out so far by the author (Földvári and Kovács-Pálffy 1993; Földvári 1997).

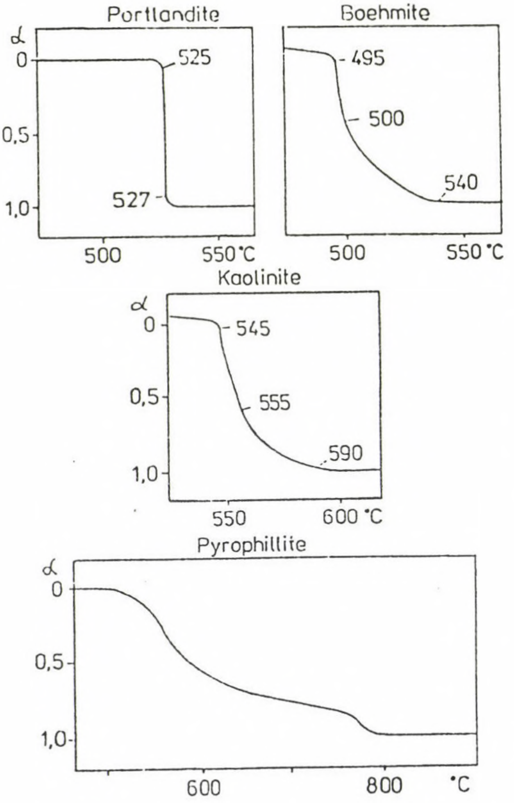

Fig. 8
Q-TG curves of portlandite, böhmite, kaolinite and pyrophyllite

The most important thermoanalytical parameters are corrected decomposition temperature and activation energy. The use of corrected (or interpolated) decomposition temperature allows the elimination of the temperature differences of a given reaction caused by the different quantity of the phases participating in the reaction. It is well known that the peak temperature of a decomposition process depends, among other things, on the quantity of the decomposed gas or vapor product because of their partial pressure. The relation between peak temperature and concentration is logarithmic (Smykatz-Kloss 1974):

$$T = c \times (\log M + T1)$$

where T = the measured temperature
M = quantity of the investigated phase
T1 = temperature of the decomposition of 1 mg of the phase
c = specific constant of reaction

An extrapolation of the measured peak temperature, considering the mass change during the decomposition process measured on the TG curve compared to a standard quantity of the decomposed products, makes the peak temperature data suitable for direct characterization and comparison (Földvári 1999).

Corrected dehydroxylation temperature (T_{corr}) of kaolinites were obtained by extrapolation of the measured dehydroxylation temperature data to 18 mg water loss during the dehydroxylation based on the empirical equation

$$T_{corr} = 42.3x + 495.5\ ^{\circ}C$$

where 495.5 °C is the dehydroxylation temperature of 1 mg of kaolinite (0.14 mg OH loss). The slope was obtained by dividing the temperature increase by the increase of the mass loss by one order of magnitude in the case of kaolinite. By doing this the data become characteristic and comparable in spite of the fact that the sample weight and kaolinite content are different from sample to sample.

Calculation of characteristic kinetic parameters of thermal reactions from thermoanalytical curves began about 40 years ago. A great variety of calculation methods was developed in the past and there is much discussion about the applicability of the methods. The two basic subjects of the debates are the mathematical procedures and their physico-chemical interpretation. Independently of the rigorous physico-chemical meaning, the virtual kinetic parameter triplets (reaction order (n), activation energy (E) and pre-exponential factor (lg A)) may be suitable for the numerical characterization of the reaction investigated. The values of kinetic parameters cannot be compared with parameter values estimated by means of other methods but under strictly defined conditions they are usually reproducible. Often a relationship may be found between the virtual kinetic parameters and certain properties of the material. For the software of the computerized Derivatograph a simple method has been developed for the estimation of the formal-kinetic parameters (Arnold et al. 1987).

The reaction order n is calculated by the Kissinger method (Kissinger 1957):

$$n = 1.26(a/b)^{1/2}$$

where a and b are the sections of the DTG baseline before and after the DTG peak maximum.

The activation energy formula (Arnold et al. 1987) is:

$$E = \frac{n \cdot \left[\ln(1-a_1) - \ln(1-a_2)\right]}{\left(1/T_1 - 1/T_2\right)} R$$

where αi are the weight percentages of the decomposed phase at the selected points

Ti = temperatures of the half values of the DTG curve (in degrees Kelvin)

R = universal gas constant.

The pre-exponential factor A is obtained by the equation

$$\log A = \log 0.2 \ \frac{R}{E} \ e^x(x^2+2x)+\log G$$

$$\text{where } x = \frac{E}{R \cdot T_3}$$

T_3 = temperature at conversion degree 0.2

G = rate of linear heating

The computation method yields acceptable results only for one step processes. In the case of overlapping processes of several steps, the calculated parameters make no sense.

The activation energy data in Table 1 reflect well the structural and OH position differences of high temperature dickite (or dickite-like) polytypes and the resulting differences in the kinetics of dickite dehydroxylation (Stoch and Waclawska 1981; Stoch 1984). The variation of values is similar to the proportion of the absorptions of the outer and the inner OH-stretching of kaolinite and dickite measured by IR spectroscopy.

Table 1
The main characteristic thermoanalytical parameters of kaolinites of different genesis

Genetic type	Geologic effect	Number of samples	T_{corr} of dehydroxylation (°C)	Activation energy (joule/mol)	Temperature of the exothermic peak (°C)
			mean	mean	mean
high temperature hydrothermal	temperature	11	651	114	1005
low temperature hydrothermal	temperature	22	578	165	996
paleosol (Devonian)	diagenesis	6	577	139	996
paleosol (Triassic)	diagenesis	3	565	144	972
low temperature weathering		61	564	133	959
bauxite		29	561	132	967
terrestrial sandstone		57	562	127	959
soil		2	556	112	940
paleosol (Pleistocene)		4	547	96	934
all		195	570	137	969

Dehydroxylation of smectite group minerals

The species of the smectite group differ from each other – even if the order of the structure is not considered – in the composition of octahedral sheet, which influences the temperature of dehydroxylation.

A decrease in electronegativity of a cation in the octahedral sheet generally results in an increase of the bonding strength and accordingly in an increase of the dissociation temperature (Földvári 1991). Table 2 summarizes the dehydroxylation temperatures of the genetically primary smectites.

Figure 9 is based on the thermoanalytical measurements on smectites varying in composition between nontronite and iron-beidellite in the Upper Pannonian maar-type basaltic bentonite, where the smectites are montmorillonite with a high iron content (Barna and Földvári 1996), and in certain sections iron-beidellite (Juhász 1989). The slope of the sample amount dependence curve is less

Table 2
Specific temperature intervals of dehydroxylation of smectite species

Subgroup	Species	Octahedral cations	Electronegativity (after Pauling)	Dehydroxylation
Dioctahedral	volkhonskoite	Cr, $Fe^{(3)}$		390-470 °C
	nontronite	$Fe^{(3)}$	1.9	400-500 °C
	beidellite	Al	1.5	550-600 °C
	montmorillonite	$Al_{0.8}Mg_{0.2}$		≈ 700 °C
Trioctahedral	sauconite	Zn(Mg, Al, $Fe^{(3)}$)	1.6	700-750 °C
	hectorite	Mg, Li		850-900 °C
	saponite	Mg	1.2	850-900 °C

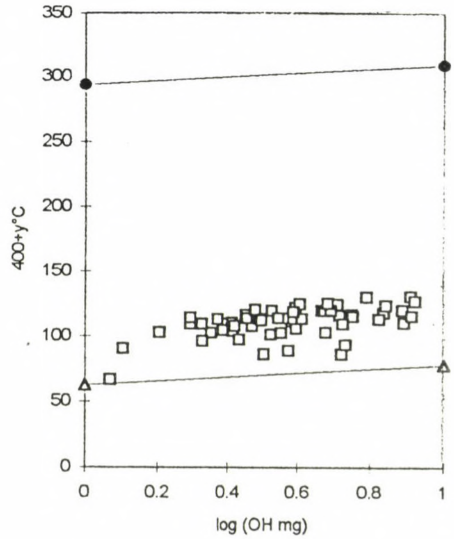

Fig. 9
Sample amount dependence curve of nontronite, Pálháza, Hungary and montmorillonite (American drilling mud) as calibration curves with the measured data of basalt bentonite, Magyargencs, Egyházaskesző, Gérce, Hungary

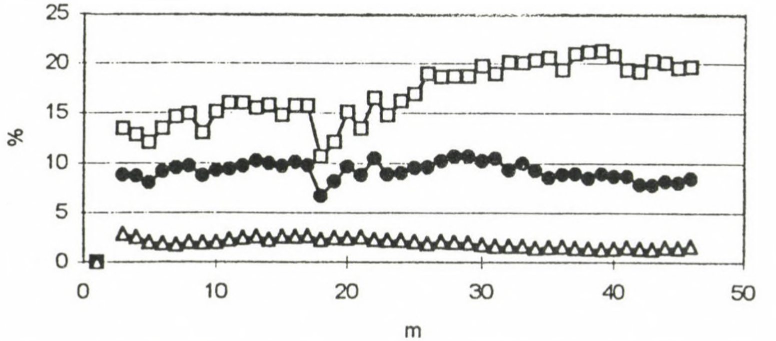

Fig. 10
Variation of Al_2O_3, Fe_2O_3 and MgO content in the section of Egyházaskesző Ekt-22 borehole, Hungary

steep than that of kaolinite (see previous section), the equation of the calibration curve for nontronite T_{corr} is 15.2x+462 °C, for the montmorillonite 15.4x+693 °C.

It can be well observed in the Egyházaskesző Ekt-22 borehole (Fig. 10) that the composition of smectite approaches that of beidellite with increasing depth. The relationship between composition and thermoanalytical data is demonstrated by the diagram showing Al_2O_3, Fe_2O_3 and MgO contents versus the proportion of molecular water/hydroxyl water contents of smectites in the samples of the Ekt-22 section (Fig. 11).

The quasi-isothermal measurement technique – without the second derivative – is suitable for the separation of the overlapping thermal reactions. The decomposition of böhmite and kaolinite often overlap between 400 and 650 °C. Fig. 12 shows the TG and DTG curves of a bauxite sample and the two different methods (DDTG and Q-TG) used for the separation of the overlapping peak. Table 3 summarizes the results of the different measurements.

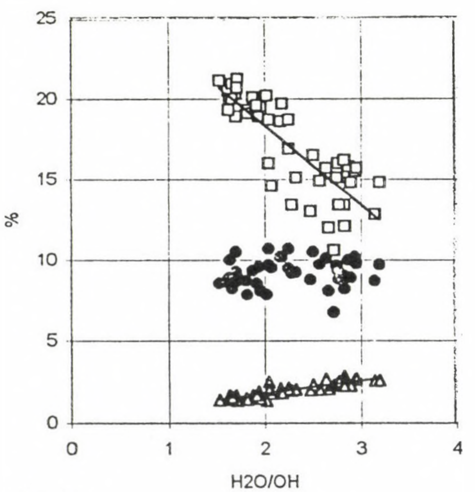

Fig. 11
Al_2O_3, Fe_2O_3 and MgO content versus proportion of molecular water/hydroxyl water contents of smectites measured by thermal analysis in the samples of the section Egyházaskesző Ekt-22, Hungary

Table 3
Results of quantitative determination of böhmite and kaolinite by different methods

	böhmite	kaolinite
TG - DTG	54–59 %	
DDTG	45 %	10 %
Q-TG - Q-DTG	44 %	11 %
XRD	42 %	11 %

Conclusions

In geology, thermal analysis is generally applied to the qualitative and quantitative determination of the mineral components of rocks. Based on the above examples it can be stated that the advanced techniques and the calculated parameters provide increased information about the nature, the structure and the specific properties of clay minerals.

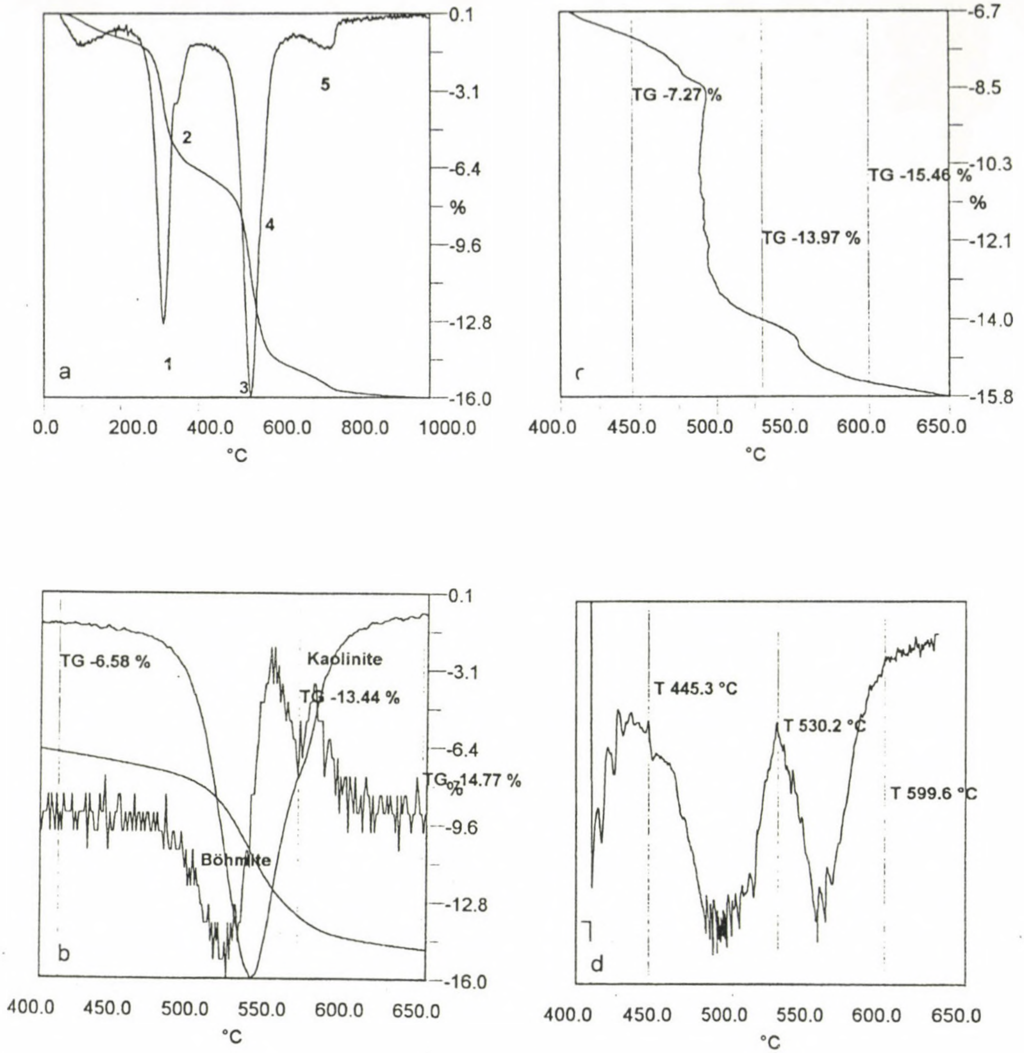

Fig. 12
a) TG and DTG curves of a bauxite sample, Nyirád, Hungary. 1. gibbsite, 2. goethite, 3. böhmite, 4. kaolinite, 5. dolomite. b) TG, DTG and DTG curves of the same sample between 400 and 650 °C. c/ quasi-isothermal TG curve of the same sample between 400 and 650 °C. d/ Q-DTG curve of the same sample

References

Arnold, M., P. Somogyvári, J. Paulik, F. Paulik 1987: The Derivatograph-C. A microcomputer-controlled simultaneous TG, DTG, DTA, TD and EGA apparatus. Part II. A simple method of estimating kinetic parameters. – Journal of Thermal Analysis, 32, pp. 679–683.

Barna, Zs., M. Földvári 1996: Thermoanalytical examinations of basaltic bentonites. – In: Olajpala, alginit, bazaltbentonit kutatása és hasznosítása 1987–1993. Alginit Alapítvány kiadása, Budapest. pp. 77–80.

Földvári, M. 1990: New possibilities in phase analysis of rocks with derivatograph-c. – Journal of Thermal Analysis, 36, pp. 1707–1715.

Földvári, M. 1991: Measurement of different water species in minerals by means of thermal derivatography – In: Series of Lecture Notes in Earth Sciences 38. Thermal Analysis in the Geosciences. – Springer Verlag, Berlin–Heidelberg–New York–London–Paris–Tokyo–Hong Kong–Barcelona–Budapest. pp. 84–100.

Földvári, M. 1997: Kaolinite genetic and thermoanalytical parameters. – Journal of Thermal Analysis, 48, pp. 107–119.

Földvári, M. 1999: The use of corrected thermal decomposition temperature in the geological interpretation I. – Journal of Thermal Analysis, 56, pp. 909–916.

Földvári, M. et al. 1988: Possibility of thermal analysis of different types of bonding of water in minerals. – Journal of Thermal Analysis, 33, pp. 121–132.

Földvári, M., P. Kovács-Pálffy 1993: A critical study on crystallinity measurement of kaolinites. – Romanian Journal of Mineralogy, 76/1, pp. 109–119.

Földvári M., P. Kovács-Pálffy, N.M. Nagy, J. Kónya 1998: The use of the second derivate of thermogravimetric curve for the investigation of exchanged interlayer cation in montmorillonite. – Journal of Thermal Analysis, 53, pp. 547–558.

Juhász, A. Z. 1989: A várkeszői bentonit típus technológiai tulajdonságai (The technological properties of the bentonite type of Várkesző). – Földtani Kutatás, 32/4, pp. 65–70.

Kissinger, H.E. 1957: Reaction kinetics in differential thermal analysis. – Anal. Chem., 29, pp. 1702–1706.

Paulik F, J. Paulik, L. Erdey 1958: The Derivatograph I. An automatic recording apparatus for simultaneously conducting differential thermal analysis, thermogravimetry and derivative thermogravimetry. – Z. Anal. Chemie, 160, pp. 241–252.

Paulik, F, J. Paulik 1971a: Complex thermoanalytical method for the simultaneous recording of T, TG, DTG, DTA, TGT, DTGT, TD and DTD curves. – Thermochimica Acta, 3, pp. 13–15.

Paulik, J., F. Paulik, 1971b: "Quasi-isothermal" thermogravimetry – Anal. Chim. Acta, 56, pp. 328–331.

Paulik, F., J. Paulik, 1972: Kinetic studies of thermal decomposition reactions under quasi-isothermal and quasi-isobaric conditions by means of the derivatograph. – Thermochimica Acta, Amsterdam, 4, pp. 189–198.

Paulik, F., J. Paulik, 1973: Investigations under quasi-isothermal and quasi-isobaric conditions by means of the derivatograph. – Journal of Thermal Analysis, London–Budapest, 5, pp. 253–270.

Paulik, F., J. Paulik 1986: Thermoanalytical examination under quasi-isothermal and quasi-isobaric conditions. – Thermochimica Acta, 100, pp. 23–59.

Paulik, F., J. Paulik, M. Arnold 1982–84: Simultaneous TG, DTG, DTA and EGA Technique for the determination of carbonate, sulphate, pyrite and organic materials in minerals, soils and rocks I., II., III. – Journal of Thermal Analysis, 25, pp. 327–340; 29, pp. 333–344, 345–351.

Paulik, J., F. Paulik, M. Arnold 1987: Derivatograph-C. A microcomputer-controlled simultaneous TG, DTG, DTA, TD and EGA apparatus. Part I. – Journal of Thermal Analysis, 32, pp. 301–331.

Schomburg, J., M. Störr 1984: Dilatometerkurvenatlas der Tonmineralrohstoffe. – Akademie-Verlag, Berlin pp. 1–88.

Smykatz-Kloss, W. 1974: Differential thermal Analysis. Application and Results in Mineralogy. – Spinger Verlag, Berlin–Heidelberg–New York. pp. 11–13.

Stoch, L. 1984: Significance of structural factors in dehydroxylation of kaolinite polytypes. – Journal of Thermal Analysis, 29, pp. 919–931.
Stoch, L., I. Waclawska 1981: Dehydroxylation of kaolinite group minerals. II. Kinetics of dickite dehydroxylation. – Journal of Thermal Analysis, 20, pp. 305–310.
Yariv, S. 1992: Wettability of Clay Minerals – In: Schrader, M. E., G.I. Loeb (Ed.): Modern approaches to Wettability: Theory and applications.– Plenum Publishing Corporation, New York. pp. 279–326.

Acta Geologica Hungarica, Vol. 43/4, pp. 463–476 (2000)

Magnetotactic bacteria and their mineral inclusions from Hungarian freshwater sediments

Mihály Pósfai, Balázs Arató
Department of Earth and Environmental Sciences
University of Veszprém

Magnetotactic bacteria produce nano-scale, intracellular magnetic minerals. The study of such minerals is of interest because it can shed light on biogenic mineral-forming processes, and on the potential contribution of biomagnets to the magnetic signal of sediments and rocks. We collected sediment and water samples from several Hungarian lakes and streams. Magnetotactic bacteria were present in all studied environments; in some samples they occurred in such large numbers that their mineral inclusions likely represent a major source for sediment magnetism. After magnetic enrichment of magnetotactic species, we characterized distinct morphological types using a light microscope. Our systematic study showed that a few bacterium types are widespread in most of the studied freshwater environments.

Using transmission electron microscopy, we studied the composition, microstructure, sizes and habits of magnetite particles from a helicoid magnetotactic bacterium from Gyöngyös stream, Szombathely. Size and shape distributions of the intracellular crystals show some distinct features that may be used for distinguishing bacterial from non-biogenic magnetite and for identifying possible mechanisms of crystal growth. In particular, the crystal size distribution (CSD) curve is highly asymmetric, consistent with previous observations on magnetite from magnetotactic bacteria. The asymmetry and our new observation of two maxima in the CSD suggest that Ostwald ripening and crystal agglomeration played important roles in the formation of the nano-scale magnetite particles.

Keywords: magnetotactic bacteria, morphological types, BCM, magnetite, crystal size distribution

Introduction

Magnetotactic bacteria grow magnetic minerals (magnetite, Fe_3O_4 or greigite, Fe_3S_4) within their cells. Since their discovery 25 years ago (Blakemore 1975), many different types of magnetotactic bacteria were found in diverse aquatic environments (Bazylinski and Moskowitz 1997); they are widespread in both freshwater and marine environments and in some sediments can be even the dominant species (Spring et al. 1993). Therefore, magnetotactic bacteria may play a significant role in the formation of magnetic iron minerals on a geologic scale; however, the importance of the contribution of bacterial minerals to the magnetic remanence of sediments and rocks is unknown.

Magnetotactic bacteria provide a striking example of biologically controlled mineralization (BCM), in which the iron oxide or sulfide crystals within the

Addresses: M. Pósfai, B. Arató: H-8201 Veszprém, P. O. Box 158, Hungary
Received: 27 March, 2000

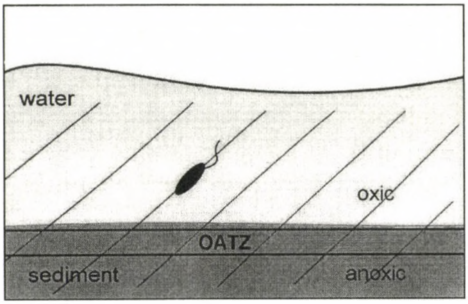

Fig. 1
A schematic representation of the use of magnetic sensing in magnetotactic bacteria. The bacterium is aligned by the Earth's magnetic field and can swim only along the magnetic field lines; thus, it does not have to search for the "up" and "down" direction, but easily finds its optimal chemical environment within the OATZ (Oxic-Anoxic Transition Zone)

bacteria grow under a high degree of biological control. The intracellular, nanometer-scale minerals are enclosed by membranes; the ensemble of the crystal and the surrounding membrane is called a magnetosome. It is likely that the growth of intracellular minerals is controlled by this membrane (Gorby et al. 1988), resulting in species or strain-specific sizes and crystal morphologies. In addition, chemical purity and typical microstructural features such as twinning in magnetite (Devouard et al. 1998) and extended defects in greigite (Pósfai et al. 1998) are characteristic of crystals from a certain bacterium strain or species.

Each intracellular crystal comprises a single magnetic domain (Bazylinski and Moskowitz 1997). These nano-magnets form chains in the cell and are arranged to produce the largest possible magnetic dipole moment, which orients the bacteria parallel to Earth's geomagnetic field lines. Since the field lines are inclined to the surface of the Earth (except at the Equator), this magnetic sensing mechanism helps the bacteria find and maintain an optimal position in the changing chemical environment of their aquatic habitat (Fig. 1).

Magnetotactic bacteria or their mineral inclusions have been unknown from Hungarian natural waters and their sediments. We initiated the present study to determine whether magnetotactic bacteria occur and how widespread they seem in distinct freshwater bodies that can be regarded typical environments of current sediment formation. In addition, our goals included the mineralogical study of magnetic crystal inclusions in bacteria from Hungarian lakes and streams. Studies of the sizes, habits, compositions, and microstructural characteristics of iron oxides and sulfides within magnetotactic bacteria are important because they provide information on biogenic mineral-forming processes. The results can also be used to define criteria for identifying bacterial crystals in geologic samples, a prerequisite for obtaining a better knowledge about the contributions of biogenic crystals to the magnetic properties of rocks.

In this paper we describe the preliminary results of our collection of magnetotactic bacteria from several lakes and streams, and report on the analysis of magnetite crystals from a magnetotactic species from Gyöngyös stream, Szombathely.

Experimental

We obtained samples from the sediment/water interface simply by filling glass jars or using a sediment sampler where the water was deep. Water depth, temperature, and pH were measured in most cases, and the concentration of dissolved iron was determined in a few cases using a Merck Aquacant rapid test kit (Table 1). Additional samples were collected on an irregular basis; these are also listed in Table 1, even though temperature, pH, or water depth were not measured for them.

We filled glass containers with sediment and water, and enriched magnetotactic bacteria by placing a bar magnet next to the side of the jar, at a level where the aerobic/anaerobic interface was suspected. The bacteria swam to the south pole of the bar magnet (the end that attracts the north-pointing needle of the compass), resulting in their enrichment near the magnet. Water and a little sediment was drawn with a pipette from next to the magnet, and magnetotactic bacteria were further enriched by attracting them to the tip of the pipette. Thus, the first drop presumably contained most magnetotactic organisms present in the pipette. This drop was placed onto a cover slip and observed as a hanging drop under the optical microscope. A bar magnet was again placed next to the drop, and magnetotactic bacteria could be observed as they were gathering at the edge of the water (Figs 2a and 2b). When the direction of the magnetic field was changed (by turning the bar magnet), magnetotactic bacteria changed their swimming direction accordingly. This behavior was used to distinguish magnetotactic species from other organisms present in the drop.

Specimens for transmission electron microscopy (TEM) were prepared from drops that contained magnetotactic bacteria by placing the enriched droplets onto holey carbon-coated copper TEM grids. No further specimen treatment was applied. The morphologies of bacteria and their mineral inclusions were studied using a Tesla TEM operated at 80-kV accelerating voltage. We analyzed the compositions of intracellular crystals using energy-dispersive X-ray spectrometry (EDS) in a Philips CM20 TEM operated at 200-kV accelerating voltage and equipped with a Noran Voyager EDS detector. In order to characterize the mineralogical compositions of lake and stream sediments, we obtained standard X-ray powder diffractograms (XRD) from several sediment samples.

Results

Occurrence and morphological types of magnetotactic bacteria

All sediment/water samples that we collected at the end of the summer and early fall of 1999 contained magnetotactic bacteria (Table 1). We included in our exploration a wide variety of natural water bodies, as far as limnological character, temperature, pH, and sediment type are concerned. The list includes the largest lake in Central Europe (Balaton), two major rivers (Tisza, Rába), and

Table 1
Sampling details and morphological types of magnetotactic bacteria as observed with a light microscope

Sampling Location	Sampling Date	Water Temp. (°C)	Water Depth (cm)	pH	Dissolved Fe (mg/l)	Dominant Minerals of the Sediment	Morphological Types of Magnetotactic Bacteria
Balaton, Örvényes	99.09.02.	21.0	150	7	1.2	carbonates	sc+, sp+, lr
Malom-tó, Tapolca	99.08.30.	19.8	80	7	0.8	carbonates	lc++
Kornyi-tó, Kővágóőrs	99.09.02.	-	60	8	-	carbonates	lr+
Belső-tó, Tihany	99.09.02.	22.5	15	8	0.2	-	lr
Külső-tó, Tihany	99.09.02.	17.0	10	8	0.8	-	lr, sc
Bonta-tó, Köveskál	99.09.01.	17.4	3	6	10.0	detrital minerals from basalt	ssc
Bika-tó, Köveskál	99.09.01.	16.2	20	5	6.5	detrital minerals from basalt	sc+, lr+
Monostori-tó, Balatonhenye	99.09.01.	16.5	10	6	6.5	-	sp+++, dc+
Fishing Pond, Balatonhenye	99.09.01.	17.0	50	7	0.8	-	lr, lc, ssc,
Pond, Salföld	99.08.30.	19.2	3	7	6.5	quartz	lr, sc+, sp+
Velencei-tó, Pákozd	99.10.11.	-	30	-	-	-	lr+, dc+
Hévíz Canal*, Hévíz	99.08.30.	29.6	100	7	-	carbonates	lr
Tisza*, Szeged	99.09.21.	-	10	-	-	-	lc+, lr+, sc+, sp+
Rába*, Körmend	99.09.29.	-	-	-	-	-	lr+, lc+
Kinizsi-forrás*, Nagyvázsony	99.09.04.	-	20	-	-	-	lc++
Gerence*, Takácsi	99.09.11.	17.1	-	5	-	-	lc+++, sp
Marcal*, Mersevát	99.09.12.	18.5	-	5	-	-	lc+++
Répce*, Csánig	99.09.12.	18.0	-	7	-	-	lc+++
Bakonyér*, Győrszemere	99.09.11.	23.1	-	7	-	-	lc+++
Gyöngyös*, Szombathely	99.10.10.	-	15	-	-	detrital minerals from metamorphic rocks	lc++++, sp

*: rivers and streams; the other items are ponds and lakes;
sc: small coccus; sp: spirillum; lr: large rod; lc: large coccus; dc: diplococcus; ssc: small slow coccus
+ signs indicate relative abundances (no sign: only a few cells; +: up to ~100 cells; ++: continuous band of bacteria at the edge of the drop; +++: several μm wide, continuous band of bacteria at the edge of the drop; ++++: >10μm wide, continuous band of bacteria at the edge of the drop)

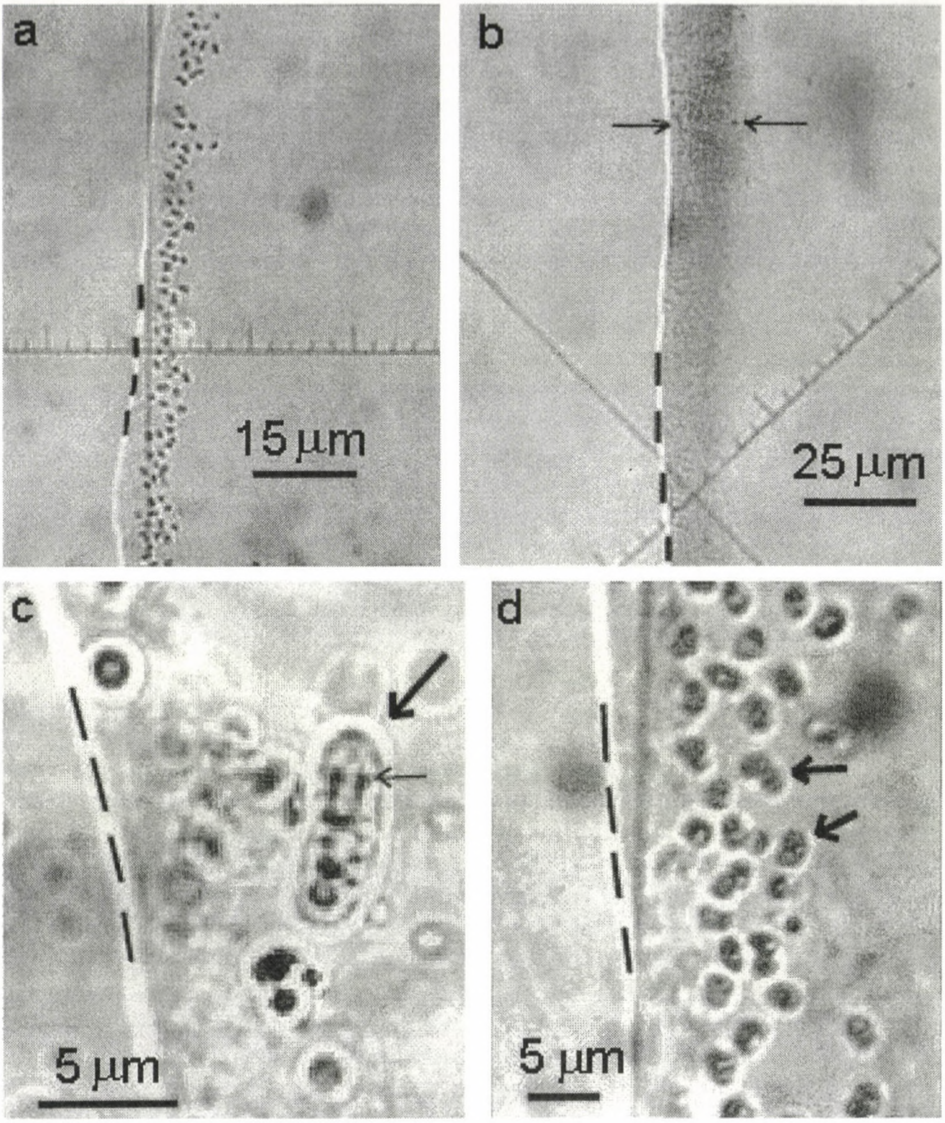

Fig. 2
Light microscope images of live magnetotactic bacteria. The nearly vertical white line in all four images (partly marked by the broken line) is the edge of the droplet (water is always to the right of the boundary line). (a) A continuous band of cocci at the edge of the drop (Malom-tó, Tapolca); such abundances are marked ++ in Table 1. (b) A thick band of magnetotactic bacteria from Marcal (between the two arrows) gathering at the drop edge; similar abundances are marked +++ in Table 1. (c) A large rod (marked by the thick arrow) from Kornyi-tó; the small arrow points to high-contrast features within the cell. (d) Large cocci (two of them arrowed) with dark-contrast spots (Malom-tó, Tapolca)

several ponds and streams. The temperature ranged from 16.2 °C (where it was measured; Gyöngyös stream was probably much colder) to 29.6 °C in the outflow of Lake Hévíz (Hévíz Canal) that is fed by hot springs. Calcareous lakes and streams (Balaton, Kornyi, Malom, Hévíz) are neutral or slightly alkaline (with a maximum pH of 8), whereas seasonal ponds on a basaltic plateau (Bonta, Bika, Monostori) are acidic (with pH between 5 and 6). Since we observed magnetotactic bacteria in all samples, and magnetotaxis requires the presence of intracellular magnetic crystals (Frankel and Blakemore 1989), our observations indicate that magnetic crystals of bacterial origin likely contribute to all studied, currently accumulating freshwater sediments.

Based on size, morphology, speed and mode of swimming, several distinct types of magnetotactic bacteria could be distinguished in the enriched droplets (Table 2). Since these bacteria are wild species and have never been cultured, we know nothing about their metabolism and cell structure. Although we plan to attempt to culture the most common morphological types in the future, the microbiological characterization of the observed bacteria is beyond the scope of this study. The light microscope observations described here are useful for identifying typical morphological types and their occurrences in different samples. Some types occur in several lakes and streams and could even belong to the same species. The characteristic features of these types are given in Table 2, and two examples are shown in Figs 2c and 2d.

The occurrence of distinct morphological types of magnetotactic cells in each sample is listed in the last column of Table 1. The + signs indicate how abundant certain types are under the optical microscope. These observations should be interpreted with caution, because the observed number of bacteria may strongly depend on sampling artifacts; we found that the number of magnetotactic cells is especially sensitive to the depth below the sediment surface from which the enriched droplet is drawn. In addition, in several samples magnetotactic bacteria occur in such large numbers that the abundance of bacteria was judged on the basis of the thickness of the band that accumulated at the edge of the droplet (see the legend to Table 1 and Figs 2a and 2b).

The listings of bacterium types in Table 1 are based on observations performed within a few hours (and at most within two days) after sampling, so the relative abundances of distinct types likely represent the original conditions in the natural environment. We kept the sediment/water samples in the laboratory in capped jars at room temperature, some containers at dimmed light or in the dark, others at natural lighting conditions. Certain bacterium types (the large rods, for example) disappeared from the samples a few days after sampling, whereas others (large cocci, for example) could be observed several months after sampling. Even when the original types survived for a long time, their relative abundances changed; for example, in the Gyöngyös sample large cocci were originally the dominant type, but small spirilla became more abundant four months after sampling.

Table 2
Morphological types and optically visible characteristics of observed magnetotactic bacteria

Type	Characteristic features
large rod	5–10 μm long, slow-moving rods; contain dark spots
large coccus	2–5 μm large, very fast-swimming cocci; contain high-contrast spots
small coccus	< 2 μm, fast-swimming cocci
small slow coccus	< 2 μm, very slow-swimming cocci
spirillum	1–2 μm long spirilla
diplococcus	2–5 μm large diplococci

As far as the distribution of distinct morphological types in different environments is concerned, most bacteria do not seem to be sensitive to temperature and pH. For example, large rods occur in both acidic and alkaline waters, both in lakes and streams, and at every measured temperature. Spirilla are also common in most samples. The only regularity we observed is that great numbers of large cocci occur in relatively cold and clean streams and lakes; in such places they may be even dominant species, particularly in Gyöngyös stream.

Morphologies and size distributions of intracellular magnetite crystals

From the many types of bacteria listed in Table 1, we studied the mineral inclusions in one magnetotactic organism, a bacterium with helicoid morphology from Gyöngyös stream. These bacteria contain chains of magnetite (Fe_3O_4) crystals, such as the one between the arrows in Fig. 3a. The mineralogical identity of the crystals was confirmed both by selected-area electron diffraction (SAED) and on the basis of EDS spectra. Apart from Fe, no other transition metals occur in the crystals; C, Ca, Si, and Cl are likely contained in the cell material, whereas the Cu peak is an artifact due to emission from the Cu specimen support grid (Fig. 4). Typical features other than magnetosomes within the bacteria include dark, round spots (two of them marked by arrows in Fig. 3b) that are amorphous and contain mostly P. Such P-containing inclusions are used for the storage of P and are not specific to magnetotactic bacteria.

In bright-field electron micrographs the intracellular magnetite crystals produce strong contrast relative to the rest of the bacterium that contains mostly light elements. Some crystals appear darker than others, owing to diffraction contrast (they are close to a symmetrical zone-axis orientation, resulting in less intensity within the direct beam that was used for forming the image). Some crystals exhibit reentrant angles (such as the one marked by the arrow in Fig. 3d), indicating the presence of twin boundaries. It is difficult to obtain an accurate percentage of twinned crystals; likely less than 10% of the total number of magnetite crystals are twinned.

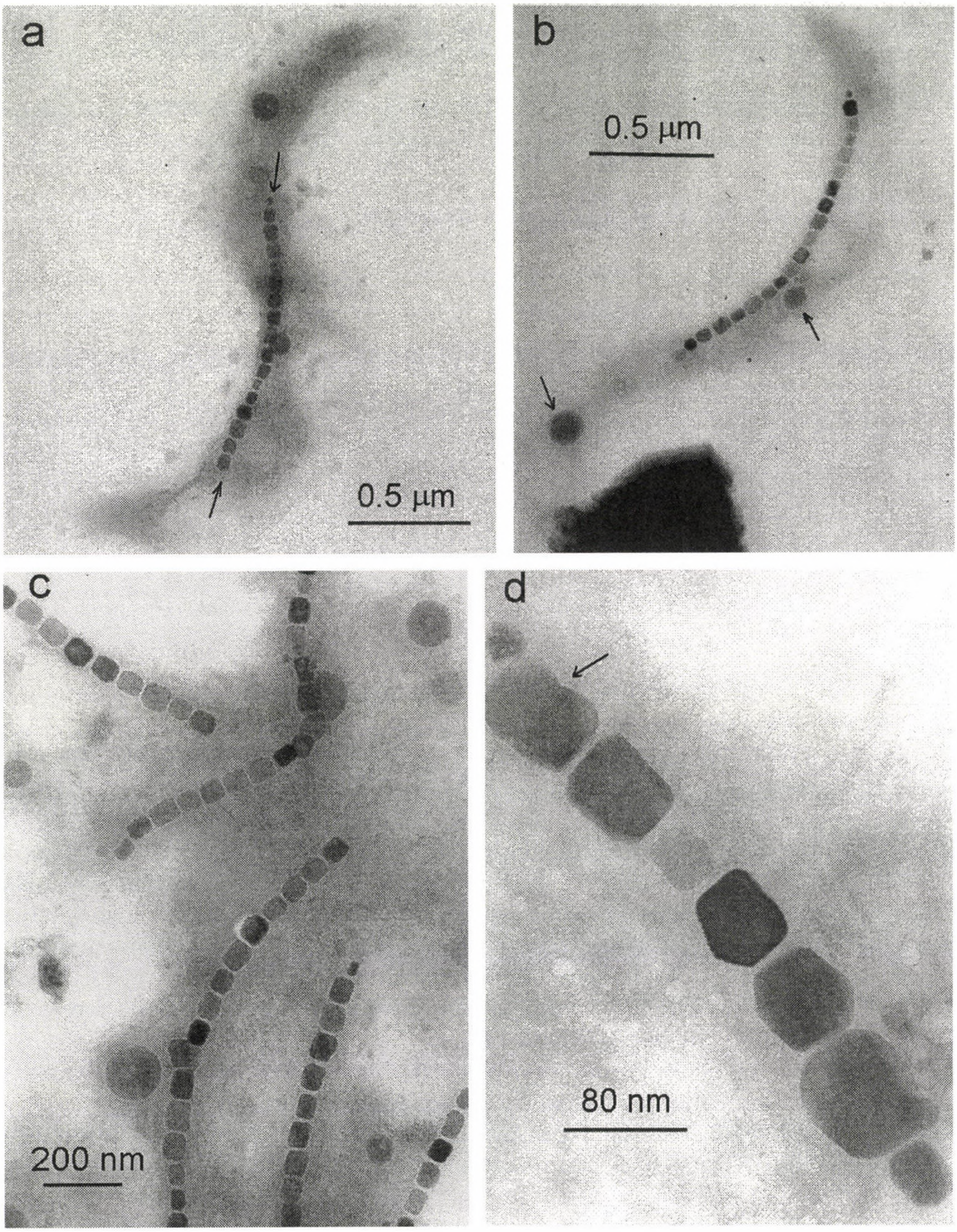

Fig. 3
Bright-field transmission electron microscope images of chains of magnetite crystals in helicoid bacteria from Gyöngyös stream, Szombathely. Individual bacteria are shown in (a) and (b), whereas several bacteria are aggregated in (c); part of a chain is shown at higher magnification in (d). The arrows mark the magnetite chain in (a), P-containing spots in (b), and a twinned crystal in (d)

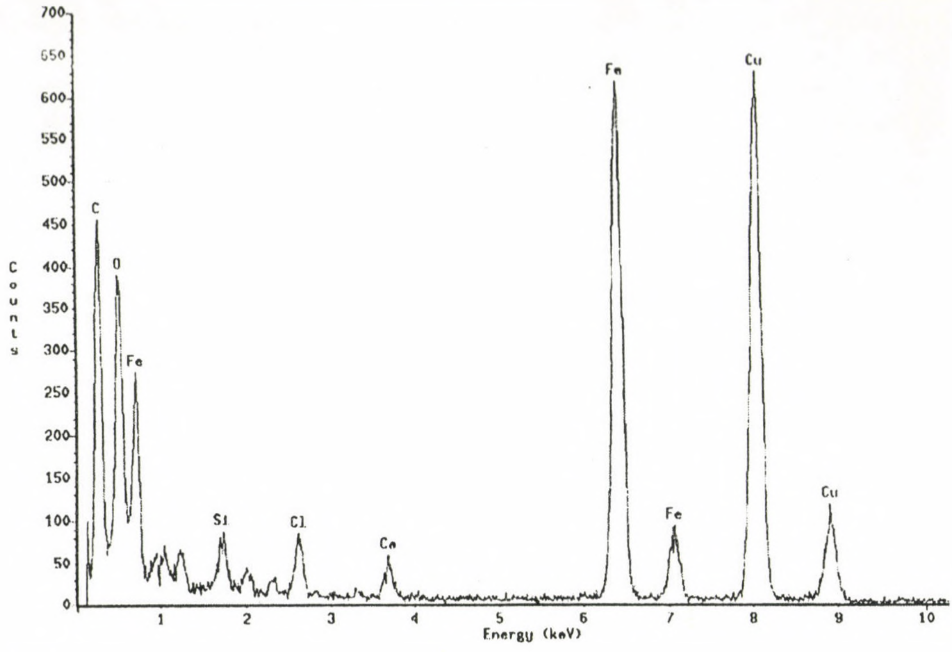

Fig. 4
A representative energy-dispersive X-ray spectrum obtained from one magnetite crystal (see text for details)

The sizes of magnetite crystals are apparently specific to the particular strain or species we examined. We measured the dimensions of magnetite particles on digitized electron micrographs (such as the ones in Figs 3a and 3b), by fitting ellipses to the outlines of the crystals. The major and minor axes of the best-fitting ellipse were taken as the length and width of the particle, respectively. The same statistical method was used by Devouard et al. (1998) for magnetite crystals from several cultured strains; thus, our results are directly comparable with previous analyses. Since the sizes of crystals were measured in two-dimensional projections, the actual values of length and width could be slightly larger than or equal to the observed ones. A total of 460 crystals were measured to produce the size distributions in Figs 5a and 5b.

The shape of the distribution histogram for the average crystal sizes (Fig. 5a) is consistent with previous results by Meldrum et al. (1993a, 1993b) and Devouard et al. (1998) in that it is quite narrow and shows a distinct asymmetry with a relatively sharp cut-off towards larger sizes. The maximum of the size distribution is between 55 and 70 nm, within the magnetic single-domain range for magnetite. A remarkable feature of the distribution histogram is a small maximum at 30–35 nm. This maximum at a small particle size is even more prominent when the distributions of length and width values are plotted separately (Fig. 5b).

At low magnification, the magnetite crystals typically look like elongated rectangles in the electron micrographs (Fig. 3). In the literature on magnetotactic bacteria such crystals were often designated "prismatic", even though this crystal form is incompatible with the cubic system to which magnetite belongs. As discussed by Devouard et al. (1998), the rectangular shapes observed in two-dimensional projections may result from combinations of common cubic forms,

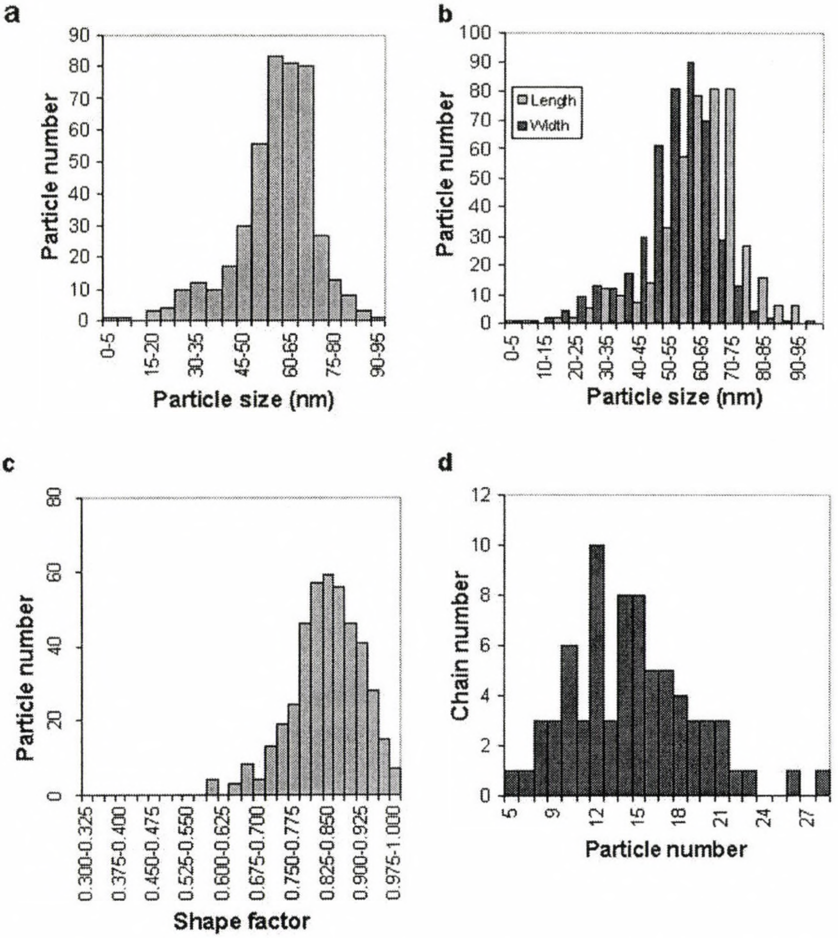

Fig. 5
(a) and (b) Size distribution histograms of magnetite crystals from a helicoid bacterium from Gyöngyös stream. Average particle sizes [(length + width)/2] are shown in (a), whereas the distributions of width and length values are given in (b). (c) Shape distribution of magnetite particles (shape factor = width/length). (d) Distribution of the number of magnetite particles in individual chains of magnetosomes

such as the cube {100}, the octahedron {111}, and the dodecahedron {110}. In fact, the characteristic angles between octahedral faces can be observed on many crystals (for example, see the third and fourth crystals from the bottom of the chain in Fig. 3d). Most crystals are likely elongated octahedra, with [111] oriented parallel to the chain. A statistical analysis of crystal shapes was performed, by taking the width/length value as the shape factor (Fig. 5c). The shape factor histogram has a relatively sharp maximum around 0.85; larger values may represent either real shapes, or result from the fact that even elongated crystals may look isometric in certain projections.

The number of magnetite crystals within individual chains varies from 5 to 28 crystals, as observed in 73 chains (Fig. 5d). When cells divide, the magnetosome chains are probably randomly split, and daughter cells inherit highly variable numbers of magnetite particles.

Discussion

The maxima in the size and shape distributions of magnetite crystals from the studied organism occur at different values than the maxima in similar distributions previously reported for magnetite from magnetotactic bacteria. The marine species MV-1 (Devouard et al. 1998), MV-2 and MV-4 (Meldrum et al. 1993b) produce smaller, whereas MC-1 (Meldrum et al. 1993a) and MC-2 (Devouard et al. 1998) produce larger crystals than MH-1. (We note that the fact that Meldrum et al. (1993a) used two types of growth media for culturing MC-1 had little effect on the sizes of magnetite crystals). The extensively-studied freshwater species *Magnetospirillum magnetotacticum* contains magnetite crystals that are smaller than 50 nm (Devouard et al. 1998), and *Magnetobacterium bavaricum* produces entirely different, bullet-shaped crystals (Hanzlik et al. 1996). MH-1 from Gyöngyös stream is likely a previously undescribed organism.

The number distribution of magnetite crystals within individual chains (Fig. 5d) is also different from those reported previously (Meldrum et al. 1993a; 1993b). When magnetotactic bacteria divide, their magnetosome chain is probably randomly split between the two daughter cells (Bazylinski and Moskowitz 1997). The maximum in the histogram around 12 crystals is apparently produced by the combined effect of the cell division process and the growth of chains that originally contained less than 12 magnetosomes.

The asymmetric size distribution of magnetite crystals from the studied organism is consistent with earlier reports about the effect of biogenic control on crystal growth. The cutoffs toward larger sizes may indicate that the crystals do not grow further once they reach their species-specific sizes. A mechanism that limits the growth of magnetite crystals may be beneficial to the bacterium because it prevents the magnetosomes from growing into the magnetic two-domain size range, which would reduce the efficiency of its magnetic sensing mechanism. On the basis of model results and a detailed analysis of experimental crystal size distributions, Eberl et al. (1998) found that several crystal growth mechanisms can be distinguished on the basis of crystal size distributions. The shapes of the size distribution histograms in Figures 5a and 5b match those model results of Eberl et al. (1998) that result from Ostwald ripening, during which the relative rate of crystal dissolution and growth is controlled by differences in specific surface area and by diffusion rate. It is possible that several crystals nucleate (typically at the ends of magnetosome chains), most of which dissolve and only one will grow to the strain-specified size at the expense of the other nuclei. In our electron micrographs there is some evidence that at least two very small crystals occur at the ends of certain magnetosome chains. Another interesting feature in the size distribution curves is the newly observed small maximum at 30–35 nm; the presence of this peak could be explained by crystal agglomeration that is known to produce multimodal size distributions (Eberl et al. 1998). Such agglomeration of growing crystals could also take place at the ends of chains, and may be responsible for the production of twinned crystals.

Although several studies reported that structural perfection is typical of bacterial magnetite, recent investigations showed that BCM magnetite can contain structural irregularities in the form of twins. On the basis of an analysis of crystals from five strains, Devouard et al. (1998) found that the frequency of twinning varied from strain to strain, and up to 40% of the magnetosomes could be twinned. The contact surface between twinned individuals was commonly irregular. Although we did not obtain high-resolution electron micrographs in this study, we could observe twinned crystals from the bacterium from Gyöngyös stream. Typically, the twins appear to have straight boundaries, making their recognition more difficult.

BCM iron minerals are of great interest as potential biomarkers. The morphological similarity of nanometer-scale magnetite and iron sulfides in the Martian meteorite ALH84001 to the same minerals produced by terrestrial magnetotactic bacteria was cited as part of the evidence for ancient life on Mars (McKay et al. 1996). Claims that magnetite particles recovered from modern and ancient sediments are of biological origin have been based on comparisons to similar grains produced by contemporary bacteria (Kirschvink and Chang 1984; Petersen et al. 1986; Stolz et al. 1986). Therefore, it is of interest whether biogenic and abiogenic magnetite crystals can be distinguished. Since microstructural features such as twinning were found to be common to both bacterial and synthetic magnetite (Devouard et al. 1998), chemical purity and narrow size and shape distributions of BCM iron minerals may be the best criteria for identifying bacterial magnetic minerals in sediments and rocks. Although little data exist about the sizes of magnetite crystals produced by inorganic processes, such crystals seem to have size distribution curves showing "tails" extending to large crystal sizes (Devouard et al. 1998). The results of this study confirm that crystal size distributions of magnetite from a certain type of a magnetotactic bacterium have characteristic features that could be used for identifying similar crystals in the geologic environment.

It is remarkable that magnetotactic bacteria occurred in every sample we studied, indicating that magnetic minerals are produced in great quantities at the sediment/water interface or within the upper few centimeters of the sediment. We will analyze the mineral inclusions in the other major morphological cell types listed in Table 1 in a similar way as was done in this study. It is unknown whether magnetite magnetosomes within dead bacteria are preserved or dissolved in the sediment as a result of diagenetic redox changes. We plan to address this problem in future studies by determining the depth profile of single-domain, bacterial crystals in sediments where we know that magnetotactic bacteria live at the sediment/water interface. The bacterial origin of the magnetite crystals will be tested by studying their size distributions. Such data are also needed for evaluating the effect of bacterial minerals on sediment magnetism.

Acknowledgements

We thank Dr. Judit Padisák for useful discussions and for help with starting the bacterium sampling. Anita Künsztler, Gizella Rasztovits, and Zsuzsanna Rezner helped to collect samples and analyzed the iron content, and Dr. Katalin Tasnády-Jelinkó provided aid with operating the Tesla TEM. Constructive reviews by Drs. Gyula Szöőr and István Vető improved the manuscript. This research was supported by a grant from the Hungarian Academy of Sciences (AKP #98-94 2.5).

References

Bazylinski, D.A., B.M. Moskowitz 1997: Microbial biomineralization of magnetic iron minerals. – In Banfield, J.F., K.H. Nealson (Eds): Geomicrobiology: Interactions between microbes and minerals. Washington, D. C.: Mineralogical Society of America, Reviews in Mineralogy, 35, pp. 181–223.

Blakemore, R.P. 1975: Magnetotactic bacteria. – Science, 190, pp. 377–379.

Devouard, B., M. Pósfai, X. Hua, D.A. Bazylinski, R.B. Frankel, P.R. Buseck 1998: Magnetite from magnetotactic bacteria: Size distributions and twinning. – Amer. Mineral., 83, pp. 1387–1399.

Eberl, D.D., V.A. Drits, J. Srodon 1998: Deducing growth mechanisms for minerals from the shape of crystal size distributions. – Amer. J. Science, 298, pp. 499–533.

Frankel, R.B., R.P. Blakemore 1989: Magnetite and magnetotaxis in microorganisms. – Bioelectromagn., 10, pp. 223–237.

Gorby, Y.A., T.J. Beveridge, R.P. Blakemore 1988: Characterization of the bacterial magnetosome membrane. – J. Bacteriol., 170, pp. 834–841.

Hanzlik, M., M. Winklhofer, N. Petersen 1996: Spatial arrangement of chains of magnetosomes in magnetotactic bacteria. – Earth. Planet. Sci. Lett., 145, pp. 125–134.

Kirschvink, J.L., S.-B. Chang 1984: Ultrafine-grained magnetite in deep-sea sediments: possible bacterial magnetofossils. – Geol., 12, pp. 559–562.

McKay, D.S., E.K. Jr. Gibson, K.L. Thomas-Keprta, H. Vali, C.S. Romanek, S.J. Clemett, X.D.F. Chillier, C.R. Maechling, R.N. Zare 1996: Search for past life on Mars: Possible relic biogenic activity in Martian meteorite ALH84001. – Science, 273, pp. 924–930.

Meldrum, F.C., S. Mann, B.R. Heywood, R.B. Frankel, D.A. Bazylinski 1993a: Electron microscopy study of magnetosomes in a cultured coccoid magnetotactic bacterium. – Proc. Roy. Soc. Lond., B251, pp. 231–236.
Meldrum, F.C., S. Mann, B.R. Heywood, R.B. Frankel, D.A. Bazylinski 1993b: Electron microscopy study of magnetosomes in two cultured vibrioid magnetotactic bacteria. – Proc. Roy. Soc. Lond., B251, pp. 237–242.
Petersen, N., T. Von Dobeneck, H. Vali 1986: Fossil bacterial magnetite in deep-sea sediments from the South Atlantic Ocean. – Nature, 320, pp. 611–615.
Pósfai, M., P.R. Buseck, D.A. Bazylinski, R.B. Frankel 1998: Reaction sequence of iron sulfides in bacteria and their use as biomarkers. – Science, 280, pp. 880–883.
Spring, S., R. Amann, W. Ludwig, K.-H. Schleifer, H. van Gemerden, N. Petersen 1993: Dominating role of an unusual magnetotactic bacterium in the microaerobic zone of a freshwater sediment. – Appl. Environ. Microbiol., 59, pp. 2397–2403.
Stolz, J.F., S.-B.R. Chang, J.L. Kirschvink 1986: Magnetotactic bacteria and single-domain magnetite in hemipelagic sediments. – Nature, 321, pp. 849–851.

Acta Geologica Hungarica, Vol. 43/4, pp. 477–492 (2000)

New results from the Kaba meteorite
Part I. Chondrules

Imre Kubovics, Kamilla Gál-Sólymos, Zuárd Ditrói-Puskás
Eötvös Loránd University, Budapest
Department of Petrology and Geochemistry

Szaniszló Bérczi
Eötvös Loránd University, Budapest
Department of General Technology

The re-examined Kaba meteorite (Hungary) is being investigated by modern research methods. The present report focuses on the EPMA studies of this carbonaceous chondrite, mainly on the chondrules. The textural features, mineralogical and chemical composition of six characteristic types of chondrules, as well as phenocrysts and matrix, indicate an extremely wide temperature range of formation (1973° K–403° K).

The multi-stage, selective condensation may have commenced at about 1973° K with the appearance of Al_2O_3, then perovskite and spinel were formed with decreasing temperature. At the end of the process magnetite, maghemite and organic compounds were the condensation products. All of these comprise the almost complete scale of condensation steps. Beside condensation and aggregation, melting and crystallization processes play a role in the chondrule formation.

Key words: carbonaceous chondrite, EPMA studies, chondrule types, white inclusion, multi-stage condensation

Introduction

The main sample of the Kaba carbonaceous chondrite that fell at the outskirts of the village of Kaba near Debrecen on April 15, 1857 has been preserved in Debrecen Calvinist College ever since. Its original weight was 2940 g. The weight of the main sample is now 2624.2 g. The meteorite was first reported by Török in 1858, and later described in 1882. Wöhler (1859) demonstrated that the chondrite contains 0.58% carbon in the form of bitumen-like hydrocarbon. Following this Török (1882) noted in connection with the carbonaceous meteorites: "Their most outstanding fame is that they contain carbon, which is the characteristic component of the plant and animal kingdom proving that in those worlds they are coming from the conditions of organic, plant and animal life do exist." And though – as is well known – this is not the case, the idea merits attention and emphasis, considering that in the sixties of the 20th century numerous researchers, e.g. Nagy et al., Claus, Meinschein, Hennessy, and others believed that they recognized structures hinting at some previous life forms in carbonaceous chondrites. The meteorite was qualified as a chondrite by Hoffer

Addresses: I. Kubovics, K. Gál-Sólymos, Z. Ditrói-Puskás: H-1088 Budapest, Múzeum krt. 4/A, Hungary
Sz. Bérczi: H-1117 Budapest, Pázmány Péter sétány 1, Hungary
Received: 16 June, 2000

(1928), who also recognized the almond-like, whitish patches of 10–15 mm length, with characteristics different from those of the main body, and which are now known to be white inclusions or Ca-Al-rich inclusions (CAIs). He, however, having no detailed studies to consult, thought them to be feldspar.

The first modern study of the meteorite was carried out by Sztrókay et al. (1961) using instrumental facilities of the time. They proved by textural analysis the dominance of the matrix (68.3%) and determined the mineral composition of the meteorite. Beside the Mg-Fe silicates characteristic of the chondrites (olivine, clinoenstatite-clinobronzite and augite) around some chondrules they found plagioclase as well. Oxide phases of two-fold genesis found in substantial quantity in the meteorite; furthermore, sulfides of predominantly pentlanditic composition and the low-quantity metal phases (1.22%) have also been analyzed and evaluated in detail. This study, although appeared forty years ago, is still a standard work on the subject.

In chronological order of falls the Kaba meteorite is the fourth registered carbonaceous chondrite on a world scale. The number of falls of this kind of meteorites has remained scarce since then. Perhaps this is the reason that only in the fifties and sixties of the 20th Century researcher's interest in the carbonaceous chondrites was conspicuously aroused, especially in the Orgueil C1-type meteorite, containing about 7% carbon. The big rate of progress was, however, due to the C3-type Allende meteorite, fallen in 1969, which is extremely rich in white inclusions. The renewed interest also focused fresh attention on the Kaba meteorite.

Twenty predominantly small pieces of the Kaba meteorite have found their way into various collections abroad. As the meteorite is of heterogeneous textural character, e.g. the distribution of the white inclusions of varying size is extremely uneven, the study of different samples can only yield divergent or partial results. The discrepancies in nomenclature (C2, C3) are partially attributable to this, besides growing criteria. The Kaba carbonaceous chondrite has been classified as C2 by Wood (1967), as C3 by Van Schmus and Wood (1967), McSween Jr. (1977) and Peck (1983), and as the more oxidized Vigarano type among the C3 by Guimon et al. (1995) on the basis of magnetite/metal rate and the form of Ni-appearance. Though they have considered the latest viewpoints even this classification cannot be regarded as final, due to contradictions among the different data.

During the eighties and nineties again numerous researchers dealt with the Kaba meteorite. The matrix olivine was studied by Kornacki and Wood (1984), the spinel-rich parts by Fegley and Post (1985), the inclusions by Liu and Schmitt (1987) and the hydrated products (minerals) by Keller and Buseck (1990).

Hua and Buseck (1995) have found that the meteorite contains fayalite (Fa=99.9%) besides forsterite, while Holmén and Wood (1987), studying mainly the inclusions, have shown that five out of six are of forsteritic composition. They were the first to identify fassaite, which has earlier been demonstrated in Allende, appearing in different forms (core, rim or intersticial in forsterite).

In the fifties and sixties intensive research with limited international cooperation was in progress and conducted by K. I. Sztrókay, covering the considerable number of meteorites in Hungary. In the meantime, however, numerous up-to-date research methods have been developed owing to the considerable progress in measuring techniques, also providing a great impetus to the study of cosmic materials worldwide. This has led to the re-examination of most meteorites, but only with limited effect on the meteorites of the Carpathian basin, including those of Hungary. That is why it has become timely and necessary to completely re-examine the meteorites of Hungary from a uniform point of view, and partly in international cooperation.

As is clear from the review, the Kaba meteorite has thus far not been neglected. Owing to its heterogeneity, however, the results, mainly with respect to the chondrules, requires completion, while the studies on the organic matter are hitherto practically insignificant. Our recent investigations have so far been focused on these two fields. In the present report results mainly concerning the chondrules (and some phenocrysts) will be dealt with.

Methodology

Electron probe microanalyses were carried out using an AMRAY 1830 I/T6 SEM equipped with both an EDAX PV9800 energy dispersive and a MICROSPEC WDX-400 wavelength dispersive X-ray spectrometer. Accelerating voltage and beam current were 15KeV and 1.5nA. The ED-measurements (mainly on grains of small size) were evaluated by the SubQuant program of the instrument and the data were normalized to 100%.

To the study of the sample effective help was provided by a mosaic map compiled of low magnification (20×) backscattered electron images covering the whole thin section (about 4 cm^2).

The entire texture, the distribution of the textural components, their relative abundance, as well as the fine-grained matrix among the chondrules, various aggregates and major opaque grains are clearly visible. This map provides valuable help in the continuation of electron probe microanalysis and in the planning of systematic study of selected textural components.

Results

In the available sample we found six types of chondrules on the basis of mineralogical composition and texture (Table 1). There are chondrules with refractory materials, the so-called white inclusions, containing spinel, perovskite and pyroxene minerals, as well as microcrystalline-amorphous material. The composite chondrules consist of spinel, plagioclase, forsterite, and diopside. The

Table 1
Texture and mineralogical composition of the Kaba meteorite

Composition of chondrules

1. chondrule with refractory materials	2. composite chondrule	3. olivine-pyroxene-spinel chondrule
spinel	spinel	forsterite
perovskite	plagioclase	clinopyroxene (partly Ti-augite)
pyroxene	forsterite	spinel
	diopside	glass

4. olivine-pyroxene chondrule	5. magnetite-metal chondrule	6. oxide-sulfide chondrule
forsterite	magnetite	magnetite
clinopyroxene (partly Al-diopside)	Fe Ni	troilite
		pentlandite

Phenocrysts

orthopyroxene	forsterite	fayalite	chromite
zoned orthopyroxene	enstatite		

Matrix

1. fayalite and fayalitic olivine, **2.** magnetite, **3.** maghemite, **4.** organic compounds

olivine-pyroxene-spinel chondrules contain forsterite, clinopyroxene (Ti-augite), glass and spinel, whereas in the olivine-pyroxene chondrule can be found forsterite, clinopyroxene (Al-diopside) and some glass. The magnetite-metal chondrules consist of magnetite and FeNi metal phases with variable composition. The oxide-sulfide chondrules are made up of magnetite, troilite, and pentlandite aggregates.

Different, sometimes zoned, phenocrysts (forsterite, fayalite, pyroxene, and chromite) can be found in the fine-grained matrix consisting of fayalite and fayalitic olivine, magnetite, maghemite and organic compounds. Furthermore, some of the characteristic chondrules are described in detail.

The distribution, size, morphology as well as structure and texture of the white inclusions are extremely varied, so their mineralogical composition is probably different as well. The most valuable information is most probably inherent in the four white inclusions of irregular shape and diameter of 1.0–1.5 cm, but is unattainable at this time for investigative purposes. The white inclusions in the sample at our disposal are in the size range of 0.1 mm, some of them of completely spherical form (Fig. 1). Their unequivocally identifiable crystalline materials are anhedral, more or less isometric perovskite and spinel. The core of the chondrule is predominantly composed of (presumably) partly micro-cryptocrystalline and partly amorphous mass, with a high Al_2O_3-content. The perovskite grains are mainly set inside this mass, in a roughly even distribution. The spinel apparently encloses the core (Fig. 2). In the outer rim pyroxene-like minerals can also be observed.

The chemical composition of the chondrule is also peculiar. The micro-crystalline-amorphous material representing the main mass is extremely rich in Al_2O_3 (69.86%), which hints at a substantial excess of alumina (Table 2). The Fe^{2+}-oxide (21.24%) and the Zn-oxide (1.21%), even if totally bound to spinel, can only bind a maximum of 31.8% Al_2O_3, consequently the alumina is in excess even if all the cations with two valences – except for the Ca – are in the spinel. This points to a substantial quantity of "free" Al_2O_3, or to the presence of corundum. This unequivocally means that the formation of the chondrule began with the high-temperature condensation of Al_2O_3.

On the basis of textural evidence it can be concluded that the condensation of perovskite of ideal composition proceeded almost simultaneously and subsequently with this, followed by the condensation of high Mg-containing spinel (see Table 2). The accretion may have commenced with this assemblage forming the core, and was later followed by the pyroxenes and the outer "black" rim (see Fig. 2) of extremely diverse composition (Table 2). Beside the rock-forming main components the rim contains phosphorous, sulfur, and chlorine. On the basis of chemical composition, this "black" rim (fine dust) may contain an iron-nickel alloy, as well as Na- and K-containing feldspar, pointing to its condensation in a wide temperature range. Consequently, the white inclusion-type chondrule is the oldest constituent of the Kaba meteorite.

The so-called composite chondrule is already predominantly composed of elongated lath-forming, or occasionally table-like, silicates (Figs 3, 4), mostly forsterite. Furthermore, clinopyroxene and anorthite are present, but the amount of spinel is also considerable (Fig. 5). The silicate minerals are in a finger-like textural relationship; the clinopyroxene and anorthite are alternately connected to the forsterite (see Fig. 5). The bigger isometric spinel grains with significant Cr_2O_3-content (12.38%; Table 3) are mainly embedded in anorthite, or are found

Table 2
Chemical composition of parts in chondrule with refractory materials (wt%)

	SiO_2	TiO_2	Al_2O_3	FeO	NiO	MgO	CaO	ZnO	K_2O	Na_2O	SO_3	Cl	P_2O_5
1.	-	58.18	-	-	-	-	41.82	-	-	-	-	-	-
2.	-	-	70.41	2.01	-	27.58	-	-	-	-	-	-	-
3.	4.59	0.66	69.86	21.24	-	-	2.44	1.21	-	-	-	-	-
4.	38.56	-	24.04	7.94	0.94	19.42	3.19	-	0.54	2.18	2.14	2.90	0.56

1: perovskite, 2: spinel, 3: matrix, 4: "black rim"

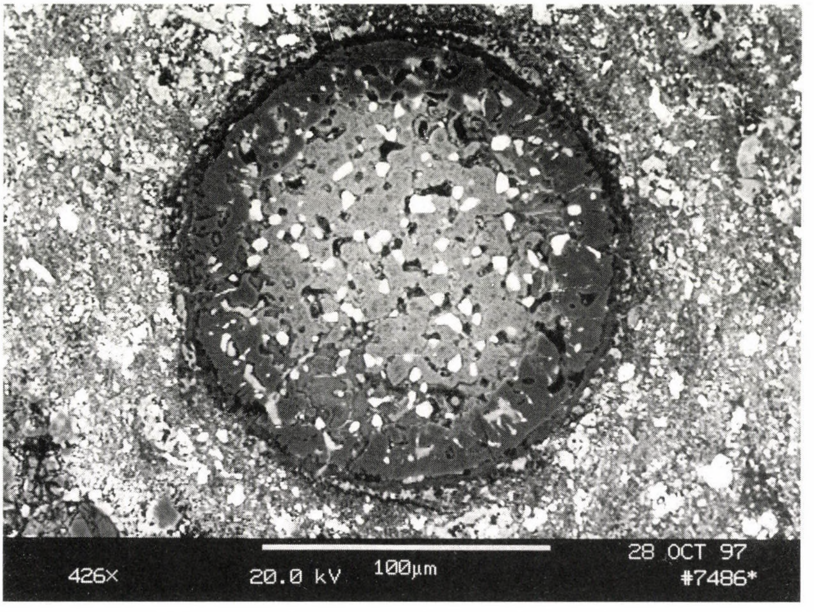

Fig. 1
BEI of chondrule with refractory materials

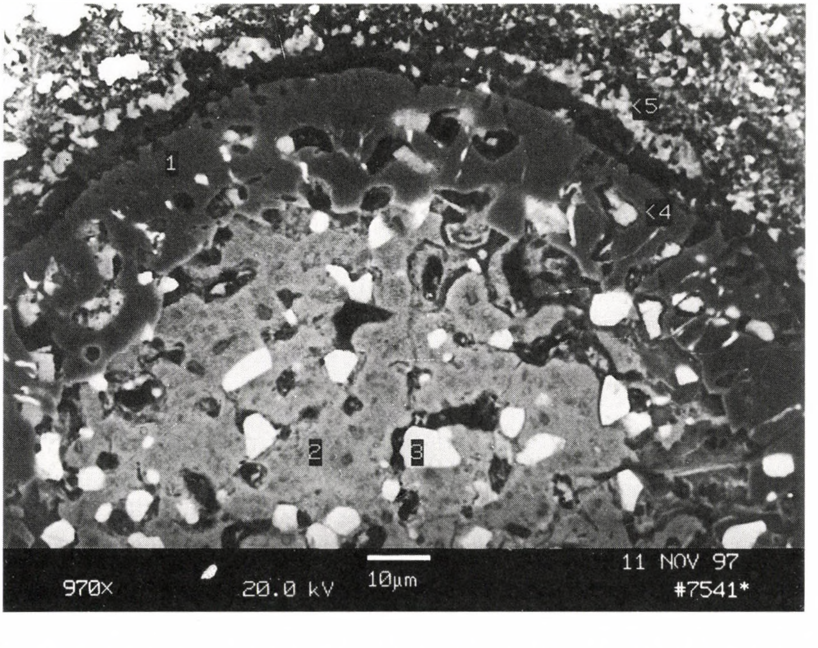

Fig. 2
Enlarged part of Fig. 1. Legend: 1. spinel; 2. microcrystalline-amorphous material; 3. perovskite

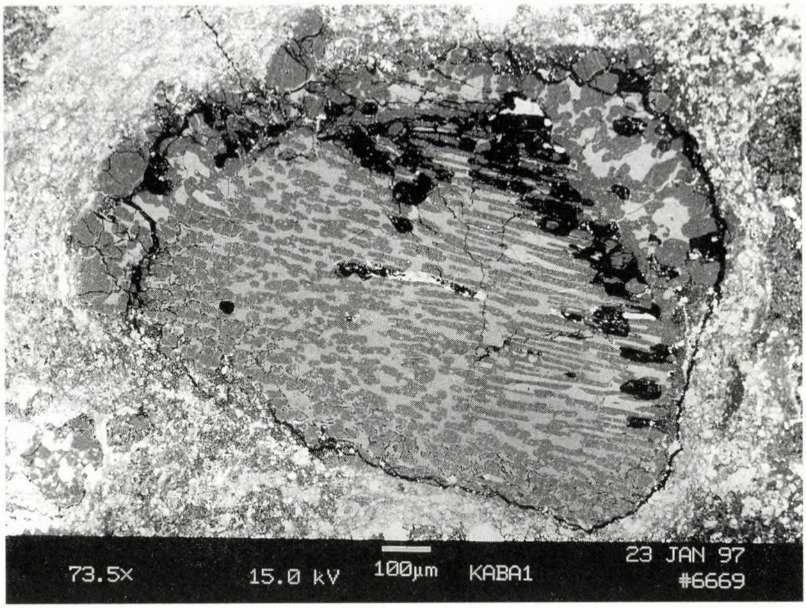

Fig. 3
BEI of composite chondrule

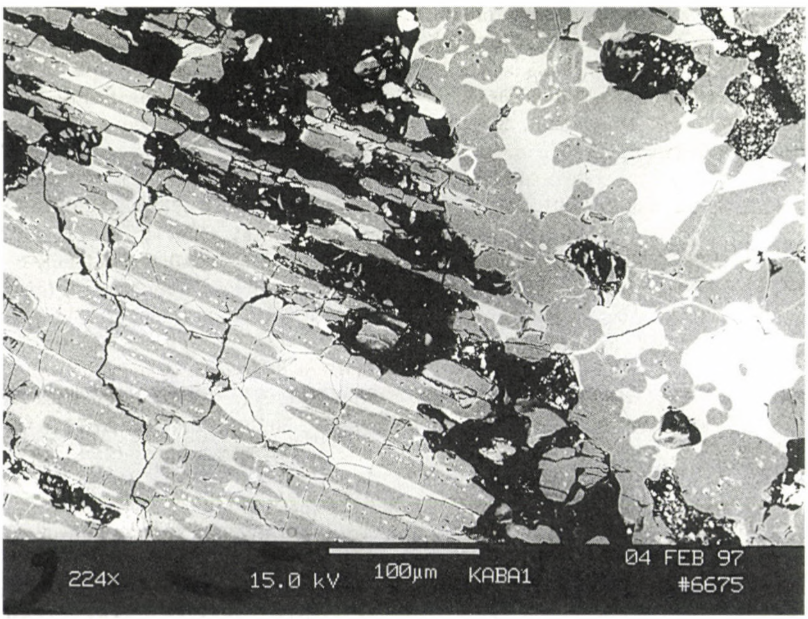

Fig. 4
Enlarged part of Fig. 3

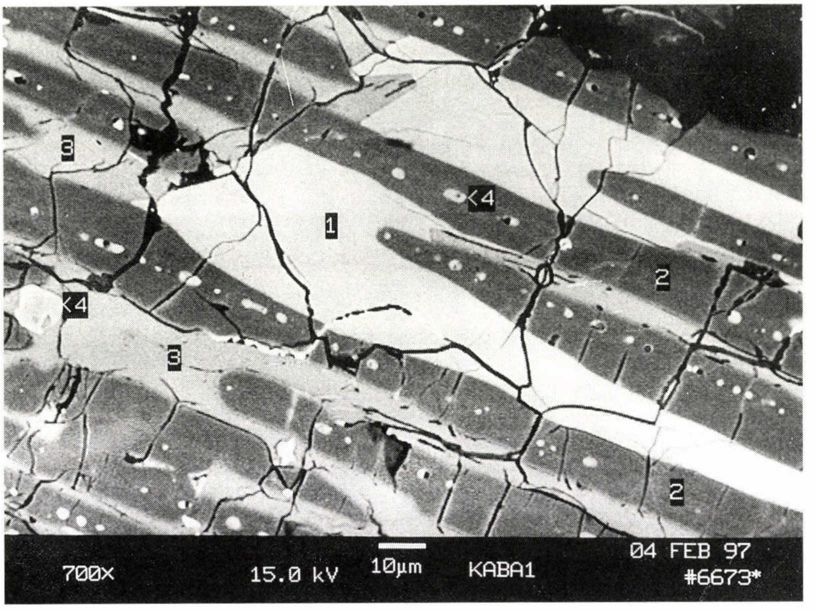

Fig. 5
Enlarged part of Fig. 4. Legend: 1. clinopyroxene; 2. forsterite; 3. plagioclase; 4. spinel

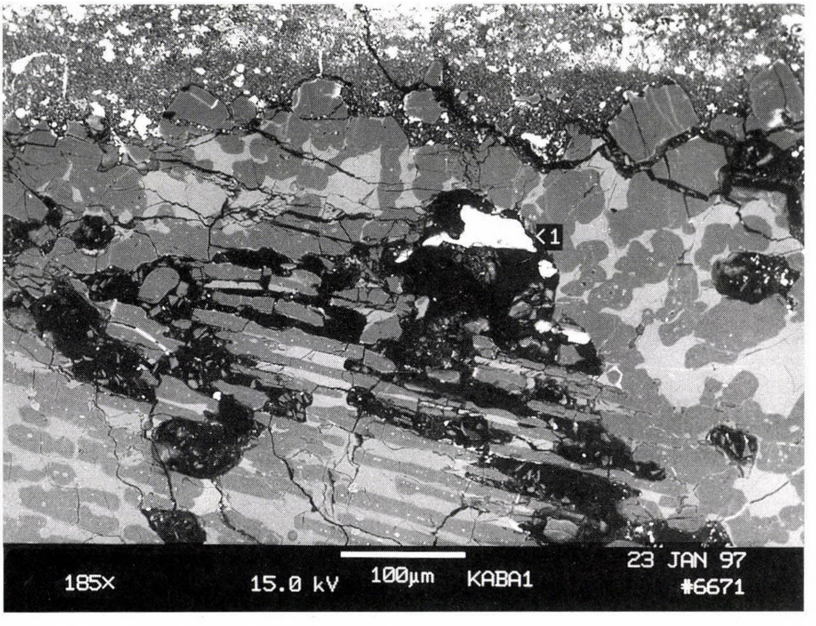

Fig. 6
Enlarged part of Fig. 3. Legend: 1. fayalite

Table 3
Chemical composition of minerals in different chondrules

	I. chondrule					II. chondrule				III. chondrule	
	1. Spl	2. Pl	3. Fo	4. Px	5. Fa	1. Spl	2. Fo	3. Px	4. Gl	1. Fo	2. Px+Gl
SiO_2	-	43.59	43.06	48.81	29.78	-	42.46	49.96	47.11	42.62	46.99
TiO_2	0.37	-	-	2.50	-	0.70	-	2.66	0.06	-	1.04
Al_2O_3	58.10	34.63	-	10.69	-	70.74	-	7.54	31.10	-	26.13
Cr_2O_3	12.38	-	0.21	0.51	-	0.13	-	0.97	-	-	0.34
FeO	2.39	0.19	1.25	0.39	69.12	-	0.68	0.63	-	0.52	0.34
MnO	-	-	-	-	1.10	-	-	-	-	-	-
MgO	26.36	-	55.05	16.38	-	28.35	56.51	15.35	2.14	56.47	4.62
CaO	0.12	21.59	0.42	20.72	-	0.09	0.34	22.28	19.58	0.38	20.55
V_2O_5	0.27	-	-	-	-	-	-	-	-	-	-

I.: composite chondrule, II.: olivine-pyroxene-spinel chondrule, III.: olivine-pyroxene chondrule
Spl: spinel, Pl: plagioclase, Fo: forsterite, Px: pyroxene, Fa: fayalite, Gl: glass

at the interface of plagioclase and forsterite, while the smaller ones form elongated strings inside forsterite (see Fig. 5). This peculiar arrangement (texture) suggests that the chemical components of these three constituents condensed simultaneously, or in a similar temperature range in the form of melt, or that they were melted during the rapid accretion succeeding the condensation. The crystallization of forsterite led to the enrichment of alumina and silica in the residual melt, hence the undersaturation of the system decreased.

Parallel with the crystallization of forsterite a considerable proportion of Al-enriched melt was separated. The spinels of string-like appearance and parallel with the elongation of forsterite were formed from the alumina (+ MgO) left behind among the skeleton crystals. This led to the further decrease of undersaturation; consequently, in the almost saturated melt, the remaining alumina may have entered the crystal lattice of high Al_2O_3-containing clinopyroxene (into positions with both four and six coordination numbers). The pyroxene contains titanium and chromium as well (Table 3). The separated alumina-rich melt, following the formation of Cr-spinel, crystallized as anorthite, probably simultaneously with the pyroxene in equilibrium system. The "pure" fayalite in the outer part of the chondrule (Fig. 6) may have formed considerably later.

The composite chondrule also contains constituents characteristic of the white inclusions, pointing to similar conditions of formation, but in a slightly lower temperature range.

The forsterite-pyroxene-spinel chondrule (Fig. 7) with a diameter of around 1 mm is predominantly composed of lath-forming forsterite, as well as Cr-bearing clinopyroxene and Ti-augite. Beside these two main constituents the amount of the high Al_2O_3-containing glass phase (Table 3) is also significant. In contrast, the proportion of spinel is subordinate. This chondrule – similarly to the previous one – was also formed from melt, but in different conditions of crystallization.

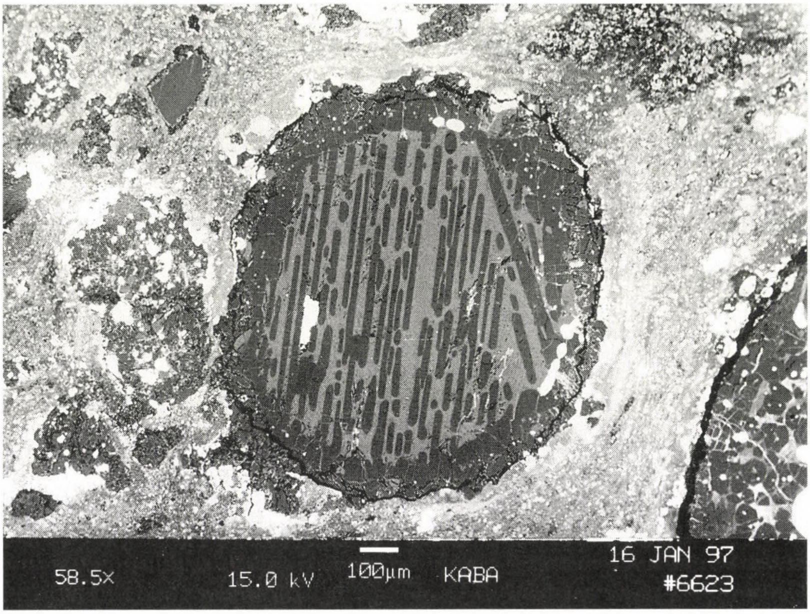

Fig. 7
BEI of olivine-pyroxene-spinel chondrule

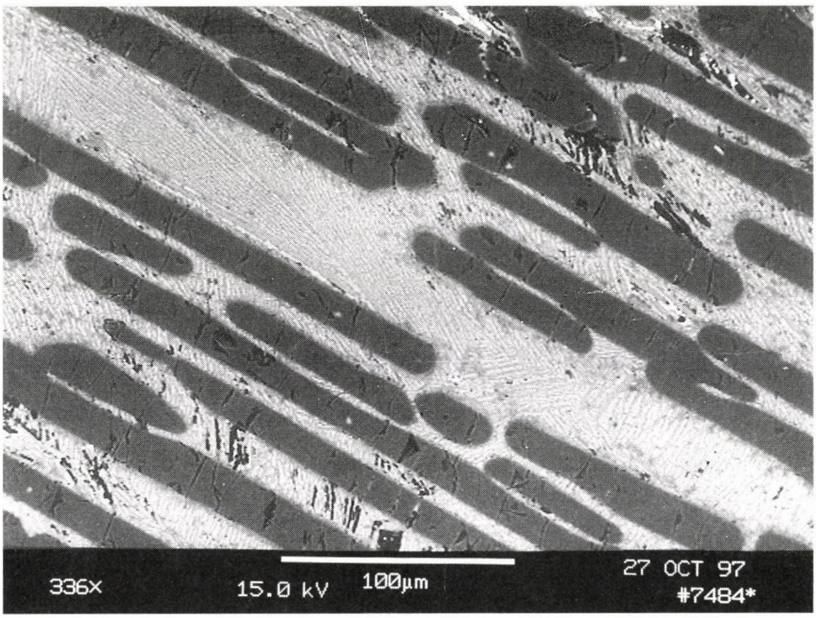

Fig. 8
Enlarged part of Fig. 7

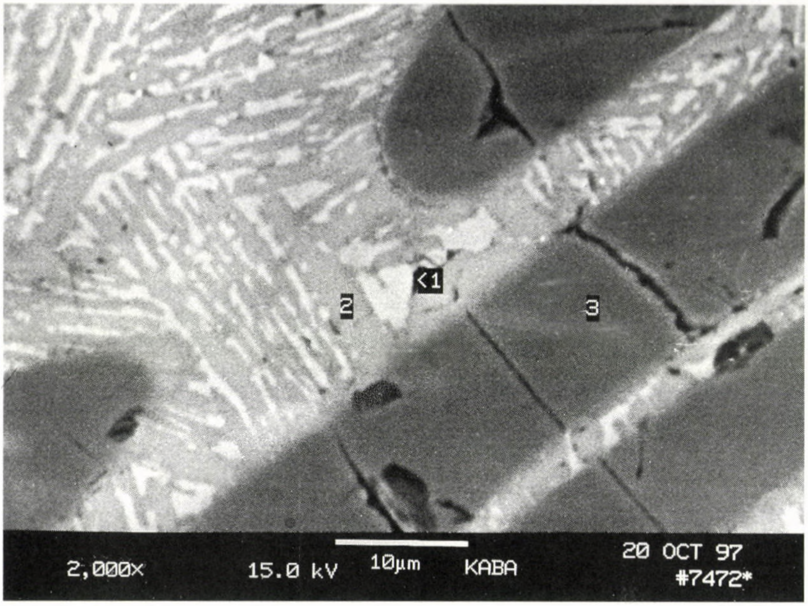

Fig. 9
Enlarged part of Fig. 7. Legend: 1. clinopyroxene; 2. glass; 3. forsterite

Following the complete crystallization of lath-forming "pure" forsterite the formation of Ti-augite commenced from the already saturated melt, but the process ceased after the formation of skeleton crystals (Figs 8, 9). This can be explained – besides the accidental and relative undercooling of the system – primarily by the chemical composition of the residual melt (Table 3). This caused the reduction of its crystallization ability, i.e. the concentration of the pyroxene-components in the melt decreased considerably in spite of slight crystallization, while the proportion of anorthite-components increased significantly. As compared to the anorthite composition, however, the proportion of silica was in excess, and may have contributed to the diminution of crystallization ability.

The core of the forsterite-pyroxene chondrule is composed of the symplectite of these two minerals (Fig. 10). The signs of resorbtion are visible on the lath-like forsterite, while the space among the crystals is mainly filled with needle-like, thready clinopyroxene rich in the Al-diopside molecule (Table 3), reflecting rapid, non-equilibrium crystallization, but some glass phase is also present (Fig. 11).

All the silicate chondrules described above were formed from melt. The heat necessary for the formation of melts may have been partly provided by the kinetic energy released during the accretion impacts, and partly by the solid-state reactions inside the accreted masses.

The forsterite has an almost completely uniform appearance and composition in the different silicate chondrules. The pyroxene, however, shows varied

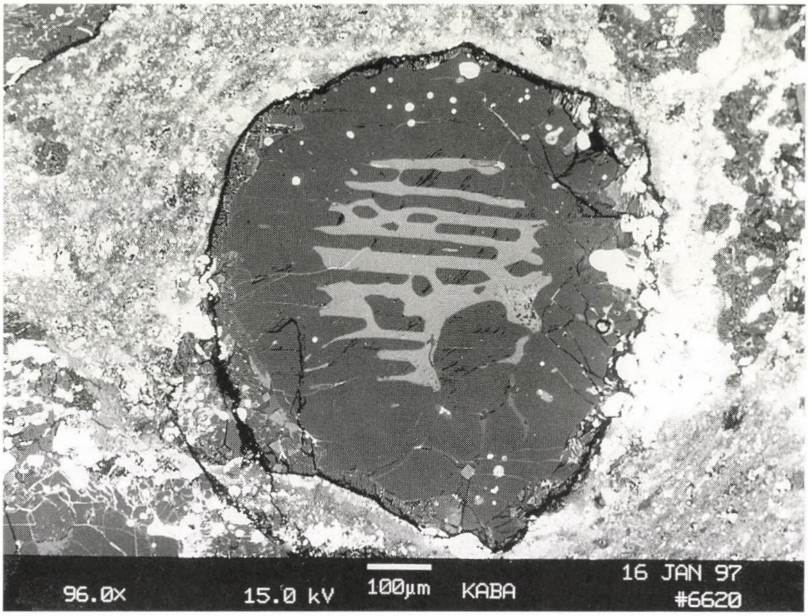

Fig. 10
BEI of olivine-pyroxene chondrule

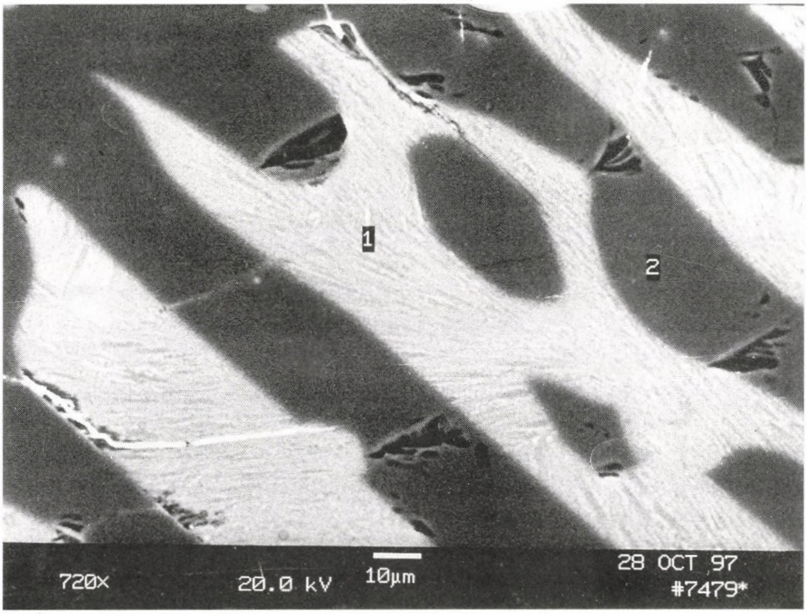

Fig. 11
Enlarged part of Fig. 10. Legend: 1. pyroxene+glass; 2. forsterite

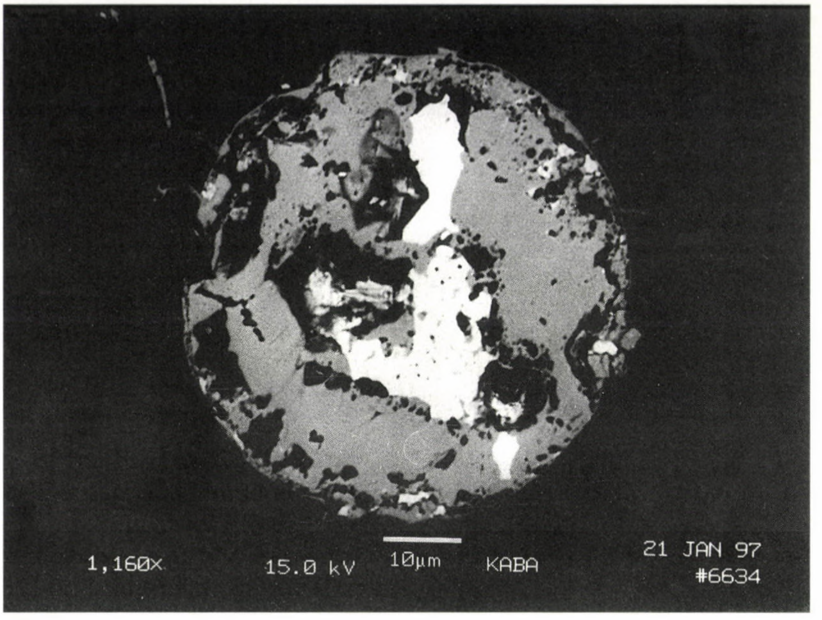

Fig. 12
BEI of magnetite-metal chondrule

appearance, is both orthorombic and monoclinic, and there are marked differences in their chemical compositions as well (see Table 3). The amount of plagioclase and spinel unambiguously decreases from the white inclusion-type chondrule toward the forsterite chondrule (and then completely disappears). consequently, the above sequence of chondrules implies their sequence of formation, i.e. decreasing temperature of formation.

The Kaba meteorite, beside the chondrules outlined above, also contains chondrules composed of either magnetite+metal (Fig. 12), or oxides+sulfides, as well as phenocrysts of various size and composition (pyroxene, forsterite, fayalite, chromite, etc.).

The phenocrysts, e.g. the olivine, are partly of clastic character and form aggregates (Fig. 13). Strong zoning may have developed in some aggregate-forming minerals and pyroxene phenocrysts (Fig. 14). This may indicate the formation mechanism of these components, namely that they could have been aggregated from the clasts produced by the collision of major cosmic bodies (planetesimals).

The very fine-grained matrix is mainly composed of olivine with ferro-hortonolitic-fayalitic composition, furthermore magnetite, maghemite and organic compounds (see Table 1). Accordingly, the olivine isomorphous series is represented by chondrule-forming forsterite of high-temperature origin, clastic chrysolite-hortonolite, as well as of fayalite, or ferrohortonolite-fayalite

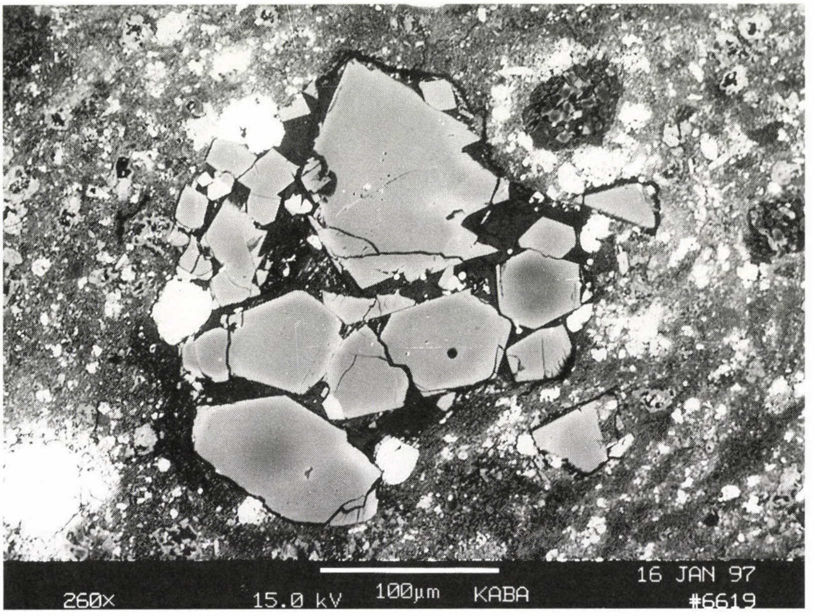

Fig. 13
BEI of zoned olivine clasts in the matrix

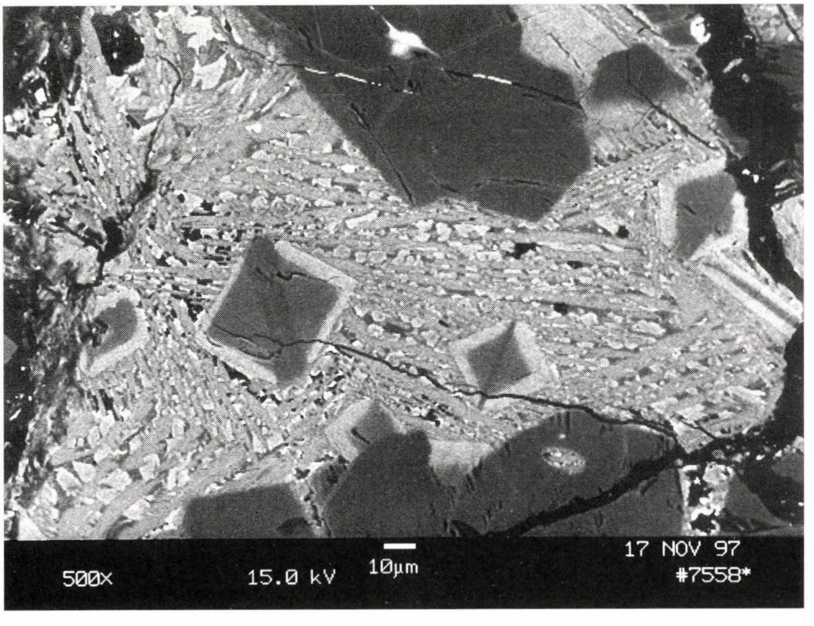

Fig. 14
BEI of zoned pyroxene phenocrysts

appearing both as phenocrysts and matrix components. Members of intermediate composition – chrysolite, hyalosiderite – are of completely subordinate importance.

Conclusion

Based on the textural features outlined above, as well as on the mineralogical and chemical compositions, the following conclusions can be drawn on the origin of the Kaba meteorite:

The temperature range of formation may have been extremely wide, from 1973° K to 403° K, with multi-stage, selective condensation, as well as accretion of both condensates of various chemical composition formed at different temperatures, and clasts formed in collision events. Constituents of high-temperature condensation and aggregation were subsequently melted to various extents. Forsterite, pyroxene and anorthite crystallized from this melt. Condensation may have commenced at about 1973° K with the appearance of Al_2O_3, was followed by the consecutive formation of perovskite and spinel, and ended with the appearances of magnetite, maghemite and organic compounds of various compositions. The Kaba meteorite, consequently, comprises the almost full scale and temperature range of multi-stage and selective (fractional) condensation products.

Acknowledgement

The Debrecen Calvinist College has provided the Kaba meteorite for cutting section, which in sincerely acknowledged. The financial support of the Research Fund of the Ministry of Education is gratefully acknowledged.

References

Claus, G., B. Nagy 1961: A Microbiological Examination of some Carbonaceous Chondrites. – Nature, 192, pp. 594–596.

Fegley, B., J.E. Post 1985: A refractory inclusion in the Kaba CV3 chondrite: Some implications for the origin of spinel-rich objects in chondrites. – Earth. Planet. Sci. Lett., 75, pp. 297–310.

Guimon, R. K. et al. 1995: Chemical and physical studies of chondrites. XII: The metamorphic history of CV chondrites and their components. – Meteoritics, 30, pp. 704–714.

Hoffer, A. 1928: A kabai meteorit története (The history of Kaba meteorite). – "Debreceni Szemle" kiadv., pp. 1–15.

Holmén, B.A., J.A. Wood 1987: Refractory inclusions in the Kaba CV3 chondrite. – Meteoritics, 22, p. 413.

Hua, X., P.R. Buseck 1995: Fayalite in the Kaba and Mokoia carbonaceous chondrites. – Geochim. Cosmochim. Acta, 59/3, pp. 563–578.

Keller, L.P., P.R. Buseck 1990: Aqueous alteration of the Kaba CV3 carbonaceous chondrite. – Geochim. Cosmochim. Acta, 54, pp. 2113–2120.

Kornacki A.S., J.A. Wood 1984: The mineral chemistry and origin of inclusion matrix and meteorite matrix in the Allende CV3 chondrite. – Geochim. Cosmochim. Acta, 48, pp. 1663–1676.

Liu, Y.G., R.A. Schmitt 1987: A chemical study of Kaba (CV3 chondrite) inclusions. – Lunar Planet. Sci., 18, pp. 560–561.
McSween Jr., H. Y. 1977: Petrographic variations among carbonaceous chondrites of the Vigarano type. – Geochim. Cosmochim. Acta, 41, pp. 1777–1790.
Meinschein, W.G. et al. 1963: Evidence in Meteorites of Former Life. – Ann. New York Acad. Sci., 108, pp. 553–579.
Nagy, B. et al. 1961: Mass Spectroscopic Analysis of the Orgueil Meteorite. Evidence for Biogenic Hydrocarbons. – Ann. New York Acad. Sci., 93, pp. 27–35.
Nagy, L. A. et al. 1969: Microstructures Approximating Hexagonal Forms (and of Unknown Origin) in the Orgueil Carbonaceous Meteorite. – Grana, 9, pp. 110–117.
Peck, J. A. 1983: Chemistry of CV3 matrix minerals and Allende chondrule olivine. – Abstract, Meteoritics, 18, pp. 373–374.
Sztrókay K. I. et al. 1961: A kabai meteorit (The Kaba meteorite). – Földt. Közl., 91/2, pp. 186–213.
Török, J. 1858: Értesités a Kaba-debreczeni lebkőről (Announcement about the Kaba-Debrecen meteorite). – Magy. Tud. Akad. Értesitője, 116.
Török, J. 1882: A Magyar Birodalom meteoritjai (Meteorites of the Hungarian Empire). – Term. Tud. Közlöny, 14, pp. 508–511.
Van Schmus, W. R., J.A. Wood 1967: A chemical-petrological classification for the chondritic meteorites. – Geochim. Cosmochim. Acta, 31, pp. 747–765.
Wood, J. A. 1967: Olivine and pyroxene compositions in Type II carbonaceous chondrites.- Geochim. Cosmochim. Acta, 31, pp. 2095–2108.
Wöhler, C. M. 1859: Die organische Substanz im Meteorsteine von Kaba. – Sitzungsberichte der mathematisch-naturwissenschaftlichen Classe der kaiserlichen Akademie der Wissenschaften. Wien, Bd. 34, pp. 7–8.

Acta Geologica Hungarica, Vol. 43/4, pp. 493–500 (2000)

History of mineralogical investigations of the Füzérradvány "illite", near Sárospatak, Hungary

István Viczián
Hungarian Institute of Geology, Budapest

The illitic material mined at Füzérradvány near Sárospatak, Tokaj Mts. (NE Hungary) was described by Maegdefrau and Hofmann in 1937 almost simultaneously with the introduction of the term "illite" by Grim et al. (1937) for the group of micaceous clay minerals. Later the mineral was called "sarospatakite" or "sarospatite". Its mixed-layer nature was recognized by Grim and Bradley (1948, 1952). In Hungary the most important mineralogical investigations were made by Professor Nemecz (1981) using thermal and X-ray diffraction methods. Dódony (1990) recognized fundamental illite particles by HRTEM. The Füzérradvány type "illite" is a common constituent of hydrothermal alteration zones in Neogene volcanic formations of the Carpathian basin (e.g. Kremnica Mts., Harghita Mts., Jász Depression), but different from the so-called hydromuscovite from Nagybörzsöny. Recently Füzérradvány "illite" became a popular standard material called "Zempleni" illite.

Key words: illite, illite/smectite, clay minerals, history of mineralogy

Introduction

The recognition and exploitation of the ceramic clay locality of Korom-hegy at Füzérradvány (Tokaj Mts.) dates back to the first half of the 19th century. In the 30s of the 20th century the material became famous as one of the first known occurrences of micaceous clay minerals. Since this time the material has been the subject of numerous investigations, both by Hungarian and foreign authors. Thanks to these studies the Füzérradvány "illite" probably became the most famous Hungarian clay mineral. In this short historical note I would like to stress the role of the first foreign authors and in particular the role of Professor Nemecz and his students in the determination of the true mineralogical nature of this material.

The early foreign investigations (1937–1948)

The Füzérradvány illite was first described by Maegdefrau and Hofmann (1937). The paper presented the results of Maegdefrau's Ph.D. thesis, dealing with clay materials of mica-like crystal structure under supervision of Professor Hofmann. He received one of his test materials from a Hungarian engineer, László Mattyasovszky. The commercial name of this ceramic material was "*kaolin*

Address: I. Viczián: H-1143 Budapest, Stefánia út 14, Hungary
Received: 13 June, 2000

of Sárospatak", because Sárospatak was the nearest well-known town and because the material was macroscopically similar to kaolin. According to his description, this material occurs "in wagon-size nests in liparite in the Hegyalja (=Tokaj) Mountains, NE Hungary". At the time the material was used in the porcelain industry because of some advantageous properties, including high potassium content. Based upon his investigations Maegdefrau renamed this material *"Glimmer von Sárospatak"* (= *"mica of Sárospatak"*).

After cleaning and preparation Maegdefrau carried out X-ray diffraction investigations using an X-ray camera and photometric registration. His X-ray pattern clearly shows the series of basal reflections at 10.09 Å etc. which he indexed as 002, 004, 006 and several *hk0* reflections, including the reflection 060 (Fig. 1). On the basis of the X-ray pattern he stated that the material has a muscovite-like structure. He carried out chemical analysis and computed the structural formula. He observed that there are only 1.41 K (Na, Ca) cations instead of the possible 2 per formula unit and supposed that the remaining sites are occupied by H_2O molecules. The thermal decomposition was determined by subsequent heating and he observed that most of "constitutional water" was lost in the interval 400 to 500 °C. In addition, the optical index of refraction, base exchange capacity and the fraction <2 μm were determined.

Maegdefrau and Hofmann compared their results on the "mica of Sárospatak" with those of a *"sericite-like mineral"* from Illinois, U. S. A., described almost simultaneously by Grim in several publications. They obtained the sample by exchange between Hofmann and Grim. This is the material to which the name *"illite"* was given by Grim et al. (1937). Their almost completely identical nature is clearly seen by comparison of the X-ray photometric curves of both minerals. In this respect *"mica of Sárospatak"* (i.e. Füzérradvány) is very closely related to the birth of the widely used mineralogical term "illite".

The newly described mineral from Sárospatak was included in a genetic system of alteration products developed by the Russian author Sedletzky (1940). He seems to be the first to use the name *"sarospatakite"* for this material. He classified the colloidal minerals into mutable (amorphous), metastable (incompletely crystalline) and stable (crystalline) compounds. In this system the *"sarospatakite"* of Maegdefrau and Hofmann (1937) was classified as a stable phase along with the *"illite"* of Grim et al. (1937) and many other clay minerals.

A somewhat shorter version of the term occurs in the review article of Maegdefrau (1941) and in a paper of Hofmann et al. (1943) in which the identity of the micaceous clay mineral *"sarospatite"* as a homogeneous mineral phase is defended. Grim (1953, p. 36) cited this paper in his book and wrote that "sarospatite has been suggested as a substitute for illite". On the other hand, Grim considered sarospatite to be "a mixture of clay minerals". However, in view of the original text of the paper of Hofmann et al. (1943), both statements of Grim seem to be erroneous. First because this paper does not mention the term illite at

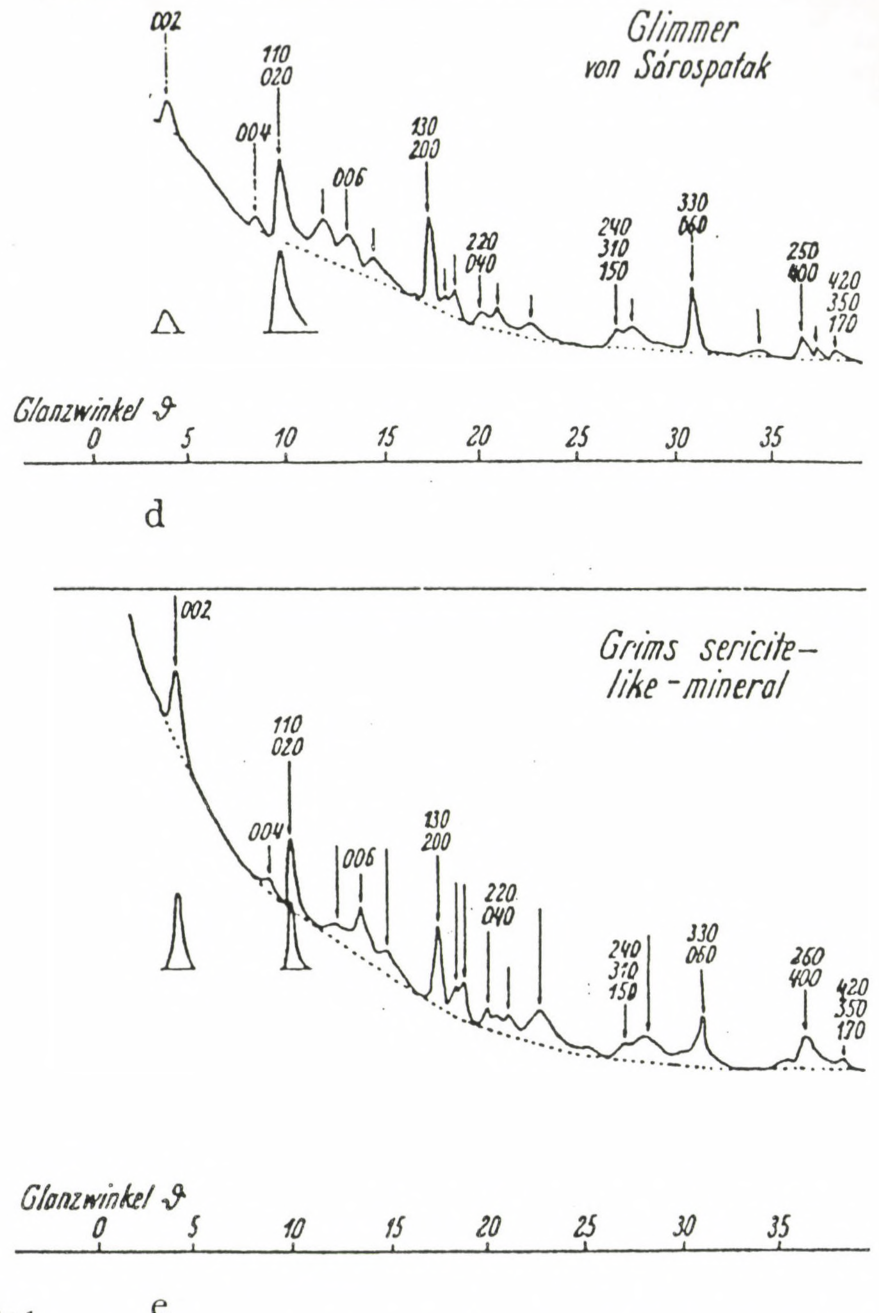

Fig. 1
Part of the photometric X-ray diffraction records of "mica of Sárospatak" and Grims "sericite-like mineral", from the paper of Maegdefrau and Hofmann (1937, Fig. 1. d–e)

all, and second because it proves by X-ray diffraction that sarospatite represents a homogeneous mineral phase instead of being a mixture of minerals.

The relation of illites to other phases of similar structure was the subject of a presentation of Grim and Bradley in the 18th International Geological Congress in London, 1948. Unfortunately, only the abstract of this paper appeared both in the Abstract Volume (1948) and in the Proceedings (1952) of the congress. *Illites* were considered to be "three-dimensionally static ... crystallizations". Those illites which we would call today "discrete" phases were opposed to the "mixed-layer crystallizations" and "*sarospatite*" was considered "to be example of mixed-layers of illite and montmorillonite". This way Grim and Bradley (1948, 1952) recognized the first time the mixed-layer nature of "sarospatite".

First period of Hungarian investigations

The first Hungarian report on the investigations of the Füzérradvány "illite" was published by Kiss and Takáts in 1963. They carried out detailed mineralogical studies (including X-ray diffraction analysis) but the main goal was to test the material as a fine ceramic raw material from technological point of view. They observed thermal loss of OH at temperatures typical both for *illites* (550–600 °C) and for montmorillonites (700 °C). The idea of Grim and Bradley (1948) on the mixed-layer character of the mineral was discussed but was finally rejected.

The first detailed description of the mineralogy of the Füzérradvány "illite" was given by Nemecz and Varju (1970). They briefly described the history of investigations and mentioned the term "*sárospatakite*" in the title in order to refer to former studies. The mode of geologic occurrence was described and shown in a geologic section. A combined hydrothermal-sedimentary genetic model was presented. The basic mineralogical properties were determined using X-ray diffractometric, thermal and chemical methods. It was shown that the composition varies from sample to sample. Nemecz recognized the *interstratified nature* of the material and estimated the proportion of the expandable layers from <10% to 26% using the Hendricks-Teller formula (Fig. 2). The d value of the basal reflection 001 varied between 10.14 Å and 11.05 Å; accordingly, the split of the 001 reflection upon ethylene glycol treatment also varied. He compared the data of this hydrothermal mineral with those collected from sedimentary rocks and found good correlation between the layer charge and equivalent K contents of these minerals.

Nemecz mentioned the Füzérradvány "illite" several times in his book "Clay Minerals" (in Hungarian in 1973 and in English in 1981; pp. 336–343 and 464–469). He recognized the *1M polytypic* modification (Fig. 2), published thermal curves and TEM photographs made by Árkosi. He also discussed the genesis in the chapter dealing with hydrothermal clays.

The mixed-layer nature of the material was more precisely determined by means of X-ray diffraction by Szegedi (1988), a student of Professor Nemecz. She

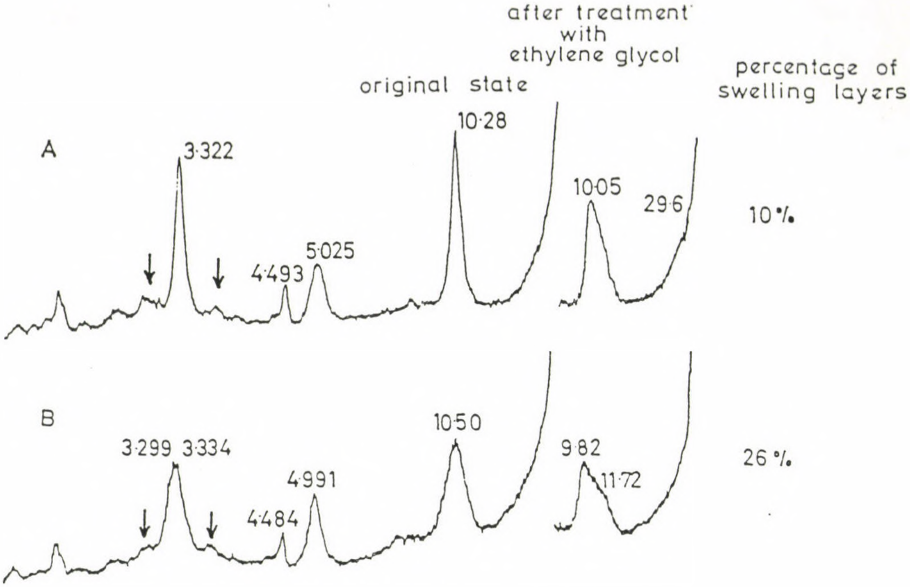

Fig. 2
Typical X-ray diffraction patterns of Füzérradvány illite from the book of Nemecz (1981, from Fig. 139), oriented specimens. Reflections typical of 1M variety are indicated by arrow. Note the split of the first basal reflection after treatment with ethylene glycol

used the direct Fourier transform method and the graphs published by Srodon (1980), and found the proportion of the expandable layers to be in the range of 10–13% and the ordering of ISII type.

Electron microscopic investigations

The first electron micrographs of *"sarospatite"* were made by Hofmann et al. (1941). The name *"sarospatakite"* occurs in the electron microscopy atlas of Beutelspacher and van der Marel (1968). In the description they list sarospatakite among "Mica minerals" and stress the "perfectly crystallized thin plates and laths" and "excellent crystallization properties" of the mineral. The locality, however, is somewhat erroneously given as "Nagybörzsony, Sarospatak, Hungary". The confusion with Nagybörzsöny is probably caused by a publication of Erdélyi et al. (1958) in which a mica-like clay mineral, hydro-muscovite-2M, is described from the locality Nagybörzsöny. However, the two materials and the two localities are completely different.

The lath-like particles of the Füzérradvány material are also included into the electron microscopy atlas of Henning and Störr (1986). The mineral is called here *"illite of Füzerradvany (sarospatakite)"*, which they consider as "a morphological exception" among "irregular montmorillonite-muscovite mixed layer minerals". These corrections in respect of the data of the former atlas may be the consequence of the detailed investigations, which were carried out by Hungarian specialists in the period between the publication of the two atlases.

Some doubts arose concerning the mixed-layer nature of the Füzérradvány "illite" by the application of the HRTEM technique. Dódony observed stacks of "several mica (muscovite) layers". These stacks were "rotated on their 001 plane ... in respect to each other". On the basis of these observations and one-dimensional electron density calculations he denied the existence of interstratification in the Füzérradvány illite (C. Sc. Thesis No. 11, 1990). This opinion was supported by Patzkó and Szántó (1983), who observed by peptization methods that in some "illite" samples from Füzérradvány the finest fraction contained only pure illite and no interstratifications were found. The discussion on these observations resembled those, which were carried out at international level following the presentation of the fundamental particle theory by Nadeau et al. (1984).

Analogous occurrences in the Carpathian basin

The views on the genesis of the Füzérradvány "illite" benefited much from the field work of the local geologic service of the mining company (Mátyás 1974, 1979a, b). Mátyás explained the formation of illite, instead of smectite, by the high K contents of the rhyolite tuffs that were altered by hydrothermal processes.

The Füzérradvány-type illitic material seems to be a common alteration product in many areas of Neogene volcanism in the Carpathian basin.

Nemecz (1981) mentioned that in the locality Mád in the Tokaj Mts. the illite zone of hydrothermal alteration consists of a mineral of the "Füzérradvány type" (pp. 450–451). Very similar mineral phases and genetic conditions were found in hydrothermally altered rhyolite tuffs of Kremnica Mts., Slovakia, in the Dolná Ves deposit (Šucha et al. 1992). Similar illite deposits are known from the Eastern Carpathians near the summit of the Harghita Mts. (Neacsu and Urcan 1978; Bobos 1993). In this locality NH_4-containing illites were found and studied by Bobos et al. (1995). NH_4, however, seems to be absent from the Füzérradvány "illite" (Srodon et al. 1992).

Füzérradvány-type mixed-layer illitic material was found in a deeply buried rhyolite tuff layer at depths of about 3100 m in the Jász depression, in the southern foreland of the Mátra Mts. (borehole Jász-I; Viczián 1985). The formation of this material was probably affected by primary hydrothermal and later burial diagenetic processes.

Recent developments

In the international mineralogical literature a new standard mineral called *"Zempleni illite"* appeared in the last ten years. The identical nature of *"Zempleni* *illite*" and Füzérradvány "illite" and the main results of its recent investigations were discussed in former papers of the present author (Viczián 1996, 1997).

The locality of Füzérradvány is becoming important not only because of its illite deposits but also because of its gold mineralization, recognized by Csongrádi et al. (1996). Molnár (2000) introduced new concepts into the study of hydrothermal alteration of the Tokaj Mts. He considers that "low sulphidation-type epithermal systems" were active in this area and "neutralization of steam-heated fluids ... resulted in illite-montmorillonite and montmorillonite zones" of alteration. The detailed application of these concepts combined with new analytical data may lead to new results in the genetic interpretation of the "illite" deposits.

References

Beutelspacher, H., H.W. van der Marel, 1968: Atlas of electron microscopy of clay minerals and their admixtures. A picture atlas. – Elsevier, Amsterdam etc. 333 p.

Bobos, I. 1993: Smectite to illite reaction in the Harghita Bai hydrothermal system (East Carpathians). – Romanian J. Min. 76/1, pp. 121–125.

Bobos, I., V. Šucha, S. Soboleva 1995: Mixed layer ammonium-illite/smectite and ammonium illite from hydrothermal system Harghita Bai – East Carpathians, Romania (abstract). – In Elsen, A. et al. (Eds): EUROCLAY '95, Leuven, Book of Abstracts pp. 384–385.

Csongrádi, J., Gy. Tungli, T. Zelenka 1996: Az utóvulkáni működés és az ércesedés kapcsolata a füzérradványi Koromhegy-Koromtetőn (Relation between the postvolcanic activities and mineralisation in the Koromhegy-Koromtető, Füzérradvány area). – Földt. Közl., 126/1, pp. 67–75. (in Hungarian)

Dódony, I. 1990: Rétegszilikátok kristálykémiai kapcsolatainak és rácsgeometriájának transzmissziós elektronmikroszkópos vizsgálata (Transmission electron microscopic investigations of crystal chemical relations and lattice geometry of layer silicates). – Kandidátusi értekezés (C. Sc. Thesis, Hungarian Academy of Sciences), Budapest, 3+115 p. (in Hungarian)

Erdélyi, J., V. Koblencz, V. Tolnay 1958: Über Hydroparagonit, ein neues Glimmermineral, sowie über seine Beziehungen zum Hydromuskovit, Natronillit und Brammallit (Hydroparagonite, a new mica mineral, and on its relations to hydromuscovite, natronillite and brammallite). – Acta Geol. Hung., 5/2, pp. 169–186.

Grim, R. E. 1953: Clay mineralogy. – McGraw-Hill, New York etc. 384 p.

Grim, R. E., W.F. Bradley 1948: The illite clay minerals (abstract). – International Geological Congress, 18th Session, Great Britain, 1948. Volume of Titles and Abstracts pp. 127–128, London.

Grim, R. E., W.F. Bradley 1952: The illite clay minerals (abstract). – International Geological Congress, Report on 18th Session, Great Britain, 1948. Part XIII, Section M. p. 302. London.

Grim, R. E. et al. 1937: The mica in argillaceous sediments. – Am. Min. 22, pp. 813–829.

Henning, K.-H., M. Störr 1986: Electron micrographs (TEM, SEM) of clays and clay minerals. – Schriftenreihe für Geol. Wiss. 25, p. 350. Akademie-Verlag, Berlin.

Hofmann, U., J. Endell, H. Maegdefrau 1943: Die Einheitlichkeit des glimmerartigen Tonminerals Sárospatit (The homogeneity of the mica-like clay mineral sarospatite). – Ber. dtsch. keram. Ges., 24, pp. 339–344.

Hofmann, U., A. Jacob, H. Loofmann 1941: Untersuchung der Tonkfraktion der Boden mit dem Elektronen-Mikroskop. – Bodenkunde und Pflanzenernährung, 25/5–6, pp. 257–271.

Kiss, L., T. Takáts 1963: A füzérradványi illitbánya anyagának ásványkőzettani vizsgálata a finomkerámiaipar szempontjából (Mineralogical investigations of the material of the

Füzérradvány illite mines with respect to the fine ceramic industry). – Építésanyagipari Központi Kutató Intézet, Tudományos Közlemények 10, pp. 1–62., 1–35. melléklet. ÉM. Építésügyi Dokumentációs Iroda, Budapest. (in Hungarian)
Maegdefrau, E. 1941: Die Gruppe der glimmertatigen Tonmineralien (The group of mica-like clay minerals). – Sprechsaal f-r Keramik – Glas – Email, 74, 39, pp. 39–372, 381–383, 393–396, 399–401 (part I).
Maegdefrau, E., U. Hofmann 1937: Glimmerartige Mineralien als Tonsubstanzen (Mica-like minerals as clay substances). – Z. Krist. 98/1, pp. 31–59.
Mátyás, E. 1974: Új illites nemesagyagbánya Füzérradványban (A recently explored high-quality clay deposit rich in illite at Füzérradvány). – Bány. Koh. L., Bányászat 107/3, pp. 187–196. (in Hungarian)
Mátyás, E. 1979a: A tokaji-hegységi ásványbányászat bányaföldtana (Mining geology of the nonmetallic mining industry in the Tokaj Mountains). – Földt. Közl., 109/3–4, pp. 488–506. (in Hungarian)
Mátyás, E. 1979b: Guide to excursion in the Tokaj Mountains. – Xth Kaolin Symposium, IGCP Project No. 23, "Genesis of Kaolin", Budapest, 1979. 63 p.
Molnár, F. 2000: Genetic aspects of mineralogy in shallow levels of low sulphidation type epithermal systems of the Tokaj Mts., NE Hungary (abstract). – In Fehér, B. et al. (Ed.): Minerals of the Carpathians Intern. Conf., Miskolc, 2000. Abstracts. Acta Min. Petr. Szeged 41, Suppl., p. 74.
Nadeau, P. H., M.J. Wilson, W.J. McHardy, J.M. Tait 1984: Interstratified clays as fundamental particles. – Science, 225, pp. 923–925.
Neacsu, G., T. Urcan 1978: 10.50 Å hydromica, a principal component of "kaolin" from the Harghita area. – Inst. Geol. Geofiz., Stud. Tehn., Ser. I, Min. Petrogr. 14, pp. 107–117.
Nemecz, E. 1973: Agyagásványok (Clay minerals). – Akadémiai Kiadó, Budapest. 507 p. (in Hungarian)
Nemecz, E. 1981: Clay Minerals. – Akadémiai Kiadó, Budapest. 547 p.
Nemecz, E., Gy. Varju 1970: Sárospatakit (Hidrotermális illit-montmorillonit) kémiai és szerkezeti sajátságai (Chemical and structural investigation of Sárospatakites, Illite/montmorillonite). – Földt. Közl., 100/1, pp. 11–22. (in Hungarian)
Patzkó, Á., F. Szántó 1983: Füzérradványi illit peptizálhatósága és organofilizálhatósága (Peptisation and organophylisation of Füzérradvány illite, abstract). – MFT Illit ankét (Symposium on Illite of the Hungarian Geological Society), Zamárdi, 1983, Program, p. 23. (in Hungarian)
Sedletzky, I. D. 1940: On the principles of classification of argillaceous minerals. – Comptes Rendus (Doklady) de l'Académie des Sciences de l'URSS 26/3, pp. 240–243.
Srodon, J 1980: Precise identification of illite/smectite interstratifications by X-ray powder diffraction. – Clays Clay Min., 28, pp. 401–411.
Srodon, J., F. Elsass, W.J. McHardy, D.J. Morgan 1992: Chemistry of illite-smectite inferred from TEM measurements of fundamental particles. – Clay Min., 27/2, pp. 137–158.
Šucha, V., I. Kraus, C. Mosser, Z. Hroncová, K.A. Soboleva, V. Širánová 1992: Mixed-layer illite/smectite from the DolnáVeshydrothermal deposit, theWestern Carpathians Kremnica Mts. – Geol. Carpathica, Ser. Clays, 1, pp. 13–19.
Szegedi, Á. 1988: Mixed layer character of "illites" from Füzérradvány, Hungary. – In Konta, J. (Ed.): Tenth Conf. on Clay Min. Petr., Ostrava, 1986, pp. 249–254. Univerzita Karlova, Praha.
Viczián, I. 1985: Diagenetic transformation of mixed-layer illite/smectites in deep zones of the Pannonian Basin (Hungary). – 5th Meeting of the European Clay Groups, Prague, Czechoslovakia, 1983, pp. 135–140. Univerzita Karlova, Praha.
Viczián, I. 1996: A füzérradványi illit vizsgálatának újabb eredményei (New results in the study of the Füzérradvány illite). – Földt. Közl., 126/2–3, pp. 263–266 (in Hungarian).
Viczián, I. 1997: Hungarian investigations on the "Zempleni" illite. – Clays Clay Min., 45/1, pp. 114–115.

Acta Geologica Hungarica, Vol. 43/4, p. 501 (2000)

Book review

UNGARN – Bergland um Budapest, Balaton-Oberland, Südbakony

Hrsg. László Trunkó. unter Mitarbeit von Pál Müller, Tamás Budai, Gábor Csillag und László Koloszár

Sammlung geologischer Führer, Band 91, Gebrüder Borntraeger, Berlin-Stuttgart, 2000

(Hungary – The mountainous region around Budapest, the Balaton Upland, and the South Bakony Mts)

Paperback pocket book, 1 sketch map, 11 black-and-white photos, 26 figures in the text

L. Trunkó left Hungary as a graduate student of geology in 1956, and eventually became curator of the Natural History Museum in Karslruhe, Germany, and University Professor. He published the Geology of Hungary in German (1969) and in English (1997), and was awarded Honorary Membership of the Hungarian Geological Society. Now with co-authors from the Geological Institute of Hungary (MÁFI, Budapest) he has edited the first foreign-language geologic field guidebook for tourists of a considerable (and touristically the most important) region of Hungary.

The first part of the book begins with a geographic and geologic introduction, and includes a relatively detailed (62-page) geologic and structural history of the region.

The second part contains 20 geologic itineraries (mainly by car), Bud 1-11 for the greater neighborhood of Budapest (northward up to Visegrád in the Danube bend) and Bal-1-9 for the Transdanubian Central Range, from the granite of the Velence Hills along the northern shore of Lake Balaton to the Tapolca Basin basalt mesas and back through the Southern Bakony Mts. (stratigraphically from the Carboniferous through the Quaternary). Particular attention has been paid to nature protection, historical and cultural highlights, and even to special Hungarian food. The text is professionally correct and up-to date, based on recent on-the-spot information, but also easily understandable for educated non-professionals.

An abridged English-language version would be very useful and most welcome.

M. Knauer-Gellai

Acta Geologica Hungarica

VOLUME 43, 2000

Akadémiai Kiadó, Budapest

ACTA GEOLOGICA HUNGARICA

Volume 43 (2000)

Contents

Number 1

Number 2

Number 3

Number 4

Printed in Hungary
Akadémiai Nyomda, Martonvásár

GUIDELINES FOR AUTHORS

Acta Geologica Hungarica is an English-language quarterly publishing papers on geological topics. Besides papers on outstanding scientific achievements, on the main lines of geological research in Hungary, and on the geology of the Alpine–Carpathian–Dinaric region, reports on workshops of geological research, on major scientific meetings, and on contributions to international research projects will be accepted.

Only original papers will be published and a copy of the Publishing Agreement will be sent to the authors of papers accepted for publication. Manuscripts will be processed only after receiving the signed copy of the agreement.

Manuscripts are to be sent to the Editorial Office for refereeing, editing, in two typewritten copies, on floppy disk with two printed copies, or by E-mail. Manuscripts written by the following word processors will be accepted: MS Word, or ASCII format. Acceptance depends on the opinion of two referees and the decision of the Editorial Board.

Form of manuscripts

The paper complete with abstract, figures, tables, and bibliography should not exceed 25 pages (25 double-spaced lines with 3 cm margins on both sides).

The first page should include:

- the title of the paper (with minuscule letters)
- the full name of the author
- the name of the institution and city where the work was prepared
- an abstract of not more than 200 words
- a list of five to ten key words
- a footnote with the postal address of the author

The SI (System International) should be used for all units of measurements.

References

In text citations the author`s name and the year of the publication between brackets should be given. The reference list should contain the family name, a comma, the abbreviation of the first name, the year of publication, and a colon. This is followed by the title of the paper. Paper titles are followed – after a long hyphen – by periodical title, volume number, and inclusive page numbers. For books the title (English version), the name of the publisher, the place of publication, and the number of pages should be given.

Figures and tables

Figures and tables should be referred to in the text. Figures are expected in the size of the final type-area of the quarterly (12.6 x 18.6) or proportionally magnified 20–25% camera ready quality. Figures should be clear line drawings or good quality black-and-white photographic prints. Colour photographs will also be accepted, but the extra cost of reproduction in colour must be borne by the authors. The author`s name and figure number should be indicated on the back of each figure. Tables should be typed on separate sheets with a number.

Proof and reprints

The authors will be sent a set of proofs. Each of the pages should be proofread, signed, and returned to the Editorial Office within a week of receipt. Twenty-five reprints are supplied free of charge, additional reprints may be ordered.

Contents